APPENDIX 1.1

PROVENIENCE VS. PROVENANCE

"Provenience" and "provenance" are closely related words. I have always understood the former term to mean a thing's *place of origin* or *source* and the latter term to mean a thing's *history* going back to and including it's origin or source. Provenance is frequently used by museum curators and art historians when discussing an object's or artwork's chain of ownership from, if possible, the time of it's discovery or creation to the present day. In archaeology, provenience can refer to two somewhat different things. There can be "archaeological provenience" (almost always referred to simply as provenience), which is both the site at which an artifact is recovered and its original location in three-dimensional space at said site, and then there can be "source provenience", which is the geographic location or area from which the raw material (rock, mineral, wood, shell, paste, temper, whatever) used to fashion the object in question was acquired. Because I was attempting to locate the raw material sources of stone or metal artifacts, I decided be a little more specific and call my work a "geologic provenience" study.

I felt confident that I was using the term provenience correctly. After all, it is in Weigand and others (1977: 24) often cited paper that the basic assumption of raw material sourcing was first made explicit as the "*Provenience* Postulate" (emphasis added). Of course I was aware from reading the literature pertaining to sourcing studies that the term provenance was used more frequently than provenience, but for the longest time I thought of this as simply an alternate spelling, perhaps one used more commonly in the UK and Europe. Then some people started to tell me that this was not an issue like *color vs. colour*. Instead, they said that I was, supposedly, using the term provenience incorrectly. But no one could tell me when, why or who decided that provenance was the correct usage, only that it was the convention. Around the time I was finalizing my dissertation I read the book Geoarchaeology by Rapp and Hill (2006) in which they plainly state (ibid: 222) that provenience is an artifact's archaeological context and provenance is an artifact's raw material source . Not really convinced but wanting to be correct, I hit ctrl-H and replaced all of the proveniences in the text of my thesis with provenances. At my dissertation defense, however, one of my committee members said that provenance was actually the incorrect usage and bluntly told me that he would not sign my thesis unless I changed it back to provenience. Since I agreed with him anyway (and wished to graduate) I happily did so.

For this book, I will continue to refer to my work as geologic provenience analyses of stone and metal artifacts. I realize that this swimming against the stream. A quick perusal of titles, abstracts and keywords using the online search engines for journals like Archaeometry, The Journal of Archaeological Science, and Geoarchaeology clearly shows that the provenance is overwhelmingly favored over provenience in published articles about artifact sourcing studies. Even so, the issue is still debated[1)] and the latter term is still sometimes used by researchers (see Grave *et al*. 2009 for a recent

1) See the following two entries in archaeologist K. Kris Hirst's blog: [http://archaeology.about.com/b/2006/05/16/provenience-provenance-lets-call-the-whole-thing-off.htm] and [http://archaeology.about.com/b/2006/05/09/provenience-or-provenance-a-poll.htm]

example). I am certain that I will be continue to be told by some (perhaps many) people that my usage of the word provenience is incorrect. But it makes much more sense to me and I don't think there will be any serious confusion because of it as to the nature of the research I am actually doing.

APPENDIX 2.1

MAJOR DIVISIONS OF GEOLOGIC TIME

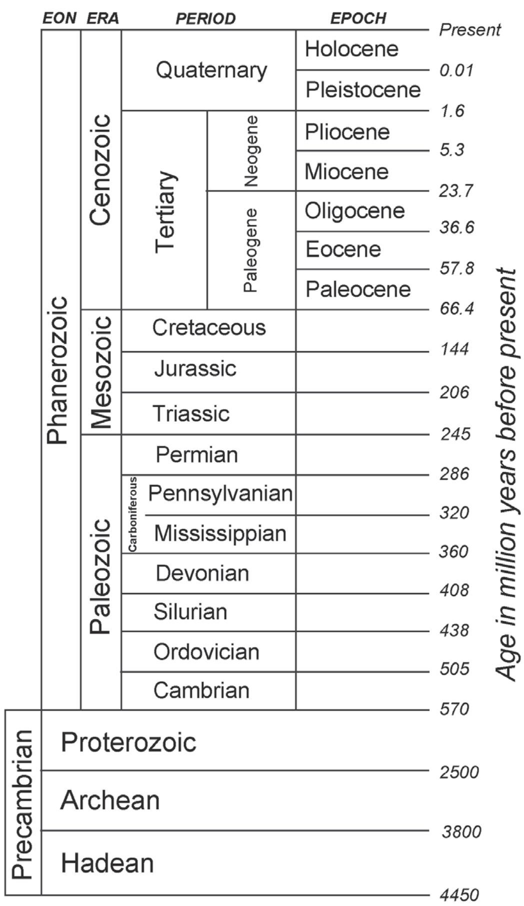

APPENDIX 2.2

REMARKS AND OBSERVATIONS ON THE ATTRITION OF STONE IN RIVERBEDS

Some scholars have suggested that certain varieties of stone used by Indus peoples may have been procured from secondary contexts, such as the beds of rivers flowing from mountain ranges, rather than from in situ geologic formations of those materials (see citations on p. 36). For example, a single, water-rounded pebble of lapis lazuli discovered at the Harappan outpost of Shortughaï in northern Afghanistan promoted the excavator of the site to speculate that some procurement activities involving that stone may have been "no more than gathering lapis in the riverbed" (Francfort 1985: 129). The riverbed in question is that of the Kokcha. It's upper reaches transect the zone where lapis lazuli occurs in the Badakshan district and the site of Shortughaï is near (5 km away) its terminal confluence with the Amu Darya (Francfort 1984b: 302). One may wonder at what point along the Kokcha's several hundred kilometer length was the pebble collected? Lapis lazuli is not a particularly hard (Mohs 5 to 6) or tough stone. It seems unlikely that a piece of it could have been rolled very far in a riverbed among tough boulders of granite and limestone before it was completely obliterated. And what about other types of softer or harder materials? Although I conducted no formal studies of the attrition rates of different kinds of stone in riverbeds (see Werrity 1992 for such as study), I tried to keep this issue in mind as I visited raw material sources and river drainages across the Greater Indus region.

In early 2001, I visited the Bannu Archaeological Project's (BAP) excavations at Lewan (Appendix 2.2 Figure 1 A) and noted among the lithic debris visible on site's surface numerous pieces of chert and jasper with rounded, weathered exteriors (Appendix 2.2 Figure 1 B). These were clearly fragments of water-worn cobbles/pebbles. When discussing potential sources of raw material for the lithic industries at Lewan and other prehistoric settlements in the western Bannu Basin, archaeologists working there have pointed to alluvial contexts in the "immediate locality" of those sites (Allchin 1981: 234), i.e., the conglomerate fans at the base of the Waziristan Hills or the beds of the region's many intermittent streams and rivers (Morris et al. 2001: 131). However, when BAP member Justin Morris and I traveled from Lewan to the nearby bed of the Tochi-Gambila river system in order to collect samples of chert/jasper (Appendix 2.2 Figure 1 C) we found very little material at all (as I recall, we came away with only a single palm-sized pebble of grayish chert). Now it's true that we didn't search that long (perhaps an hour) and that the bed of river was dry and dusty (if it had been wet it would have certainly been much easier to spot chert/jasper pebbles). Under better conditions and with more time, ancient peoples with greater experience than we would have almost certainly been more successful. Even so, the Tochi-Gambila river system, at least at the point on it where Justin Morris and I searched, is not exactly brimming chert or jasper. Perhaps the richer source areas lay closer to or within the hills of Waziristan, which were visible from the bed of the Tochi, 12 km to the west (Appendix 2.2 Figure 2).

Later that same year, while conducting geologic sampling in North Waziristan, I visited three jasper outcrops in the region that lay some 50 to 70 km due west of the Bannu Basin sites (Appendix 2.2 Figure 3). Red jasper at occurs at Barzai (Appendix 2.2 Figure 4 A; see also Figure 6.3 A & B) and large boulders of the material erode directly into the adjacent stream

Appendix 2.2 Figure 1.1 **[A]** Bannu Archaeological Project excavations at the site of Lewan. **[B]** A red jasper pebble fragment on the surface of Lewan. **[C]** Searching for chert and jasper in the bed of the Tochi River.

bed or nala (Appendix 2.2 Figure 4 B). Another red jasper outcrop is found at Masha Alga (Appendix 2.2 Figure 4 C) and brecciated jasper-chalcedony occurs at Sadgai (see Figure 6.3 C & D). Importantly, the nalas along which each of these occurrences are located eventually drain into the Tochi River. We had to drive our jeep along these intermittent stream beds to get to and from the sources. As we drove away from the outcrops, the size and amount of jasper fragments visible in the nalas dropped of quickly and, in fact, became, fairly rare after only a few kilometers. By the time I walked a transect of the Tochi River bed (Appendix 2.2 Figure 4 D) just east of the town of Miran Shah (this was still well within the Waziristan

Appendix 2.2 Figure 1.2 Looking toward the hills of North Waziristan from the bed of the Tochi River.

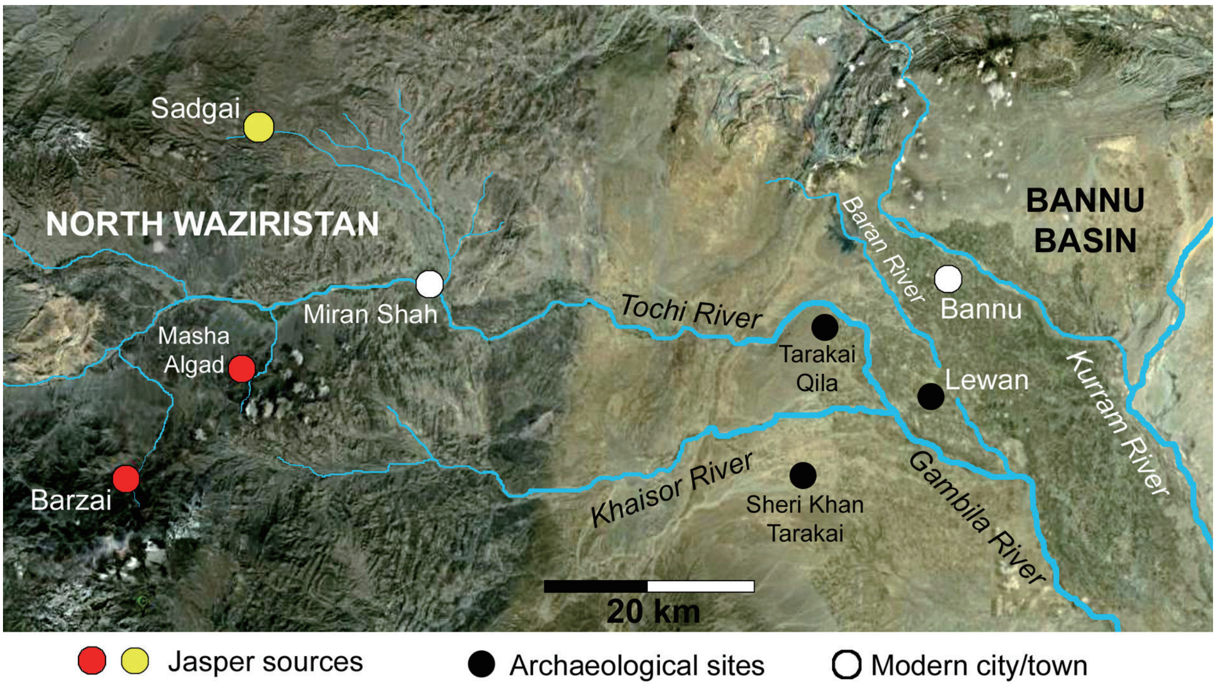

Appendix 2.2 Figure 1.3 Map of North Waziristan and the western Bannu Basin showing the archaeological sites, geologic sources, modern towns and rivers discussed in this appendix.

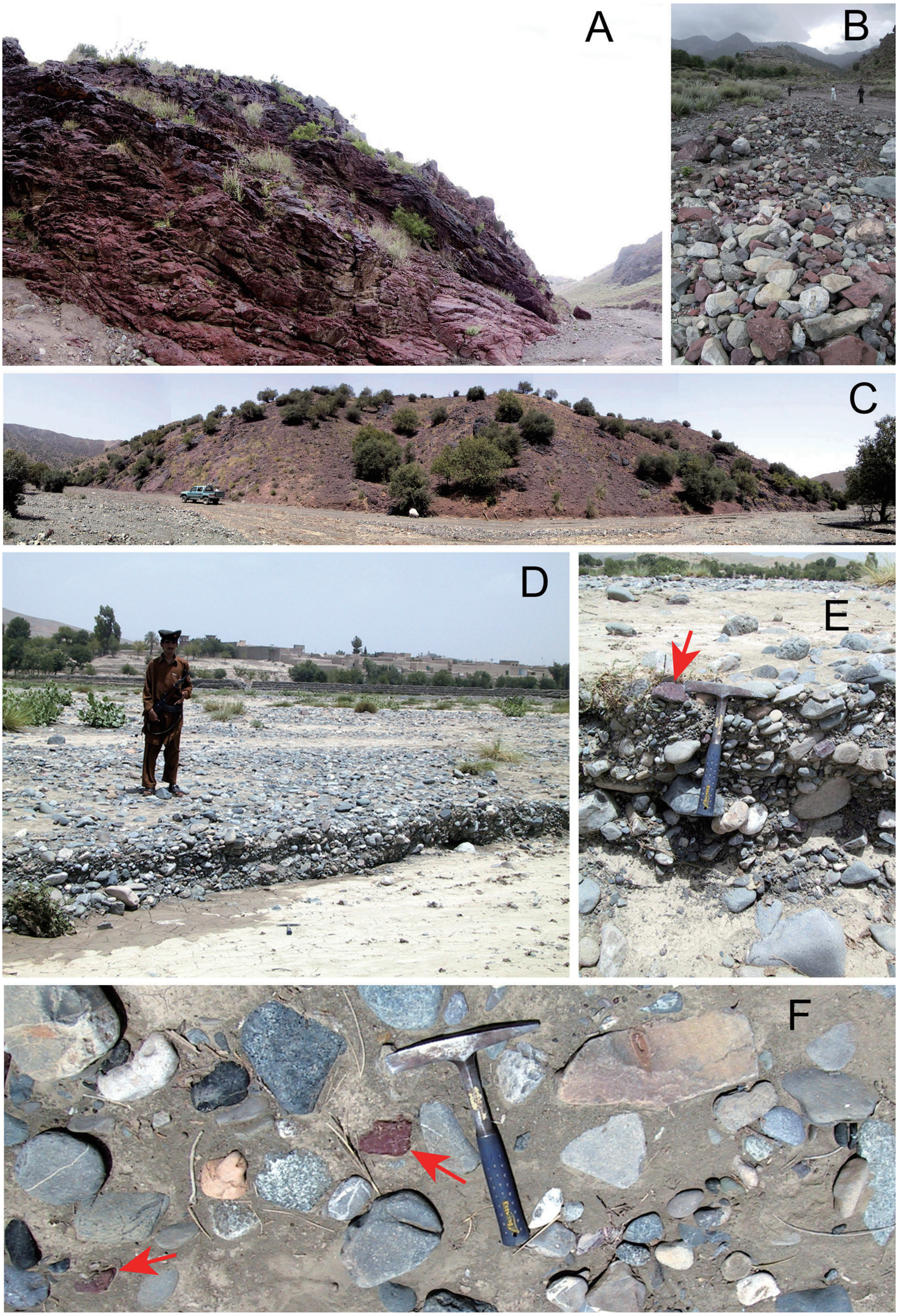

Appendix 2.2 Figure 1.4 Observations of jasper in North Waziristan. **[A]** The jasper outcrop at Barzai. **[B]** Jasper boulders in the nala adjacent to the Barzai outcrop. **[C]** The jasper outcrop at Masha Alga. **[D]** Searching for jasper in the Tochi River bed just east of Miran Shah. **[E]** A jasper fragment (arrow) in the Tochi near Miran Shah. **[F]** More red jasper fragments (arrows) at the same location.

Appendix 2.2 Figure 1.5 A water-rolled steatite fragment from the streambed directly below the steatite deposit at Daradar, Kurram Agency, FATA.

Hills, around 45 km west of Lewan), I was only able to find a few fragments of jasper (Appendix 2.2 Figure 4 E & F). Although cursory, I feel fairly confident in this qualitative assessment as it was done not long after a rain and the red jasper fragments I saw stood out prominently.

Based these observations and others, my conclusion is that alluvial fans or riverbeds at the bases of mountain ranges are good sources only for tough materials like sandstone, quartzite and granite. Although stone like chert and jasper can also sometimes be found in such contexts, to have a reliable supply of large, good quality pieces of those raw materials it is necessary to travel fairly close to the original source. For softer or more fracture-prone types of rock it's a non-starter. To reach the Daradar steatite deposit (see Figure 7.18) in the Kurram Agency, FATA, I had to travel the last several kilometers up a steep boulder filled streambed. It was only within sight of the source (less than a 100 meters from it) that I began to observe water-rounded pieces of steatite (Appendix 2.2 Figure 5). If you're going to travel that far you may as well go all of the way. Ancient peoples making the arduous journey up the Kokcha River Valley in order to acquire a valuable stone like lapis lazuli certainly would have collected water-rolled pebbles of the material whenever they encountered them. It is highly likely that such opportunistic procurement happened relatively near the actual deposits and that the ancient peoples would have then continued on to the mining areas themselves.

APPENDIX 3.1

MOHS' MINERAL HARDNESS SCALE

Hardness	***Mineral***
1	Talc
2	Gypsum
3	Calcite
4	Fluorite
5	Apatite
6	Orthoclase Feldspar
7	Quartz
8	Topaz
9	Corundum
10	Diamond

APPENDIX 4.1

X-RAY DIFFRACTION ANALYSES OF HARAPPAN ROCK AND MINERAL ARTIFACTS - MAJOR AND MINOR PHASES

(*MINOR PHASES DETERMINED BY EMPA)

Artifact	*Description*	*Major Phase*	*Minor Phase(s) / [SG]*
H2000/9999-108	alabaster fragment	Gypsum	
H2000/9999-131	alabaster fragment	Gypsum	
H95/4943-8	copper mineral	Malachite	
H90/3126-1	copper mineral	Malachite	
H90/3022-98	copper mineral	Malachite	
H90/2070-12	copper mineral	Chalcocite	
H90/3008-13	copper mineral	Chalcocite	
H90/3008-14	copper mineral	Chalcocite	
H94/4999-529	copper mineral	Chalcocite	
H2000/2090-49	"Ernestite"	Mullite	quartz, rutile, hematite, zircon*
H2000/3317-2	"Ernestite"	Mullite	cristobolite, titanohematite*, zircon*, phosphate*
H2000/3317-3	"Ernestite"	Mullite	cristobolite, titanohematite*, zircon* phosphate*
H2000/3317-4	"Ernestite"	Mullite	quartz, rutile, hematite
H2000/9999-81	green pebble frag.	Quartz	albite*
H90/2076-6	green pebble frag.	Quartz	epidote*, albite*, sphene*
H90/3000-30	green pebble frag.	Quartz	epidote, rutile*
H90/3207-14	green pebble frag.	Quartz	felspar*, epidote*, albite*
H98/8499-351	green pebble frag.	Quartz	albite*
H88/182-14	green pendent	Nephrite (tremolite)	chromite
H2000/9999-126	green rock fragment	Quartz	tremolite
H97/6977-7	green rock fragment	Fluorite	
H96/6303-4	green rock fragment	Prehnite	
H2000/9999-92	green rock fragment	Quartz	
H95/4960-88	green rock fragment	Quartz	
H2000/8990-1	green rock fragment	Quartz	
H94/4999-213	green rock fragment	Turquoise	
H2000/9999-87	green rock fragment	Vesuvianite	[SG = 3.33]
H2000/9999-88	green rock fragment	Vesuvianite	[SG = 3.29]
H2000/9999-89	green rock fragment	Vesuvianite	[SG = 3.32]
H2000/9999-90	green rock fragment	Vesuvianite	grossular / [SG = 3.32]
H2000/9999-93	green rock fragment	Vesuvianite	[SG = 3.28]
H90/2076-7	green rock fragment	Vesuvianite	[SG = 3.23]

Artifact	*Description*	*Major Phase*	*Minor Phase(s) / [SG]*
H90/2080-1	green rock fragment	Vesuvianite	grossular, clinochlore / [SG = 3.28]
H90/3000-31	green rock fragment	Vesuvianite	[SG = 3.23]
H90/3011-153	green rock fragment	Vesuvianite	clinochlore [SG = 3.29]
H90/3200-36	green rock fragment	Vesuvianite	clinochlore / [SG = 3.19]
H90/3208-147	green rock fragment	Vesuvianite	clinochlore / [SG = 3.29]
H90/3220-4	green rock fragment	Vesuvianite	clinochlore / [SG = 3.31]
H94/4374-19	green rock fragment	Vesuvianite	[SG = 3.27]
H94/4999-4	green rock fragment	Vesuvianite	clinochlore / [SG = 3.28]
H94/4999-5	green rock fragment	Vesuvianite	clinochlore / [SG = 3.27]
H95/4922-79	green rock fragment	Vesuvianite	clinochlore / [SG = 3.29]
H95/4922-81	green rock fragment	Vesuvianite	clinochlore / [SG = 3.32]
H95/5760-54	green rock fragment	Vesuvianite	clinochlore / [SG = 3.23]
H95/5764-74	green rock fragment	Vesuvianite	clinochlore / [SG = 3.26]
H96/6958-41	green rock fragment	Vesuvianite	grossular, clinochlore / [SG = 3.32]
H98/8499-353	green rock fragment	Vesuvianite	clinochlore* [SG = 3.32]
H94/5310-36	green rock fragment	Clinochlore	vesuvianite / [SG = 2.98]
H96/7129-1	green rock fragment	Clinochlore	vesuvianite / [SG = 3.16]
H2000/9999-91	green rock fragment	Grossular	vesuvianite*, clinochlore / [SG = 3.45]
H94/5106-8	green rock fragment	Grossular	vesuvianite / [SG = 3.45]
H94/4999-23	green rock fragment	Lizardite	
H89/2006-159	green rock fragment	Lizardite	
H2000/9508-2	green bead	Clinochrysotile	
H96-7730-15	red bead	Kaolinite	hematite
H2000/9999-77	lapis Lazuli fragment	Lazurite	calcite
H2000/9999-74	lapis Lazuli fragment	Lazurite	calcite
H90/3011-1	lead mineral	Galena	
H2000/2102-1726	lead mineral	Galena	stibnite
H2000/2226-111	lead mineral	Galena	stibnite
H2000/9999-73	lead mineral	Galena	stibnite
H90/8857-1	lead mineral	Cerrusite	anglesite
H99/8755-152	lead mineral	Cerrusite	anglesite
H2000/2139-141	lead mineral	Cerrusite	anglesite
H90/3193-6	lead mineral	Massicot	
H94/5530-13	limestone fragment	Calcite	
H2000/9999-122	ochre fragment	Goethite	
H2000/2227-65	ochre fragment	Hematite	
H90/3073-34	ochre fragment	Hematite	

APPENDIX 4.2

REPRESENTATIVE XRD SCANS

A. Steatite fragment H2000/2084-1, Talc (T = talc peak).

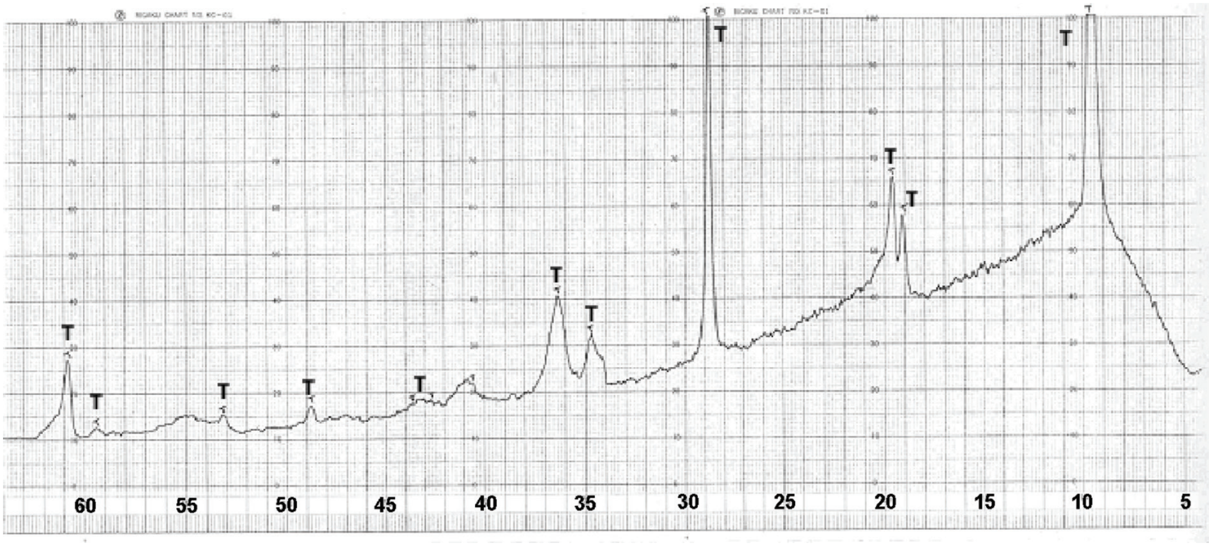

B. Steatite fragment H2000/8983-3, Talc (T) with Quartz (Q = quartz peak).

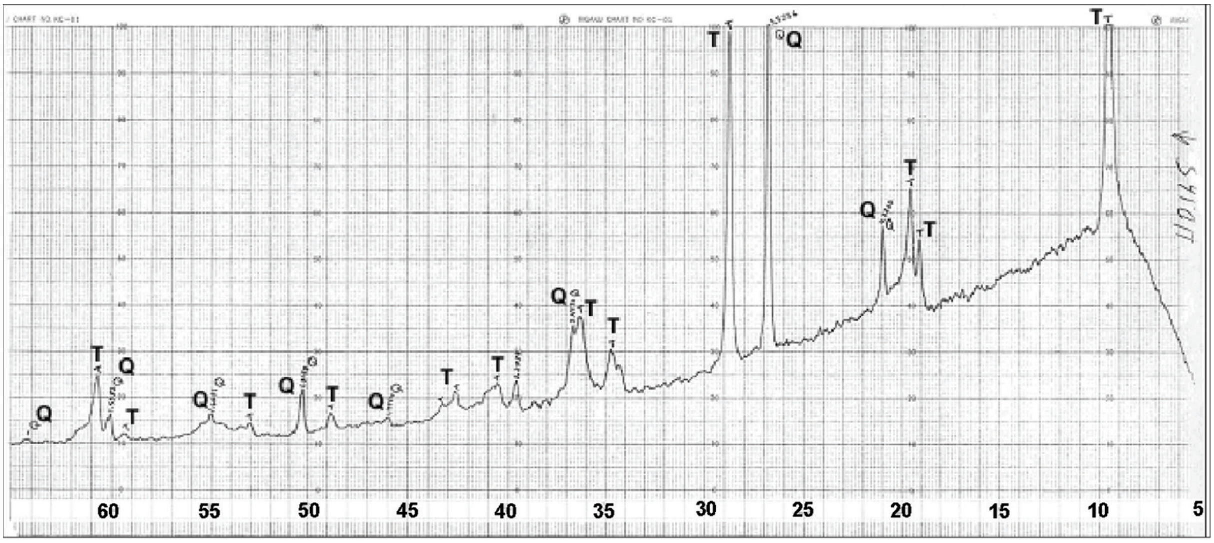

C. Steatite fragment H95/5729-99, Talc (T) with Dolomite (D = dolomite peak).

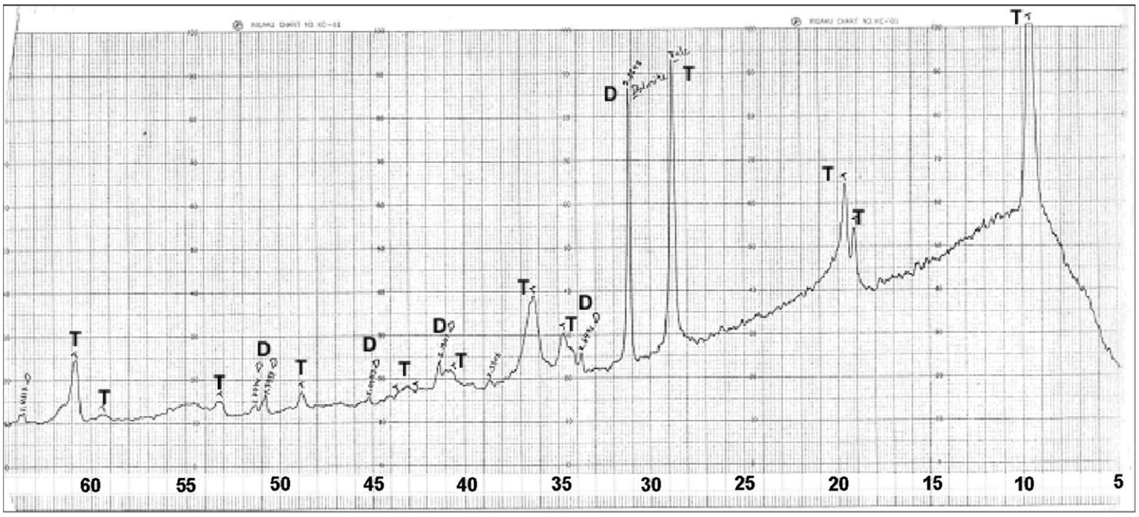

D. Copper ore fragment H90/2070-12, (C = Chalcocite peak).

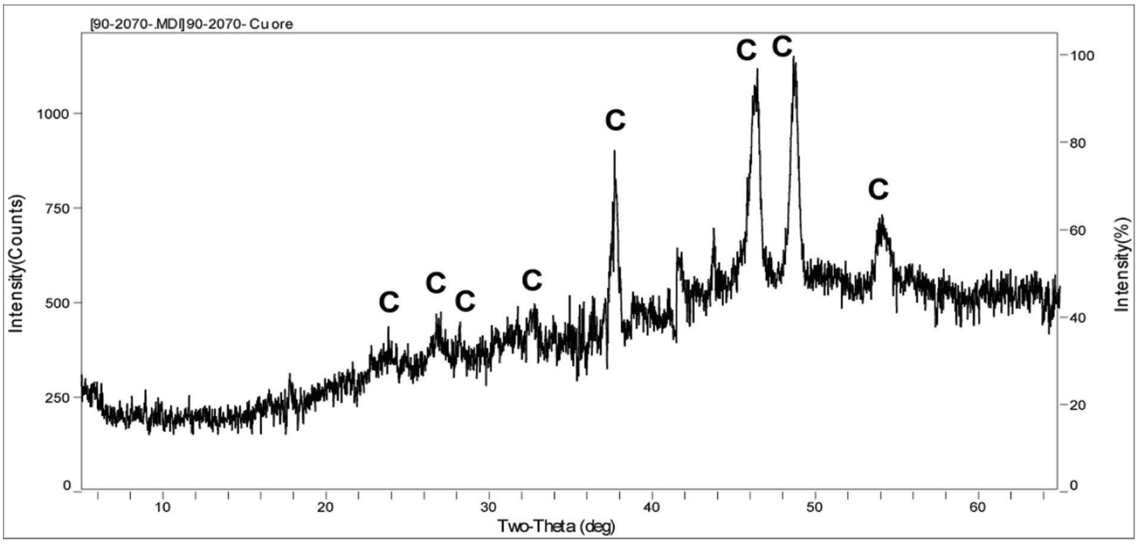

E. Copper ore fragment H95/4943-8, (M = Malachite peak).

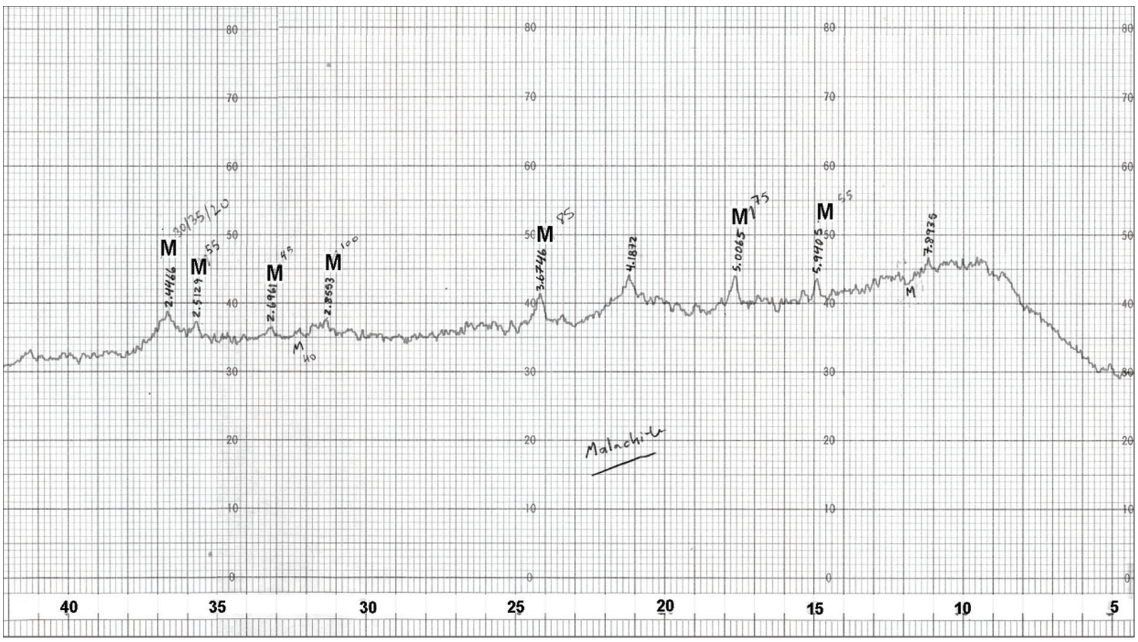

F. Composite of four XRD scans of vesuvianite-grossular garnet fragments, (G = Grossular peak, V = Vesuvianite peak. C – Chlorite peak).

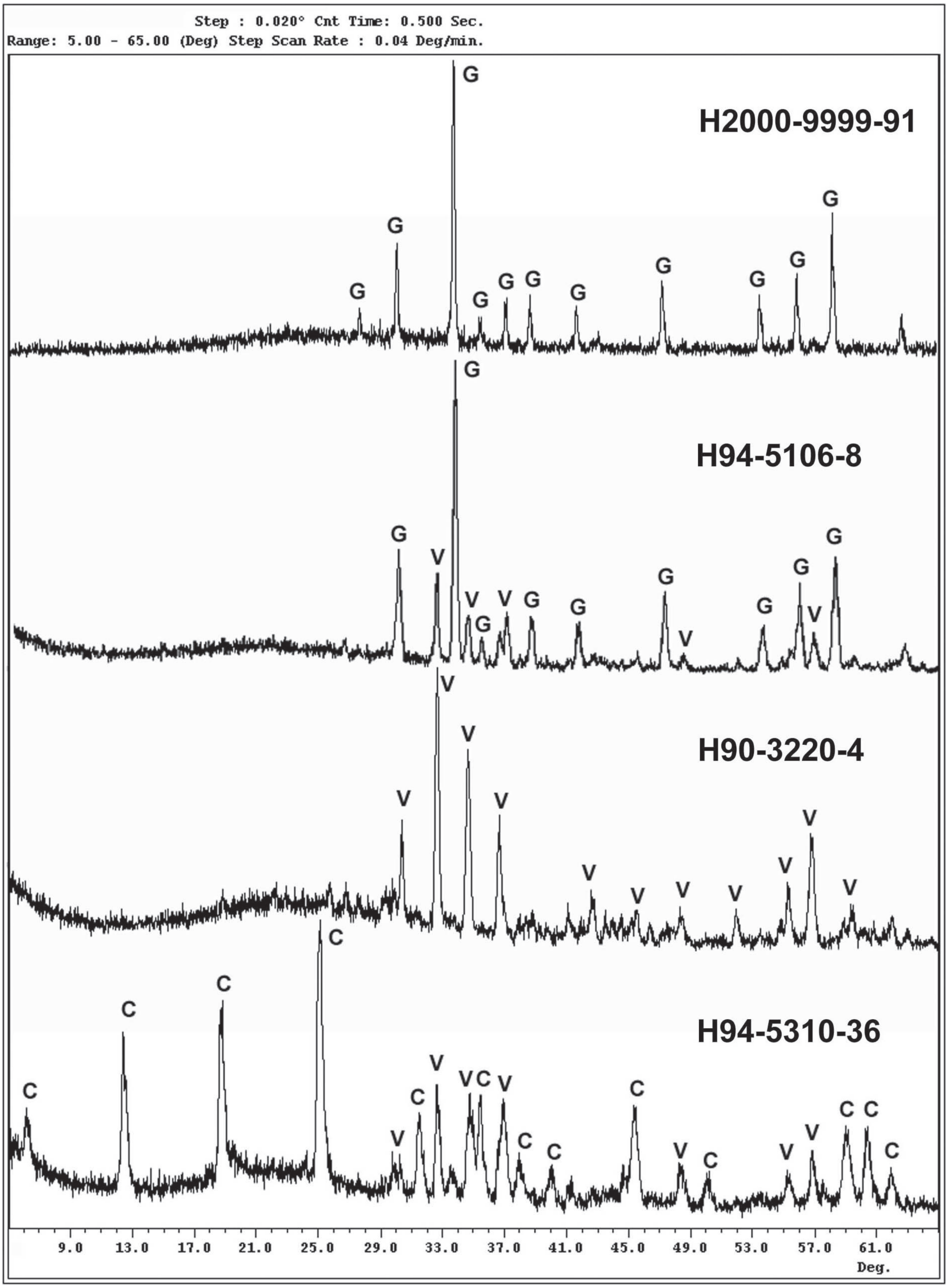

G. Alabaster fragment H2000/9999-130, (G = Gypsum peak).

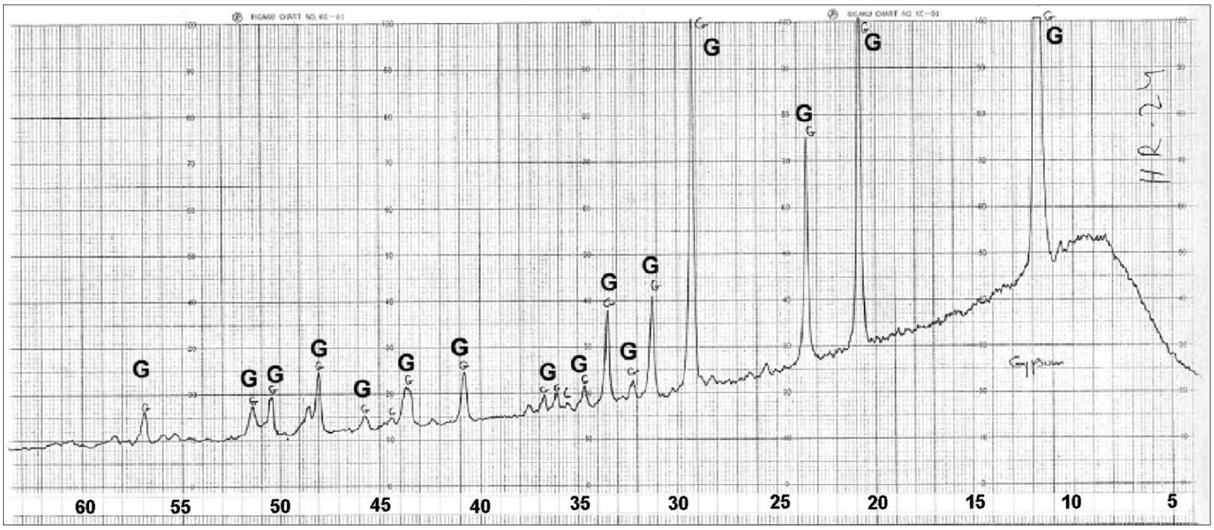

H. Lapis lazuli blocklet H2000/9999-77, (L = Laurite peak, D = Diopside peak).

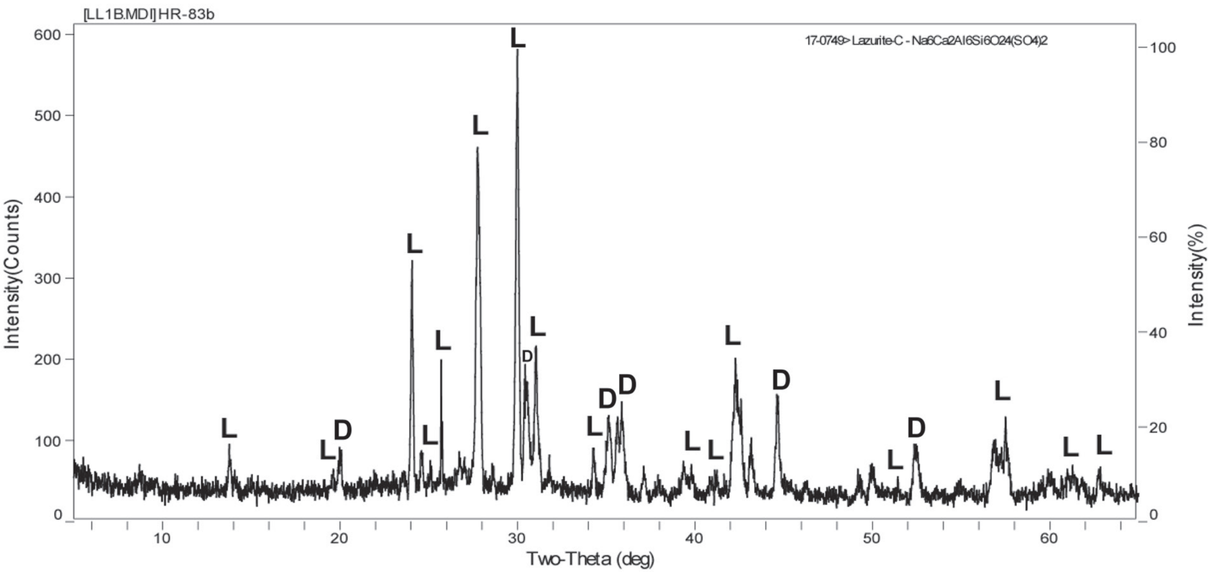

I. “Ernestite” fragment H2000/3317-4, (Q = Quartz peak, M = Mullite peak, R = Rutile peak, H = Hematite peak).

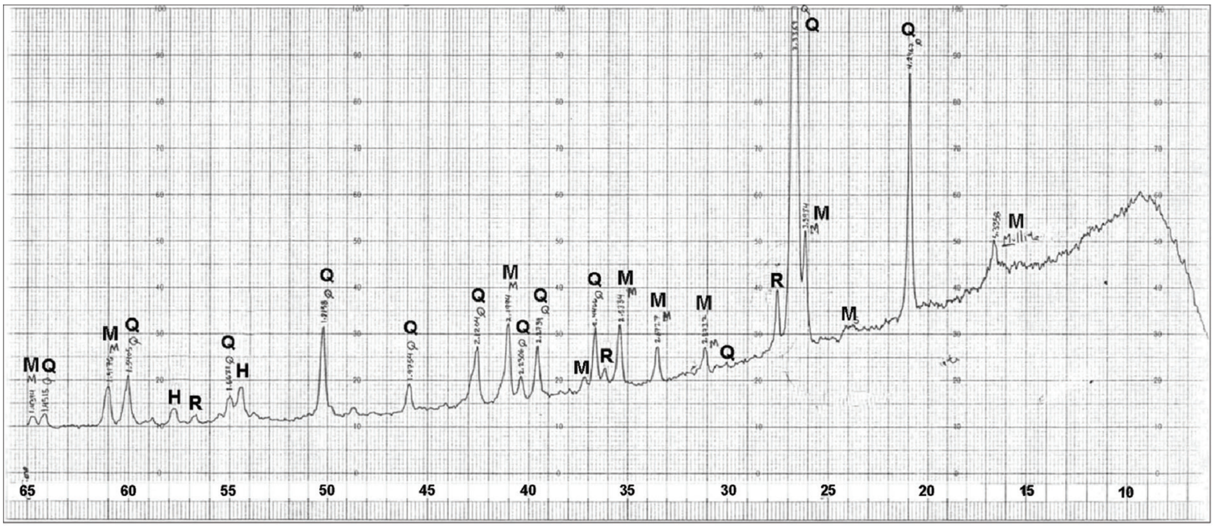

J. "Ernestite" fragment H2000/3317-3, (M = Mullite peak, C = Cristobalite peak).

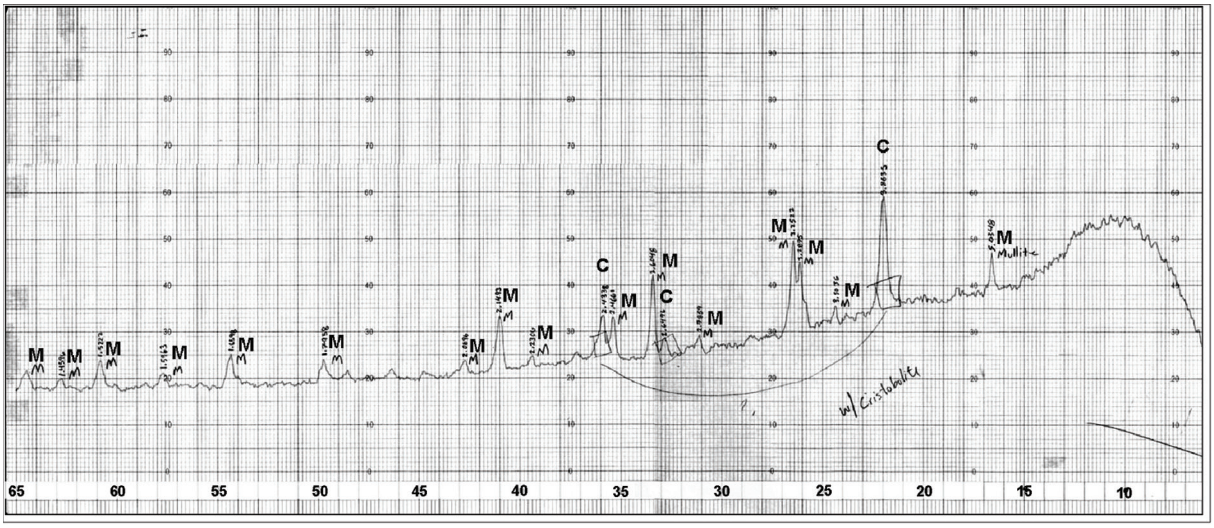

K. "Ochre" fragment H90/3073-7,4 (H = Hematite peak).

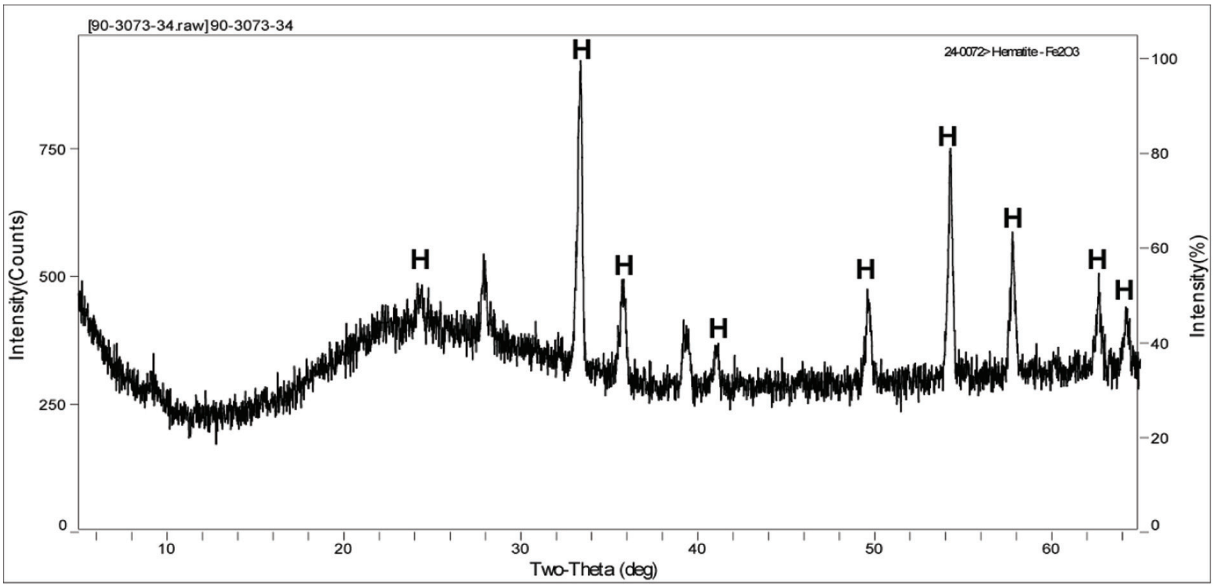

L. "Ochre" fragment H2000/9999-122, (G = Goethite peak).

M. Lead ore fragment H90/3011-147, (G = Galena peak, A = Stibnite (Antimony peak).

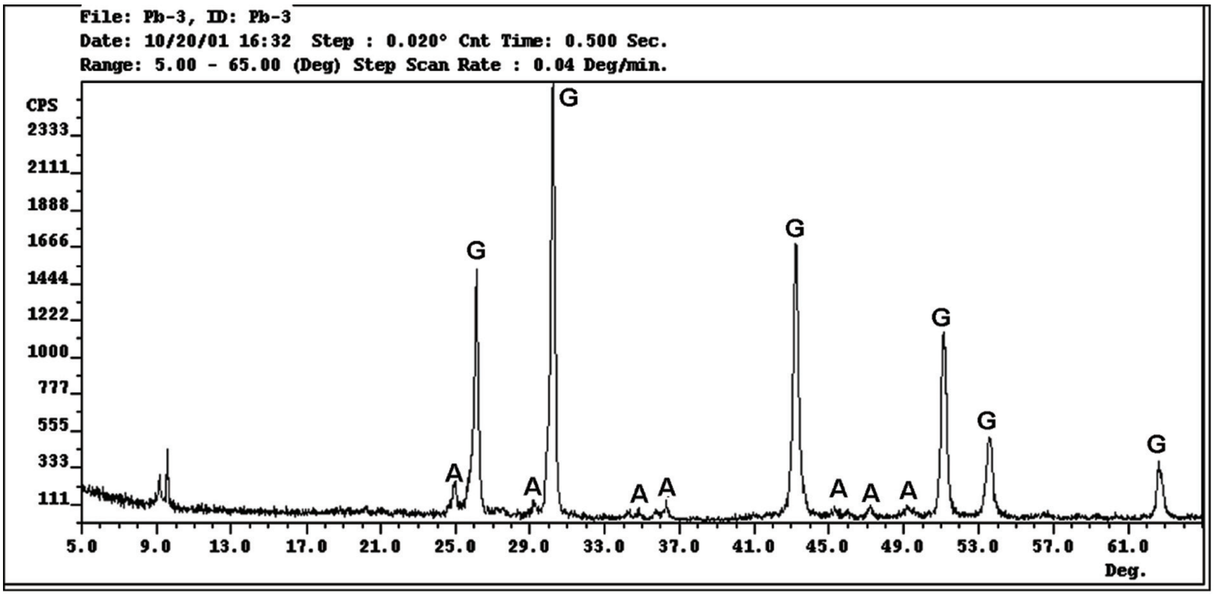

N. Lead ore fragment H99/8857-1, (C = Cerussite peak, A = Anglesite peak).

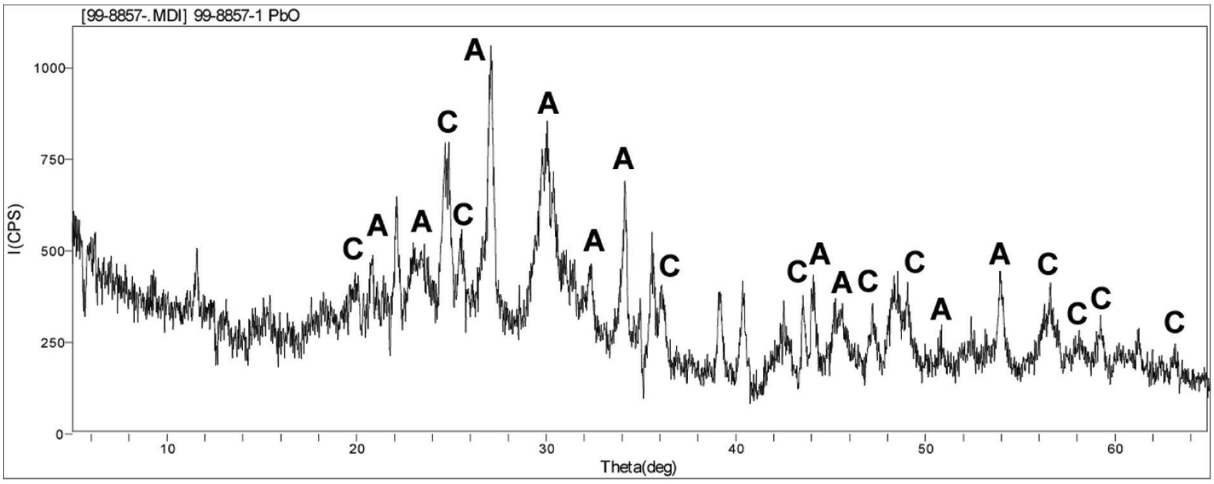

O. Lead ore fragment H90/3193-6, (M = Massicot peak).

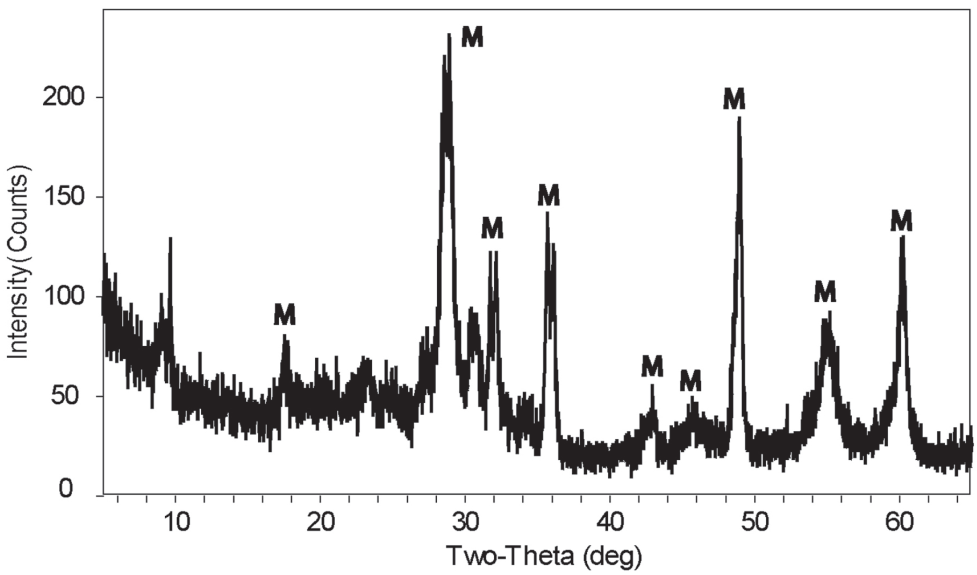

P. Serpentine fragment H94/4999-23, (L = Lizardite peak).

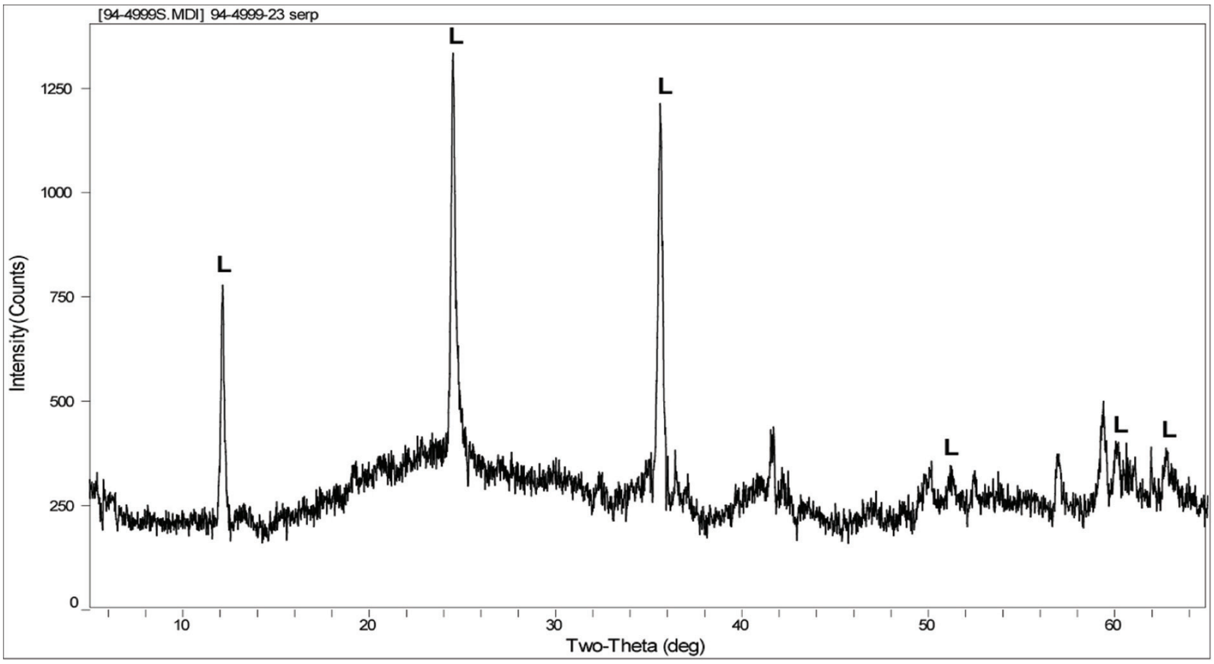

Q. Serpentine bead H2000/9508-2, (C = Clinochrysotile peak).

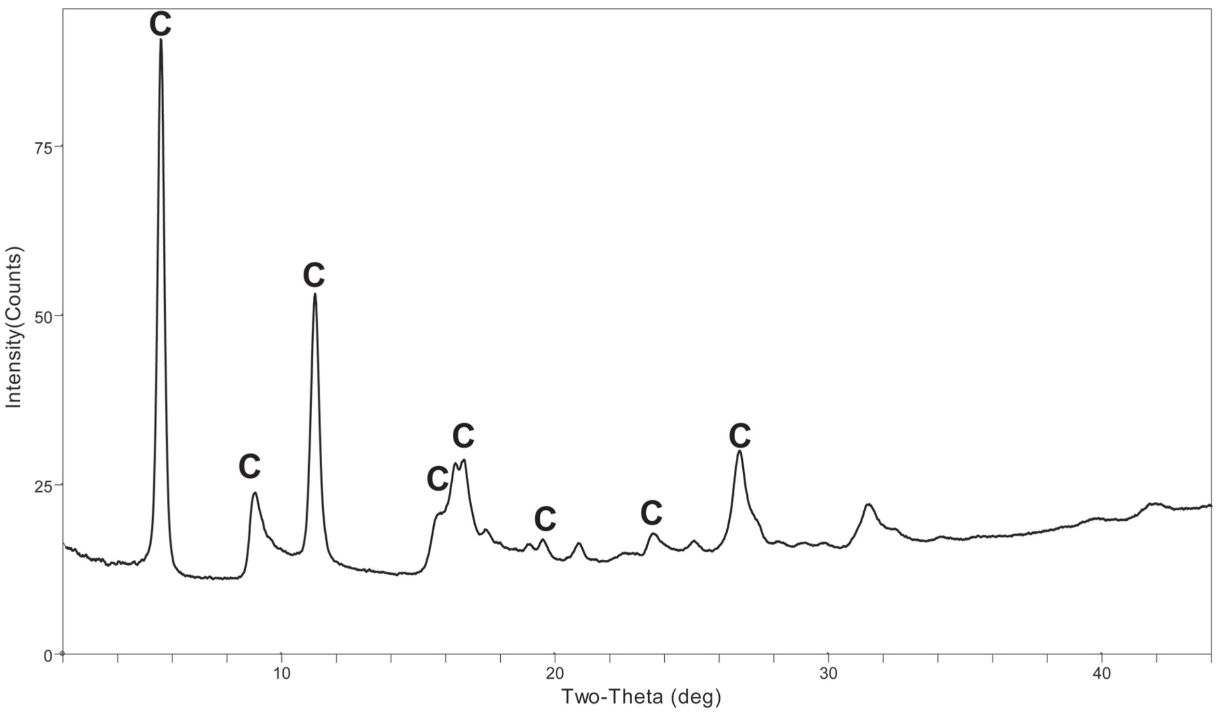

R. Calcite fragment H2000/2110-77, (C = Calcite peak).

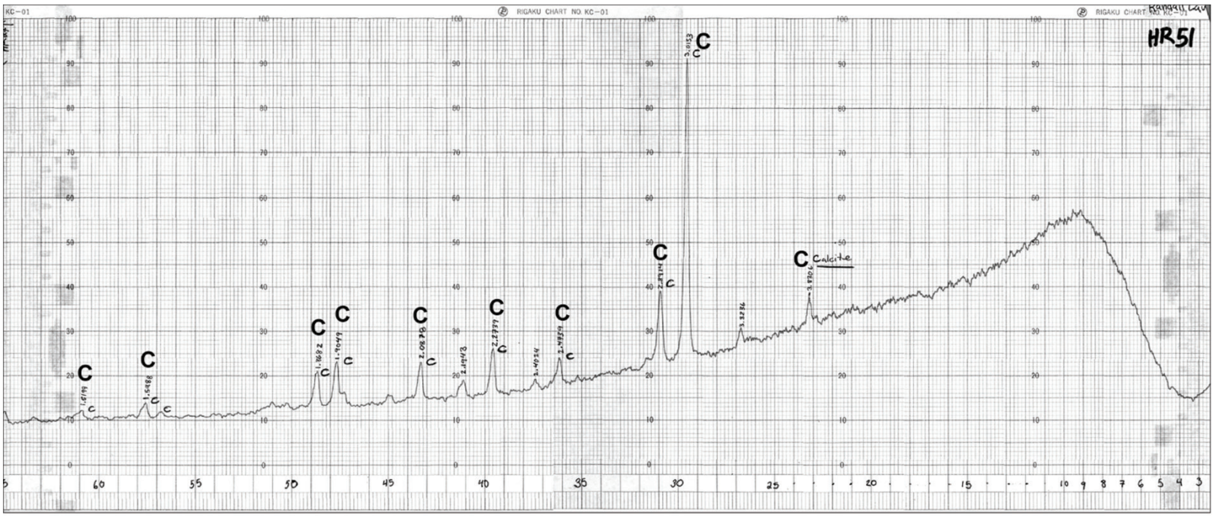

S. Fluorite fragment H97/6977-7, (F = Fluorite peak).

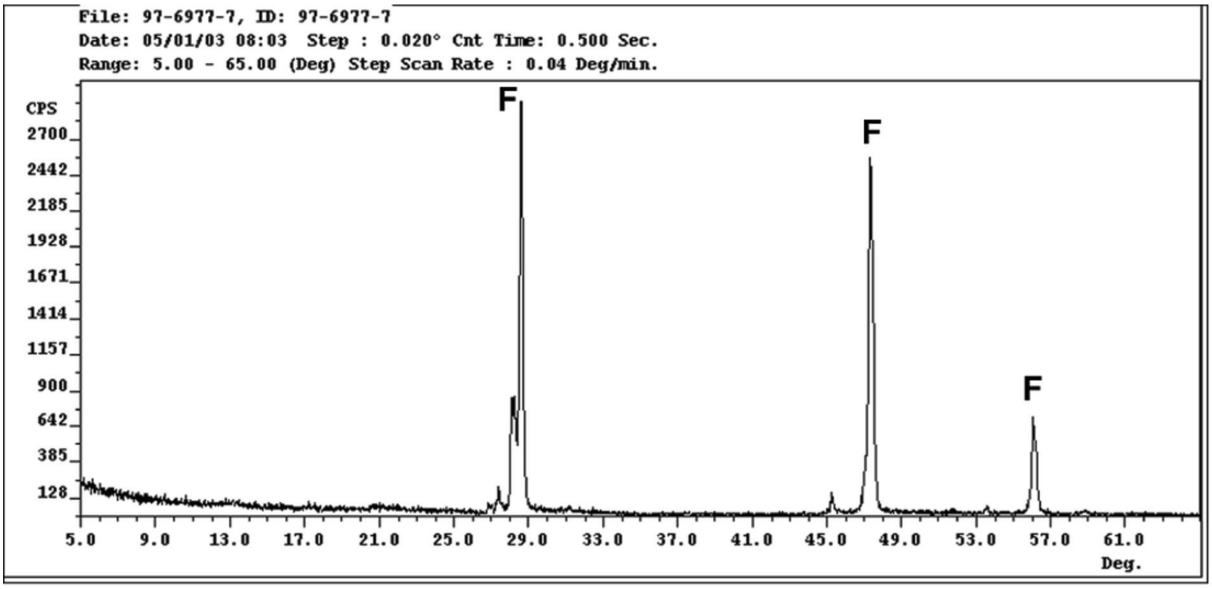

T. Mica fragment H87/62, (M = Muscovite peak).

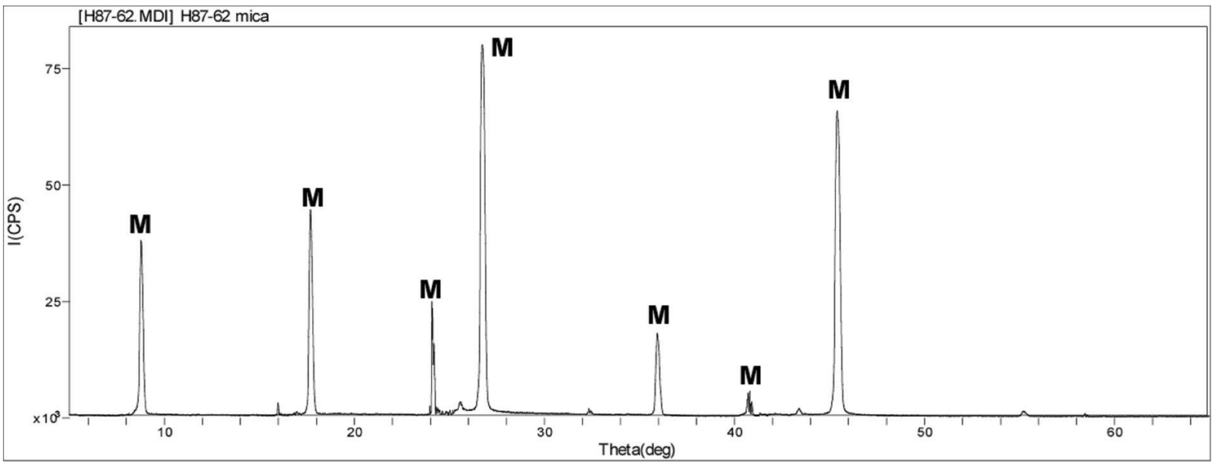

U. Prehnite fragment H96/6303-475, (P = Prehnite peak).

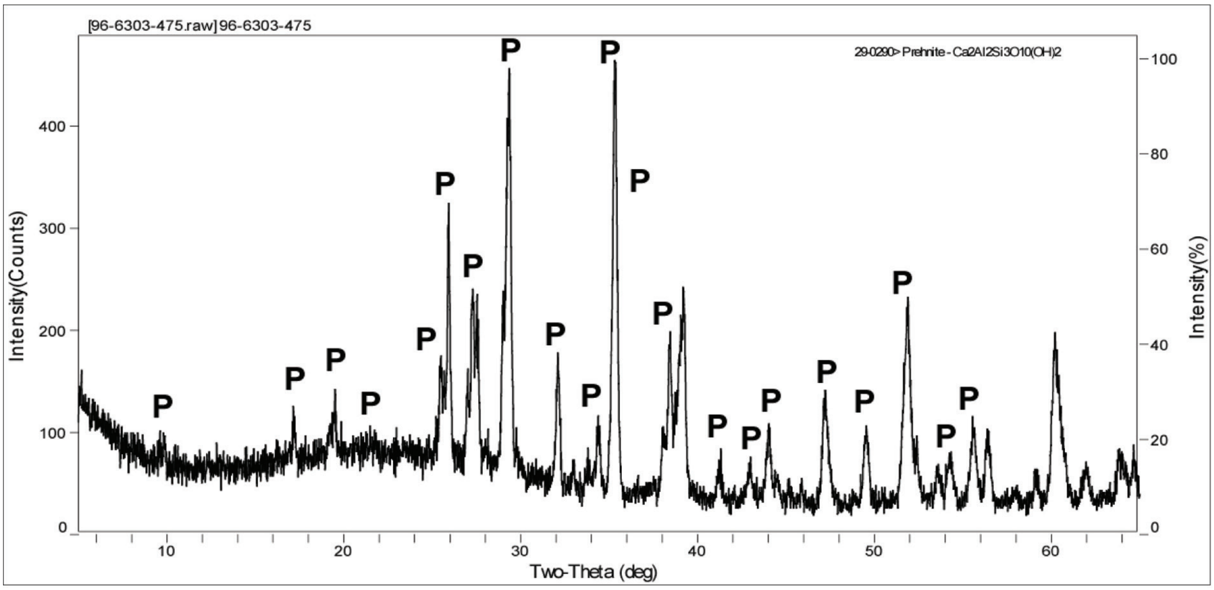

V. Sulfur fragment H96/6219-43, (S = Sulfur peak).

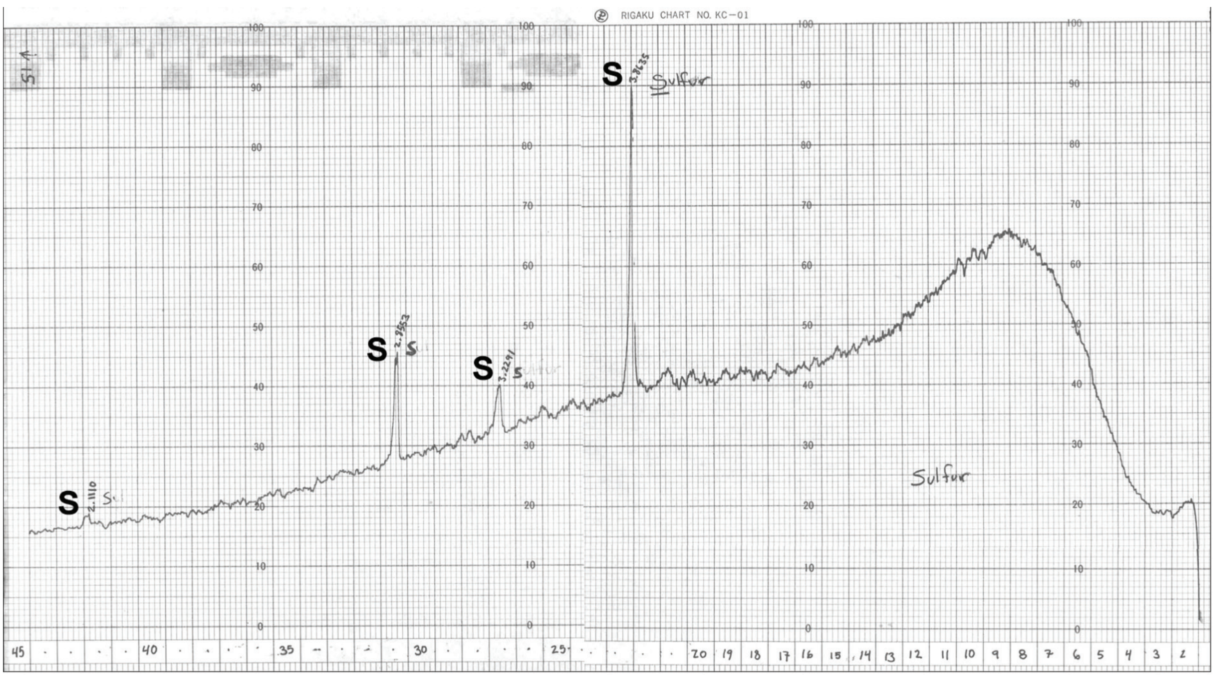

W. Turquoise fragment H94/4999-213, (T = Turquoise peak).

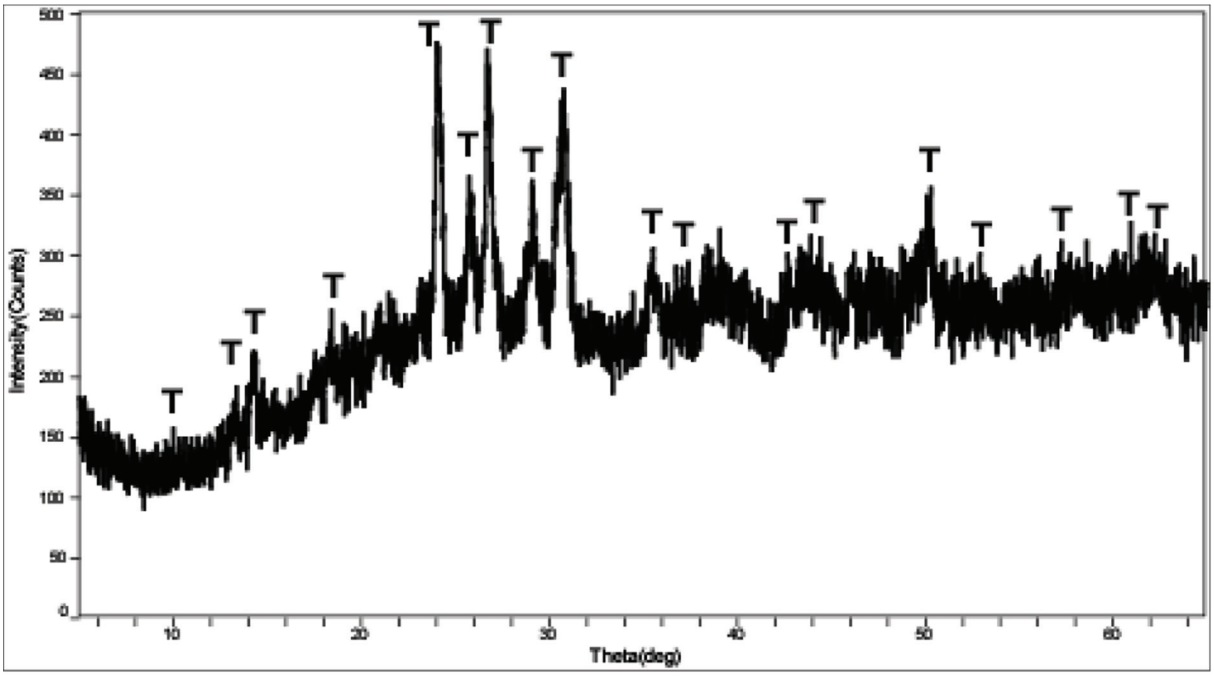

X. Chagai “turquoise” sample from J.-F. Jarrige, (Q = Quartz peak).

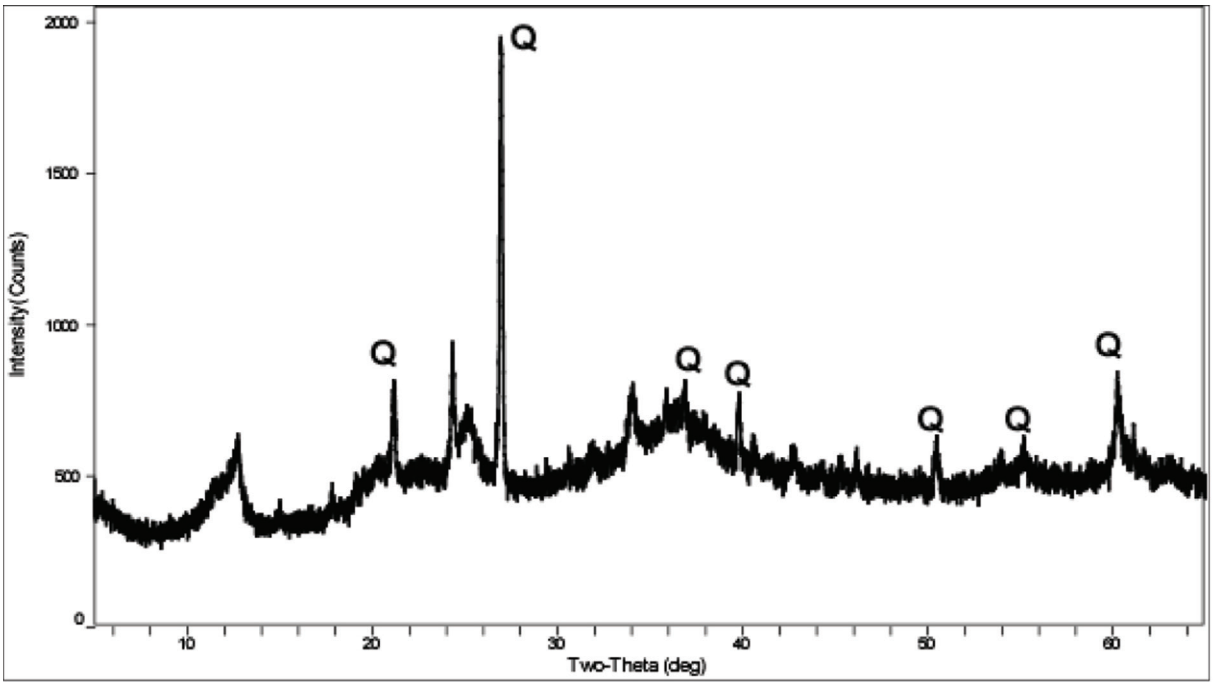

APPENDIX 4.3

CHARACTERIZATION OF TWO BASALT ARTIFACTS USING EMPA

Basalt is a dense, dark-colored volcanic rock that is composed mainly of plagioclase and pyroxene minerals, but which may sometimes contain significant amounts of olivine (Lapidus and Winstanley 1990: 53). By using EMPA to study the chemical compositions of clinopyroxene crystals in samples, geologists can often identify the tectonic settings (continental, island arc, ocean floor) in which rocks of this kind most probably formed (LeBas 1962; Nisbet and Pearce 1977). Leanne Mallory-Greenough and others (1998) successfully employed this method to characterize and determine the regional geologic provenience of minute pieces of basalt temper in an Egyptian potsherd. Two fragments of basalt recovered from surface contexts at Harappa were selected for exploratory EMPA (Appendix 4.3 Figure 1) to see if similar results could be achieved for artifacts from an Indus Civilization site. Both artifacts were examined using the electron microprobe's back-scatter electron (BSE) imaging and wavelength dispersive spectrometry (WDS) features.

The first artifact examined – H2000/9999-127 (pictured in the third image of Figure 4.4 B), is a large basalt flake that appears to have broken from a pestle or rubbing-stone. The BSE image (Appendix 4.3 Figure 1 A) shows that pyroxene minerals (gray phases) partially surround lathe-like plagioclase crystals (lightest phases), giving the stone a slightly *sub-ophitic* texture (Shelley 1993: Figure 1.17a) that is somewhat reminiscent of *dolerite* (the intrusive equivalent to basalt). WDS scans were made on clinopyroxene crystals at 16 different points extending across the sample. The second artifact examined – H2000/9999-128 (not pictured), is a small, non-diagnostic chunk of basalt. Its BSE image (Appendix 4.3 Figure 1B) revealed a much finer, inter-granular texture than that of the first example, one that is quite typical of basalts (ibid.: Figure 1.31b). For this sample, WDS scans were made on 15 different clinopyroxene crystals. Eight oxides were measured and the results of all scans were averaged for each artifact. These data are reported in Appendix 4.3 Figure 1 C.

One way that geologists classify igneous rocks like basalt is according their *alkalinity* – a term which, in this instance, refers to the relative abundance of silica to sodium or potassium- rich minerals in a sample (McBirney 2007: 38-45). The silica and aluminum composition of clinopyroxene crystals in a basalt sample has been shown to be indicative of the alkalinity of the magma from which it formed (LeBas 1962). Using the averages of their measured SiO_2 and Al_2O_3 abundances, the Harappan artifacts are plotted on Appendix 4.3 Figure 1 D in relation to dashed lines that demarcate the approximate boundaries between sub-alkaline, alkaline and peralkaline volcanic rocks (ibid.). Both fall clearly into the *sub-alkaline* category. Basalts of this kind are the most common rocks in oceanic crust (Lapidus and Winstanley 1990: 510) and so the artifacts might very well have originated in one of the ophiolite sequences (obducted oceanic crust) found intermittently to the north and west of the Indus Basin. However, sub-alkaline basalts are known to sometimes occur in volcanic formations associated with continental and island-arc settings.

Using canonical discriminant analysis and data on the same eight oxides measured here, Nisbet and Pearce (1977) compared a large set (n = 329) of volcanic rocks from four different geologic settings: OFB – ocean floor basalts; VAB – volcanic arc (or active continental margin) basalts; WPT – within-plate (continental) tholeiitic basalts; and WPA – within-plate alkali basalts. Reasonably good

Appendix 4.3 Figure 1 EMPA characterization of two basalt fragments from Harappa.

A. BSE image of H2000/9999-127.

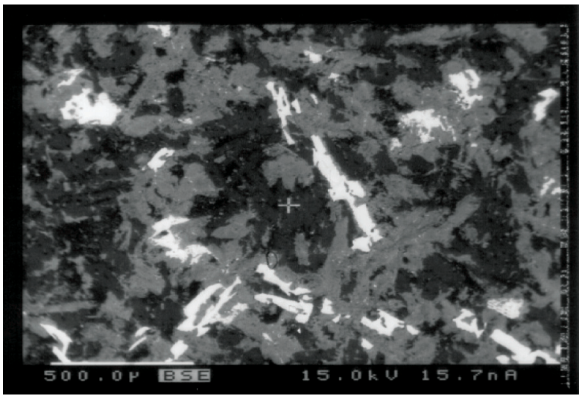

B. BSE image of H2000/9999-128.

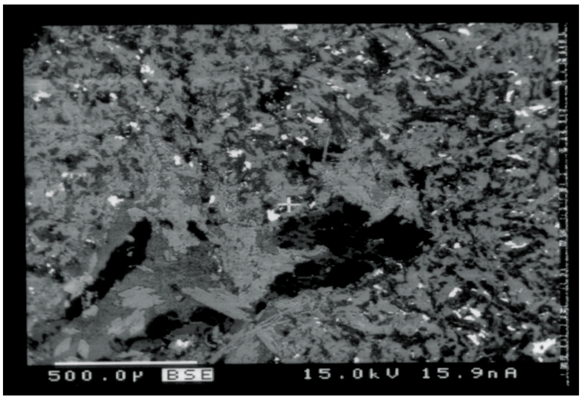

C. Composition of clinopyroxene of crystals in the two basalt fragments.

	H2000/9999-127 (average of 16 analysis points)	**H2000/9999-128 (average of 15 analysis points)**
Al_2O_3	2.07	4.28
CaO_2	14.56	11.04
FeO_2	17.63	14.19
MgO_2	13.02	14.82
MnO_2	0.43	0.26
Na_2O	0.26	0.44
SiO_2	49.92	50.73
TiO_2	0.87	0.30
totals	98.80	96.23

D. Silica/alumina plot of Harappan basalt fragments clinopyroxenes compositions (boundaries after LeBas 1962).

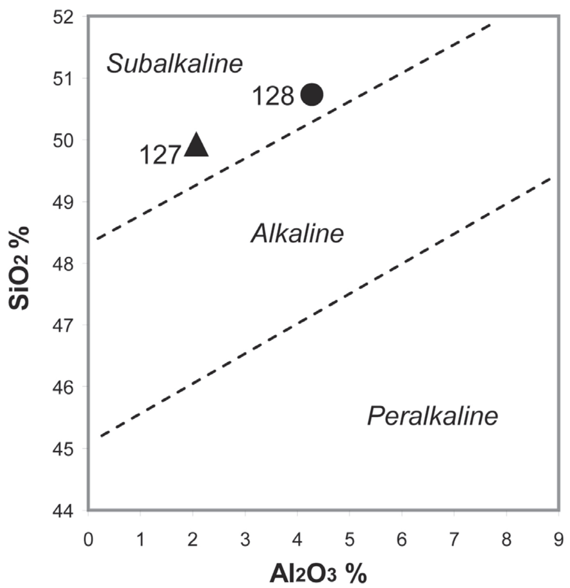

E. Harappan basalt artifact clinopyroxene composition data plotted in relation to basalts from different tectonic settings. (Functions and boundaries after Nisbet and Pearce 1977)

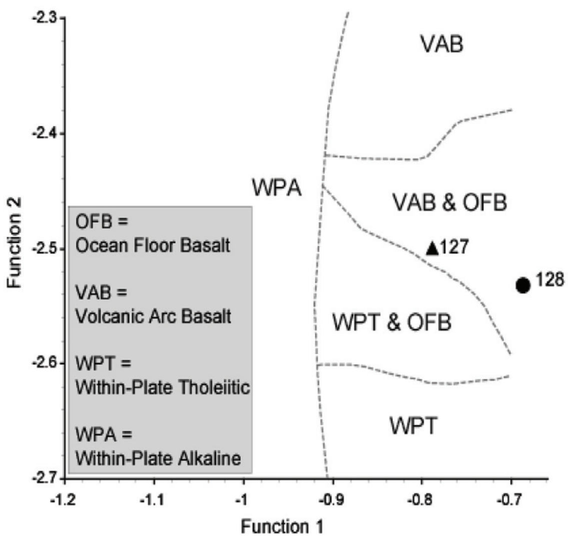

separation between the four grouped sub-sets was achieved (the average correct classification success rate was around 70%) and, using the first and second discriminant functions, they created a visual plot with boundaries roughly demarking the zones where samples from the various geologic settings fell (ibid.: 153). Mallory-Greenough and others used a version of this plot (1998: Figure 6) in their effort to identify the geologic provenience of basalt temper fragments. I have created another version (Appendix 4.3 Figure 1 E) upon which the two Harappan basalt artifacts are plotted using the discriminant functions published by Nisbet and Pearce (1977: 152). Both samples fall within the combined VAB and OFB zone.

This preliminary study indicates that the two fragments of dark-colored stone examined here are sub-alkaline basalts that likely came from volcanic formations associated with either oceanic crust (ophiolites) or subduction zones (at island arcs or active continental margins). Although this leaves open a wide range of potential geologic sources around northwestern South Asia (most of them on the northern and western margins of the Greater Indus Valley region), it is possible to state, with reasonable confidence, that these artifacts are probably *not* related to the continental flood basalts of peninsular India and Gujarat known as the Deccan Traps. Whole rock analysis (Mallory-Greenough and Greenough 2004) and potassium-argon dating (Weinstein-Evron *et al*. 1995) have shown promise in helping to more narrowly define the probable regional provenience of basalt artifacts and may eventually be employed in future studies on these and other objects made of that stone from Harappa.

APPENDIX 4.4

THE LAPIS LAZULI QUESTION

INTRODUCTION

"Where did the lapis lazuli come from?" This was the first question that the late Prof. Farzand Durrani asked me at a gathering at the University of Peshawar back in 2000. He, of course, knew of Georgina Herrmann's seminal study (1968) in which she had evaluated all of the reported sources of lapis lazuli in the Old World and concluded that deposits in northern Afghanistan's Badakhshan Province were almost certainly the only ones exploited in ancient times. He had assumed the raw stone for the hundreds of lapis lazuli artifacts he had excavated at the Early Harappan settlement of Rehman Dheri on Pakistan's Gomal Plain (Durrani *et al*. 1995) originated in that region, around 475 km due north of the site. In recent years, however, there had been reports of another potential source in the Chagai Hills of western Balochistan Province, Pakistan. Prof. Durrani was, therefore, quite interested to learn if this "new" source, which was said to be located some 675 km to the west-southwest of Rehman Dheri, was genuine. I did not have a satisfactory answer for him at the time. I said that I too had heard of this supposed source but was having a difficult time finding any detailed information on it at all. I told him that I would work on the question.

Now 10 years later, I have reached the same conclusion that Georgina Herrmann did four decades ago – deposits in the Badakhshan region of northern Afghanistan would have been the *only* viable sources of lapis lazuli for peoples in ancient northwestern South Asia or their contemporaries in the Near East. It is highly improbable that this important luxury material occurs in the Chagai Hills. Examples of lapis lazuli that have been attributed to that area were, in all likelihood, actually derived from the Badakhshan deposits. In this appendix, I discuss the research and analyses that have led me to these conclusions. Appendix 4.4 Figure 1 is a map with insets that shows the regions, lapis lazuli sources (both genuine and questionable) and sites that are mentioned in this discussion.

LAPIS LAZULI IN ANCIENT SOUTH ASIA

The earliest evidence for the use of lapis lazuli in South Asia (or anywhere else) comes from Mehrgarh, where a few small beads were unearthed in burials dating to the seventh millennium BC (Jarrige 1991b: 41). By the time Harappa was founded, roughly three thousand years later, this stone was being transported through exchange networks that brought it to sites across Balochistan (Besenval 2000: 170; Hargreaves 1929: 33-34; Tosi and Vidale 1990), the NWFP (Khan *et al*. 1991a: 58-59) and into Cholistan (Dogar 2001: 11). Finished lapis lazuli objects and debris fragments from early Ravi Phase strata at Harappa indicate that the fourth millennium BC residents of that site on the Punjab Plain were also participants in those exchange networks and acquired at least some of that stone in raw form.

Lapis lazuli was traded over an even wider area of northwestern South Asia during the Harappan Period (for information on sites where it has been found see Asthana 1993: 271-273; Chakrabarti 1978; Lahiri 1992; and Ratnagar 2004: 185-193). However, artifacts made from this material tend not to be found in great abundance at those sites where they are present (a few notable exceptions are mentioned below). Case in

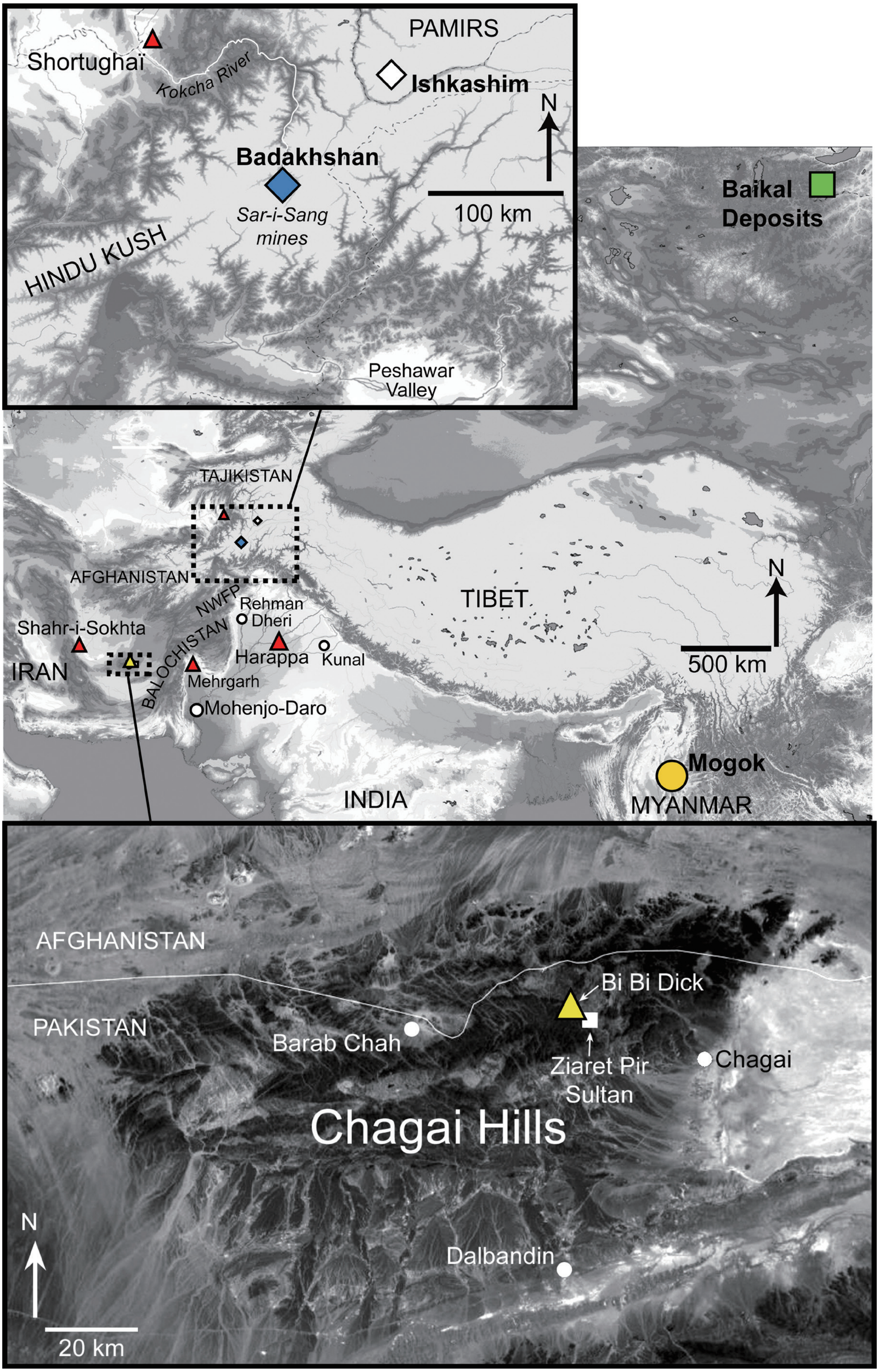

Appendix 4.4 Figure 1 Archaeological sites and lapis lazuli sources discussed in this appendix.

Appendix 4.4 Figure 2 Spatial and temporal distribution of lapis lazuli artifacts at Harappa.

Context	*fragments, manufacturing debris and unfinished beads*	*finished beads, pendants or ring*
Period 1	3(AB)	1(AB)
Period 2	1(E)	6(AB) 4(E)
Period 3A	ø	21(AB) 3(E)
Period 3B	ø	4(E) 1(ET) 1(cemetery)
Period 3C	2(E) 1(cemetery) 5(ET) 1(F)	8(AB) 7(E) 2(ET) 1(cemetery) 5(F)
Period 4/5	ø	2 (AB)
surface & disturbed deposits	5(AB) 12(E) 5(ET) 3(F) 12(other)	30(AB) 16(E) 2(ET) 2(F) 8(other)
total	**50**	**124**

point – Mohenjo-daro, which was located at the nexus of long-distance trade routes and was home to a large population of affluent elites who, presumably, sought to differentiate themselves through the consumption of exotic materials. Only a pitiful few (perhaps less than a dozen in total) lapis lazuli artifacts have been recovered at this, the largest Indus city (Mackay 1931c: 525; Mackay 1938: 499; Pracchia *et al.* 1985: 236; Bondioli *et al.* 1984: 24). Because of its apparent limited use there and at most other Indus Civilization sites, the stone is often thought of as being a material that, for various reasons (discussed by Shaffer 1982: 193; Kenoyer 1998: 96; Vidale 1989b: 180), was "never as highly esteemed in India as in ancient Egypt or Mesopotamia" (Buddruss 1980: 26). Such assessments are probably fair. The tremendous value that some ancient Near Eastern societies placed on lapis lazuli during the fourth and third millenniums BC and the large amounts of that material they consumed is clearly evident in the textual and archaeological records of that region (von Rosen 1988, 1990). The high demand for this stone in Mesopotamia seems to have been an important stimulus for trade across the Iranian plateau during that time (Sarianidi 1971; Tosi 1974a) and a key aspect of the economies of certain settlements located in that region – most notably Shahr-i-Sokhta, a Helmand Tradition site where large quantities of lapis lazuli were evidently prepared for export (Tosi 1974a: 15).

The utilization of lapis lazuli by Indus Civilization peoples was, in comparison to their contemporaries to the west, undeniably less intense. Even so, I am hesitant to believe that it was an unimportant or even a particularly rare material during the Harappan Period (although its greatly limited use at a settlement as large and centrally located as Mohenjo-daro is problematic) simply because it is found across such a wide area and, at a few sites at least, it was rather abundant. The 104 debris fragments found in Harappan levels at Shortughaï in northern Afghanistan (Francfort 1989: 145, 173) appear to indicate that, during the Harappan Period at least, Indus peoples had direct access to (some have suggested even controlled - see Asthana 1993: 273; Ratnagar 2004: 189) a major source of that material located in the nearby Badakhshan region (discussed below). Nearly 500 lapis lazuli beads and fragments were recovered at Rehman Dheri (Durrani *et al.* 1995a) and more than 5500 were part of a single large cache at Kunal in Haryana (Khatri and Acharya 1997: 86). I have recently recorded 125 beads made from this stone and several debris fragments (two of which were confirmed using XRD to be lazurite) among excavated materials from the site of Dholavira in

Gujarat. At Harappa, lapis lazuli artifacts have been recovered from every one of the site's chronological phases and sub-phases (Appendix 4.4 Figure 2). The largest sub-assemblage dates to Period 3C, from which 23 finished objects and nine debris fragments have been recovered. That lapis lazuli was, in general, used sparingly by Indus Civilization peoples is less important in terms of the current study than the fact that Harappans appear to have had good access to it and that it was present at many sites. Identifying the potential geologic source(s) of such a widely used stone is the main concern here.

POTENTIAL HARAPPAN LAPIS LAZULI SOURCES

Lazurite – the constituent of lapis lazuli that gives the rock its blue color – is a rare mineral in nature (Hogarth and Griffen 1976b: 2). Where it is found, it typically occurs as specks, masses and, occasionally, crystals in zones of marble formed where impure limestone was metasomatized by intrusive granitic rocks (Deer *et al.* 1992: 502). The only *well-documented* lazurite/lapis lazuli sources in Asia are: the Sar-i-Sang area deposits in the Badakhshan District, Afghanistan (Bowersox and Chamberlin 1995: Chapter 3; Faryad 2002; Kulke 1974; Herrmann 1968: 22-27; Wyart *et al.* 1981; Yurgenson and Sukharev 1985); a very small occurrence in the Ishkashim region of the Pamir Mountains, Tajikistan (Ivanov and Sapozhnikov 1985: 14-18; Lutniski 1955; Ostroumov *et al.* 2002; Sapozhnikov 1992); and a series of deposits in Siberia southwest of Lake Baikal (Bauer 1904: 442-444; Hogarth 1970; Ivanov 1976; Ivanov and Sapozhnikov 1985: 5-14; Ostwald 1963). By well-documented I mean that there are published photographs of the deposits, maps and precise geographic coordinates, descriptions of mining areas and of mining activities, geologic section drawings, studies of the host rocks and numerous mineralogical analyses of lapis lazuli samples from those locations. There is not a shred of doubt that these occurrences actually exist. Deposits said to be located in the Ural Mountains of Russia and the Mogok area of Myanmar (Bender 1983: 208; Brown and Judd 1896: 213; da Cunha 1989: 69-70), although poorly documented, are likely genuine given the suitable geology of those regions and the analysis of samples said to be from those source areas that seem to be geochemically distinctive (see the sulfur isotope analysis below as well as Casanova 1992 and Zöldföldi *et al.* 2006). Various older reports and rumors of lapis lazuli occurrences in India, Iran and Egypt are, however, almost certainly spurious (Aston *et al.* 2000: 39; Herrmann 1968: 27; Irvine 1841: 162; Karanth 2000: 209). Just over two decades ago, a deposit supposedly located in the Chagai Hills of western Balochistan, Pakistan was first brought to the attention of scholars (Jarrige 1988: 28). It is now frequently cited as a potential source for the lapis lazuli used in antiquity (Kenoyer 1998: 96; Lahiri 1992: 22; Possehl 1999: 236; Ratnagar 2004: 185) and samples purported to be from there have even been used in recent geologic provenience studies of artifacts (Casanova 1997) and pigments (Ballirano and Maras 2006) made from that stone. An occurrence in western Balochistan would, *if genuine*, have tremendous implications for studies of trade and interaction between the ancient peoples of the Indus region, eastern Iran and southern Afghanistan. However, there are many reasons to doubt that lapis lazuli actually exists in the Chagai Hills.

DOUBTS ABOUT A SOURCE OF LAPIS LAZULI IN THE CHAGAI HILLS

The first direct mention of lapis lazuli in the Chagai Hills of which I am aware[1)] are those relating to explorations in the region during the mid-

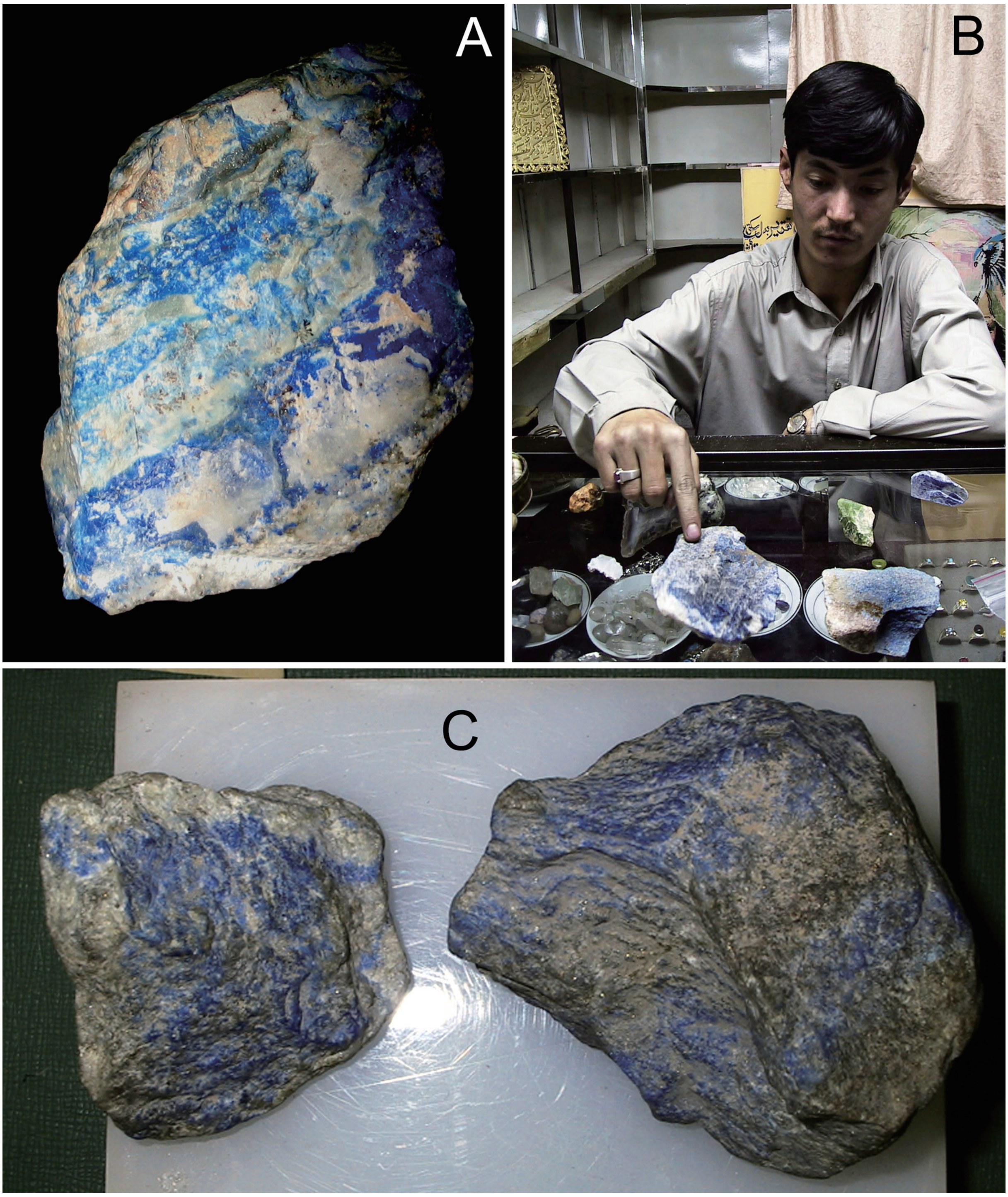

Appendix 4.4, Figure 3 Lapis lazuli purported to be from the Chagai Hills, Balochistan. **[A]** Sample of "Chagai Hills" lapis lazuli given to Jean-François Jarrige by Usman Hassan. **[B]** "Chagai Hills" lapis lazuli for sale at Abdul Karim's rock shop, Liaqat Bazaar, Quetta, Balochistan. **[C]** Lapis lazuli samples in the GSP-Quetta Museum labeled "Brab Chah, Chagai."

1980s by Jean-François Jarrige, leader of the French Archaeological Mission to Pakistan, and Usman Hassan, a now deceased Pakistani ex-military officer who was a friend of Jarrige's and who had a keen interest in archaeology (Jarrige 1988: 28; Jarrige and Hassan 1989: 160-162). The deposit they reported is said to exist at a location called Bi Bi Dick, approximately 56 km north of Dalbandin, near the Pakistan-Afghanistan border. Jarrige himself never actually visited the location (Jean-François Jarrige *personal communication* 2003) but somehow Hassan obtained samples said to be from there, some of which he gave to Jarrige (Appendix 4.4, Figure 3 A). Those samples were analyzed by the Geological Survey of Pakistan and confirmed to be genuine lapis lazuli (Khan *et al*. 1985). Whether or not Hassan himself actually visited the supposed source to collect the samples is unclear. Jarrige believes that he may have but no account of the source/mine was ever given such as the one Hassan published about old lead workings in the Khuzdar District (Hassan 1989). Nor is there any mention of it be found in Hassan's posthumously published collection of observations on the archaeology and history of Balochistan (Hassan 2002).

I have conducted exhaustive searches of the geologic literature relating the Chagai Hills but, to date, have found no reference to either lazurite or lapis lazuli in that region. I have spoken with numerous geologists at the Geological Survey of Pakistan (GSP), at the University of Balochistan-Quetta, and several working for private firms operating in the Chagai Hills region about the possibility of lapis lazuli being found there but most had never even heard of such an occurrence. The few that had seriously doubted that it actually existed. Nearly everyone questioned if it were even geologically possible for lapis lazuli to form in the Chagai Hills, which are mostly composed of andesitic volcanic rocks (Bannert 1995: 19). Lazurite forms in metamorphosed limestones and then only under exceptional conditions (thus its rarity). Rich polymetallic (copper, lead, zinc, molybenite and gold) ores occur in and to the west of the Chagai Hills and, because of that, the region is one of the better surveyed and mapped parts of Balochistan (Allan Spector and Associates Ltd. 1981; Dykstra and Birnie 1979; Hunting Survey Corporation 1960; Nagell 1975; Taghizadeh 1974; Vredenburg 1901). However, there is no mention of lazurite or lapis lazuli in any of the geologic literature related to that region. I consulted the published GSP map that covers the area around Bi Bi Dick (Ziaret Pir Sultan quad sheet 34 C/7) where the source is said to be located and others covering adjacent areas (Barab Chah quad sheet 34 C/3 and Chagai quad sheet 34 C/11). Metamorphic rocks are not found there. Plainly stated, lapis lazuli should not occur in the Chagai Hills given what is known about the geology of the region. The samples attributed to a source near Bi Bi Dick that Usman Hassan had analyzed by the GSP were most definitely genuine lapis lazuli, however. How could Hassan have obtained that stone from the Chagai Hills if it were geologically unlikely for it to occur there? Dr. Wazir Khan of the GSP-Quetta offered a possible explanation (*personal communication* 2001). He related that a tremendous amount of narcotics smuggling and other clandestine trade took place across the Pakistan-Afghanistan border in western Balochistan, particularly through the rugged Chagai Hills region. Marble, travertine and other types of stone are frequently brought to Quetta from Afghanistan and, rather than having to pay duty on imported goods, those transporting the stone attribute it to sources in the Chagai District. Lapis lazuli from "Chagai" can be found in the bazaars of Quetta, I have even purchased some (Appendix 4.4 Figure 3 B). Dr. Khan suggested that Hassan's samples may have been some of this smuggled material.

Confusing matters further, there are two samples of lapis lazuli in the museum at the GSP headquarters in Quetta (Appendix 4.4 Figure 3 C) that are labeled "Brab Chah, Chagai" I questioned the curator of the museum and other members of the Survey about these samples and learned that they were donated by a former GSP administrator. I was told that this person (who I will not name here) did not do fieldwork in the Chagai Hills and, in fact, was never known to have travelled west of Quetta. They said it is highly

1) There are reports of lapis lazuli in the Balochistan region going back to the 1800s (see Ball *et al*. 1881: 529) but none specifically identify the Chagai Hills region.

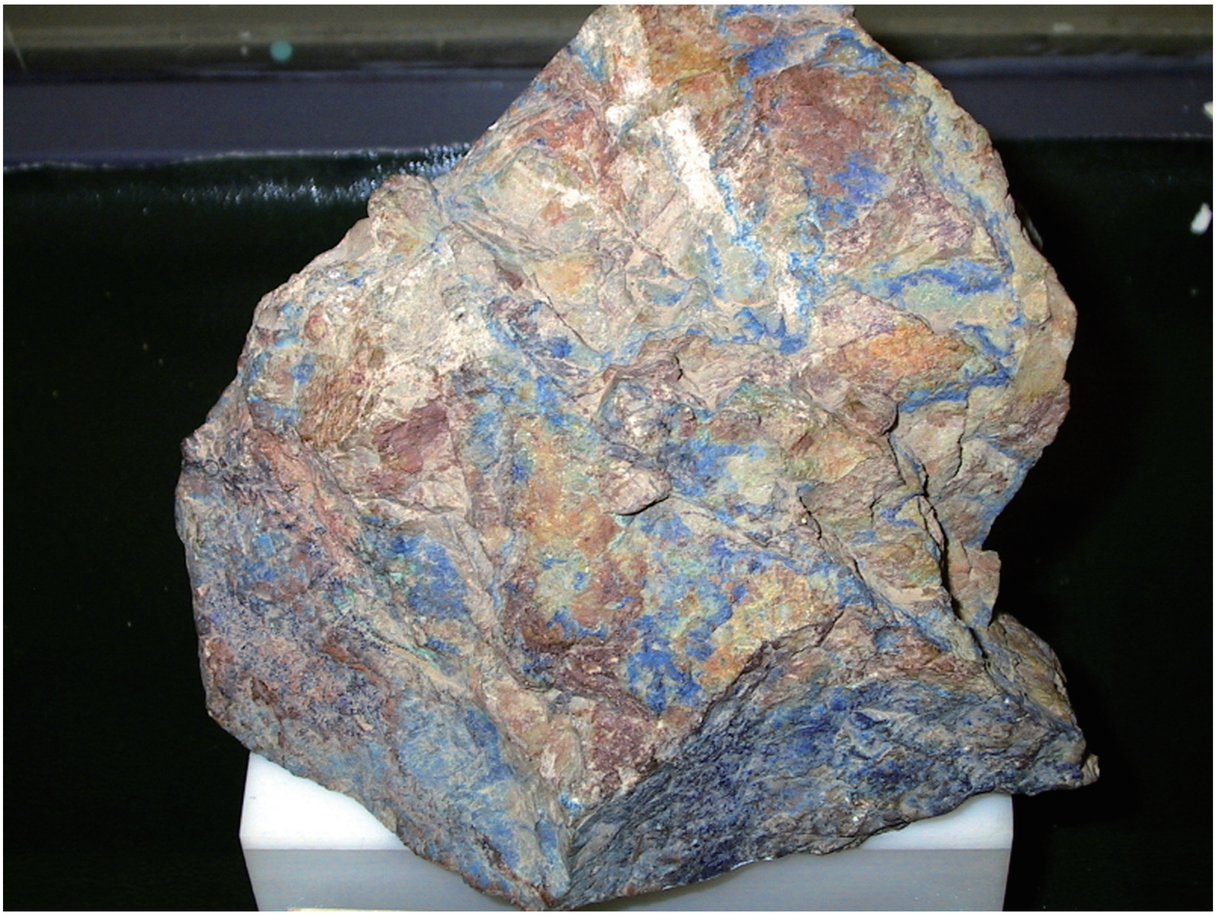

Appendix 4.4 Figure 4 Azurite (hydrated copper carbonate) sample from Koh-i-Dalil, Chagai District, Balochistan that is very lazurite-like in appearance.

unlikely that the former administrator collected the samples personally and, thus, their provenance is, like other examples of "Chagai Hills" lapis lazuli, questionable.

The story does not end there. In the 1990s, Michèle Casanova used atomic absorption spectrometry to compare lapis lazuli artifacts from proto-historic sites in Iran (Shahr-i-Sokhta and Tépé Sialk) to geologic samples from several sources in Asia including eleven purported to be from the Chagai Hills (Casanova 1992, 1997; Delmas and Casanova 1990). More recently, Ballirano and Maras (2006) used Raman spectroscopy to compare a sample of *ultramarine* (a blue pigment made from powdered lazurite) from Michelangelo's fresco "The Last Judgment" to small sets of lapis lazuli samples from Sar-i-Sang (n=3) and the supposed Chagai Hills source (n=5). These researchers obtained the "Chagai Hills" samples that they analyzed from Prof. Maurizio Tosi who was in possession of a collection of lapis lazuli, supposedly from that region, given to him in the 1980s by Emmanuel Lizioli – an Italian living in Pakistan who had business investments in the onyx marble (variegated calcite) quarries of the western Chagai District (Maurizio Tosi *personal communication* 2005). Sadly, like Usman Hassan, Mr. Lizioli is no longer living and he left no record of how he obtained the samples. For this reason, the provenance of the "Chagai Hills" lapis lazuli samples analyzed in these recent studies should be considered very uncertain.

In 1984, Prof. Tosi visited the Chagai Hills region and attempted to reach the lapis lazuli "source" reported there. Although he was unsuccessful due to the troubled nature of the area, the local inhabitants that he spoke with at the village of Barab Chah near the Afghanistan border "were quite plain in declaring that blue stone" could be found in the area (Maurizio Tosi *personal communication* 2006). There is no particular reason to doubt that those locals were being anything other than truthful with Prof. Tosi and I am quite sure that they believed the "blue stone" they told him of to be *lazhward* (دروژال – the Persian word for lapis lazuli that is also used in the various languages spoken in Pakistan). However, through my own personal experience I have come to realize that many people (even some jewellers) are apt to call any variety of bluish-colored rock "lazhward." The "blue stone" that the people at Barab Chah were referring to was, in all probability, *azurite* – a hydrated copper carbonate. As pointed out above, copper mineralization occurs throughout the Chagai Hills region. Geologists that do fieldwork there have shown me samples (Appendix 4.4 Figure 4) and photographs of zones of brilliant blue azurite and apple-green chrysocolla (*personal communication* – Abdul Razique and Razzaq Abdul-Manan of Tethyan Copper Limited and the Center of Excellence in Mineralogy, University of Balochistan-Quetta). Those copper minerals can easily be (and frequently are) mistaken for semi-precious stones like lapis lazuli and turquoise and are sometimes even used as simulants for them (da Cuhna 1989: 116-17). The same geologists also told me that old pits where azurite and malachite have been extracted in the past can be found at a place called Ziaret Pir Sultan, which just so happens to be located within a few kilometers of the supposed lapis lazuli source at Bi Bi Dick. It is quite probable that accounts of a "lazhward" source in this part of the Chagai Hills actually refer to old those workings or ones like them. Rumors of an occurrence there would have no doubt gained credence when genuine lapis lazuli smuggled from Afghanistan ended up in the bazaars of Quetta and was attributed to this region. Although that is how it may have happened, it is impossible to know for certain. In any case, the existence of lapis lazuli in the Chagai Hills region remains unconfirmed and, geologically speaking, highly unlikely if not impossible.

Michèle Casanova's provenience study of lapis lazuli artifacts, although groundbreaking, produced results that were largely inconclusive. The artifacts she analyzed from Shahr-i-Sokhta variously appeared to be related to samples from northern Afghanistan, Tajikistan and the "Chagai Hills" (Casanova 1992: 56). While it is conceivable that material from multiple deposits might be found at that site, the actual assignment of the artifacts to sources was simply not convincing. The same can be said of the study of ultramarine from "The Last Judgment," which produced results that Ballirano and Maras themselves described (2006: 997) as "dubious." My reservations about accepting the provenience determinations made in these two studies lie not with the researchers' methods but with their datasets. The first and most obvious weakness is the great uncertainty surrounding the origins of "Chagai Hills" lapis lazuli samples. It seems highly probable that those particular samples were derived from one of the Badakhshan region deposits in northern Afghanistan and came into Lizioli's possession (and eventually Tosi's) via business associates or other contacts in the Chagai District. Although it is true that in both studies there were some geochemical differences between the "Chagai Hills" samples and those from other sources examined, such differences could easily be due to natural variation between individual deposits *within* the Badakhshan region itself. Lapis lazuli is mined there at multiple points along an intermittent zone of mineralization that is approximately 20 km long (Hermann 1968: 22-24). Keisch and Callahan conducted a sulfur isotope study (1976) of ultramarine that included geologic samples from the Badakhshan deposits and their results suggested that there was a great deal of isotopic variability along that zone. Therein is a second area of weakness in both Casanova's and Ballirano and Maras' datasets – the number of samples and their representativeness. The potential range of chemical variability across the extensive Badakhshan lapis lazuli deposits simply cannot be adequately assessed based on the small number of samples they analyzed from that source (seven by the former and three by the latter). It is not even clear if their samples represented a single mine or several individual ones. The same is true, for that matter, of the Badakhshan lapis lazuli samples that showed so much isotopic variability in Keisch and Callahan's study. They wrote that "it would be of considerable interest to analyze samples from each of the mines in Badakhshan" (Keisch and Callahan 1976: 518).

One final word on this matter: By being skeptical of a lapis lazuli source in the Chagai Hills it is not my intention to impugn the reliability of those who originally provided samples attributed to that region (Hassan and Lizioli) or to find fault with Casanova or Ballirano and Maras, who did outstanding work given the number and nature of the geologic samples available to them. I just believe that this ancient luxury stone is too important to accept anything less than well-documented confirmation that another source of it existed. It would be thrilling if it could be confirmed that lapis lazuli actually occurred in the Chagai Hills. If the stone did somehow form in the Chagai Hills then there is reason to expect[2] that it would be chemically and/or isotopically distinguishable from that occurring in the Badakhshan region. The existence of two viable sources would have tremendous implications for studies of ancient trade and interaction from South Asia to Egypt. But all of the available evidence presented strongly suggests that lapis lazuli does not and cannot exist in the Chagai Hills. Even so, additional geologic fieldwork in the region and further analytical studies of samples are always warranted.

2) The oldest rock formations in the Chagai Hills date to the later Cretaceous Period (ca. 145 to 65 Ma) while the Badakhshan lapis lazuli deposits occur in ca. 2700-2400 Ma Archean rock (Faryad 2002: 726).

A SULFUR ISOTOPE STUDY OF LAPIS LAZULI ARTIFACTS AND SOURCE SAMPLES

The sample set

Both Jean-François Jarrige and Maurizio Tosi generously provided me with samples of the "Chagai Hills" lapis lazuli that they had obtained from Hassan and Lizioli respectively. During my research work in Quetta, I had also purchased a few pieces that ostensibly came from the same region. I wished to compare this "Chagai Hills" lapis lazuli to samples from confirmed sources in order to determine if they were geochemically distinct in any way. Keisch and Callahan's excellent study (1976) showed that there often were clear differences (ibid: Fig. 3) in the sulfur isotope composition of samples from different sources (for instance between those from occurrences in Afghanistan, Russia and Chile). If the "Chagai Hills" samples were isotopically distinct then, perhaps, there could be a source in that region after all. Such differences would, at the very least, suggest that there probably is somewhere a second viable source of lapis lazuli for Indus Civilization peoples. In order to test this possibility, a small set geologic source samples and artifacts was assembled (Appendix 4.4 Figure 5).

Back in 1999, when I was in Irkutsk, Russia nearby Lake Baikal, I purchased a number of raw lapis lazuli samples that I was told were from the sources documented in the Sayan Mountains, which are located immediately to the southwest of the lake. A few years later, during my various research periods in Peshawar, Pakistan, I obtained numerous pieces of the stone that I could be fairly certain had been brought to the city's bazaars directly from sources in the Badakhshan region. And recently, I bought a piece of lapis lazuli from a rock dealer in Vienna that is supposed to be from one of the sources in the Mogok region of Myanmar. The irony that, since I did not collect them myself, the provenances of these geologic source samples are, in reality, not that much better

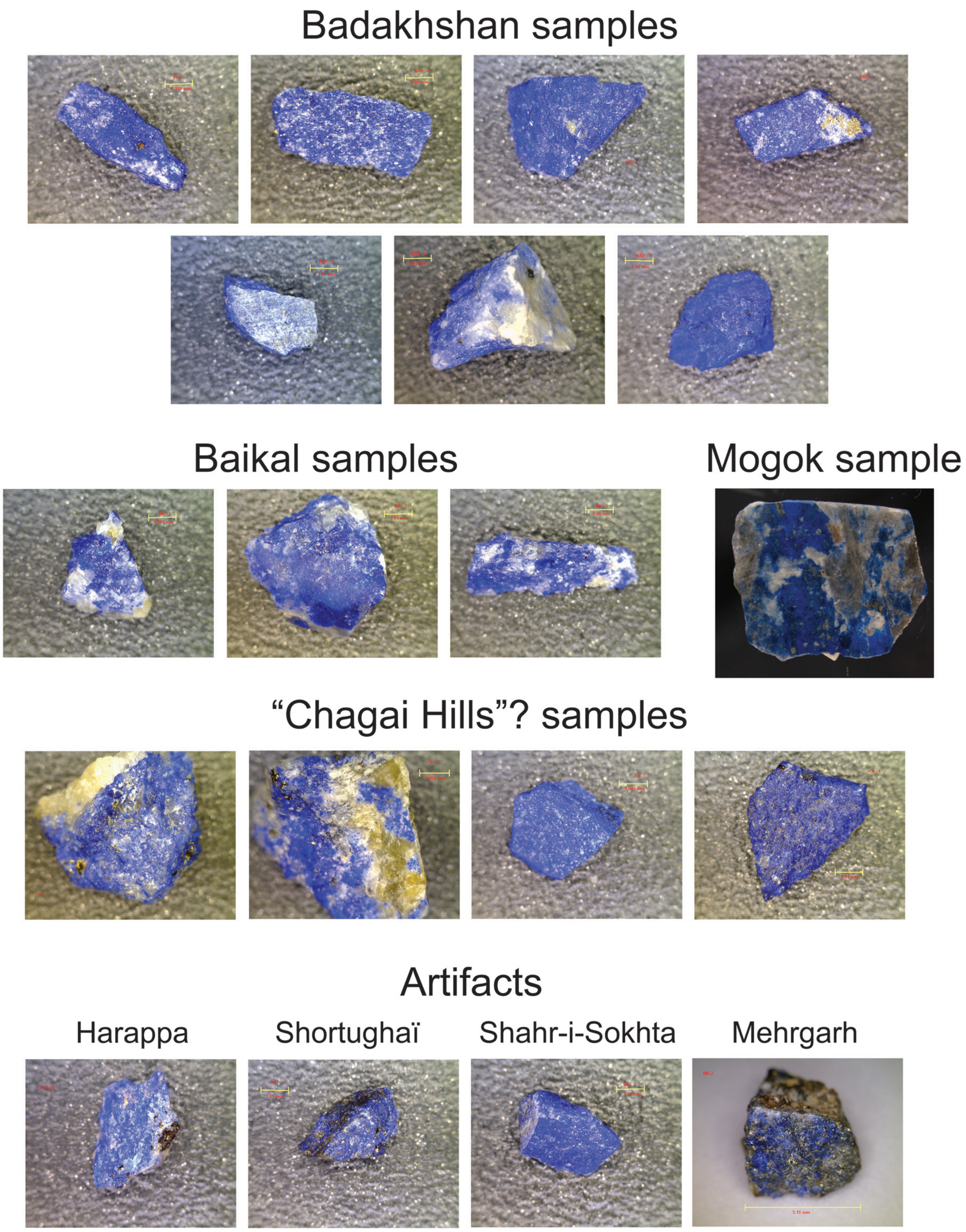

Appendix 4.4 Figure 5 Lapis lazuli source samples and artifacts isotopically assayed for this study.

than those from the “Chagai Hills” is not lost on me. However, at least for the Baikal and Badakhshan samples, I did obtain them from merchants in cities where one would expect that genuine materials from those sources would be gathered and sold (in the case of Peshawar this is well known to be true). As for Wilhelm Niemetz’s rock shop in Vienna, I can only say that he had an exceptional collection of specimens from around the world including many from Myanmar.

I also analyzed lapis lazuli artifacts from four archaeological sites for this study. Jean-François

Appendix 4.4 Figure 6 $\delta^{34}S$ ‰ and $\delta^{18}O$ ‰ values for lapis lazuli source samples and artifacts.

sample	source/site	$\delta^{34}S$ ‰	$\delta^{18}O$ ‰
BAD-1	Badakhshan, Afghanistan	16.7	19.7
BAD-2	Badakhshan, Afghanistan	16.8	20.2
BAD-2P	Pyrite extracted from BAD-2	12.2	not analyzed
BAD-3	Badakhshan, Afghanistan	19.0	20.6
BAD-4	Badakhshan, Afghanistan	23.1	19.4
BAD-5	Badakhshan, Afghanistan	16.3	no sample left
BAD-6	Badakhshan, Afghanistan	14.5	15.3
BAD-7	Badakhshan, Afghanistan	23.4	15.2
BK-1	Baikal, Russia	41.3	18.8
BK-2	Baikal, Russia	54.8	19.0
BK-3	Baikal, Russia	52.8	19.3
CH-1	Chagai Hills? - Purchased in Quetta	18.9	19.7
CH-1P	Pyrite from extracted from CH-1	12.3	not analyzed
CH-2	Chagai Hills? - Jarrige/Hassan sample	19.3	20.3
CH-3	Chagai Hills? - Tosi/Lizzioli sample	13.5	19.3
CH-4	Chagai Hills? - Tosi/Lizzioli sample	15.2	19.0
Burma-1	Mogok area, Myanmar	4.5	not analyzed
Burma-2	Mogok area, Myanmar	4.1	not analyzed
HR-82	Harappa, Pakistan	24.5	20.3
SIS-1	Shahr-i-Sokhta, Iran	19.4	18.3
SHT-1	Shortughaï, Afghanistan	16.7	19.4
MR-2	Mehrgarh, Pakistan	13.3	15.5

Jarrige kindly provided debris fragments from both the Indus Tradition settlement of Mehrgarh and the Harappan site of Shortughaï. If stone from the Chagai Hills of western Balochistan was traded into the Indus region then some of it is very likely to have ended up at Mehrgarh, which is located at the foot of the most prominent pass connecting the Balochistan highlands to the Indus Valley. A Chagai Hills lapis lazuli source, if it really existed, would have also been significantly closer and more accessible to peoples at that site than deposits in the Badakhshan region (300 km due west of Mehrgarh over reasonably traversable terrain versus over 800 km due north over some of the most dangerous mountain passes on earth). The site of Shortughaï in northern Afghanistan sits near the lower reaches of the Kokcha River, the upper reaches of which run directly through the Sar-i-Sang lapis lazuli mines. Out of all Harappan sites, it is there that one would most expect to find stone from the Badakhshan area deposits. Maurizio Tosi kindly provided a fragment recovered during his excavations of Shahr-i-Sokhta in eastern Iran. This site is again significantly closer to the supposed Chagai Hills source. Finally, a lapis lazuli fragment that was surface find from Harappa was analyzed.

Altogether, the set of lapis lazuli samples

(Appendix 4.4 figures 5 and 6) consisted of a single fragment from each of the four archaeological sites just discussed and 18 geologic samples. Seven of the geologic samples were from the Badakhshan deposits, three were from the Baikal deposits, one was from the Mogok area and four were attributed to a source in the Chagai Hills (one purchased in Quetta by me, one from Jarrige and two from Tosi). Material from two opposite sides of the Mogok lapis lazuli sample was removed for two separate analyses. Pyrite crystals from two of the geologic samples were extracted (for reasons discussed below) and analyzed separately as well. Sulfur isotope analysis, which is relatively inexpensive and fast, was the method selected based on Keisch and Callahan's successful study (1976).

Sample preparation and analysis

Lapis lazuli almost invariably contains inclusions of pyrite. After a conversation on this matter with Massimo Vidale in 2007, it was decided that an attempt should be made to separate the pyrite from the lazurite in each sample prior to analysis. The reasoning was that sulfur isotope characteristics of the lazurite (sodium calcium aluminum silicate sulfur sulfate) and pyrite (iron sulfide) components of lapis lazuli might not necessarily be the same. This would not be a significant problem if the proportions of these minerals were identical from sample to sample. However, the amount of pyrite in lapis lazuli can vary considerably (see the photographs of the samples in Appendix 4.4 Figure 5), even within a single specimen. Let us assume for the moment that the sulfur isotope values for pyrite and lazurite within individual samples and deposits are indeed different from one another. If two pieces of lapis lazuli from the same source were analyzed, one of which contained a few flecks of pyrite while the other was rife with it, then the sulfur isotope composition of heterogeneous samples taken from the two pieces would likely be different as well. It was because of this possibility that it was deemed prudent to try, inasmuch as was possible, to separate the two minerals.

Each lapis lazuli sample was ground to a fine powder in an agate mortar. The powders were then placed into individual plastic vials that had wide mouths and conical-shaped bottoms. Enough purified water was added to the vials to cover the powder with at least 1 cm of liquid. Vials were then covered and placed into a shallow ultrasonic bath that thoroughly mixed the contents. The lids were removed and the vials were put into a drying box overnight so that the water could evaporate. Pyrite has a specific gravity of around 5.1 while the density of lazurite is between 2.3 and 2.4. It was hoped that the much denser pyrite would collect in the constricted bottoms of the vials while the lighter lazurite would settle toward the top. There are other methods to separate the pyrite that involve magnetizing it by heating so that it could be removed using a magnet (Uslu and Arol 2003). The problem is that some of the sulfur that would be needed for isotopic analysis would probably be driven off in the process (Gunter 1909: 117). In the end, the method used here seemed to work reasonably well. The blue powder that settled at the top seemed to be free of pyrite, unlike the grayer blue residue that collected at the bottom of the vial.

It was decided to test the theory that lazurite and pyrite in a single specimen might have different sulfur isotope values. Material from two of the geologic samples (BAD-2 and CH-1) was coarsely ground and pyrite crystals were removed by hand to be analyzed separately.

Sulfur analysis of the sample set was conducted by Dr. Chris Eastoe at the Isotope Geochemistry Laboratory, University of Arizona. Each sample was dissolved in HCl and then a $BaCl_2$ solution was added to precipitate $BaSO_4$, which as then filtered and dried (Isotope Geochemistry Laboratory 2004). Sulfur dioxide gas was extracted from the $BaSO_4$ by combustion with V_2O_5 (Yanagisawa and Sakai 1983) in a Costech elemental analyzer. From that gas $\delta^{34}S$ values were measured a Finnigan Delta PlusXL continuous flow gas-ratio mass spectrometer. International sulfur standards OGS-1 and NBS123 were used along with several other sulfide and sulfate materials that have been compared between laboratories. Based on repeated use of internal standards the precision was estimated to be ± 0.15 or better (Chris Eastoe *personal communication* 2004). The results of the sulfur isotope analyses of the geologic and archaeological samples are listed in the third column of Appendix 4.4 Figure 6. They are expressed using the notation $\delta^{34}S$ ‰, which represents the per mil (‰) deviation in the $^{34}S/^{32}S$ ratio measured in the sample compared to that measured in the Canyon Diablo Troilite (CDT) meteorite international standard (Eckhardt 2001: 514). Oxygen isotope analysis was also conducted by Dr. Eastoe on most of the samples in the set. Those results, although listed here in the fourth column of Appendix 4.4 Figure 6, did not prove to have any value in terms of differentiating the various samples by their geologic sources.

Results

The results of the sulfur isotope analysis of the geologic and archaeological lapis lazuli sample set are plotted in Appendix 4.4 Figure 7. It is immediately clear that the Badakhshan, Baikal and Mogok source samples are very distinct from one another. The $\delta^{34}S$ ‰ values of the seven Badakhshan lazurite samples range from 14.5 to 23.4 (a variation of 8.9), the three Baikal samples ranges from 41.3 to 54.8 (a variation of 13.5) and the Mogok sample that was analyzed twice ranged from 4.1 to 4.5 (a variation of 0.4 in a single specimen). The "Chagai Hills" lazurite samples, which range from $\delta^{34}S$ ‰ 13.5 to 19.3, overlap significantly with those from the Badakhshan region. The either means that the source from which they came has the same isotopic characteristics as the lapis lazuli deposits of northern Afghanistan or that they are actually from the Badakhshan region. Given what we know of about the geology of the Chagai Hills and the questionable provenances of the samples themselves, I believe the latter scenario to be more likely.

So if we discount the "Chagai Hills" samples as representative of a separate source (which at this point I have) then all four of the archaeological lapis lazuli fragments appear most closely related to samples from the Badakhshan region. The $\delta^{34}S$ ‰ value for the Harappa fragment is slightly greater (by 1.1) than the highest Badakhshan sample value while the fragment from Mehrgarh is slightly lower (by 1.2) than the lowermost value. However, it is doubtful that the analysis of a mere seven geologic samples captured the full range of isotopic variation exhibited across that extensive source area. The incorporation of additional samples from the Badakhshan deposits will very likely extend the range of variation for that source area and encompass isotopic values of the Harappa and Mehrgarh artifacts.

The distinct isotopic characteristics of the Mogok sample suggests that it is genuinely representative of a separate lapis lazuli source. Moreover, none of samples from the multiple deposits (in Afghanistan, Tajikistan, Russia, Italy, Chile and the USA) analyzed by Keisch and Callahan have similar sulfur isotope values (see Keisch and Callahan: Fig. 3). This specimen is probably indeed from a source in Myanmar. Analyses of additional samples are obviously needed, however. The range of isotopic variation will almost certainly expand when further assays of the Myanmar source are conducted. If the specimen analyzed here happens to be on the lower range of variation and the source varies similarly to the Badakhshan and Baikal occurrences, then the higher range of the Mogok source sulfur isotope values could overlap with the lower ones of Badakhshan.

Interestingly and importantly, the pyrite crystals extracted from two lapis lazuli samples in the set (these are noted with black symbols and are labeled on Appendix 4.4 Figure 7) did indeed have sulfur isotope values that were different from those of the lazurite components in the very same specimens (also

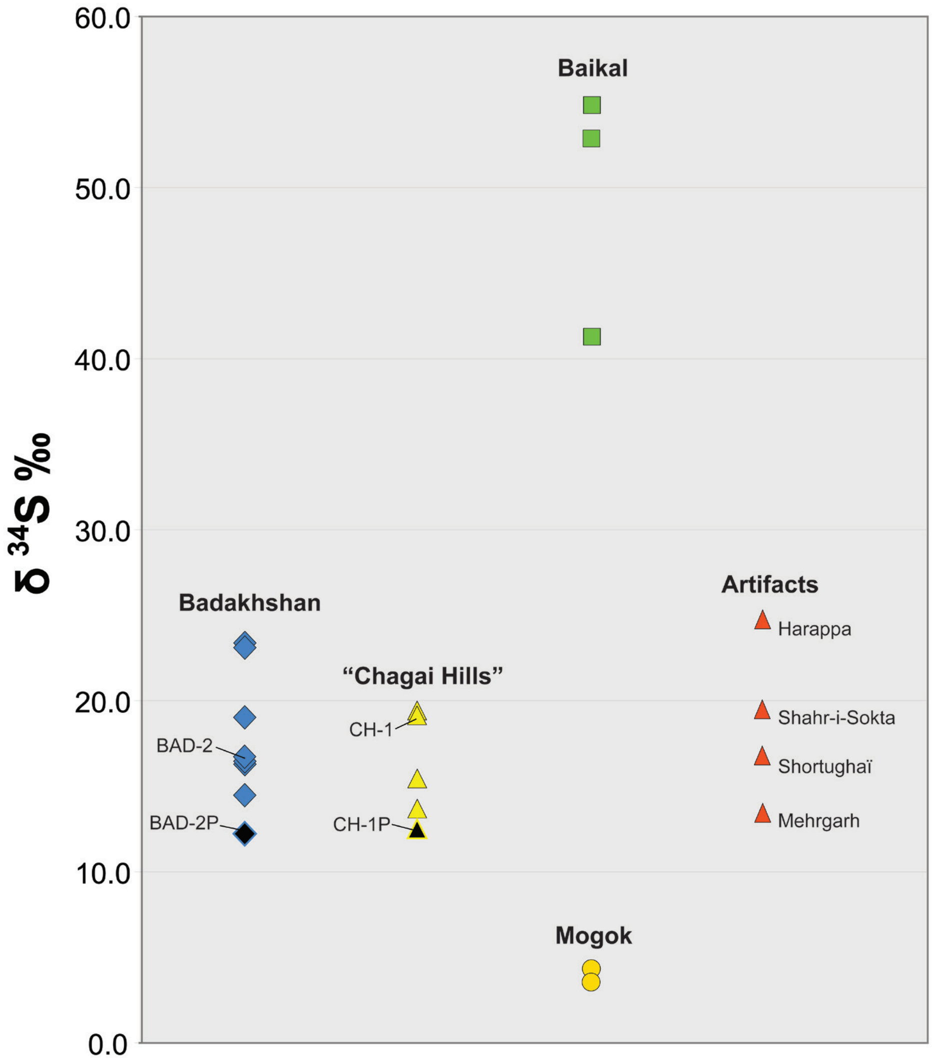

Appendix 4.4 Figure 7 Sulfur isotope values ($\delta^{34}S$ ‰) plotted for lapis lazuli source samples and artifacts.

labeled on Appendix 4.4 Figure 7). Pyrite from the Badakhshan sample (BAD-2 / BAD-2P) had a $\delta^{34}S$ ‰ value that was 4.6 lower while that for "Chagai Hills" sample (CH-1 / CH-1P) was 6.6 lower. Although this is not enough difference to result in a misclassification of artifacts between the sources examined here, it is significant because it shows that the amount of pyrite in a specimen will probably affect the results. So it is indeed advisable to separate it out inasmuch as possible. After the analyses presented here were completed, I learned (in Craddock 2009: 412) that for their study Keisch and Callahan actually analyzed pyrite from lapis lazuli samples rather than the lazurite component (this is not stated in their 1976 paper on the subject). Had I known, I too would have done this. While the separation technique I used seemed to work reasonably well, I could not be certain that I extracted all of the pyrite from the lazurite. Extracting the small but highly visible crystals would have been much easier and would have likely resulted in a purer sample.

The sulfur isotope results published by Keisch and Callahan became clearer once I understood that they had analyzed extracted pyrite and I discovered that the sulfur isotope values for that mineral were generally lower than they are for lazurite in the same samples. In their published chart of the isotopic ranges for the lapis lazuli sources they analyzed (Keisch and Callahan 1976: Fig. 3), both the Baikal and Badakhshan occurrences had somewhat lower values than I detected in my analyses of lazurite from those same sources. My results would have likely been more or less the same as theirs had I analyzed extracted pyrite instead.

RECENT LAPIS LAZULI PROVENIENCE RESEARCH USING OTHER TECHNIQUES

The question "Where does lapis lazuli come from?" continues to intrigue scholars. This was actually the title of a fairly recent paper by Zöldföldi and others (2006). Using non-destructive prompt gamma activation analysis (PGAA), they studied lapis lazuli samples from sources in Afghanistan, Russia (Baikal and the Ural Mountains) and Chile. They found the Ural and Chilean samples to be quite distinct but had more trouble differentiating Afghanistan and Baikal samples. More recently, Smith and Klinshaw (2009) examined the infrared spectra of lazurite in lapis lazuli samples from Afghanistan, Canada, Myanmar, Lake Baikal, Tajikistan, and the Ural Mountains. They found that a weak band in the spectra at 2340 cm^{-1}, which had once been considered to be a marker of stone from the Badakhshan region (Derrick *et al.* 1999: 137), was actually present in lapis lazuli from several other source areas and, thus, was not a good indicator of raw material from Afghanistan. Also recently, Lo Giudice and others (2009) employed cathodoluminescence (CL), scanning electron microscopy (SEM) and micro-Raman spectroscopy in their study of lapis lazuli samples from Afghanistan, Tajikistan, Chile, and the Baikal area. Among other things, they found that Tajikistan source samples exhibit several distinct features ("an additional luminescence band at 690 nm ... a cancrinite phase with a strong UV emission and a vibronic structure with ZPL at 2.55 eV" – Lo Giudice and others 2009: 2217) and Baikal samples can be distinguished by their unusually high barium and strontium contents.

These recent studies are important because, although none have proven to differentiate the lapis lazuli deposits of Asia any better than sulfur isotope analysis, some of the methods employed in them could be used in combination with sulfur isotope analysis when an overlap between two sources occurred. I am specifically referring to the small lapis lazuli deposit located at Ishkashim in the Pamir Mountains of Tajikistan. It is my feeling that this occurrence was probably too minor and too inaccessible (situated at 4600 meters in elevation on a precipitous cliff face – Ivanov and Sapozhnikov 1985: 17) to have been a very important source. However, it is located only around 130 km northeast of the Sar-i-Sang mines, which themselves are pretty high up (ca. 2500 meters – Wyart *et al.* 1981: 187) and not easily reached. The Ishkashim deposit, therefore, should not be disregarded entirely. The single sample from that source analyzed by Keisch and Callahan had a value of around $\delta^{34}S$ ‰ 13, which is near the middle of the range (ca. $\delta^{34}S$ ‰ 10 to 18) of the isotopic variation that they defined for the Badakhshan deposit (see Keisch and Callahan 1976: Figure 3). For future studies, it might be possible to differentiate Badakhshan lapis lazuli from that of the Ishkashim deposit by keying in on one of the several distinct features of raw material from the latter that were identified by Lo Giudice and others (2009).

CONCLUSION

Based on the evidence and analysis presented above, my answer to Prof. Durrani's question today would be that the Sar-i-Sang deposits in the Badakhshan region of northern Afghanistan would likely have been the only viable sources of lapis lazuli for Harappans or their contemporaries in the Near East. I base the latter part of this statement, in part, on that fact that in their paper, Keisch and Callahan related (1976: 518) that they had "also analyzed some samples of archeological interest that were found in

Mesopotamia and are reported to be 3000 to 4000 years old." Although they did not note the names the sites from which the artifacts originated, they did state that the lapis lazuli "also probably came from Afghanistan" (ibid).

APPENDIX 4.5

THE "ERNESTITE" PROBLEM

"ERNESTITE"

I have had numerous debates (sometimes impassioned but always good-natured and constructive) with Dr. Mark Kenoyer regarding the problem of the nature and origins of "Ernestite" – a type of rock that Harappans used to make drill bits for perforating hard stone beads. Kenoyer feels that it is some unusual type of metamorphic rock, which perhaps has not been previously described by geologists. It was for this reason that he and Massimo Vidale (Kenoyer and Vidale 1992) gave it the informal designation "Ernestite" in honor of Ernest Mackay (*Mackayite* was already being used for another mineral) who first described drill bits from Chanhu-daro made of this material (Mackay 1937: 6-7). I have had the opportunity to conduct a series of follow-up analyses of "Ernestite" and have come to a different, albeit still provisional, conclusion. My research suggests that "Ernestite" is probably a type of *indurated tonstein flint clay* that has been deliberately heated in order to produce or enhance properties in the stone that made it a highly effective material for drilling hard stone beads. In this appendix, I present my case for making this designation.

Let me begin by restating and expanding my introduction to the material from Chapter 4. "Ernestite" is an extremely fine-grained stone with dark-brown to black patches and/or dendritic veins in a khaki-colored matrix (see examples of raw "Ernestite" from Harappa in Appendix 4.5 Figure 1). It is hard (easily scratching quartz but not topaz giving it a Mohs hardness of at least 7 but less than 8), very tough (does not break or fracture easily) and fairly dense (SG ranging from ≈ 2.8 for the khaki-colored matrix to ≈ 3.2 for the brown-black portion). It was made into drill bits, many of which have a distinctive constricted cylindrical form (Appendix 4.5 Figure 2). These were used by Indus beadmakers to perforate hard stone (namely microcrystalline silicates and vesuvianite-grossular). As far as I have been able to determine, drill bits made from this rock and having this distinctive form are nearly unique[1)] to the Indus Civilization sites. Ernest Mackay (1937) first discovered them among bead-making materials at the site of Chanhu-daro in Sindh (Appendix 4.5 Figure 3). Drill bits of the exact same shape, along with the raw material used to make them, were later identified at Harappa and Mohenjo-daro (Kenoyer and Vidale 1992). A huge number are present in the stone and metal artifact assemblage of Dholavira[2)] (Bisht and Prabhakar 2008). I have seen "Ernestite" drill bits in collections of excavated materials from Harappan sites elsewhere in Gujarat like Kanmer, Shikarpur, Khirsara and Lothal. I fully expect that many more such artifacts will be discovered as old collections are re-examined and new Harappan sites are excavated.

The raw material from which these drill bits are made would *seem* to be similarly unique. Using XRD and EMPA, Kenoyer and Vidale (1992) characterized it as a metamorphic rock composed of quartz, sillimanite-mullite and hematite-titanium oxide phases. Unable at the time to identify a known

1) A single drill of this description was found at the city of Ur in Mesopotamia, leading Ernest Mackay to speculate that it was "not at all unlikely that bead-making in Sumer was carried on by Indian craftsmen" (1943: 212).

2) The exquisitely fashioned black constricted cylindrical drill bit from Dholavira that is published (as jasper) in the catalog for the 2000 "Indus Civilization Exhibition" in Tokyo (NHK 2000: 106, Figure 598) is one of them.

Appendix 4.5 Figure 1 Raw "Ernestite" fragments from Harappa.

Appendix 4.5 Figure 2 Constricted cylindrical drill bits made from "Ernestite".

Appendix 4.5 Figure 3 "Ernestite" drill bits and long biconical carnelian beads from the site of Chanhu-daro. Photo by J. M. Kenoyer, with permission from the Boston Museum of Fine Arts.

rock type with those phases, they proposed the name "Ernestite."

For this study, four "Ernestite" fragments recovered on Mound E at Harappa (H2000/2090-49, H2000/3317-2 to 4) were selected for study using XRD and EMPA with the hope that further characterization might shed new light on the identity of this stone, its geologic origins, potential sources and the properties that made is the most effective material available to Harappans for drilling hard-stone beads.

XRD ANALYSIS OF "ERNESTITE"

Two of the four "Ernestite" samples (H2000/2090-49 and H2000/3317-4) examined using XRD were mainly made up of the khaki-colored primary matrix and had only small patches of the black-brown material. These samples displayed diffraction peaks showing that they were composed primarily of quartz and mullite-sillimanite (see Appendix 4.2 I for one of these scans). Minor peaks indicative of *hematite* (iron oxide) and *rutile* (titanium oxide) were also present. *Mullite* and *sillimanite* are actually two separate aluminum silicate minerals that have nearly identical XRD peak profiles (Brown 1980: Table 6.21; Varley 1968: 3). The XRD profiles of the two samples were ambiguous – meaning that they seemed to have peaks characteristic of both minerals and could have been interpreted as either. The same was true of the Mohenjo-daro sample analyzed by Kenoyer and Vidale, which they characterized using a combined term – "sillimanite-mullite" (1992: 507). It is possible that both minerals exist in the samples or, perhaps, than an aluminum silicate phase intermediate to mullite and sillimanite is present (Cameron 1976; Bradley and Roussin 1932). It is also possible that what has been detected in the XRD scans is a poorly crystallized, early stage of mullite formation (Chakraborty *et al.* 2003).

The remaining two "Ernestite" samples (H2000/3317-2 & H2000/3317-3) were composed largely of the darker material that occurs in veins and patches. The XRD scans unambiguously showed it was the mineral mullite that was present in these fragments (see Appendix 4.2 J for one of these scans). Peaks for quartz, hematite and rutile (present in the previous two samples) were not to be found, however. Instead, strong peaks for *cristobalite* – the high temperature polymorph of quartz, were evident.

The minerals in these samples provide important clues into the possible origins of "Ernestite." Sillimanite occurs in highly metamorphosed *argillaceous* (clay-rich) rocks known as *pelites* (Deer *et al*. 1992: 52). It is not an uncommon mineral and can be found in rocks of this type occurring at points throughout the Himalayas of northern Pakistan and India (Das 1984; Khan *et al*. 1997) as well as across Rajasthan (Bhattacharyya 1980; Goel and Chaudhari 1979). Mullite also forms in metamorphosed argillaceous rocks (Deer *et al.* 1992: 54) but, in contrast to sillimanite, it is an exceedingly rare mineral in nature. To my knowledge, no natural occurrences in South Asia have ever been reported. Mullite is, however, a very common man-made mineral. It is both an intentionally produced *refractory* material (a substance able to withstand high temperatures without melting or vitrifying) and a byproduct of certain high-temperature crafts and industries. Mullite can be synthesized when the other aluminum silicate minerals (sillimanite, kyanite and andalusite) are heated to temperatures exceeding 1350°C (Industrial Minerals 1998: 139). However, mullite also forms when aluminum-rich clays (such as *kaolinite*) and claystones are subjected to sufficient heat – generally this is around 1100°C but may be somewhat higher or lower depending on the composition of the raw material, the atmosphere and firing dynamics (Brindley and Nakahira 1959; Castelein *et al*. 2001: 2369; MacKenzie *et al*. 1996; Russell 1965; Saunders 1958; Schneider *et al*. 1994: 107). Interestingly and importantly, experimental heating studies (Dubois *et al*. 1995; Donley 1955: 3; Liu 1990: 5; Lundin 1958; Russell 1965: 45; Worrall 1975: 16) of kaolinitic clay bodies reveal that amorphous silica, which is freed during kaolinite-to-mullite conversion, will crystallize as cristobalite. This has been observed at temperatures as low as 1100°C (Brindley and Nakahira 1959). The mineral quartz alone will also convert to cristobalite when heated. Experimental studies (using controlled atmospheres and sample purities) have shown that this conversion occurs slowly between 900°C and 1200°C and rapidly after 1300°C (Sosman 1965: 132-133). Like mullite, cristobalite is a common mineral byproduct in certain high-temperature craft industries. Cristobalite has been previously detected in studies of Harappan high-temperature craft industries such as stoneware bangles (Vidale 2000: 90), faineance objects (McCarthy and Vandiver 1991: 502) and steatite beads (Barthélémy de Saizieu 1994: 56).

The advanced pyrotechnological capabilities of Indus craftspeople are well-documented (Miller 1999) and the presence of these two high-temperature minerals in the "Ernestite" samples analyzed here would seem to suggest that it may have been yet another of the many materials that Harappans heat treated. If it was, then what type of stone might the original material have been? Further characterization studies were conducted using EMPA in order to address this question.

EMPA OF "ERNESTITE"

The four "Ernestite" samples from Harappa, as well as the one from Mohenjo-daro studied by Kenoyer and Vidale in 1992, were examined using the backscatter electron (BSE) imaging, energy dispersive spectrometry (EDS) and wavelength dispersive spectrometry (WDS) capabilities of the electron microprobe. Appendix 4.5 figure 4 and 5 are labeled BSE images of portions of two of the "Ernestite" fragments, which may serve as visual references as I

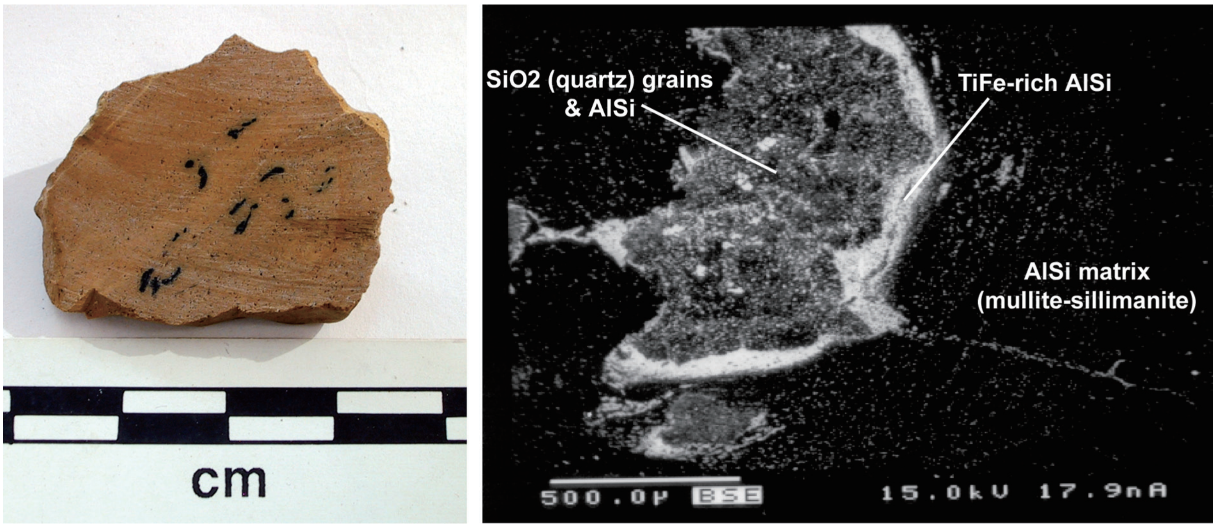

Appendix 4.5 Figure 4 “Ernestite” fragment H2000/2090-49 (left). BSE image of black patch (right).

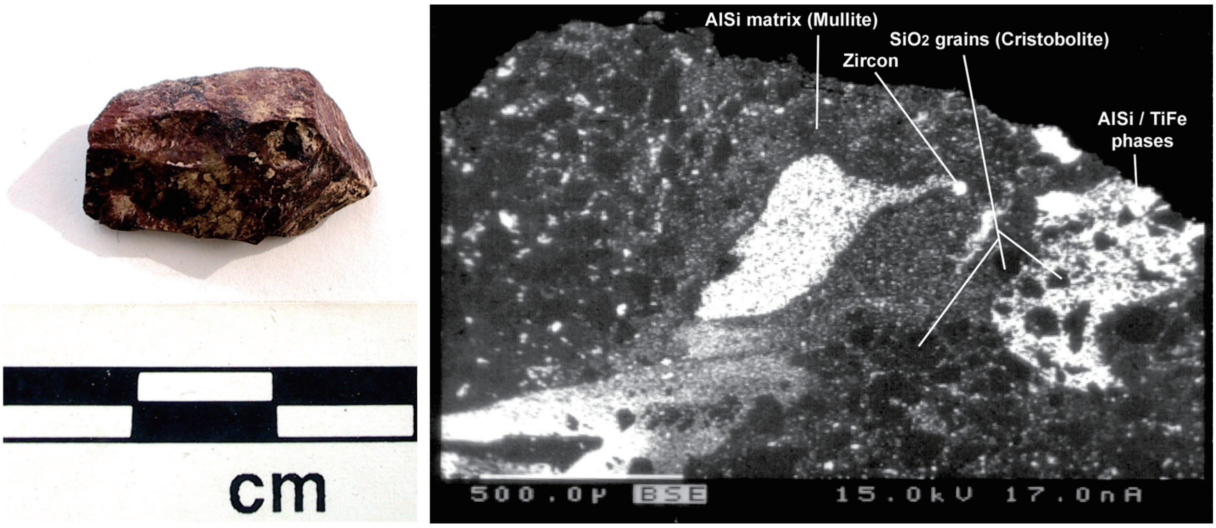

Appendix 4.5 Figure 5 “Ernestite” fragment H2000/3317-2 (left). BSE image of main body (right).

discuss the mineral phases and inclusions (labeled on the figures) that, in most cases, were detected in each of the five samples. Appendix 4.5 Figure 6 is a table of WDS scans that were selected to represent the phases and inclusions identified.

WDS scans of the primary, khaki-colored matrix (the darker phases in the BSE images) of “Ernestite” showed it to be composed of clay-sized (< 2 μm) or smaller particles of an aluminum silicate (Al-Si) mineral. This would be the phase identified in the XRD scans as mullite or mullite-sillimanite. The darker matrix (lighter phases in the BSE images) that occurs in veins and patches is also an Al-Si phase. However, in some samples this matrix is rich in hematite (iron oxide) and/or contains small phases or inclusions hematite and rutile (titanium oxide). In other samples, an oxide of titanium and iron called *titanohematite* is interspersed among the darker Al-Si matrix. Titanohematite only begins to form at temperatures of around 1050°C (Deer *et al.* 1992: 541). It is highly significant that this phase is evident in the same samples (H2000/3317-2 & H2000/3317-3) in which two other high-temperature minerals (mullite and cristobalite) were identified using XRD.

Among the light and dark Al-Si matrixes that make up the main body of ernestite are sub-euhedral grains and fragments of SiO_2 up to 100 μm in size. These are the quartz or cristobalite phases detected in the XRD analyses (EMPA cannot differentiate the two of types of quartz as they are chemically identical polymorphs). Using EDS scans only, small (≈ 20 μm) inclusions of zircon (the brightest white spots on the BSE image) were identified, as well as occasional minute phosphate phases that contained the rare earth elements (REEs) yttrium (Y) and cerium (Ce). The texture of "Ernestite," as seen in the BSE images also provides clues to its possible origin. The stone's matrix is composed of randomly oriented clay-sized Al-Si particles into which fairly well-sorted sub-euhedral grains and fragments of SiO_2 are set. These are detrital attributes that point to a rock of sedimentary origin. There is no evidence of characteristics one would expect to see if this was a metamorphosed rock such as foliation, deformation or re-crystallization. Nor are there any obvious metamorphic minerals such as are evident in the massive, compact rock composed of altered sillimanite found near Rewa in northern Madhya Pradesh (Banerjee and Sirgar 1961). Remnants of the prismatic, needle-like structure that is characteristic of sillimanite in thin-section (MacKenzie and Adams 1994: 180-181) can clearly been seen in the Rewa rock (Banerjee and Sirgar 1961: Figure 1). Nothing of the sort is evident in the BSE images of "Ernestite," however. This suggests that the somewhat ambiguous "mullite-sillimanite" phases detected in two samples using XRD is almost certainly *not* heat-transformed sillimanite. Instead, those phases most likely represent a poorly crystallized, early stage of mullite formed from the heating of the clay-sized Al-Si material that makes up the stone's matrix.

WHAT IS "ERNESTITE"?

Based on results of the XRD and EMPA characterization studies, I believe that "Ernestite" is a variety of *claystone* known as a *tonstein* and that it was heat-treated by Harappans to produce properties in the stone that made it an extremely effective material for drilling hard stone beads. In this section, I present my case for making this designation.

Claystone (sometimes called clayrock) is a general term for *non-fissile* sedimentary rocks (those that are not laminated and do not split along bedding planes) that are composed of *indurated* (a term synonymous with lithified or cemented) "clay-size silicate minerals" (Blatt 1992: 490; Lapidus and Winstanley 1990: 108). "Ernestite" – a tough, non-fissile stone primarily made up of clay-sized Al-Si particles, clearly falls into this category. Claystones vary in their origins, compositions and degrees of induration (Loughnan 1978). The variety known as *flint clay* is composed mainly of tightly interlocking kaolinite crystals (Moore and Reynolds 1997: 143), which makes it extremely tough and gives it a very fine-grained to microcrystalline texture along with a conchoidal to sub-conchoidal fracture (Keller 1968). The stone is named as it is because, obviously, these traits provide it with physical properties and an appearance that mimics flint (chert). It can easily be knapped like that material and then further shaped by grinding and engraving. In many parts of ancient North America, flint clay was a popular stone for making ornaments, effigies and, significantly, smoking pipes (Emerson and Hughes 2000; Hughes *et al*. 1998; Wisseman *et al*. 2002). Using a claystone of this sub-variety, Harappans could have easily fashioned constricted cylindrical drills by the chipping and grinding method described by Vidale (2000: 56).

Most flint clays are also *fire clays* (although not all fire clays are as highly indurated as flint clay). A fireclay is a common refractory material composed of an aluminous clay mineral (normally *kaolinite*) with small amounts of free silica (quartz) and other impurities (of which iron oxide and anatase are of particular importance here), which can withstand temperatures as high as 1750°C without vitrifying or deforming (Dodd and Murfin 1994: 120-121, 125; Lapidus and Winstanley 1990: 215). Although

Appendix 4.5 Figure 6 Select WDS scans of "Ernestite" fragments

	Light Matrix	Darker Matrix	Fe Phase (Hematite)	Ti Phase (Rutile)	Titanohematite Phase	SiO_2 Phase
MgO	0.05	0.20	0.18	0.00	0.26	0.00
Al_2O_3	39.25	48.10	6.36	0.50	4.94	0.19
SiO_2	59.28	40.56	7.25	0.30	1.24	98.57
CaO	0.04	0.59	0.03	0.00	0.00	0.00
TiO_2	0.21	0.25	1.56	95.66	33.39	0.08
MnO	0.00	0.00	0.07	0.01	0.06	0.00
FeO	1.07	4.61	74.45	1.00	51.85	0.22
Na_2O	0.06	0.90	0.01	0.00	0.00	0.00
K_2O	0.08	0.64	0.01	0.01	0.02	0.01
Cr_2O_3	0.01	0.02	0.30	0.07	0.14	0.00
total	***100.04***	***95.87***	***90.21***	***97.55***	***91.89***	***99.07***

kaolinite peaks were not detected in the XRD analyses, there are multiple lines of evidence, in addition to its appearance, toughness and texture, which suggests that "Ernestite" is a type of indurated kaolinitic fire clay that has been heat-treated. To begin with, as has been previously discussed, the heating of aluminous clays and claystones produces very characteristic high-temperature minerals. After 600°C, the structure of kaolinite becomes disordered and, in a *solid-state* (Castelein *et al.* 2001; Russell 1965), passes through several amorphous (or nearly amorphous) forms (Leonard 1977) until it begins to re-organize as mullite starting at around 1100° C. The mullite phases detected in the "Ernestite" samples are composed of clay-sized Al-Si particles that, in all likelihood, were once kaolinite, but that have been transformed in this way. Similarly, cristobalite is a common by byproduct of heated refractory clays (Davison and Heystek 1979). The phases of that mineral evident in the "Ernestite" samples with well-crystallized mullite could be a product of kaolinite-to-mullite conversion and/or the high-temperature transformation of natural quartz impurities contained within the original claystone – perhaps a combination both. It is also possible that cristobalite was a component of the original, unheated stone (discussed further below).

Other mineral impurities detected in the samples provide supporting evidence that "Ernestite" is a type indurated fire clay and help to explain the variation that is seen between the phase compositions of the stone's lighter and darker Al-Si matrixes. Iron oxide is an important minor component of fireclays (especially in levels greater than three percent) because it enhances mullite formation by acting as a fluxing element with aluminum silicate (Keller 1968: 116). It was not at all surprising, therefore, when EMPA indicated the darker Al-Si matrix of "Ernestite," which exhibited the best developed peaks for mullite in the XRD scans, had refractory levels of iron oxide (Appendix 4.5 Figure 6 column 3). Mullite was more poorly-developed in the samples composed of the lighter-colored Al-Si matrix, which had lower concentrations of iron oxide (Appendix 4.6 Figure 2 column 2). Another common impurity in fireclay is *anatase* (TiO_2), which is the low temperature polymorph of rutile. Anatase converts to rutile after being heated above 730°C (Deer *et al*. 1992: 550). The rutile that was detected using XRD in the two lighter matrix "Ernestite" samples is *perhaps* heat-transformed anatase (it may also have been present in the original, unheated stone – see below). This anatase/rutile would have contributed the titanium component of the high-temperature titanohematite phases detected in the darker matrix samples. The zircon inclusions and phosphate phases containing REEs that were detected using EMPA provide still more clues to the identity and origin of "Ernestite." Fire clays were formed in swampy, non-marine environments either from the accumulation of detrital kaolinitic sediments or from the in-situ kaolinitazation of fallen volcanic-ash (Admakin 2002; Keller 1968; Loughnan 1978). The term *tonstein* is widely used to denote the variety formed in the latter manner (Bohor and Triplehorn 1993). The first studies that I read regarding claystones of this type were eye-opening, because it was as if I was reading descriptions of "Ernestite." Tonsteins possess *all* of the properties that I have outlined above for fire clays *as well as* zircon inclusions and phosphate phases with concentrations of REEs – two traits that are indicative of their volcanic parentage (Bohor and Triplehorn 1993; Hower et. al 1999). In fact, cristobalite and rutile derived from the diagenesis of volcanic ash are also lithogenetic indicators of tonsteins (Admakin 2001: 24). It is therefore possible that those two minerals were original components of "Ernestite" and did not form due to heating (although heating of the stone still took place as demonstrated by the presence of mullite and titanohematite). Because tonsteins formed in swampy, plant-rich environments, they frequently contain casts of rootlets and other organic materials, which give them a mottled appearance (Bohor and Triplehorn 1993: 26-27). This may account for the characteristic appearance[3] of "Ernestite", with its dark patches and dendritic veining.

In summary, the appearance, toughness, texture (both macroscopic and microscopic) and composition of "Ernestite" are all consistent with the category of highly indurated claystone known as flint clay. Most flint clays are also kaolinitic fire clays that, when subjected to sufficient heat, produce a very characteristic mineral – mullite, which is highly uncommon in nature but a ubiquitous byproduct of high-temperature crafts and industries involving aluminous clays and claystones. Its presence, along with titanohematite phases, strongly suggests that "Ernestite" was *deliberately* heated. Cristobalite and rutile phases detected in the stone may also be products of heat-treatment. Or, they could be further evidence of its volcanic parentage, which is clearly indicated by the presence of zircon inclusions and REE-rich phosphate phases. Kaolinitic claystone formed from the diagenesis of volcanic ash fallen in a swampy, non-marine environment is known as a tonstein. This is what "Ernestite" appears to be.

At least that is my working hypothesis. I have been unable to find any reference to another type of naturally occurring sedimentary, igneous, or metamorphic rock possessing the same combination of characteristics reported here. Of course it is entirely possible that "Ernestite" is a variety of stone that has not previously been encountered and described by geologists. I consider that to be very unlikely, however. Its physical properties are highly consistent with a tonstein, which belongs to a category of kaolinitic claystones that are well known to geologists. The changes kaolinitic materials undergo when heated are equally well-documented and well understood. Although studies will continue, *a highly indurated tonstein flint clay that has been heat-*

3) The "Ernestite" drill bit and raw material assemblage at Dholavira is much more macroscopically variable, which may indicate that the beadmakers of that site may have dwelled near the source or sources of this stone and exported only a certain sub-variety of it to craftsmen at Harappan settlements elsewhere.

treated is the most fitting characterization that can be made for "Ernestite" at this time. The concern now is to determine where exactly Harappans might have acquired raw material of this kind.

WHERE DOES "ERNESTITE" COME FROM?

Tonsteins are variable in terms of their color, texture, mineral constituents and degree of induration (Bohor and Triplehorn 1993). Identifying the precise occurrence(s) that was used as a raw material source for "Ernestite" drills will require a great deal of exploration and sample testing. The latter will be necessary because if "Ernestite" was heat-treated (I believe the evidence demonstrates that it was) then it is very likely that the original, unheated tonstein, wherever it is located, will have somewhat different visual and physical properties, as any substance composed primarily of clay minerals does prior to being fired. Samples collected from potential sources will first need to be experimentally heated to determine if the physical appearance and properties of "Ernestite" can be replicated. Then they will need to be fashioned into drills to evaluate their effectiveness at perforating hard stone such as agate and vesuvianite-grossular. The problem of locating potential sources is made somewhat easier by the fact that tonsteins and other fire clays were formed in swampy, non-marine environments rich in organic matter and so are almost invariably found in association with coal beds (Bohor and Triplehorn 1993; Loughnan 1978: 380; Hoehne 1976).

Although the term "tonstein" has, up until now, rarely been used in the geologic literature of South Asia, occurrences of claystones or fire clay seams in coal beds have been noted in many different areas around the Greater Indus region (Bender 1995b: 276; Kazmi 1995a: 206-218; Talati and Desai 1978). In the spring of 2003, I traveled throughout northern Gujarat examining and sampling the many fire clay deposits of that area (Bhatti and Chavda 1977; Rahalkar and Madhukara 1980). One occurrence that I was particularly hopeful might be a raw material source for "Ernestite" is located near Guneri (Chavda and Joshi 1990) in the Lakhpat district of western Kutch, not far (≈ 20 km) from where a Harappan Period site has been identified (IAR 1960-61: 8). The samples of dark gray-colored fire clay collected from that location and the four others I visited in northern Saurashtra, were extremely fine-grained but rather soft (as compared to "Ernestite"). After being fired at 1200°C for one hour, their colors ranged from light khaki to an almost pure white and, although they became significantly harder, they were light in weight and somewhat brittle. Although these deposits obviously did not provide the raw material that I was seeking, the overall physical appearance of samples from them, aside from their color, in many ways resembled the larger fragments of "Ernestite" recovered at Harappa. This further convinced me that Harappans were using a variety of sedimentary claystone to make constricted cylindrical drill bits, rather than a metamorphic rock. I simply had not yet located a coal bed containing a tonstein claystone that was sufficiently indurated to begin with. Other potential occurrences can be found in every province of Pakistan (Kazmi *et al*. 1990; Shah *et al*. 1990; Warwick and Husain 1990). Some of those where refractory clays and claystones are noted (Baqri 1978) lay deeply buried and so would not have been accessible to Harappans. Coal beds are, however, exposed on the western flanks of the Kirthar Range in Sindh (Blanford 1879: 192-193) and I have been told (S.R.H. Baqri *personal communication* 2004) that very hard, flint-like claystones can be found in the vicinity of Sehwan. Claystone seams in accessible coal beds are also reported in the western and central part of the Salt Range (Shah 1980: 82-84; Whitney *et al*. 1990: 3).

Although the search for Ernestite" will continue in all of the above areas, my feeling at this stage is that the Harappan source likely lies somewhere in northern

Gujarat. I have recorded over 1200 "Ernestite" drill bits in my studies of the collection of excavated materials from the site of Dholavira. Compare this to the 75 artifacts in total (both drill bits and debris) that have been recovered at Harappa. The shear abundance of "Ernestite" at Dholavira would seem to indicate that beadmakers there had access to a local (on Khadir Island) or regional (elsewhere in Kutch) source of the stone.

"ERNESTITE" AS A DRILL-MAKING MATERIAL

What properties did heat-treated tonstein flint clay possess that appealed to Harappan beadmakers? Experimental studies by Kenoyer and Vidale (1992) have shown that it would have been possible for them to perforate a hard stone like carnelian almost three times faster using an "Ernestite" drill bit than it would have been using one made from a microcrystalline silicate like jasper or chert ("Ernestite" abraded carnelian at an average rate of 2.37 mm per hour compared to .83 mm per hour for green jasper). This unequal drilling efficiency probably has little to do with differences in hardness between the two materials. Quartz has a Mohs hardness of around 7 and so does mullite – the hardest major mineral in "Ernestite" (zircon has a hardness of 7.5 but there is not enough of it in the stone to have contributed significantly to its cutting effectiveness). The properties that make "Ernestite" much more effective than chert or jasper for drilling hard stone beads are its *durability*, *strength* and *heat-resistance*.

Harappans would have found drills made of a microcrystalline silicate to be more than effective tools for perforating steatite, lapis lazuli, serpentine or any other variety of stone with a Mohs hardness of less than 7. However, as Kenoyer and Vidale discovered (1992: 504-505), when used on a stone of equal hardness such as agate, both the shaft of the drill and the hole of the bead being perforated wear to a high polish. Abrading effectiveness rapidly diminishes as this occurs. In contrast, the inter-locking clay-sized Al-Si particles of "Ernestite" make it an extremely durable (wear-resistant) material. In the 1930s, C.H. Desch carried out a drilling experiment (noted in Mackay 1943: 211) on carnelian using a bit recovered from the site of Harappan Period site of Chanhu-daro in Sindh. At the time, the bit was thought to be made of chert but it is now known be composed of "Ernestite." After drilling carnelian to a depth of 1 mm in around 20 minutes (an abrading rate roughly comparable to what Kenoyer and Vidale recorded for "Ernestite"), Desch found the wear on the tool "to be very slight" (ibid.). Scanning electron microcopy (SEM) studies by Kenoyer and Vidale (1992: 508) revealed that drills made of durable "Ernestite" do not become polished during use like microcrystalline silicates. Instead, they maintain a rough micro-surface and, thus, an undiminished cutting capacity.

In addition to being durable, "Ernestite" is an extremely well-bonded material, which can be made into drills that, although delicate-looking, are very strong. Perforating the distinctively Harappan style of long (≈ 7 to 10 cm) carnelian beads was accomplished using a graduated series of three or four long and progressively thinner "Ernestite" drill bits (Kenoyer and Vidale 1992: 511). One example that Ernest Mackay reported (1943: 211 *footnote* and Plate LXXXVI b, #8, drill e) from Chanhu-daro was 1.5 inches (3.81 cm) in length but only 0.12 inches (3.05 mm) in diameter. Although fashioning a drill bit of similar dimensions out of chert or jasper would have been possible, such a tool would likely not have lasted for long under the stress of drilling as the "raw material is very brittle and tends to flake very easily and snap" (Kenoyer and Vidale 1992: 503).

Microcrystalline silicate drills are also plagued by frequent incidences of spalling due to the heat generated by the friction of drilling, as well as a tapered design that makes cooling the tool during use difficult (Kenoyer and Vidale 1992: 505). Tiny heat-spalled drill bit tips made of jasper and chert are very common finds in areas at Harappa where hard stone beads were made (Meadow *et al*. 2001: 7). A tool made from a refractory material like tonstein flint clay, on the other hand, would be extremely resistant to the effects of heat. The biggest testament to this is that no heat-spalled "Ernestite" drill tips have ever been found at Harappa (J.M. Kenoyer *personal communication* 2002).

The "secret" to "Ernestite's" durability, strength and resistance to heat is mullite. The remarkable mechanical and refractory properties of this mineral are well-documented (Osendi and Baudín 1996; Mah and Mazdiyasni 1983; Schneider *et al* 1994; Schneider and Komarneni 2005). Mullite "imparts uniformly high strength" to those materials in which it forms, as well as a "high resistance to thermal spalling, i.e, resistance to breaking or cracking when heated" to extreme temperatures (Keller 1968: 119-120). There is a modern industry devoted to deliberately synthesizing it for applications that require a material having this specific combination of properties (Industrial Minerals 1998; Johnstone and Johnstone 1961; Schneider and Komarneni 2005). Mullite would not have been originally present in the tonstein(s) used as a raw material for "Ernestite." That stone likely attracted the attention of Harappans looking for drill-making material because it was already a tough, highly indurated rock (as most flint clays are). Sometime around the middle part of the Integration Era (ca. Period 3B at Harappa), perhaps even earlier, it was discovered that by heating tonstein flint clay to a temperature that probably exceeded 1100°C it was possible to produce or enhance properties (discussed above) in the rock that made it a superior material for drilling hard stone beads. Although Harappans could not have known that the reason for this was that its structure of tightly inter-locking kaolinite crystals was being made even stronger and more heat-resistant by the solid-state transformation of those crystals into mullite, they were evidently well aware of which parts of the stone had most benefited from the heat-treatment. The majority of finished "Ernestite" drill bits recovered at Harappa and other Indus sites were made largely or entirely from the stone's less abundant black matrix, which the XRD scans showed have the best developed mullite phases.

CONCLUSION

There is still great deal of work to be done on the "Ernestite" problem. Although I feel strongly that the identification "tonstein flint clay that has been heat-treated" is, currently, the best explanation for the macroscopic, mineralogical and mechanical characteristics possessed by "Ernestite," I realize that many (including myself) will not be entirely convinced of this until a source of tonstein flint clay is located in the Greater Indus region, material from that sources is heated to temperatures that should result in the formation of mullite, then that heat-treated material is fashioned by chipping and grinding into replicas of Harappan constricted cylindrical drill bits and finally it is shown that those drills are capable of perforating agate or vesuvianite-grossular at a rate of better than 2 mm an hour or better without breaking or spalling. If that can be done and the resulting material *looks* like "Ernestite" then I will be convinced.

ADDENDUM - A SMALL TEST

Having read the above section, Prof. Kenoyer felt that I had not adequately demonstrated that "Ernestite" was heat-treated. He suggested that I heat a piece of it in a muffle furnace to a temperature hot enough for mullite and cristobalite to form (≈ 1100 to 1200° C) in order to see if its appearance changed. He argued that if the material had been previously heat-

Appendix 4.5 Figure 7 Before and after images of an "Ernestite" chip that has been heated to 1200° C.

treated in this way then its appearance after being re-heated should remain unchanged. So I took a small (≈ 1.75 x 2.75 cm) chip off of one of the larger pieces of "Ernestite" and heated it slowly (a dynamic firing where the temperature was steadily raised 200° C per hour) to 1200° C. The chip was allowed to dwell at 1200° C for two hours after which the furnace was turned completely off and left to cool slowly overnight.

The next day the "Ernestite" chip was removed from the cooled furnace and examined. Appendix 4.5 Figure 7 is a composite photo that shows the chip's unheated appearance (left) next to how it looked after being fired slowly to 1200° C (right). There is a *slight* difference in the before and after images. The khaki-colored matrix is a shade lighter as are some patches of the darker matrix. I can think of two reasons why the stone's color might have become slighter lighter. Firstly, the chip is from an artifact that has been buried for 4000 plus years. "Ernestite" is dense, yes, but is still basically a claystone that is somewhat permeable. "Ernestite" artifacts may actually have darkened slightly over the last four millennia as they picked up organics from the moisture laden soils at Harappa. Firing the chip may have simply burned off some of the organics it picked up. Moreover (and secondly) the muffle furnace was an oxygen-rich environment. "Ernestite" contains iron phases, the heaviest concentrations of which are in the darker portions of the stone. Had the chip been fired in a reducing atmosphere then the iron oxides in it might have remained dark or, perhaps, even become darker.

In the end, the chip's appearance was little changed and the firing experiment was inconclusive. In my opinion, the biggest testament to "Ernestite's" heat-treatment by Harappans remains the presence of mullite and cristobalite – two minerals that are rare nature (even rarer together) but are common in clays and claystones heated to high temperatures.

APPENDIX 4.6

A LATE HARAPPAN KAOLINITE BEAD

DISCOVERY

Trench 38 (Appendix 4.6 Figure 1 A) was placed on the north side of Mound AB in one of the few areas at Harappa where Late Harappan (Period 5) or "Cemetery H" Phase architecture was still, more or less, intact after the extensive brick robbing of the mid-1800s (Kenoyer 2005b: 32-37). During the 1996 excavation season, a small pot that had been buried in the floor of house (Appendix 4.6 Figure 1 B) from this period was recovered. The interior of the pot (Appendix 4.6 Figure 1 C) was carefully excavated by J.M. Kenoyer (Appendix 4.6 Figure 1 D) and found to contain a cache of 133 beads (Appendix 4.6 Figure 1 E). These artifacts have provided a number of insights into trade and technology during the Late Harappan Period (ibid: 37-39). Of particular interest is object H96/7330-15 – a small red bead (indicated by a red arrow on Appendix 4.6 Figure E).

IDENTIFICATION

The red bead in question was initially thought to be as carnelian but closer examination (Appendix 4.6 Figure 1 F) suggested that it might actually be an early form of glass (Kenoyer 2005a: 167; Kenoyer 2005b: 37-38). It has a polished, glassy sheen and a dark bubbly-looking patch that seemed as if it could have been the vestiges of the glass manufacturing process. This would have made the bead the earliest evidence for glass-making in South Asia. However, its identification as glass was only provisional until such time as further, positive analyses could be conducted. With the permission of Dr. Fazal Dad Kakar, Director-General, Department of Archaeology and Museums, Government of Pakistan, the bead was brought to the University of Wisconsin-Madison in 2009 for non-desctructive analysis using variable pressure scanning electron microscopy (VP-SEM) and X-ray diffraction (XRD).

VP-SEM

The variable pressure scanning electron microscope (VP-SEM) is a wonderful tool for non-destructive characterization of artifacts. With it is possible to micro-image samples without having to first coat them with a current conducting material such as carbon or gold, as is necessary with conventional scanning electron microscopy (SEM). Moreover, the Hitachi S-3400N VP-SEM at the Eugene Cameron Electron Microprobe Lab in the Department of Geoscience, University of Wisconsin-Madison is equipped with a Thermo Electron energy dispersive spectrometer (EDS) and so it is possible to do qualitative evaluations of the composition of the artifacts being examined.

Analysis of the red bead focused on and around the dark bubbly patch (seen in visible light in Appendix 4.6 Figure 2 A). Back-scatter electron imaging (BSE) of that area (Appendix 4.6 Figure 2 B) revealed that the main body of the object, while fairly smooth and homogenous, is spotted with a few large and many small depressions or pits filled with a substance having a relatively low atomic number (the pits appear dark gray or black because materials with low atomic numbers appear darkest in BSE images while those with higher ones appear brighter). The bubbly patch is made up of spherical nodules or concretions with an atomic number much higher than the main body or the pitted area (thus they appear white in the BSE image).

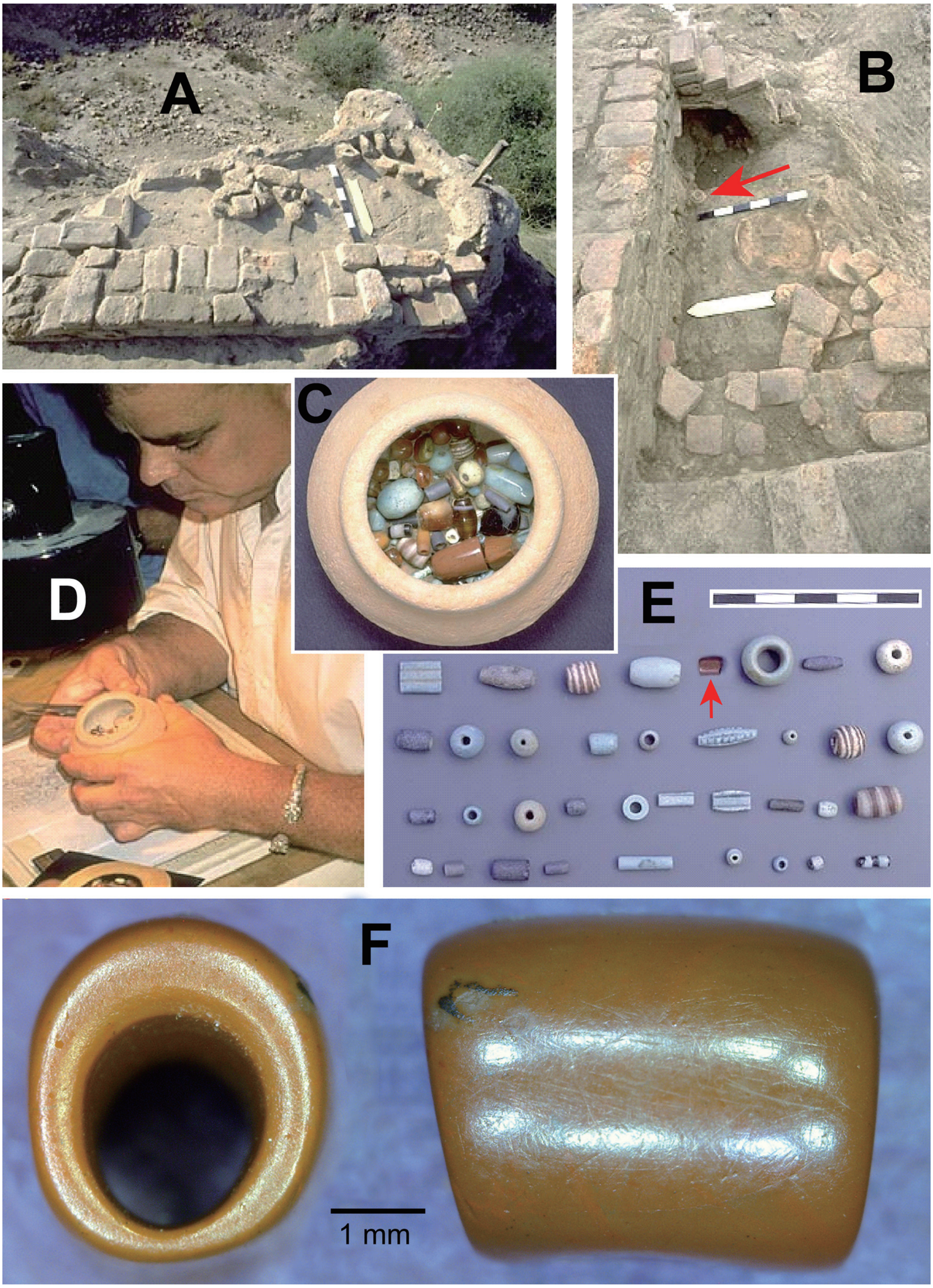

Appendix 4.6 Figure 1 **[A]** During the excavation of Trench 38 on the north side of Mound AB. **[B]** a small pot (indicated by a red arrow) was found embedded in a Late Harappan (Period 5) house floor. **[C]** The pot contained a cache of beads, **[D]** which were carefully excavated by J.M. Kenoyer. **[E]** Among the artifacts found in the pot was a small red bead (indicated by a red arrow) **[F]** with a polished, glassy sheen and a dark bubbly-looking patch (visible on the upper left corner of the right-hand view of the bead).

Images A through E are from the website Harappa.com and are used with the permission of J.M. Kenoyer.

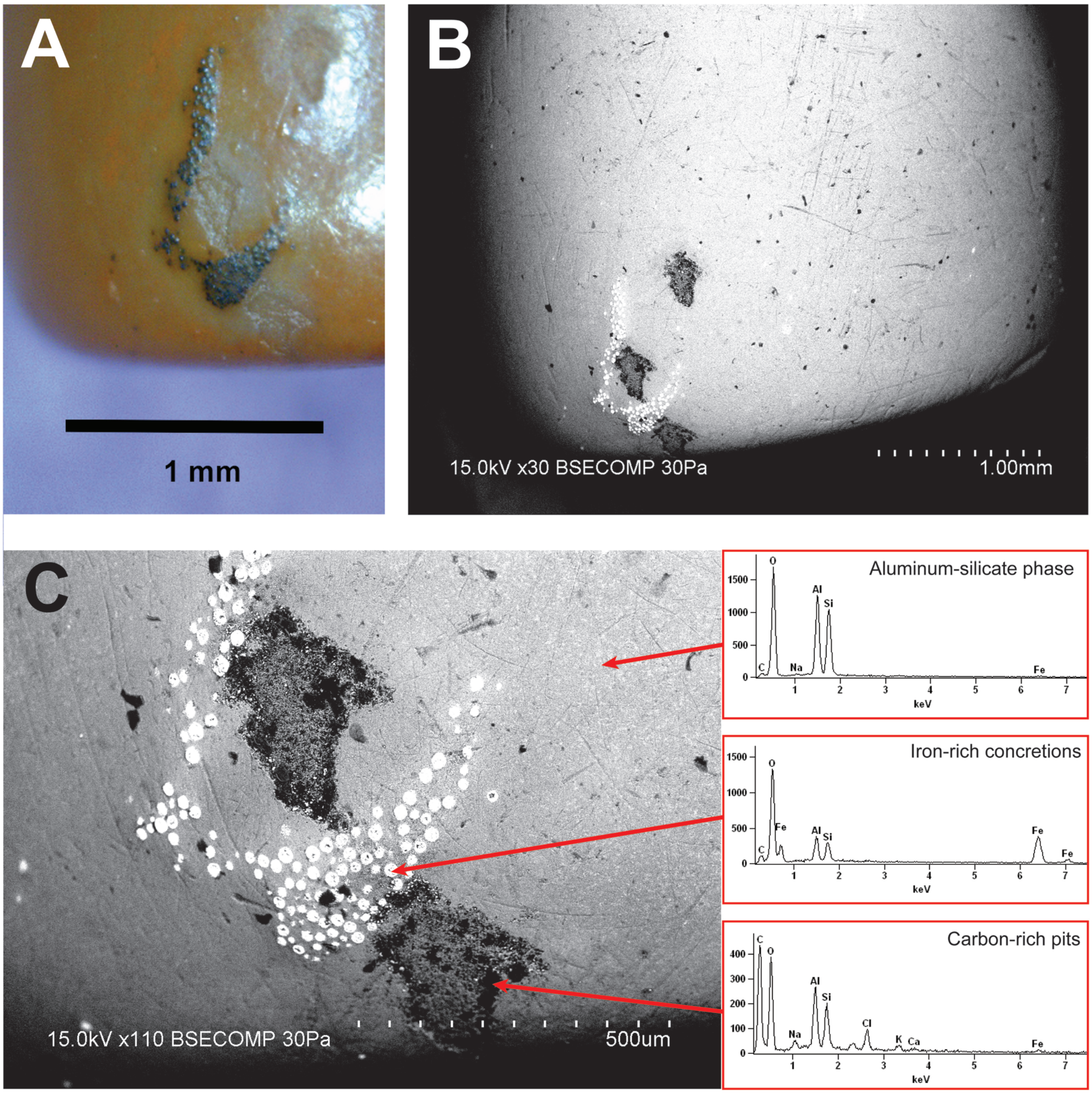

Appendix 4.6 Figure 2 **[A]** Visible light image of the small red bead's black patch. **[B]** BSE image of the small red bead's black patch showing that it is made up of spherical concretions. **[C]** EDS spectra of bead's primary matrix, the spherical concretions and tiny pits/depressions in the bead's surface.

EDS scans were made of three points on the red bead (Appendix 4.6 Figure 2 C). These revealed that the main body of the object was an aluminum silicate mineral of some kind, the spherical concretions making up the dark bubbly patch were rich in iron, and the pits were high in carbon. It was immediately obvious that the artifact was *not* a glass bead. What it was made from was not entirely clear, however. The aluminum silicate composing the main body of the bead could have been any number of minerals including kyanite, sillimanite, andalusite, mullite, kaolinite and pyrophyllite. The concretions were thought to be hematite and the pits might have contained graphite. Positive mineralogical identification of these phases would require a different technique.

XRD

In September of 2009, the S.W. Bailey Memorial XRD Laboratory in the Department of Geoscience, University of Wisconsin-Madison acquired a state-of-the-art Rigaku Rapid II XRD (Appendix 4.6 Figure

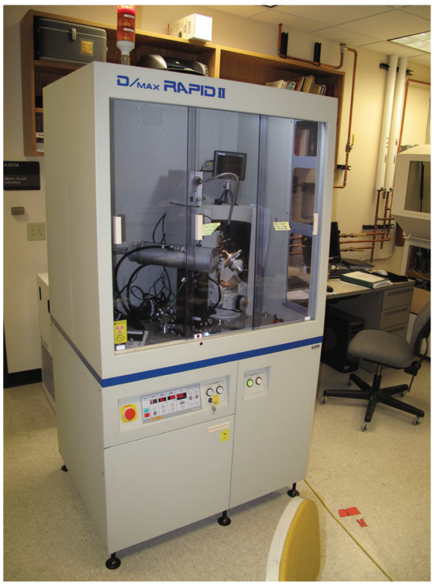

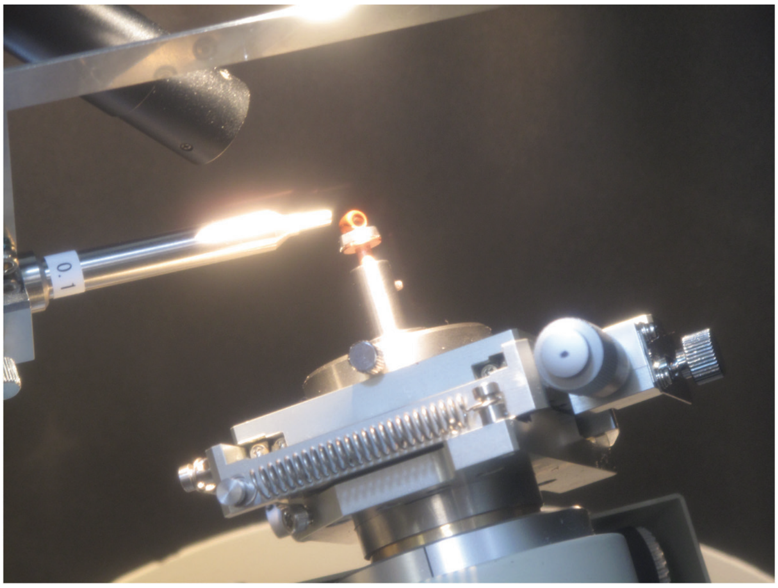

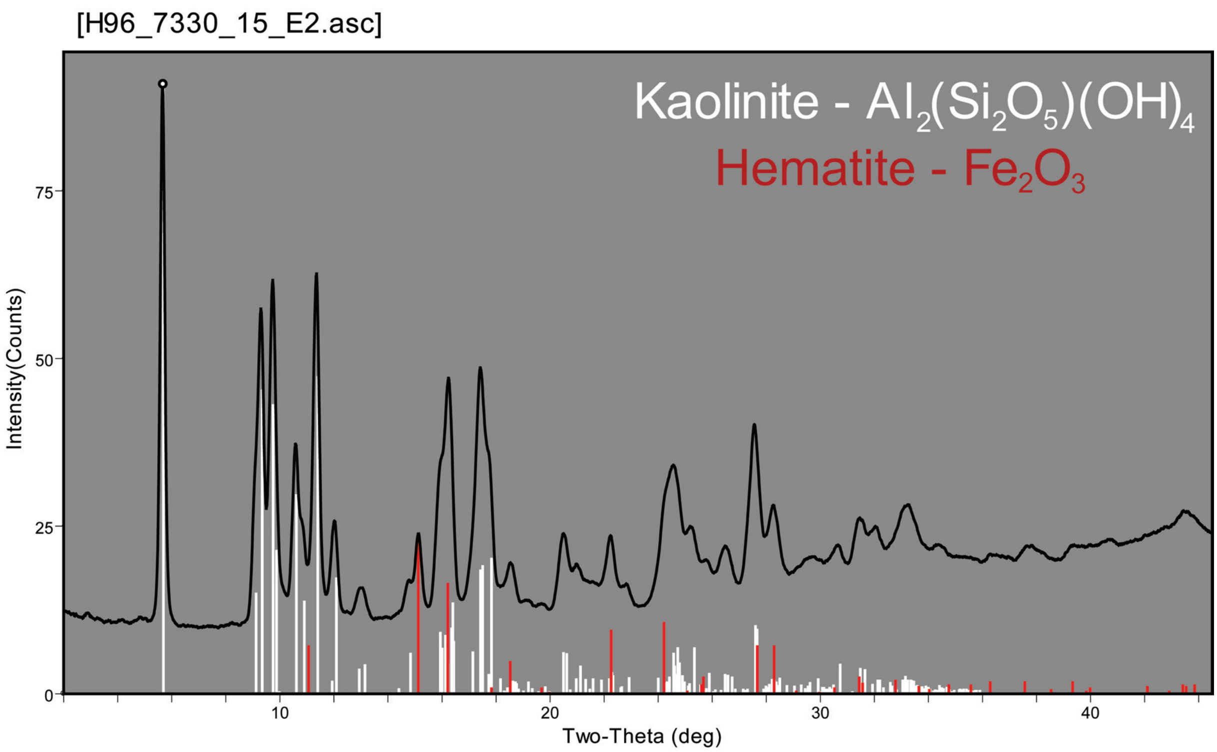

Appendix 4.6 Figure 3 None-destructive XRD analysis of the Late Harappan red bead using the Rigaku Rapid II (top images). XRD spectrum (bottom) of the bead's primary matrix – kaolinite with a minor hematite phase.

3 *top left*). With this instrument, points down to 20 nanometers in size can be nondestructively analyzed on a sample, such as the late Harappan bead, in situ (Appendix 4.6 Figure 3 *top right*). Multiple scans of the red bead were made but all were basically the same. A representative scan is presented here (Appendix 4.6 Figure 3 *bottom*) The results indicate that bead is mainly composed of the mineral *kaolinite* (aluminum silicate hydroxide). Small peaks indicating the presence of hematite (iron oxide) were detected in every scan, but kaolinite always dominated, even in scans that were centered directly on the iron-rich spherical concretions. No minerals with a carbon component were detected. Thus, the carbon detected

in the pits is probably an amorphous carbon substance like wood ash rather than a mineral like graphite.

CONCLUSION

The tiny red bead from the Late Harappan bead cache that was once thought to be glass now appears to have been made from a solid piece of indurated hematitic kaolinite. Kaolinite is a clay mineral which, in its form that develops plasticity when mixed with water, is widely used in the production of ceramics (Keller 1982; King 2009). However, the mineral can also occur in indurated (hardened) forms called *claystones* that will not slake in water and develop plasticity (Keller 1968; Loughnan 1978). We can be certain that bead was fashioned from a natural claystone rather than molded from a plastic clay that was then harded by heat (fired) because the act of heating transforms kaolinite into entirely new mineral phases – beginning around 550°C *metakaolinite* starts to form, a *spinel* phase is formed at 920°C, and finally *mullite* forms at around 1100°C (Bellotto *et al*. 1995a, 1995b). Had the bead been heated (if it was a ceramic bead) then one of these mineral phases would have been detected by XRD rather than kaolinite. As for the Fe-rich spherical concretions and hematite phases detected in the artifact, iron oxides are very common natural impurities in kaolinite bodies (Malden and Meads 1967). The reddish color of the bead is quite clearly related to the presence of iron and, thus, the raw material can aptly be described at hematitic kaolinite.

APPENDIX 4.7

THE IDENTIFICATION, CHARACTERIZATION AND POTENTIAL SOURCES OF A NEPHRITE JADE AMULET RECOVERED FROM THE CEMETERY AREA AT HARAPPA

DESCRIPTION AND DISCOVERY

A semi-translucent, spinach-green colored truncated conical amulet (Appendix 4.7 Figure 1 *left*) was recovered from a cemetery area debris layer that directly overlaid a burial pit dated to Period 3B. Although the artifact may or may not date to that period, there is no question that it is from the Harappa Phase. Hundreds of objects (sometimes called "gamesmen") of the exact same form have been discovered at Indus Civilization sites but none are known from sites of earlier or later periods. The majority of such amulets are made from black basalt. Examples composed of other kinds of stone, including steatite, serpentine, alabaster, limestone and vesuvianite-grossular, are also found. The amulet under discussion here – artifact H88/182-14 – is notable for its high polish (especially around its grooved "neck") and distinctive black spots (Appendix 4.7 Figure 1 *right*).

IDENTIFICATION AND CHARACTERIZATION

The amulet was originally thought to be composed of *serpentine* and was listed as such in the catalogue of the *Great Cities, Small Treasures* exhibit (Kenoyer 1998: 208) that came to the United States in 1998. This was an apt designation based on the object's visual characteristics alone. However, during my density testing of all green-colored stone artifacts from Harappa (described in Chapter 9) it was determined that the amulet had a specific gravity (SG) of 3.0, which is too dense to be serpentine (SG 2.7 to 2.8) or *quartz* (SG 2.6) and too light to be the *jadeite* form of jade (SG 3.24 to 3.43). A few examples of vesuvianite from Harappa with SG values of around 3.0 have been recorded but these are highly weathered debris fragments that have numerous fractures filled with chlorite. The material composing the amulet in question is unweathered and flawless. It also possesses a much deeper green color than is typical for vesuvianite-grossular and has a high, very "jade-like" polish. As it turns out, SG 3.0 is precisely the density of the tremolite-actinolite form of jade known as *nephrite* and so I provisionally designated the amulet as such in my dissertation (Law 2008a: 164-167). Further analyses were needed to confirm this identification, however. With the kind permission of Dr. Fazal Dad Kakar, Director-General, Department of Archaeology and Museums, Government of Pakistan, the artifact was brought to the University of Wisconsin-Madison in early 2010 for non-destructive identification and characterization using XRD and VP-SEM.

XRD

The amulet was analyzed on the Rigaku Rapid II XRD in the Department of Geosciences, University of Wisconsin-Madison (Appendix 4.7 Figure 2 A). As nephrite jade is a variable rock in the tremolite-actinolite series (it is actually "nearly pure tremolite" with "variable amount of actinolite" – Liu 2010: 249), the XRD spectrum from this analysis was compared to the peak profiles for both end-member minerals (Appendix 4.7 Figure 2 B & C). All peaks in the amulet's spectrum were found to correspond very

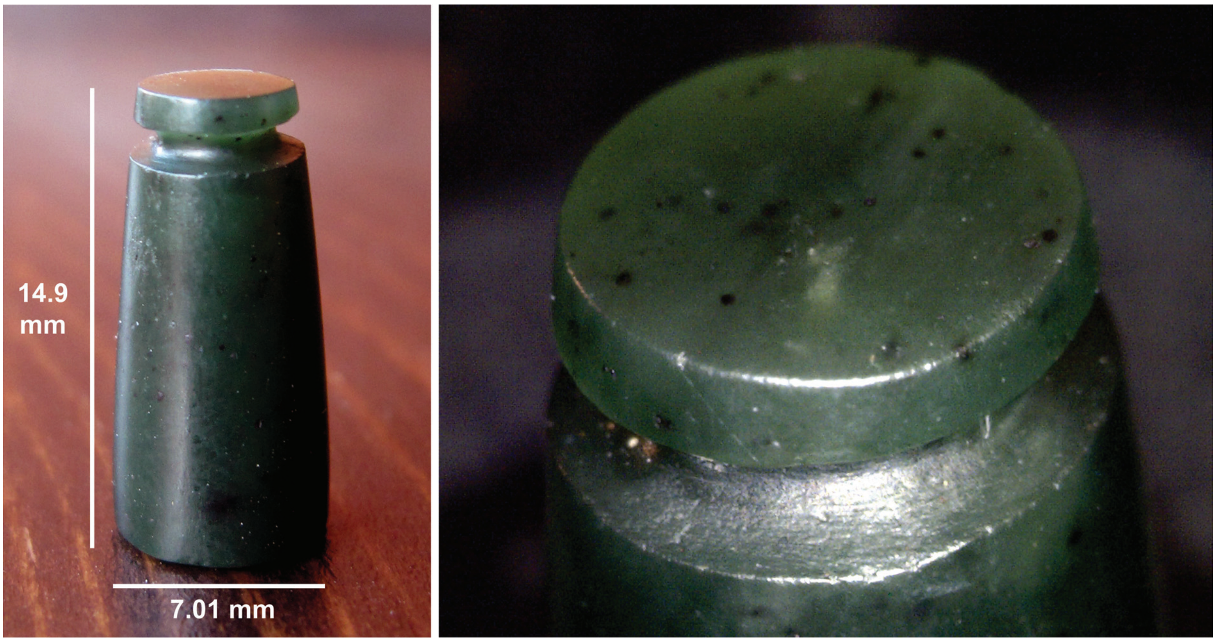

Appendix 4.7 Figure 1 Left - The semi-translucent, spinach-green colored truncated conical amulet – artifact H88/182-14 – recovered from a cemetery area debris layer at Harappa.
Right - Detail of the amulet's grooved neck and black inclusions.

well to those of both actinolite and tremolite, which confirmed that it was indeed a rock that series.

For the next step, the amulet's XRD spectrum was compared to the spectra of several known examples of nephrite (Appendix 4.7 Figure 2 D). Two samples of that stone from the source near the city of Khotan (Hetian) in western China were analyzed along with samples from the Sayan Mountains of southern Siberia, Russia and the Granite Mountains of central Wyoming, USA. The peak profile of the amulet's spectrum closely matched those of each of these nephrite samples.

VP-SEM

Further characterization of the amulet was conducted on the VP-SEM in the Department of Geosciences, University of Wisconsin-Madison. One distinquishing characteristic of nephrite is the tightly woven, matted fibrous texture it exhibits in microscopic images of fresh breaks and in petrographic thin sections (for examples see Bradt *et al* 1973: Figure 1 *top* and Twilley 1992: Figure 1). The highly polished surface of the Harappan amulet, which is evident in the BSE of the upper portion of the object (Appendix 4.7 Figure 3 A), largely obscures the natural texture of the stone. However, there are a few small unpolished areas (one is noted as E & F on the image) in which the rough surface of the raw material is visible. Close BSE imaging of one of these areas revealed a nephrite-like texture of tightly woven, matted fibrous crystals (Appendix 4.7 Figure 3 E & F).

Appendix 4.7 Figure 3 B is a BSE image of a portion of the top surface of the amulet on which several of stone's black inclusions are visible (these appear bright white on the image). EDS scans were made in this area of the amulet's primary phase and one of the inclusions (at the points noted as C & D respectively on the image). The peaks of Mg, Si, Fe and Ca evident in the spectrum of the primary phase (Appendix 4.7 Figure 3 C) are wholly consistent with nephrite (calcium magnesium iron silicate hydroxide). The peaks of Al, Fe and Cr evident in the spectrum of the inclusion (Appendix 4.7 Figure 3 D) are indicative of an aluminum-rich chromite (spinel) phase. Spinel-chromite inclusions such as these are not at all uncommon in nephrite (Hobbs 1982) and

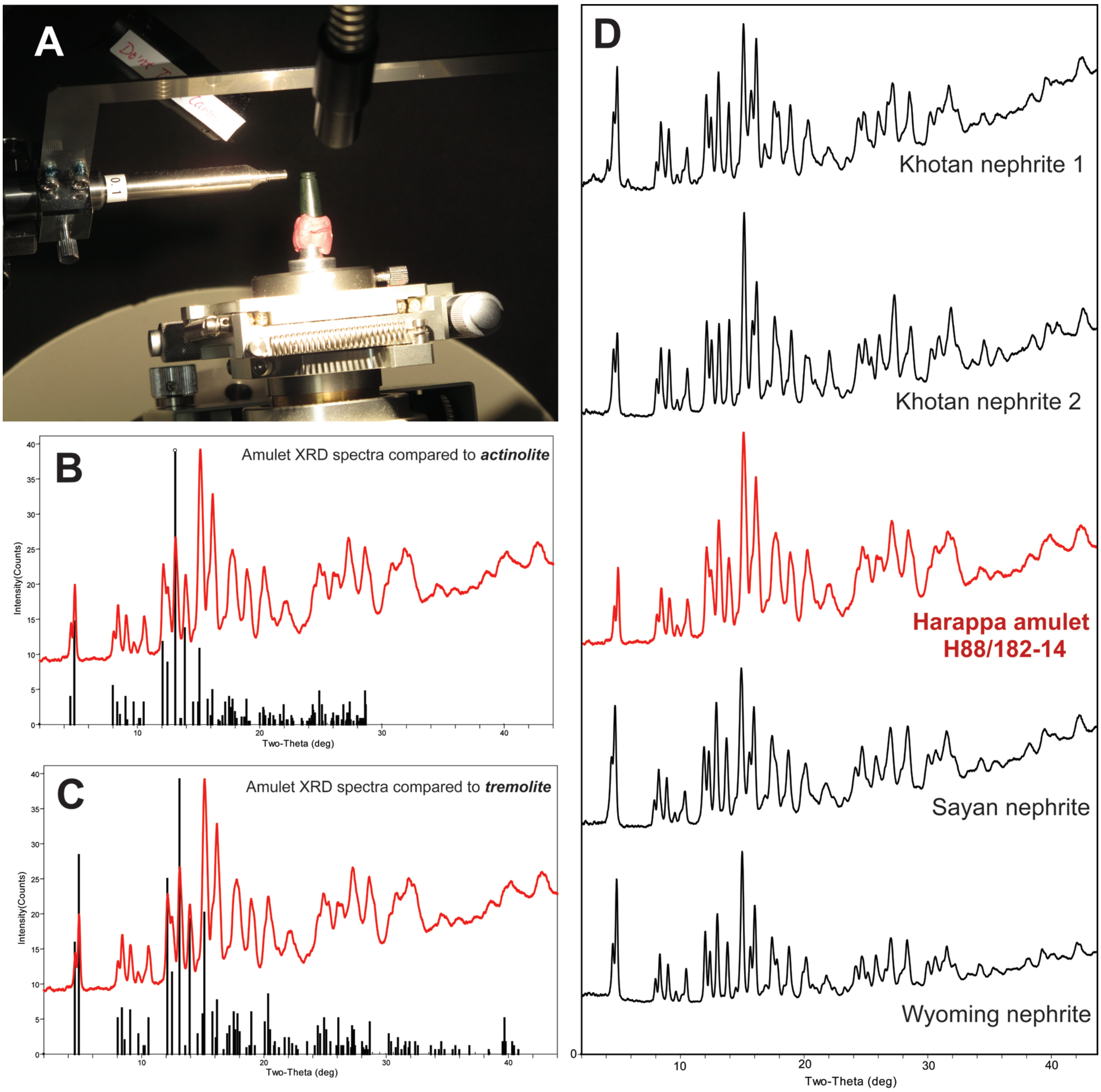

Appendix 4.7 Figure 2 **[A]** The amulet being non-destructively analyzed on the Rigaku Rapid II XRD. **[B]** The amulet's XRD spectrum compared to peaks for the mineral actinolite. **[C]** The amulet's XRD spectrum compared to peaks for the mineral tremolite. **[D]** The amulet's XRD spectrum was compared to the spectra of nephrite samples from Khotan, Sayan Mountains and Wyoming.

variations in their chemistry can sometimes even be used differentiate sources of the stone (Iizuka *et al.* 2005).

Conclusion

The semi-translucent, spinach-green colored truncated conical amulet recovered in the cemetery area at Harappa is almost certainly composed of nephrite jade. The macroscopic appearance, density, mineralogy, and microscopic texture of the stone from which the ornament is made are all consistent with that identification. This makes the amulet the first and, thus far, only positively confirmed jade artifact at an Indus Civilization site. The question now is – from what source did Harappans acquire this stone?

POTENTIAL SOURCES

Jade is found in many locations across Asia

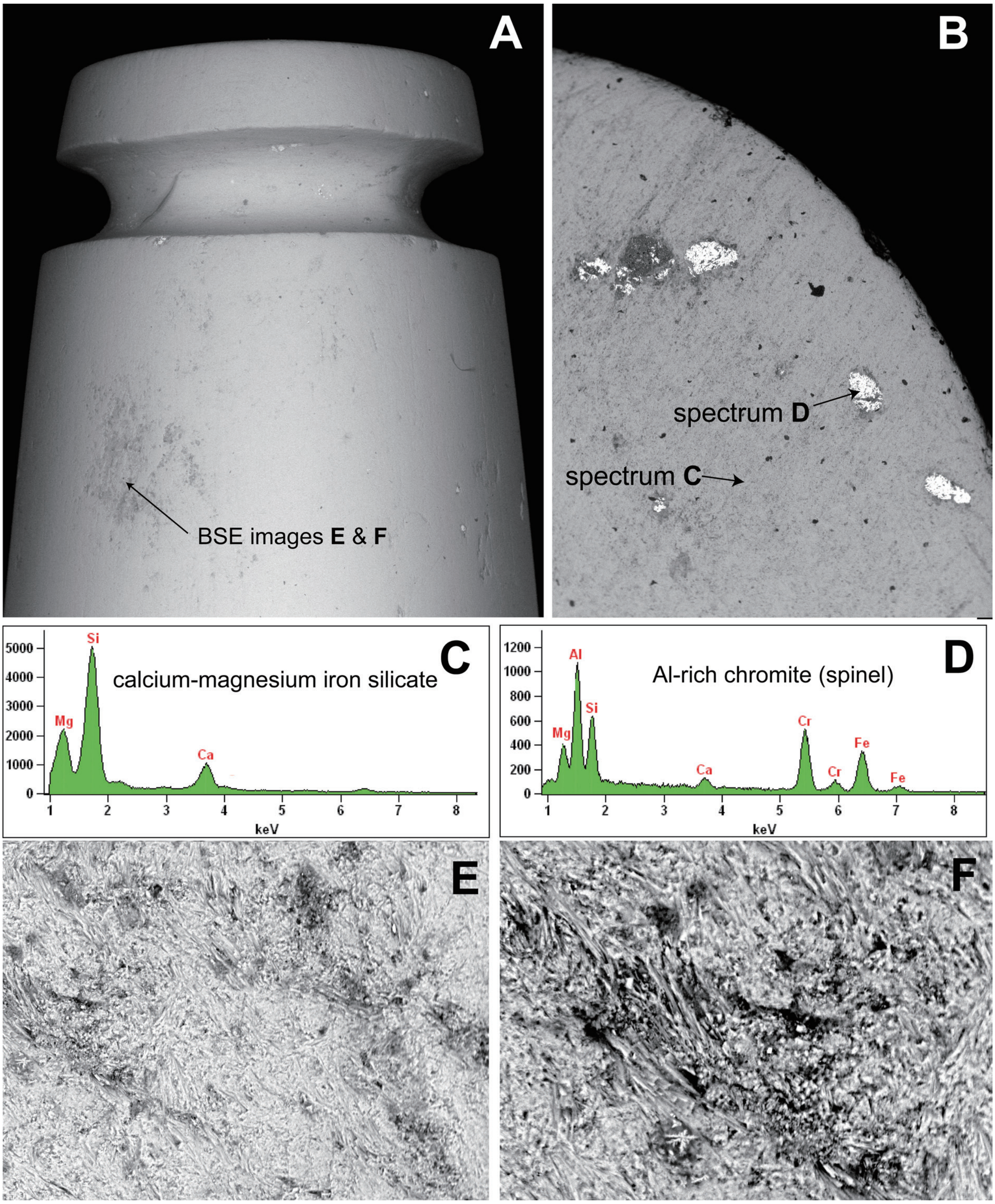

Appendix 4.7 Figure 3 VP-SEM/EDS analysis of the amulet. **[A]** BSE images of the upper portion of the amulet showing the unpolished locations (points E & F) where detailed BSE images were made. **[B]** BSE image of the top surface of the amulet showing the black inclusions (which are white in the image) and locations (points C & D) where EDS scans were made. **[C]** EDS spectrum of the amulet's main phase. **[D]** EDS spectrum of the amulet's black inclusions. **[E & F]** BSE details of an unpolished area on the amulet where the fibrous texture of the natural stone is unobscured.

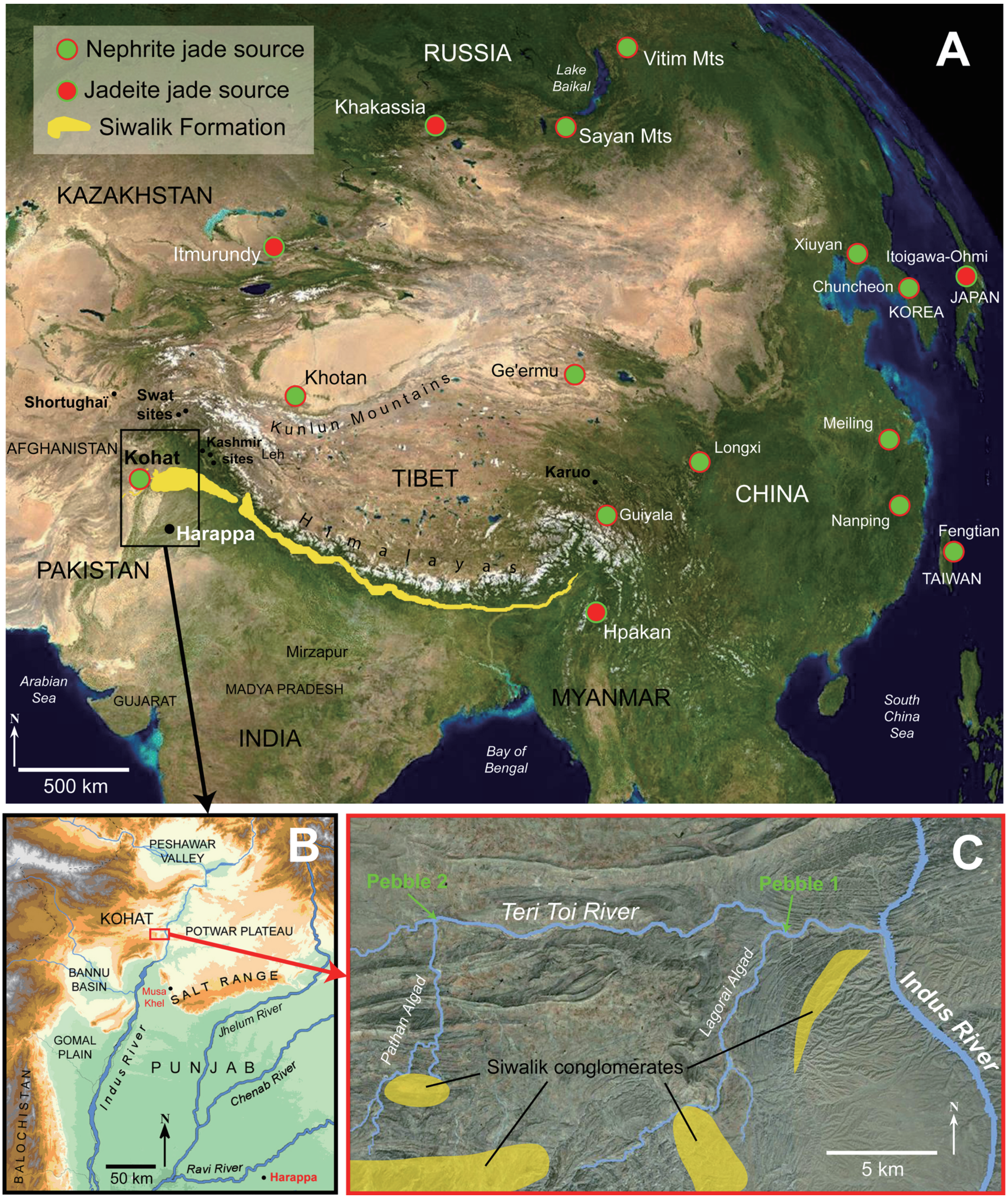

Appendix 4.7 Figure 4 **[A]** Map of the Asian jade sources, archaeological sites and geologic formations discussed in this section. **[B]** Map of the upper Indus Valley Region. **[C]** The Teri Toi River area, Kohat with the locations where B.C.M Butler collected nephrite pebbles noted and the approximately locations of the Siwalik conglomerates highlighted (after Butler 1963a: Figure 5).

(Appendix 4.7 Figure 4 A). Although several occurrences have been reported within the Indian Subcontinent, nearly all of those either have been demonstrated to not actually exist or remain to be positively confirmed. Krishnaswamy stated (1979: 499) that jade could be found in Tamil Nadu, Madhya Pradesh and Gujarat. An examination of his primary source material, however, suggests that these are not actually sources of either jadeite or nephrite. For example, he cites C.S. Middlemiss (1921: 69)

Appendix 4.7 Figure 5 Nephrite jade cobbles for sale in the Khotan bazaar, July 1997.

who described two types of material in northeast Gujarat (a translucent white pyroxene and a pale green tremolite-amphibole) that, when polished, were very "handsome" and "jade-like." Middlemiss even suggested that they might make good ornamental stone. He also, however, made it clear that neither material was dense enough to qualify as true jade. F.R. Mallet reported jade (presumably nephrite) in the Mirzapur area of what is today the state of Madhya Pradesh (Mallet 1872: 22) but this was later shown by K.P. Sinor (1923) to have been a misidentification. Somewhat more recently, Singh and Gupta reported (1987) jadeite pods within the ultramafic rocks of the Shyok Ophiolite, Leh District, Jammu and Kashmir. A more detailed mineralogical analysis is needed to confirm that the material from that locality is genuine jade, however.

The only positive identification of jade in South Asia thus far was made by geologist B.C.M. Butler of Oxford University (Butler 1963a, 1963b). He collected two pebbles from the bed of the Teri Toi river in the Kohat District, NWFP, which lies some 320 km north-northwest of Harappa (Appendix 4.7 Figure 4 B & C). Using a combination of thin-section petrography and XRD, Butler determined that both were composed of nephrite jade. He believed (but was not able to confirm) that the pebbles had to have eroded from nearby conglomerate beds of the Middle to Upper Siwaliks as there were no *in situ* metamorphic formations in the area from which they could have originated (Butler 1963a: 389-390). If he was correct, then it is conceivable that nephrite, although perhaps rare, might be found at various other points across the extensive Siwalik Formation (highlighted in yellow on Appendix 4.7 Figure 4 A) where conglomerates containing metamorphic clasts also occur (Brozović and Burbank 2000; Cheema *et al*. 1977: 89-98). Most significantly in terms of the present study, Butler recorded (1963a: 387-389) that the larger of the nephrite pebbles had a translucent "spinach-green" appearance and tiny black inclusions of spinel – exactly like that of the Harappan amulet! The description of the smaller pebble – "pale greenish-white" (ibid.: 386), is somewhat reminiscent of the light-green colored jade beads and pendants recovered to the north of Kohat from the prehistoric sites of Ghalegay and Loebanr in the Swat Valley of the NWFP (Stacul 1987: 75). Still, it is possible that those ornaments, as well at the amulet from Harappa, are made from nephrite jade derived from a different source altogether.

Elsewhere across Asia, nephrite occurs near Lake Baikal, Russia in both the Sayan Mountains and the Vitim Mountains (Kolesnik 1970; O'Donoghue 2006: 341); it has been reported in Oman in the Bawshir – al-Khuwair area (el-Shazly and al-Belushi 2004), at Wadi al-Ain (Thesiger 1948: 14) and at Fanja, Wadi Hatta and Semail (Guba 2007: 320); the source at Chuncheon, South Korea is one of the largest in the world (Yui and Kwon 2002); material from the Fengtian deposit of eastern Taiwan has been traded across southeast Asia for 3000 years (Hung *et al*. 2007); in China, deposits of genuine nephrite have been documented at Xiuyan in Liaoning Province (Wang *et al*. 2002), at Longxi in Sichuan Province (Wang *et al*. 1990), at Meiling in Jiangsu Province (Zhong 1995), at Nanping in Fujian Province (Tang *et al*. 1997), at Ge'ermu in Qinghai Province (Kong *et al*. 1997), and in the Guiyala area of the Tibet Autonomous Region (Chen 1999). The most extensive nephrite jade source area in China – and the most pertinent with regard to the current study – is in the vicinity of Khotan (Hetian) in Xinjiang Province. Nearly 20 individual occurrences have been documented to south of that city across the Kunlun Mountain Range (for a map of these locations see Liu *et al* 2010: Figure 1 a). Jade from this region was being exploited since at least since the Neolithic Period (Bai and Wu 2002) and it still today fills the bazaars of the region (Appendix 4.7 Figure 5).

After Kohat, the deposits of the Khotan area are the nephrite occurrences nearest to Harappa. Although "near" in this case means over 900 km to the north-northwest across the highest mountains on earth, the existence of the Indus Civilization outpost of Shortughaï in northern Afghanistan (Francfort 1984b) amply demonstrates that Harappans had the ability to travel to regions beyond the high ranges of northwestern South Asia when they so desired. On the other hand, the acquisition of Khotan nephrite (if that is what the amulet is composed of) could have been indirect and carried out through trade with the non-Harappa peoples inhabiting northern highland regions such as Swat and Kashmir. These so-called "Northern Neolithic" groups had clear affinities with the cultures of Inner and East Asia (Fairservis 1975: 312-318; Stacul 1994) and, in some instances (Stacul 1987: 75), used jade themselves. One site that exhibits strong material culture parallels with those groups is Karuo in eastern Tibet (Xu 1991). Indirect, long-distance interaction with the inhabitants of that settlement and others like it could conceivably have provided Harappans access to jade from eastern Tibet or even China.

Despite of the existence of many potential jade sources and evidence for links across the Tibetan Plateau, I feel that the Kohat nephrite occurrence is the most likely source of the raw material used to fashion the nephrite amulet from Harappa. Indus Civilization peoples were dwelling a mere 75 km south of the Teri Toi River at Musa Khel and the Indus River, which would have been and important transitway between the Punjab Plain and the northern reaches of the Subcontinent, passes almost directly adjacent to the source. Most importantly, the amulet is macroscopically and mineralogically comparable to one of the nephrite pebbles B.C.M. Butler collected there. Additional geologic samples will need to be acquired and further analytical studies will need to be undertaken in order to confirm that Teri Toi area of Kohat was indeed the source, however.

POSSIBILITIES FOR FUTURE STUDIES

The nephrite amulet from Harappa is a complete, one-of-a-kind artifact and, therefore, any future provenience studies will have to involve non-descructive or, at least, minimally invasive methods. Utilizing both proton induced X-ray emission (PIXE) and laser raman spectroscopy (LRS), Gan and others (2008) were able to determine that jades from the Shang Dynasty site of Yinxu probably were not derived from the Hetain source area. Using a VP-SEM coupled with an EDS to examine the composition of spinel-chromite inclusions, Iizuka and others (2005) determined that nephrite artifacts excavated at a site in the Philippines were analogous to jade from the Fengtian sources in Taiwan. Casadio and others (2007) employed a suite of non-invasive methods (Raman microspectroscopy, visible reflectance spectroscopy and XRD) to characterize jade artifacts and experimental samples. Much of the data they collected are useful for provenience studies.

If nephrite manufacturing debris or broken artifacts that can be sampled are eventually recovered at Harappa then, perhaps, provenience analyses could be undertaken using successfully employed invasive methods such as ICP-MS (Chen *et al* 2000), EMPA (Iizuka and Hung 2005), argon isotope (Ar-Ar) dating (Chou *et al*. 2009) and strontium isotope analysis (Adams *et al*. 2007). Current research indicates that nephrite deposits form due to the metamorphic or metasomatic alteration of either serpentinite or dolomitic marble (Harlow and Sorensen 2005; Lui *et al*. 2010: 249-250). Thus, like I show for steatite in Chapter 7 of this book, it should be possible to determine, using any of variety of techniques, which type of deposit an artifact comes from by examining the abundances of elements in it such as Ni, Cr, Fe and Mn. In this way certain deposits could be ruled out as potential sources.

APPENDIX 5.1

ALL QUERNS AND MULLERS (WHOLE AND FRAGMENTARY) RECOVERED FROM EXCAVATIONS AND SURVEYS AT HARAPPA FROM 1986 TO 2004

In the tables below each artifact is first listed by year, lot and record number.

The location from which an artifact was recovered is noted by mound (AB, E, ET, F or LW [low western]), operation (Op.), area (CEM = cemetery, MS = Mughal Sarai) or trench number (for certain off-mound trenches).

An artifact's context is noted by period number (1, 2, 3A, 3B, 3C, 4 or 5) if it was recovered from secure deposits. Context is noted as "S&D" if it came from either surface or disturbed deposits. In rare instances (such as miscellaneous finds turned in by workmen) an artifact's context is not available (n/a).

Designated material type is listed as Pab sandstone (PAB), Delhi quartzite (DQ), Kirana Hills stone (KH) gray sandstone (GSS) or unknown (UNK).

The weight of each artifact is provided in grams.

year	*lot*	*record*	*location*	*context*	*material*	*grams*
86	0.002	27	E	S&D	GSS	290
86	0.004	37	E	S&D	DQ	338
86	0.004	38	E	S&D	GSS	174
86	0.005	96	E	S&D	PAB	462
86	0.006	58	E	S&D	DQ	72
86	0.006	57	E	S&D	UNK	247
86	0.024	216	E	S&D	DQ	143
86	0.024	218	E	S&D	DQ	1000
86	0.024	213	E	S&D	GSS	434
86	0.024	214	E	S&D	PAB	283
86	0.024	215	E	S&D	PAB	228
86	0.024	219	E	S&D	PAB	133
86	0.029	10	LW	S&D	PAB	685
86	0.033	16	E	S&D	UNK	67
86	0.042	63	E	S&D	DQ	8
86	0.042	64	E	S&D	DQ	6
86	0.042	66	E	S&D	DQ	5
86	0.042	67	E	S&D	DQ	3
86	0.042	65	E	S&D	PAB	6
86	0.043	42	E	S&D	GSS	242
86	0.043	41	E	S&D	UNK	327
86	0.043	44	E	S&D	UNK	132
86	0.047	21	E	S&D	DQ	19
86	0.047	22	E	S&D	DQ	14
88	329	6	E	3C	UNK	38
88	330	3	E	S&D	PAB	832
88	334	9	E	S&D	PAB	208.7
88	340	9	E	3C	PAB	33.7
88	343	41	E	S&D	DQ	765
88	343	63	E	S&D	PAB	365.5

year	*lot*	*record*	*location*	*context*	*material*	*grams*
86	0.047	23	E	S&D	DQ	6
86	0.126	27	AB	S&D	PAB	77
86	0.126	28	AB	S&D	UNK	57
87	3	31	CEM	S&D	UNK	126
87	11	21	CEM	3C	GSS	330
87	33	2	CEM	3C	UNK	435
87	50	1	CEM	3C	UNK	236.2
87	62	68	CEM	3C	DQ	164
87	73	22	CEM	3C	PAB	124
87	127	8	CEM	3C	GSS	173
87	130	1	CEM	3C	UNK	287
87	141	4	CEM	3C	UNK	179
87	144	1	CEM	3B	UNK	72
88	210	1	CEM	S&D	UNK	254.8
88	241	5	CEM	S&D	DQ	127.6
87	300	10	n/a	n/a	PAB	139.7
87	303	11	E	3C	GSS	255
87	303	12	E	3C	PAB	290
88	321	15	E	S&D	PAB	211
88	321	2	E	S&D	UNK	93.5
88	321	14	E	S&D	UNK	132.5
88	322	6	E	S&D	UNK	1490
88	324	2	E	3C	GSS	177.3
88	326	16	E	3C	PAB	649.7
87	518	50	AB	S&D	GSS	677
87	518	47	AB	S&D	PAB	187
87	518	48	AB	S&D	PAB	354
87	518	49	AB	S&D	UNK	434
87	525	51	AB	S&D	UNK	927
87	525	108	AB	S&D	DQ	74.5

year	*lot*	*record*	*location*	*context*	*material*	*grams*
88	343	64	E	S&D	PAB	68
88	343	65	E	S&D	UNK	158
88	344	96	E	3C	GSS	75.5
88	348	12	E	3C	DQ	3200
88	348	2	E	3C	PAB	293.5
88	348	17	E	3C	PAB	124
88	348	20	E	3C	UNK	248.9
88	348	28	E	3C	UNK	248
88	353	17	E	3C	PAB	3200
88	354	66	E	3C	PAB	113.5
88	355	48	E	3C	UNK	192.5
88	358	12	E	3C	PAB	750
88	363	11	E	S&D	UNK	65
88	365	11	E	S&D	DQ	1074
88	365	11	E	S&D	DQ	1074
88	365	10	E	S&D	PAB	1450
88	433	1	CEM	3C	PAB	36
88	433	20	CEM	3C	UNK	57.5
88	436	7	CEM	3C	UNK	120.5
88	436	37	CEM	3C	UNK	29
87	501	2	AB	S&D	UNK	97.5
87	502	5	AB	S&D	UNK	89
87	503	23b	AB	S&D	PAB	400
87	503	23	AB	S&D	UNK	235.8
87	505	49	AB	S&D	PAB	336
87	508	21	AB	3C	DQ	53.5
87	508	23	AB	3C	DQ	346.6
87	508	20	AB	3C	PAB	698
87	513	4	AB	S&D	GSS	151.1
87	514	22	AB	3C	DQ	204
87	514	11	AB	3C	GSS	572
87	514	10	AB	3C	UNK	524.5
87	514	11	AB	3C	UNK	104.3
87	515	13	AB	S&D	GSS	1146
87	516	13	AB	S&D	DQ	166.7
87	516	20	AB	S&D	GSS	326.7
87	516	14	AB	S&D	UNK	393
87	518	15	AB	S&D	GSS	319.8
87	518	38	AB	S&D	GSS	220
88	734	4	E	3C	PAB	733.5
88	746	7	E	S&D	PAB	302.5
88	752	3	E	3C	PAB	385
88	767	34	E	3B	UNK	36.2
88	767	35	E	3B	UNK	36.1
88	769	1	E	3B	PAB	359
88	781	2	E	3B	PAB	426.5
88	783	29	E	3B	UNK	310
88	797	36	E	3A	GSS	227
88	802	52	E	3C	PAB	25
88	802	53	E	3C	PAB	24
88	1000	5	E	3A	UNK	74.5
89	1013	9	E	S&D	KH	351
89	1015	21	Op.6	S&D	UNK	156
89	1015	22	Op.6	S&D	UNK	152
89	1018	15	Op.6	S&D	PAB	590
89	1024	18	E	3A	UNK	296.4
89	1027	29	Op.6	S&D	PAB	118
87	525	161	AB	S&D	PAB	997
87	525	162	AB	S&D	PAB	374.5
87	525	163	AB	S&D	PAB	105
87	525	164	AB	S&D	UNK	114
87	525	165	AB	S&D	PAB	677
87	525	166	AB	S&D	UNK	22.7
87	525	167	AB	S&D	UNK	35.7
87	525	168	AB	S&D	PAB	73.5
87	525	175	AB	S&D	UNK	394.5
88	528	37	AB	S&D	PAB	116.9
88	528	57	AB	S&D	PAB	167
88	528	56	AB	S&D	UNK	92
88	538	6	AB	3C	PAB	170.5
88	540	3	AB	3C	PAB	465
88	546	2	AB	3C	UNK	145.5
88	553	3	AB	3C	PAB	454
88	559	21	AB	3C	UNK	432
88	572	21	AB	3C	PAB	120
89	586	10	AB	3C	PAB	294
94	634	1	AB	S&D	KH	118.3
94	645	10	AB	S&D	PAB	995
94	651	1	AB	S&D	PAB	400
94	658	1	AB	S&D	PAB	228
94	699	8	AB	S&D	DQ	9.3
94	699	1	AB	S&D	KH	173.3
88	700	36	E	S&D	PAB	356
88	703	7	E	3C	UNK	101.8
88	703	15	E	3C	UNK	178
88	709	36	E	S&D	PAB	356
88	712	1	E	S&D	UNK	134
88	714	17	E	S&D	DQ	385
88	714	25	E	S&D	DQ	464
88	725	75	E	3C	PAB	391.5
88	725	77	E	3C	PAB	512.5
88	725	82	E	3C	PAB	324
88	725	86	E	3C	PAB	458.2
88	725	125	E	3C	PAB	6500
88	725	128	E	3C	PAB	7
88	731	8	E	S&D	PAB	370.5
89	1115	5	E	3A	GSS	147
89	1115	6	E	3A	KH	322
89	1120	11	E	S&D	KH	305
89	1121	31	E	S&D	KH	27.5
89	1121	32	E	S&D	PAB	33.2
89	1121	13	E	S&D	UNK	57.7
89	1124	7	E	2	KH	72.8
89	1135	1	E	2	UNK	86.9
89	1136	1	E	2	KH	62.5
90	1142	15	E	S&D	UNK	613
90	1147	4	E	3A	UNK	60.8
90	1147	20	E	3A	UNK	234
90	1150	18	E	2	PAB	30
90	1150	19	E	2	PAB	124
90	1152	29	E	3A	KH	187.7
90	1153	42	E	S&D	KH	160.7
90	1156	74	E	2	KH	185.6
90	1156	75	E	2	KH	134.6

year	lot	record	location	context	material	grams
89	1038	25	Op.6	S&D	DQ	186
89	1038	24	Op.6	S&D	PAB	128
89	1046	30	E	2	KH	30.6
89	1046	31	E	2	KH	39.4
89	1054	130	E	S&D	KH	63.6
89	1056	13	E	2	DQ	43.1
89	1056	2	E	2	UNK	102.8
89	1060	112	E	S&D	KH	198.7
89	1060	113	E	S&D	KH	839
89	1060	110	E	S&D	UNK	78.1
89	1060	111	E	S&D	UNK	215.3
89	1067	85	E	S&D	KH	114
89	1067	35	E	S&D	PAB	151
89	1067	34	E	S&D	UNK	130.4
89	1072	11	Op.6	S&D	UNK	28.3
89	1075	22	E	S&D	GSS	163
89	1075	21	E	S&D	UNK	244.4
89	1078	8	E	S&D	GSS	126.4
89	1083	31	E	S&D	KH	157
89	1084	6	Op.6	S&D	PAB	154
89	1087	3	E	S&D	UNK	87.4
89	1091	13	E	S&D	PAB	109
89	1101	4	E	3A	KH	249
89	1104	4	E	S&D	UNK	159
89	1105	9	E	S&D	KH	320
89	1107	13	E	S&D	PAB	502
89	1110	4	E	S&D	UNK	747
90	1187	20	E	2	KH	48.7
90	1187	21	E	2	KH	157.5
90	1187	22	E	2	UNK	260
90	1189	7	E	2	UNK	99.9
90	1191	13	E	2	KH	52.7
90	1191	14	E	2	KH	37.8
90	1191	15	E	2	KH	14.9
90	1191	16	E	2	KH	4.8
90	1191	17	E	2	KH	65.8
90	1191	18	E	2	KH	39.4
90	1191	20	E	2	KH	339
90	1191	25	E	2	KH	21.2
90	1191	28	E	2	KH	85.8
90	1191	19	E	2	UNK	180.2
90	1197	11	E	2	KH	79.6
90	1197	12	E	2	KH	159.3
90	1197	17	E	2	KH	40.4
90	1198	16	E	2	KH	80.5
90	1198	19	E	2	KH	12.2
90	1200	40	E	2	KH	79.9
90	1200	41	E	2	KH	326
90	1200	42	E	2	KH	49.6
90	1200	43	E	2	KH	252
90	1200	44	E	2	KH	152.3
90	1200	45	E	2	KH	95.3
90	1200	76	E	2	KH	20.4
90	1200	77	E	2	KH	5.9
90	1200	12	E	2	UNK	181.4
90	1207	9	E	2	KH	80.2
90	1207	8	E	2	UNK	89.6

year	lot	record	location	context	material	grams
90	1157	75	E	S&D	PAB	19.3
90	1157	1	E	S&D	SR	347.7
90	1157	67	E	S&D	UNK	6.6
90	1163	1	E	2	UNK	607.5
90	1164	21	E	2	KH	135.8
90	1170	32	E	2	KH	457.5
90	1170	34	E	2	KH	90.6
90	1174	16	E	2	KH	203
90	1174	17	E	2	KH	209
90	1175	25	E	2	KH	20.8
90	1175	25	E	2	KH	26.2
90	1175	26	E	2	KH	89
90	1175	31	E	2	KH	211.9
90	1177	5	E	2	KH	506
90	1177	6	E	2	KH	210.2
90	1178	28	E	3A	KH	54.1
90	1180	15	E	2	KH	42.8
90	1180	16	E	2	KH	64.4
90	1181	16	E	2	KH	141.6
90	1181	17	E	2	KH	144.7
90	1181	28	E	2	KH	76.4
90	1182	82	E	2	KH	28.5
90	1183	4	E	2	KH	113.4
90	1187	16	E	2	KH	25
90	1187	17	E	2	KH	50
90	1187	18	E	2	KH	70.6
90	1187	19	E	2	KH	59.2
90	1302	4	E	2	KH	12
90	1303	18	E	2	UNK	34.5
89	2000	65	E	S&D	PAB	904
89	2000	66	E	S&D	UNK	112.5
89	2005	16	E	3A	UNK	8.3
89	2005	65	E	3A	UNK	63.8
89	2006	134	E	S&D	UNK	599
89	2014	4	E	3B	PAB	35.6
89	2033	5	E	3B	PAB	92.1
89	2047	1	E	3A	KH	162
89	2052	9	E	3B	UNK	247.4
90	2071	9	E	S&D	KH	39
2000	2087	7	E	S&D	PAB	251
2000	2101	60	E	S&D	UNK	59
2000	2102	310	E	S&D	DQ	50
2000	2102	928	E	S&D	DQ	80.8
2000	2102	1561	E	S&D	DQ	146.6
2000	2102	905	E	S&D	PAB	500
2000	2102	906	E	S&D	PAB	953
2000	2102	1558	E	S&D	PAB	42.5
2000	2102	1559	E	S&D	PAB	85.3
2000	2102	1562	E	S&D	PAB	126.6
2000	2102	904	E	S&D	UNK	374
2000	2102	926	E	S&D	UNK	54.7
2000	2102	1560	E	S&D	UNK	90.6
2000	2104	138	E	S&D	DQ	153.2
2000	2104	93	E	S&D	PAB	132
2000	2104	94	E	S&D	PAB	61.6
2000	2104	96	E	S&D	PAB	34.2
2000	2104	139	E	S&D	PAB	212.7

year	*lot*	*record*	*location*	*context*	*material*	*grams*
90	1210	6	E	2	UNK	6.3
90	1215	40	E	2	KH	4.3
90	1216	38	E	2	UNK	4.8
90	1218	16	E	2	UNK	26.7
90	1223	6	E	2	KH	153
90	1223	1	E	2	KH	200
90	1224	6	E	2	KH	98
90	1228	3	E	2	KH	1.5
90	1228	4	E	2	KH	0.9
90	1232	4	E	2	KH	193.7
90	1232	6	E	2	KH	4.6
90	1234	1	E	2	KH	18.3
90	1235	1	E	2	KH	1
90	1260	33	E	S&D	KH	102
90	1260	34	E	S&D	UNK	219
2000	2110	328	E	S&D	UNK	252
2000	2111	73	E	S&D	UNK	227.8
2000	2112	66	E	S&D	DQ	39.4
2000	2112	64	E	S&D	KH	284.9
2000	2112	67	E	S&D	KH	36.6
2000	2112	65	E	S&D	PAB	129.2
2000	2113	54	E	S&D	UNK	103.7
2000	2114	63	E	S&D	PAB	217.1
2000	2114	78	E	S&D	UNK	14.2
2000	2115	48	E	S&D	PAB	219.8
2000	2115	49	E	S&D	PAB	280
2000	2115	70	E	S&D	PAB	392
2000	2121	110	E	S&D	DQ	148.5
2000	2121	198	E	S&D	DQ	202
2000	2121	108	E	S&D	PAB	1302
2000	2121	109	E	S&D	PAB	258.8
2000	2121	111	E	S&D	PAB	74.8
2000	2121	112	E	S&D	PAB	475
2000	2121	113	E	S&D	PAB	145.9
2000	2121	114	E	S&D	PAB	213
2000	2121	115	E	S&D	PAB	234.7
2000	2121	116	E	S&D	PAB	188.1
2000	2121	117	E	S&D	PAB	974
2000	2121	118	E	S&D	UNK	363
2000	2123	16	E	S&D	KH	617
2000	2123	33	E	S&D	PAB	107.3
2000	2123	17	E	S&D	UNK	682
2000	2133	1	E	S&D	PAB	140.2
2000	2133	27	E	S&D	UNK	16.3
2000	2133	28	E	S&D	UNK	3.6
2000	2139	147	E	S&D	DQ	20.3
2000	2139	149	E	S&D	DQ	18.1
2000	2139	143	E	S&D	PAB	2021.9.5
2000	2139	145	E	S&D	PAB	83.2
2000	2139	151	E	S&D	PAB	388
2000	2139	152	E	S&D	PAB	581
2000	2139	144	E	S&D	UNK	24.8
2000	2139	146	E	S&D	UNK	46.6
2000	2139	148	E	S&D	UNK	57.2
2000	2140	8	E	3A	PAB	102.6
2000	2149	35	E	S&D	PAB	387
2000	2149	36	E	S&D	UNK	254.5
2000	2105	2	E	S&D	DQ	458
2000	2105	3	E	S&D	PAB	137.7
2000	2110	37	E	S&D	DQ	123
2000	2110	72	E	S&D	DQ	114.1
2000	2110	74	E	S&D	DQ	36.7
2000	2110	33	E	S&D	PAB	149
2000	2110	34	E	S&D	PAB	161.5
2000	2110	36	E	S&D	PAB	100.8
2000	2110	38	E	S&D	PAB	278
2000	2110	40	E	S&D	PAB	237.5
2000	2110	73	E	S&D	PAB	35.9
2000	2110	319	E	S&D	PAB	432
2000	2110	320	E	S&D	PAB	263
2000	2110	39	E	S&D	UNK	300
2000	2110	326	E	S&D	UNK	116.2
2000	2151	72	E	S&D	PAB	53.3
2000	2157	20	E	3B	UNK	139.6
2000	2158	9	E	3B	KH	96.7
2000	2165	35	E	S&D	PAB	104.3
2000	2165	36	E	S&D	PAB	98.2
2000	2165	37	E	S&D	PAB	130.1
2000	2174	315	E	S&D	DQ	121.5
2000	2174	319	E	S&D	DQ	787
2000	2174	317	E	S&D	PAB	1396
2000	2174	318	E	S&D	PAB	2006
2000	2174	320	E	S&D	PAB	549
2000	2174	854	E	S&D	PAB	170.1
2000	2174	911	E	S&D	PAB	1734
2000	2174	912	E	S&D	PAB	153.7
2000	2174	913	E	S&D	PAB	633
2000	2174	914	E	S&D	PAB	888
2000	2174	915	E	S&D	PAB	125.7
2000	2174	916	E	S&D	PAB	198.4
2000	2174	917	E	S&D	PAB	240.1
2000	2174	918	E	S&D	PAB	251
2000	2174	919	E	S&D	PAB	158.5
2000	2174	922	E	S&D	PAB	303
2000	2174	976	E	S&D	PAB	2445
2000	2174	977	E	S&D	PAB	2084
2000	2174	316	E	S&D	UNK	130.9
2000	2174	708	E	S&D	UNK	72.1
2000	2174	910	E	S&D	UNK	85.5
2000	2174	921	E	S&D	UNK	227.8
2000	2174	923	E	S&D	UNK	95.4
2000	2174	924	E	S&D	UNK	266.9
2000	2194	51	E	S&D	UNK	137
2000	2215	23	E	S&D	PAB	321
2000	2226	157	E	S&D	DQ	195.3
2000	2226	173	E	S&D	DQ	31.7
2000	2226	174	E	S&D	PAB	407
2000	2226	175	E	S&D	PAB	105.7
2000	2226	179	E	S&D	PAB	562
2000	2226	180	E	S&D	PAB	1906
2000	2226	177	E	S&D	UNK	40.2
2000	2226	178	E	S&D	UNK	233.1
2000	2227	66	E	S&D	DQ	32
2000	2227	64	E	S&D	PAB	136.7

year	*lot*	*record*	*location*	*context*	*material*	*grams*
2000	2150	1	E	S&D	PAB	195
2000	2151	70	E	S&D	DQ	11.2
2000	2151	71	E	S&D	PAB	64
2000	2227	377	E	S&D	PAB	117
2000	2227	63	E	S&D	UNK	3.7
2000	2227	375	E	S&D	UNK	72.8
2000	2229	23	E	3B	UNK	42.6
2000	2232	1	E	3B	PAB	130
2000	2235	1	E	3B	PAB	152
2000	2312	30	E	3A	DQ	278.5
2000	2312	31	E	3A	DQ	34.9
2000	2338	8	E	3A	PAB	326
2000	2358	28	E	S&D	DQ	12.4
2000	2358	29	E	S&D	PAB	15.3
2000	2358	30	E	S&D	PAB	9.8
2000	2358	27	E	S&D	UNK	265.1
2000	2359	76	E	S&D	KH	48.2
2000	2361	97	E	S&D	KH	142
2000	2362	7	E	S&D	PAB	243.1
2001	2375	13	E	S&D	PAB	408.5
2001	2378	4	E	3C	PAB	1064
2001	2381	14	E	3C	KH	262
2001	2381	15	E	3C	PAB	458.5
2001	2393	1	E	3B	PAB	499
2001	2416	1	E	S&D	UNK	443.8
2001	2416	2	E	S&D	UNK	51.9
2000	2501	2	E	S&D	UNK	309
2000	2502	2	E	S&D	DQ	560
2000	2502	4	E	S&D	GSS	241
2000	2502	1	E	S&D	PAB	265.5
2000	2502	3	E	S&D	PAB	139.7
2000	2717	37	E	S&D	DQ	79.6
2000	2719	26	E	S&D	UNK	37.9
2000	2720	21	E	S&D	UNK	52.9
2000	2725	17	E	3C	DQ	21.6
2000	2726	1	E	3C	PAB	497
2000	2726	2	E	3C	UNK	240.5
2000	2727	19	E	3C	UNK	59.8
2000	2727	21	E	3C	UNK	81.5
2000	2728	1	E	3C	DQ	445
2000	2728	2	E	3C	PAB	150
2000	2753	21	E	3C	DQ	62.9
2000	2755	23	E	3C	PAB	30.8
2000	2755	25	E	3C	UNK	100
2000	2758	18	E	3C	UNK	562
2000	2762	25	E	3C	PAB	222.4
2000	2763	28	E	3C	UNK	92.8
2000	2776	39	E	3C	DQ	374
90	3037	47	E	S&D	PAB	67.4
90	3038	8	E	3B	UNK	29.2
90	3040	31	E	S&D	PAB	1253
90	3040	32	E	S&D	PAB	834
90	3040	33	E	S&D	PAB	672
90	3040	34	E	S&D	PAB	1583
90	3040	35	E	S&D	PAB	625
90	3040	2	E	S&D	UNK	271.9
90	3042	20	E	S&D	GSS	179.5

year	*lot*	*record*	*location*	*context*	*material*	*grams*
2000	2227	67	E	S&D	PAB	7.2
2000	2227	374	E	S&D	PAB	171.4
2000	2227	376	E	S&D	PAB	324
2000	2777	31	E	3C	KH	77.7
2000	2782	7	E	S&D	PAB	6
2000	2784	5	E	3C	PAB	258.3
2000	2784	35	E	3C	UNK	162.9
2000	2789	25	E	3C	DQ	310
2000	2794	1	E	3C	DQ	804
2000	2795	1	E	3C	UNK	268
2000	2824	21	E	3C	GSS	1265
2000	2824	22	E	3C	PAB	510
2000	2824	23	E	3C	PAB	115.6
2000	2824	24	E	3C	PAB	209
2000	2825	20	E	3C	GSS	721
2000	2836	15	E	3C	PAB	279.6
2000	2840	12	E	3C	UNK	17.4
2000	2853	12	E	3C	PAB	48.3
2000	2853	13	E	3C	PAB	35.1
2000	2855	8	E	3C	UNK	202.2
2001	2906	2	E	3B	PAB	327.2
2001	2911	11	E	3B	DQ	92.3
2001	2913	157	E	3B	PAB	716.8
2001	2913	158	E	3B	PAB	50
2001	2920	3	E	S&D	PAB	22.9
2001	2920	4	E	S&D	PAB	941.6
2001	2921	6	E	S&D	PAB	244.2
2001	2939	43	E	3B	UNK	253.1
2001	2940	1	E	3B	PAB	3000
2001	2940	2	E	3B	PAB	343.8
2001	2944	37	E	3B	PAB	79.6
2001	2944	38	E	3B	PAB	80.2
90	3000	8	n/a	n/a	DQ	450
90	3001	10	E	S&D	PAB	275
90	3007	2	E	S&D	DQ	60.9
90	3011	52	E	S&D	PAB	40.7
90	3011	53	E	S&D	PAB	575.2
90	3011	51	E	S&D	UNK	500
90	3014	15	E	S&D	PAB	745.5
90	3022	31	E	S&D	UNK	180.5
90	3025	23	E	S&D	PAB	523.3
90	3025	24	E	S&D	PAB	174.8
90	3025	25	E	S&D	UNK	131.8
90	3026	36	E	S&D	UNK	72.8
90	3028	82	E	S&D	DQ	72.8
90	3028	16	E	S&D	UNK	1310
90	3028	64	E	S&D	UNK	164.6
90	3037	46	E	S&D	PAB	160.4
90	3221	21	E	S&D	DQ	160.6
90	3221	4	E	S&D	PAB	398
90	3222	27	E	3C	PAB	1358
90	3222	57	E	3C	PAB	378.5
90	3222	26	E	3C	UNK	137
90	3222	55	E	3C	UNK	81.8
90	3223	2	E	3C	PAB	124
90	3223	12	E	3C	UNK	106
90	3230	3	E	3C	DQ	239.1

year	*lot*	*record*	*location*	*context*	*material*	*grams*
90	3042	3	E	S&D	PAB	438
90	3043	1	E	S&D	PAB	404.5
90	3063	6	E	3B	GSS	60.8
90	3064	17	E	3B	DQ	108.8
90	3068	3	E	S&D	GSS	242.1
90	3068	82	E	S&D	UNK	191.2
90	3079	6	E	3B	PAB	138.3
90	3089	13	E	3A	PAB	36.7
90	3091	2	E	3C	UNK	51.6
90	3094	3	E	3C	GSS	924.5
90	3094	2	E	3C	PAB	170.2
90	3094	2	E	3C	UNK	150.9
90	3101	11	E	S&D	PAB	167
90	3101	12	E	S&D	PAB	94.5
90	3104	1	E	S&D	PAB	195.7
90	3104	27	E	S&D	UNK	155.5
90	3106	18	E	3C	DQ	85.5
90	3106	4	E	3C	UNK	324
90	3107	2	E	3C	PAB	168.8
90	3107	7	E	3C	UNK	132.8
90	3109	15	E	3C	UNK	17.5
90	3111	2	E	3C	GSS	477.7
90	3113	1	E	3C	KH	104.7
90	3115	62	E	3C	PAB	85.2
90	3117	1	E	3C	PAB	4200
90	3132	8	E	3C	UNK	40
90	3138	3	E	3B	PAB	2000
90	3151	24	E	3B	PAB	322.3
90	3173	12	E	S&D	SR	75.7
90	3186	14	E	3A	KH	20.6
90	3188	29	E	S&D	PAB	102.7
90	3188	39	E	S&D	PAB	988.5
90	3188	28	E	S&D	UNK	181
90	3191	19	E	S&D	PAB	122
90	3191	20	E	S&D	UNK	164.6
90	3221	5	E	S&D	DQ	244.8
93	3516	36	E	S&D	PAB	100
93	3517	5	E	S&D	PAB	66.3
93	3527	1	E	3C	PAB	8200
93	3527	2	E	3C	UNK	519
93	3527	3	E	3C	UNK	359.5
93	3527	4	E	3C	UNK	117
93	3530	37	E	S&D	DQ	75.4
93	3530	38	E	S&D	DQ	41.5
93	3530	48	E	S&D	DQ	19.1
93	3530	51	E	S&D	DQ	1053
93	3530	52	E	S&D	PAB	55.3
93	3530	39	E	S&D	SR	24.2
93	3532	97	E	S&D	DQ	247.5
93	3532	98	E	S&D	DQ	194.8
93	3532	99	E	S&D	DQ	103.3
93	3532	100	E	S&D	UNK	129.8
93	3533	94	E	S&D	DQ	35.9
93	3533	95	E	S&D	DQ	8.8
93	3533	96	E	S&D	DQ	3.1
93	3533	90	E	S&D	PAB	52.2
93	3533	91	E	S&D	PAB	25.1

year	*lot*	*record*	*location*	*context*	*material*	*grams*
90	3240	6	E	3C	PAB	259.5
90	3241	3	E	3C	PAB	366.5
90	3247	46	E	S&D	GSS	343.5
90	3247	43	E	S&D	PAB	290.2
90	3247	44	E	S&D	PAB	92.2
90	3247	45	E	S&D	PAB	127.7
90	3247	1	E	S&D	UNK	254
90	3253	22	E	3B	GSS	918
90	3253	17	E	3B	PAB	411
90	3253	18	E	3B	PAB	229.4
90	3253	19	E	3B	PAB	717.7
90	3253	20	E	3B	PAB	34.1
90	3253	16	E	3B	UNK	54
90	3265	4	E	S&D	PAB	68.7
90	3266	3	E	3B	PAB	375.5
90	3266	4	E	3B	UNK	103.6
90	3277	2	E	3A	PAB	109
90	3281	16	E	3A	UNK	154.4
90	3289	1	E	3A	PAB	892
90	3290	25	E	S&D	PAB	9.5
90	3290	24	E	S&D	UNK	171.1
90	3291	6	E	3C	PAB	1252
2000	3311	1	E	3C	UNK	248.5
2000	3315	1	E	3C	UNK	3761
90	3400	3	E	3B	UNK	137.5
90	3406	15	E	3B	PAB	167.2
90	3430	2	E	3C	UNK	183.8
93	3501	6	E	S&D	UNK	124.8
93	3502	42	E	S&D	PAB	33.4
93	3504	19	E	3C	PAB	50.9
93	3505	16	E	S&D	DQ	655
93	3506	62	E	S&D	DQ	96.8
93	3506	61	E	S&D	PAB	270.9
93	3506	67	E	S&D	PAB	127
93	3511	14	E	S&D	PAB	92
93	3515	8	E	3C	KH	2
93	3556	10	E	3C	DQ	26.2
93	3556	8	E	3C	UNK	23.5
93	3557	7	E	S&D	DQ	73.8
93	3559	2	E	3C	GSS	6.5
93	3563	15	E	3C	PAB	79.7
93	3564	2	E	3C	UNK	39.6
93	3565	16	E	3C	DQ	9.5
93	3567	3	E	3C	DQ	18.9
93	3574	9	E	3C	PAB	19.2
93	3575	10	E	3C	PAB	18.4
93	3575	24	E	3C	PAB	6.9
93	3596	23	E	3C	PAB	2
93	3601	27	E	3B	KH	105.6
93	3602	19	E	3B	PAB	232.9
93	3604	4	E	3B	UNK	24.7
93	3606	46	E	3B	PAB	5.6
93	3614	6	E	2	PAB	149.6
93	3623	1	E	3C	UNK	73.5
93	3641	12	E	3B	KH	76
93	3644	7	E	3B	UNK	17.6
93	3645	67	E	3B	KH	25.4

year	*lot*	*record*	*location*	*context*	*material*	*grams*
93	3533	100	E	S&D	PAB	18.7
93	3533	101	E	S&D	PAB	53.8
93	3534	15	E	S&D	DQ	11.4
93	3534	29	E	S&D	UNK	7.4
93	3535	30	E	S&D	PAB	228
93	3535	50	E	S&D	UNK	248.3
93	3536	6	E	S&D	UNK	95.9
93	3536	7	E	S&D	UNK	53.3
93	3537	37	E	S&D	DQ	57.4
93	3537	38	E	S&D	DQ	171
93	3537	39	E	S&D	DQ	111.2
93	3537	35	E	S&D	PAB	132.6
93	3537	36	E	S&D	UNK	90.1
93	3538	43	E	3C	PAB	39.4
93	3539	8	E	3C	DQ	98.1
93	3541	51	E	3C	PAB	608.5
93	3541	52	E	3C	PAB	73
93	3544	27	E	3C	PAB	75.6
93	3545	18	E	3C	PAB	912.5
93	3548	11	E	3C	PAB	33.9
93	3552	23	E	S&D	PAB	67.9
93	3555	31	E	S&D	DQ	914
93	3555	32	E	S&D	PAB	103
93	3556	9	E	3C	DQ	108.7
93	3803	101	E	S&D	UNK	46.5
93	3804	57	E	S&D	PAB	1076
93	3804	58	E	S&D	PAB	124.5
93	3804	23	E	S&D	UNK	46.3
93	3804	54	E	S&D	UNK	63.7
93	3804	55	E	S&D	UNK	29.8
93	3806	71	E	3C	UNK	96.8
93	3809	13	E	3C	DQ	98.9
93	3811	4	E	3C	DQ	144.7
93	3812	10	E	3C	UNK	74.6
93	3813	3	E	3C	UNK	43.2
93	3814	8	E	3C	UNK	126.8
93	3829	3	E	S&D	GSS	1486
93	3830	1	E	S&D	DQ	84.7
93	3830	2	E	S&D	DQ	40.1
93	3831	7	E	S&D	DQ	718.3
93	3831	8	E	S&D	DQ	858.3
93	3832	8	E	S&D	PAB	39.7
93	3833	11	E	S&D	UNK	118.9
93	3834	6	E	S&D	DQ	35.9
93	3834	7	E	S&D	PAB	170
93	3834	8	E	S&D	UNK	77.6
93	3835	8	E	S&D	DQ	69.4
93	3835	10	E	S&D	PAB	263.4
93	3836	25	E	S&D	DQ	52.1
93	3836	29	E	S&D	DQ	205.3
93	3836	4	E	S&D	PAB	21.2
93	3836	26	E	S&D	PAB	56.9
93	3836	30	E	S&D	PAB	161.8
93	3836	31	E	S&D	PAB	176.6
93	3836	24	E	S&D	UNK	52
93	3838	12	E	S&D	PAB	416.7
93	3839	33	E	S&D	DQ	510

year	*lot*	*record*	*location*	*context*	*material*	*grams*
93	3649	9	E	3A	KH	156.6
93	3700	40	E	S&D	DQ	236.5
93	3700	41	E	S&D	UNK	36.4
93	3704	11	E	3C	DQ	189
93	3705	5	E	S&D	DQ	52.6
93	3705	4	E	S&D	UNK	365
93	3707	13	E	3C	PAB	33.6
93	3709	21	E	S&D	DQ	65.5
93	3709	22	E	S&D	DQ	72.2
93	3709	15	E	S&D	PAB	95.8
93	3710	14	E	3C	DQ	84.5
93	3710	28	E	3C	DQ	45.8
93	3710	27	E	3C	PAB	63
93	3710	30	E	3C	PAB	29.3
93	3710	29	E	3C	UNK	7.7
93	3714	4	E	3C	PAB	439
93	3716	11	E	3C	PAB	19.5
93	3739	36	E	S&D	DQ	65.4
93	3802	7	E	S&D	DQ	88
93	3802	9	E	S&D	DQ	52.4
93	3802	6	E	S&D	PAB	222.4
93	3802	8	E	S&D	UNK	131.5
93	3803	37	E	S&D	DQ	214.1
93	3803	35	E	S&D	PAB	245.5
93	3864	9	E	3C	DQ	116.7
93	3864	10	E	3C	DQ	132.4
93	3864	21	E	3C	PAB	191.7
93	3864	23	E	3C	PAB	122.6
93	3865	37	E	3C	GSS	107
93	3865	29	E	3C	PAB	104.7
93	3865	44	E	3C	PAB	106.8
93	3865	4	E	3C	UNK	165.9
93	3866	8	E	3C	PAB	31.1
93	3866	32	E	3C	UNK	123.6
93	3866	40	E	3C	UNK	10.5
93	3866	41	E	3C	UNK	91.9
93	3867	48	E	3C	UNK	19.3
93	3868	11	E	3C	DQ	63.7
93	3868	12	E	3C	DQ	66.2
93	3869	47	E	3C	DQ	30.4
93	3869	52	E	3C	DQ	34.2
93	3869	5	E	3C	UNK	447.4
93	3873	12	E	S&D	DQ	8.5
93	3876	6	E	S&D	PAB	252.6
94	3879	8	E	S&D	DQ	91.3
94	3879	9	E	S&D	DQ	4.5
94	3879	23	E	S&D	DQ	19.6
94	3879	21	E	S&D	KH	59.4
94	3879	22	E	S&D	PAB	22.7
93	3887	10	E	3C	GSS	130.7
93	3888	22	E	3C	UNK	23.7
93	3890	15	E	3C	DQ	112.6
93	3891	20	E	3C	DQ	119.8
93	3891	24	E	3C	DQ	95
93	3891	25	E	3C	GSS	221.1
93	3892	14	E	3C	DQ	25.5
93	3892	57	E	3C	DQ	583.5

year	lot	record	location	context	material	grams
93	3839	35	E	S&D	DQ	17.6
93	3839	69	E	S&D	DQ	211.8
93	3839	37	E	S&D	PAB	62.3
93	3839	38	E	S&D	PAB	117.9
93	3839	36	E	S&D	UNK	53.2
93	3840	1	E	3C	DQ	76.1
93	3841	17	E	S&D	DQ	76.5
93	3860	2	E	S&D	DQ	22
93	3861	2	E	S&D	DQ	37.6
93	3862	7	E	S&D	PAB	40.3
93	3863	20	E	S&D	DQ	44.4
93	3863	19	E	S&D	UNK	56.8
93	3892	73	E	3C	UNK	55.2
94	3899	3	E	S&D	UNK	143.3
94	3899	4	E	S&D	UNK	130.5
94	3903	29	E	S&D	PAB	21.2
94	3903	34	E	S&D	PAB	117.2
94	3904	25	E	3C	PAB	204.6
94	3904	26	E	3C	PAB	109.6
94	3904	29	E	3C	UNK	74.5
94	3904	43	E	3C	UNK	117.4
94	3912	7	E	3C	UNK	40
94	3917	15	E	3C	PAB	66.9
94	3918	2	E	3C	DQ	99.1
94	3921	4	E	3C	PAB	121.5
94	3922	4	E	3C	UNK	120.4
94	3924	19	E	3C	DQ	912.5
94	3931	6	E	3C	PAB	94.9
94	3931	8	E	3C	PAB	11.3
94	3935	25	E	3C	DQ	115.2
94	3935	26	E	3C	DQ	62.7
94	3935	27	E	3C	DQ	46.4
94	3935	29	E	3C	DQ	19.7
94	3935	28	E	3C	PAB	27.8
94	3935	30	E	3C	PAB	15.9
94	3940	2	E	S&D	DQ	47
94	3942	1	E	3C	DQ	602.3
94	3942	2	E	3C	DQ	936.1
94	3946	61	E	3C	DQ	108
94	3946	62	E	3C	PAB	92
94	3947	19	E	3C	UNK	600
94	3951	29	Tr.21	S&D	PAB	185.9
94	3965	32	Tr.21	3B	PAB	108
94	3966	6	Tr.21	3B	PAB	632.3
94	3984	59	E	S&D	UNK	136.5
94	3985	41	E	3C	DQ	52.5
94	3985	42	E	3C	DQ	18
94	3987	36	E	3C	PAB	149
94	3989	11	E	3C	PAB	75.9
94	3998	11	E	3C	PAB	145.8
93	4004	8	ET	S&D	UNK	28.9
93	4016	10	ET	S&D	PAB	750
93	4016	9	ET	S&D	UNK	283.5
93	4030	6	ET	S&D	PAB	206.1
93	4041	1	ET	S&D	UNK	57.6
93	4046	1	ET	3B	PAB	559.9
93	4051	2	ET	S&D	PAB	419.9

year	lot	record	location	context	material	grams
93	3892	59	E	3C	DQ	18.5
93	3892	60	E	3C	DQ	13.4
93	3892	61	E	3C	DQ	60.6
93	3892	62	E	3C	DQ	34.7
93	3892	63	E	3C	DQ	77.9
93	3892	64	E	3C	DQ	47.5
93	3892	74	E	3C	DQ	67.4
93	3892	13	E	3C	PAB	392.4
93	3892	66	E	3C	PAB	14.6
93	3892	67	E	3C	PAB	82.5
93	3892	75	E	3C	PAB	237.6
93	3892	65	E	3C	UNK	53.9
93	4051	12	ET	S&D	PAB	223
93	4065	73	ET	3B	KH	11.7
93	4065	71	ET	3B	PAB	928.5
93	4065	72	ET	3B	PAB	46.4
93	4069	9	ET	3B	PAB	296.3
93	4069	10	ET	3B	PAB	310.2
93	4074	33	ET	3C	PAB	399
93	4090	14	ET	3B	PAB	28.1
93	4098	16	ET	3B	PAB	2800
93	4099	2	ET	3B	KH	64.4
93	4100	3	ET	3C	UNK	164
93	4100	13	ET	3C	UNK	29.3
93	4106	41	ET	3C	GSS	43.1
93	4111	10	ET	3C	UNK	120
93	4128	7	ET	3B	PAB	149.6
93	4161	22	ET	3B	KH	64.8
93	4193	38	ET	3C	GSS	18.1
93	4200	23	ET	S&D	UNK	216.3
93	4213	1	ET	S&D	PAB	1219
93	4250	24	ET	3B	PAB	972.5
93	4255	5	ET	S&D	PAB	138
93	4302	19	E	3B	PAB	22
93	4314	2	ET	S&D	PAB	161.3
93	4325	1	E	2	PAB	470
93	4330	4	E	3B	PAB	309
93	4330	14	E	3B	PAB	199
93	4335	10	E	2	PAB	1178
93	4341	5	E	2	UNK	6.1
95	4411	18	ET	S&D	UNK	164.2
95	4415	15	ET	S&D	PAB	260.6
95	4415	16	ET	S&D	PAB	94.3
95	4416	34	ET	3C	PAB	536.5
95	4423	78	ET	S&D	GSS	274.2
95	4423	32	ET	S&D	PAB	33.1
95	4427	14	ET	S&D	UNK	256.7
95	4433	31	ET	S&D	UNK	175.1
95	4442	5	ET	3C	PAB	150.4
95	4445	381	ET	S&D	PAB	182.2
95	4461	3	ET	3C	PAB	423.9
95	4463	2	ET	3C	PAB	421.1
95	4463	3	ET	3C	PAB	773.9
95	4463	4	ET	3C	PAB	527.6
95	4463	5	ET	3C	PAB	1722
95	4466	45	ET	S&D	PAB	626.6
95	4466	65	ET	S&D	PAB	23

year	lot	record	location	context	material	grams
95	4466	66	ET	S&D	PAB	7.1
95	4468	1	E	3B	PAB	436
95	4484	1	E	3A	PAB	374
95	4545	9	ET	3B	UNK	68
95	4565	2	ET	3B	PAB	2980
95	4572	1	ET	3B	UNK	717.4
95	4587	1	ET	3B	PAB	224.2
95	4606	35	ET	3B	PAB	312.3
95	4607	47	ET	S&D	DQ	242
95	4607	7	ET	S&D	KH	306
95	4609	208	ET	S&D	DQ	261.7
95	4609	40	ET	S&D	PAB	794.3
95	4609	41	ET	S&D	PAB	90
95	4609	44	ET	S&D	PAB	659.5
95	4609	45	ET	S&D	PAB	594.2
95	4609	124	ET	S&D	PAB	173
95	4609	181	ET	S&D	PAB	112.5
95	4611	14	ET	3B	PAB	16
95	4613	3	ET	3B	PAB	336.5
95	4613	43	ET	3B	PAB	185.2
95	4614	44	ET	3B	DQ	201.3
95	4614	1	ET	3B	PAB	190.8
95	4614	42	ET	3B	PAB	158.2
95	4614	43	ET	3B	PAB	154.7
95	4614	46	ET	3B	PAB	138.8
95	4614	40	ET	3B	UNK	180
95	4615	2	ET	3C	PAB	153.5
95	4623	38	ET	S&D	DQ	291.1
95	4623	114	ET	S&D	DQ	58.5
95	4623	23	ET	S&D	PAB	345.9
95	4623	113	ET	S&D	PAB	375.5
95	4623	115	ET	S&D	PAB	30
95	4623	119	ET	S&D	PAB	418.3
95	4624	5	ET	3C	PAB	63.7
95	4647	66	ET	S&D	DQ	77
95	4647	19	ET	S&D	PAB	170.8
95	4651	3	ET	S&D	PAB	80.5
95	4654	18	ET	3B	PAB	21.9
95	4665	1	ET	3B	PAB	992.8
95	4667	1	ET	S&D	PAB	1419
95	4667	14	ET	S&D	PAB	213.7
95	4669	4	ET	3B	DQ	1160
95	4669	6	ET	3B	PAB	288.3
95	4681	11	ET	3B	PAB	362.9
95	4687	2	ET	3B	GSS	300.2
95	4725	6	ET	3C	PAB	778.4
95	4726	110	ET	3C	DQ	562.3
95	4726	112	ET	3C	DQ	6
95	4726	212	ET	3C	DQ	176
95	4726	215	ET	3C	GSS	10.5
95	4726	113	ET	3C	PAB	394
95	4726	213	ET	3C	UNK	344.6
95	4726	214	ET	3C	UNK	3.98
95	4728	214	ET	3C	GSS	255.5
95	4731	6	ET	3C	DQ	13.5
95	4733	52	ET	3C	DQ	52
95	4733	23	ET	3C	GSS	161.5

year	lot	record	location	context	material	grams
95	4687	1	ET	3B	UNK	438.7
94	4700	4	ET	S&D	DQ	27.9
94	4700	6	ET	S&D	DQ	131.5
94	4700	7	ET	S&D	DQ	70.6
94	4700	8	ET	S&D	DQ	15.4
94	4700	10	ET	S&D	DQ	34.8
94	4700	5	ET	S&D	PAB	133.9
94	4700	9	ET	S&D	UNK	15.1
94	4701	6	ET	S&D	DQ	40.9
94	4701	7	ET	S&D	DQ	37.8
94	4702	31	ET	S&D	DQ	29.8
94	4702	32	ET	S&D	DQ	43.8
94	4702	33	ET	S&D	DQ	19.6
94	4702	34	ET	S&D	DQ	31.4
94	4702	12	ET	S&D	PAB	30.5
94	4702	30	ET	S&D	PAB	143.5
94	4702	11	ET	S&D	UNK	92.9
94	4704	47	ET	3C	DQ	22.6
94	4704	30	ET	3C	GSS	61.5
94	4707	10	ET	S&D	DQ	394.4
94	4707	17	ET	S&D	PAB	7
94	4707	33	ET	S&D	UNK	21.7
94	4712	8	ET	3C	UNK	200.5
94	4714	10	ET	3C	PAB	44.4
95	4716	4	ET	S&D	DQ	1577
95	4716	3	ET	S&D	PAB	71.4
95	4719	84	ET	3C	DQ	13
95	4719	85	ET	3C	DQ	10
95	4719	171	ET	3C	PAB	106
95	4719	172	ET	3C	PAB	148.7
95	4719	82	ET	3C	UNK	31.99
95	4719	83	ET	3C	UNK	10.5
95	4719	113	ET	3C	UNK	127
95	4719	114	ET	3C	UNK	101.6
95	4720	112	ET	3C	DQ	740.5
95	4721	4	ET	3C	DQ	224.9
95	4721	5	ET	3C	DQ	177.6
95	4721	132	ET	3C	DQ	57.2
95	4721	3	ET	3C	UNK	188.2
95	4721	6	ET	3C	UNK	208
95	4721	133	ET	3C	UNK	54.5
95	4723	108	ET	3C	PAB	285.6
95	4723	111	ET	3C	PAB	134
95	4724	15	ET	3C	PAB	31.3
95	4724	86	ET	3C	PAB	1012
95	4916	139	ET	3C	UNK	48.2
95	4917	9	ET	3C	DQ	83.4
95	4917	20	ET	3C	GSS	66.8
95	4917	10	ET	3C	UNK	136.1
95	4918	5	ET	3C	PAB	244.9
95	4918	12	ET	3C	PAB	54.2
95	4919	13	ET	3C	DQ	42.4
95	4919	14	ET	3C	DQ	671.6
95	4919	15	ET	3C	PAB	143.1
95	4919	16	ET	3C	PAB	266
95	4919	26	ET	3C	PAB	79
95	4920	3	ET	3C	PAB	19.3

year	lot	record	location	context	material	grams
95	4733	22	ET	3C	UNK	110
95	4734	4	ET	3C	GSS	315
95	4734	40	ET	3C	PAB	185
95	4737	2	ET	3C	PAB	467.5
95	4738	7	ET	3C	PAB	370
95	4738	5	ET	3C	UNK	23.5
95	4740	2	ET	3C	PAB	664.5
95	4741	1	ET	3C	DQ	235
95	4743	1	ET	3C	DQ	278
95	4751	5	ET	3C	DQ	88.5
95	4751	19	ET	3C	PAB	44.5
95	4752	8	ET	3C	DQ	602.5
94	4803	1	ET	S&D	DQ	478.6
94	4803	2	ET	S&D	DQ	647.3
94	4805	3	ET	S&D	DQ	257.1
94	4810	251	ET	3C	PAB	13.5
94	4819	9	ET	S&D	DQ	540.2
94	4819	7	ET	S&D	UNK	492.4
94	4824	6	ET	3C	KH	421
94	4857	6	ET	S&D	PAB	102.7
94	4860	25	ET	S&D	UNK	354
94	4860	27	ET	S&D	UNK	86.8
95	4910	40	ET	3C	DQ	11.9
95	4910	41	ET	3C	DQ	23.9
95	4910	42	ET	3C	DQ	19
95	4910	39	ET	3C	UNK	3.8
95	4911	16	ET	3C	PAB	198
95	4911	113	ET	3C	PAB	592
95	4913	10	ET	3C	UNK	102
95	4913	11	ET	3C	UNK	18.3
95	4916	51	ET	3C	DQ	55.2
95	4916	52	ET	3C	PAB	175.8
95	4916	50	ET	3C	UNK	18.7
95	4960	23	ET	S&D	UNK	12.8
95	4961	4	ET	3C	GSS	280.7
95	4961	2	ET	3C	PAB	189
95	4961	3	ET	3C	PAB	335
95	4961	5	ET	3C	PAB	1111
95	4962	124	ET	S&D	GSS	11.3
95	4963	6	ET	3C	DQ	492
95	4963	38	ET	3C	DQ	304.7
95	4970	54	ET	3C	DQ	134.2
95	4973	4	ET	3C	DQ	29.3
95	4973	15	ET	3C	DQ	338.5
95	4973	3	ET	3C	UNK	58.2
95	4974	86	ET	3C	UNK	1435
95	4976	1	ET	3C	PAB	62.9
95	4978	42	ET	3C	PAB	533.4
95	4980	6	ET	S&D	PAB	300
95	4980	7	ET	S&D	UNK	130.5
95	4980	8	ET	S&D	UNK	1125
95	4981	59	ET	S&D	GSS	128.4
95	4981	38	ET	S&D	PAB	468.3
95	4981	39	ET	S&D	PAB	117.5
95	4981	40	ET	S&D	PAB	234.7
95	4981	60	ET	S&D	PAB	388.7
95	4981	66	ET	S&D	UNK	77.5

year	lot	record	location	context	material	grams
95	4921	25	ET	3C	DQ	8.9
95	4921	26	ET	3C	DQ	31.6
95	4921	31	ET	3C	PAB	38.9
95	4921	139	ET	3C	PAB	108.7
95	4922	4	ET	3C	PAB	318.5
95	4922	18	ET	3C	PAB	57
95	4922	75	ET	3C	PAB	2500
95	4923	101	ET	3C	UNK	17
95	4926	215	ET	3C	PAB	539
95	4933	16	ET	S&D	PAB	88
95	4934	107	ET	S&D	UNK	91
95	4935	20	ET	S&D	DQ	27
95	4935	44	ET	S&D	UNK	46.3
95	4936	19	ET	3C	UNK	75.9
95	4940	107	ET	3C	DQ	42.6
95	4940	75	ET	3C	PAB	184.9
95	4940	109	ET	3C	UNK	309.9
95	4941	6	ET	3C	DQ	246.6
95	4942	4	ET	S&D	PAB	190.3
95	4942	3	ET	S&D	UNK	916.1
95	4943	34	ET	S&D	DQ	347.1
95	4943	51	ET	S&D	DQ	33.5
95	4943	12	ET	S&D	GSS	60.5
95	4943	57	ET	S&D	PAB	57.4
95	4945	35	ET	3C	PAB	533.6
95	4949	1	ET	S&D	UNK	8.3
95	4949	2	ET	S&D	UNK	87.2
95	4950	1	ET	3C	PAB	142.7
95	4952	45	ET	3C	DQ	104.3
95	4953	171	ET	3C	KH	126.7
95	4953	208	ET	3C	UNK	2.5
95	4954	2	ET	3C	PAB	77.3
95	4960	28	ET	S&D	DQ	149.8
94	5044	11	MS	S&D	DQ	28.3
94	5044	9	MS	S&D	PAB	73.4
94	5044	10	MS	S&D	UNK	138.8
94	5046	50	MS	3C	DQ	29
94	5051	1	MS	S&D	UNK	500
94	5063	78	MS	3C	UNK	17.1
94	5070	1	MS	3C	DQ	30.2
94	5076	41	MS	3C	DQ	16.5
94	5076	40	MS	3C	UNK	161.1
94	5076	42	MS	3C	UNK	179.7
94	5084	3	MS	3C	PAB	234
94	5101	1	E	3C	PAB	324
94	5101	29	E	3C	UNK	527.5
95	5142	21	E	S&D	PAB	679.8
95	5144	12	E	3C	DQ	105.6
95	5144	166	E	3C	DQ	745.2
95	5144	11	E	3C	UNK	219.2
95	5145	20	E	3C	DQ	431.1
95	5145	96	E	3C	DQ	177.5
95	5145	71	E	3C	KH	311.7
95	5145	62	E	3C	PAB	567.4
95	5145	63	E	3C	UNK	63.4
95	5145	97	E	3C	UNK	62.9
95	5146	62	E	3C	DQ	54.2

year	lot	record	location	context	material	grams
95	4982	102	ET	S&D	DQ	76.6
95	4982	2	ET	S&D	PAB	507.3
95	4982	122	ET	S&D	PAB	60.6
95	4982	123	ET	S&D	UNK	22.5
95	4986	40	ET	S&D	KH	201.7
95	4986	37	ET	S&D	PAB	447
95	4986	1	ET	S&D	UNK	21.9
95	4988	44	ET	3C	PAB	4988
95	4989	91	ET	3C	DQ	45.1
95	4989	4	ET	3C	GSS	397.9
95	4989	47	ET	3C	PAB	321
95	4989	48	ET	3C	PAB	252.9
95	4991	2	ET	3C	DQ	106
95	4991	1	ET	3C	PAB	104.8
95	4992	3	ET	3C	GSS	644.2
93	5024	23	MS	3C	UNK	335.8
93	5030	32	MS	3C	GSS	307.7
94	5039	13	MS	3C	PAB	159.7
94	5039	15	MS	3C	UNK	225
94	5040	17	MS	S&D	PAB	99.8
94	5042	33	MS	3C	DQ	138.3
94	5200	17	MS	S&D	PAB	111.5
94	5200	18	MS	S&D	PAB	86.5
94	5200	19	MS	S&D	PAB	20.8
94	5202	5	MS	S&D	DQ	163.6
94	5204	4	MS	S&D	UNK	34.3
94	5207	1	MS	S&D	DQ	168
94	5251	31	ET	S&D	DQ	60.5
94	5251	32	ET	S&D	PAB	29
94	5344	1	ET	3B	UNK	5500
94	5406	6	ET	S&D	PAB	732.9
94	5501	28	ET	3B	DQ	446.6
94	5502	61	ET	3B	GSS	279.7
94	5505	1	ET	3B	PAB	288.1
95	5517	8	ET	3B	PAB	62.7
95	5526	10	ET	3B	GSS	802
95	5602	13	ET	S&D	DQ	234.6
95	5602	12	ET	S&D	PAB	331.1
95	5603	34	ET	S&D	DQ	34.8
95	5604	15	ET	S&D	UNK	34.2
95	5606	22	ET	S&D	PAB	20.6
95	5607	18	ET	S&D	PAB	210.7
95	5614	21	ET	S&D	PAB	58.7
95	5614	22	ET	S&D	PAB	1052
95	5616	1	ET	3B	PAB	244.3
95	5625	4	ET	3B	PAB	126.2
95	5625	21	ET	3B	PAB	448.3
95	5625	22	ET	3B	PAB	405.2
95	5629	8	ET	S&D	PAB	318
95	5631	18	ET	3B	PAB	431.1
95	5669	8	ET	3B	DQ	108.7
95	5684	31	ET	3B	UNK	181
95	5685	13	ET	3B	PAB	816.7
95	5702	17	ET	S&D	DQ	5.4
95	5702	68	ET	S&D	DQ	715.8
95	5702	4	ET	S&D	UNK	6.1
95	5709	101	ET	S&D	DQ	188.8

year	lot	record	location	context	material	grams
95	5146	95	E	3C	GSS	3000
95	5146	60	E	3C	UNK	233
95	5149	167	E	S&D	DQ	118.6
95	5149	168	E	S&D	PAB	276
95	5150	32	E	3C	DQ	83.3
95	5150	33	E	3C	DQ	34.4
95	5150	1	E	3C	PAB	186.5
95	5151	1	E	3C	DQ	196.2
95	5152	23	E	3C	KH	602.2
95	5153	3	E	3C	DQ	37
95	5153	2	E	3C	UNK	323.3
95	5153	4	E	3C	UNK	49.6
95	5171	1	E	3C	PAB	45
95	5175	4	E	3C	PAB	329.9
95	5176	1	E	3C	PAB	312.9
95	5181	1	E	3C	DQ	545.4
95	5181	2	E	3C	UNK	203.1
95	5184	24	E	3C	PAB	255
95	5184	3	E	3C	UNK	70
95	5188	9	E	3C	UNK	1133
95	5195	5	E	3C	PAB	282
95	5711	30	ET	3C	KH	9.2
95	5711	31	ET	3C	KH	6.6
95	5711	33	ET	3C	KH	34
95	5712	79	ET	S&D	UNK	366.1
95	5713	118	ET	S&D	DQ	240
95	5713	70	ET	S&D	GSS	193.6
95	5714	11	ET	3C	DQ	16
95	5718	58	ET	S&D	UNK	64
95	5720	7	ET	3C	UNK	75.9
95	5720	50	ET	3C	UNK	56.3
95	5723	10	ET	3C	DQ	129
95	5724	49	ET	3C	DQ	143.8
95	5726	80	ET	3C	DQ	34.1
95	5726	15	ET	3C	PAB	797.1
95	5728	58	ET	3C	DQ	34.1
95	5728	59	ET	3C	DQ	14
95	5728	10	ET	3C	KH	87.4
95	5729	220	ET	3C	DQ	90.5
95	5729	74	ET	3C	PAB	193
95	5729	78	ET	3C	PAB	82
95	5732	23	ET	3C	DQ	193.8
95	5735	74	ET	S&D	PAB	444
95	5735	75	ET	S&D	UNK	278
95	5737	21	ET	3C	DQ	33
95	5740	23	ET	3C	DQ	104.3
95	5740	24	ET	3C	PAB	359
95	5741	45	ET	3C	DQ	71
95	5741	46	ET	3C	DQ	9
95	5741	47	ET	3C	GSS	116
95	5741	49	ET	3C	PAB	150
95	5741	50	ET	3C	UNK	586
95	5743	13	ET	3C	DQ	135.6
95	5745	16	ET	S&D	DQ	135
95	5745	1	ET	S&D	UNK	144
95	5745	3	ET	S&D	UNK	170
95	5745	17	ET	S&D	UNK	105.2

year	*lot*	*record*	*location*	*context*	*material*	*grams*
95	5709	112	ET	S&D	DQ	90.4
95	5709	100	ET	S&D	GSS	490.7
95	5709	102	ET	S&D	UNK	443.7
95	5709	113	ET	S&D	UNK	623
95	5710	77	ET	S&D	DQ	19.5
95	5710	78	ET	S&D	DQ	6.7
95	5710	79	ET	S&D	PAB	166
95	5711	32	ET	3C	DQ	4
95	5711	29	ET	3C	KH	9
95	5751	98	ET	3C	UNK	83.7
95	5753	56	ET	3C	DQ	18.3
95	5753	57	ET	3C	DQ	61
95	5757	24	ET	3C	PAB	209.8
95	5759	24	ET	3C	UNK	279.5
95	5760	52	ET	3C	DQ	6.5
95	5760	50	ET	3C	GSS	90.4
95	5760	53	ET	3C	KH	6.4
95	5760	18	ET	3C	UNK	283.2
95	5762	1	ET	3C	DQ	289.9
95	5764	2	ET	3C	DQ	59.6
95	5764	73	ET	3C	DQ	44.8
95	5767	1	ET	3C	PAB	41.5
95	5778	1	ET	3C	PAB	137.7
95	5778	1	ET	3C	PAB	483.7
95	5789	7	ET	3C	DQ	586.5
95	5802	1	ET	3C	PAB	50.5
95	5802	8	ET	3C	PAB	163.1
95	5802	172	ET	3C	PAB	214.8
95	5802	134	ET	3C	UNK	40
95	5807	56	ET	3C	DQ	35.5
95	5807	264	ET	3C	DQ	2400
95	5807	265	ET	3C	KH	11.5
95	5807	54	ET	3C	PAB	229.6
95	5807	58	ET	3C	PAB	304
95	5807	57	ET	3C	UNK	12.5
95	5807	263	ET	3C	UNK	56.1
95	5807	266	ET	3C	UNK	17.5
95	5810	60	ET	3C	PAB	140.3
96	5832	22	ET	3C	PAB	238.6
96	5837	26	ET	3C	GSS	139.8
96	5837	27	ET	3C	PAB	302.6
96	5837	25	ET	3C	UNK	222.5
96	5840	5	ET	3C	PAB	199.7
96	5851	2	ET	3C	PAB	1282
95	5855	12	ET	3C	PAB	4500
95	5856	1	ET	3C	UNK	82.9
96	5860	5	ET	3C	PAB	789.8
96	5863	2	ET	3C	GSS	133
95	5868	25	ET	3C	PAB	576.5
95	5872	1	ET	3C	PAB	1123
95	5876	1	ET	3C	DQ	2569
95	5900	41	ET	3C	PAB	506.5
95	5902	8	ET	3C	GSS	1082
95	5902	9	ET	3C	PAB	1141
96	6351	5	ET	3C	GSS	876.5
96	6351	6	ET	3C	UNK	817.2
95	6503	32	ET	3C	PAB	694

year	*lot*	*record*	*location*	*context*	*material*	*grams*
95	5746	89	ET	3C	DQ	23
95	5746	88	ET	3C	UNK	51
95	5747	12	ET	3C	DQ	159
95	5749	10	ET	3C	DQ	821.5
95	5749	11	ET	3C	DQ	121.3
95	5749	12	ET	3C	DQ	39.4
95	5750	32	ET	3C	DQ	634.8
95	5750	1	ET	3C	KH	105.3
95	5751	30	ET	3C	DQ	86.1
94	6009	1	F	S&D	DQ	338.3
96	6199	1	n/a	n/a	GSS	152.1
96	6201	1	ET	S&D	DQ	1741
96	6201	2	ET	S&D	GSS	385
96	6202	2	ET	S&D	DQ	1132
96	6202	3	ET	S&D	GSS	118.7
96	6211	34	ET	S&D	UNK	31.5
96	6219	66	ET	S&D	DQ	929
96	6219	85	ET	S&D	GSS	48.3
96	6219	88	ET	S&D	PAB	405
96	6220	9	ET	S&D	DQ	266.3
96	6220	10	ET	S&D	UNK	329.5
96	6222	62	ET	S&D	UNK	267.5
96	6223	29	ET	3C	DQ	57.3
96	6223	28	ET	3C	UNK	140
96	6224	45	ET	S&D	DQ	161.3
96	6224	44	ET	S&D	UNK	83
96	6226	9	ET	3C	DQ	60.5
96	6226	8	ET	3C	UNK	268.4
96	6230	13	ET	3C	GSS	303.3
96	6231	83	ET	S&D	DQ	11.4
96	6234	10	ET	S&D	DQ	386.7
96	6234	11	ET	S&D	UNK	275.3
96	6237	2	ET	3C	DQ	124.5
96	6237	1	ET	3C	UNK	161.5
96	6239	1	ET	S&D	PAB	351.1
96	6239	2	ET	S&D	UNK	10.1
96	6244	56	ET	S&D	DQ	41.7
96	6244	55	ET	S&D	GSS	93.8
96	6244	2	ET	S&D	PAB	575
96	6251	1	ET	3C	DQ	228.8
96	6251	18	ET	3C	DQ	564.3
96	6251	2	ET	3C	UNK	84.4
96	6251	4	ET	3C	UNK	146
96	6251	25	ET	3C	UNK	4.5
96	6251	26	ET	3C	UNK	16.7
96	6254	2	ET	3C	KH	130
96	6255	2	ET	3C	PAB	268.5
96	6255	3	ET	3C	PAB	143.3
96	6255	1	ET	3C	UNK	379
96	6256	1	ET	3C	GSS	656
96	6257	1	ET	3C	PAB	810.3
96	6300	22	ET	S&D	GSS	181
96	6303	73	ET	S&D	GSS	103.2
96	6310	153	ET	3C	UNK	44.4
95	7013	1	AB	S&D	DQ	1081
95	7015	1	AB	3C	PAB	623.6
95	7015	2	AB	3C	UNK	350

year	*lot*	*record*	*location*	*context*	*material*	*grams*
95	6503	67	ET	3C	PAB	75.6
95	6512	29	ET	2	PAB	257.6
95	6525	13	ET	3C	DQ	42.1
95	6525	24	ET	3C	PAB	217.4
95	6527	1	ET	2	PAB	157.2
95	6532	8	ET	2	PAB	143.2
95	6538	38	ET	2	KH	38.4
95	6547	3	ET	3C	DQ	105
95	6605	2	ET	3C	UNK	61.3
95	6612	1	ET	3C	GSS	171.7
95	6619	1	ET	3C	PAB	530.5
97	6645	5	ET	3B	PAB	383.5
97	6686	17	ET	3B	PAB	253.3
95	6703	2	E	3C	DQ	80
95	6703	1	E	3C	UNK	106.3
95	6716	1	E	3C	UNK	129
95	6716	2	E	3C	UNK	80
96	6821	18	E	S&D	KH	2992
96	6821	128	E	S&D	UNK	458
96	6821	135	E	S&D	UNK	39.7
96	6838	2	E	3C	GSS	207
96	6838	38	E	3C	PAB	191.8
96	6838	39	E	3C	PAB	198.5
96	6862	23	E	3C	UNK	214
96	6864	25	E	3C	PAB	654.8
96	6868	28	E	3C	DQ	121.7
96	6868	35	E	3C	PAB	972.4
96	6876	25	E	3C	GSS	23.5
96	6882	14	E	3C	PAB	766.1
96	6884	9	E	3C	PAB	266
96	6912	10	E	3C	UNK	450
96	6923	7	E	3C	PAB	254.3
96	6963	15	E	3C	DQ	318.1
96	6972	3	E	3C	PAB	669
96	6972	4	E	3C	PAB	261.8
97	6989	15	E	S&D	UNK	309.5
97	6989	16	E	S&D	UNK	190.5
95	7000	11	AB	S&D	UNK	297.5
95	7002	12	AB	S&D	PAB	749.3
95	7003	17	AB	S&D	KH	27.5
95	7004	14	AB	S&D	DQ	158.7
95	7004	12	AB	S&D	UNK	18.7
96	7232	46	F	3C	PAB	73.9
96	7243	26	F	S&D	UNK	2.5
96	7243	69	F	S&D	UNK	219
96	7248	2	F	3C	PAB	79.3
96	7254	53	F	3B	PAB	365.2
96	7256	41	F	3B	PAB	43.4
96	7257	54	F	3B	KH	211.5
96	7257	52	F	3B	UNK	187.9
96	7257	53	F	3B	UNK	209.9
96	7257	55	F	3B	UNK	69.5
96	7263	6	F	3C	UNK	1118
96	7291	1	F	3B	PAB	294.5
96	7310	17	AB	5	DQ	3
96	7317	1	AB	5	UNK	659.2
96	7319	1	AB	4	KH	347.2
96	7329	3	AB	5	UNK	121.2

year	*lot*	*record*	*location*	*context*	*material*	*grams*
95	7016	11	AB	3C	UNK	42.9
96	7101	13	E	S&D	DQ	14.4
96	7103	11	E	S&D	GSS	9.2
96	7103	12	E	S&D	PAB	91.5
96	7103	13	E	S&D	PAB	117.3
96	7103	24	E	S&D	PAB	201.7
96	7103	14	E	S&D	UNK	225.5
96	7103	15	E	S&D	UNK	50.8
96	7104	139	E	S&D	UNK	59
96	7109	1	E	3C	KH	1161
96	7113	3	E	S&D	DQ	120.2
96	7113	4	E	S&D	GSS	18.5
96	7114	1	E	S&D	DQ	230.6
96	7114	4	E	S&D	UNK	416.3
96	7115	15	E	3C	DQ	251.7
96	7115	14	E	3C	PAB	214
96	7115	13	E	3C	UNK	143
96	7118	53	E	3C	UNK	2.6
96	7121	84	E	3C	UNK	7.3
96	7123	5	E	3C	PAB	623.6
96	7123	4	E	3C	UNK	144.3
96	7144	7	E	3C	PAB	165.3
96	7148	43	E	3C	UNK	89.5
96	7149	78	E	S&D	UNK	15.5
96	7150	6	E	S&D	DQ	261.7
96	7150	22	E	S&D	DQ	22.9
96	7155	9	E	3C	UNK	13.2
96	7156	19	E	3C	UNK	76.6
96	7201	12	F	S&D	UNK	3189
96	7202	5	F	S&D	DQ	151.3
96	7203	8	F	S&D	DQ	198
96	7205	2	F	S&D	DQ	1850
96	7205	11	F	S&D	DQ	1954
96	7209	40	F	S&D	GSS	189.7
96	7210	14	F	S&D	UNK	219.8
96	7212	4	F	S&D	PAB	295.2
96	7218	6	F	S&D	KH	25.2
96	7227	34	F	3C	DQ	111
96	7227	35	F	3C	PAB	362.1
96	7229	5	F	3C	UNK	27.8
96	7230	2	F	S&D	DQ	917.2
96	7230	34	F	S&D	DQ	152.9
96	7466	13	AB	2	KH	3600
96	7467	297	AB	3A	KH	682.4
96	7467	298	AB	3A	KH	976
96	7467	299	AB	3A	KH	1146
96	7467	302	AB	3A	UNK	127.5
96	7482	1	AB	2	KH	168.9
96	7482	5	AB	2	KH	153.4
96	7490	39	AB	2	KH	4.5
96	7490	40	AB	2	KH	5
96	7490	38	AB	2	UNK	25
96	7491	7	AB	1	KH	99.7
96	7491	9	AB	1	UNK	1
96	7492	4	AB	1	KH	32.9
96	7492	5	AB	1	KH	20
96	7493	5	AB	1	KH	81
96	7493	4	AB	1	UNK	259

year	*lot*	*record*	*location*	*context*	*material*	*grams*
96	7333	28	AB	5	GSS	10.7
96	7333	31	AB	5	PAB	184.9
96	7344	1	AB	5	DQ	10.9
96	7351	9	AB	5	UNK	4
96	7355	9	AB	5	DQ	53.5
96	7356	57	AB	4	DQ	24.5
96	7356	61	AB	4	DQ	70
96	7356	60	AB	4	GSS	122.5
96	7356	54	AB	4	PAB	72.2
96	7356	58	AB	4	UNK	18.8
96	7357	4	AB	5	DQ	666.3
96	7357	2	AB	5	UNK	251.6
96	7359	6	AB	4	KH	164.8
96	7373	3	AB	4	UNK	80
96	7375	15	AB	4	DQ	160.3
96	7375	8	AB	4	UNK	47.8
96	7401	19	AB	3A	UNK	228.8
96	7402	88	AB	3A	PAB	1160
96	7403	6	AB	3A	PAB	253
96	7419	35	AB	2	KH	29.8
96	7423	84	AB	2	KH	39
96	7423	3	AB	2	UNK	114.5
96	7423	93	AB	2	UNK	12.3
96	7431	9	AB	2	UNK	400
96	7451	2	AB	S&D	PAB	44.5
96	7460	8	AB	2	KH	253.8
96	7460	7	AB	2	UNK	242.1
96	7460	48	AB	2	UNK	4.5
96	7462	6	AB	2	KH	1321
99	7631	16	F	3C	UNK	174
99	7631	17	F	3C	UNK	151
99	7631	28	F	3C	UNK	53.3
99	7633	8	F	3C	DQ	892.8
99	7633	9	F	3C	PAB	289
99	7635	15	F	3C	UNK	216.4
99	7635	56	F	3C	UNK	477
99	7643	5	F	3C	DQ	255.6
99	7643	4	F	3C	PAB	218.4
99	7647	1	F	3C	GSS	800.9
99	7648	2	F	3C	UNK	950.4
99	7666	7	F	S&D	DQ	2270
99	7666	8	F	S&D	DQ	2690
99	7666	9	F	S&D	DQ	1696
99	7666	24	F	S&D	DQ	1266
99	7666	25	F	S&D	DQ	657
99	7666	5	F	S&D	GSS	1013
99	7666	16	F	S&D	GSS	311.5
99	7666	28	F	S&D	GSS	763
99	7666	17	F	S&D	KH	185.7
99	7666	10	F	S&D	PAB	1866
99	7666	12	F	S&D	PAB	588
99	7666	15	F	S&D	PAB	375
99	7666	22	F	S&D	PAB	1341
99	7666	23	F	S&D	PAB	1158
99	7666	26	F	S&D	PAB	1161
99	7666	6	F	S&D	UNK	571.1
99	7666	11	F	S&D	UNK	370.5
99	7666	13	F	S&D	UNK	1016

year	*lot*	*record*	*location*	*context*	*material*	*grams*
96	7495	10	AB	1	KH	72.5
96	7496	13	AB	1	KH	119.9
96	7496	14	AB	1	KH	68.3
96	7497	17	AB	1	KH	287.5
96	7498	4	AB	1	KH	2750
96	7498	5	AB	1	KH	153
96	7500	25	AB	1	KH	31.9
96	7503	2	AB	1	KH	189.9
96	7512	161	AB	1	KH	346.5
97	7603	1	F	3C	PAB	430
97	7607	26	F	3C	GSS	15.2
97	7608	1	F	3C	DQ	2595
97	7608	2	F	3C	PAB	111.2
97	7617	10	F	3C	PAB	467
97	7617	11	F	3C	UNK	57
97	7619	19	F	3C	DQ	22.1
99	7631	4	F	3C	DQ	913.5
99	7631	5	F	3C	DQ	176.5
99	7631	6	F	3C	DQ	128.5
99	7631	9	F	3C	DQ	2500
99	7631	11	F	3C	DQ	1262
99	7631	13	F	3C	DQ	466
99	7631	18	F	3C	DQ	84
99	7631	15	F	3C	GSS	330
99	7631	3	F	3C	PAB	1258
99	7631	8	F	3C	PAB	3500
99	7631	12	F	3C	PAB	874
99	7631	10	F	3C	UNK	1409
99	7631	14	F	3C	UNK	422
99	7792	5	AB	3C	UNK	91.5
99	7793	1	AB	3C	PAB	50.2
99	7798	4	AB	3C	DQ	20
99	7798	3	AB	3C	KH	68.3
97	7814	8	ET	S&D	PAB	1016
97	7816	1	ET	S&D	PAB	252.5
97	7817	1	ET	S&D	DQ	498
97	7817	1	ET	S&D	UNK	332
97	7819	21	ET	3B	DQ	290
97	7819	2	ET	3B	PAB	326
97	7824	52	ET	3B	UNK	104.6
97	7825	8	ET	3B	PAB	9000
97	7835	1	ET	3B	PAB	348.8
97	7844	1	ET	S&D	PAB	115.7
97	7851	20	ET	3B	PAB	1170
97	8025	4	E	3B	KH	26.6
97	8053	21	E	3C	UNK	428.2
97	8081	3	E	3C	PAB	408.7
97	8105	6	E	S&D	PAB	384
97	8107	12	E	3C	PAB	250.9
97	8107	13	E	3C	PAB	580.4
97	8107	22	E	3C	PAB	1040
97	8107	55	E	3C	PAB	311
97	8108	1	E	3C	PAB	1277
97	8109	1	E	S&D	DQ	400
97	8110	3	E	S&D	PAB	353.6
97	8110	4	E	S&D	PAB	322.4
97	8111	33	E	3C	DQ	362.1
97	8111	34	E	3C	UNK	105.7

year	lot	record	location	context	material	grams
99	7666	14	F	S&D	UNK	133
99	7666	20	F	S&D	UNK	1202
99	7666	21	F	S&D	UNK	809.8
99	7666	27	F	S&D	UNK	590.8
99	7666	35	F	S&D	UNK	518.8
98	7680	3	F	3C	PAB	300
97	7701	182	AB	3C	GSS	182
97	7715	6	AB	S&D	UNK	308
97	7715	10	AB	S&D	UNK	7000
97	7740	3	AB	S&D	DQ	231.2
97	7743	1	AB	S&D	PAB	80.9
97	7781	24	AB	S&D	PAB	157.3
97	7784	804	AB	S&D	UNK	111.9
99	7790	2	AB	3C	UNK	95.4
99	7790	15	AB	3C	UNK	202.2
99	7791	8	AB	3C	UNK	250.3
98	8161	49	E	3C	DQ	784.1
98	8161	23	E	3C	UNK	165.2
98	8163	11	E	3C	PAB	499.5
98	8163	12	E	3C	PAB	67.5
98	8163	8	E	3C	UNK	317.5
98	8165	17	E	S&D	PAB	730
98	8165	32	E	S&D	PAB	1247
98	8165	104	E	S&D	PAB	207
98	8165	105	E	S&D	PAB	558.8
98	8165	126	E	S&D	PAB	379.7
98	8165	16	E	S&D	UNK	53.9
98	8165	33	E	S&D	UNK	1204
98	8165	99	E	S&D	UNK	93.5
98	8165	100	E	S&D	UNK	136.1
98	8165	101	E	S&D	UNK	73
98	8165	103	E	S&D	UNK	260.4
98	8165	124	E	S&D	UNK	260.9
98	8166	12	E	S&D	PAB	449.4
98	8166	13	E	S&D	UNK	173
98	8167	4	E	3C	PAB	116.6
98	8169	97	E	3C	PAB	468.7
98	8170	20	E	3C	UNK	27.5
98	8170	21	E	3C	UNK	114
98	8172	24	E	S&D	UNK	127.6
98	8173	40	E	S&D	DQ	544
98	8173	42	E	S&D	DQ	173.5
98	8173	90	E	S&D	DQ	159.7
98	8173	91	E	S&D	DQ	105.7
98	8173	92	E	S&D	DQ	47.8
98	8173	39	E	S&D	GSS	269.6
98	8173	41	E	S&D	PAB	782.3
98	8173	99	E	S&D	UNK	300
98	8173	99	E	S&D	UNK	313
98	8175	13	E	3C	PAB	121.5
98	8175	14	E	3C	PAB	105.9
98	8176	111	E	3C	DQ	260
98	8176	25	E	3C	PAB	576
98	8176	26	E	3C	UNK	49.8
98	8176	45	E	3C	UNK	274.9
98	8183	15	E	3C	UNK	339.7
98	8183	16	E	3C	UNK	137.1
98	8185	8	E	3C	PAB	281.2

year	lot	record	location	context	material	grams
97	8113	4	E	3C	DQ	66.6
97	8113	3	E	3C	PAB	151
97	8115	14	E	3C	DQ	1057
97	8115	13	E	3C	GSS	405.8
97	8115	15	E	3C	PAB	1478
97	8115	40	E	3C	UNK	142.3
97	8121	4	E	3C	PAB	1700
98	8154	12	E	3C	DQ	81.7
98	8154	11	E	3C	UNK	188.9
98	8158	44	E	3C	DQ	470
98	8158	75	E	3C	DQ	600.1
98	8158	3	E	3C	PAB	346.1
98	8158	63	E	3C	UNK	127.7
98	8158	79	E	3C	UNK	195.9
98	8159	36	E	3C	DQ	181.5
98	8159	37	E	3C	PAB	243.3
97	8201	4	E	3B	GSS	761.5
97	8245	1	E	3C	PAB	1260
98	8301	81	AB	S&D	GSS	277
98	8301	64	AB	S&D	KH	199.5
98	8301	66	AB	S&D	UNK	300
98	8301	163	AB	S&D	UNK	200
98	8302	36	AB	S&D	PAB	58.2
98	8302	35	AB	S&D	UNK	185.3
98	8303	37	AB	S&D	UNK	47.7
98	8303	39	AB	S&D	UNK	5.4
98	8304	2	AB	S&D	KH	116.1
98	8305	82	AB	S&D	DQ	1.2
98	8305	10	AB	S&D	KH	1.25
98	8305	8	AB	S&D	UNK	82.9
98	8305	9	AB	S&D	UNK	386.8
98	8305	65	AB	S&D	UNK	120.3
98	8305	81	AB	S&D	UNK	1.9
98	8306	26	AB	S&D	DQ	565.3
98	8306	262	AB	S&D	DQ	151.6
98	8306	84	AB	S&D	GSS	150.9
98	8306	198	AB	S&D	GSS	32.4
98	8306	221	AB	S&D	KH	363
98	8306	27	AB	S&D	UNK	334.6
98	8306	167	AB	S&D	UNK	249.5
98	8306	219	AB	S&D	UNK	208.2
98	8306	261	AB	S&D	UNK	75.7
98	8306	262	AB	S&D	UNK	105.9
98	8306	263	AB	S&D	UNK	137.3
98	8308	57	AB	3C	DQ	232.1
98	8308	9	AB	3C	UNK	93.1
98	8308	32	AB	3C	UNK	1610
98	8309	1	AB	3C	GSS	104.5
98	8310	110	AB	3C	DQ	1.5
98	8310	127	AB	3C	UNK	250.8
98	8310	154	AB	3C	UNK	321.3
98	8311	7	AB	3C	KH	38.2
98	8311	8	AB	3C	KH	19.8
98	8313	159	AB	S&D	DQ	53.5
98	8314	16	AB	3C	KH	19.5
98	8315	6	AB	3C	UNK	332.2
98	8315	7	AB	3C	UNK	140.8
98	8315	8	AB	3C	UNK	57.1

year	*lot*	*record*	*location*	*context*	*material*	*grams*
98	8198	22	E	3C	DQ	57.9
98	8198	23	E	3C	DQ	373.3
98	8198	25	E	3C	DQ	115.8
98	8322	126	AB	3C	KH	77.8
98	8322	124	AB	3C	UNK	20.2
98	8322	125	AB	3C	UNK	7.7
98	8323	50	AB	3C	UNK	89.4
98	8326	124	AB	3C	DQ	186
98	8326	125	AB	3C	KH	41.9
98	8328	23	AB	3C	DQ	269.5
98	8331	73	AB	S&D	DQ	31
98	8331	37	AB	S&D	UNK	200
98	8332	15	AB	S&D	DQ	201
98	8332	3	AB	S&D	KH	557.9
98	8332	16	AB	S&D	UNK	100
98	8334	84	AB	S&D	PAB	138
98	8334	2	AB	S&D	UNK	3000
98	8334	6	AB	S&D	UNK	117.7
98	8334	7	AB	S&D	UNK	150.5
98	8336	87	AB	3C	GSS	304.2
98	8340	13	AB	3C	GSS	198.3
98	8341	44	AB	3C	DQ	13.5
98	8341	53	AB	3C	DQ	81.4
98	8341	54	AB	3C	DQ	62.7
98	8347	129	AB	3C	DQ	135.3
98	8366	12	AB	3B	PAB	285.3
98	8375	74	AB	3B	UNK	48.2
98	8377	6	AB	3B	UNK	593.7
98	8380	3	AB	3C	KH	6.9
99	8385	27	AB	S&D	KH	34.4
99	8387	110	AB	S&D	UNK	145
99	8388	133	AB	S&D	PAB	240.1
99	8388	120	AB	S&D	UNK	225.3
99	8388	121	AB	S&D	UNK	36
99	8393	140	AB	3C	GSS	216.5
99	8394	22	AB	S&D	DQ	207
99	8394	45	AB	S&D	PAB	322
99	8394	24	AB	S&D	UNK	10.9
99	8394	33	AB	S&D	UNK	76.3
99	8394	44	AB	S&D	UNK	170.3
99	8394	46	AB	S&D	UNK	830
99	8395	58	AB	S&D	UNK	280.9
99	8395	73	AB	S&D	UNK	173.8
99	8395	74	AB	S&D	UNK	48.2
99	8398	16	AB	3B	KH	154.5
98	8404	114	AB	S&D	DQ	234.7
98	8404	1083	AB	S&D	DQ	71.5
98	8404	1090	AB	S&D	DQ	59.5
98	8428	33	AB	2	KH	4.2
98	8429	19	AB	2	KH	82.2
98	8430	24	AB	2	KH	333.6
98	8430	25	AB	2	KH	143.7
98	8430	26	AB	2	KH	94.9
98	8430	27	AB	2	KH	40.9
98	8430	28	AB	2	KH	44.3
98	8430	23	AB	2	UNK	90
98	8430	59	AB	2	UNK	117.9
98	8431	5	AB	2	KH	102.7

year	*lot*	*record*	*location*	*context*	*material*	*grams*
98	8321	6	AB	3C	GSS	235.5
98	8322	2	AB	3C	DQ	125
98	8322	118	AB	3C	DQ	377.2
98	8404	1091	AB	S&D	DQ	13.2
98	8404	1092	AB	S&D	DQ	12.4
98	8404	1096	AB	S&D	DQ	2.3
98	8404	1139	AB	S&D	DQ	545
98	8404	113	AB	S&D	KH	180.4
98	8404	115	AB	S&D	KH	129.7
98	8404	116	AB	S&D	KH	50
98	8404	120	AB	S&D	KH	322
98	8404	160	AB	S&D	KH	888.8
98	8404	356	AB	S&D	KH	1280
98	8404	1088	AB	S&D	KH	67.7
98	8404	1089	AB	S&D	KH	26.8
98	8404	1093	AB	S&D	KH	267
98	8404	1094	AB	S&D	KH	25.9
98	8404	1095	AB	S&D	KH	3.7
98	8404	1082	AB	S&D	PAB	370
98	8404	1084	AB	S&D	PAB	162.5
98	8404	1085	AB	S&D	PAB	73
98	8404	1087	AB	S&D	PAB	48.4
98	8404	117	AB	S&D	UNK	33.5
98	8404	119	AB	S&D	UNK	1006
98	8404	127	AB	S&D	UNK	393
98	8404	191	AB	S&D	UNK	450
98	8404	1086	AB	S&D	UNK	98.2
98	8404	1140	AB	S&D	UNK	423
98	8408	12	AB	2	KH	4.5
98	8409	48	AB	2	KH	182.9
98	8412	154	AB	3A	KH	99.9
98	8412	260	AB	3A	KH	39.7
98	8412	193	AB	3A	PAB	75
98	8412	208	AB	3A	PAB	156.3
98	8412	209	AB	3A	PAB	720.7
98	8412	124	AB	3A	UNK	65.1
98	8412	125	AB	3A	UNK	131.5
98	8412	166	AB	3A	UNK	750
98	8412	194	AB	3A	UNK	157.7
98	8412	207	AB	3A	UNK	72.3
98	8413	31	AB	2	KH	63.4
98	8416	2	AB	3A	UNK	3.8
98	8416	11	AB	3A	UNK	286.7
98	8424	13	AB	2	KH	31.5
98	8427	23	AB	2	KH	158.9
98	8427	24	AB	2	PAB	176.8
98	8428	27	AB	2	KH	1224
98	8428	28	AB	2	KH	15.4
99	8492	38	AB	2	KH	148.3
99	8492	39	AB	2	KH	161.9
99	8492	233	AB	2	KH	11.4
99	8492	234	AB	2	KH	284.8
99	8492	235	AB	2	KH	25.8
99	8492	246	AB	2	KH	158.3
99	8492	247	AB	2	KH	22.2
99	8492	248	AB	2	KH	72.1
99	8492	249	AB	2	KH	82.7
99	8492	250	AB	2	KH	90.3

year	lot	record	location	context	material	grams
98	8432	50	AB	2	KH	138.7
98	8433	11	AB	2	PAB	318.5
98	8433	40	AB	2	UNK	23.4
98	8436	11	AB	2	KH	64.5
98	8436	12	AB	2	KH	65.4
98	8436	13	AB	2	KH	68.7
98	8436	14	AB	2	KH	79.8
98	8436	27	AB	2	KH	2500
98	8436	29	AB	2	KH	18.2
98	8437	16	AB	2	PAB	51.8
98	8439	26	AB	S&D	KH	103.1
98	8439	27	AB	S&D	UNK	46.3
98	8439	70	AB	S&D	UNK	10.4
98	8440	80	AB	S&D	KH	34.5
98	8440	3	AB	S&D	UNK	100.3
98	8440	79	AB	S&D	UNK	218.5
98	8452	6	AB	2	KH	67.3
98	8461	7	AB	2	UNK	33.5
98	8463	1	AB	2	KH	154.7
98	8480	11	AB	1	KH	34.8
98	8482	8	AB	1	KH	132.4
98	8486	30	AB	2	KH	364.4
98	8486	31	AB	2	KH	187.5
98	8486	3	AB	2	UNK	170.5
98	8486	29	AB	2	UNK	66.8
98	8487	37	AB	2	KH	27
98	8487	38	AB	2	KH	216.5
98	8490	102	AB	2	DQ	22
99	8490	99	AB	2	KH	17
99	8490	100	AB	2	KH	65
99	8490	101	AB	2	KH	24
99	8490	121	AB	2	KH	114
99	8492	35	AB	2	KH	290
99	8492	36	AB	2	KH	136.3
99	8492	37	AB	2	KH	129.1
98	8551	1	AB	1	KH	86.2
98	8554	3	AB	1	GSS	28.3
98	8562	28	AB	1	UNK	269.9
98	8576	1	AB	1	KH	176.2
98	8582	17	AB	1	KH	89.4
98	8588	10	AB	1	KH	3.8
98	8588	11	AB	1	KH	18.8
98	8590	3	AB	1	KH	520.5
98	8600	10	F	S&D	GSS	970
98	8600	9	F	S&D	PAB	520
98	8600	31	F	S&D	PAB	240
98	8601	10	F	S&D	DQ	142
98	8601	9	F	S&D	UNK	71
98	8602	8	F	S&D	DQ	300
98	8602	7	F	S&D	UNK	152.9
98	8603	46	F	S&D	DQ	42.4
98	8603	47	F	S&D	PAB	292.7
98	8603	48	F	S&D	PAB	133.3
98	8603	5	F	S&D	UNK	115
98	8604	21	F	S&D	PAB	1101
98	8607	1	F	S&D	DQ	6000
98	8607	56	F	S&D	DQ	639.9
98	8607	55	F	S&D	UNK	29.3

year	lot	record	location	context	material	grams
99	8492	251	AB	2	KH	115
99	8492	252	AB	2	KH	139.8
99	8492	253	AB	2	KH	66.8
99	8492	15	AB	2	UNK	146.8
99	8493	13	AB	2	KH	130.1
98	8499	174	AB	2	UNK	2103
98	8499	295	AB	2	UNK	1332
98	8501	6	AB	1	UNK	20.3
98	8502	7	AB	1	PAB	19.2
98	8503	8	AB	1	KH	7.7
98	8503	9	AB	1	KH	149.8
98	8509	9	AB	1	KH	7.1
98	8509	9	AB	1	KH	18.4
98	8511	31	AB	1	KH	25.7
98	8515	9	AB	1	GSS	76
98	8517	3	AB	1	KH	18.1
98	8517	4	AB	1	KH	31.4
98	8518	8	AB	1	KH	172.1
98	8518	9	AB	1	KH	80.5
98	8518	10	AB	1	KH	63.6
98	8518	17	AB	1	KH	65.3
98	8518	18	AB	1	KH	49.5
98	8518	19	AB	1	KH	38
98	8518	20	AB	1	KH	34.5
98	8518	21	AB	1	KH	23.5
98	8518	22	AB	1	KH	20.2
98	8518	23	AB	1	KH	12.5
98	8525	5	AB	1	KH	6.3
98	8528	4	AB	1	KH	43.3
98	8530	11	AB	1	UNK	137.4
98	8531	1	AB	1	KH	120
98	8531	2	AB	1	UNK	105.5
98	8532	2	AB	1	KH	95
98	8533	7	AB	1	DQ	80.2
98	8544	8	AB	1	KH	1491
98	8663	22	F	3C	DQ	184.5
98	8667	41	F	3C	DQ	558
98	8667	42	F	3C	DQ	122.5
98	8668	26	F	3C	UNK	41.5
98	8669	13	F	S&D	PAB	102.3
98	8673	15	F	S&D	UNK	167.3
98	8679	7	F	3C	PAB	529.3
98	8684	7	F	3C	UNK	116.4
98	8707	2	F	3C	UNK	3.3
98	8717	4	F	3C	PAB	7.8
98	8727	3	F	3C	DQ	180.6
98	8727	5	F	3C	GSS	244.2
98	8727	4	F	3C	UNK	184.8
98	8727	7	F	3C	UNK	1570
2000	8750	8	F	S&D	UNK	125
2000	8753	16	F	S&D	DQ	185.7
99	8754	34	F	3C	DQ	208.1
99	8754	35	F	3C	DQ	98.7
99	8754	33	F	3C	KH	258.9
99	8754	2	F	3C	PAB	800.5
99	8754	36	F	3C	UNK	264.5
99	8754	37	F	3C	UNK	7.4
99	8755	74	F	3C	DQ	50.6

year	lot	record	location	context	material	grams
98	8609	9	F	3C	UNK	991.5
98	8616	24	F	S&D	UNK	346
98	8617	1	F	3C	DQ	55.7
98	8619	5	F	3C	DQ	20.6
98	8625	10	F	3C	DQ	90.5
98	8625	9	F	3C	UNK	282
98	8630	55	F	3C	UNK	50
98	8636	1	F	3C	DQ	57
98	8639	3	F	3C	UNK	321.5
98	8641	8	F	3C	DQ	58.3
98	8641	7	F	3C	GSS	598.4
98	8641	9	F	3C	PAB	807.7
98	8642	2	F	3C	GSS	2266
98	8642	4	F	3C	KH	204
98	8642	5	F	3C	UNK	607
98	8645	3	F	3C	UNK	56.3
98	8649	15	F	3C	DQ	58.8
98	8652	2	F	3C	PAB	27.5
98	8654	24	F	3C	PAB	123
98	8660	3	F	3C	UNK	38.5
98	8662	2	F	3C	UNK	115.3
98	8662	8	F	3C	UNK	72.5
99	8757	214	F	3C	UNK	92.9
99	8758	4	F	3C	UNK	40
99	8758	5	F	3C	UNK	87.8
99	8758	6	F	3C	UNK	87.6
99	8758	7	F	3C	UNK	39.8
99	8760	155	F	3C	KH	34.3
99	8760	39	F	3C	UNK	24.7
99	8760	42	F	3C	UNK	83.7
99	8760	43	F	3C	UNK	31.9
99	8760	44	F	3C	UNK	68.4
99	8763	77	F	3C	PAB	157
99	8763	40	F	3C	UNK	43.7
99	8763	41	F	3C	UNK	57.5
99	8763	74	F	3C	UNK	7.2
99	8763	78	F	3C	UNK	335
99	8764	122	F	S&D	DQ	598
99	8764	144	F	S&D	DQ	13.7
99	8764	173	F	S&D	DQ	7.2
99	8764	136	F	S&D	PAB	1.7
99	8764	140	F	S&D	UNK	137.6
99	8764	142	F	S&D	UNK	3.7
99	8764	145	F	S&D	UNK	36.8
99	8764	171	F	S&D	UNK	4.6
99	8764	174	F	S&D	UNK	44.5
99	8764	245	F	S&D	UNK	57.8
99	8764	266	F	S&D	UNK	8.8
99	8774	70	F	3C	DQ	177.1
99	8774	12	F	3C	GSS	199
99	8774	86	F	3C	KH	16
99	8774	67	F	3C	UNK	2.1
99	8774	87	F	3C	UNK	78
99	8775	32	F	3C	GSS	33.9
99	8775	33	F	3C	UNK	21
99	8776	62	F	3C	DQ	382.5
99	8776	121	F	3C	KH	128.2
99	8776	63	F	3C	PAB	963.9

year	lot	record	location	context	material	grams
99	8755	82	F	3C	DQ	257.5
99	8755	77	F	3C	GSS	813.5
99	8755	81	F	3C	GSS	346.5
99	8755	79	F	3C	KH	304.5
99	8755	75	F	3C	PAB	44.2
99	8755	78	F	3C	PAB	350.8
99	8755	83	F	3C	UNK	31.1
99	8756	69	F	3C	GSS	545.5
99	8756	87	F	3C	GSS	131.8
99	8756	43	F	3C	PAB	133.9
99	8756	45	F	3C	PAB	249.4
99	8756	46	F	3C	PAB	711
99	8756	80	F	3C	PAB	641.3
99	8756	84	F	3C	PAB	227.8
99	8756	40	F	3C	UNK	178
99	8756	42	F	3C	UNK	95.9
99	8756	44	F	3C	UNK	193.1
99	8757	78	F	3C	DQ	446.5
99	8757	79	F	3C	DQ	83.7
99	8757	80	F	3C	DQ	280.5
99	8757	81	F	3C	UNK	169.3
99	8757	82	F	3C	UNK	51.9
99	8777	40	F	3C	UNK	43.7
99	8777	41	F	3C	UNK	12.1
99	8777	42	F	3C	UNK	13.8
99	8778	50	F	3C	UNK	84.3
99	8778	51	F	3C	UNK	28.9
99	8779	24	F	3C	DQ	165
99	8780	46	F	3C	DQ	631.7
99	8780	66	F	3C	DQ	6.3
99	8780	47	F	3C	UNK	56.7
99	8780	73	F	3C	UNK	20.5
99	8788	28	F	3C	PAB	470.8
99	8795	20	F	3C	DQ	231.7
99	8795	21	F	3C	UNK	121.9
99	8796	23	F	3C	DQ	3.5
99	8796	31	F	3C	DQ	254.7
99	8796	30	F	3C	UNK	712
99	8806	28	E	S&D	UNK	18.6
99	8821	32	E	3C	DQ	384.4
99	8821	33	E	3C	DQ	570.9
99	8821	23	E	3C	GSS	980.6
99	8827	18	E	3C	KH	978.8
99	8828	7	E	S&D	PAB	70.5
99	8829	31	E	S&D	DQ	39.4
99	8830	2	E	S&D	PAB	390.1
99	8830	3	E	S&D	PAB	80.9
99	8831	4	E	S&D	DQ	49.6
99	8831	5	E	S&D	PAB	1059
99	8832	1	E	3C	DQ	584.3
99	8834	9	E	3C	DQ	1490
99	8840	1	E	S&D	PAB	375.7
99	8843	7	E	S&D	PAB	149.6
99	8844	9	E	S&D	DQ	43.2
99	8845	12	E	S&D	UNK	31.8
99	8846	3	E	S&D	UNK	107.1
99	8857	6	E	3C	DQ	9.1
99	8858	34	E	3C	UNK	21.5

year	lot	record	location	context	material	grams
99	8776	120	F	3C	PAB	844
99	8776	46	F	3C	UNK	246.3
99	8776	117	F	3C	UNK	5500
99	8777	39	F	3C	GSS	17.9
99	8777	26	F	3C	UNK	8.7
99	8777	27	F	3C	UNK	150.6
99	8777	28	F	3C	UNK	149.8
99	8777	37	F	3C	UNK	44.5
99	8777	38	F	3C	UNK	5.4
99	8860	13	E	3C	PAB	174.3
99	8864	72	E	S&D	DQ	979
99	8864	69	E	S&D	UNK	99.3
99	8864	70	E	S&D	UNK	51.5
99	8864	71	E	S&D	UNK	82.3
99	8866	9	E	3C	PAB	237.5
99	8867	39	E	3C	DQ	130.7
99	8871	4	E	3C	DQ	137.1
99	8884	2	E	S&D	DQ	490.4
99	8884	3	E	S&D	UNK	378
99	8887	13	E	S&D	DQ	22.2
99	8889	16	E	3C	PAB	733
99	8890	31	E	3C	DQ	35.7
99	8890	82	E	3C	KH	378
99	8890	74	E	3C	PAB	923
99	8890	80	E	3C	PAB	391
99	8890	99	E	3C	PAB	454
99	8890	32	E	3C	UNK	66.8
99	8890	33	E	3C	UNK	81.1
99	8894	20	E	S&D	DQ	583
99	8896	20	E	3C	UNK	26.6
99	8898	1	E	3C	UNK	110.1
99	8907	1	AB	1	UNK	205
99	8936	15	AB	2	KH	53.5
99	8938	54	AB	S&D	KH	42.1
99	8938	55	AB	S&D	KH	170.1
99	8939	229	AB	S&D	DQ	665.8
99	8939	230	AB	S&D	DQ	178.7
99	8939	232	AB	S&D	DQ	130.2
99	8939	236	AB	S&D	DQ	66.4
99	8939	237	AB	S&D	DQ	28.1
99	8939	243	AB	S&D	DQ	592.5
99	8939	231	AB	S&D	PAB	109.9
99	8939	244	AB	S&D	PAB	309.5
99	8939	245	AB	S&D	PAB	323.5
99	8939	246	AB	S&D	PAB	351
99	8939	238	AB	S&D	UNK	43.7
99	8939	241	AB	S&D	UNK	87.1
99	8939	242	AB	S&D	UNK	65.8
99	8939	247	AB	S&D	UNK	155
99	8939	248	AB	S&D	UNK	43.5
99	8939	249	AB	S&D	UNK	9.2
99	8939	250	AB	S&D	UNK	3.2
99	8939	258	AB	S&D	UNK	31
99	8940	12	AB	S&D	KH	220
2001	9059	5	E	3C	UNK	351
2001	9059	7	E	3C	UNK	533
2001	9065	7	E	3C	UNK	25
2001	9067	39	E	S&D	PAB	107

year	lot	record	location	context	material	grams
99	8858	38	E	3C	UNK	294
99	8859	51	E	3C	DQ	267
99	8859	46	E	3C	KH	32.1
99	8859	8	E	3C	PAB	343.3
99	8859	47	E	3C	PAB	370
99	8859	49	E	3C	PAB	133.3
99	8859	45	E	3C	SR	116
99	8859	48	E	3C	UNK	29.4
99	8860	14	E	3C	GSS	227.2
99	8940	5	AB	S&D	UNK	765.3
99	8940	9	AB	S&D	UNK	778
99	8940	10	AB	S&D	UNK	863.8
99	8940	11	AB	S&D	UNK	286.9
99	8940	33	AB	S&D	UNK	10.5
99	8941	61	AB	2	PAB	225.5
99	8941	63	AB	2	UNK	297.7
99	8943	61	AB	2	KH	72.3
99	8944	81	AB	2	KH	90.5
99	8944	82	AB	2	KH	26
99	8944	85	AB	2	KH	45.3
99	8950	24	AB	2	PAB	192.1
99	8954	11	AB	2	UNK	78.5
99	8960	11	AB	2	KH	70.7
99	8960	12	AB	2	KH	105.8
99	8961	18	AB	2	KH	177.8
99	8963	1	AB	2	KH	155
99	8963	13	AB	2	KH	326.5
99	8963	14	AB	2	KH	260
2000	8983	53	AB	2	KH	100.2
2000	8983	54	AB	2	KH	55.9
2000	8984	81	AB	2	KH	726
2000	8990	117	AB	2	GSS	141.2
2000	8990	84	AB	2	UNK	16.1
2000	8990	118	AB	2	UNK	118
2000	8990	120	AB	2	UNK	44.4
2000	8996	27	AB	2	KH	1171
2001	9004	12	E	S&D	DQ	64.5
2001	9004	18	E	S&D	DQ	231
2001	9004	16	E	S&D	PAB	558
2001	9004	8	E	S&D	UNK	130.8
2001	9006	1	E	S&D	DQ	290.6
2001	9007	20	E	S&D	UNK	146.1
2001	9010	21	E	3C	UNK	512.3
2001	9017	3	E	3C	PAB	95.5
2001	9043	3	E	3C	DQ	43
2001	9044	13	E	3C	PAB	513
2001	9051	6	E	3C	PAB	663.5
2001	9051	14	E	3C	PAB	43.8
2001	9051	23	E	3C	PAB	54.3
2001	9056	20	E	3C	UNK	104.7
2001	9057	14	E	3C	PAB	234
2001	9059	6	E	3C	PAB	51.3
2001	9059	75	E	3C	PAB	277
2001	9059	76	E	3C	PAB	234
99	9401	38	AB	S&D	UNK	38.5
99	9401	39	AB	S&D	UNK	3.4
99	9406	1	AB	3B	DQ	991.6
99	9406	2	AB	3B	DQ	660.7

year	*lot*	*record*	*location*	*context*	*material*	*grams*
2001	9069	2	E	3C	PAB	113.8
2001	9076	4	E	3C	DQ	304
2001	9076	2	E	3C	UNK	251.9
2001	9079	24	E	3C	GSS	303
2001	9079	21	E	3C	PAB	1071
2001	9079	20	E	3C	UNK	1148
2001	9091	7	E	3C	PAB	342
2001	9091	8	E	3C	PAB	1462
2001	9091	10	E	3C	UNK	1202
2001	9091	54	E	3C	UNK	140
2001	9092	2	E	3C	GSS	3000
2001	9097	1	E	3C	PAB	1394
99	9103	2	F	3C	UNK	15.7
99	9108	39	F	3C	PAB	340.7
99	9110	39	F	3C	DQ	88.8
99	9110	40	F	3C	DQ	41
99	9110	41	F	3C	DQ	27.9
99	9110	21	F	3C	UNK	24.7
99	9112	15	F	3C	DQ	271.8
99	9113	43	F	3C	DQ	248.2
99	9113	44	F	3C	DQ	234.1
99	9115	30	F	3C	DQ	3.6
99	9120	20	F	3C	DQ	218.8
99	9120	19	F	3C	GSS	165.1
99	9120	18	F	3C	UNK	4.5
99	9129	2	F	3C	DQ	11
99	9131	1	F	3C	UNK	123
99	9203	1	F	S&D	DQ	188.1
99	9203	2	F	S&D	DQ	133
99	9203	3	F	S&D	DQ	126
99	9205	16	F	3C	DQ	261
99	9205	17	F	3C	UNK	158.7
99	9210	20	F	S&D	PAB	8.8
99	9211	17/18	F	S&D	PAB	63.5
99	9237	1	F	3C	PAB	724.8
99	9241	1	F	3C	UNK	291.6
99	9400	12	AB	S&D	UNK	8.3
99	9400	14	AB	S&D	UNK	622.3
99	9401	33	AB	S&D	UNK	12.5
99	9401	34	AB	S&D	UNK	10
99	9401	37	AB	S&D	UNK	29
99	9604	45	E	S&D	PAB	201.8
99	9604	46	E	S&D	PAB	425.5
99	9606	46	E	S&D	DQ	142.7
99	9606	47	E	S&D	DQ	744
99	9606	49	E	S&D	DQ	177.2
99	9606	48	E	S&D	PAB	177.7
99	9606	50	E	S&D	PAB	106.1
2001	9611	67	E	3C	DQ	94
2001	9611	66	E	3C	GSS	28.6
2001	9611	68	E	3C	UNK	17.6
2001	9612	103	E	3C	DQ	127.3
2001	9612	108	E	3C	DQ	303
2001	9612	104	E	3C	GSS	117.4
2001	9612	106	E	3C	GSS	198.5
2001	9612	107	E	3C	PAB	623.7
2001	9613	5	E	3C	PAB	249.3
2001	9613	6	E	3C	PAB	80.9

year	*lot*	*record*	*location*	*context*	*material*	*grams*
99	9408	38	AB	3B	UNK	375.4
99	9409	8	AB	3B	KH	398.5
99	9413	124	AB	S&D	KH	151.7
99	9413	74	AB	S&D	UNK	44.5
99	9413	75	AB	S&D	UNK	46
99	9413	76	AB	S&D	UNK	22.7
99	9413	77	AB	S&D	UNK	24.9
99	9413	78	AB	S&D	UNK	232.9
99	9413	121	AB	S&D	UNK	35.5
99	9413	122	AB	S&D	UNK	18
99	9413	123	AB	S&D	UNK	44.3
99	9421	1	AB	3B	KH	29.3
99	9432	23	AB	S&D	UNK	30.8
99	9432	35	AB	S&D	UNK	645.2
99	9435	7	AB	3B	UNK	35.5
2000	9438	26	AB	S&D	KH	35
2000	9438	27	AB	S&D	KH	130.9
2000	9438	28	AB	S&D	KH	38.4
2000	9438	29	AB	S&D	KH	126.5
2000	9438	31	AB	S&D	KH	27.7
2000	9438	8	AB	S&D	UNK	28.2
2000	9438	32	AB	S&D	UNK	44
2000	9440	2	AB	S&D	UNK	91.1
2000	9444	3	AB	3B	KH	46.6
2000	9504	40	AB	2	KH	94
2000	9507	39	AB	2	UNK	111.1
2000	9511	21	AB	2	KH	19.4
2000	9511	1	AB	2	PAB	72
2000	9514	14	AB	2	KH	84.5
2000	9514	96	AB	2	UNK	167.6
2000	9522	72	AB	3A	KH	179.7
2000	9522	71	AB	3A	PAB	563
2000	9555	11	AB	2	DQ	12
2000	9559	3	AB	2	DQ	49.4
2000	9586	14	AB	2	KH	34.8
2000	9588	37	AB	2	GSS	112.2
2000	9588	36	AB	2	KH	105.4
99	9600	8	E	S&D	KH	779.6
99	9600	1	E	S&D	UNK	3565
99	9600	9	E	S&D	UNK	1486
99	9604	44	E	S&D	KH	338
99	9722	11	F	3C	GSS	418.5
99	9722	12	F	3C	GSS	183.5
99	9722	31	F	3C	GSS	238
99	9722	10	F	3C	KH	396
99	9722	13	F	3C	UNK	170.3
99	9724	49	F	3C	UNK	120.4
99	9729	88	F	3C	UNK	42.5
99	9729	92	F	3C	UNK	67
99	9729	93	F	3C	UNK	50
99	9742	5	F	3C	UNK	9.4
99	9742	14	F	3C	UNK	14.3
99	9743	11	F	S&D	DQ	802
99	9743	21	F	S&D	GSS	140
99	9743	12	F	S&D	PAB	216
99	9749	11	F	3C	DQ	180
99	9752	4	F	3C	PAB	423.7
99	9756	24	F	3C	DQ	912.1

year	lot	record	location	context	material	grams
2001	9613	13	E	3C	PAB	21.6
2001	9613	32	E	3C	PAB	67.5
2001	9613	2	E	3C	UNK	530.5
2001	9614	6	E	3C	DQ	245.8
2001	9614	5	E	3C	PAB	1238
2001	9615	80	E	3C	DQ	113.1
2001	9615	1	E	3C	UNK	329.9
99	9700	21	F	S&D	UNK	56.3
99	9700	22	F	S&D	UNK	34.5
99	9700	23	F	S&D	UNK	62.5
99	9700	24	F	S&D	UNK	93.8
99	9702	54	F	3C	DQ	52.8
99	9702	70	F	3C	DQ	192.7
99	9702	68	F	3C	PAB	2.9
99	9702	69	F	3C	UNK	3.7
99	9704	12	F	S&D	KH	229.7
99	9704	10	F	S&D	UNK	863.5
99	9704	11	F	S&D	UNK	300
99	9704	36	F	S&D	UNK	23.4
99	9714	9	F	3C	PAB	285
99	9714	1	F	3C	UNK	99.1
99	9714	3	F	3C	UNK	202.4
99	9714	4	F	3C	UNK	128.3
99	9715	3	F	3C	UNK	169.6
99	9716	59	F	S&D	KH	44.5
99	9716	17	F	S&D	UNK	230.4
99	9718	24	F	3C	DQ	292.1
99	9718	3	F	3C	UNK	135.1
2000	9843	3	F	3C	PAB	447
2000	9844	1	F	3C	UNK	347
2000	9845	17	F	3C	DQ	148.2
2000	9846	21	F	3C	UNK	62.6
2000	9862	18	F	3C	UNK	87.1
2000	9863	5	F	3C	UNK	222.8
2000	9865	2	F	3C	UNK	193.7
2000	9879	2	F	3C	UNK	76
2000	9880	76	F	3C	DQ	227.9
2000	9880	77	F	3C	DQ	295
2000	9880	48	F	3C	UNK	4.9
2000	9880	58	F	3C	UNK	35.5
2000	9880	72	F	3C	UNK	122.9
2000	9881	13	F	3C	UNK	122.9
2000	9890	5	F	3C	DQ	18.4
2003	9904	1	AB	3C	DQ	203
2003	9904	23	AB	3C	DQ	292.2
2003	9904	24	AB	3C	DQ	579
2003	9904	26	AB	3C	DQ	871
2003	9904	27	AB	3C	DQ	1619
2003	9904	29	AB	3C	DQ	449
2003	9904	44	AB	3C	DQ	235.7
2003	9904	6	AB	3C	GSS	965.6
2003	9904	34	AB	3C	GSS	67.5
2003	9904	36	AB	3C	GSS	536.8
2003	9904	3	AB	3C	PAB	539.1
2003	9904	4	AB	3C	PAB	538
2003	9904	5	AB	3C	PAB	796.7
2003	9904	7	AB	3C	PAB	350
2003	9904	14	AB	3C	PAB	2500

year	lot	record	location	context	material	grams
99	9756	25	F	3C	DQ	397
99	9756	26	F	3C	DQ	210.8
99	9756	20	F	3C	GSS	41.3
99	9756	27	F	3C	PAB	35
99	9763	34	F	3C	UNK	22
99	9773	13	F	3C	UNK	111.3
99	9778	7	F	3C	UNK	150
99	9779	19	F	3C	DQ	22.4
99	9788	1	F	3C	UNK	3.6
99	9788	5	F	3C	UNK	291.8
2000	9807	12	F	3C	DQ	35.2
2000	9810	78	F	3C	DQ	281.7
2000	9810	41	F	3C	PAB	353
2000	9812	1	F	3C	DQ	27
2000	9812	2	F	3C	DQ	26.1
2000	9812	4	F	3C	UNK	76.4
2000	9818	12	F	3C	GSS	354
2000	9818	14	F	3C	PAB	18
2000	9818	15	F	3C	UNK	155.9
2000	9822	8	F	3C	DQ	16
2000	9822	9	F	3C	UNK	85.1
2000	9829	18	F	3C	PAB	300.3
2000	9839	16	F	3C	DQ	36.5
2000	9840	12	F	3C	UNK	45.8
2000	9841	7	F	3C	DQ	201.8
2000	9841	1	F	3C	GSS	1800
2000	9841	4	F	3C	UNK	298
2000	9841	6	F	3C	UNK	30.2
2003	9904	11	AB	3C	UNK	264.9
2003	9904	22	AB	3C	UNK	456
2003	9904	28	AB	3C	UNK	1565
2003	9904	32	AB	3C	UNK	2500
2003	9904	33	AB	3C	UNK	364
2003	9904	35	AB	3C	UNK	523
2003	9904	37	AB	3C	UNK	385
2003	9904	40	AB	3C	UNK	375
2003	9904	41	AB	3C	UNK	791.9
2003	9904	43	AB	3C	UNK	147.9
2004	9905	5	AB	3C	KH	4000
2000	9919	1	AB	2	UNK	220.7
2000	9919	2	AB	2	UNK	366
2000	9924	1	AB	2	DQ	270.8
2000	9932	2	AB	2	UNK	88.3
2000	9964	26	AB	2	KH	92.8
2000	9964	3	AB	2	PAB	168.2
2000	9973	1	AB	2	KH	31.1
2000	9999	56	n/a	n/a	PAB	3500
2000	9999	160	n/a	n/a	UNK	567
2000	9999	165	n/a	n/a	PAB	290.8
2001	9999	166	n/a	n/a	UNK	86.5
2000	10000	1	F	3C	PAB	31.2
2000	10011	1	F	3C	PAB	392
2000	10025	5	F	3C	UNK	69.9
2000	10030	1	F	3C	UNK	31
2000	10031	6	F	3C	PAB	377
2000	10036	3	F	3C	DQ	182
2000	10044	21	F	3C	DQ	124.1
2000	10047	5	F	3C	DQ	230.8

year	*lot*	*record*	*location*	*context*	*material*	*grams*
2003	9904	17	AB	3C	PAB	236
2003	9904	18	AB	3C	PAB	507
2003	9904	19	AB	3C	PAB	204
2003	9904	20	AB	3C	PAB	678
2003	9904	21	AB	3C	PAB	417.2
2003	9904	25	AB	3C	PAB	1090
2003	9904	30	AB	3C	PAB	572
2003	9904	31	AB	3C	PAB	1054
2003	9904	38	AB	3C	PAB	466.4
2003	9904	39	AB	3C	PAB	279
2003	9904	42	AB	3C	PAB	1158
2003	9904	2	AB	3C	UNK	278.7
2003	9904	8	AB	3C	UNK	690
2003	9904	9	AB	3C	UNK	348
2003	9904	10	AB	3C	UNK	1082
2001	11505	7	E	S&D	UNK	52.4
2001	11505	20	E	S&D	UNK	70.1
2001	11505	21	E	S&D	UNK	72.9
2001	11521	1	E	3C	DQ	436
2001	11522	1	E	3C	PAB	126.5
2001	11527	2	E	3C	UNK	213.3
2001	11529	1	E	3C	DQ	439.5
2001	11531	1	E	3C	PAB	1037
2001	11534	12	E	3C	DQ	256.7
2001	11535	1	E	3C	UNK	544.8
2001	11542	18	E	S&D	UNK	193
2001	11549	17	E	3C	UNK	52.3
2001	11559	48	E	3C	DQ	491
2001	11560	17	E	3C	PAB	95
2001	11568	1	E	3C	UNK	141.3
2001	11577	1	E	S&D	PAB	52.1
2001	11581	10	E	3C	PAB	240.2

year	*lot*	*record*	*location*	*context*	*material*	*grams*
2000	10047	4	F	3C	UNK	166
2000	10048	2	F	3C	DQ	2500
2000	10050	20	F	3C	DQ	172
2000	10063	5	F	3C	DQ	870
2000	10067	1	F	3C	DQ	1322
2000	10067	2	F	3C	DQ	1332
2000	11000	7	AB	2	KH	28.4
2000	11005	1	AB	2	UNK	55.7
2000	11060	16	AB	1	KH	1
2000	11060	17	AB	1	KH	1
2000	11060	15	AB	1	UNK	5.6
2000	11079	12	AB	2	KH	23.6
2000	11084	1	AB	1	PAB	236.8
2001	11500	1	E	S&D	UNK	17.3
2001	11504	2	E	S&D	DQ	856
2001	11701	26	E	S&D	PAB	2500
2001	11751	82	E	S&D	DQ	46
2001	11751	37	E	S&D	PAB	373.9
2001	11751	38	E	S&D	PAB	201.6
2001	11751	80	E	S&D	PAB	507
2001	11756	45	E	3C	UNK	112
2001	11760	4	E	3C	PAB	285
2001	11761	18	E	3C	DQ	11.2
2001	11761	14	E	3C	PAB	408.6
2001	11800	21	E	S&D	UNK	505
2001	11801	26	E	S&D	DQ	8
2001	11901	1	E	3C	PAB	583
2001	11909	2	E	3C	PAB	257.7
2001	11919	6	E	3C	UNK	29.9
2001	11920	11	E	3C	PAB	778.7
2001	11920	12	E	3C	UNK	1780

APPENDIX 5.2

GRINDINGSTONES IN THE HARAPPA MUSEUM FROM PRE-1986 EXCAVATIONS

Most of the querns and mullers in the Harappa Museum Reserve Collection from pre-1986 exactions were marked with a Harappa Museum number (HM#). Many were also stenciled with an old excavation number. Those without any numbers were given a temporary one (T#).

Museum / temp #	*stenciled #*	*material*	*grams*
HM#1524		UNK	1500
HM#65	980	PAB	5000
HM#67		GSS	20000
HM#68	3498	PAB	1250
HM#HPA93	HPA222.92	UNK	1750
HM#10410		UNK	21000
HM#10420		PAB	4000
HM#10438		UNK	20500
HM#10447		UNK	2500
HM#10452		UNK	3500
HM#10453		UNK	14000
HM#10455	980	PAB	5500
HM#10456		DQ	4500
HM#10457		PAB	1250
HM#10458		GSS	11000
HM#10459		GSS	11250
HM#10460	319	PAB	4500
HM#10461	37	DQ	15500
HM#10462	8841	GSS	7250
HM#10463		GSS	3000
HM#10464		PAB	11500
HM#10465	8327	UNK	14500
HM#10466	334	UNK	9000
HM#10467		DQ	11000
HM#10471		PAB	6500
HM#10472		UNK	14000
HM#10473		GSS	6500
HM#10474		GSS	7500
HM#10475	319	PAB	10000
HM#10477		UNK	14000
HM#10479		UNK	10250
HM#10480	630	UNK	5500
HM#10481	347	UNK	3500
HM#10482		DQ	3500
HM#10483	3034	UNK	6000
HM#10484	982	PAB	1750
HM#10485		PAB	2250
HM#10530	2775	DQ	1250
HM#10533	2400	UNK	1000
HM#10536	54.395	GSS	4000
HM#10537		UNK	1000
HM#10538		GSS	2000
HM#10546	318	PAB	10500
HM#10547		PAB	1500
HM#10549		GSS	2500
HM#10550		UNK	1250

Museum / temp #	*stenciled #*	*material*	*grams*
HM#10486		GSS	7250
HM#10487	3773	PAB	6500
HM#10488	300	DQ	7000
HM#10489	360	PAB	13250
HM#10491		PAB	10000
HM#10492	3753	DQ	14000
HM#10493		GSS	8000
HM#10494		PAB	10000
HM#10496		GSS	11500
HM#10497		UNK	9500
HM#10498		DQ	9000
HM#10500/1	8641	PAB	6500
HM#10502		UNK	4500
HM#10504		PAB	3500
HM#10505		GSS	1000
HM#10506		DQ	1000
HM#10507		PAB	1500
HM#10508		UNK	2000
HM#10509	14031	PAB	3000
HM#10510		PAB	2500
HM#10511		GSS	2750
HM#10512	1719	PAB	3500
HM#10513		UNK	2500
HM#10515		PAB	2000
HM#10516		DQ	1250
HM#10517	36	DQ	3000
HM#10518	9291	GSS	2500
HM#10519		GSS	2000
HM#10520		GSS	2250
HM#10521	319	PAB	5000
HM#10522		GSS	2500
HM#10523		UNK	1500
HM#10524		UNK	1250
HM#10525		UNK	1500
HM#10527		GSS	3500
HM#10528		UNK	2250
HM#10529	12842	UNK	1250
HM#10532	12648	GSS	500
T#44		GSS	12500
T#46		UNK	10000
T#48		GSS	1500
T#49		UNK	2500
T#50		UNK	4000
T#57	80798	GSS	9000
T#58		GSS	6750
T#59		UNK	7000

Museum / temp #	*stenciled #*	*material*	*grams*
T#2	557R	UNK	750
T#3		UNK	535
T#4		GSS	563
T#5		GSS	442
T#6		UNK	506
T#7		UNK	409
T#8		PAB	266
T#9		PAB	313
T#10		GSS	506
T#11		GSS	335
T#12		GSS	424
T#13		UNK	737
T#14		UNK	712
T#15		UNK	852
T#16		UNK	500
T#18		PAB	1110
T#19		UNK	1520
T#20		UNK	1250
T#27	PII43/9705	UNK	1500
T#28		GSS	1250
T#29		UNK	927
T#30		UNK	1750
T#31		UNK	1000
T#32		GSS	1500
T#33		UNK	6000
T#34		UNK	4000
T#35		GSS	2750
T#36		GSS	2500
T#37		GSS	4250
T#38		GSS	4500
T#39		UNK	4500
T#40		UNK	9000
T#41		UNK	9000
T#42		UNK	11500
T#43		GSS	3500

Museum / temp #	*stenciled #*	*material*	*grams*
T#60		UNK	22500
T#61	HPA92-93	PAB	7250
T#62	HPA_ET/24	PAB	18000
T#63	982	PAB	4000
T#64	1719	UNK	4750
T#66		GSS	8000
T#69	318	PAB	11500
T#70	980	PAB	3750
T#71	3989	PAB	9750
T#72		UNK	10500
T#73		UNK	5000
T#74		PAB	1000
T#75		DQ	1500
T#76		DQ	1170
T#77		UNK	5250
T#78		DQ	4000
T#79		DQ	843
T#80		GSS	769
T#81		UNK	1300
T#82		DQ	1000
T#83		GSS	1250
T#84		DQ	1000
T#85		UNK	2250
T#86		PAB	2000
T#87		DQ	1750
T#88	982	PAB	9000
T#89		DQ	3500
T#90		DQ	3500
T#91		UNK	5000
T#92		PAB	4500
T#93		PAB	13250
T#94	319	PAB	7500
T#95	3634	DQ	1000
T#129		UNK	5000
T#131		UNK	7000

APPENDIX 6.1

ELEMENTAL CONCENTRATIONS FOR 9 BLACK CHERT ARTIFACTS FROM HARAPPA

(parts per million)

Figure 6.1 #	Artifact	Period	Trench	Al	Ce	Co	Cr	Eu	Fe	La	Mn	Na	Sc	Sm	V
23	H98/8546-5	1	39	3760	1.541	1.644	12.25	0.126	1542	0.984	31.52	1161	1.061	0.284	5.37
24	H98/8489-25	2	39	2438	1.475	0.413	18.21	0.136	773	1.471	15.80	579	0.268	0.241	19.84
20	H98/8554-18	1	39	3832	1.523	2.133	14.75	0.231	2615	0.977	29.43	1168	1.175	0.298	8.09
22	H98/8558-4	1	39	4263	2.279	1.614	9.44	0.139	1981	1.440	25.34	1379	1.113	0.338	6.67
18	H96/7517-1	1	39	3258	1.406	1.791	10.46	0.145	1928	0.851	25.79	920	0.928	0.268	5.57
19	H96/7490-42	2	39	2345	0.732	0.501	15.67	0.125	1105	0.528	9.50	489	0.165	0.114	14.98
16	H89/1062-9	2	52	2872	1.178	1.782	12.83	0.199	1634	0.732	34.09	786	0.965	0.223	6.20
17	H2000/9598-4	2	39	2531	0.778	0.450	9.96	0.134	781	0.689	7.16	693	0.129	0.131	8.94
21	H2001/2925-17	S&D	54	1826	2.904	0.425	4.73	0.144	575	1.100	5.24	199	0.174	0.369	7.21

APPENDIX 6.2

ELEMENTAL CONCENTRATIONS FOR BLACK CHERT SAMPLES FROM THE BOLAN PASS AND JAMMU

(parts per million)

Location	Sample	Al	Ce	Co	Cr	Eu	Fe	La	Mn	Na	Sc	Sm	V
Dozan, Balochistan	BOLAN-1	2306	1.34	0.569	8.86	0.122	1166	1.664	35.98	259	0.297	0.31	6.66
Dozan, Balochistan	BOLAN-2	2450	1.517	0.388	9.69	0.133	733	2.341	11.12	333	0.458	0.379	8.99
Dozan, Balochistan	BOLAN-3	3022	1.782	2.941	4.87	0.141	2292	1.385	38.64	550	0.536	0.391	2.12
Dozan, Balochistan	BOLAN-4	1887	1.14	0.457	8.53	0.122	1310	1.935	20.38	172	0.302	0.236	9.18
Dozan, Balochistan	BOLAN-5	4059	3.435	1.956	9.23	0.202	2855	4.227	253.1	752	0.879	0.694	7.02
Dozan, Balochistan	BOLAN-6	4216	3.519	0.974	9.88	0.264	1767	6.338	28.1	847	1.136	0.997	9.23
Dozan, Balochistan	BOLAN-7	2374	0.917	0.472	8.28	0.126	706	1.402	9.17	278	0.274	0.204	5.08
Dozan, Balochistan	BOLAN-8	2532	1.005	0.581	8.83	0.122	1179	1.764	20.88	290	0.356	0.248	5.27
Dozan, Balochistan	BOLAN-9	2089	1.194	0.333	7.94	0.126	1098	1.94	19.77	169	0.271	0.24	7.12
Dozan, Balochistan	BOLAN-10	2287	1.391	0.451	13.29	0.139	1554	2.461	13.14	309	0.425	0.299	9.14
Mari nala, Jammu	JAMM-1	2273	0.201	0.433	4.01	0.067	1048	0.224	11.44	73	0.059	0.034	1.58
Mari nala, Jammu	JAMM-2	5568	1.621	1.639	6.13	0.131	3253	1.33	115.8	550	0.863	0.195	4.02
Mari nala, Jammu	JAMM-3	2672	0.504	0.472	2.26	0.069	825	0.305	10.09	90	0.11	0.044	1.46
Mari nala, Jammu	JAMM-4	2535	0.243	0.497	2.72	0.082	724	0.294	8.05	79	0.094	0.034	1.37
Mari nala, Jammu	JAMM-5	2582	3.948	0.345	2.34	0.104	476	2.527	8.91	282	0.615	0.396	1.28
Jangleghari, Jammu	JAMM-6	4662	0.79	0.745	3.02	0.089	1144	0.559	12.34	219	0.335	0.105	2.96
Jangleghari, Jammu	JAMM-7	3903	0.293	0.635	3.12	0.086	1321	0.26	17.7	285	0.291	0.073	4.08
Jangleghari, Jammu	JAMM-8	5326	9.827	0.423	3.68	0.114	689	5.88	7.39	235	0.183	0.59	3.72
Jangleghari, Jammu	JAMM-9	5251	2.345	0.858	4.22	0.117	1698	1.649	65.81	1388	0.707	0.272	6.15
Jangleghari, Jammu	JAMM-10	2290	0.346	0.374	2.58	0.082	881	0.285	11.32	124	0.099	0.058	0.79

APPENDIX 6.3

ELEMENTAL CONCENTRATIONS FOR BLACK CHERT SAMPLES FROM SAKESAR LIMESTONE, SALT RANGE

(parts per million)

Location	Sample	Al	Ce	Co	Cr	Eu	Fe	La	Mn	Na	Sc	Sm	V
Nammal Gorge, Salt Range	SRNG-1	2133	0.981	0.388	14.44	0.122	914	0.928	11.53	659	0.162	0.193	9.87
Nammal Gorge, Salt Range	SRNG-2	2517	0.900	0.539	21.97	0.097	1442	0.874	9.84	477	0.215	0.181	21.00
Nammal Gorge, Salt Range	SRNG-3	2282	0.771	0.453	15.13	0.103	1129	0.84	10.47	500	0.152	0.182	11.90
Nammal Gorge, Salt Range	SRNG-4	2433	0.925	0.576	24.86	0.117	1801	0.958	12.46	377	0.267	0.187	38.88
Nammal Gorge, Salt Range	SRNG-5	2204	1.063	0.437	16.90	0.117	1192	1.229	10.25	338	0.202	0.267	18.87
Nammal Gorge, Salt Range	SRNG-6	2259	0.795	0.486	16.80	0.092	1166	0.913	14.48	482	0.197	0.157	19.38
Nammal Gorge, Salt Range	SRNG-7	2474	0.912	0.518	16.90	0.074	1409	0.907	10.89	421	0.192	0.160	20.11
Nammal Gorge, Salt Range	SRNG-8	2333	0.886	0.417	13.29	0.09	678	0.879	7.25	339	0.217	0.182	17.06
Nammal Gorge, Salt Range	SRNG-9	2270	1.041	0.518	17.20	0.088	1085	1.061	14.99	431	0.241	0.186	18.95
Nammal Gorge, Salt Range	SRNG-10	2179	0.645	0.661	26.57	0.092	2999	0.875	31.91	667	0.176	0.198	10.91
Buri Khel, Salt Range	SRBK-6	2334	0.753	0.535	19.57	0.101	1587	0.678	18.73	322	0.184	0.146	12.53
Buri Khel, Salt Range	SRBK-7	2200	1.002	0.476	14.61	0.129	913	0.658	8.58	349	0.192	0.149	12.07
Buri Khel, Salt Range	SRBK-8	2386	1.108	0.423	14.44	0.113	913	0.799	9.51	333	0.214	0.200	11.69

APPENDIX 6.4

ELEMENTAL CONCENTRATIONS FOR TAN-GRAY CHERT ARTIFACTS FROM HARAPPA AND NAGWADA (BOTTOM ROW)

(parts per million)

Figure 6.1 #	Artifact	Period	Trench	Al	Ce	Co	Eu	Fe	La	Mn	Na	Sc	U	V
5	H98/8482-13	1	39	2044	2.338	1.003	0.141	1748	1.170	11.01	644	0.268	7.52	23.01
12	H96/7531-4	1	39	1914	3.021	0.513	0.126	1617	0.837	13.25	435	0.22	11.18	13.73
11	H96/7500-30	1	39	2429	0.548	0.375	0.101	610	0.494	4.26	689	0.073	0.93	7.04
15	H98/8429-24	2	39	8678	1.320	0.430	0.097	1228	0.714	33.43	439	0.231	3.34	37.24
13	H2000/9984-12	2	39	1841	0.876	0.507	0.119	994	0.829	65.98	278	0.193	2.14	5.36
14	H98/8417-1	2/3	39	1779	2.300	0.533	0.101	916	0.593	7.88	823	0.173	10.08	9.29
6	H2000/2125-17	3A	54	2054	3.038	0.879	0.076	1412	0.922	23.85	957	0.137	12.72	18.95
7	H2000/2300-24	3A	54	1794	4.124	0.419	0.140	737	1.048	19.25	583	0.169	18.06	7.74
9	H2000/2312-27	3A	54	1702	1.938	0.427	0.137	891	0.721	7.90	718	0.132	7.60	9.08
8	H97/7781-46	3B	42	2103	1.696	0.540	0.128	1030	0.775	21.07	374	0.239	5.31	5.44
10	H97/7778-17	3B	42	1853	1.754	0.375	0.073	769	0.503	8.01	520	0.139	8.04	6.60
1	H2001/2939-27	3B	54	1841	8.355	0.680	0.127	1142	1.505	7.64	617	0.162	30.94	31.91
2	H2001/2920-77	3B	54	1664	0.774	0.390	0.117	513	0.704	25.68	448	0.159	1.80	4.56
3	H2001/2920-76	3B	54	1746	6.947	0.429	0.099	644	1.398	3.34	699	0.165	28.08	14.81
4	H2001/2943-7	3B	54	1735	3.578	0.422	0.110	818	0.912	4.08	889	0.163	14.53	9.37
NGW	NGW	Harappan	n/a	8342	2.884	0.391	0.110	902	1.102	67.15	451	0.20	10	46.32

APPENDIX 6.5

ELEMENTAL CONCENTRATIONS FOR TAN-GRAY CHERT SAMPLES FROM FOUR ROHRI HILLS LOCATIONS

(parts per million)

Location	Sample	Al	Ce	Co	Eu	Fe	La	Mn	Na	Sc	U	V
Adam Sultan	RHAS-1	2153	1.499	0.391	0.128	799	0.533	5.08	656	0.324	2.78	7.34
Adam Sultan	RHAS-2	2186	1.003	0.461	0.126	1164	0.925	12.23	579	0.320	2.17	6.95
Adam Sultan	RHAS-3	2150	1.198	0.437	0.061	1280	0.479	7.94	619	0.311	2.84	8.40
Adam Sultan	RHAS-4	2356	1.116	0.514	0.150	1584	1.183	15.25	759	0.364	1.96	9.31
Adam Sultan	RHAS-5	2228	1.051	0.455	0.080	1099	0.506	6.78	654	0.309	3.02	8.09
Kot Diji	RHKD-1	2136	2.110	1.158	0.129	1588	1.076	72.28	292	0.325	4.32	10.88
Kot Diji	RHKD-2	2213	1.938	0.477	0.136	933	1.173	23.57	413	0.521	2.50	13.20
Kot Diji	RHKD-3	2532	1.286	2.019	0.103	5160	0.882	60.2	367	0.474	3.81	36.91
Kot Diji	RHKD-4	1996	0.460	0.971	0.091	2517	0.541	12.77	544	0.366	1.69	19.19
Kot Diji	RHKD-5	2357	2.172	0.967	0.155	1786	1.298	41.37	538	0.449	1.71	12.66
Rohri	RHR-1	1737	0.777	0.355	0.116	1142	0.514	10.44	427	0.135	3.09	8.50
Rohri	RHR-2	1622	5.648	0.469	0.076	1651	1.127	10.55	266	0.171	23.01	8.64
Rohri	RHR-3	1721	1.509	0.535	0.116	2172	0.818	11.52	185	0.136	5.60	20.30
Rohri	RHR-4	1892	1.280	0.523	0.093	2161	0.706	15.31	271	0.235	5.22	9.44
Rohri	RHR-5	1572	1.279	0.493	0.084	1134	0.628	9.06	504	0.160	4.13	11.02
Kandarki	RHK-1	1946	1.632	0.677	0.083	2009	0.448	22.88	225	0.244	6.47	9.79
Kandarki	RHK-2	2071	1.643	0.762	0.072	2742	0.554	20.99	207	0.278	7.52	10.94
Kandarki	RHK-3	2024	1.514	0.793	0.097	2812	0.503	28.13	257	0.268	6.37	10.62
Kandarki	RHK-4	1979	1.349	0.892	0.101	3812	0.692	45.91	196	0.206	5.31	9.37
Kandarki	RHK-5	2041	2.853	0.663	0.071	2057	0.819	16.86	229	0.246	13.12	10.84

APPENDIX 6.6

ELEMENTAL CONCENTRATIONS FOR TAN-GRAY CHERT SAMPLES FROM BALOCHISTAN, THE NWFP AND THE PUNJAB

(parts per million)

Location	Sample	Al	Ce	Co	Eu	Fe	La	Mn	Na	Sc	U	V
Balochistan - Kalat - Gunga	Aub138-1	12924	0.349	0.415	0.081	1046	0.315	40.15	218	0.073	0.28	6.86
Balochistan - Kalat - Gunga	Aub138-2	13274	0.348	0.316	0.087	628	0.334	15.62	217	0.054	0.23	4.12
Balochistan - Kalat - Gunga	Aub138-3	2624	0.737	0.536	0.102	1223	1.294	7.18	322	0.203	0.45	1.49
Balochistan - Kalat - Gunga	Aub138-4	14108	0.580	0.527	0.110	1653	1.195	53.11	404	0.299	0.45	17.61
Balochistan - Kalat - Gunga	Aub138-5	32205	3.268	2.264	0.156	4191	2.974	248.34	1410	1.336	1.37	66.87
NWFP - Mohmand Agency	MMA-1	2221	2.839	0.702	0.104	1697	1.013	27.94	323	0.226	12.27	19.53
NWFP - Mohmand Agency	MMA-2	1678	2.520	0.466	0.109	890	1.063	33.91	189	0.171	11.61	14.65
NWFP - Mohmand Agency	MMA-3	1606	2.789	0.610	0.112	1286	1.015	34.32	176	0.158	11.01	14.12
NWFP - Mohmand Agency	MMA-4	363	2.412	0.425	0.242	1566	2.160	4.07	190	0.217	4.91	2.72
NWFP - Mohmand Agency	MMA-5	6738	1.099	0.369	0.127	925	1.260	85.85	141	0.169	2.00	23.73
NWFP - Mohmand Agency	MMA-6	1569	1.933	0.381	0.130	732	1.124	16.96	136	0.161	4.72	5.75
NWFP - Mohmand Agency	MMA-7	1841	2.352	0.572	0.110	1616	0.778	22.61	175	0.127	9.72	16.09
NWFP - Mohmand Agency	MMA-8	1690	2.983	0.448	0.101	1124	1.045	29.59	217	0.188	10.65	21.79
Punjab - Salt Range - Buri Khel	SRBK-1	2145	1.043	0.420	0.174	1782	1.231	12.24	197	0.149	0.98	8.26
Punjab - Salt Range - Buri Khel	SRBK-2	1917	1.724	0.365	0.174	1436	2.008	14.28	159	0.230	1.02	6.22
Punjab - Salt Range - Buri Khel	SRBK-3	2390	0.599	0.428	0.121	1159	0.589	9.46	229	0.146	0.79	9.32
Punjab - Salt Range - Buri Khel	SRBK-4	2093	0.957	0.402	0.123	840	1.077	8.85	187	0.161	0.85	6.35
Punjab - Salt Range - Buri Khel	SRBK-5	1973	0.895	0.402	0.120	1323	0.926	11.09	152	0.140	0.73	6.15

APPENDIX 6.7

STANDARDIZED CANONICAL DISCRIMINANT FUNCTION COEFFICIENTS FOR FIGURES IN CHAPTER 6 GENERATED USING CANONICAL DISCRIMINANT ANALYSIS

Figure 6.18	*Function 1*	*Function 2*
Log Al	-1.79	-1.246
Log Ce	2.046	-3.226
Log Co	1.299	1.036
Log Cr	0.949	-0.693
Log Eu	0.496	0.569
Log La	-1.596	3.698
Log Mn	-0.733	-0.056
Log Sc	-0.312	0.007
Log V	0.82	0.339

Figure 6.30	*Function 1*	*Function 2*
Log Al	1.688	1.425
Log Ce	.953	-.993
Log Co	.546	-1.242
Log Eu	-.530	.256
Log Fe	.594	1.213
Log La	.289	-.905
Log Mn	-.933	.320
Log Na	.348	.735
Log Sc	-.285	.809
Log U	-1.321	1.738
Log V	-1.217	-2.230

Figure 6.31	*Function 1*	*Function 2*
Log Al	.142	1.559
Log Ce	-.401	.361
Log Co	-1.608	-.877
Log Eu	.204	.068
Log Fe	1.190	1.502
Log La	.125	-.635
Log Mn	.238	-.373
Log Na	.123	.604
Log Sc	-.865	-.064
Log U	1.095	.233
Log V	-.157	-1.386

APPENDIX 7.1

TYPE, CONTEXT AND CDA PREDICTION INFORMATION FOR THE UNFIRED STEATITE ARTIFACTS FROM HARAPPA ANALYZED FOR THIS STUDY (*BEAD BLANKS)

Artifact (year/lot-record)	Type	Mound / Area	Trench / Op.	Period	CDA predicted group membership (PGM)			
					full set 1st PGM	parent-rock 1st & 2nd PGM	11 dolomitic 1st PGM	regional dolomitic 1st PGM
H87/33-02	F	Cemetery	Op. 1	3C	SB	SB / SKK	SB	Sherwan
H87/86-228	F	Cemetery	Op. 1	3C	SB	SB / JKK	SB	S.RAJ
H87/86-229	F	Cemetery	Op. 1	3C	SB	SB / JKK	SB	S.RAJ
H87/86-236	F	Cemetery	Op. 1	3C	SB	JKK / SB	SB	Sherwan
H87/237-86	F	Cemetery	Op. 1	S&D	SB	SB / ATM	SB	Sherwan
H88/340-24	F	E	Op. 3	S&D	PD	RKA / PD	PD	PD
H89/1018-13	D	AB / E	53	S&D	SKK	SKK / SB	SKK	Sherwan
H89/1121-5	A	E	52	S&D	SKK	SKK / SC	SKK	Sherwan
H2000/2230-14	C	E	54	3B	SB	SB / RSA	SB	Sherwan
H2000/2230-15	C	E	54	3B	SB	SB / LKPD	LKPD	LKPD
H2000/2230-16	C	E	54	3B	JAMPT	JAMPT / RSA	JAMPT	JAMPT
H2000/2230-17	B	E	54	3B	JAMPT	JAMPT / SB	JAMPT	Sherwan
H2000/2301-176*	B	E	54	3A	SB	JAMPT / SB	JAMPT	Sherwan
H2000/2301-177*	B	E	54	3A	JAMPT	JAMPT / SB	JAMPT	JAMPT
H2001/2373-10	C	E	54	3B	RSA	RSA / SB	SKK	Sherwan
H2000/2753-17	E	E	55	3C	SB	SB / PD	PD	PD
H2000/2774-14	G	E	55	3C	SKK	SC / SKK	SC	Sherwan
H2000/2774-15	C	E	55	3C	SB	PD / SKK	SKK	PD
H2000/2789-30	C	E	55	3C	SKK	SKK / SB	SKK	Sherwan
H2000/2880-16	D	E	55	3C	ATM	ATM / RSA	SKK	JAMPT
H2001/2913-12	E	E	57	3B	SKK	SKK / SB	SKK	Sherwan
H2001/2920-7	C	E	57	S&D	SB	SB / SKK	SKK	Sherwan
H2001/2922-6	A	E	57	S&D	SB	SB / SKK	SB	Sherwan
H2001/2939-25	G	E	57	3B	LKPD	JAMPT / BESH	LKPD	LKPD
H90/3030-55	E	E	58	S&D	JAMPT	JAMPT / RSA	JAMPT	Sherwan
H90/3068-50	A	E	58	S&D	SB	SB / RSA	SB	PD
H90/3290-17	D	E	59	S&D	SB	SB / SKK	SB	Sherwan
H93/3534-13	F	E	2	S&D	SKK	RSA / SB	LKPD	Sherwan
H93/3710-16	F	E	3	3C	SB	SB / SKK	SB	Sherwan
H93/3710-70	F	E	3	3C	SB	JKK / SB	LKPD	LKPD
H93/3808-52	A	E	5	S&D	SB	SB / SKK	SKK	Sherwan
H93/3869-24	A	E	7	3C	SB	PD / SB	SKK	PD
H95/4453-22	D	E	11	S&D	SB	SB / SKK	SB	Sherwan

Artifact (year/lot-record)	Type	Mound / Area	Trench / Op.	Period	CDA predicted group membership (PGM)			
					full set 1st PGM	parent-rock 1st & 2nd PGM	11 dolomitic 1st PGM	regional dolomitic 1st PGM
H95/4613-42	A	ET	10	3B	SB	SKK / SB	SKK	Sherwan
H95/4615-94	A	ET	10	3C	SB	SKK / SB	SKK	Sherwan
H95/4723-2	B	ET	19	3C	SB	LKPD / RDP	LKPD	LKPD
H95/4726-101	A	ET	19	3C	LKPD	SB / PD	SB	PD
H95/4746-7	A	ET	19	3C	SB	SB / PD	SB	PD
H95/4751-8	E	ET	19	3C	SB	LKPD / ATM	SKK	Sherwan
H95/4919-62	D	ET	28	3C	ATM	RDP / SC	RDP	Jhunjhunu
H95/4950-4	A	ET	28	3C	RDP	SB / SKK	SKK	Sherwan
H95/4954-18	E	ET	28	3C	SB	SB / SKK	SKK	Sherwan
H95/4961-176	A	ET	28	3C	SB	SB / SKK	SKK	Sherwan
H94/5135-34	E	E	7 / 8	3C	SB	SB / SKK	SB	Sherwan
H95/5184-1	A	E	7 / 8	3C	SB	SB / SKK	SB	Sherwan
H95/5713-145	C	ET	32	S&D	SB	SB / PD	SB	Sherwan
H95/5734-31	C	ET	32	3C	SB	PD / SB	PD	PD
H95/5747-125	B	ET	32	3C	PD	SB / SKK	SB	Sherwan
H95/5749-97	C	ET	32	3C	SB	RSA / SB	SKK	Sherwan
H95/5759-25	E	ET	32	3C	SB	SB / PD	SB	PD
H95/5763-19	A	ET	32	3C	SB	SB / SKK	SB	Sherwan
H95/5802-5	A	ET	28	3C	SB	LKPD / BESH	LKPD	LKPD
H95/5803-25	B	ET	28	3C	LKPD	LKPD / BESH	LKPD	LKPD
H95/5820-11a	A	ET	28	3C	LKPD	PD / SB	PD	PD
H96/5837-18	B	ET	28	3C	PD	SB / LKPD	SB	LKPD
H96/6218-8	C	ET	35	S&D	LKPD	SKK / PD	SKK	PD
H96/6219-44	D	ET	35	S&D	SB	SB / LKPD	SB	Sherwan
H96/6234-2	C	ET	35	S&D	SB	SB / SKK	SB	Sherwan
H96/6257-21	A	ET	35	3C	SB	SB / SKK	SKK	Sherwan
H95/6509-97	B	E / ET	11	2	SB	JAMPT / RSA	JAMPT	JAMPT
H96/7105-8	A	E	36	3C	JAMPT	SKK / SB	SKK	Sherwan
H96/7106-27	G	E	36	3C	SKK	LKPD / RDP	LKPD	LKPD
H96/7118-9	A	E	36	3C	LKPD	LKPD / BESH	LKPD	LKPD
H96/7153-14	D	E	36	S&D	LKPD	SB / SKK	SB	Sherwan
H96/7156-14	G	E	36	3C	SB	SB / LKPD	SB	Sherwan
H96/7239-26	A	F	37	3C	SB	SB / SKK	SB	Sherwan
H96/7256-43	B	F	37	3B	SB	SKK / SB	SKK	Sherwan
H96/7257-46*	B	F	37	3B	SKK	PD / SB	PD	PD
H96/7333-22	A	AB	38	5	PD	SC / SC	SC	Sherwan
H96/7358-11	A	AB	38	5	SC	LKPD / SKK	LKPD	LKPD
H96/7401-63	F	AB	39	S&D	SC	SC / RDP	SC	Sherwan

Artifact (year/lot-record)	Type	Mound / Area	Trench / Op.	Period	CDA predicted group membership (PGM)			
					full set 1st PGM	parent-rock 1st & 2nd PGM	11 dolomitic 1st PGM	regional dolomitic 1st PGM
H96/7410-1	E	AB	39	2/3A	SKK	SKK / SB	SKK	Sherwan
H96/7410-2	E	AB	39	2/3A	SKK	SKK / SB	SKK	Sherwan
H96/7414-46	A	AB	39	2	SC	SC / SKK	SC	Sherwan
H96/7414-47	A	AB	39	2	JAMPT	JAMPT / LKPD	JAMPT	JAMPT
H96/7467-658*	A	AB	39	S&D	SKK	SB / JJG	ATM	S.RAJ
H96/7467-790	A	AB	39	S&D	RSA	RDA / SKK	SKK	Sherwan
H96/7531-16	A	AB	39	1	ATM	ATM / SB	ATM	Sherwan
H97/7619-3	C	F	41	3C	SB	SB / LKPD	SB	Sherwan
H99/7636-8	E	F	41	3C	JJK	JKK / ATM	RSA	Jhunjhunu
H99/7637-32	G	F	41	3C	JJK	JKK / RDP	LKPD	Jhunjhunu
H99/7638-1	G	F	41	3C	JJK	JKK / ATM	SB	Sherwan
H99/7649-42	A	F	41	3C	SB	SB / SKK	SB	Sherwan
H97/7780-10	E	AB	42	3B	SC	SC / SC	SB	Sherwan
H97/7780-8	A	AB	42	3B	SC	SC / SC	SC	Sherwan
H97/7780-9	A	AB	42	3B	SB	SB / SKK	SB	Sherwan
H97/7784-156	A	AB	42	3A	SKK	SKK / SC	SKK	Sherwan
H97/7784-157	F	AB	42	3A	RSA	RSA / LKPD	LKPD	LKPD
H97/7784-158	A	AB	42	3A	LKPD	LKPD / SB	LKPD	LKPD
H97/7784-159	A	AB	42	3A	SC	SC / SKK	SKK	Sherwan
H97/7784-16	A	AB	42	3A	RSA	RDA / SKK	RSA	Sherwan
H97/7784-17	A	AB	42	3A	JAMPT	JAMPT / SKK	SKK	JAMPT
H97/7784-18	A	AB	42	3A	USK	USK / SKK	USK	Uttaranchal
H97/7784-19	A	AB	42	3A	SC	SC / SKK	SC	Sherwan
H97/7784-20	A	AB	42	3A	USK	USK / SKK	USK	Sherwan
H97/7784-21	B	AB	42	3A	SB	SB / SKK	SB	Sherwan
H97/7784-22	C	AB	42	3A	JAMPT	JAMPT / SB	JAMPT	JAMPT
H97/7784-23	C	AB	42	3A	SB	SB / SKK	SKK	Sherwan
H97/7784-24	C	AB	42	3A	SKK	SKK / UB	SKK	Sherwan
H97/7784-25	A	AB	42	3A	JAMPT	JAMPT / SKK	SKK	JAMPT
H97/7784-27	A	AB	42	3A	LBW1	LBW1 / LBW2	-	-
H97/7784-28	B	AB	42	3A	SB	SB / SKK	SB	Sherwan
H97/7784-29	B	AB	42	3A	SC	LKPD / SC	SC	JAMPT
H97/7784-30	E	AB	42	3A	SB	SB / SKK	SKK	Sherwan
H97/7784-31	F	AB	42	3A	SC	SC / RDP	SC	LKPD
H99/7794-3	B	AB	42	3C	SB	SB / LKPD	SB	Sherwan
H98/8342-3	F	AB	39	3C	SC	SB / LKPD	SB	Sherwan
H98/8355-2	A	AB	39	3B	SB	SC / SKK	SC	Sherwan
H98/8364-5	F	AB	39	3B	SB	SB / SKK	SKK	Sherwan
H98/8407-39	E	AB	39	2	RSA	SB / SC	SB	Sherwan
H98/8407-40	A	AB	39	2	SC	RSA / USK	RDP	Uttaranchal
H98/8410-12	A	AB	39	2	SC	SC / SKK	SC	Sherwan

Artifact (year/lot-record)	Type	Mound / Area	Trench / Op.	Period	CDA predicted group membership (PGM)			
					full set 1st PGM	parent-rock 1st & 2nd PGM	11 dolomitic 1st PGM	regional dolomitic 1st PGM
H98/8486-50	A	AB	39	2	SKK	SC / SKK	SC	Sherwan
H98/8487-32	E	AB	39	2	JAMPT	SKK / SC	SKK	Sherwan
H98/8487-33	A	AB	39	2	PD	JAMPT / USK	JAMPT	JAMPT
H99/8490-103	B	AB	39	2	SC	PD / SKK	PD	PD
H99/8492-229	E	AB	39	2	SKK	SC / SKK	SC	Sherwan
H99/8497-3	E	AB	39	2	LKPD	SKK / SC	SKK	Sherwan
H98/8668-2*	E	F	43	3C	KOT	KOT / ZTT	-	-
H99/8760-77	F	F	43	3C	ATM	ATM / JKK	ANB	Jhunjhunu
H99/8956-1	A	AB	39	2	JAMPT	JAMPT / USK	SKK	Sherwan
H2000/8983-44	E	AB	39	2	LKPD	LKPD / SC	SC	Sherwan
H2000/8992-1	E	AB	39	2	JAMPT	JAMPT / RSA	JAMPT	JAMPT
H2000/8997-4	A	AB	39	2	JAMPT	JAMPT / USK	JAMPT	JAMPT
H2000/9442-2	E	AB	39	3B	SC	UB / SC	SC	Sherwan
H2000/9443-6	A	AB	39	3B	SKK	SKK / SC	SKK	Sherwan
H2000/9443-7	B	AB	39	3B	JAMPT	JAMPT / RSA	JAMPT	JAMPT
H2000/9445-1	G	AB	39	3B	ANB	ANB / ATM	ANB	Jhunjhunu
H2000/9445-2	G	AB	39	3B	LKPD	LKPD / SC	SC	LKPD
H2000/9447-5	A	AB	39	3B	SKK	SKK / SC	SC	Sherwan
H2000/9514-93	E	AB	39	2	JAMPT	JAMPT / SB	SB	JAMPT
H99/9737-22	A	F	43	3C	SB	SB / PD	SKK	PD
H99/9747-33	B	F	43	3C	SB	SKK / SB	SKK	Sherwan
H99/9756-16	A	F	43	3C	SB	SB / SKK	SB	Sherwan
H99/9779-4	A	F	43	3C	SB	SB / LKPD	SB	Sherwan
H2000/9840-8	E	F	43	3C	SB	SB / SC	SB	Sherwan
H2000/9973-13	C	AB	39	2	JAMPT	JAMPT / RSA	JAMPT	JAMPT
H2000/11001-6	A	AB	39	1	JAMPT	JAMPT / RSA	JAMPT	JAMPT
H2001/11562-26	F	E	11	S&D	SB	ATM / SB	SB	Sherwan
H2001/11923-9	C	E	11	3C	SB	SB / PD	SB	Sherwan
H90/3208-68**	A	E	59	3C	PD	PD/DGT	PD	PD

APPENDIX 7.2

STEATITE DEPOSITS IN PAKISTAN AND INDIA SAMPLED FOR THIS STUDY

Region	District / Agency	Deposit	Source code	Coordinates	Parent-Rock
Balochistan	Las Bela	Wayaro 1 (Duddo mine)	LBW1	≈ N 26° 02', E 66° 39'	Ultramafic
Balochistan	Las Bela	Wayaro 2 (Thaddi mine)	LBW2	≈ N 26° 00', E 66° 37'	Ultramafic
Balochistan	Zhob	Urgasai Nasir, Muslimbagh Ophiolite	ZUN	≈ N 30° 52', E 67° 39'	Ultramafic
Balochistan	Zhob	Takhahen, Muslimbagh Ophiolite	ZTAK	≈ N 30° 43', E 67° 52'	Ultramafic
Balochistan	Zhob	Tor Tangi, Muslimbagh Ophiolite	ZTT	≈ N 30° 56', E 67° 49'	Ultramafic
FATA	Kurram	Safed Koh (Parachinar-Daradar)	PD	≈ N 33° 57', E 70° 14'	Dolomite
FATA	Mohmand	Sakhakot-Qila Ophiolite (Kot)	KOT & Kot (MP)	≈ N 34° 27', E 71° 43'	Ultramafic
FATA	Khyber	Landi Kotal (Prang Dera)	LKPD	≈ N 34° 00', E 71° 05'	Dolomite
NWFP	Swat	Tangir mine (Besham-Derai area)	BESH	≈ N 35° 55', E 72° 50'	Dolomite
NWFP	Hazara	Sherwan - Khanda Khu	SKK	≈ N 34° 11', E 73° 03'	Dolomite
NWFP	Hazara	Sherwan - Bandi	SB	≈ N 34° 12', E 73° 02'	Dolomite
NWFP	Hazara	Sherwan - Chelethar	SC	≈ N 34° 12', E 73° 02' 30"	Dolomite
NWFP	Chitral	near Tar village, Shi Shi Valley	CHT	≈ N 35° 43', E 71° 57'	Ultramafic
Jammu	Udhampur	Painthal	JAMPT	N 32° 59.695, E 74° 59.097	Dolomite
Uttaranchal	Bageshwar	Chatikhet to Dungri to Kanda	UB	N 29° 52.286, E 79° 51.198	Dolomite
Uttaranchal	Bageshwar	Saling	US	N 30° 01.086, E 79° 56.742	Dolomite
Uttaranchal	Bageshwar	Shishi Khani	USK	N 29° 48.678, E 79° 46.374	Dolomite
Gujarat	Sarbarkantha	Dev Mori – Bhiloda & Kundol	DMB & DMK	N 23° 36.276, E 73° 23.050	Ultramafic
Gujarat	Panchmahal	Gandhra	GPM	N 22° 27.449, E 73° 41.372	Dolomite

Region	District / Agency	Deposit	Source code	Coordinates	Parent-Rock
Rajasthan	Alwar	Nangalhari-Bairaswas	ANB	N 27° 27.003, E 76° 24.209	Dolomite
Rajasthan	Alwar	Samra	ASM	N 27° 11.254, E 76° 13.929	Dolomite
Rajasthan	Alwar	Teori	ATM	N 27° 24.070, E 76° 08.880	Dolomite
Rajasthan	Jaipur	Degota	DGT	N 27° 06.122, E 76° 14.995	Dolomite
Rajasthan	Jhunjhunu	Chirani-ki-Dhani	JJC	N 28° 00.643, E 75° 48.522	Dolomite
Rajasthan	Jhunjhunu	Gurda	JJG	N 27° 48.847, E 75° 38.419	Dolomite
Rajasthan	Jhunjhunu	Kho	JJK	N 27° 47.218, E 75° 37.948	Dolomite
Rajasthan	Dungarpur	Deola	RDP	N 23° 53.762, E 74° 21.052	Dolomite
Rajasthan	Dungarpur	Manpur	RMP	N 23° 51.328, E 73° 45.714	Ultramafic
Rajasthan	Dungarpur	Shala Shah Thana	RST	N 24° 03.222, E 73° 40.115	Ultramafic
Rajasthan	Rajsamand	Karoli	RKA	N 24° 51.731, E 73° 45.499	Dolomite
Rajasthan	Rajsamand	Rabcha	RRA	N 24° 53.786, E 73° 47.074	Dolomite
Rajasthan	Udaipur	Dev Pura	RDV	N 24° 18.182, E 73° 46.715	Dolomite
Rajasthan	Udaipur	Kali Ghadi mine	RKG	≈ N 24° 07', E 73° 40'	Ultramafic
Rajasthan	Udaipur	Rishab-der	RRD	≈ N 24° 02', E 73° 38'	Ultramafic
Rajasthan	Udaipur	near Salumbar	RSA	N 24° 07.204, E 74° 07.356	Dolomite
Rajasthan	Udaipur	Shiv Bola mine	RSB	≈ N 24° 03', E 73° 38'	Ultramafic
Rajasthan	Udaipur	Khadi Ghati mine	RSH	≈ N 23° 59', E 73° 47'	Ultramafic

APPENDIX 7.3

INAA DATA FOR STEATITE SAMPLES COLLECTED FROM DEPOSITS IN PAKISTAN AND INDIA.

Data in parts per million (PPM)

Sample	Al	Co	Cr	Eu	Fe	La	Mn	Na	Sc	V	Zn
ANB-01	10838	3.9488	10.59	0.05794	11394	0.11851	19.309	8070.88	0.0914	14.73	51.54
ANB-02	3132	7.3863	18.501	0.09754	16045	0.45252	29.321	1535.31	1.0496	27.033	41.686
ANB-03	8829	5.6125	27.046	0.09216	13640	0.73486	29.457	6347.02	0.8313	34.387	27.745
ANB-04	7410	5.8687	14.154	0.10109	13597	0.66108	24.943	5285.76	0.3912	28.835	37.634
ANB-05	3091	3.4451	26.685	0.43534	11673	7.81245	25.551	74367.16	0.3194	14.189	20.415
ANB-06	22469	0.3813	2.237	0.3038	70	0.48679	17.283	18026.28	0.0108	11.905	14.381
ANB-07	4773	4.4095	7.093	0.08936	14249	0.18589	26.341	3288.62	0.3825	13.995	45.756
ANB-08	6040	5.0426	13.26	0.09656	14669	0.35191	23.527	5162.58	0.2676	14.967	47.48
ANB-09	2328	4.5184	6.484	0.10308	15652	0.12945	30.896	1238.02	0.7509	12.448	46.318
ANB-10	1749	6.296	2.247	0.08499	15789	0.25353	26.296	613.34	0.2643	14.709	45.772
ASM-01	5041	62.0628	2.915	0.23708	38576	3.89395	119.895	607.59	6.1815	21.671	37.106
ASM-02	6884	82.9666	2.914	0.06382	37394	0.12002	53.078	900.75	2.4121	15.407	33.901
ASM-03	6102	52.2559	1.932	0.89868	38991	16.74099	80.896	656.7	7.9921	27.205	12.812
ASM-04	2822	51.9297	2.884	0.26342	29682	0.06561	49.394	473.77	1.4676	11.472	68.865
ASM-05	41383	72.0259	49.15	0.21734	65274	0.44792	218.157	660.62	29.7642	166.489	137.797
ASM-06	2960	53.3159	3.713	0.31987	30370	0.11255	55.553	459.96	1.4998	12.165	70.003
ASM-07	4970	66.6679	3.141	0.27488	41526	0.21308	80.665	586.59	5.0374	23.166	87.085
ASM-08	33971	20.3045	5.084	0.32132	41635	4.06409	97.341	14805.97	4.1106	26.794	84.438
ASM-09	7119	82.8355	3.964	0.13809	38061	0.16251	55.816	974.15	3.1366	14.85	84.884
ASM-10	65164	22.2235	3.077	1.60397	38030	2.13848	124.022	25641.84	25.3054	72.457	142.649
ATM-01	1677	6.2143	2.813	0.07908	20473	0.22484	25.001	390.68	0.3548	5.183	6.095
ATM-02	5810	2.1351	14.64	0.09001	32356	0.31447	41.247	3644.99	0.6938	7.196	6.275
ATM-03	5159	14.9285	10.38	0.07973	28458	0.27459	22.405	3328.93	0.6876	12.313	3.8
ATM-04	3889	1.5232	15.73	0.05143	31239	0.16566	35.516	2273.82	0.7773	7.15	22.18
ATM-05	6721	3.3619	17.187	0.04968	26144	0.29461	41.465	3225.97	0.52	9.717	32.15
ATM-06	5730	2.6302	18.141	0.07411	26532	0.14313	38.372	3462.39	0.708	7.576	29.552
ATM-07	9607	1.5114	5.15	0.17968	20752	0.39987	30.897	6358	3.2441	25.09	35.433
ATM-08	2768	2.8818	15.25	0.32287	21113	4.71459	25.715	1228.56	1.3072	4.128	98.035
ATM-09	3756	2.9824	19.677	0.06657	23758	0.2293	33.263	1789.4	0.5454	6.506	139.586
ATM-10	8376	1.9656	21.103	0.09169	33995	0.27174	47.483	5491.45	0.6311	12.428	52.167
BESH-01	2239	8.139	6.345	0.05292	14530	0.2215	82.44	219.3	0.1118	4.788	568.6
BESH-02	2257	6.908	2.858	0.05239	11990	0.2898	87.76	179.2	0.189	5.007	434.8
BESH-03	3139	2.064	2.489	0.04839	8117	0.3212	48.53	139.2	0.0947	2.744	531.9
BESH-04	71670	11.02	8.56	0.04323	44940	0.3287	487.6	296.5	0.5624	55.65	1296
BESH-05	3643	1.865	1.965	0.03865	2861	0.1833	9.407	279.7	0.2165	2.726	43
BESH-06	3445	1.464	1.382	0.03483	5227	0.1617	54.12	165.7	0.0633	3.581	385.8
CHT-05	105750	20.1943	120.602	0.27555	19625	0.55821	939.388	611.05	9.7798	38.55	13.247
CHT-06	5938	116.4152	2884.07	0.08195	43116	0.43713	486.602	166.03	3.8576	24.764	15.172
CHT-07	4602	100.327	2201.815	0.08196	41532	0.83485	513.342	185.47	4.4241	20.801	11.143
CHT-08	3309	95.8852	1084.921	0.2157	42565	1.35871	1069.746	136.54	6.9632	18.399	13.617
CHT-09	7353	118.8686	2890.156	0.19991	42785	0.38929	538.488	134.39	6.8112	49.121	16.443
CHT-10	10114	101.4568	2551.579	0.08495	35019	0.81213	502.177	136.86	3.29	27.145	12.231
CHT-11	107126	79.1107	130.3	0.06972	57412	0.0254	995.937	154.67	2.2985	9.9	20.765
CHT-12	4467	94.7426	2246.069	0.08479	39322	0.43779	470.692	161.75	3.3723	22.757	12.124
CHT-13	107120	47.0076	854.304	0.09972	30458	0.77108	1113.708	222.22	25.6847	73.995	16.853
CHT-14	114231	39.0685	585.932	0.13376	30470	1.82156	1172.146	179.6	23.9586	77.056	16.036
CHT-15	107996	17.6785	93.941	0.14288	17011	0.13516	981.748	4771.21	6.0683	23.332	15.953
CHT-16	7886	52.5927	1001.07	0.05159	36690	0.15301	289.861	131.79	5.6678	29.849	8.673
CHT-17	5249	92.6355	3230.896	0.19414	49392	0.24402	501.981	149.64	4.1732	32.134	14.29

Sample	Al	Co	Cr	Eu	Fe	La	Mn	Na	Sc	V	Zn
CHT-18	6080	108.8336	2335.358	0.31449	41961	0.39644	523.869	130.7	6.6138	34.36	15.347
CHT-19	5240	96.6386	3822.27	0.21664	48799	0.38621	519.646	138.69	3.6297	29.835	24.565
CHT-20	1521	27.1111	399.325	0.22573	17480	0.02248	147.894	203.58	2.3574	4.388	8.673
DGT-01	10669	6.0233	13.351	0.18205	8559	0.28125	21.665	226.72	4.3521	15.589	7.858
DGT-02	6703	7.6544	4.305	0.1176	13183	0.11123	38.973	237.82	2.5701	12.083	7.886
DGT-03	9187	6.469	11.263	0.10631	6614	0.19383	23.168	206.25	2.3182	12.165	6.9
DGT-04	16087	14.8073	10.463	0.08876	17581	0.28503	43.289	235.76	5.5005	28.033	9.31
DGT-05	7106	4.67	7.774	0.15633	3893	0.29221	21.524	219.67	1.8603	10.558	6.297
DGT-06	8457	4.861	7.84	0.09832	4156	0.04864	13.788	222.64	2.0799	13.015	3.478
DGT-07	3448	9.2071	3.588	0.11251	14814	0.14959	44.825	312.87	1.1908	6.467	7.178
DGT-08	2883	6.9818	0.829	0.10871	6783	0.03726	18.495	265.13	1.0948	5.572	6.274
DGT-09	10254	15.5073	11.945	0.12889	17041	0.2382	33.675	250.97	3.7338	16.161	48.875
DGT-10	9762	5.0405	12.938	0.17957	4672	2.44249	9.477	240.51	3.0705	13.624	55.805
DMB-01	9513	84.7546	1426.757	0.14157	27827	0.14541	126.587	137.19	4.714	20.145	84.789
DMB-02	7540	86.5644	1286.542	0.09382	28275	0.13249	122.483	236.04	3.9437	18.922	83.137
DMK-01	9025	50.7741	941.29	0.06221	19443	0.03357	398.081	108.67	3.0674	24.211	9.745
DMK-02	3126	55.953	923.911	0.10377	23669	0.10086	175.869	157.69	2.7086	12.054	10.73
DMK-03	1945	64.8495	187.698	0.08588	28092	0.04729	246.996	167.09	0.7702	3.661	23.205
DMK-04	7331	67.5889	1095.566	0.12478	29451	0.02708	276.361	140.55	1.4461	16.281	18.978
DMK-05	9726	72.9098	1291.936	0.08284	30920	0.03825	277.173	187.79	5.7345	22.016	11.968
DMK-06	6589	77.828	1126.932	0.09159	32582	0.03555	257.156	159.3	5.273	18.443	11.963
DMK-07	6328	60.0072	1370.227	0.11073	32866	0.05718	226.01	147.65	5.8568	23.149	11.444
DMK-08	5029	87.129	1631.007	0.13266	30083	0.05934	278.276	157.09	3.1263	17.79	13.005
DMK-10	3828	96.9284	1628.703	0.08653	32379	0.04035	253.713	162.39	3.3557	15.465	12.12
DMK-11	6680	90.6609	1716.564	0.11786	37669	0.05292	310.524	175.81	5.1705	29.491	102.259
DMK-12	18079	74.7236	2491.719	0.09747	38212	0.07968	386.375	120.61	5.6655	38.142	100.534
DMK-13	6697	96.1327	1494.2	0.0863	33717	0.08049	319.308	161.22	4.7049	15.306	102.422
DMK-14	6098	90.6916	1671.748	0.08014	36766	0.07244	318.308	149.75	4.6683	29.821	57.39
DMK-15	7713	83.6133	1541.921	0.08714	35100	0.07953	238.198	183.59	6.0348	22.563	72.089
DMK-16	3225	55.6025	791.463	0.0832	19492	0.05119	137.389	88.17	2.5608	6.481	69.765
DMK-17	5706	92.1768	1170.556	0.06766	30559	0.0727	297.37	212.33	2.9652	13.617	82.295
DMK-18	76891	98.897	3065.504	0.06562	63635	0.11517	872.518	150.57	10.1874	91.289	109.359
DMK-20	8093	84.8584	1796.771	0.10074	35358	0.15849	319.981	129.71	6.5988	29.382	93.062
GPM-01	5423	8.4175	10.122	0.50112	45689	1.11776	1304.832	204.77	1.5511	13.204	8.091
GPM-02	24289	23.1947	26.854	0.35009	23633	17.94244	50.918	263.98	1.3009	37.809	9.167
GPM-03	9627	24.8549	24.57	0.14107	19216	1.2355	36.125	218.12	0.4534	14.297	5.547
GPM-04	3752	24.0747	10.587	0.12255	18928	0.22539	118.464	218.97	0.3317	6.994	4.621
GPM-05	7668	19.366	14.075	0.28667	20726	4.46669	37.266	210.07	0.4143	11.93	7.647
GPM-06	5999	15.6893	8.417	0.10437	17532	0.58996	29.731	192.49	0.3097	9.737	7.407
GPM-07	8133	19.3785	13.304	0.25141	21316	4.34528	36.563	206.06	0.4585	14.519	4.98
GPM-08	1498	18.5584	25.875	0.12068	29505	0.05865	54.423	285.49	0.0747	10.443	39.973
GPM-09	4279	19.22	8.61	0.19906	36804	0.23435	147.245	360.61	1.1449	14.331	31.427
GPM-10	5561	36.8421	25.899	0.16076	29597	0.45556	54.699	353.48	0.5022	7.632	7.623
GPM-11	18993	14.8698	61.788	0.46786	26801	6.35172	56.388	205.27	0.9813	48.626	64.933
GPM-12	7446	19.5151	12.835	0.33685	21322	4.06235	42.238	198.83	0.4171	10.7	42.227
GPM-13	1781	8.3863	10.379	0.12722	19072	0.12013	51.999	205.65	0.9786	12.944	51.959
GPM-14	1335	12.6894	4.039	0.10503	21446	0.05999	74.57	196.98	0.0397	9.987	216.002
GPM-15	22140	28.7355	25.059	0.31456	24413	7.25684	123.649	197.34	1.1818	33.229	69.755
GPM-16	10669	22.1336	15.308	0.2314	20895	6.09588	37.484	218.02	0.4693	14.147	35.495
GPM-17	22519	8.5138	25.909	0.4299	27974	4.20658	69.799	186.57	2.2795	37.216	62.572
GPM-18	14257	22.9619	25.549	0.31974	22123	11.46318	36.009	239.07	0.6139	18.512	38.234
GPM-19	85546	45.6732	208.263	2.15307	61127	64.98015	226.23	283.9	6.8655	173.279	127.264
GPM-20	10051	13.7382	17.975	0.36369	22320	1.32386	40.08	225.71	1.327	21.891	58.115
JAMPT-01	1379	0.833	3.804	0.07126	9150	0.10014	12.848	189.04	0.0403	1.059	21.178
JAMPT-02	1247	8.2883	6.595	0.07072	38615	0.17226	21.009	179.33	0.0356	1.283	132.905
JAMPT-03	1499	0.5007	0.795	0.07731	14379	0.0715	34.591	234.9	0.0313	1.024	42.897
JAMPT-04	1237	0.7343	0.741	0.08361	17375	0.05548	11.869	144.93	0.0236	0.879	37.654
JAMPT-05	1008	0.6014	0.602	0.07076	15601	0.06094	9.419	162.48	0.011	0.736	30.932

Sample	Al	Co	Cr	Eu	Fe	La	Mn	Na	Sc	V	Zn
JAMPT-06	1312	0.6122	1.141	0.06523	13932	0.04025	13.107	173.56	0.022	0.86	16.417
JAMPT-07	1075	0.4282	0.624	0.07321	6567	0.05699	7.349	155.13	0.0219	0.841	19.32
JAMPT-08	1156	0.4964	0.446	0.07473	14706	0.05947	8.836	165.15	0.0171	0.757	27.459
JAMPT-09	1174	0.4168	0.68	0.06992	5232	0.08573	8.023	177.25	0.0346	0.657	26.997
JAMPT-10	1334	0.3708	0.5	0.06937	9528	0.05464	6.995	180.79	0.0223	1.023	25.009
JAMPT-11	1093	0.2597	1.882	0.08931	5597	0.04213	5.976	168.91	0.0272	0.705	15.003
JAMPT-12	1144	0.2401	0.471	0.06716	7817	0.01537	6.731	183.36	0.0243	0.469	14.549
JAMPT-13	1145	0.2698	1.544	0.06486	4570	0.02788	6.138	159.5	0.0247	0.975	15.477
JAMPT-14	1136	0.2078	0.727	0.05722	9072	0.02466	7.328	164.36	0.0366	1.213	15.572
JAMPT-15	1461	0.6933	0.537	0.06947	13019	0.03613	9.81	360.55	0.0188	0.794	18.599
JAMPT-16	1117	0.2918	0.751	0.05119	4755	0.0436	6.677	197.6	0.0231	0.756	15.213
JAMPT-17	1157	0.2158	0.522	0.07858	7256	0.0226	6.683	155.56	0.0196	0.806	13.54
JAMPT-18	1309	0.5034	0.947	0.0683	15084	0.02816	10.079	207.54	0.0143	0.618	20.928
JAMPT-19	1252	0.5468	1.002	0.06902	14749	0.02474	11.595	172.46	0.0159	0.775	20.737
JAMPT-20	1261	0.5621	1.069	0.07926	10466	0.09022	77.548	199.55	0.0366	1.116	35.229
JJC-01	6990	0.1853	0.33	0.04307	44	0.0534	154.999	322.91	0.0031	18.148	40.135
JJC-02	9246	6.0981	4.845	0.08487	14310	0.11995	157.802	340.18	2.9137	21.823	33.726
JJC-03	1758	0.2027	0.314	0.05447	47	0.06793	133.854	283.87	0.0035	3.316	48.914
JJC-04	2243	0.2351	0.353	0.04411	33	0.05856	114.642	266.95	0.0041	4.651	43.524
JJC-05	2623	0.3619	2.491	0.35008	54	0.49835	116.724	275.82	0.0149	6.455	22.291
JJC-06	8952	0.3187	2.359	0.34139	70	0.50709	156.497	263.83	0.012	20.164	17.807
JJC-07	2102	0.3348	2.89	0.38883	48	0.45103	109.128	269.15	0.0134	12.832	18.612
JJC-08	5299	0.3794	2.419	0.35955	81	0.58381	137.744	252.38	0.0156	14.179	18.696
JJC-09	6518	14.0348	19.601	0.45997	29285	121.5312	154.907	16319.96	2.3598	8.874	14.725
JJC-10	13627	12.7119	55.899	0.50571	29840	15.606	189.93	12565.6	5.5855	34.026	15.437
JJG-01	24526	3.9645	17.9	0.12391	15274	3.87767	87.915	232.67	2.9505	43.847	19.097
JJG-02	31808	0.1741	0.386	0.04072	36	0.04949	103.295	197.85	0.0043	72.347	46.122
JJG-03	19978	3.5207	12.767	0.14479	15193	1.51699	98.624	180.98	1.9723	43.19	30.886
JJG-04	33843	9.5106	45.377	0.17243	35365	4.71019	107.383	131.62	8.027	72.892	47.839
JJG-05	14324	7.2124	25.284	0.12033	30075	0.276	90.922	233.52	3.0565	28.216	68.592
JJG-06	41385	8.3865	53.056	0.29927	44328	4.54264	132.624	263.58	7.4134	64.043	82.375
JJG-07	29566	8.0928	38.079	0.22674	42270	3.84057	142.426	180.17	4.1784	53.333	76.196
JJG-08	70593	8.5728	48.814	0.59401	58928	3.91057	207.489	146.86	15.8474	118.727	108.747
JJG-09	31927	7.2202	11.035	0.09705	40467	0.16359	143.197	173.91	3.0742	40.962	88.855
JJG-10	28399	8.1931	35.435	0.50814	39406	16.65383	118.204	241.17	4.7817	47.249	43.502
JJK-01	3685	1.5753	1.563	0.05508	9231	0.04987	70.293	180.6	0.199	8.964	74.401
JJK-02	9728	3.3094	15.843	0.06036	18837	0.32648	69.267	191.34	1.6718	62.173	25.558
JJK-03	1541	0.2276	0.383	0.05303	30	0.04577	50.93	144.2	0.0053	5.093	6.201
JJK-04	9180	3.222	21.099	0.1403	19488	0.22823	67.95	244.11	1.9481	74.254	57.605
JJK-05	4954	2.1792	10.648	0.11419	15938	0.1372	44.129	224.29	0.6567	15.755	91.888
JJK-06	4680	2.8266	8.905	0.08363	14772	0.07184	54.351	229.28	0.8224	11.835	89.123
JJK-07	4302	4.1537	4.475	0.11697	20532	0.19185	59.809	263.57	0.369	5.968	266.065
JJK-08	14232	4.292	30.599	0.1115	22809	0.20238	84.792	254.2	2.3877	105.191	61.789
JJK-09	2227	3.8478	6.223	0.09316	20382	0.04504	50.226	217.11	0.2755	12.34	141.149
JJK-10	8797	3.5129	14.861	0.09683	18827	0.17594	61.967	232.05	1.4878	76.901	86.732
Kot(MP-1)	2224	84.15	1370	0.3512	42290	0.4218	325.2	120.3	6.14	22.75	57.54
Kot(MP-2)	11890	89.55	1828	0.455	41910	0.06993	182.7	123.6	6.013	38.13	64.48
Kot(MP-3)	9966	85.24	1553	0.4414	42190	0.06743	210.2	95.51	5.297	31.26	60.18
Kot(MP-4)	1445	81.17	2616	0.4146	39760	0.06211	229	52.98	1.672	23.41	96.78
KOT-01	10279	113.6252	4662.838	0.47283	71332	0.09096	1020.337	140.8	3.1707	262.556	30.659
KOT-02	53791	83.8528	1244.02	0.51041	37434	0.08981	591.108	161.8	6.9744	88.666	15.921
KOT-03	15370	80.674	2125.4	0.49256	42682	0.09401	209.666	156.7	6.6963	23.692	15.845
KOT-04	62687	103.0556	2546.115	0.51432	43187	0.0898	885.357	169.11	3.5859	136.785	15.27
KOT-05	7121	87.4994	1451.672	0.57215	35729	0.08799	750.593	167.94	3.6289	70.172	9.443
KOT-06	4617	88.82	1602	1.297	35770	0.1033	115	100.5	2.477	14.81	41.18
KOT-07	35610	94.41	3627	2.567	46870	0.05429	555.5	146.7	4.574	107	44.25
KOT-08	7249	78.21	1341	2.519	42010	0.05985	374	191.8	6.299	66.71	33.18

Sample	Al	Co	Cr	Eu	Fe	La	Mn	Na	Sc	V	Zn
KOT-09	20820	83.82	1367	1.722	38630	0.07753	465.3	213.4	8.406	56.93	34.08
KOT-10	20290	102.8	3201	0.4078	46990	0.05813	376	176.7	4.287	58.37	38.76
KOT-11	21940	104.1	3291	0.3911	48490	0.0676	325.1	102.4	4.372	50.08	37.92
KOT-12	19628	92.7521	2402.644	0.08404	47647	1.00427	375.772	127.32	14.3725	55.517	55.978
KOT-13	16008	85.888	1802.188	0.07151	41634	0.87432	341.235	126.68	11.0025	43.475	51.601
KOT-14	2568	89.6967	3299.438	0.05287	45061	0.63052	413.515	144.35	1.9482	43.783	150.44
KOT-15	28960	106.6857	5386.251	0.06334	56553	0.83591	451.561	169.64	5.4215	98.399	77.618
KOT-16	25264	102.4266	3539.983	0.05471	48325	0.80864	368.535	132.62	5.4055	55.365	52.277
LBW1-01	10660	59.19	1864	0.08683	23610	0.5173	142.1	758	8.342	31.64	11.06
LBW1-02	7436	41.91	1974	0.09187	16530	7.333	61.96	443.9	8.863	29.02	10.56
LBW1-03	3059	46.61	777.6	0.05207	13680	0.02384	44.93	246.3	2.19	13.98	4.723
LBW1-04	3034	43.8	843.2	0.04536	12080	6.337	28	369.3	2.328	10.58	7.056
LBW1-05	2558	49.59	463.9	0.08829	16230	0.0439	38.18	371.7	3.071	6.412	10.93
LBW1-06	3617	51.4	1042	0.1002	16170	0.05558	124.8	649	2.465	13.03	11.66
LBW1-07	3749	6.491	248.6	0.03634	1910	0.02159	65.07	158.8	1.106	13.02	5.711
LBW1-08	3958	27.07	1292	0.1028	9074	0.07589	72.03	626.5	4.915	17	11.2
LBW1-09	3501	43.13	1055	0.08619	13170	0.02603	24.79	400.8	3.098	12.94	10.42
LBW1-10	3248	26.25	708.6	0.09374	8610	0.05953	68.74	664.4	3.638	11.05	10.47
LBW2-01	1232	31.4654	6.137	0.03603	10011	0.12838	22.476	447.95	0.3155	1.706	7.006
LBW2-02	11688	56.1296	3863.705	0.10088	17940	0.33392	55.316	1604.29	15.9825	55.378	15.986
LBW2-03	1372	36.3546	9.285	0.03629	9804	0.12717	20.708	618.21	0.2633	1.176	5.357
LBW2-04	1660	53.0697	111.371	0.04283	15897	0.16725	34.424	755.26	0.5807	2.231	8.672
LBW2-05	2100	87.9788	405.484	0.06212	22286	0.23746	39.51	1308.92	1.85	4.668	12.607
LBW2-06	1906	46.2385	11.993	0.05484	12980	0.15548	18.246	919.94	0.5179	4.225	9.03
LBW2-07	3731	75.4578	1644.424	0.0724	19356	0.25201	44.295	1757.21	3.8246	16.088	13.461
LBW2-08	3471	77.0846	1020.591	0.07091	19851	0.26522	50.84	1574.25	3.0339	10.61	12.883
LBW2-09	2455	54.9975	1735.822	0.06796	16819	0.2671	38.334	1689.31	5.1673	11.811	13.381
LBW2-10	3616	81.0977	582.736	0.06905	22328	0.29036	52.205	1882.59	4.7158	13.003	14.7
LKPD-01	2051	0.3951	0.788	0.05787	1660	0.16213	95.797	174.46	0.0326	1.381	184.104
LKPD-02	1538	2.3073	0.875	0.05326	8403	0.1397	84.793	199.83	0.0774	1.958	422.641
LKPD-03	2109	3.1554	1.525	0.05194	7896	0.14352	25.502	338.9	0.2482	6.269	190.661
LKPD-04	1921	2.2941	1.296	0.06186	8433	0.14596	85.461	190.35	0.0845	2.609	402.98
LKPD-05	4285	1.5973	2.489	0.05774	6349	0.17328	31.139	336.65	0.4567	11.052	164.716
LKPD-06	2322	0.4071	1.309	0.05971	1677	0.14938	61.943	191.1	0.0344	2.407	186.883
LKPD-07	2034	0.37	0.963	0.05757	3071	0.1666	23.069	438.97	0.3495	4.941	148.966
LKPD-08	35547	0.6907	1.348	0.05251	3874	0.28324	156.189	188.66	1.8086	7.207	131.423
LKPD-09	54080	0.5053	5.901	0.29823	4981	3.03927	216.854	179.41	1.3464	11.733	156.365
LKPD-10	47133	0.703	1.1	0.13176	4669	7.01164	201.454	161.14	3.1181	8.916	94.654
LKPD-11	2200	0.2177	0.591	0.46942	2570	0.04167	103.658	165.17	0.0346	1.252	40.244
LKPD-12	74984	0.5204	0.88	0.48371	4534	1.28103	327.576	177.24	2.6154	12.668	26.948
LKPD-13	10140	0.2617	0.744	0.45007	3787	0.0258	89.243	402.87	0.373	24.489	20.984
LKPD-14	8210	2.4173	0.557	0.45439	8814	0.03559	119.224	428.89	0.7501	17.36	18.662
LKPD-15	99602	0.4038	0.808	0.49246	3303	0.09141	446.06	223.34	1.4668	21.341	22.068
LKPD-16	3747	0.9298	7.391	0.3593	5010	0.1431	30.83	328.2	0.3951	11.82	148.7
LKPD-17	4805	1.139	7.493	1.434	5172	0.1837	29.39	321.7	0.4798	14.56	148.7
LKPD-18	2207	1.322	7.598	0.9421	6460	0.2588	10.47	116.4	0.7434	5.121	146.7
LKPD-19	7085	1.477	6.421	1.014	6741	0.2308	33.94	312.2	0.7042	20.43	138.3
LKPD-20	2208	0.4501	1.753	0.9406	1471	0.04287	47.36	178.9	0.0372	1.85	130.4
PD-01	1708	2.0044	0.791	0.05249	1470	0.25221	1.576	192.06	0.0715	1.907	31.22
PD-02	1762	24.0847	1.267	0.06126	27885	0.32545	77.307	212.95	0.15	2.364	190.765
PD-03	1687	0.8221	0.585	0.0515	770	0.35255	2.133	212.97	0.0471	1.205	15.468
PD-04	1719	2.5871	1.762	0.06186	4086	1.71931	5.96	177.04	0.0323	1.834	33.842
PD-05	1649	1.2068	0.707	0.05036	1121	0.26823	5.567	179.2	0.019	1.339	49.572
PD-06	2011	1.547	0.969	0.05174	1938	0.2444	4.627	243.83	0.0414	3.216	29.786
PD-07	1785	1.6196	0.873	0.05185	1427	1.10195	2.256	304.84	0.0305	2.678	9.692
PD-08	1755	1.0971	0.758	0.03522	678	0.05414	2.098	193.62	0.0371	1.676	9.562
PD-09	1687	2.2671	0.723	0.02724	1478	0.13537	2.251	333.59	0.0601	1.727	8.395

Sample	Al	Co	Cr	Eu	Fe	La	Mn	Na	Sc	V	Zn
PD-10	1634	1.9469	1.07	0.02631	4469	0.09727	2.385	347.6	0.1025	1.891	8.301
PD-11	1901	13.3491	1.884	0.04549	9939	0.02515	6.556	213.79	0.0895	4.86	43.288
PD-12	1838	6.3418	1.454	0.05649	3572	0.03023	3.386	226.66	0.0253	1.474	16.003
PD-13	3385	2.1819	1.731	0.04645	1423	1.38453	7.321	229.33	0.0929	3.427	51.006
PD-14	1531	1.6763	1.514	0.05012	3215	0.02343	3.549	232.32	0.0517	1.565	60.547
PD-15	1669	0.8269	0.877	0.05848	711	0.08888	1.124	244.46	0.0555	1.626	36.693
PD-16	1636	0.6701	1.327	0.0456	599	0.01505	1.573	233.02	0.0305	2.092	33.997
PD-17	1864	6.6076	1.66	0.05783	3730	0.02943	3.135	253.33	0.0205	1.41	69.406
PD-18	1443	1.0907	1.7	0.04861	817	0.23827	1.36	210.08	0.018	1.232	54.408
PD-19	1586	1.508	1.059	0.0457	3323	0.04488	2.753	163.88	0.0444	1.556	63.227
PD-20	1675	1.4727	1.505	0.04203	2525	0.0915	2.43	178.06	0.0498	2.348	67.608
RDP-01	5271	4.3582	6.633	0.08545	9816	0.07692	38.649	190.92	0.5778	8.007	32.223
RDP-02	4017	5.3453	11.976	0.21093	9244	0.97501	139.822	174.22	0.9065	7.178	36.126
RDP-03	1827	2.1209	1.287	0.12915	8172	0.37762	49.829	136.72	0.4865	4.354	27.368
RDP-04	2222	3.7109	2.236	0.09766	9009	0.29137	31.201	175.5	0.3351	5.978	34.155
RDP-05	16128	3.6427	24.507	0.28277	9790	11.34843	28.445	210.79	2.4715	29.819	29.303
RDP-06	25674	5.1891	19.756	0.16445	13951	0.89244	96.172	144.96	3.6496	38.567	34.924
RDP-07	6060	7.022	8.102	0.18126	12505	0.72266	199.698	282.53	1.4424	10.709	27.21
RDP-08	2194	3.1073	4.06	0.06276	7655	0.19639	21.792	155.31	0.4748	4.235	32.6
RDP-09	3993	3.6526	5.685	0.10229	9492	0.666	29.303	141.79	0.8559	5.87	25.754
RDP-10	5393	2.6156	7.629	0.28016	8265	6.02314	30.581	170.28	0.7634	8.998	15.855
RDP-11	14130	1.001	1.932	0.6374	2349	6.835	93.57	409	4.714	68.05	31.07
RDP-12	5914	1.066	1.259	0.5266	2030	1.016	47.38	494.9	1.764	32.72	27.36
RDV-01	1276	2.4106	2.889	0.06526	5421	4.19301	17.907	171.61	0.0174	0.728	252.903
RDV-03	1429	1.815	1.44	0.08685	9155	6.20208	29.915	211.25	0.0123	1.3	265.764
RDV-04	1185	4.7467	12.954	0.08755	7060	6.30798	161.048	191.87	0.0154	1.476	226.255
RDV-05	1702	2.0008	1.913	0.10625	4599	5.85611	17.732	288.6	0.0104	2.885	242.49
RDV-06	1713	1.9793	1.656	0.07648	4845	5.32474	16.932	264.39	0.0155	1.455	210.027
RDV-07	1770	2.1028	2.56	0.10252	4540	6.25825	14.528	255.05	0.0128	2.049	252.823
RDV-08	2051	2.6776	5.734	0.08093	7739	7.94283	18.702	269.81	0.0722	2.893	286.477
RDV-09	1439	3.0189	2.445	0.06672	7703	7.14964	31.822	204.4	0.0224	1.031	280.178
RDV-10	2092	2.5326	6.563	0.11189	7603	12.04493	21.418	247.51	0.0537	3.022	268.293
RKA-01	36172	23.83	50.719	0.16931	33503	1.50299	200.752	463.67	11.7137	87.37	48.14
RKA-02	91679	25.2074	156.835	0.45671	45416	8.79662	191.203	243.28	24.5474	178.612	61.182
RKA-03	34650	23.9842	73.438	0.2052	29006	1.30315	93.675	398.14	10.5958	72.636	43.974
RKA-04	50546	23.9374	114.613	0.30406	38445	6.18829	167.121	230.42	16.5218	100.02	53.707
RKA-05	31487	23.902	70.71	0.41156	27138	11.61102	106.731	472.39	9.8072	71.977	12.736
RKA-06	41174	24.4836	83.459	0.11351	32260	2.05011	107.38	460.43	12.9429	81.43	13.144
RKA-07	56076	24.6131	144.295	0.2681	40377	8.75675	173.149	368.64	17.8488	110.471	15.011
RKA-08	58897	28.6735	103.171	0.23479	41109	4.81383	130.934	394.48	15.5174	98.947	14.308
RKA-09	8412	16.9576	61.345	0.9113	11031	28.87787	32.796	496.9	3.1146	28.916	11.431
RKA-10	50454	24.9277	101.51	0.25482	37012	7.75869	160.896	419.23	15.1434	110.402	14.195
RKA-11	53340	54.19	29.97	0.4953	47750	0.5519	79.43	186	15.01	123.2	51.65
RKA-12	184400	0.5864	35.26	2.415	744	29.34	7.861	7881	31.44	144	46.86
RKA-13	41710	39.21	2.555	1.889	46280	1.674	60.43	65.5	20.13	66.25	40.54
RKA-14	34190	65.27	125.1	2.623	46150	10.88	72.37	121.9	15.63	96.07	38.12
RKA-15	79640	28.44	4.366	0.5778	29210	1.206	120.7	310.8	12.71	123.8	72.2
RKA-16	70870	30.31	5.881	1.424	31840	27.91	101.6	291.5	12.25	104.3	76.12
RKA-17	72770	53.54	67.71	0.4946	44240	3.493	103.8	299.6	14.64	181.8	84.91
RKA-18	67490	52.78	62.47	1.636	45120	1.075	108.1	251.7	14.21	161.7	38.92
RKA-19	172100	0.6079	31.54	0.5417	962	32.71	8.845	7923	30.91	117.3	64.66
RKA-20	220300	39.52	4.618	0.691	42080	0.3581	283.8	228.6	15.68	343.1	50.73
RKG-01	6740	109.2	2033	0.08467	50120	0.5585	220	132.9	6.802	28.66	89.53
RKG-02	4630	93.52	6092	0.08067	66190	0.5236	577.3	217	3.383	42.26	182.2
RKG-03	1076	81.86	20.62	0.05123	13750	0.3278	100.7	123	0.162	0.911	104.1
RKG-04	3206	86.5	509.5	0.06472	24670	0.3737	240.4	216.5	1.497	5.731	195.6
RKG-05	4855	97.44	5259	0.07609	47980	0.5145	693.3	188.4	3.174	35.09	690.4
RKG-06	6467	88.6	478.6	0.06296	13770	0.4438	102.9	189.7	3.034	5.919	53.51

Sample	Al	Co	Cr	Eu	Fe	La	Mn	Na	Sc	V	Zn
RKG-07	8234	80.42	1072	0.06796	18100	0.4962	154.9	152.3	4.837	5.722	41.72
RKG-08	2951	85.83	51.22	0.05545	13900	0.4317	99.46	172.5	1.79	3.492	34.3
RKG-09	2240	76.79	180.3	0.04474	13700	0.3831	136.2	240	0.7921	1.311	71.97
RKG-10	2337	71.64	186.6	0.04882	15490	0.4018	130.5	140.7	0.8817	2.454	75.01
RMP-01	95930	140.9543	3120.007	0.13284	61589	0.07326	299.7	176.44	25.1114	89.29	110.933
RMP-02	5609	93.8105	334.921	0.06213	25243	0.03468	96.6	172.02	2.6496	5.836	173.674
RMP-03	1159	84.4118	36.212	0.05137	12809	0.02912	30.09	167.39	0.1221	1.012	397.125
RMP-04	1306	92.9248	179.179	0.06767	32388	0.03678	42.37	164.56	0.2388	2.979	352.102
RMP-05	1548	70.7914	23.901	0.07887	18185	0.03158	69.47	147.12	0.4034	1.966	301.214
RMP-06	12800	86.0983	1575.066	0.06071	30355	0.04108	82.42	163.01	3.3739	16.09	161.729
RMP-07	6784	76.8377	1349.078	0.05603	32551	0.04453	82.93	157.85	5.1664	18.31	84.601
RMP-08	1556	99.1805	324.494	0.06336	24466	0.03499	45.52	158.41	0.406	6.668	348.01
RMP-09	3636	93.0251	309.342	0.05786	24417	0.04311	416.754	158.9	2.8966	4.976	118.074
RMP-10	102417	137.4092	321.927	0.10759	60126	0.08274	497.692	169.43	19.6657	100.077	231.025
RRA-01	3308	3.1163	7.46	0.0618	2521	7.98333	6.077	137.63	0.1325	6.214	82.884
RRA-02	4687	3.3231	10.984	0.09033	2574	11.61522	41.167	156.31	0.7305	9.587	48.053
RRA-03	2382	2.0251	22.369	0.09453	2890	10.63241	7.645	205.73	0.7376	11.197	48.425
RRA-04	1349	2.2966	1.538	0.07258	1314	7.70511	2.72	129.56	0.0158	3.05	87.835
RRA-05	3513	51.623	321.92	0.06383	24467	9.7252	40.133	139.62	0.9675	5.791	98.802
RRA-06	7531	61.6732	1556.495	0.05523	31276	13.81008	98.632	98.34	3.7643	16.61	42.225
RRA-07	2781	3.2286	4.685	0.07349	9525	5.25564	25.934	310.8	0.0952	2.642	306.807
RRA-08	7287	58.1925	851.218	0.06945	25694	13.65727	50.964	165.79	3.7636	13.189	38.802
RRA-09	2082	2.9701	8.525	0.07206	2246	4.15094	8.014	157.1	0.1576	5.243	72.619
RRA-10	1429	2.8026	1.376	0.05494	1651	4.33986	4.391	135.53	0.0244	3.043	93.597
RRD-01	1959	83.5705	468.532	0.05942	23530	0.21717	94.923	1472.26	0.8505	2.716	49.058
RRD-02	1348	70.2287	34.474	0.05255	18239	0.20317	166.615	1541.41	0.3647	1.351	36.55
RSA-01	1297	3.6641	1.631	0.05424	15934	5.11319	64.912	195.12	0.0136	1.301	246.869
RSA-02	1320	5.1421	1.383	0.06165	13638	6.36928	22.37	120.57	0.0118	2.38	89.875
RSA-03	1214	6.0493	1.43	0.09701	16179	0.04524	21.12	165.31	0.0098	1.577	80.478
RSA-04	1137	6.4652	2.669	0.05618	15802	0.06352	17.49	162.24	0.018	1.814	68.272
RSA-05	1179	5.796	1.1	0.06665	13160	0.03395	21.52	164.18	0.0107	1.635	94.933
RSA-06	1111	7.2579	2.135	0.06912	16361	0.07084	21.25	169.79	0.0137	1.779	97.477
RSA-07	619	3.6217	2.628	0.15386	12578	0.67927	390.2	137.55	0.0726	2.3	56.689
RSA-08	1313	5.1216	1.245	0.05699	14005	0.01753	22.74	179.86	0.0142	2.641	98.067
RSA-09	1396	4.4707	1.96	0.06763	18552	0.08618	37.54	238.48	0.0184	1.404	150.88
RSA-10	835	4.2234	2.743	0.13425	12130	0.50953	272.8	150.6	0.0553	1.994	94.474
RSA-11	4224	5.481	0.832	0.4715	14760	0.1645	65.41	427.3	0.0548	12.79	81.72
RSA-12	1909	1.646	2.129	0.8867	4381	0.0237	15.01	257.4	0.0252	1.895	201
RSA-13	6204	0.8008	0.476	0.4404	1967	0.02182	23.69	472.2	0.0515	10.51	66.55
RSA-14	2758	0.9182	0.841	0.4617	1610	0.02737	10.18	131.1	0.0404	5.05	29.67
RSB-01	3842	88.98	1013	0.08024	31280	0.9057	313.3	146.3	2.786	10.56	30.9
RSB-02	5575	92.45	2055	0.09512	47530	0.09053	918.2	161.3	6.275	25.71	12.16
RSB-03	5010	88.05	978	0.06875	31170	0.1414	295.1	134.2	4.022	13.75	10.93
RSB-04	16990	85.51	2208	0.08434	37780	0.453	520.8	136.3	9.399	23.11	12.52
RSB-05	5190	91.71	1698	0.06604	36250	0.02811	332.4	141.4	3.136	22.69	27.19
RSB-06	5191	89.22	1779	0.06471	34040	0.03105	331.7	138.4	3.053	21.13	23.67
RSB-07	6175	98.21	1697	0.09682	40680	0.03449	1172	160.9	6.43	19.27	16.94
RSH-01	1810	93.02	263.6	0.07499	22140	0.02323	253.6	186.3	1.546	4.055	29.56
RSH-02	5376	76.61	46.75	0.0814	14070	0.02304	117.8	161.4	5.152	8.225	11.39
RSH-03	4720	76.13	47.18	0.08208	13750	0.02431	101.9	163.2	5.055	7.079	9.588
RSH-04	1755	96.95	456.4	0.08034	28640	0.02116	268	177.6	1.331	9.136	30.8
RSH-05	1730	97.15	388	0.07673	28000	0.02098	248.7	181.7	1.558	7.915	26.19
RST-02	996	70.2683	41.3	0.08989	17621	9.29932	46.893	107.45	0.178	0.634	124.05
RST-03	10017	70.404	1434.462	0.09214	27893	32.16222	98.268	101.36	5.1225	20.524	44.897
RST-04	1176	71.9147	15.751	0.06928	14639	20.5445	54.799	164.44	0.0815	0.974	143.533
RST-05	1139	73.5815	37.453	0.07457	12412	21.21967	22.748	119.42	0.2337	0.827	83.93
RST-06	1757	73.7518	170.759	0.06494	21493	22.92109	29.325	122.4	0.7184	2.157	64.934
RST-07	1135	74.3835	19.241	0.08463	13982	22.65678	68.949	137.4	0.092	1.007	146.543

Sample	Al	Co	Cr	Eu	Fe	La	Mn	Na	Sc	V	Zn
RST-08	6471	58.6065	863.937	0.09531	30108	30.80349	99.724	104.4	4.7977	12.239	42.486
RST-09	1127	72.6273	24.131	0.06839	12781	10.17662	48.925	162.17	0.0634	0.908	114.055
RST-10	7889	86.8858	1217.922	0.06623	18104	16.40526	19.418	96.35	6.2831	14.163	29.159
SB-01	13164	1.0651	4.558	0.09999	3967	0.22757	9.365	251.51	0.2577	9.379	38.473
SB-02	541	1.0158	0.966	0.22407	1995	0.06909	1.863	353.81	0.3421	1.143	25.852
SB-03	917	1.4161	1.289	0.19728	3602	0.11686	1.737	273.45	0.1769	2.456	32.784
SB-04	1970	1.1915	0.759	0.19231	2929	0.02745	7.11	255.39	0.1066	2.528	34.394
SB-05	1581	2.9249	3.338	0.23264	5573	1.17349	0.949	172.69	0.1836	3.965	31.463
SB-06	1773	0.9407	0.692	0.08388	2856	0.07853	6.754	247.38	0.1556	3.369	57.218
SB-07	21308	1.0883	15.135	0.15438	4606	0.33459	11.774	294.8	0.4185	13.66	53.352
SB-08	2245	1.9204	1.482	0.07875	2719	1.31363	7.922	208.9	0.1512	5.996	36.161
SB-09	9219	1.595	4.05	0.09071	3672	2.2706	7.379	175.63	0.2255	6.973	48.052
SB-10	3043	1.7456	1.952	0.07052	2823	2.14967	13.311	160.48	0.1906	4.272	45.149
SC-01	1681	0.9669	2.308	0.25428	2338	0.44635	2.799	248.97	0.9594	4.004	26.098
SC-02	472	1.3294	2.696	0.6222	3118	58.19955	3.048	241.38	0.7902	1.801	23.082
SC-03	2205	0.9621	1.235	0.22107	2850	0.07625	15.716	242.39	0.1877	3.922	35.439
SC-04	2787	1.3421	5.309	0.30503	3925	2.41489	1.917	320.67	1.3106	3.708	23.514
SC-05	1880	2.0954	1.352	0.09015	6047	0.08207	45.448	277.36	0.1517	1.964	39.57
SC-06	13974	1.2766	8.474	0.16673	4250	5.01052	9.134	394.45	1.401	18.719	53.125
SC-07	46462	1.5069	28.55	0.24325	7206	12.29991	17.947	256.16	2.0544	37.647	38.148
SC-08	1596	1.7055	0.912	0.24535	2715	0.03291	8.034	259.64	0.1601	1.802	13.489
SC-09	44776	1.5764	25.995	0.4053	6741	11.59144	19.667	251.75	1.9938	41.231	17.787
SC-10	1545	3.216	2.164	0.08887	2255	2.57413	5.231	141.56	0.7177	5.415	18.987
SKK-02	2298	1.1315	1.423	0.18733	2650	1.87836	3.025	240.59	0.1163	1.695	42.527
SKK-03	4994	2.7071	4.523	0.08432	2609	2.29653	4.396	256	0.2136	9.593	41.467
SKK-04	3407	1.1562	3.553	0.08582	3202	2.32511	6.534	288.87	0.2235	7.184	39.147
SKK-05	1715	1.0525	2.131	0.19509	2982	0.11037	4.123	342.78	0.1924	3.108	43.932
SKK-06	604	1.024	0.991	0.26006	2259	1.86413	1.152	3080.09	0.1092	0.55	80.241
SKK-07	6687	1.021	1.258	0.47719	2377	1.5094	13.73	226.92	0.1036	2.902	5.687
SKK-08	1985	1.1378	1.154	1.24236	2393	1.67625	3.953	255.42	0.1203	2.434	34.678
SKK-09	1823	0.9898	1.18	0.0788	2377	2.76853	5.08	266.46	0.1091	1.519	47.38
SKK-10	2448	1.2815	2.502	0.09656	2232	2.8764	3.77	173.84	0.1213	1.369	80.801
SKK-11	18534	2.1003	9.144	0.08488	3985	6.92138	12.534	189.77	0.3506	12.595	42.354
UB(UC-1)	34008	12.9314	26.976	0.26189	10111	19.37513	29.739	146.28	4.0062	35.27	33.446
UB(UC-2)	1394	1.8742	1.573	0.0675	3162	0.11939	7.132	123.6	0.0514	1.459	68.8
UB(UC-3)	1376	9.985	3.941	0.1956	5592	1.23314	349.471	106.04	0.4717	3.032	38.901
UB(UD-1)	8725	5.6373	10.667	0.17525	10188	6.13346	52.707	189.75	1.8476	11.659	24.819
UB(UD-2)	1169	3.174	2.399	0.14179	6144	0.45597	11.71	106.78	0.0858	1.008	99.514
UB(UD-3)	1419	2.1278	2.96	0.10602	7217	0.3521	113.061	171.79	0.3511	3.834	293.667
UB(UK-1)	1029	8.1314	1.209	0.06563	5261	0.06132	2.729	115.67	0.0602	1.307	26.421
UB(UK-2)	84882	5.2631	67.294	1.07047	34855	59.23943	15.234	153	15.4225	88.665	56.41
UB(UK-3)	60518	7.1686	62.073	0.89535	30869	38.48763	7.242	98.43	11.8641	64.533	50.243
UB(UK-4)	11644	7.5949	11.549	0.29688	10588	5.96033	9.58	163.5	2.086	13.203	26.881
UB(UK-5)	1330	3.7672	1.91	0.08689	4918	0.55289	4.541	106.41	0.3364	1.756	27.036
US-01	3821	1.9382	6.175	0.10456	2336	2.08466	45.715	397.75	0.5942	4.215	24.647
US-02	1393	2.5004	5.241	0.06818	2875	0.20543	3.054	173.34	1.0279	12.425	38.338
US-03	868	2.2831	1.72	0.05245	2562	0.08819	1.464	105.07	0.6915	7.536	17.8
USK-01	3757	8.9359	13.642	0.08328	18343	0.16158	17.218	113.58	0.3478	4.377	31.244
USK-02	1314	5.5032	1.051	0.0943	16638	0.11904	22.325	99.63	0.4377	1.169	18.786
USK-03	15176	22.2518	32.629	0.79592	25341	4.25442	22.979	100.08	0.9056	11.333	9.747
USK-04	973	5.1286	0.773	0.06945	15131	0.04643	26.782	95.16	0.0384	0.839	40.611
USK-05	1183	5.3961	0.963	0.07703	17360	0.06154	13.731	167.85	0.2293	1.089	24.59
USK-06	1018	5.2903	0.74	0.0912	16636	0.05224	15.798	159.51	0.09	1.057	40.508
USK-07	6404	9.752	9.242	0.16252	18830	0.31446	16.505	162.18	0.5947	5.902	21.675
USK-08	21622	21.5134	37.054	1.20747	26159	9.50274	28.792	210.42	0.9692	21.048	10.316
USK-09	1012	5.575	2.587	0.07126	17944	0.0404	21.042	149.69	0.1553	2.2	31.18
USK-10	1043	7.3798	3.394	0.09823	16626	0.06327	13.575	174.2	0.1873	0.91	34.501
ZTAK-01	915	4.229	8.264	0.06154	19580	0.04406	207.6	266.5	0.0717	1.595	24.06

Sample	Al	Co	Cr	Eu	Fe	La	Mn	Na	Sc	V	Zn
ZTAK-02	990	2.903	8.555	0.06317	12530	0.01483	296.8	134.9	0.0402	1.265	24.17
ZTAK-03	1229	2.814	7.071	0.05227	19120	0.0209	159.4	266.1	0.0439	1.283	35.57
ZTAK-04	1281	34.89	9.232	0.05443	33720	0.03144	107.7	155.2	0.8555	2.611	8.579
ZTAK-05	1700	33.45	117.9	0.1063	21650	0.07776	237.8	196.2	1.581	4.736	13.99
ZTAK-06	1349	16.04	6.998	0.08312	23210	0.04347	226.5	210.1	0.4538	2.474	14.87
ZTAK-07	1231	22.98	9.301	0.04559	16780	0.03208	23.45	263.4	0.2581	2.45	17.75
ZTAK-08	1207	12.6	9.527	0.1183	18540	0.04724	194.4	196.5	0.2852	2.38	14.49
ZTAK-09	1373	11.32	14.82	0.1511	19290	0.06931	204	214.4	0.5196	2.801	18.73
ZTAK-10	1063	7.957	7.066	0.04318	16840	0.02711	24.98	313.8	0.0886	2.142	17.4
ZTT-01	1892	52.45	4920	0.06615	54550	0.4955	669.8	148.6	2.819	47	54.05
ZTT-02	1523	41.72	2236	0.05878	65420	0.4757	172.3	126.9	3.129	22.82	34.81
ZTT-03	1592	37.38	3326	0.05382	39190	0.4193	235	137.4	1.45	24.53	61.87
ZTT-04	1514	50.34	2518	0.06244	63500	0.5315	160.5	62.1	3.543	20.45	39.84
ZTT-05	1633	170.1	4098	0.09201	53870	0.8138	423.6	121.1	5.233	36.27	56.92
ZTT-06	1080	53.7	222.5	0.03786	30280	0.3958	273.9	165.9	0.6289	5.898	36.2
ZTT-07	1612	0.5841	2.241	0.17215	2334	0.13854	3.7	98.7	0.0936	1.761	108.51
ZTT-08	1204	54.42	1084	0.08185	81060	0.5746	138.5	102.9	3.725	11.11	91.31
ZTT-09	1972	45.81	3716	0.06229	47770	0.4524	48.01	56.4	2.681	32.99	83.48
ZTT-10	1070	36.5	86.14	0.04869	40970	0.3786	26.24	102.9	0.2334	1.674	111.8
ZUN-01	1120	12.4797	15.578	0.03722	4410	0.08514	4.23	442.06	0.1168	3.214	20.79
ZUN-02	1086	15.2697	1.404	0.05056	7417	0.07985	4.679	534.62	0.0837	2.04	24.86
ZUN-03	1089	19.2626	16.37	0.05061	7964	0.09622	42.143	452	0.4978	5.37	18.331
ZUN-04	1489	52.1921	13.663	0.06762	19529	0.15153	88.132	748.29	0.9862	3.471	30.739
ZUN-05	2840	103.5938	2778.927	0.08621	46592	0.28995	122.946	1311.32	4.9705	45.031	65.753
ZUN-06	2138	71.1968	1539.828	0.06887	37333	0.24959	106.126	1179.33	4.5573	20.27	30.152
ZUN-07	1323	24.0303	32.658	0.03064	17219	0.12811	19.32	668.5	0.5629	14.672	27.439
ZUN-08	1360	40.0954	445.997	0.06363	18490	0.13738	30.91	839.51	0.5906	11.126	38.723
ZUN-09	1218	19.101	16.659	0.04888	13395	0.29179	5.224	11933.54	0.2376	11.167	23.207
ZUN-10	1339	28.2447	88.08	0.05245	14907	0.29558	11.433	13367.44	0.353	10.075	24.894

APPENDIX 7.4

INAA DATA FOR STEATITE ARTIFACTS FROM HARAPPA

Elemental data in parts per million (PPM)

Artifact (year/lot-rec)	Al	Co	Cr	Eu	Fe	La	Mn	Na	Sc	V	Zn
H87/33-02	2048	0.6936	2.012	0.0692	3658	0.16965	4.075	569.98	0.0531	3.622	93.79
H87/86-228	1803	1.753	6.358	0.06166	3928	0.16071	9.868	417.28	0.0964	4.27	112.141
H87/86-229	2087	1.2263	2.577	0.0554	4689	0.17738	12.586	477.79	0.0671	3.887	102.267
H87/86-236	2085	0.8963	2.8	0.06142	4477	0.15191	12.228	504.37	0.1688	4.562	138.319
H87/237-86	2160	0.7003	2.667	0.05617	5019	0.15229	4.626	675.22	0.0594	4.045	97.469
H88/340-24	1565	8.7269	8.26	0.05768	2302	0.12548	6.918	355.27	0.0425	3.376	75.202
H89/1018-13	1491	0.5875	1.092	0.05933	2154	0.1729	2.772	304.81	0.0332	0.834	76.968
H89/1121-5	9444	0.8239	6.74	0.43926	2878	15.36836	4.039	693.28	1.4736	4.571	62.038
H2000/2230-14	1566	0.5745	2.339	0.3222	2530	0.0322	5.329	477.1	0.0407	2.171	113.2
H2000/2230-15	1796	0.3977	6.596	0.2777	2578	0.113	6.788	404.1	0.0735	3.864	175.6
H2000/2230-16	1540	0.2525	0.992	0.48474	2116	0.08471	12.33	424.51	0.035	2.193	10.747
H2000/2230-17	964	0.5984	4.444	0.49046	3228	0.09129	3.698	474.61	0.0457	1.197	15.049
H2000/2301-176	1614	0.3186	1.176	0.50474	2440	0.11467	5.805	365.22	0.0548	2.501	10.691
H2000/2301-177	1675	0.4263	1.812	0.46841	2968	0.11826	4.349	435.86	0.0685	3.264	13.189
H2001/2373-10	1527	0.9361	0.89	0.12273	4391	0.0222	9.209	600.57	0.0312	0.864	166.649
H2000/2753-17	1704	0.6088	0.713	0.06119	1639	0.03378	12.172	516.82	0.0356	0.831	33.62
H2000/2774-14	25996	2.4339	16.812	0.27295	7037	33.85512	17.498	961.72	1.6237	36.504	15.681
H2000/2774-15	1777	0.6635	0.63	0.09948	1640	0.05545	3.349	604.26	0.0877	0.721	16.766
H2000/2789-30	1915	0.6296	1.015	0.12053	3000	0.07677	5.179	668.02	0.0303	0.73	31.703
H2000/2880-16	2178	0.7311	1.602	0.0621	2924	0.08398	22.701	744.61	0.0269	1.188	28.404
H90/3030-55	1551	0.6282	0.746	0.08979	5127	0.03268	6.408	408.17	0.0226	0.924	130.403
H90/3068-50	1596	0.8657	1.411	0.0607	3877	0.03733	5.183	585.77	0.0246	1.455	88.372
H90/3208-68	1414	3.48	1.612	0.4496	2479	0.03604	2.481	550.7	0.0734	1.075	20.16
H90/3290-17	1561	0.6749	1.405	0.16116	1778	0.04251	2.082	737.58	0.0654	1.904	85.343
H93/3534-13	2001	1.0981	3.055	0.14927	4282	0.19795	14.556	971.62	0.0652	2.52	147.739
H93/3710-16	1516	0.4904	1.976	0.07162	2517	0.0626	6.046	552.65	0.0594	1.645	59.855
H93/3710-70	1747	0.6235	3.74	0.07846	2673	0.08883	9.024	719.89	0.1316	4.178	216.293
H93/3808-52	1535	0.5978	0.705	0.11724	1757	0.03949	2.866	584.69	0.0595	0.938	83.005
H93/3869-24	1545	0.948	0.713	0.0534	2080	0.07567	6.785	431.07	0.0501	0.903	73.704
H95/4453-22	1468	0.6378	0.936	0.07793	2988	0.02537	5.263	532.65	0.03	0.92	128.348
H95/4613-42	1626	0.4385	0.498	1.14059	1480	0.04576	6.963	669.88	0.0721	1.332	35.312
H95/4615-94	1897	1.0672	1.057	0.08311	3835	0.20093	8.262	660.78	0.1029	1.215	63.778
H95/4723-2	1328	0.5706	2.034	0.05157	2667	0.16767	27.227	707.18	0.1308	1.543	64.732
H95/4726-101	1910	0.4867	1.063	0.04422	1694	0.06002	4.057	708.36	0.0364	1.595	84.159
H95/4746-7	1516	0.6595	0.687	0.05577	2212	0.0283	1.82	541.39	0.0358	1.167	103.45
H95/4751-8	1885	0.5744	0.819	0.11345	2635	0.13825	20.026	1041.44	0.0939	1.643	32.813
H95/4919-62	1185	0.7353	1.672	0.07132	2359	0.49272	51.771	564.43	0.2421	1.981	13.615
H95/4950-4	1673	0.66	0.537	0.12262	2845	0.02256	4.6	609.57	0.0379	1.105	36.725
H95/4954-18	1322	0.4472	0.974	0.09818	1938	0.02474	3.828	647.4	0.0331	0.813	22.447
H95/4961-176	1433	0.6354	0.779	0.11414	3345	0.04042	3.845	682.24	0.0503	1.064	23.343
H94/5135-34	1990	0.391	7.257	0.14091	1226	0.098	2.279	507.23	0.129	1.821	72.69
H95/5184-1	1254	0.5649	0.969	0.08989	2155	0.02363	3.77	327.9	0.032	0.84	103.985
H95/5713-145	1810	0.7737	1.266	0.06631	2268	0.03384	7.164	697.78	0.1004	1.636	89.964
H95/5734-31	1590	1.2582	1	0.07435	2617	0.03433	4.885	608.96	0.0404	1.268	100.125
H95/5747-125	1529	0.5098	1.075	0.06686	2639	0.03519	4.464	489.91	0.0291	1.161	63.928
H95/5749-97	1363	0.7542	0.635	0.08768	3423	0.03623	4.201	643.82	0.0161	1.046	122.396
H95/5759-25	1636	0.712	0.851	0.04045	2842	0.03462	3.704	567.39	0.0323	1.587	77.658
H95/5763-19	1571	0.8232	0.758	0.07527	2626	0.04487	10.005	750.27	0.0431	1.799	141.979

Artifact (year/lot-rec)	Al	Co	Cr	Eu	Fe	La	Mn	Na	Sc	V	Zn
H95/5802-5	2091	0.8686	0.809	0.4075	3753	0.08015	66.755	620.2	0.0589	0.985	82.87
H95/5803-25	1655	0.7372	1.692	0.14813	6033	0.11117	174.265	703.34	0.0581	0.897	288.355
H95/5820-11a	1261	0.6224	1.077	0.08811	1363	0.03201	1.892	477.13	0.0148	0.86	105.058
H96/5837-18	1326	0.3213	0.528	0.12375	1978	0.02819	4.856	539.61	0.0388	0.962	191.366
H96/6218-8	1592	1.1237	0.673	0.128	3572	0.09552	2.989	1138.76	0.0787	1.109	24.592
H96/6219-44	1309	0.4862	0.668	0.06733	1922	0.03336	11.306	458.98	0.0391	0.965	37.301
H96/6234-2	1303	0.4887	0.607	0.07568	2316	0.0272	4.065	392.41	0.0314	0.773	97.483
H96/6257-21	1430	1.0858	0.545	0.14628	4108	0.02347	3.656	467.05	0.0325	0.836	168.416
H95/6509-97	1958	0.4702	1.517	0.07118	4777	0.10161	22.064	722.29	0.023	1.582	41.605
H96/7105-8	1835	0.5276	0.645	1.15691	2313	0.05698	4.923	593.76	0.0537	1.082	42.632
H96/7106-27	1574	0.3944	0.804	0.07924	2250	0.39446	88.955	593.87	0.1138	1.932	97.271
H96/7118-9	1717	0.7717	1.605	0.1395	2492	0.37042	61.076	661.47	0.0771	1.86	141.859
H96/7153-14	2054	0.8125	1.224	0.07762	4670	0.0741	6.651	906.99	0.1039	1.653	126.13
H96/7156-14	1714	0.3722	1.675	0.09426	2597	0.05294	5.61	447.65	0.1029	1.39	68.086
H96/7239-26	1780	0.6479	1.934	0.07958	2038	0.09767	4.859	529.28	0.1028	1.587	17.117
H96/7256-43	1537	0.6898	0.913	0.13925	3190	0.12141	8.093	505.38	0.0545	0.802	23.826
H96/7257-46	4060	0.7658	2.596	0.04421	2098	0.03628	2.383	782.5	0.0265	1.31	27.685
H96/7333-22	4291	0.8249	1.927	0.12301	2395	0.58948	9.824	683.5	1.0023	2.159	38.809
H96/7358-11	2105	0.9389	1.213	0.12895	3465	0.23081	19.331	880.46	0.0807	1.881	141.163
H96/7401-63	17284	1.2007	23.644	0.28853	4619	10.60924	22.63	682.77	2.2431	14.211	18.2
H96/7410-1	543	0.4993	1.524	1.195	2470	0.07171	1.064	154.5	0.0619	0.567	15.33
H96/7410-2	1598	0.5093	1.614	0.22257	2531	0.06751	2.844	429.15	0.0437	0.911	88.935
H96/7414-46	8029	0.7899	5.574	0.21674	2249	2.19513	6.818	656.71	0.8936	6.146	54.917
H96/7414-47	1857	0.5334	1.637	0.5947	4501	f3208	33.72	652.3	0.0789	1.201	16.79
H96/7467-658	88516	2.329	113.877	2.477	12741	63.574	45.889	2722.55	8.224	64.292	43.999
H96/7467-790	1667	0.7843	0.836	0.1335	2202	0.08082	17.419	766.14	0.0303	1.355	28.503
H96/7531-16	2071	0.8768	5.165	0.09811	4541	0.11687	4.681	1270.88	0.0891	1.759	41.952
H97/7619-3	1655	0.3622	3.502	0.10151	2614	0.18101	6.656	438.45	0.103	2.435	102.207
H99/7636-8	2124	1.2381	1.807	0.06132	6026	0.24069	58.721	534.99	0.0779	16.563	98.514
H99/7637-32	1853	1.445	1.633	0.04334	4703	0.16588	35.718	415.95	0.0976	3.219	122.39
H99/7638-1	1869	0.4164	2.611	0.10212	4935	0.11426	4.396	479.11	0.091	12.891	71.325
H99/7649-42	1970	0.7385	1.528	0.12647	2681	0.04569	5.374	529.31	0.0688	2.122	154.091
H97/7780-10	1603	0.5884	0.719	0.10167	2123	0.09512	4.09	687.75	0.4052	1.764	63.166
H97/7780-8	3186	0.8741	2.777	0.07543	2160	0.22341	7.285	486.41	0.5741	1.684	74.104
H97/7780-9	1566	0.429	2.361	0.04539	1860	0.21949	4.498	795.76	0.0511	1.472	125.591
H97/7784-156	2053	0.8499	0.836	0.5271	2849	5.32711	5.474	473.19	0.368	1.012	9.679
H97/7784-157	5922	0.6855	1.363	0.382	5327	0.02745	27.82	1240	0.0529	3.268	85.38
H97/7784-158	8606	0.794	0.704	0.6222	4137	0.03545	16.42	2096	0.7103	5.714	68.53
H97/7784-159	18390	0.9886	3.241	0.5797	2606	1.87	8.889	3009	1.317	11.82	49.26
H97/7784-16	1983	0.6449	0.702	0.4285	3939	0.02739	4.329	494	0.0119	0.897	147.3
H97/7784-17	1757	0.4613	1.467	0.50166	2628	0.06017	3.02	527.33	0.0518	0.861	10.816
H97/7784-18	1664	1.0544	4.001	0.54321	2415	0.07093	5.113	514.83	0.0363	0.648	10.209
H97/7784-19	9294	1.4114	6.768	0.53097	4495	3.51956	4.131	663.97	1.6514	4.731	6.293
H97/7784-20	1881	1.2938	3.631	0.50932	2057	0.03803	3.115	421.69	0.0495	0.864	9.737
H97/7784-21	1612	52.08	3192	0.1046	55550	0.5403	32.35	15090	3.567	18.15	64.04
H97/7784-22	1884	0.2482	1.374	0.49488	2878	0.06257	3.104	511.5	0.0965	1.445	6.524
H97/7784-23	1863	0.5209	1.233	0.328	2688	0.07389	3.323	400	0.1574	1.032	130.3
H97/7784-24	19440	1.676	15.71	0.3225	5417	9.882	11.63	646.3	2.107	3.188	78.86
H97/7784-25	1560	0.458	0.829	0.46907	2315	0.05173	3.012	455.18	0.0401	0.813	10.109
H97/7784-27	2104	13.225	81.349	0.49928	1861	0.28395	4.99	496.58	0.6556	2.831	6.574
H97/7784-28	2054	0.478	1.415	0.5038	2696	0.05971	4.46	591.89	0.0961	2.201	9.067
H97/7784-29	1910	0.4477	1.656	0.47837	2512	0.12922	18.28	544.17	0.1083	1.69	9.351
H97/7784-30	513	0.4103	1.39	0.13002	2989	0.0309	1.103	450.69	0.0513	0.442	88.492
H97/7784-31	617	0.4982	5.937	0.3469	2330	1.131	9.594	142.6	0.1273	0.832	119.4
H99/7794-3	4600	0.2839	2.942	0.08072	3717	0.17823	4.555	340.42	0.1448	6.035	142.601
H98/8342-3	7107	1.035	8.298	0.17775	3715	7.42393	5.943	797.95	1.4574	5.82	11.459
H98/8355-2	1888	0.5139	1.232	0.10985	2867	0.05477	1.446	709.22	0.0816	1.462	64.64

Artifact (year/lot-rec)	Al	Co	Cr	Eu	Fe	La	Mn	Na	Sc	V	Zn
H98/8364-5	2051	0.4365	1.221	0.05151	2313	0.11733	4.458	557.29	0.1947	1.906	55.086
H98/8407-39	1778	0.9304	4.195	1.265	1728	0.2508	53.41	442.1	0.0579	1.64	13.68
H98/8407-40	1269	1.111	3.121	1.31	2116	1.988	1.648	106.9	1.316	1.024	7.676
H98/8410-12	9141	1.1994	9.302	0.23644	2627	6.47423	8.383	691.46	1.1734	5.834	43.818
H98/8486-50	1718	1.287	5.323	0.3346	3235	2.556	1.362	174.6	0.6837	1.516	105.6
H98/8487-32	1907	0.4496	0.698	0.848	2740	0.0549	3.669	483.3	0.0284	0.762	9.459
H98/8487-33	760	1.7753	9.249	0.16709	1329	0.06247	1.402	424.39	0.0222	0.575	102.432
H99/8490-103	241	0.5523	2.182	0.107	1602	0.28657	3.488	668.31	0.0984	0.44	95.468
H99/8492-229	1068	0.5015	1.139	1.114	810	0.3548	5.865	340.5	0.0698	1.193	13.77
H99/8497-3	1465	0.5716	1.987	0.15151	2199	0.40107	26.21	490.13	0.1389	1.539	76.924
H98/8668-2	1825	24.986	671.41	0.88296	33729	0.14137	59.035	443.16	1.3826	9.412	317.395
H99/8760-77	2185	0.6666	4.872	0.06074	7353	0.08911	7.656	1099.17	0.0375	17.62	85.628
H99/8956-1	582	0.6865	1.05	1.339	4824	0.06759	2.152	222.8	0.0584	0.583	22.83
H2000/8983-44	1686	0.428	0.994	0.5192	2389	0.3261	26.45	668.4	0.1156	2.401	14.82
H2000/8992-1	2129	0.267	1.082	1.034	5480	0.08161	8.968	524.1	0.0369	1.329	11.48
H2000/8997-4	1993	0.3954	0.652	1.055	2793	0.04022	4.007	476.3	0.036	0.913	12.34
H2000/9442-2	6493	1.4664	6.495	0.19253	2491	4.01521	12.58	347.38	0.7164	3.745	67.164
H2000/9443-6	13130	1.0476	6.338	0.31612	3968	12.67332	5.966	598.01	1.2442	6.264	47.379
H2000/9443-7	1136	0.33	2.319	1.021	9097	0.05017	3.527	255.6	0.0424	0.946	10.14
H2000/9445-1	54600	0.4794	1.643	1.636	3285	0.06579	600	10000	0.075	90	11.19
H2000/9445-2	392	0.5189	1.437	0.21518	3615	0.15337	13.21	519.23	0.1468	0.424	91.974
H2000/9447-5	7535	1.402	14.37	1.157	4953	18.94	4.595	293	1.941	3.008	11.03
H2000/9514-93	1964	0.4098	1.126	0.07465	2718	0.05535	4.49	468.36	0.0535	1.092	18.043
H99/9737-22	1331	1.0386	0.682	0.1272	2807	0.02977	1.344	367.15	0.0248	0.969	149.973
H99/9747-33	1715	0.6065	0.709	0.1186	2869	0.10796	5.54	738.14	0.0553	1.347	127.436
H99/9756-16	1487	0.5775	1.039	0.06759	2551	0.02069	4.48	486.93	0.038	1.37	149.495
H99/9779-4	1496	0.5006	1.104	0.10644	3218	0.03175	4.131	446.97	0.0705	2.233	163.126
H2000/9840-8	22771	1.7333	19.051	0.12146	7585	0.38133	11.975	785.5	1.2201	15.289	141.286
H2000/9973-13	657	0.2368	0.75	0.9334	3267	0.1066	19.39	150.7	0.0175	0.767	18.9
H2000/11001-6	1990	0.4956	1.194	0.192	5136	0.0648	6.8318	502.81	0.0555	5.661	27.62
H2001/2913-12	1920	0.8082	0.754	0.31509	3359	0.14078	7.871	801.75	0.0484	1.113	74.926
H2001/2920-7	1111	0.6078	0.886	0.12777	3045	0.03029	3.725	361.35	0.0387	0.737	120.657
H2001/2922-6	1414	0.5917	0.556	0.05952	2376	0.05637	5.415	293.21	0.039	0.934	98.276
H2001/2939-25	1550	0.9066	1.644	0.07531	8401	0.31191	179.866	384.3	0.1217	1.916	95.45
H2001/11562-26	2158	0.5767	2.124	0.12408	2657	0.07452	6.15	790.88	0.0694	3.373	18.882
H2001/11923-9	1834	0.6998	1.133	0.09334	2047	0.03676	4.341	599.76	0.099	1.063	23.414

APPENDIX 7.5
INAA DATA FOR UNFIRED STEATITE ARTIFACTS FROM MOHENJO-DARO (MD)

Elemental data in parts per million (PPM)

Sample / Area	Parent-rock 1st & 2nd PGM	Al	Co	Cr	Eu	Fe	La	Mn	Na	Sc	V	Zn
MD-S1 / DK-A	SB / SKK	1744	0.2975	1.628	0.08737	2181	0.11994	4.882	709.45	0.0628	1.591	30.013
MD-S2 / DK-A	PD / SKK	2106	0.8963	1.627	0.07933	2438	0.08497	5.947	936.66	0.0394	1.353	45.075
MD-S3 / DK-A	SKK / SB	2140	0.6876	3.459	0.08595	3229	0.19026	9.672	775.72	0.0795	1.278	26.517
MD-S4 / DK-A	ATM / SB	1481	0.8113	3.792	0.0629	3316	0.10597	4.724	852.45	0.0756	2.505	31.386
MD-S5 / DK-A	ATM / SKK	1441	0.8831	1.853	0.09926	5241	0.23115	6.751	1214.59	0.0697	1.47	34.255
MD-S6 / DK-A	ATM / ANB	1553	0.9122	1.345	0.08971	1956	0.13561	5.746	1686.97	0.0544	2.723	21.419
MD-S7 / Moneer	SB / SKK	820	0.8168	1.331	0.07102	5367	0.04619	2.88	679.55	0.099	1.471	30.777
MD-S8 / Moneer	ATM / SB	1858	1.0956	1.348	0.04398	4215	0.08384	7.104	1318.33	0.072	2.539	30.532
MD-S9 / Moneer	ANB / ATM	3361	1.6533	2.889	0.08035	4775	1.30215	23.849	7552.83	0.389	5.474	35.939
MD-S10 / Moneer	PD / GMP	1828	4.44	1.837	0.07191	3923	0.30075	16.615	300.98	0.1155	3.508	18.608
MD-S11 / Moneer	SB / SC	1671	0.6067	1.92	0.06065	2389	0.1423	9.755	326.63	0.0801	1.646	25.208
MD-S12 / DK-A	SC / SB	1938	0.4789	1.838	0.07169	2302	0.36967	13.907	526.06	0.1618	3.004	19.741
MD-S13 / DK-A	RDP / ATM	1613	0.6379	1.55	0.06836	2793	0.42014	151.612	1090.83	0.2931	1.703	12.789
MD-S14 / DK-A	PD / SKK	4063	1.204	3.688	0.06431	2483	0.10103	8.315	531.95	0.0384	1.623	46.903
MD-S15 / DK-A	SB / SKK	1539	0.4198	3.213	0.05401	2984	0.32981	8.809	381.28	0.0875	1.799	30.494

APPENDIX 7.6
INAA DATA FOR UNFIRED STEATITE ARTIFACTS FROM MEHRGARH (MR) AND NAUSHARO (NS)

Elemental data in parts per million (PPM)

Sample [artifact context / number]	Al	Co	Cr	Eu	Fe	La	Mn	Na	Sc	V	Zn
MR-s1 [MR4 Atelier]	2143	0.2647	15.234	0.10067	609	0.1043	8.222	979.05	0.1783	20.02	6.816
MR-s2 [MR4 Atelier]	1847	0.2706	12.179	0.10085	439	0.099	5.676	860.26	0.1486	15.21	6.593
MR-s3 [MR4 Atelier]	2629	0.2604	26.586	0.08776	961	0.1291	5.179	1198.54	0.285	23.35	8.364
MR-s4 [MR4 Atelier]	1945	0.2434	37.275	0.0755	523	0.379	4.763	1350.85	0.1789	66.95	4.277
MR-s5 [MR4 Atelier]	1403	0.1697	18.895	0.0732	356	0.4688	6.261	1037.41	0.1335	68.82	5.582
MR-s6 [MR4 Atelier]	1786	0.1874	20.7595	0.0855	584	0.1371	5.681	1409.39	0.2706	105.7	7.646
MR-s7 [MR4 Atelier]	1987	0.4336	40.389	0.0946	1135	0.2655	8.8041	1476.75	0.2175	84.12	7.618
MR-s8 [MR.99.03.145.12]	2553	0.4108	15.326	0.0956	477	0.4933	14.28	1183.66	0.1702	26.26	7.327
MR-s9 [MR.00.3S.508.08]	3468	174.66	7407.3	0.0966	66212	0.116	294.9	208.78	2.1511	30.7	37.097
MR-s10 [MR.00.03.390]	3430	0.4513	41.0334	0.4934	1078	0.1338	5.548	1198.18	0.3797	83.05	11.278
MR-s11 [MR.00.03.109.115]	62049	71.218	387.088	0.0519	112956	15.754	1876.2	190.48	104.7	574.5	12.001
MR-s12 [MR.98.03.87.02]	3184	0.8116	42.3403	0.0945	1970	0.0865	13.181	2201.85	0.3861	72.1	6.662
MR-s13 [MR.00.03.183.219]	1386	41.617	1472.49	0.0835	34553	0.0845	38.83	308.17	1.2495	7.882	17.41
NS-s1 [NS.90.09.21.02]	1408	118.14	1826.7	0.06186	12059	0.1655	135.03	428.62	1.203	9.199	14.256

APPENDIX 7.7

INAA DATA FOR UNFIRED STEATITE ARTIFACTS FROM GOLA DHORO (GD), NAGWADA (NGW), UNKNOWN LORALAI SITE (LOR), TEPE HISSAR (TH) AND MITATHAL (MTL)

Elemental data in parts per million (PPM)

Sample	Al	Co	Cr	Eu	Fe	La	Mn	Na	Sc	V	Zn
GD-s1	11371	85.764	2546.5	0.3223	35012	0.07018	132.05	1892.7	2.2341	23.132	62.057
NGW-s1	8243	57.7813	894.3	0.07159	23523	0.03659	313.105	133.47	4.3543	25.202	10.412
LOR-s1	191700	0.352	7.579	3.358	3070	36.58	6.941	250.4	3.61	8.385	30.25
LOR-s2	2174	48.2109	4262.9	0.0925	43246	0.5044	106.2584	427.34	2.9106	33.7013	16.785
TH-s1	1336	6.1175	1.2358	0.1375	28101	0.3156	88.1441	951.29	0.0571	4.819	128.74
TH-s2	36727	1.1252	84.56	0.1183	13020	4.8644	32.5707	745.67	4.0722	102.23	10.286
TH-s3	1219	3.4656	1.7806	0.138	14026	1.009	163.3491	332.54	0.101	1.5844	101.64
TH-s4	1221	2.8522	0.9222	0.0932	7627	0.0502	27.5931	1122.9	0.0657	1.9529	22.322
MTL-1	2272	2.264	2.87	4.018	1939	0.9789	16.23	1457	0.0614	9.567	16.13

APPENDIX 7.8

STANDARDIZED CANONICAL DISCRIMINANT FUNCTION COEFFICIENTS FOR SCATTERPLOTS IN CHAPTER 7 GENERATED USING CANONICAL DISCRIMINANT ANALYSIS

Figures 7.31 & 7.32	Function 1	Function 2
Log Al	.062	-.504
Log Co	1.303	.937
Log Cr	.605	-1.100
Log Eu	-.089	-.043
Log Fe	-1.363	-.884
Log La	-.442	.318
Log Mn	.278	-.239
Log Na	.237	.452
Log Sc	.513	.573
Log V	-.449	.940
Log Zn	.072	.198

Figure 7.34	Function 1	Function 2
Log Al	.791	.059
Log Co	-.091	-.547
Log Cr	.423	.097
Log Eu	.442	.350
Log Fe	.256	.372
Log La	.200	1.120
Log Mn	.363	-.147
Log Na	-.753	-.054
Log Sc	-.418	-.551
Log V	-.657	-.224
Log Zn	.261	-.321

Figure 7.35	Function 1	Function 2
Log Al	-.333	-.670
Log Co	1.599	-.657
Log Cr	-.369	.226
Log Eu	-.069	-.042
Log Fe	-1.829	.676
Log La	-.120	-.213
Log Mn	.199	.671
Log Na	.382	.612
Log Sc	1.005	-.670
Log V	.373	.896
Log Zn	.261	-.081

Figure 7.38	Function 1	Function 2
Log Al	-.515	-.295
Log Co	.670	-1.114
Log Cr	.323	.353
Log Eu	-.313	-.071
Log Fe	-.826	1.306
Log La	-.134	-.037
Log Mn	.307	.269
Log Na	.724	.479
Log Sc	.661	-.455
Log V	.206	.119
Log Zn	-.071	-.347

Figure 7.39 A & B	Function 1	Function 2
Log Al	-.803	-.248
Log Co	.317	1.304
Log Cr	.226	-.129
Log Eu	-.106	-.299
Log Fe	-.545	-.550
Log La	-.019	.099
Log Mn	.800	-.489
Log Na	.157	.597
Log Sc	-.122	-.087
Log V	1.011	.290
Log Zn	.302	-.333

Figure 7.45	Function 1	Function 2
Log Al	.611	.670
Log Co	-.272	1.176
Log Cr	.079	-.450
Log Eu	.597	.371
Log Fe	.621	-1.218
Log La	.160	-.083
Log Mn	1.092	.018
Log Na	-1.241	-.088
Log Sc	-.073	.178
Log V	-.616	.098
Log Zn	.613	.273

Figure 7.47	Function 1	Function 2
Log Al	-1.462	-.304
Log Co	.189	1.060
Log Cr	-.985	-.069
Log Eu	-.209	-.704
Log Fe	.152	-1.252
Log La	.293	.155
Log Mn	.146	-.216
Log Na	-.497	.515
Log Sc	-.054	.646
Log V	1.808	.208
Log Zn	1.083	.689

Figure 7.48	Function 1	Function 2
Log Al	.082	.919
Log Co	-.097	-.316
Log Cr	-.194	-.547
Log Eu	.136	-.112
Log Fe	.067	1.018
Log La	-1.137	-.183
Log Mn	-.052	-1.084
Log Na	.201	.108
Log Sc	.884	.414
Log V	-.251	-.746
Log Zn	.383	.820

APPENDIX 7.9

CLUSTER ANALYSIS (COMPLETE LINKAGE) OF ALL STEATITE ARTIFACTS AND GEOLOGIC SAMPLES

Section A

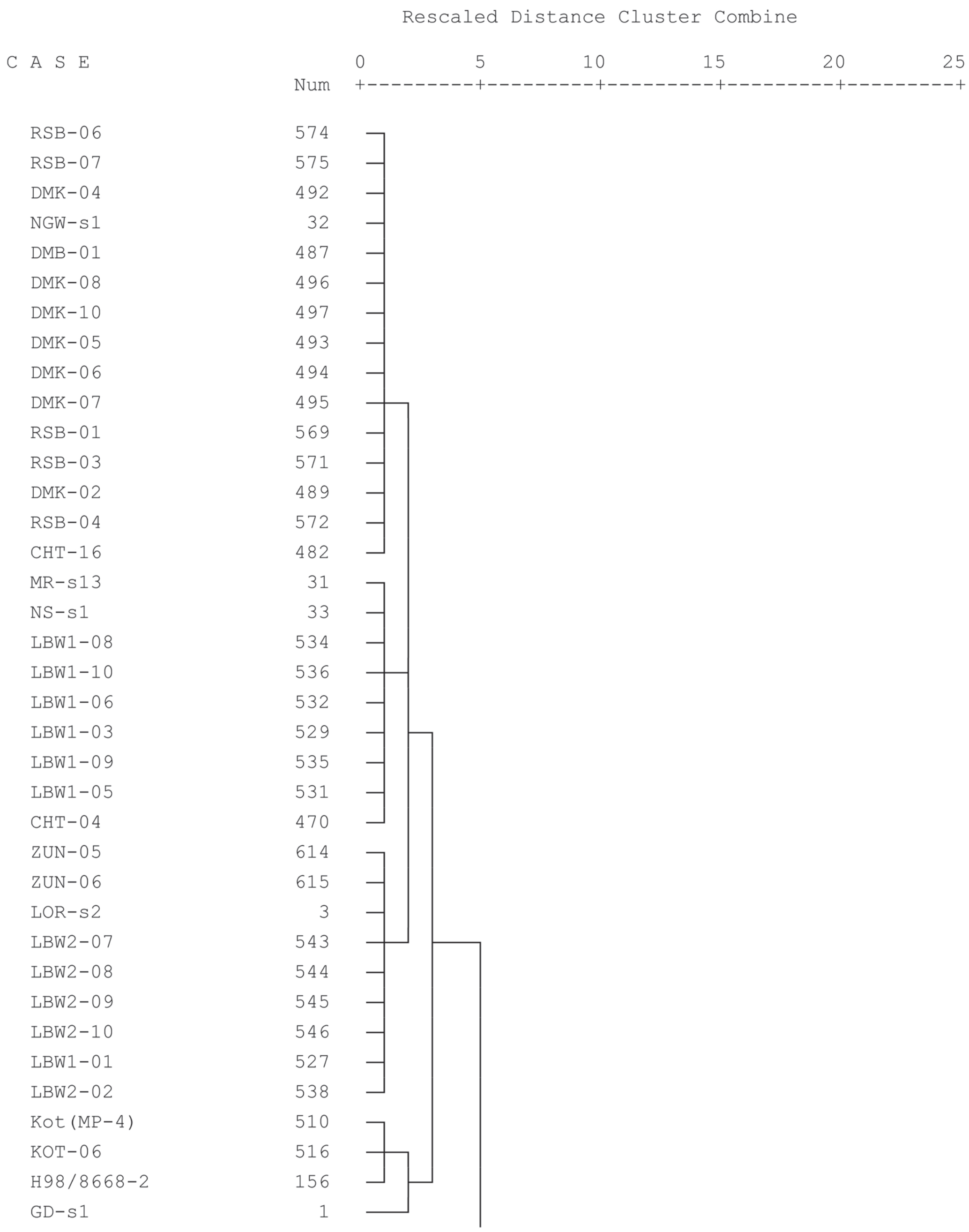

Section B

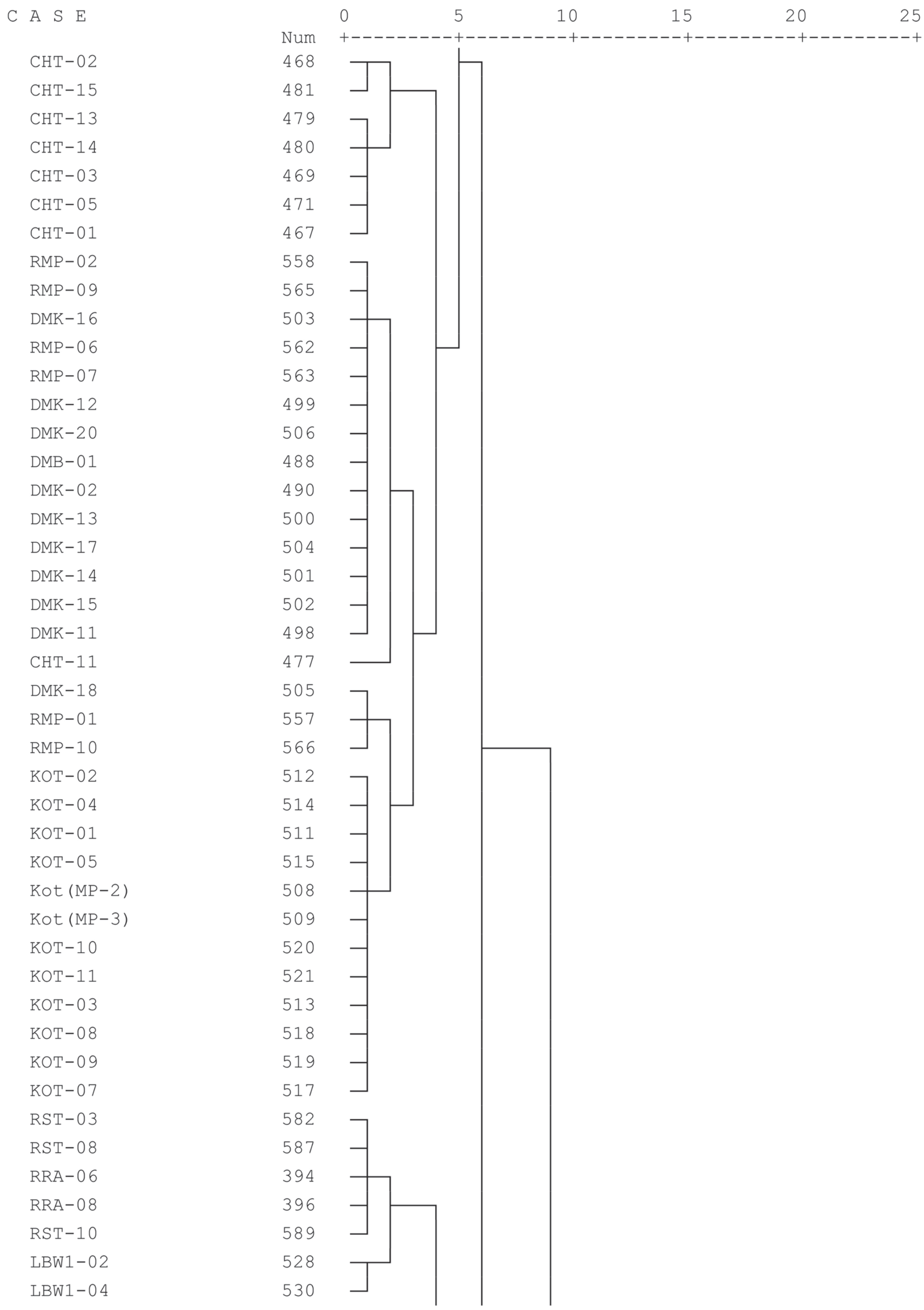
C A S E
Num
0
5
10
15
20
25
CHT-02 468
CHT-15 481
CHT-13 479
CHT-14 480
CHT-03 469
CHT-05 471
CHT-01 467
RMP-02 558
RMP-09 565
DMK-16 503
RMP-06 562
RMP-07 563
DMK-12 499
DMK-20 506
DMB-01 488
DMK-02 490
DMK-13 500
DMK-17 504
DMK-14 501
DMK-15 502
DMK-11 498
CHT-11 477
DMK-18 505
RMP-01 557
RMP-10 566
KOT-02 512
KOT-04 514
KOT-01 511
KOT-05 515
Kot(MP-2) 508
Kot(MP-3) 509
KOT-10 520
KOT-11 521
KOT-03 513
KOT-08 518
KOT-09 519
KOT-07 517
RST-03 582
RST-08 587
RRA-06 394
RRA-08 396
RST-10 589
LBW1-02 528
LBW1-04 530

Section C

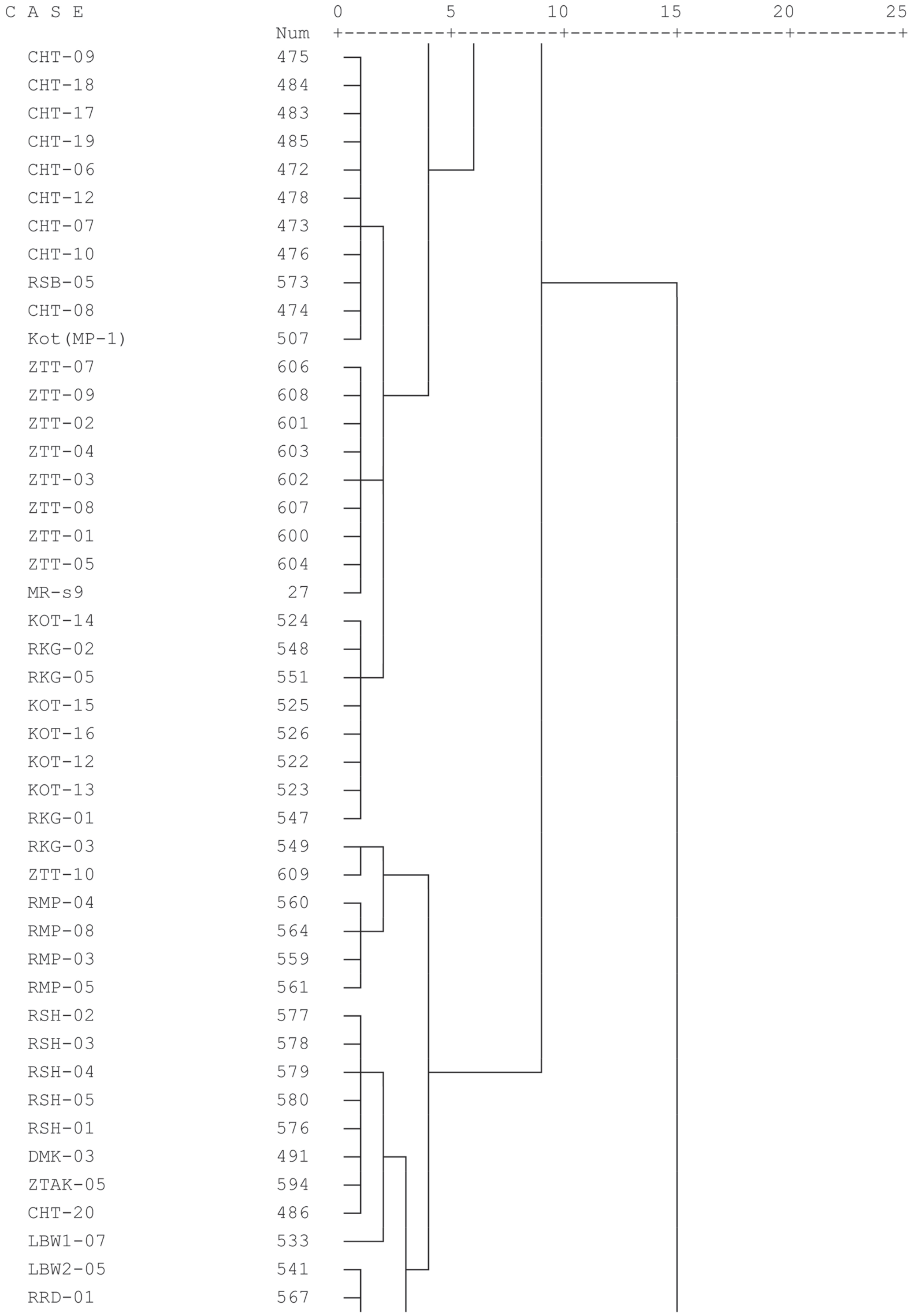
C A S E
Num
0
5
10
15
20
25
CHT-09 475
CHT-18 484
CHT-17 483
CHT-19 485
CHT-06 472
CHT-12 478
CHT-07 473
CHT-10 476
RSB-05 573
CHT-08 474
Kot(MP-1) 507
ZTT-07 606
ZTT-09 608
ZTT-02 601
ZTT-04 603
ZTT-03 602
ZTT-08 607
ZTT-01 600
ZTT-05 604
MR-s9 27
KOT-14 524
RKG-02 548
RKG-05 551
KOT-15 525
KOT-16 526
KOT-12 522
KOT-13 523
RKG-01 547
RKG-03 549
ZTT-10 609
RMP-04 560
RMP-08 564
RMP-03 559
RMP-05 561
RSH-02 577
RSH-03 578
RSH-04 579
RSH-05 580
RSH-01 576
DMK-03 491
ZTAK-05 594
CHT-20 486
LBW1-07 533
LBW2-05 541
RRD-01 567

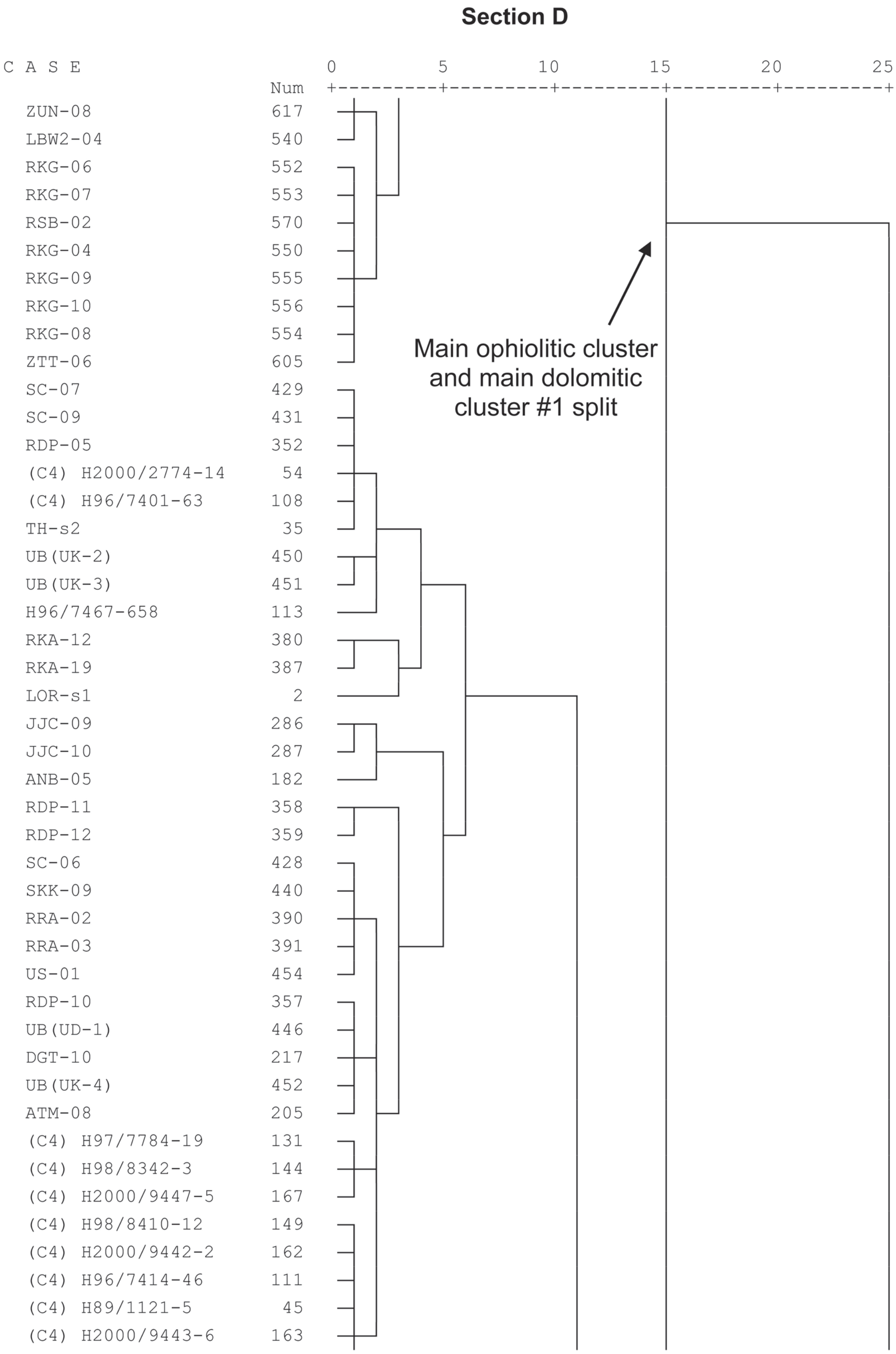
Section D
C A S E
Num
0
5
10
15
20
25
ZUN-08 617
LBW2-04 540
RKG-06 552
RKG-07 553
RSB-02 570
RKG-04 550
RKG-09 555
RKG-10 556
RKG-08 554
ZTT-06 605
SC-07 429
SC-09 431
RDP-05 352
(C4) H2000/2774-14 54
(C4) H96/7401-63 108
TH-s2 35
UB(UK-2) 450
UB(UK-3) 451
H96/7467-658 113
RKA-12 380
RKA-19 387
LOR-s1 2
JJC-09 286
JJC-10 287
ANB-05 182
RDP-11 358
RDP-12 359
SC-06 428
SKK-09 440
RRA-02 390
RRA-03 391
US-01 454
RDP-10 357
UB(UD-1) 446
DGT-10 217
UB(UK-4) 452
ATM-08 205
(C4) H97/7784-19 131
(C4) H98/8342-3 144
(C4) H2000/9447-5 167
(C4) H98/8410-12 149
(C4) H2000/9442-2 162
(C4) H96/7414-46 111
(C4) H89/1121-5 45
(C4) H2000/9443-6 163
Main ophiolitic cluster
and main dolomitic
cluster #1 split

Section E

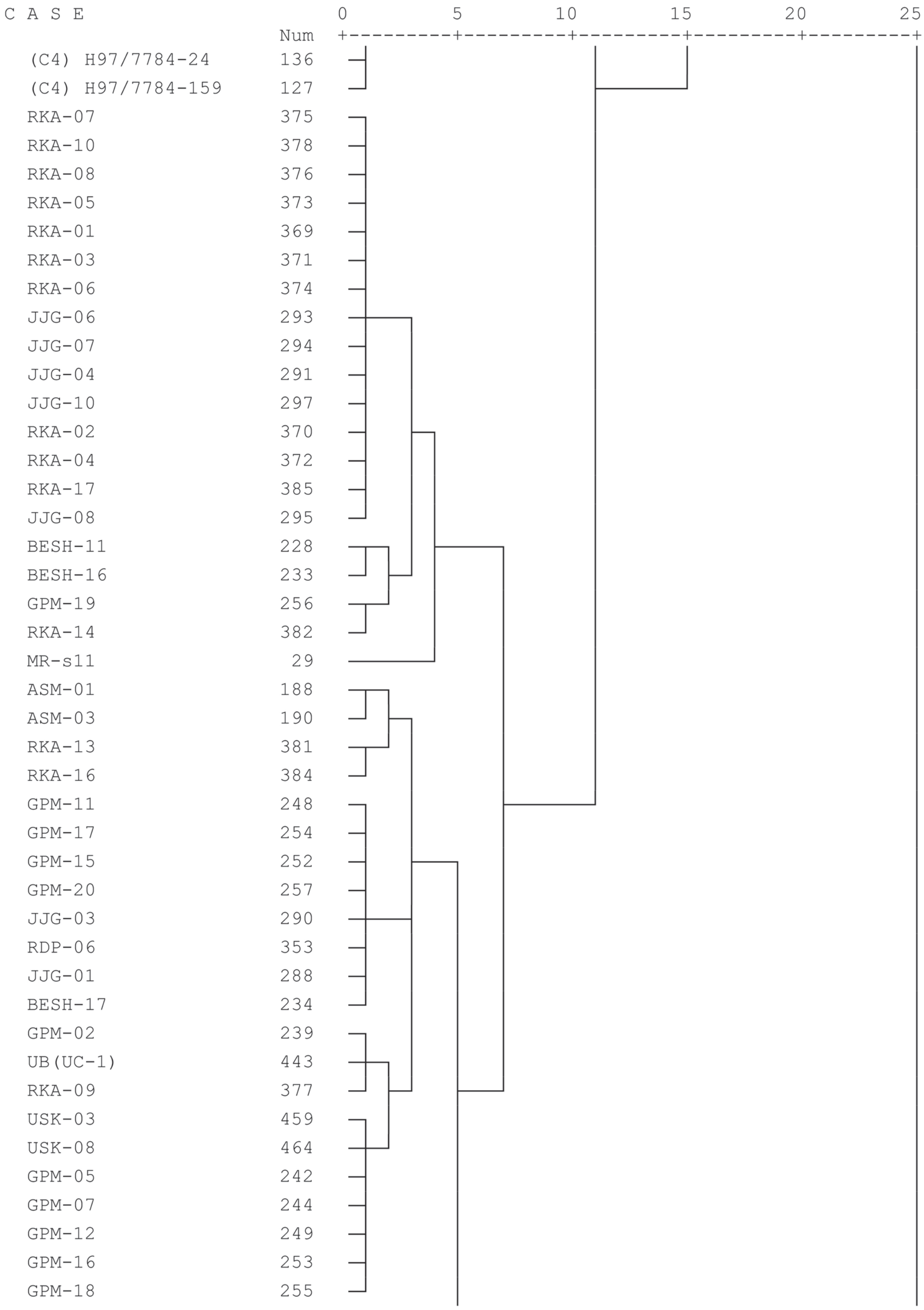
C A S E
Num
0 5 10 15 20 25
(C4) H97/7784-24 136
(C4) H97/7784-159 127
RKA-07 375
RKA-10 378
RKA-08 376
RKA-05 373
RKA-01 369
RKA-03 371
RKA-06 374
JJG-06 293
JJG-07 294
JJG-04 291
JJG-10 297
RKA-02 370
RKA-04 372
RKA-17 385
JJG-08 295
BESH-11 228
BESH-16 233
GPM-19 256
RKA-14 382
MR-s11 29
ASM-01 188
ASM-03 190
RKA-13 381
RKA-16 384
GPM-11 248
GPM-17 254
GPM-15 252
GPM-20 257
JJG-03 290
RDP-06 353
JJG-01 288
BESH-17 234
GPM-02 239
UB(UC-1) 443
RKA-09 377
USK-03 459
USK-08 464
GPM-05 242
GPM-07 244
GPM-12 249
GPM-16 253
GPM-18 255

Section F

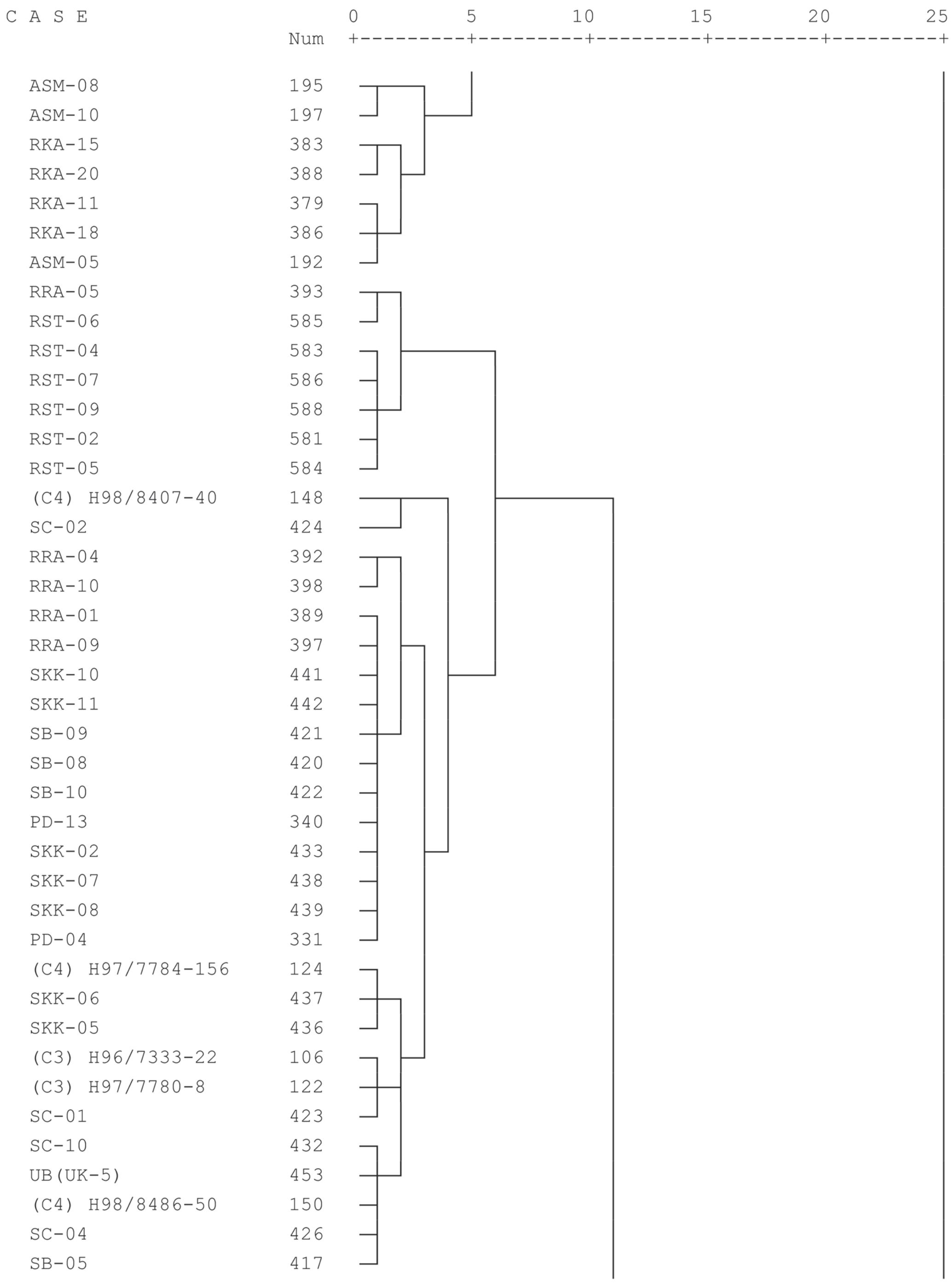
C A S E
Num
0 5 10 15 20 25
ASM-08 195
ASM-10 197
RKA-15 383
RKA-20 388
RKA-11 379
RKA-18 386
ASM-05 192
RRA-05 393
RST-06 585
RST-04 583
RST-07 586
RST-09 588
RST-02 581
RST-05 584
(C4) H98/8407-40 148
SC-02 424
RRA-04 392
RRA-10 398
RRA-01 389
RRA-09 397
SKK-10 441
SKK-11 442
SB-09 421
SB-08 420
SB-10 422
PD-13 340
SKK-02 433
SKK-07 438
SKK-08 439
PD-04 331
(C4) H97/7784-156 124
SKK-06 437
SKK-05 436
(C3) H96/7333-22 106
(C3) H97/7780-8 122
SC-01 423
SC-10 432
UB(UK-5) 453
(C4) H98/8486-50 150
SC-04 426
SB-05 417

Section G

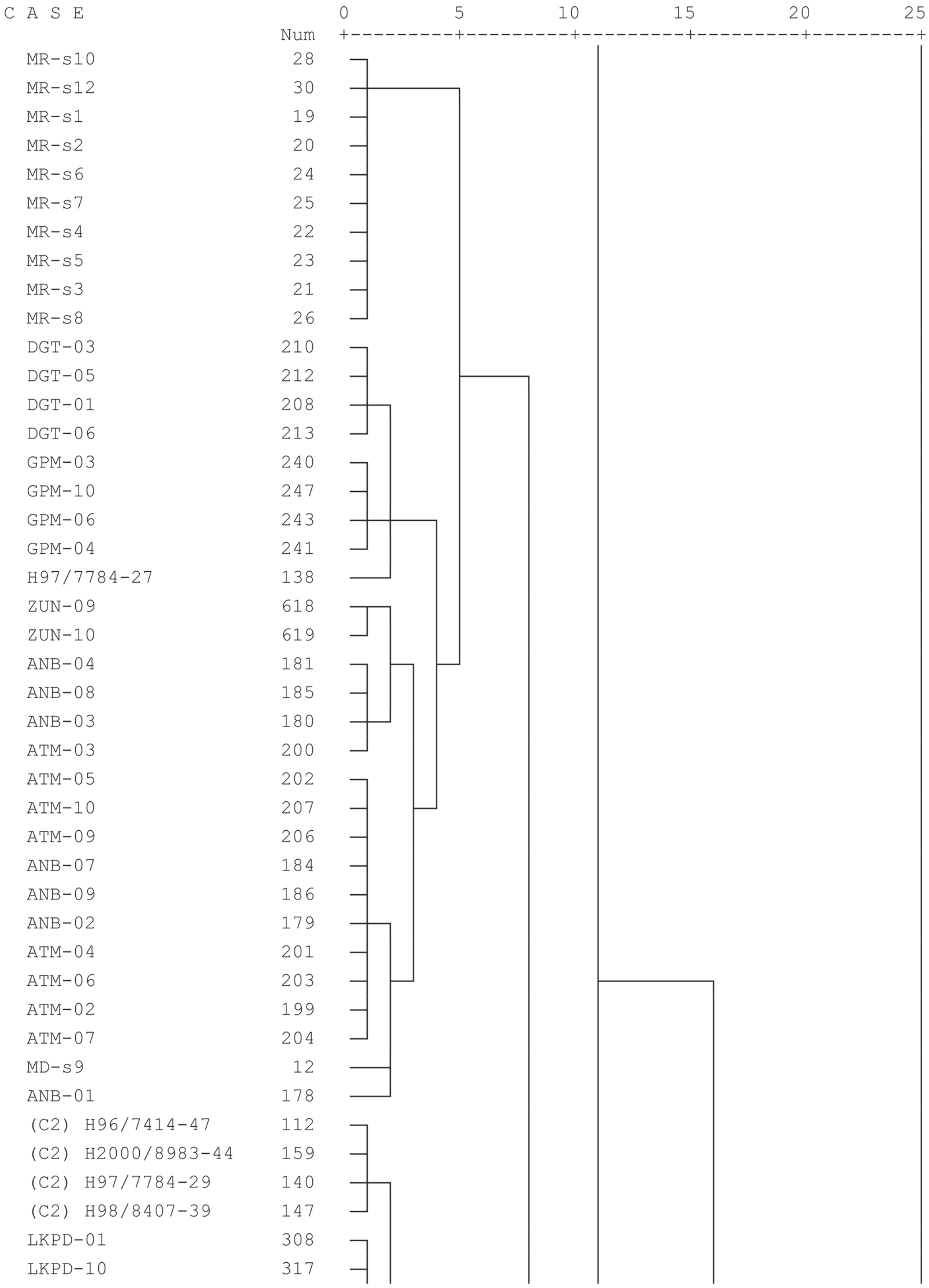
C A S E
Num
0
5
10
15
20
25
MR-s10 28
MR-s12 30
MR-s1 19
MR-s2 20
MR-s6 24
MR-s7 25
MR-s4 22
MR-s5 23
MR-s3 21
MR-s8 26
DGT-03 210
DGT-05 212
DGT-01 208
DGT-06 213
GPM-03 240
GPM-10 247
GPM-06 243
GPM-04 241
H97/7784-27 138
ZUN-09 618
ZUN-10 619
ANB-04 181
ANB-08 185
ANB-03 180
ATM-03 200
ATM-05 202
ATM-10 207
ATM-09 206
ANB-07 184
ANB-09 186
ANB-02 179
ATM-04 201
ATM-06 203
ATM-02 199
ATM-07 204
MD-s9 12
ANB-01 178
(C2) H96/7414-47 112
(C2) H2000/8983-44 159
(C2) H97/7784-29 140
(C2) H98/8407-39 147
LKPD-01 308
LKPD-10 317

Section H

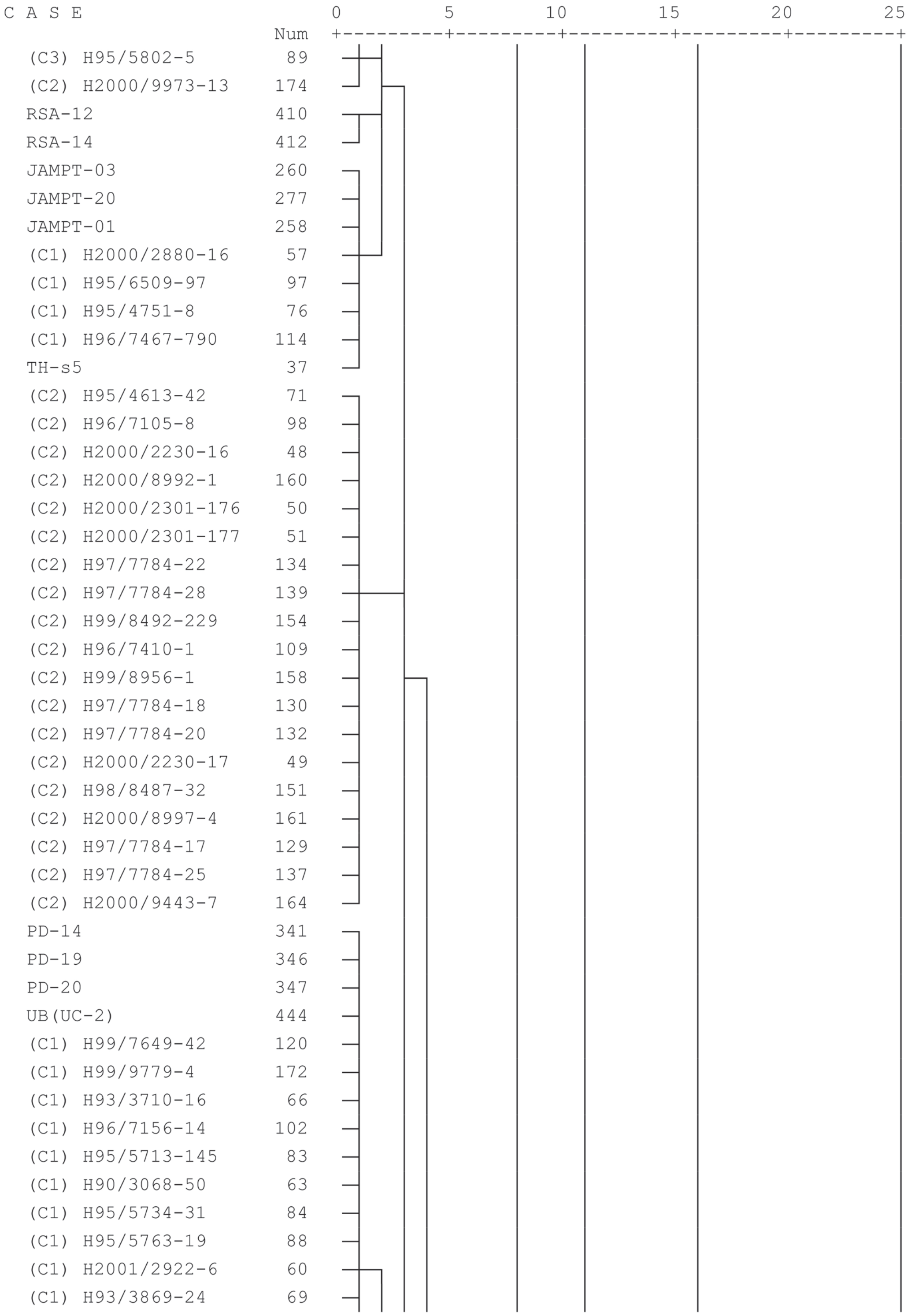
C A S E
Num
0
5
10
15
20
25
(C3) H95/5802-5 89
(C2) H2000/9973-13 174
RSA-12 410
RSA-14 412
JAMPT-03 260
JAMPT-20 277
JAMPT-01 258
(C1) H2000/2880-16 57
(C1) H95/6509-97 97
(C1) H95/4751-8 76
(C1) H96/7467-790 114
TH-s5 37
(C2) H95/4613-42 71
(C2) H96/7105-8 98
(C2) H2000/2230-16 48
(C2) H2000/8992-1 160
(C2) H2000/2301-176 50
(C2) H2000/2301-177 51
(C2) H97/7784-22 134
(C2) H97/7784-28 139
(C2) H99/8492-229 154
(C2) H96/7410-1 109
(C2) H99/8956-1 158
(C2) H97/7784-18 130
(C2) H97/7784-20 132
(C2) H2000/2230-17 49
(C2) H98/8487-32 151
(C2) H2000/8997-4 161
(C2) H97/7784-17 129
(C2) H97/7784-25 137
(C2) H2000/9443-7 164
PD-14 341
PD-19 346
PD-20 347
UB(UC-2) 444
(C1) H99/7649-42 120
(C1) H99/9779-4 172
(C1) H93/3710-16 66
(C1) H96/7156-14 102
(C1) H95/5713-145 83
(C1) H90/3068-50 63
(C1) H95/5734-31 84
(C1) H95/5763-19 88
(C1) H2001/2922-6 60
(C1) H93/3869-24 69

Section I

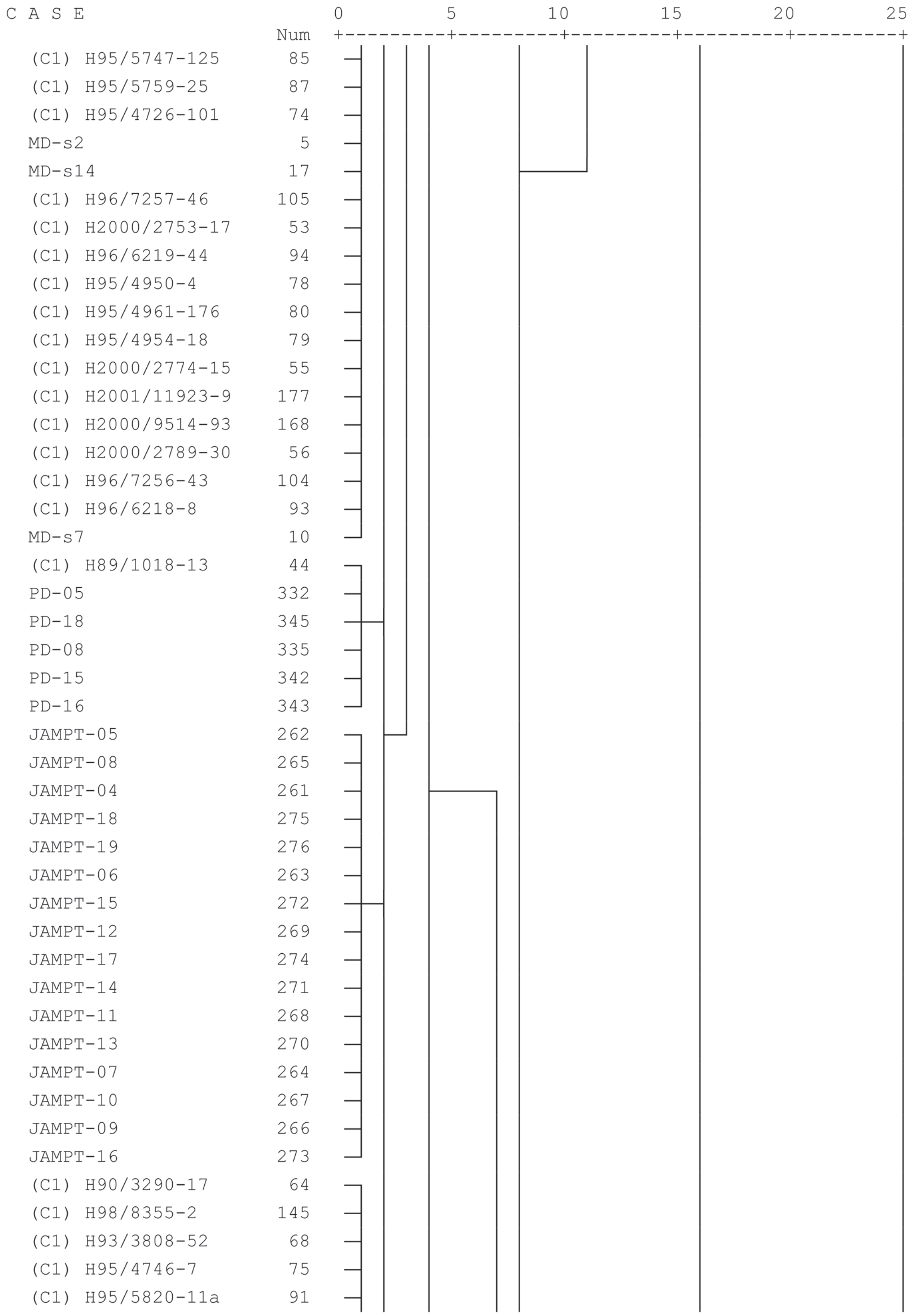
C A S E
Num
0 5 10 15 20 25
(C1) H95/5747-125 85
(C1) H95/5759-25 87
(C1) H95/4726-101 74
MD-s2 5
MD-s14 17
(C1) H96/7257-46 105
(C1) H2000/2753-17 53
(C1) H96/6219-44 94
(C1) H95/4950-4 78
(C1) H95/4961-176 80
(C1) H95/4954-18 79
(C1) H2000/2774-15 55
(C1) H2001/11923-9 177
(C1) H2000/9514-93 168
(C1) H2000/2789-30 56
(C1) H96/7256-43 104
(C1) H96/6218-8 93
MD-s7 10
(C1) H89/1018-13 44
PD-05 332
PD-18 345
PD-08 335
PD-15 342
PD-16 343
JAMPT-05 262
JAMPT-08 265
JAMPT-04 261
JAMPT-18 275
JAMPT-19 276
JAMPT-06 263
JAMPT-15 272
JAMPT-12 269
JAMPT-17 274
JAMPT-14 271
JAMPT-11 268
JAMPT-13 270
JAMPT-07 264
JAMPT-10 267
JAMPT-09 266
JAMPT-16 273
(C1) H90/3290-17 64
(C1) H98/8355-2 145
(C1) H93/3808-52 68
(C1) H95/4746-7 75
(C1) H95/5820-11a 91

Section J

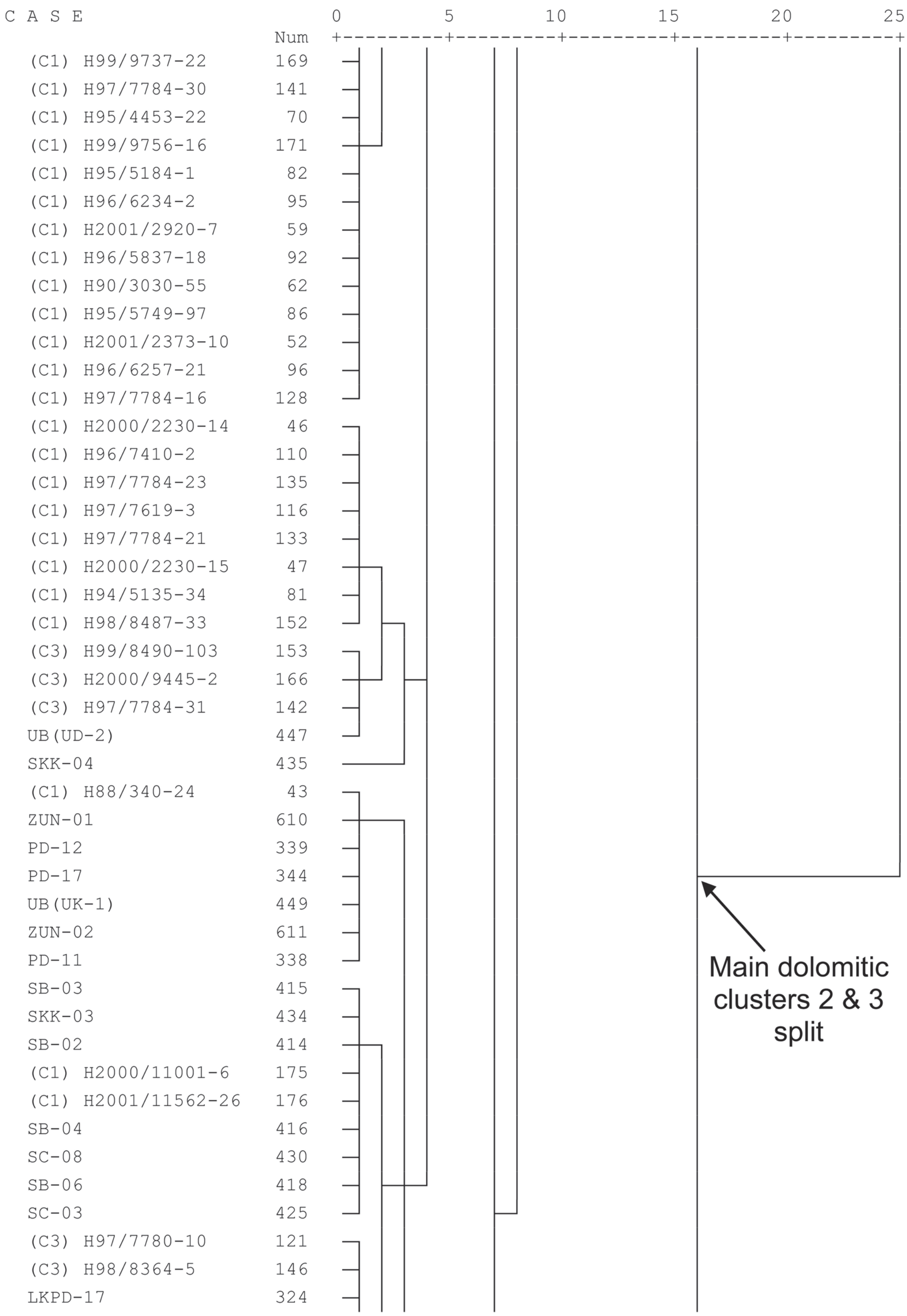
C A S E
Num
0
5
10
15
20
25
(C1) H99/9737-22 169
(C1) H97/7784-30 141
(C1) H95/4453-22 70
(C1) H99/9756-16 171
(C1) H95/5184-1 82
(C1) H96/6234-2 95
(C1) H2001/2920-7 59
(C1) H96/5837-18 92
(C1) H90/3030-55 62
(C1) H95/5749-97 86
(C1) H2001/2373-10 52
(C1) H96/6257-21 96
(C1) H97/7784-16 128
(C1) H2000/2230-14 46
(C1) H96/7410-2 110
(C1) H97/7784-23 135
(C1) H97/7619-3 116
(C1) H97/7784-21 133
(C1) H2000/2230-15 47
(C1) H94/5135-34 81
(C1) H98/8487-33 152
(C3) H99/8490-103 153
(C3) H2000/9445-2 166
(C3) H97/7784-31 142
UB(UD-2) 447
SKK-04 435
(C1) H88/340-24 43
ZUN-01 610
PD-12 339
PD-17 344
UB(UK-1) 449
ZUN-02 611
PD-11 338
SB-03 415
SKK-03 434
SB-02 414
(C1) H2000/11001-6 175
(C1) H2001/11562-26 176
SB-04 416
SC-08 430
SB-06 418
SC-03 425
(C3) H97/7780-10 121
(C3) H98/8364-5 146
LKPD-17 324
Main dolomitic clusters 2 & 3 split

Section K

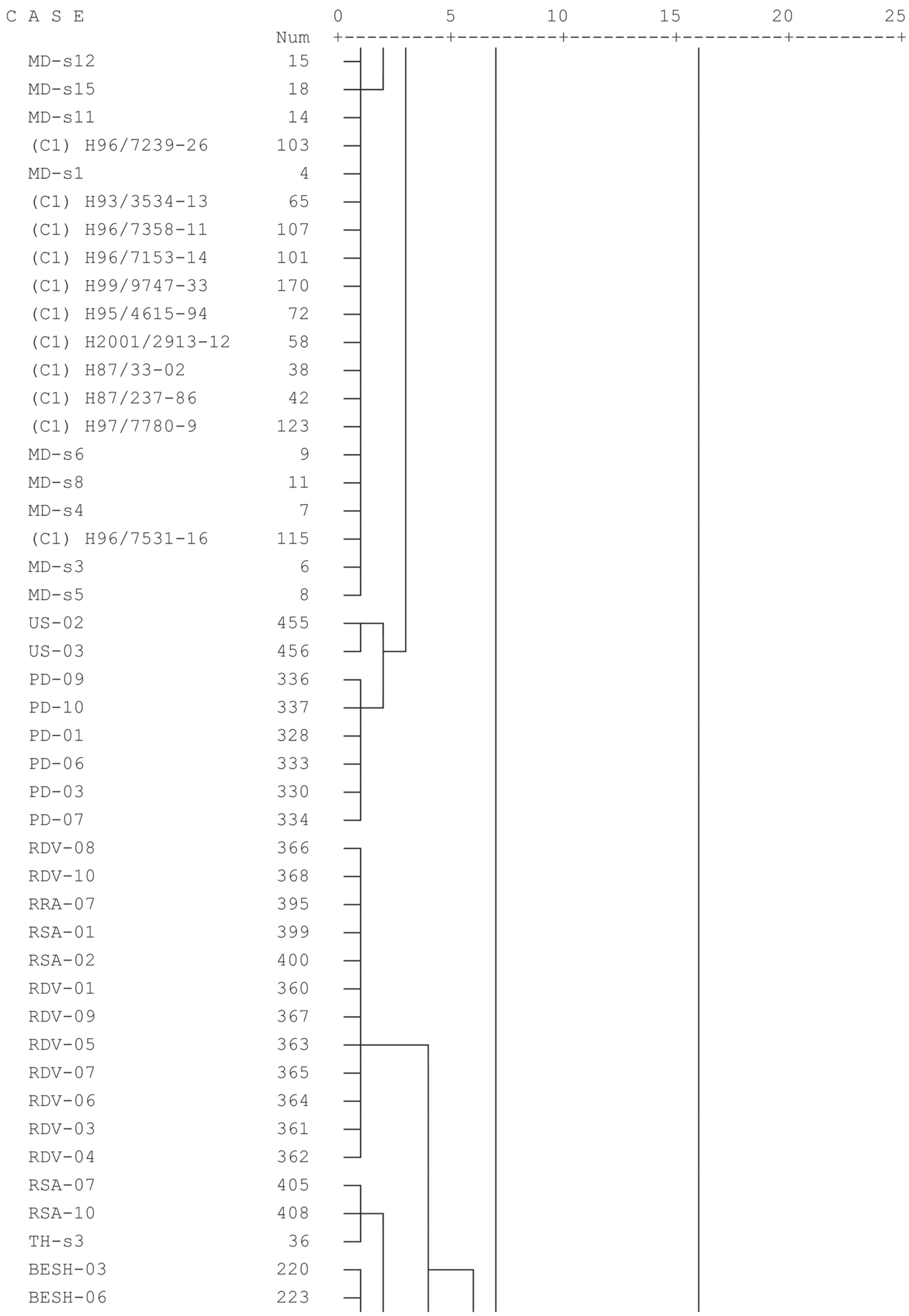
C A S E
Num
0 5 10 15 20 25
MD-s12 15
MD-s15 18
MD-s11 14
(C1) H96/7239-26 103
MD-s1 4
(C1) H93/3534-13 65
(C1) H96/7358-11 107
(C1) H96/7153-14 101
(C1) H99/9747-33 170
(C1) H95/4615-94 72
(C1) H2001/2913-12 58
(C1) H87/33-02 38
(C1) H87/237-86 42
(C1) H97/7780-9 123
MD-s6 9
MD-s8 11
MD-s4 7
(C1) H96/7531-16 115
MD-s3 6
MD-s5 8
US-02 455
US-03 456
PD-09 336
PD-10 337
PD-01 328
PD-06 333
PD-03 330
PD-07 334
RDV-08 366
RDV-10 368
RRA-07 395
RSA-01 399
RSA-02 400
RDV-01 360
RDV-09 367
RDV-05 363
RDV-07 365
RDV-06 364
RDV-03 361
RDV-04 362
RSA-07 405
RSA-10 408
TH-s3 36
BESH-03 220
BESH-06 223

Section L

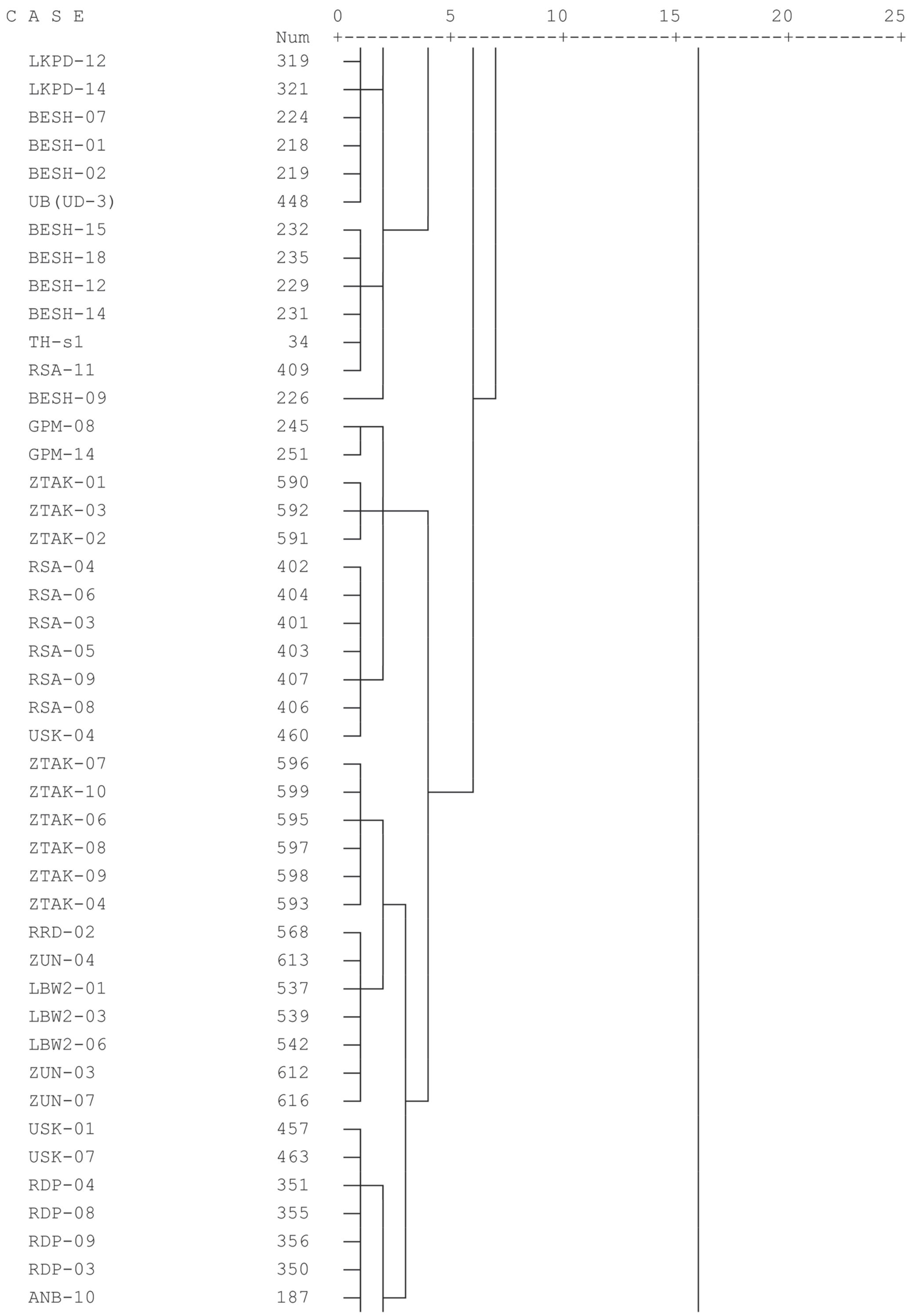
C A S E
Num
0
5
10
15
20
25
LKPD-12 319
LKPD-14 321
BESH-07 224
BESH-01 218
BESH-02 219
UB(UD-3) 448
BESH-15 232
BESH-18 235
BESH-12 229
BESH-14 231
TH-s1 34
RSA-11 409
BESH-09 226
GPM-08 245
GPM-14 251
ZTAK-01 590
ZTAK-03 592
ZTAK-02 591
RSA-04 402
RSA-06 404
RSA-03 401
RSA-05 403
RSA-09 407
RSA-08 406
USK-04 460
ZTAK-07 596
ZTAK-10 599
ZTAK-06 595
ZTAK-08 597
ZTAK-09 598
ZTAK-04 593
RRD-02 568
ZUN-04 613
LBW2-01 537
LBW2-03 539
LBW2-06 542
ZUN-03 612
ZUN-07 616
USK-01 457
USK-07 463
RDP-04 351
RDP-08 355
RDP-09 356
RDP-03 350
ANB-10 187

Section M

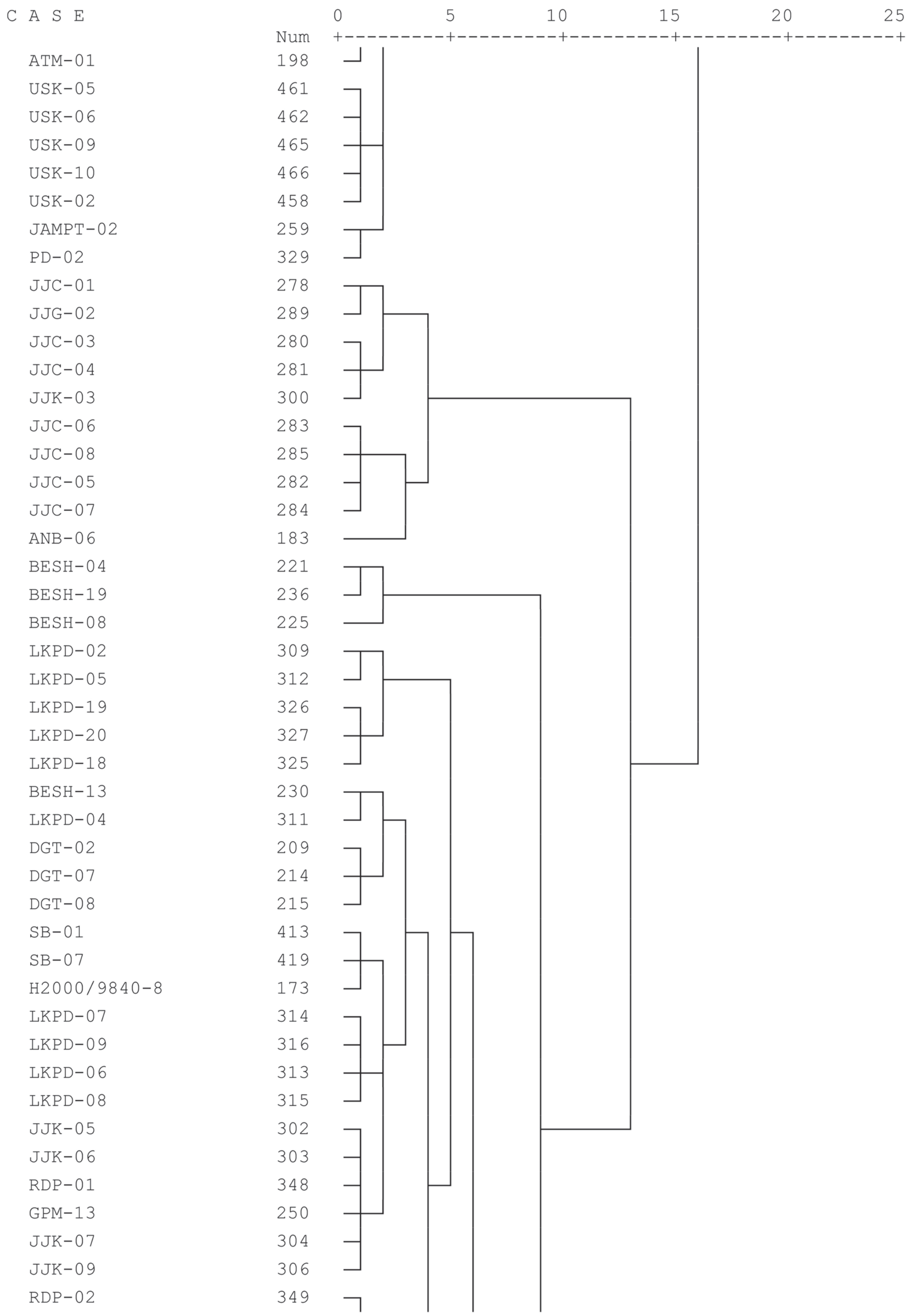
C A S E
Num
0 5 10 15 20 25
ATM-01 198
USK-05 461
USK-06 462
USK-09 465
USK-10 466
USK-02 458
JAMPT-02 259
PD-02 329
JJC-01 278
JJG-02 289
JJC-03 280
JJC-04 281
JJK-03 300
JJC-06 283
JJC-08 285
JJC-05 282
JJC-07 284
ANB-06 183
BESH-04 221
BESH-19 236
BESH-08 225
LKPD-02 309
LKPD-05 312
LKPD-19 326
LKPD-20 327
LKPD-18 325
BESH-13 230
LKPD-04 311
DGT-02 209
DGT-07 214
DGT-08 215
SB-01 413
SB-07 419
H2000/9840-8 173
LKPD-07 314
LKPD-09 316
LKPD-06 313
LKPD-08 315
JJK-05 302
JJK-06 303
RDP-01 348
GPM-13 250
JJK-07 304
JJK-09 306
RDP-02 349

Section N

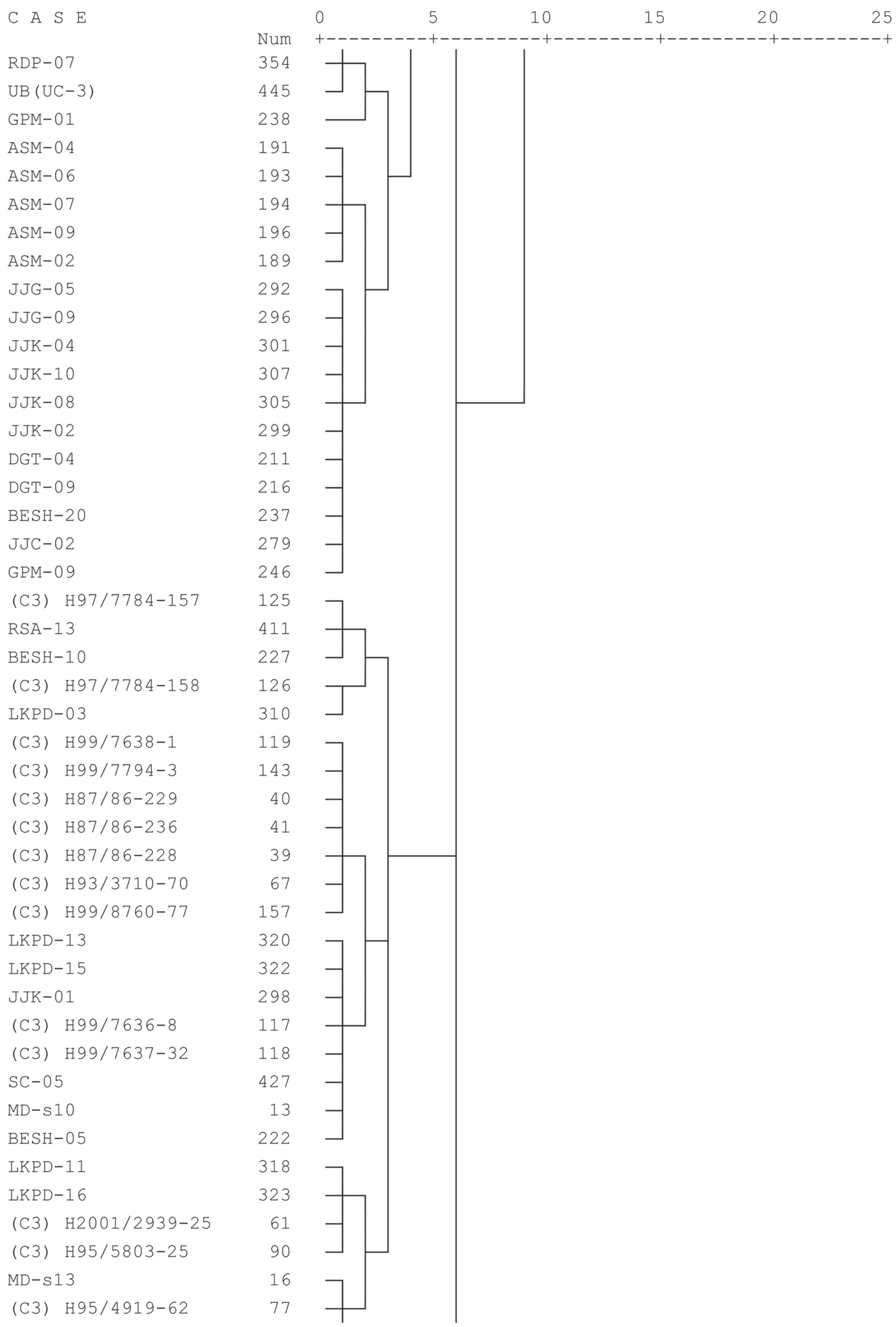
C A S E
Num
0 5 10 15 20 25
RDP-07 354
UB(UC-3) 445
GPM-01 238
ASM-04 191
ASM-06 193
ASM-07 194
ASM-09 196
ASM-02 189
JJG-05 292
JJG-09 296
JJK-04 301
JJK-10 307
JJK-08 305
JJK-02 299
DGT-04 211
DGT-09 216
BESH-20 237
JJC-02 279
GPM-09 246
(C3) H97/7784-157 125
RSA-13 411
BESH-10 227
(C3) H97/7784-158 126
LKPD-03 310
(C3) H99/7638-1 119
(C3) H99/7794-3 143
(C3) H87/86-229 40
(C3) H87/86-236 41
(C3) H87/86-228 39
(C3) H93/3710-70 67
(C3) H99/8760-77 157
LKPD-13 320
LKPD-15 322
JJK-01 298
(C3) H99/7636-8 117
(C3) H99/7637-32 118
SC-05 427
MD-s10 13
BESH-05 222
LKPD-11 318
LKPD-16 323
(C3) H2001/2939-25 61
(C3) H95/5803-25 90
MD-s13 16
(C3) H95/4919-62 77

Section O

```
C A S E                    0         5        10        15        20        25
                     Num   +---------+---------+---------+---------+---------+

  (C3) H96/7106-27    99
  (C3) H96/7118-9    100
  (C3) H95/4723-2     73
  (C3) H99/8497-3    155
  H2000/9445-1       165
```

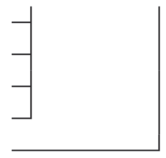

APPENDIX 7.10

CLUSTER ANALYSIS (COMPLETE LINKAGE) OF 140 STEATITE ARTIFACTS FROM HARAPPA

Section A

Artifact #	Period	Mound	Trench	1st / 2nd PGM	Type
H2000/2753-17	3C	E	Tr.55	PD / SB	E
H96/6219-44	S&D	ET	Tr.35	SB / SKK	D
H95/4950-4	3C	ET	Tr.28	SKK / SB	A
H95/4961-176	3C	ET	Tr.28	SKK / SB	A
H95/4954-18	3C	ET	Tr.28	SKK / SB	E
H2000/2774-15	3C	E	Tr.55	SKK / PD	C
H2001/11923-9	3C	E	Tr.11	SB / SKK	C
H2000/9514-93	2	AB	Tr.39	SB / JAMPT	E
H2000/2789-30	3C	E	Tr.55	SKK / SB	C
H96/7256-43	3B	F	Tr.37	SKK / SB	B
H96/6218-8	S&D	ET	Tr.35	SKK / SB	C
H96/7239-26	3C	F	Tr.37	SB / SC	A
H2001/11562-26	S&D	E	Tr.11	SB / SC	F
H96/7531-16	1	AB	Tr.39	ATM / SKK	A
H96/7257-46	3B	F	Tr.37	PD / SKK	B
H90/3290-17	S&D	E	Tr.59	SB / SKK	D
H98/8355-2	3B	AB	Tr.39	SKK / SB	A
H93/3808-52	S&D	E	Tr.5	SKK / SB	A
H95/4746-7	3C	ET	Tr.19	SB / SKK	A
H95/5820-11a	3C	ET	Tr.28	PD / SKK	A
H99/9737-22	3C	F	Tr.43	SKK / SB	A
H97/7784-30	3A	AB	Tr.42	SKK / SB	E
H95/4453-22	S&D	E	Tr.11	SB / SKK	D
H99/9756-16	3C	F	Tr.43	SB / SKK	A
H95/5184-1	3C	E	Tr.7/8	SB / SKK	A
H96/6234-2	S&D	ET	Tr.35	SB / SKK	C
H2001/2920-7	S&D	E	Tr.57	SKK / SB	C
H96/5837-18	3C	ET	Tr.28	SB / LKPD	B
H90/3030-55	S&D	E	Tr.58	JAMPT / RSA	E
H95/5749-97	3C	ET	Tr.32	SKK / SB	C
H2001/2373-10	3B	E	Tr.54	SKK / SB	C
H96/6257-21	3C	ET	Tr.35	SKK / SB	A
H97/7784-16	3A	AB	Tr.42	RSA / SKK	A
H2000/2230-14	3B	E	Tr.54	SB / LKPD	C
H96/7410-2	2/3	AB	Tr.39	SKK / SB	E
H97/7784-23	3A	AB	Tr.42	SKK / SB	C
H97/7619-3	3C	F	Tr.41	SB / LKPD	C
H97/7784-21	3A	AB	Tr.42	SB / SKK	B
H2000/2230-15	3B	E	Tr.54	LKPD / SB	C
H94/5135-34	3C	E	Tr.7/8	SB / SC	E
H99/7649-42	3C	F	Tr.41	SB / SKK	A
H99/9779-4	3C	F	Tr.43	SB / LKPD	A
H93/3710-16	3C	E	Tr.3	SB / SKK	F
H96/7156-14	3C	E	Tr.36	SB / SKK	G
H95/5713-145	S&D	ET	Tr.32	SB / SKK	C
H90/3068-50	S&D	E	Tr.58	SB / SKK	A
H95/5734-31	3C	ET	Tr.32	PD / SB	C
H95/5763-19	3C	ET	Tr.32	SB / LKPD	A
H2001/2922-6	S&D	E	Tr.57	SB / SKK	A
H93/3869-24	3C	E	Tr.7	SKK / PD	A
H95/5747-125	3C	ET	Tr.32	SB / SKK	B
H95/5759-25	3C	ET	Tr.32	SB / PD	E
H95/4726-101	3C	ET	Tr.19	SB / SKK	A
H87/33-02	3C	CEM	CEM	SB / SKK	F
H87/237-86	S&D	CEM	CEM	SB / SKK	F
H97/7780-9	3B	AB	Tr.42	SB / SKK	A
H89/1018-13	S&D	AB/E	Tr.53	SKK / SB	D
H93/3534-13	S&D	E	Tr.2	LKPD / SB	F
H96/7358-11	5	AB	Tr.38	LKPD / SKK	A
H96/7153-14	S&D	E	Tr.36	SB / SKK	D
H99/9747-33	3C	F	Tr.43	SKK / SB	B
H95/4615-94	3C	ET	Tr.10	SKK / SB	A
H2001/2913-12	3B	E	Tr.57	SKK / SB	E
H2000/2880-16	3C	E	Tr.55	SKK / SB	D
H95/6509-97	2	E/ET	Tr.11	JAMPT / RSA	B
H95/4751-8	3C	ET	Tr.19	SKK / SB	E
H96/7467-790	S&D	AB	Tr.39	SKK / SB	A
H2000/11001-6	1	AB	Tr.39	JAMPT / RSA	A
H88/340-24	S&D	E	Op. 3	PD / SB	F
H98/8487-33	2	AB	Tr.39	PD / SKK	A

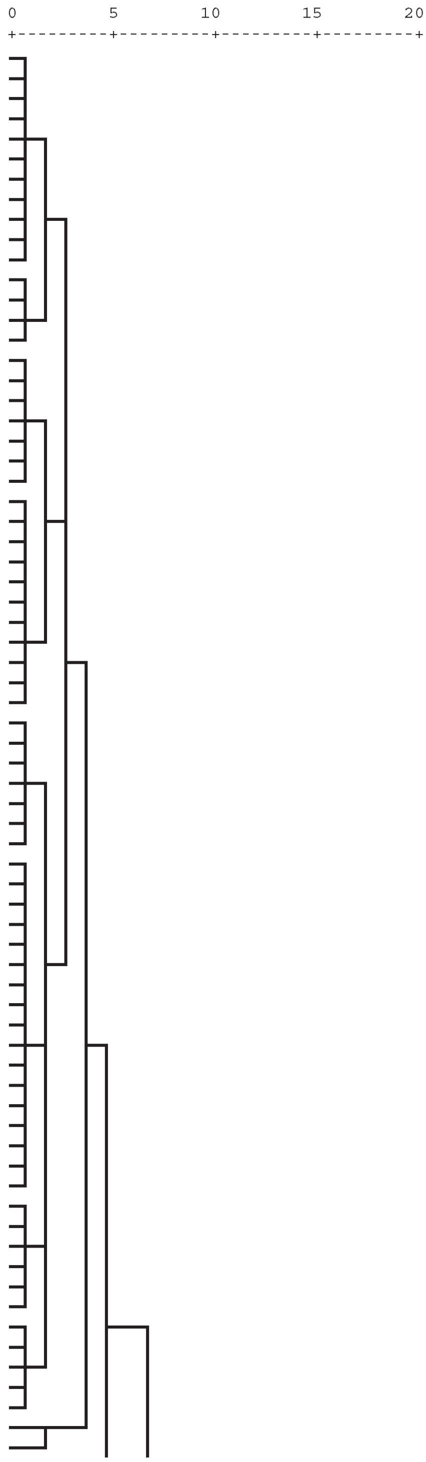

Section B

H96/7414-47	2	AB	Tr.39	JAMPT / LKPD	A
H2000/8983-44	2	AB	Tr.39	SC / LKPD	E
H97/7784-29	3A	AB	Tr.42	SC / SKK	B
H98/8407-39	2	AB	Tr.39	RDP / USK	E
H2000/9973-13	2	AB	Tr.39	JAMPT / RSA	C
H95/4613-42	3B	ET	Tr.10	SKK / SB	A
H96/7105-8	3C	E	Tr.36	SKK / SB	A
H2000/2230-16	3B	E	Tr.54	JAMPT / RSA	C
H2000/8992-1	2	AB	Tr.39	JAMPT / RSA	E
H2000/2301-176	3A	E	Tr.54	JAMPT / SB	B
H2000/2301-177	3A	E	Tr.54	JAMPT / SB	B
H97/7784-22	3A	AB	Tr.42	JAMPT / SKK	C
H97/7784-28	3A	AB	Tr.42	SB / SKK	B
H99/8492-229	2	AB	Tr.39	SKK / SC	E
H96/7410-1	2/3A	AB	Tr.39	SKK / SB	E
H99/8956-1	2	AB	Tr.39	SKK / JAMPT	A
H97/7784-18	3A	AB	Tr.42	USK / SKK	A
H97/7784-20	3A	AB	Tr.42	USK / SKK	A
H2000/2230-17	3B	E	Tr.54	JAMPT / SKK	B
H98/8487-32	2	AB	Tr.39	JAMPT / SKK	E
H2000/8997-4	2	AB	Tr.39	JAMPT / SKK	A
H97/7784-17	3A	AB	Tr.42	SKK / JAMPT	A
H97/7784-25	3A	AB	Tr.42	SKK / JAMPT	A
H2000/9443-7	3B	AB	Tr.39	JAMPT / USK	B
H99/7636-8	3C	F	Tr.41	RSA / LKPD	E
H99/7637-32	3C	F	Tr.41	LKPD / SB	G
H99/7638-1	3C	F	Tr.41	SB / JAMPT	G
H99/7794-3	3C	AB	Tr.42	SB / LKPD	B
H87/86-229	3C	CEM	CEM	SB / RSA	F
H87/86-236	3C	CEM	CEM	SB / LKPD	F
H87/86-228	3C	CEM	CEM	SB / SC	F
H93/3710-70	3C	E	Tr.3	LKPD / SB	F
H99/8760-77	3C	F	Tr.43	ANB /RSA	F
H95/5802-5	3C	ET	Tr.28	LKPD / RSA	A
H97/7784-157	3A	AB	Tr.42	LKPD / RSA	F
H97/7784-158	3A	AB	Tr.42	LKPD / SB	A
H2001/2939-25	3B	E	Tr.57	LKPD / RDP	G
H95/5803-25	3C	ET	Tr.28	LKPD / RSA	B
H99/8490-103	2	AB	Tr.39	SC / SKK	B
H2000/9445-2	3B	AB	Tr.39	SC / LKPD	G
H97/7784-31	3A	AB	Tr.42	SC / LKPD	A
H96/7106-27	3C	E	Tr.36	LKPD / RDP	G
H96/7118-9	3C	E	Tr.36	LKPD / RDP	A
H95/4723-2	3C	ET	Tr.19	LKPD / RDP	B
H99/8497-3	2	AB	Tr.39	LKPD / SC	E
H95/4919-62	3C	ET	Tr.28	RDP / SC	D
H97/7780-10	3B	AB	Tr.42	SB / SC	E
H98/8364-5	3B	AB	Tr.39	SB / SC	F
H96/7333-22	5	AB	Tr.38	SC / SKK	A
H97/7780-8	3B	AB	Tr.42	SC / SB	A
H2000/9445-1	3B	AB	Tr.39	ANB / ATM	G
H97/7784-156	3A	AB	Tr.42	SKK / SC	A
H98/8407-40	2	AB	Tr.39	SC / SKK	A
H98/8486-50	2	AB	Tr.39	SKK / SC	A
H98/8410-12	2	AB	Tr.39	SC / SKK	A
H2000/9442-2	3B	AB	Tr.39	SC / SKK	E
H96/7414-46	2	AB	Tr.39	SC / SKK	A
H89/1121-5	S&D	E	Tr.52	SKK / SC	A
H2000/9443-6	3B	AB	Tr.39	SKK / SC	A
H97/7784-24	3A	AB	Tr.42	SKK / SC	C
H97/7784-159	3A	AB	Tr.42	SKK / SC	A
H2000/2774-14	3C	E	Tr.55	SC / RDP	G
H96/7401-63	S&D	AB	Tr.39	SC / RDP	F
H97/7784-19	3A	AB	Tr.42	SC / SKK	A
H98/8342-3	3C	AB	Tr.39	SC / SKK	F
H2000/9447-5	3B	AB	Tr.39	SC / SKK	A
H97/7784-27	3A	AB	Tr.42	LBW1 / LBW2	A
H2000/9840-8	3C	F	Tr.43	SB / SC	E
H98/8668-2	3C	F	Tr.43	KOT / ZTT	E
H96/7467-658	S&D	AB	Tr.39	ATM / SC	A

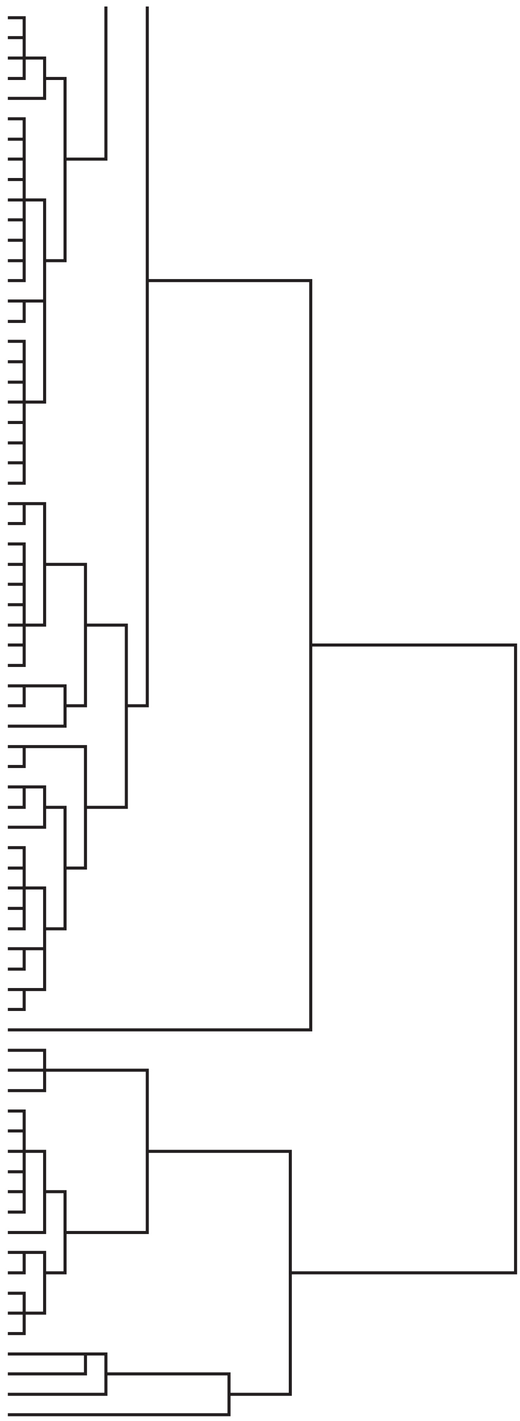

APPENDIX 7.11

CLUSTER ANALYSIS (COMPLETE LINKAGE) OF ALL 177 STEATITE ARTIFACTS

Section A

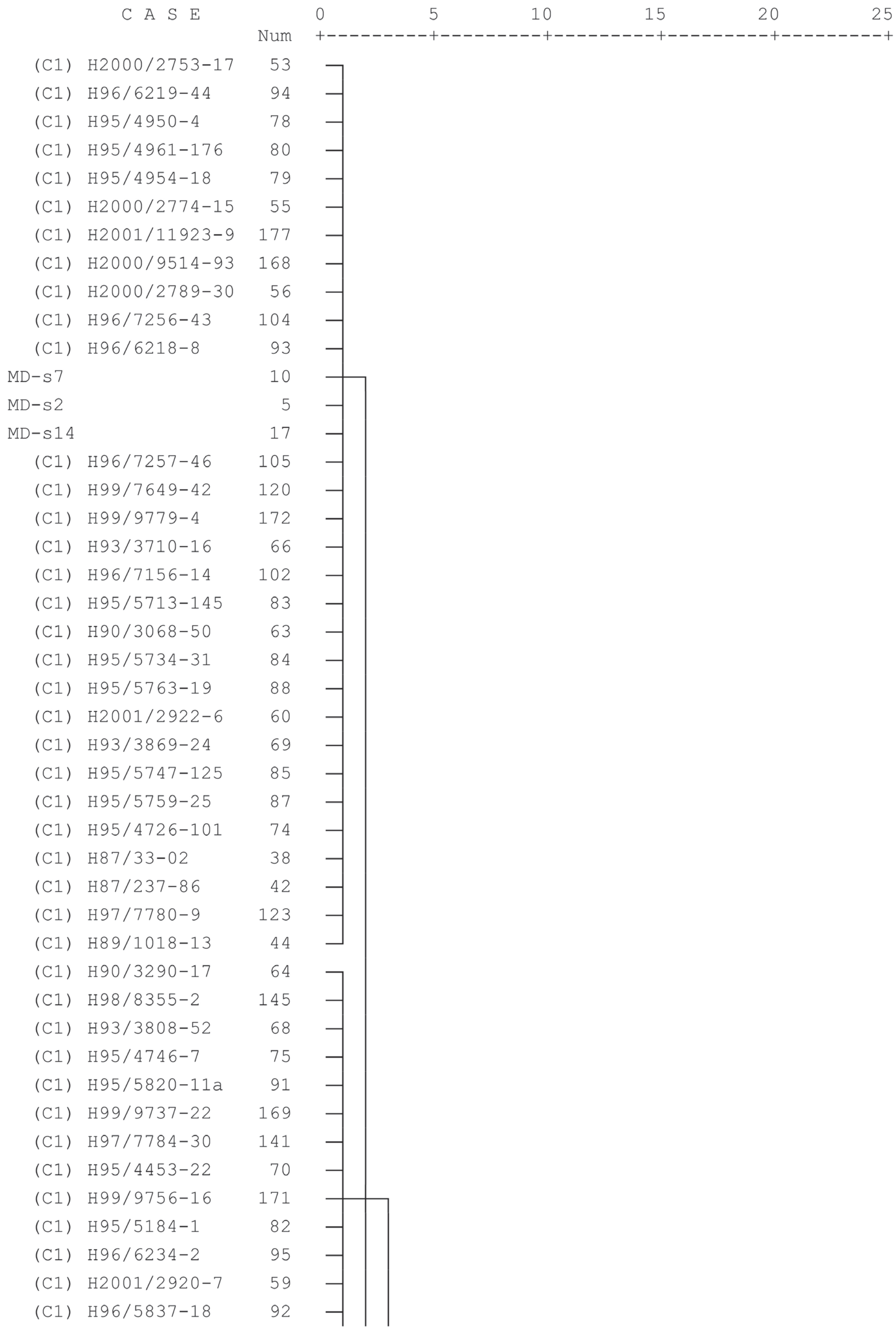

Section B

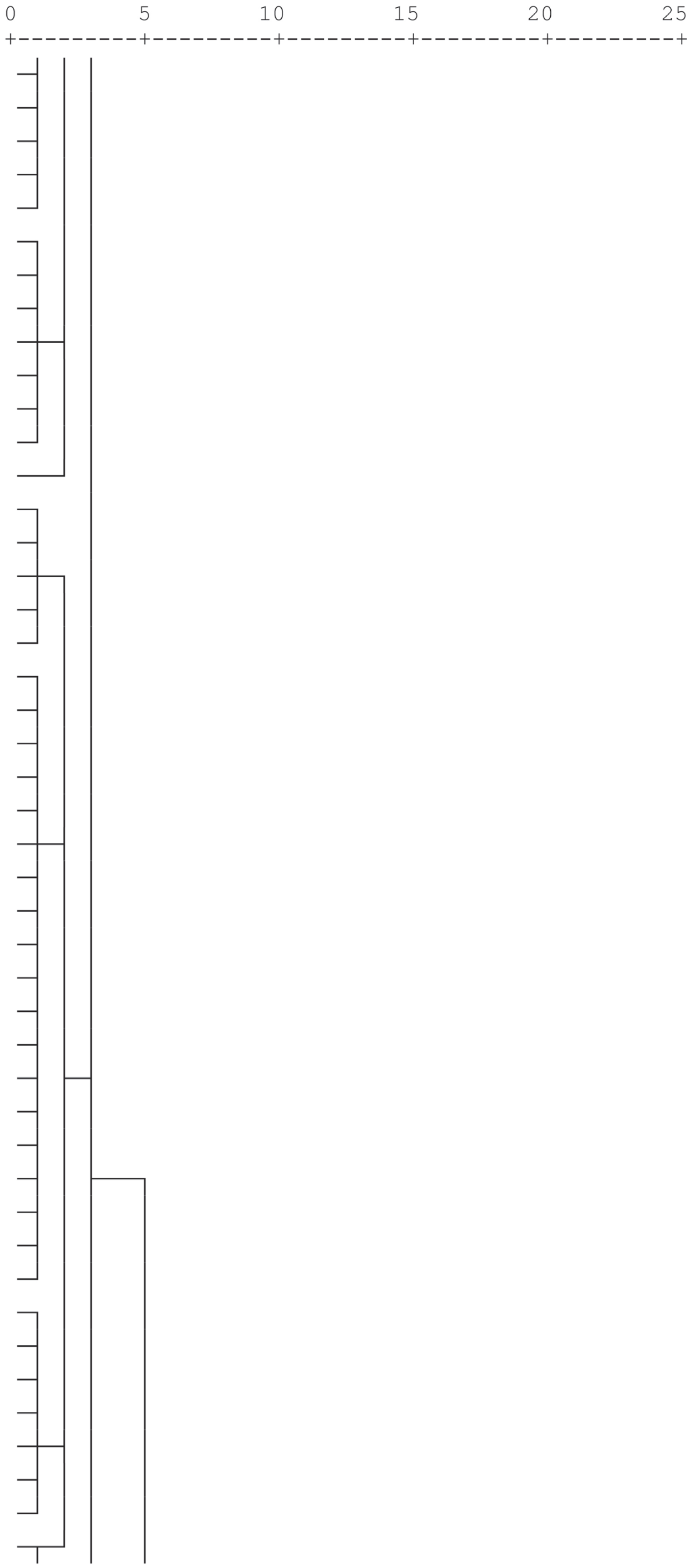

C A S E	
(C1) H90/3030-55	62
(C1) H95/5749-97	86
(C1) H2001/2373-10	52
(C1) H96/6257-21	96
(C1) H97/7784-16	128
(C1) H2000/2230-14	46
(C1) H96/7410-2	110
(C1) H97/7784-23	135
(C1) H97/7619-3	116
(C1) H97/7784-21	133
(C1) H2000/2230-15	47
(C1) H94/5135-34	81
(C1) H98/8487-33	152
(C1) H2000/2880-16	57
(C1) H95/6509-97	97
(C1) H95/4751-8	76
(C1) H96/7467-790	114
TH-s5	37
(C1) H93/3534-13	65
(C1) H96/7358-11	107
(C1) H96/7153-14	101
(C1) H99/9747-33	170
(C1) H95/4615-94	72
(C1) H2001/2913-12	58
MD-s12	15
MD-s15	18
MD-s11	14
(C1) H96/7239-26	103
MD-s1	4
(C1) H2000/11001-6	175
(C1) H2001/11562-2	176
MD-s6	9
MD-s8	11
MD-s4	7
(C1) H96/7531-16	115
MD-s3	6
MD-s5	8
(C3) H99/7638-1	119
(C3) H99/7794-3	143
(C3) H87/86-229	40
(C3) H87/86-236	41
(C3) H87/86-228	39
(C3) H93/3710-70	67
(C3) H99/8760-77	157
MD-s10	13

Section C

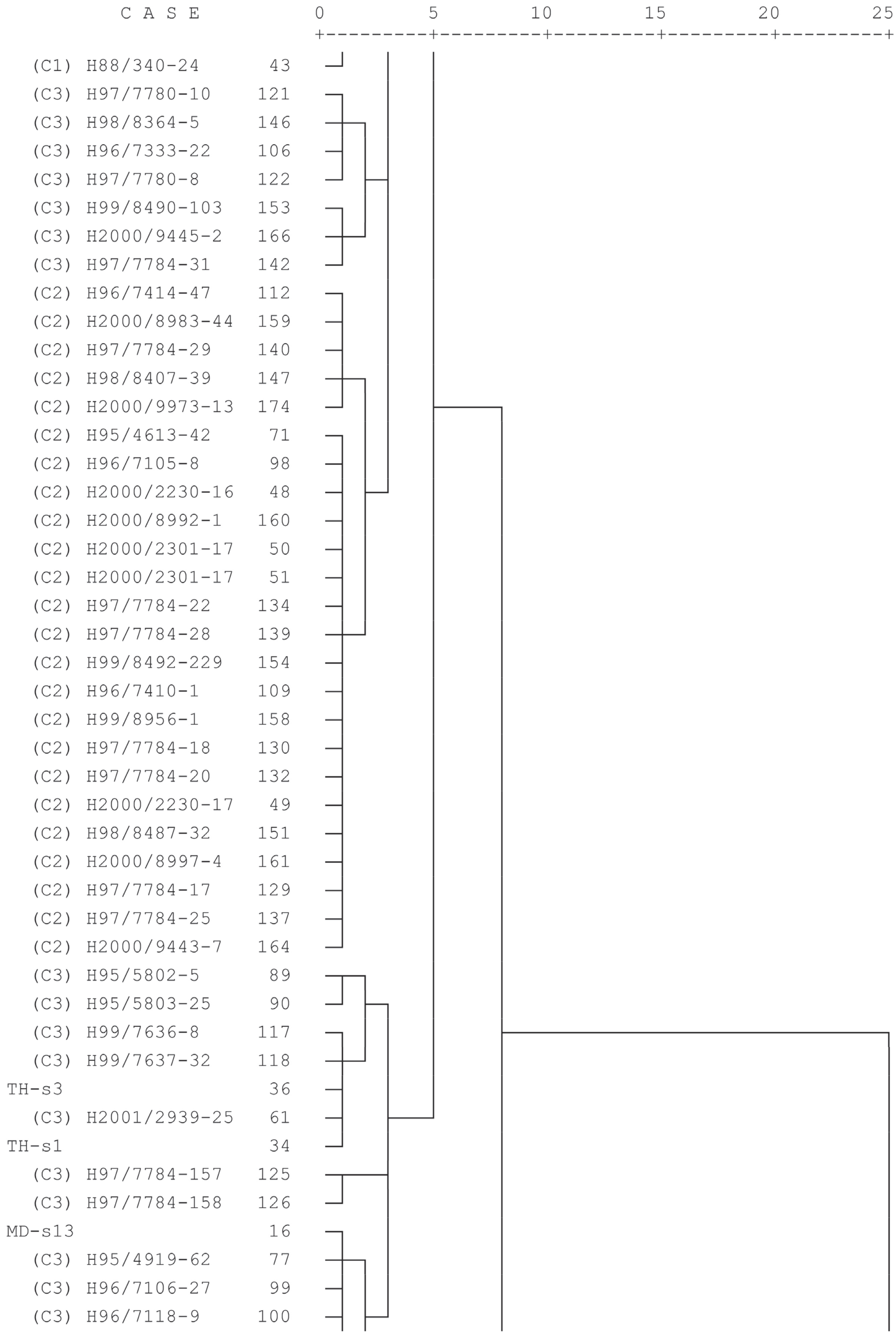
C A S E
0
5
10
15
20
25
(C1) H88/340-24 43
(C3) H97/7780-10 121
(C3) H98/8364-5 146
(C3) H96/7333-22 106
(C3) H97/7780-8 122
(C3) H99/8490-103 153
(C3) H2000/9445-2 166
(C3) H97/7784-31 142
(C2) H96/7414-47 112
(C2) H2000/8983-44 159
(C2) H97/7784-29 140
(C2) H98/8407-39 147
(C2) H2000/9973-13 174
(C2) H95/4613-42 71
(C2) H96/7105-8 98
(C2) H2000/2230-16 48
(C2) H2000/8992-1 160
(C2) H2000/2301-17 50
(C2) H2000/2301-17 51
(C2) H97/7784-22 134
(C2) H97/7784-28 139
(C2) H99/8492-229 154
(C2) H96/7410-1 109
(C2) H99/8956-1 158
(C2) H97/7784-18 130
(C2) H97/7784-20 132
(C2) H2000/2230-17 49
(C2) H98/8487-32 151
(C2) H2000/8997-4 161
(C2) H97/7784-17 129
(C2) H97/7784-25 137
(C2) H2000/9443-7 164
(C3) H95/5802-5 89
(C3) H95/5803-25 90
(C3) H99/7636-8 117
(C3) H99/7637-32 118
TH-s3 36
(C3) H2001/2939-25 61
TH-s1 34
(C3) H97/7784-157 125
(C3) H97/7784-158 126
MD-s13 16
(C3) H95/4919-62 77
(C3) H96/7106-27 99
(C3) H96/7118-9 100

Section D

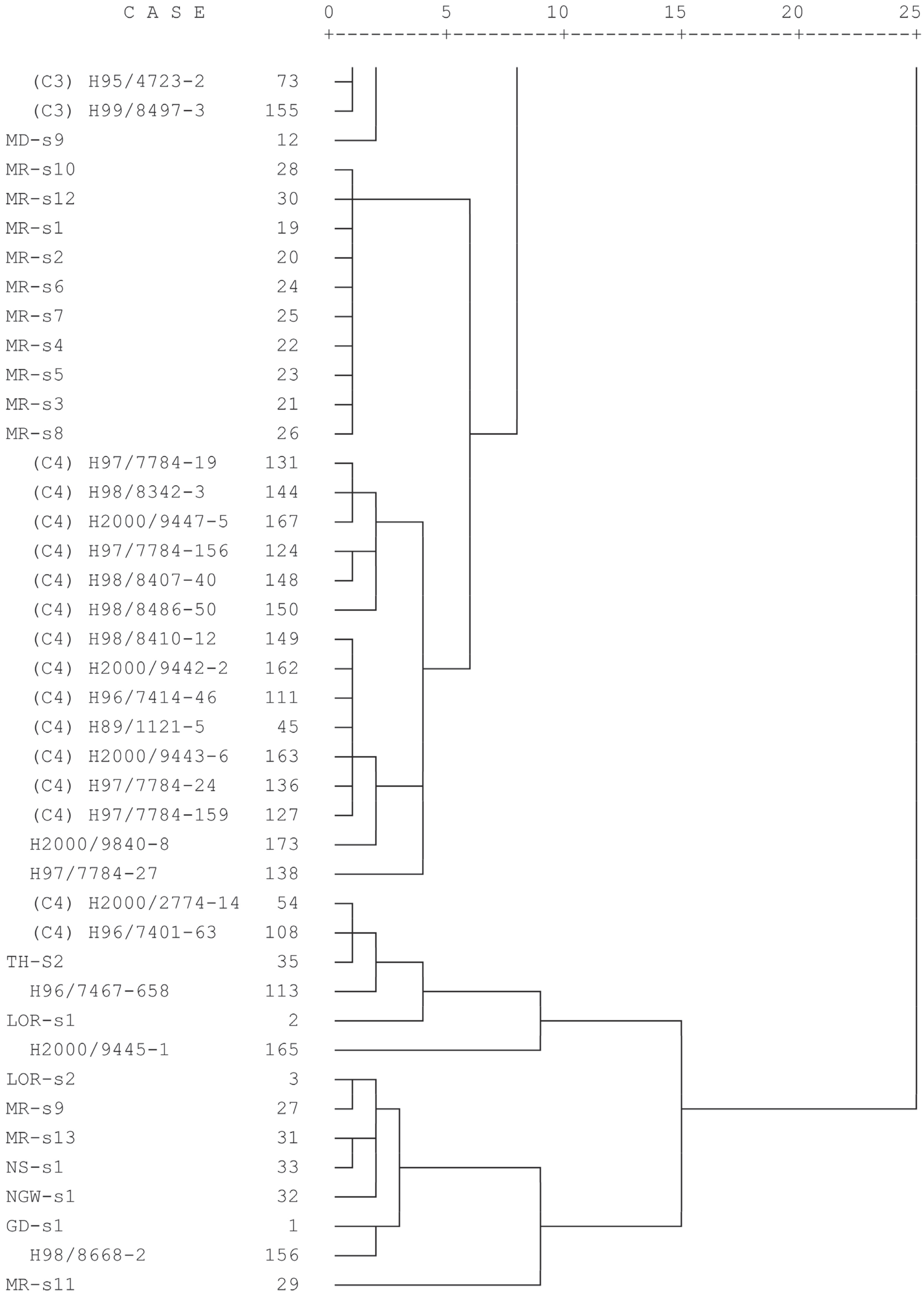
C A S E
0
5
10
15
20
25
(C3) H95/4723-2 73
(C3) H99/8497-3 155
MD-s9 12
MR-s10 28
MR-s12 30
MR-s1 19
MR-s2 20
MR-s6 24
MR-s7 25
MR-s4 22
MR-s5 23
MR-s3 21
MR-s8 26
(C4) H97/7784-19 131
(C4) H98/8342-3 144
(C4) H2000/9447-5 167
(C4) H97/7784-156 124
(C4) H98/8407-40 148
(C4) H98/8486-50 150
(C4) H98/8410-12 149
(C4) H2000/9442-2 162
(C4) H96/7414-46 111
(C4) H89/1121-5 45
(C4) H2000/9443-6 163
(C4) H97/7784-24 136
(C4) H97/7784-159 127
H2000/9840-8 173
H97/7784-27 138
(C4) H2000/2774-14 54
(C4) H96/7401-63 108
TH-S2 35
H96/7467-658 113
LOR-s1 2
H2000/9445-1 165
LOR-s2 3
MR-s9 27
MR-s13 31
NS-s1 33
NGW-s1 32
GD-s1 1
H98/8668-2 156
MR-s11 29

APPENDIX 7.12

NOTES ON EXPERIMENTAL HEATING OF BLACK STEATITE FROM MEHRGARH

In May of 2004, Dr. Jean-François Jarrige and Catherine Jarrige kindly provided me with a small set of steatite artifacts from the site of Mehrgarh for use in geologic provenience analyses and experimental heating studies. Among the set were a number of jet-black bead roughouts and fragments that, along with several hundred other such artifacts, had been recovered from an MR4 atelier dating to the early Chalcolithic Period (Mehrgarh IIB – ca. 5000 BC) (Jarrige 1981: 99). Seven of the atelier artifacts were examined using INAA (Chapter 7 – Figure 7.7 A, MR-s1 through MR-s7) and determined to likely represent steatite from a single dolomitic deposit that is, perhaps, located in central Balochistan. It had already been established in previous studies conducted by Barthélémy de Saizieu and Bouquillon (1994, 1997) that this type of steatite became white when heated. As part my effort to understand the properties that made steatite from certain sources desirable to Indus craftspeople, I decided to further document the macroscopic and mineralogical changes that "Mehrgarh Black" steatite undergoes as it is heat-treated.

A large fragment of the "Mehrgarh Black" steatite (Appendix 7.12, Figure 1 *top*) was selected for the heating experiment. Although I did not know it at the time, the fragment had a calcite phase in addition to the main talc phase (XRD was not performed until after the initial firings were complete and I had not read Vidale's 1995 article in which he also documented this secondary phase). Had I known this, I would not have used that particular fragment as I was mainly interested in documenting the decomposition of talc into enstatite and cristobolite. Barthélémy de Saizieu and Bouquillon's XRD (1994: Figure 3.4) analysis of black steatite from Mehrgarh had indicated that it was entirely talc.

The fragment I chose was cut into 16 chips (Appendix 7.12, Figure 1 *bottom*). For the first round of firings, nine chips (Set One) were heated separately in a muffle furnace at different temperatures for exactly one hour each. The numbers 4 through 12, which correspond to the temperature that each was subjected to – 400°C to 1200°C in increments of 100°C, were scratched on their surfaces. Length, width and thickness measurements were made for each chip in Set One before and after the firings (Appendix 7.12, Figure 2). This was a *static* firing in that each chip was placed into the furnace when the experimental temperature was reached and then removed immediately after the one hour. XRD was conducted on the unfired fragment and then on each fired chip (Appendix 7.12, Figure 3) to determine if and how its mineral composition had been altered by the heat to which it had been subjected. Based on the results provided by Set One, a second set (Set Two) of seven samples was static fired for three-hour periods at temperatures between 600°C and 1200°C.

XRD OF THE UNFIRED "MEHRGARH BLACK" STEATITE SAMPLE

Both talc and calcite phases are evident in the raw sample. In their unfired state the steatite chips have a dark gray appearance with a matte textured surface.

Observations SET ONE

MGR 400°C @ 1 hr

Talc and calcite phases. The intensity of the major calcite peak has dropped slightly indicating that it is

Appendix 7.12 Figure 1 The black steatite fragment from the MR4 atelier used in this experimental study (top) and the two sets of chips cut from it before and after heating.

already beginning to decompose. The macroscopic appearance of the steatite remained unchanged.

MGR 500ºC @ 1 hr

Talc and calcite phases. The intensity of the major calcite peak continues to diminish as that mineral decomposes. The talc phase remains practically unaltered. The appearance of the steatite remained unchanged.

MGR 600ºC @ 1 hr

Talc and calcite phases. The intensity of the major calcite peak continues to diminish as that mineral decomposes. The talc phase is still largely unaltered.

Appendix 7.12 Figure 2 Mehrgarh Black Steatite Heating Experiment – SET ONE

				Before Heat-treatment					
STEATITE CHIP	4	5	6	7	8	9	10	11	12
LENGTH (mm)	8.5	8.29	9.18	8.24	8.6	9.29	8.69	9.6	9.76
WIDTH (mm)	5.13	5.11	5.87	6.45	5.86	6.32	7	7.09	6.4
THICKNESS (mm)	1.61	1.92	1.19	1.67	2.1	1.89	1.81	1.49	1.91
WEIGHT(g)	0.1502	0.1998	0.1571	0.2024	0.2595	0.2712	0.2543	0.2687	0.2998
				After Heat-treatment					
TEMPERATURE	400°C	500°C	600°C	700°C	800°C	900°C	1000°C	1100°C	1200°C
LENGTH (mm)	8.48	8.26	9.17	8.15	8.57	9.35	8.76	10.01	10.05
WIDTH (mm)	5.1	5.1	5.87	6.51	5.87	6.38	7.15	7.26	6.74
THICKNESS (mm)	1.61	1.92	1.18	1.67	2.11	1.92	1.84	1.54	2.01
WEIGHT(g)	0.1495	0.1992	0.1563	0.1979	0.2482	0.2358	0.2071	0.2184	0.2431
				Change					
VOLUME	-0.82%	-0.56%	-0.95%	-0.17%	0.30%	3.21%	4.67%	10.35%	14.12%
WEIGHT	-0.47%	-0.30%	-0.51%	-2.22%	-4.35%	-13.05%	-18.56%	-18.72%	-18.91%

The appearance of the steatite remained unchanged.

MGR 700°C @ 1 hr

Talc and calcite phases. The intensity of the major calcite peak continues to diminish as that mineral decomposes. The talc phase is largely unaltered. The appearance of the steatite remained largely unchanged although a few light gray-white patches are evident.

MGR 800°C @ 1 hr

Talc and calcite phases. The intensity of the major calcite peak continues to diminish as that mineral decomposes and several of the minor calcite peaks have disappear. The talc phase is beginning to show signs that that decomposition has begun. Much of the steatite chip is now mottled with gray-white patches.

MGR 900°C @ 1 hr

Talc with minor calcite and enstatite phases. A single, much diminished calcite peak remains. Peaks indicating the formation of enstatite are now evident. The appearance of the steatite is now a cloudy gray-white with spots of pure white.

MGR 1000°C @ 1 hr

Enstatite with a minor talc phase. The calcite has entirely decomposed. Most of the steatite has converted to enstatite leaving only a few minor peaks. The appearance of the steatite is now white with spots and streaks of gray-white.

MGR 1100°C @ 1 hr

Enstatite with a minor talc phase. Enstatite is well formed while a few minor peaks for talc remain. The steatite is now almost entirely white.

MGR 1200°C @ 1 hr

Enstatite with cristobolite and a minor talc phase. Mostly well-formed enstatite. A few minor peaks for talc remain and strong peaks for cristobolite are now present. The steatite is entirely white.

In the one hour static firings of this particular black steatite sample the conversion of talc to enstatite began somewhere between 800°C and 900°C (closer

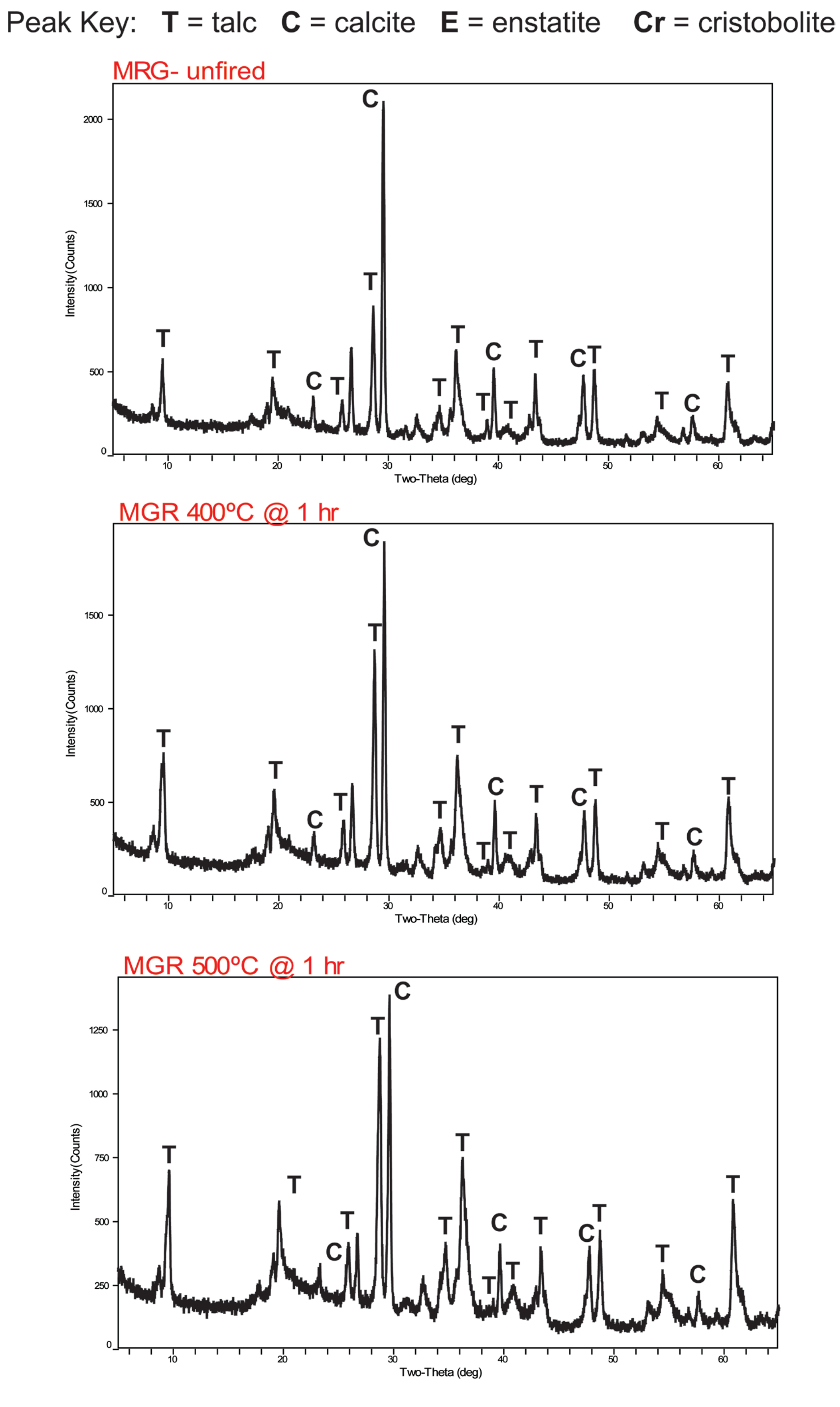

Appendix 7.12, Figure 3 XRD scans of experimental steatite chips

to the latter judging from the peak intensities). Enstatite was fully developed by 1100°C. Cristobalite phases did not appear until temperatures approached 1200°C. A more or less fully white color was not achieved until temperatures of around 1000°C to 1100°C were reached. Although the overall drop in weight (≈ -19%) and volume (≈ -14%) was fairly significant by 1200°C, little deformation or cracking of the chips was evident.

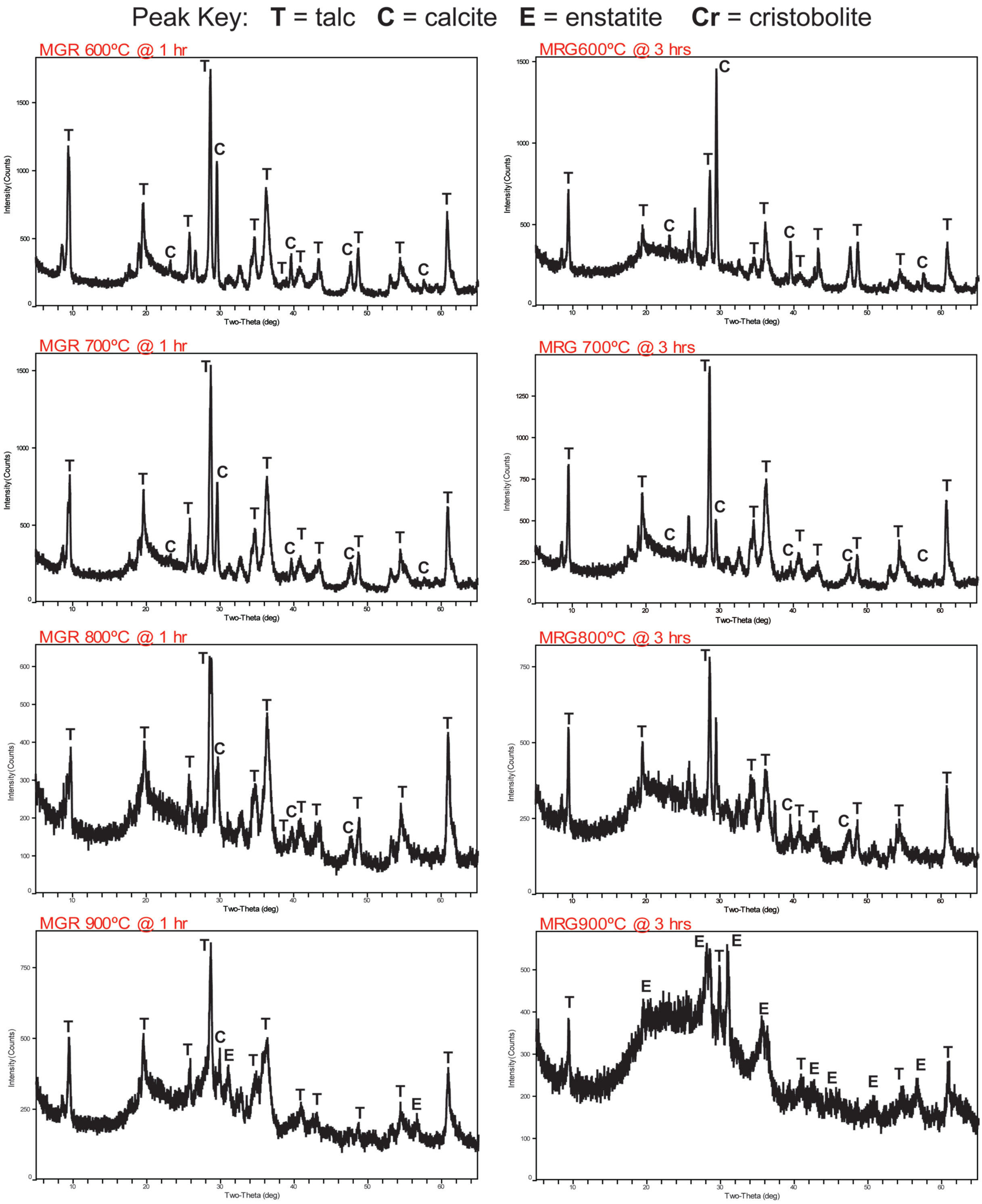

Appendix 7.12, Figure 3 (cont.) XRD scans of experimental steatite chips

Observations SET TWO

MGR 600°C @ 3 hrs

Talc and calcite phases. The intensity of the major calcite peak is actually much stronger here than it was in the sample that had only been heated for one hour at 600°C. A few light gray patches are evident on the chip.

MGR 700°C @ 3 hrs

Talc and calcite phases. The intensity of the major calcite peak has diminished significantly as that mineral decomposes. The talc phase is largely unaltered from before. A few light gray-white patches are evident on the steatite chip.

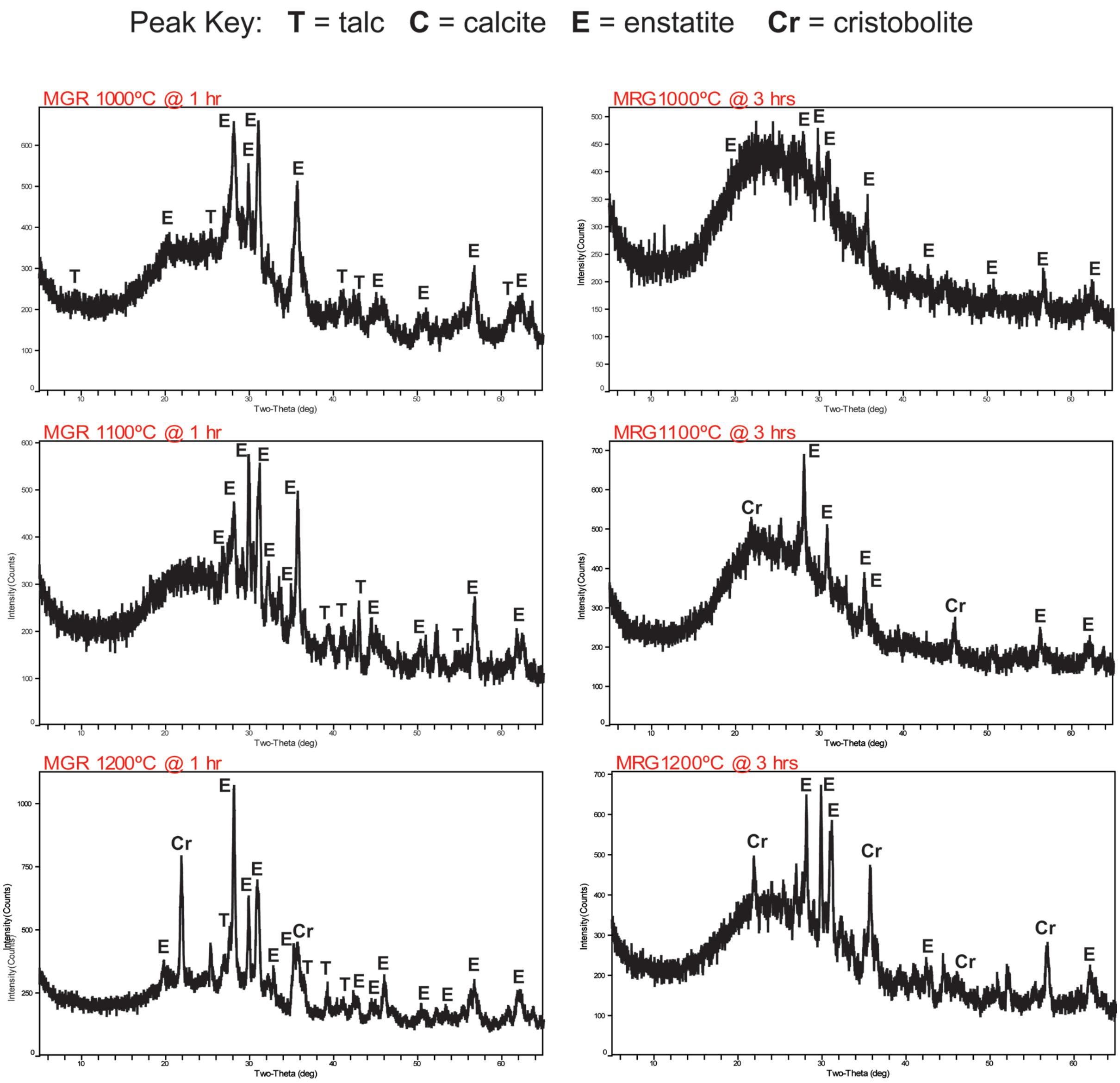

Appendix 7.12, Figure 3 (cont.) XRD scans of experimental steatite chips

MGR 800ºC @ 3 hrs

Talc and calcite phases. The calcite has almost entirely decomposed. Most of the steatite chip is now mottled with gray-white patches.

MGR 900ºC @ 3 hrs

Enstatite with talc. The calcite is entirely gone and the talc has undergone conversion to enstatite leaving only minor peaks behind. The appearance of the steatite is now a cloudy gray-white with spots of white

MGR 1000ºC @ 3 hrs

Enstatite. The remaining talc has entirely decomposed. The appearance of the steatite is now white with a few gray-white spots and streaks.

MGR 1100ºC @ 3 hrs

Enstatite with a minor cristobolite phase. The appearance of the steatite chip is now entirely white.

MGR 1200ºC @ 3 hrs

Enstatite and cristobolite phases. The macroscopic appearance of the steatite chip is now entirely white.

The XRD scans of Set Two indicate that, in general, longer firing times produce more developed and, in some cases, slightly earlier mineral phase changes. Enstatite still does not appear until around 900°C but it shows better peak development. Talc entirely was completely gone by 1000°C whereas it had never entirely decomposed in the 1-hour firings. Cristobolite now appears at 1100°C and is well formed by 1200°C. The appearance of the steatite still does not fully transform into a pure white color until around 1000°C to 1100°C.

APPENDIX 7.13

XRD CHARACTERIZATION OF SIX WHITE BEADS FROM MEHRGARH

Along with the unfired steatite artifacts discussed in the previous appendix (7.12), Dr. Jean-François Jarrige and Catherine Jarrige also provided me with six tiny white beads from Mehrgarh periods I and II levels for characterization using XRD. The scans for these beads can be found on the next page (Appendix 7.13, Figure 1) along with a peak key.

Three of the Period I beads (MR.99.03.74, MR.98.03.10 and MR.98.03.53) were determined to be composed of *aragonite* – a calcium carbonate similar to calcite. The XRD patterns of the remaining three revealed them to be made from talcose materials with characteristics consistent with those reported by Barthélémy de Saizieu and Bouquillon's in their study (1994) of Mehrgarh steatite beads from the same periods. Bead MR3 178 (from Period I) is composed

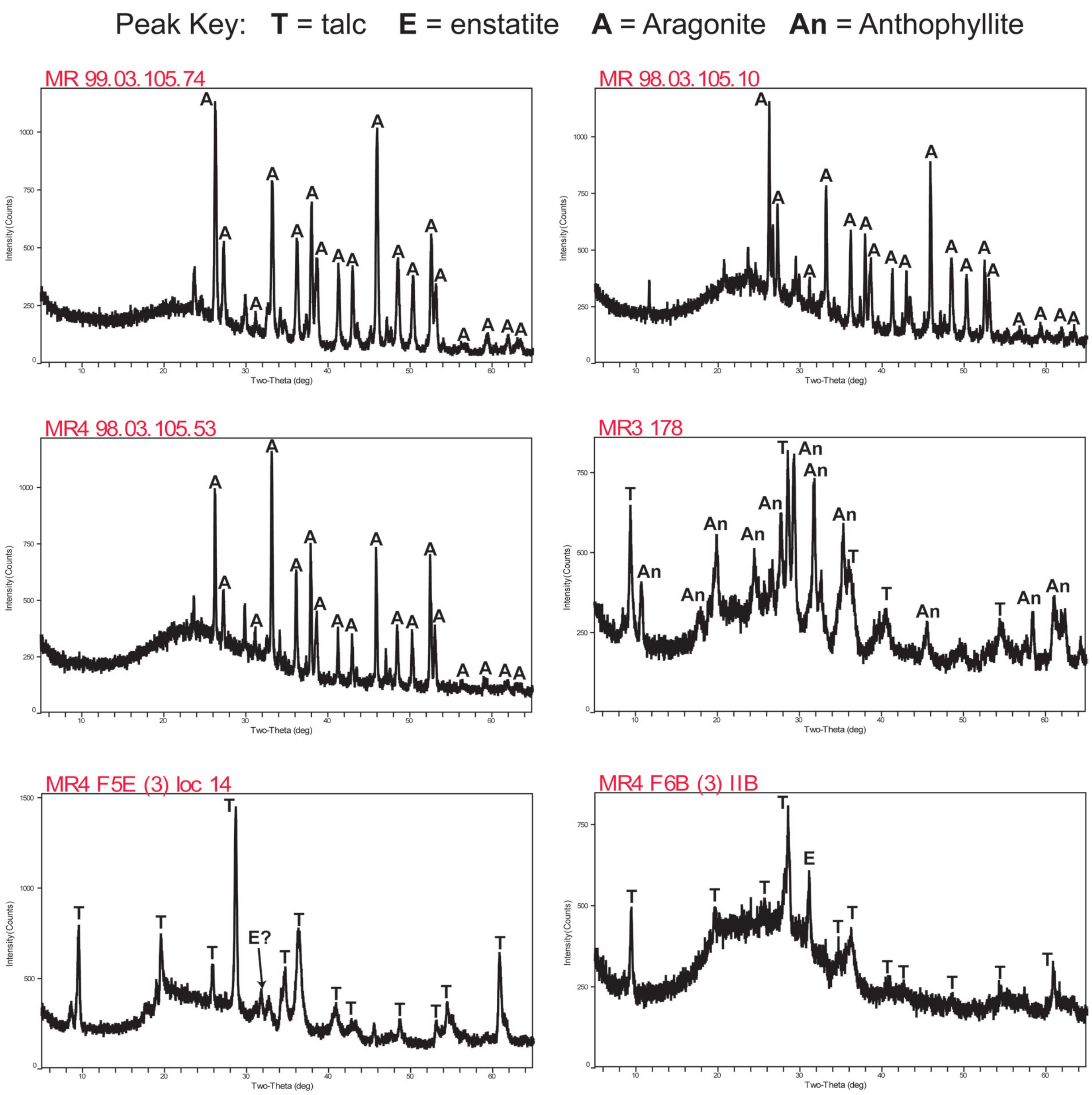

Appendix 7.13 Figure 1 XRD scans of six white steatite beads from Mehrgarh

mainly of *anthophyllite* with secondary phases of talc. Anthophyllite is an asbestos-like mineral that, because it occurs in both ultramafic igneous and dolomitic sedimentary rocks (Deer *et al*. 1992: 235), is not particularly helpful for determining the stone's geologic provenience. The nearest reported natural occurrence is in the Sakhakot-Qila ophiolite of the Mohmand Agency, FATA (Ahmed 1987b). The mineral could, however, be related to the thermal decomposition of talc to enstatite. In experimental heating studies of talc, Greenwood reported (1963) the formation and breakdown of an intermediate stage of anthophyllite between 667° ± 8°C and 745° ± 10°C.

Scans of the final two white beads (MR4 F5E (3) loc 15 and MR4 F6B (3) IIB), which are both from Period IIB, revealed talc peaks and a few minor enstatite peaks. After comparing those scans to the ones produced in the experimental heating study of the Mehrgarh black steatite fragment (Appendix 7.12), I would estimate that the beads were fired at a temperature between 800 and 900°C – probably closer to 900°C given the presence but poorly developed appearance of the enstatite peaks. That temperature is consistent with Barthélémy de Saizieu and Bouquillon's previous estimate (1994: 51) for fired steatite beads of this period.

APPENDIX 7.14

XRD AND EMPA CHARACTERIZATION OF STEATITE BEADS FROM HARAPPA, LORALAI AND GOLA DHORO

The thermal decomposition of the mineral talc into enstatite and cristobolite can provide an accurate indication of the temperatures achieved during the firing of steatite artifacts. In this appendix, steatite beads from three sites are characterized using XRD and EMPA.

For the first round of analyses, XRD was conducted on fragments of two artifacts that had clearly been fashioned from solid pieces of steatite. One was of a disc bead (Appendix 7.14, Figure 1 *top left*) from Harappa that was in a bag of miscellaneous surface finds from Mound E (H94/4999). Linear marks from the saw used to cut the solid steatite were still visible on the surfaces of the fragments. The second artifact analyzed was a broken tubular bead fragment (Appendix 7.14, Figure 1 *top right*) provided by Syed Ghani of the Geological Survey of Pakistan-Quetta. It was said to be from a mound in the Loralai District of Balochistan that is in the general vicinity of the Early Harappan site of Rana Ghundai (Ross

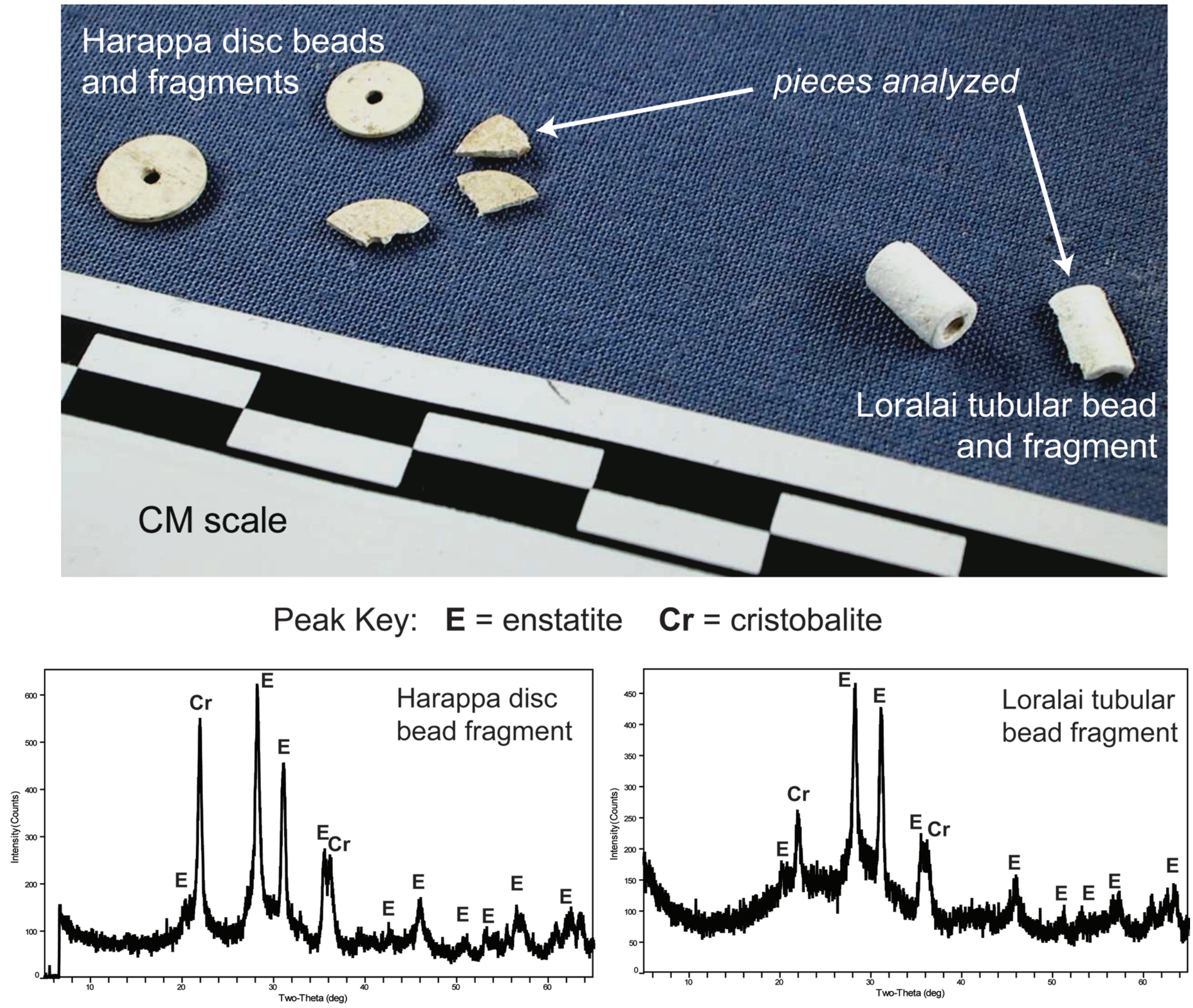

Appendix 7.14 Figure 1 Steatite beads from Harappa and a prehistoric site in the Loralai District, Balochistan (top) and their respective XRD spectrums (bottom).

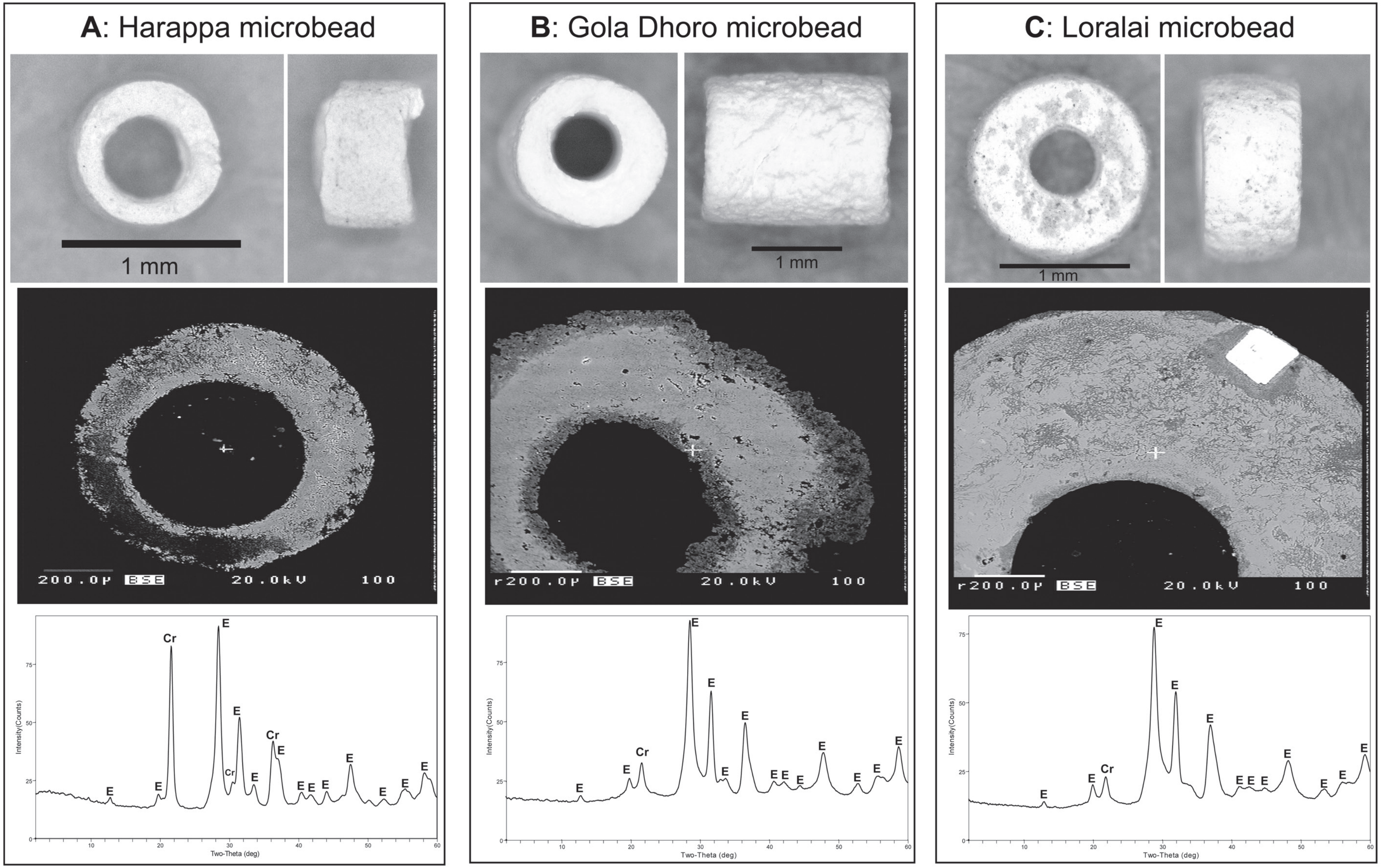

Appendix 7.14 Figure 2 Steatite microbeads from Harappa **[A]**, Ghola Dhoro **[B]** and Loralai, BSE images of their sections and their Rigaku II-made XRD spectrums **[C]**.

1946). Marks from the made during the grinding of the steatite raw material prior to firing were faintly visible on the bead fragment's surface.

The XRD spectrum of the disc bead fragment from Harappa (Appendix 7.14, Figure 1 *bottom left*) indicates that it is composed of enstatite (E) and cristobolite (CR). The cristobolite is very well developed suggesting that a firing temperature of close to 1200°C was achieved (compared the scan of the disc bead to that for experimental sample from Mehrgarh [Appendix 7.12, Figure 3] that was fired for 1 hour at 1200°C). The scan of the Loralai tubular bead fragment (Appendix 7.14, Figure 1 *bottom right*) shows that it is also composed of enstatite and cristobolite. However, the cristobalite is not as well-developed as it is in the disc bead from Harappa. This probably indicates that a firing temperature of only around 1100°C was reached (compared the scan for the Loralai bead fragment to that for the Mehrgarh sample [Appendix 7.12, Figure 3] that was fired for 3 hours at 1100°C).

A second round of analyses were conducted on steatite "microbeads" from Harappa, the site of Gola Dhoro in Gujarat and the unnamed mound in Loralai (Appendix 7.14, Figure 2 A, B & C). Exactly how Indus craftspeople created extremely small ornaments such as these is poorly understood. Some researchers have speculated that they were made by carving and drilling blanks of solid steatite that were then reduced by grinding while others have argued that they were fashioned from a paste composed of talc powder and a clay mineral binding medium (see Vidale 2000: 64-66 for a more detailed review of the various theories regarding the manufacture of these objects). I tend to favor the former hypothesis based on my limited characterizations of the three microbeads using EMPA. The BSE images of the beads' sections suggest that there is solid steatite beneath their heavily weathered surfaces. The Loralai bead even has a complete calcite crystal within its matrix (recall that calcite was detected in the raw steatite sample from Mehrgarh analyzed for Appendix 7.12), which, quite obviously, had to have formed in situ. Also, EDS scans made at various points across the beads' sections detected no evidence of aluminum that would indicate they were composed of a talc mixed with a small amount of clay. These observations are cursory, however. The problem of the manufacture of Harappan microbeads remains, as Massimo Vidale has stated (2000: 66) very much "open to further archaeometric analysis and debate".

The results of the XRD analyses, on the other hand, are quite clear: the three Harappan microbeads are high-fired ornaments. Cristobalite as was detected in all of them and was especially well-developed in the example from Harappa. Hegde and others (1982) likewise detected a cristobalite phase in the microbeads they analyzed from the site of Zekhada in Gujarat. It now seems clear then that by the third millennium BC, craftspeople in many parts of the Indus realm were heating steatite to temperatures that exceeded 1100°C and, perhaps, approached 1200° C.

APPENDIX 7.15

EMPA, VP-SEM AND XRD OBSERVATIONS OF A STEATITE SEAL BOSS FROM HARAPPA

INTRODUCTION

In Appendix 7.16, I will show that certain types of steatite become pure white when heated (fired) without having been subjected to any form of pre-treatment whatsoever. It is clear that some Harappan seals were made from this type of material as there are broken examples in which the interior is exposed to reveal that they have become white throughout. However, many other seals have thin, enamel-like white exteriors covering non-white or unfired steatite interiors. These have obviously been subjected to a surface treatment of some kind. The exact nature of that treatment is poorly understood, however (Miller 1999: 309). Some researchers have proposed that a thin glaze or slip was applied to seals (Mackay 1931d; Sana Ullah 1931) while others have argued that they were subjected to some kind of surface whitening agent, perhaps an alkaline solution (Beck 1934; Kenoyer 1998; Vidale 2000; Wheeler 1968: 101). In this appendix, I present observations made of the surface and interior of a steatite seal boss – the perforated knob that is found on the reverse sides of seals – using electron microprobe analysis (EMPA), a variable-pressure scanning electron microscope (VP-SEM) with an energy dispersive spectrometer (EDS) and X-ray diffraction (XRD) analysis. Although the results of these analyses do not definitively establish

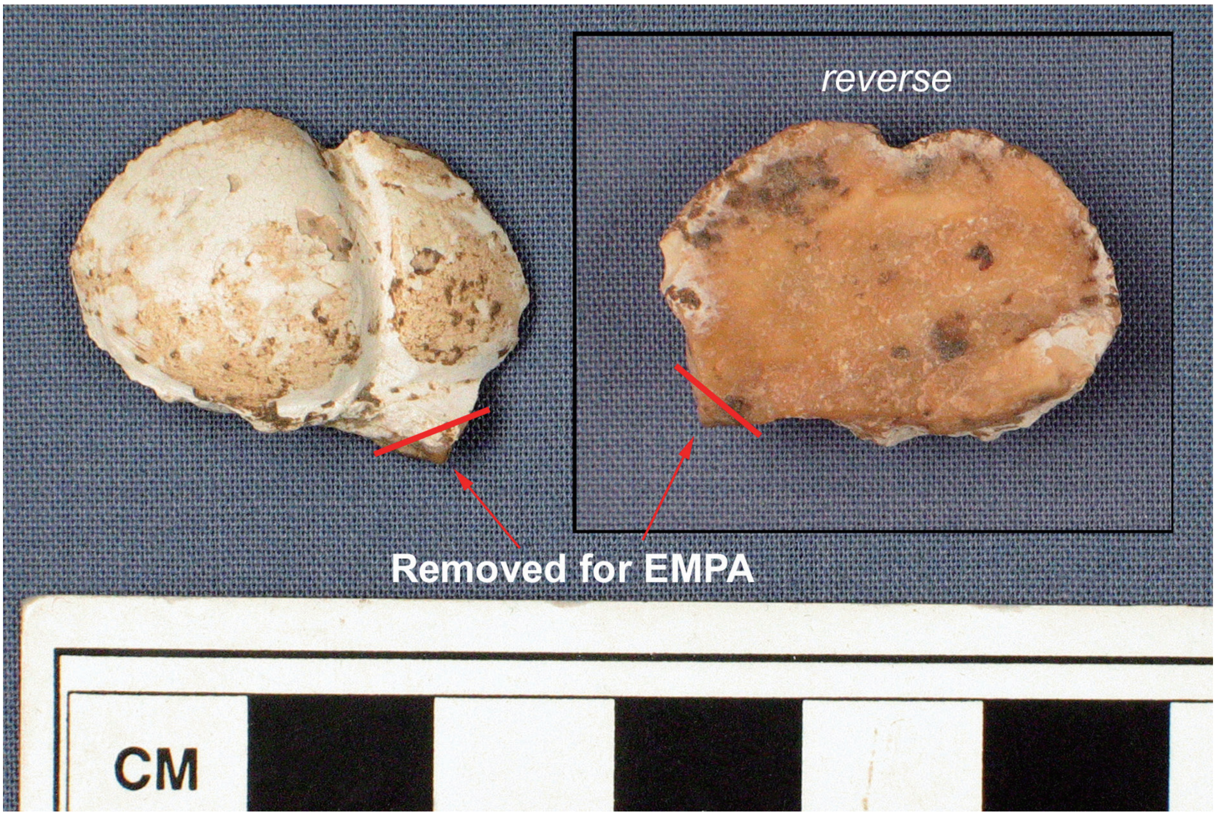

Appendix 7.15 Figure 1 The "glazed" exterior (left) and unfired or "raw" steatite interior (right) of the seal boss with the piece removed for EMPA noted in red.

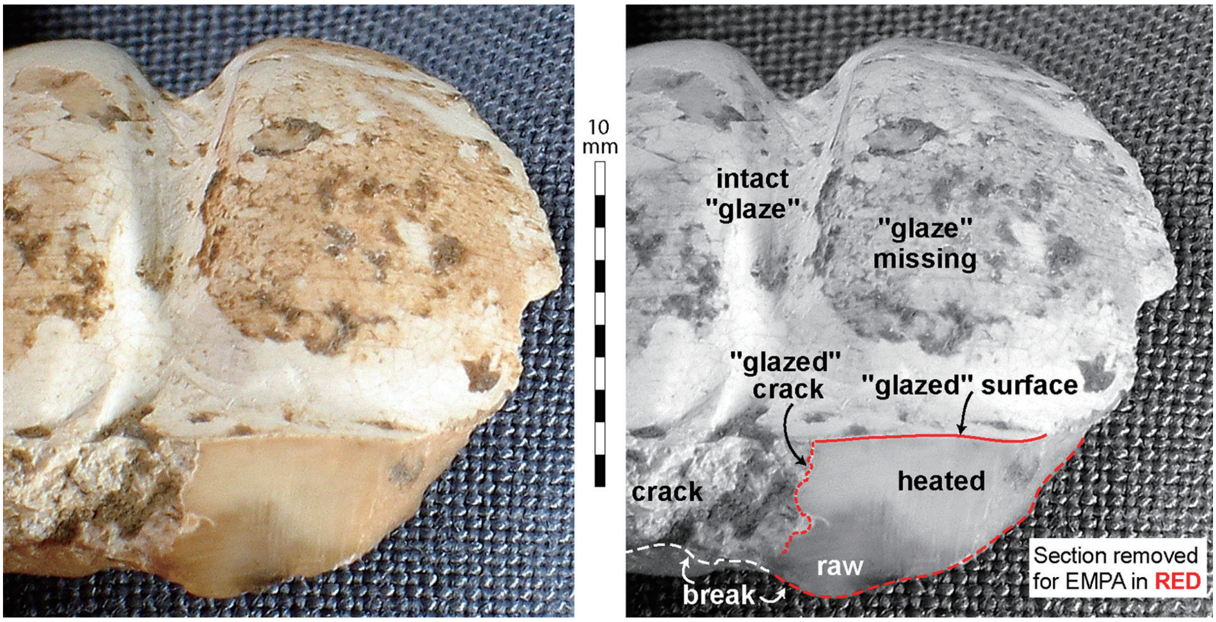

Appendix 7.15 Figure 2 View of the steatite seal boss and the section cut (left) and features on the boss / section labeled (right).

how the white surfaces of steatite seals were created, they do, in my opinion, lend strong support to the view that the objects were covered with a thin talcose slip.

BOSS DESCRIPTION AND SUMMARY OF PAST WORK ON SEAL SURFACE TREATMENTS

Artifact H90/3208-68 (Appendix 7.15 Figure 1) is a portion of a boss that broke away, in antiquity, from a steatite seal (see Figure 7.5 F right in Chapter 7 of this book for a reconstruction what it probably looked like prior to breaking off). It was recovered in Period 3C levels in Trench 59 on the south side of Mound E at Harappa. A sample of unfired steatite was removed from the boss' underside for INAA analysis. The results (listed in Appendix 7.1) indicate that the raw material is most closely related to steatite from the Daradar (PD) deposit in the Kurram Agency, FATA.

The exterior surface of the boss is white and is rife with fine cracks that are reminiscent of a glaze that has undergone crazing. In places this "glaze" (if indeed that is what it is) has fallen away to reveal the off-white fired steatite subsurface beneath it. The khaki-colored unfired or "raw" steatite that the seal was carved from is visible on the broken reverse side of the boss. Heat-treatment (presumably) has altered the raw steatite from the surface to a depth of between one and four millimeters. This discolored (light khaki-colored zone) can be most clearly seen in the section exposed when a sliver of the seal was removed for EMPA (Appendix 7.15 Figure 2). A rough fractured area at the base of the boss is the remains of a substantial crack (labeled "crack" on Appendix 7.15 Figure 2 right) in the body of the seal. It clearly existed during the manufacture of this object as it exhibits the same "glaze" and/or treatment as the surface of the seal. This crack is probably is the reason (or part of the reason) why the boss broke from the seal body. That could have happened during manufacture or the crack may have weakened the boss causing it to snap off later.

In his study of seals from Mohenjo-daro, the Archaeological Survey of India's chemist K.B.M. Sana Ullah concluded (1931: 688) that the exterior of those artifacts was coated with a talcose slip. An analysis of the surface layer of one (ibid.: 689, Table 1 #8) indicated that it was primarily composed of

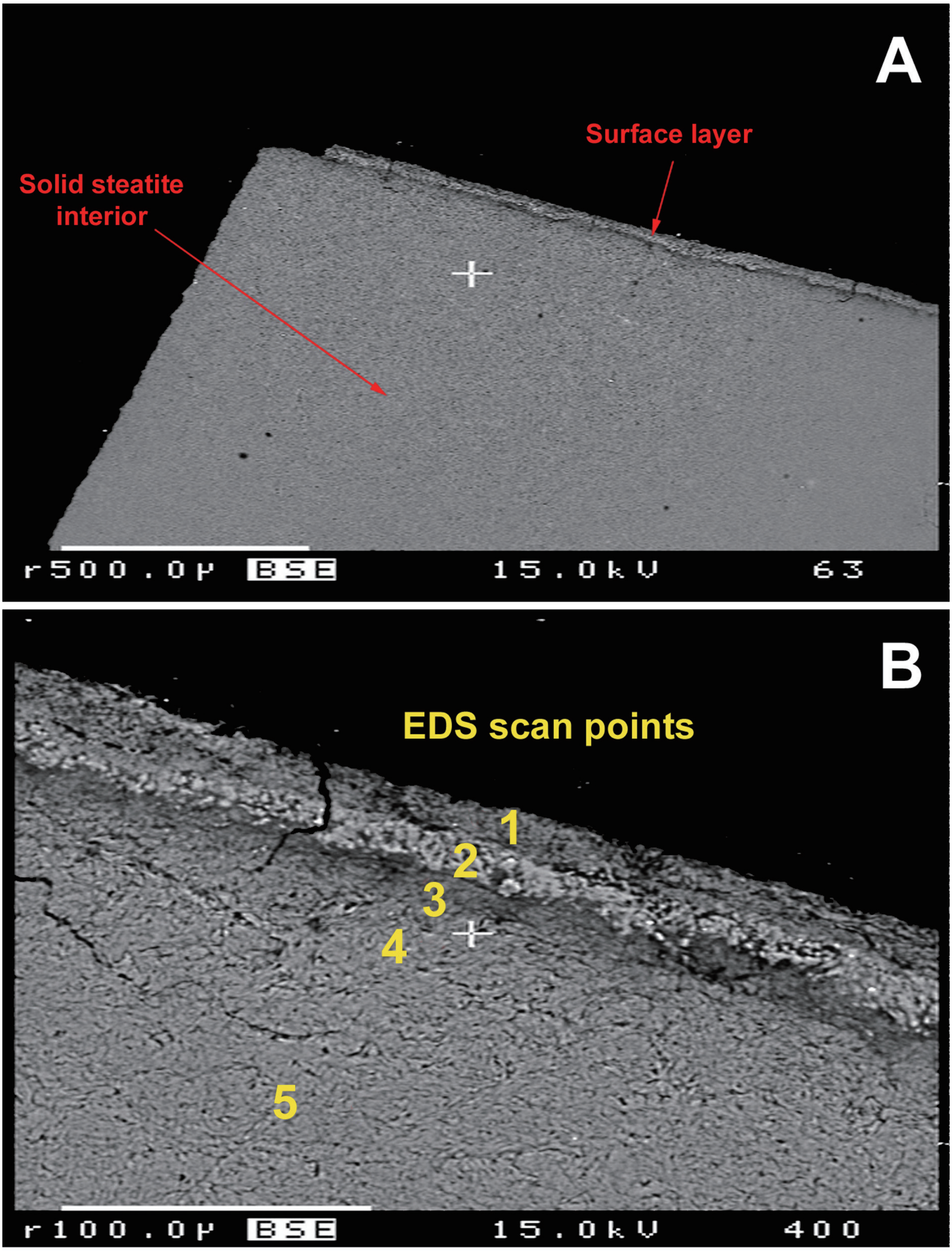

Appendix 7.15 Figure 3 EMPA of the seal boss. **[A]** BSE image of boss section. **[B]** BSE detail of the surface layer and the EDS scan locations.

magnesium silicate with only a trace amount (1.8%) of water. This layer is almost certainly talc that has thermally decomposed to enstatite. Sana Ullah proposed that the slip was made from powdered steatite that has been previously fired (this was already enstatite). A trace amount alumina and ferric oxide (2.4% total) was also detected in the surface layer. This may indicate that a minute quantity of iron-rich clay was added to the talcose slip, perhaps as a binder. However, in his experimental attempts to replicate the white surface, Sana Ullah instead added "silicate of soda" (sodium silicate – Na_2SiO_3) to powdered fired steatite. He found that this method produced "durable coatings, similar to the ones on the seals" (ibid.: 688).

Based on thin-section studies of Harappan seals, Horace Beck concluded (1934: 80-81) that "the surface had not been added as a paste, but that the seals had been carved completely from a block of steatite, and then treated with an alkali and heated." Both Kenoyer (1998: 73) and Vidale (2000: 62) concur that, rather than being covered by an applied slip/glaze, the seals were subjected to some type of alkaline mixture – perhaps calcium carbonate ($CaCO_3$ or "free lime") and potassium hydroxide, (KOH or "potash"), prior to firing. A slip, it is argued (Mark Kenoyer personal communication 2004), would obscure the finely carved details and minute manufacturing marks that are plainly visible on surfaces of seals. Soaking them in an alkaline solution and then applying heat would essentially "bleach" the surface leaving any details/marks intact.

In order to evaluate the two different explanations for the white exterior of Harappan seals – i.e, glaze vs. surface treatment, observations of the seal boss were made using EMPA, VP-SEM and XRD.

EMPA

EMPA of the seal boss described above was conducted in January 2005. A small piece that is actually a remnant of the flat reverse side of seal rather than of the boss itself was sawn from the artifact (red lines and arrows on Appendix 7.15 Figure 1 indicate the portion that was removed). This piece (≈ 7 mm in width) was prepared according to the methods outlined in the EMPA section of Chapter 3. The section left by its removal is displayed and labeled in Appendix 7.15 Figure 2. A thin white layer is plainly visible on the seal surface portion of the section as well as along the contours of the crack on its left hand side. The contrast between the heated portion of the seal body and its unaltered steatite interior is likewise evident in the section.

Appendix 7.15 Figures 3 shows two back scattered electron (BSE) images of the prepared seal sample. In image A, a surface layer approximately 35 microns (0.035 millimeter) thick stands in contrast to the homogenous steatite of the seal's immediate subsurface interior. Image B is a detail of that layer. Three sub-layers are visible (labeled on the figure as 1, 2 and 3) each of which is approximately ten microns or so in width. The seal body immediately beneath the surface layers is labeled "4" and a point around 100 microns in depth is labeled "5" on the figure. At each of the five points a scan was performed using the probe's EDS, which provided fast, qualitative chemical characterizations. The composition of the material at each point was exclusively <u>magnesium silicate</u>. There were no peaks observable peaks in the EDS spectrum that would indicate the presence of potassium, calcium, sodium, aluminum (indicative of clay minerals), lead or any other substance that might conceivably have been added or applied as a binder, flux or colorant. Based on this, it was decided on not to calibrate the probe with mineral standards (a time consuming process) and conduct quantitative assays using its wavelength dispersive spectrometer (WDS).

Compositionally, the seal's surface layer appears identical to its interior. This could then be seen as support for Mackay's assertion (1931d: 379) "that the coating upon these seals is made of the same material as the seals themselves," that is, talc/enstatite. On the other hand, if the seal's original carved steatite surface was bleached using an alkali treatment and then heated, its basic mineralogical composition (magnesium silicate) might not have been altered very much or even at all. These initial EDS assessments, therefore, could not really provide an answer to the

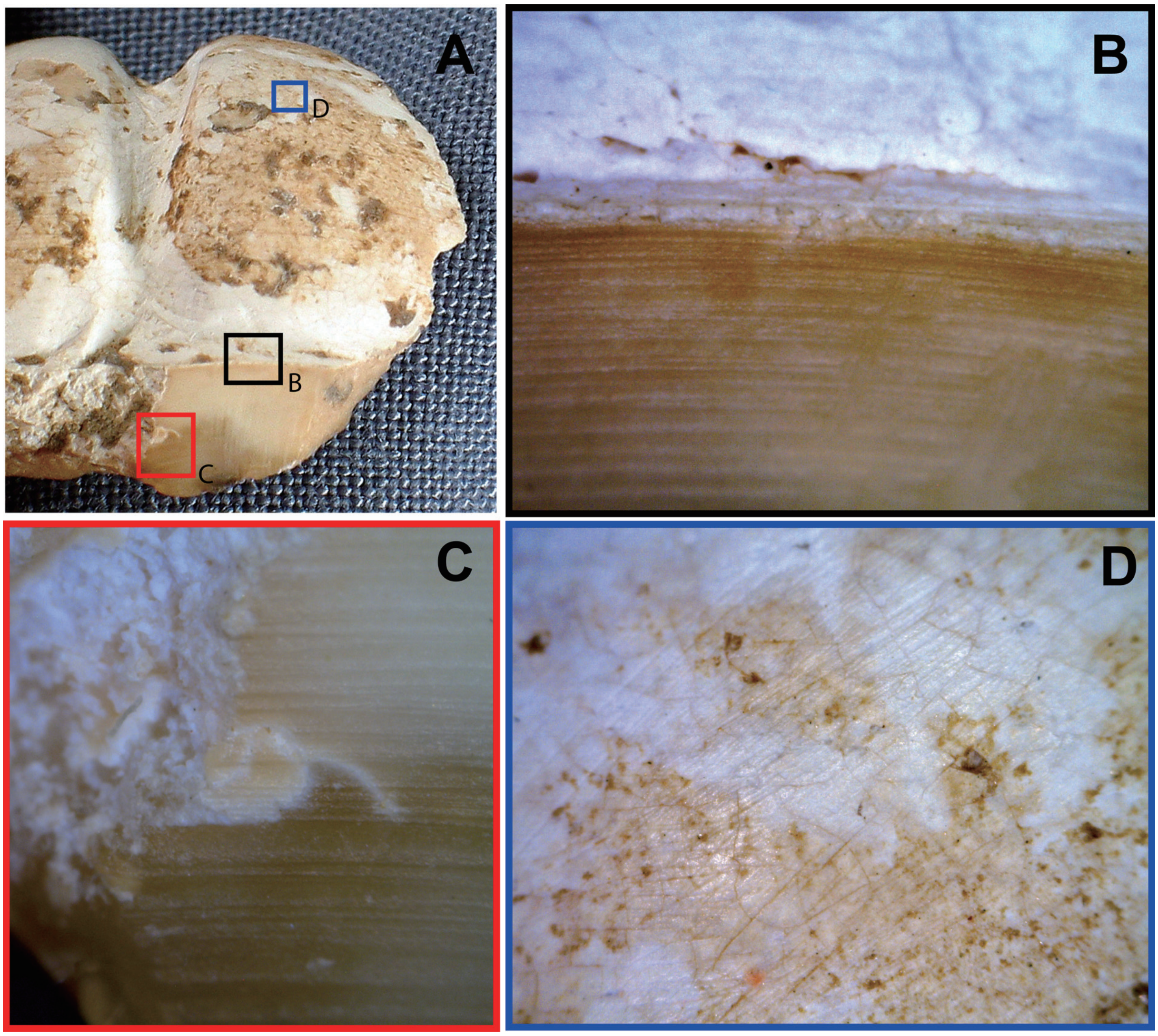

Appendix 7.15 Figure 4 **[A]** Three areas on the seal boss chosen for BSE imaging and qualitative compositional analysis using the VP-SEM/EDS. **[B]** Visible light detail of the surface layer in section. **[C]** Visible light detail of the micro-crack in the seal body. **[D]** Visible light detail of a patchy area on the seal boss' surface.

glaze vs. treatment question.

The BSE images were more revealing. Looking at Appendix 7.15 Figure 3 B, it is evident that although the platy interlocking grains of the seal's interior lighten (darken on the BSE image) as layer 3 begins, the texture remains homogenous through layer 3 up to layer 2. After that point the texture suddenly becomes much coarser. It seems to me that if there is an applied surface it probably begins at this sharp layer 2 to 3 boundary. Layer 3 may then be the original carved surface of the seal that has undergone some form of alteration due to its fusion the Layer 2. Note that the indicated micro-crack runs from the surface through layer 3. This probably explains why as the "glaze" scales off it often takes some of the original carved surface with it.

What of that original carved surface of the seal? Would not a slip obscure details and manufacturing marks? It would if a "wet glaze" (Miller 1999: 308) that was too thick and viscous was applied to a seal. However, it is possible to produce extremely fine and fluid steatite slips (Grosjean 1999). If layer marked "3" is assumed to be the original seal surface then the remaining "glaze" is only around 20 microns (0.02 millimeter) in thickness. A slip that thin could have adhered to the contours of carved details and

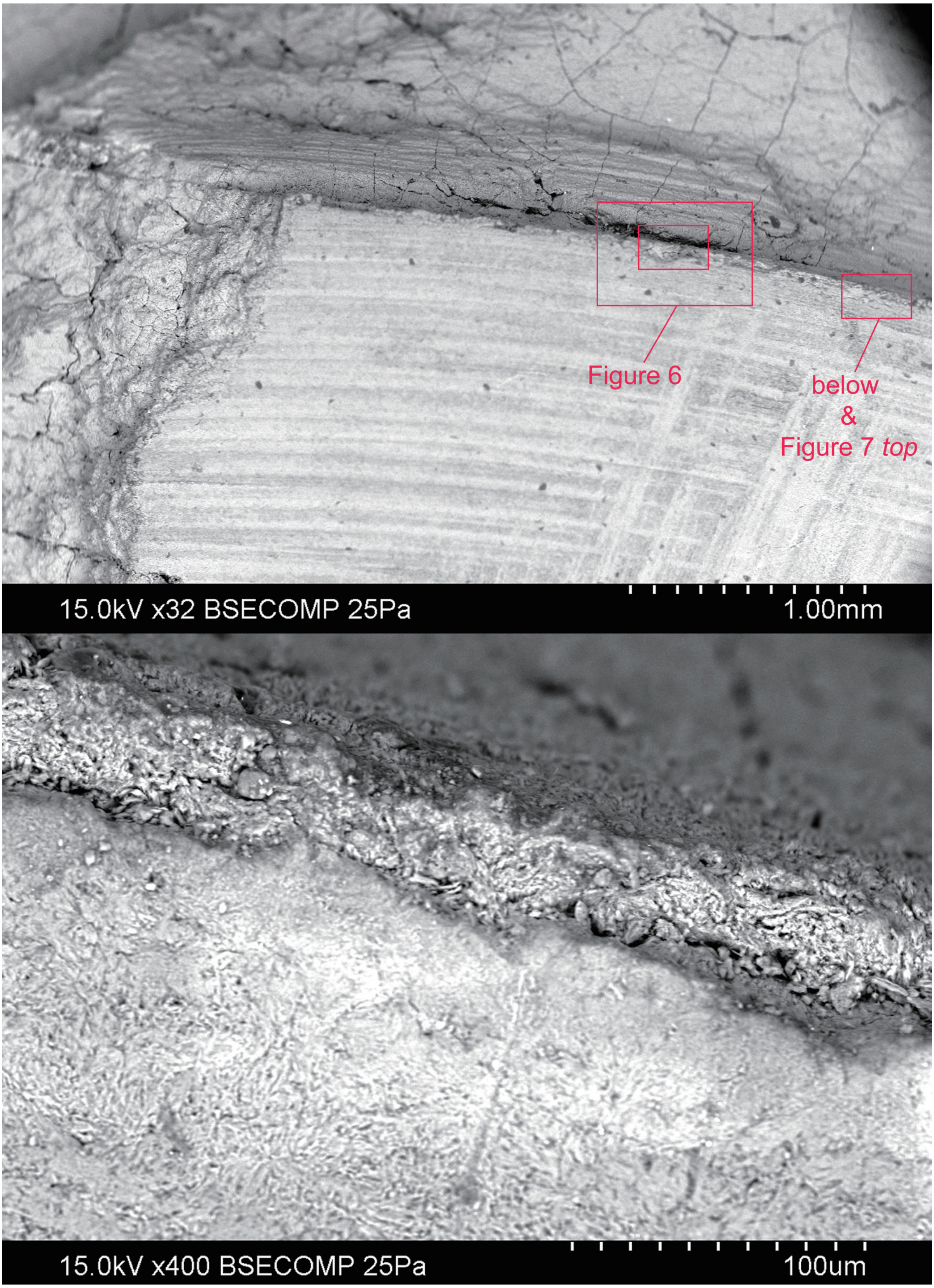

Appendix 7.15 Figure 5 Top - Two areas in which detailed BSE imaging and/or EDS of the seal boss' surface layer in section was conducted. Bottom - BSE image detail of the first area examined.

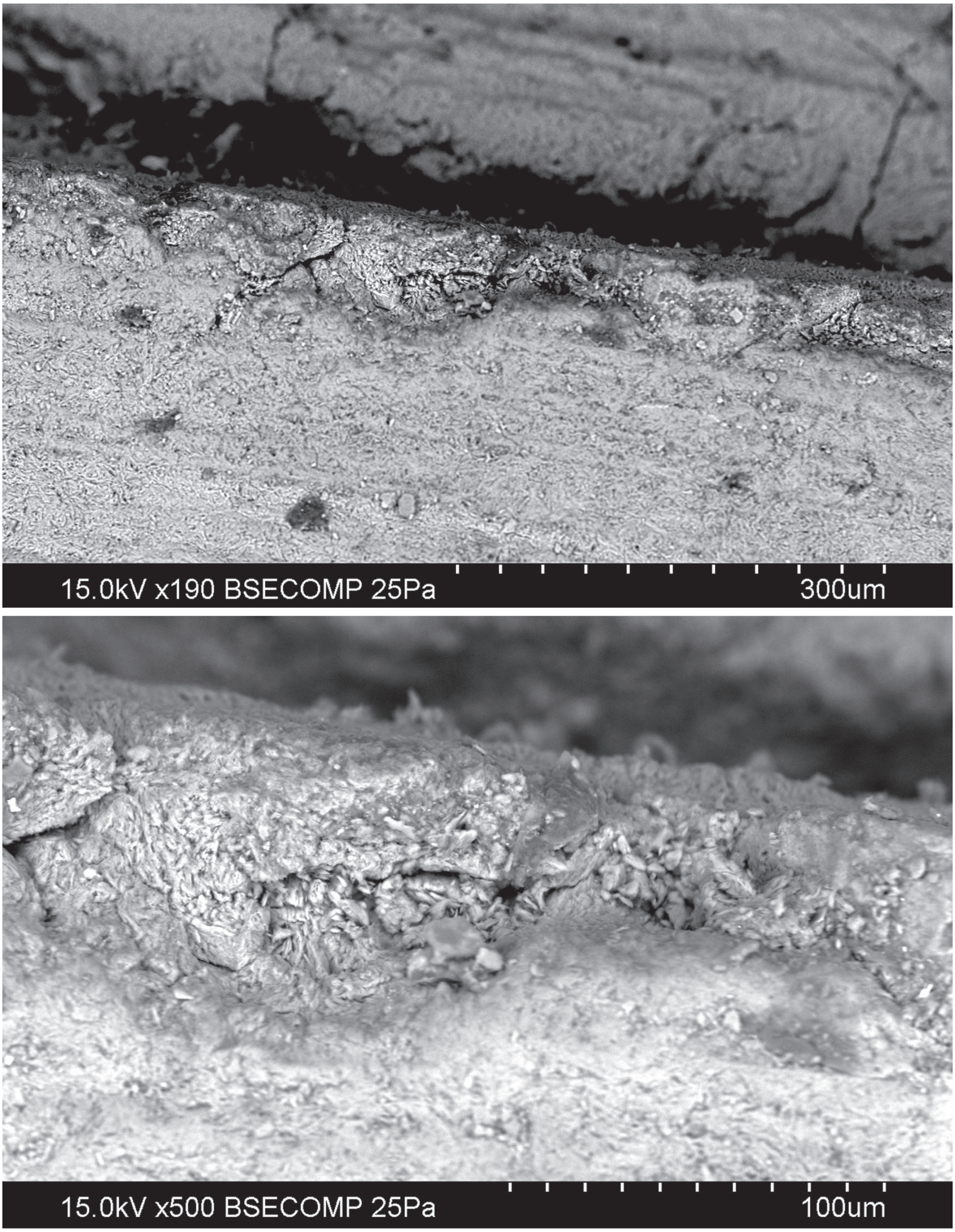

Appendix 7.15 Figure 6 Full view and detail of the second area examined on the seal boss' surface layer in section.

manufacturing marks and still left them visible. It also probably could have worked its way into and coated the crack that is evident in the seal body (labeled on Appendix 7.15 Figure 1 C), something that Beck argued (1934: 81) an applied paste would not have done.

VP-SEM / EDS

The cursory EMPA of the seal boss provided somewhat equivocal results and so follow-up studies were conducted on the VP-SEM in December 2009. There were several advantages to using this technique. The entire artifact could be placed into the instrument's vacuum chamber; it did not need to be coated with a conducting layer; and it was possible to easily and quickly move the different areas on the object to make observations. Three areas (Appendix 7.15 Figure 4 A) were chosen for BSE imaging and qualitative compositional analysis using the instrument's EDS. The first (Appendix 7.15 Figure 4 B) was along the same thin surface layer that was exposed in section when a small piece of the boss was cut for EMPA. The second (Appendix 7.15 Figure 4 C) was around a micro-crack coming off the large "glazed" break-crack that, in visible light images, appeared to filled with a white substance similar to that covering the seal's surface. It was hoped that if the seal had been placed into a liquid medium (a bleach, slip, or glaze) during its manufacture then some of that material might be preserved in a fissure in the solid steatite such as this. The third area examined (Appendix 7.15 Figure 4 D) was the surface of the boss itself in a patchy place where the white exterior was both intact and had fallen away.

Surface layer in section

Detailed BSE imaging of the seal boss' surface layer in section was conducted in two areas (identified on Appendix 7.15 Figure 5 top). Unlike boss piece examined using EMPA, which was finely polished prior to analysis, the section imaged on the VP-SEM was rough and the concentric marks from the circular saw used to removed the piece were visible. Nevertheless, a distinct boundary between the solid, compact steatite of the seal body and the looser material of the surface layer is evident in the first area observed (Appendix 7.15 Figure 5 bottom). The solid steatite directly below and following the contours of that boundary appears in the BSE image as a thin (5 to 10 microns), slightly gray phase. This corresponds to the Layer 3 in the earlier EMPA and would seem to be the original surface of the seal prior to the application of the final surface layer. The discoloration is probably a reaction zone created when the applied material fused or bonded with the solid steatite. In some places along the boundary there are gaps (dark areas in the BSE image) where the applied layer either did not fully adhere to the carved surface or has begun to break away.

Appendix 7.15 Figure 6 shows two views (a full view - top, and a detail - bottom) of the second area imaged. This area was chosen because of a deep undulation, which could be a carving groove, in the solid steatite along the boundary where it meets the surface layer. The thin gray reaction zone observed in there first area is present again here and closely follows the contour of the undulation/groove. The difference between the solid steatite of the seal interior and the surface layer is also again striking. Although both are composed of platy crystals, those in the seal body are very tightly packed while those making up the surface layer are loose and randomly oriented. The latter almost seem to have flowed viscously into the deep groove. It is difficult to imagine what this layer could be other than applied material.

A series of 12 EDS (Appendix 7.15 Figure 7 top) scans were made along the first section of the surface layer that was imaged. Scans 1 to 3 were centered on points within the solid steatite of the seal body; scans 4 to 8 were made in the thin gray phase that at the

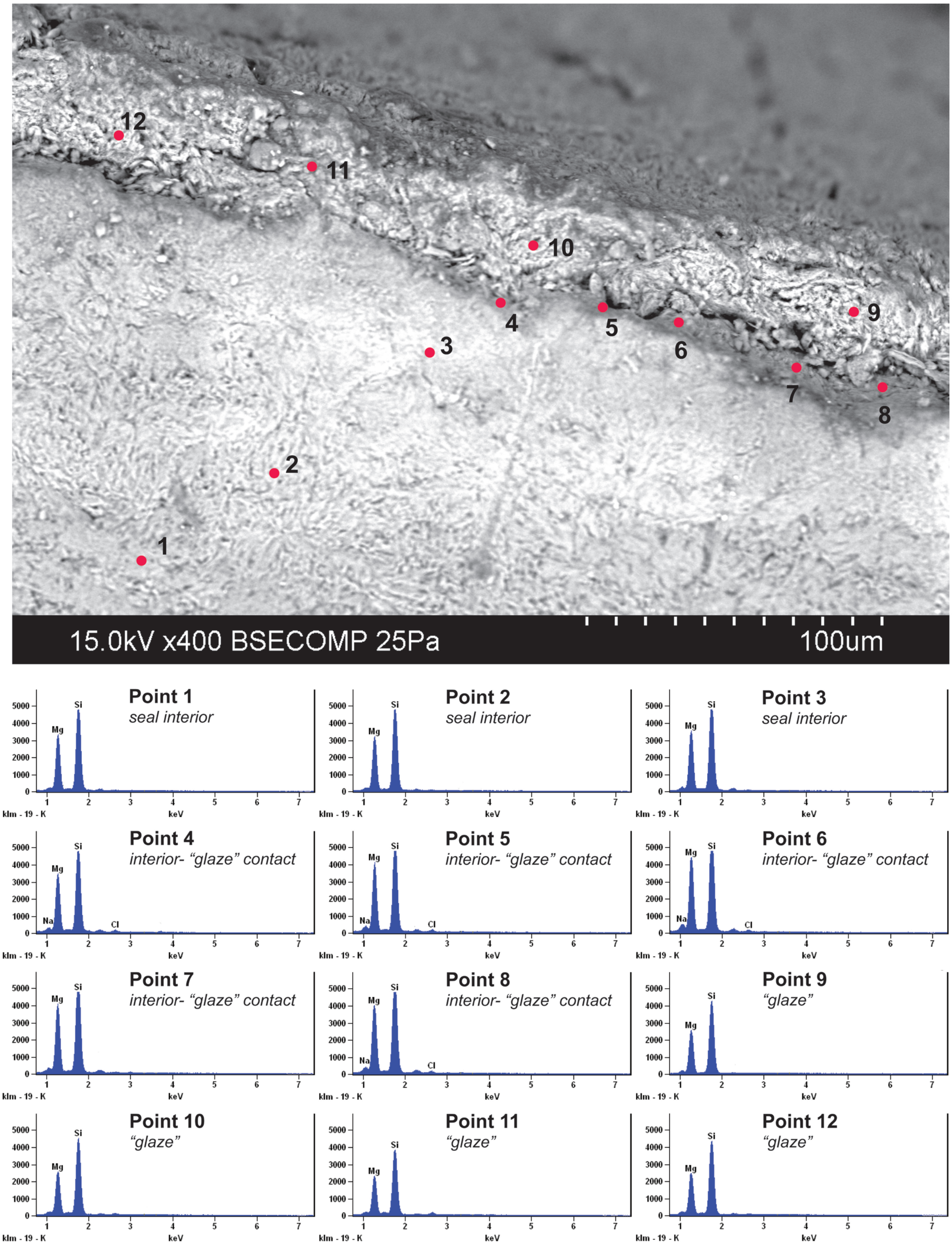

Appendix 7.15 Figure 7 Top - The 12 points where EDS scans were made in the first area examined on the seal boss' surface layer in section. Bottom - The spectra for the 12 EDS scans.

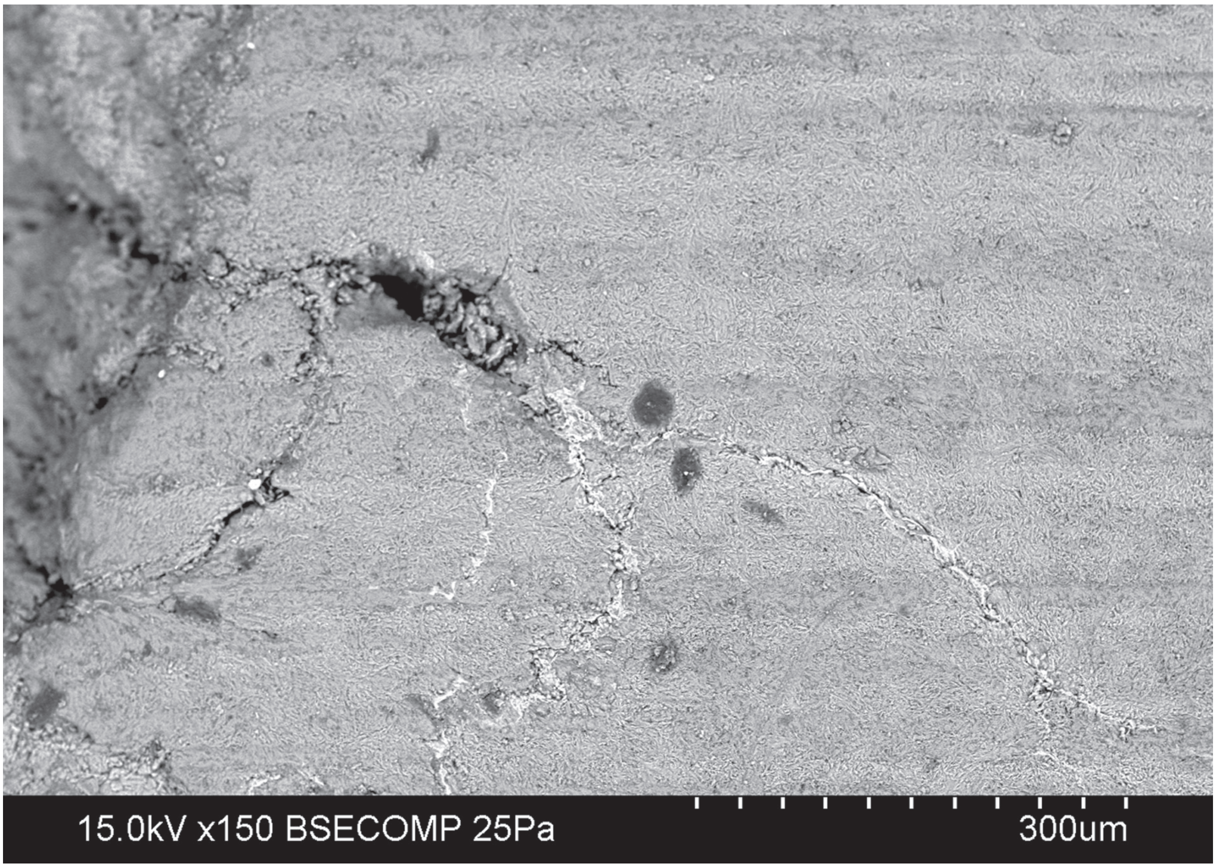

Appendix 7.15 Figure 8 BSE image of the micro-crack in the seal boss' interior.

edge of the original seal surface that appears to be a reaction zone; and scans 9 to 12 were made at points along and within the loose material of the surface layer. The spectra for all 12 (Appendix 7.15 Figure 7 bottom) are practically identical. Like the initial EDS scans made during the earlier EMPA, those made on the VP-SEM indicated that all phases were composed solely of magnesium silicate. This was not unexpected for the scans centered on solid steatite but it was somewhat surprising with regard to the surface layer. The layer was clearly composed of talcose material but there was, again like in the EMPA, no suggestion of chemical phases that could have been remnants of fluxes, binders, or bleaches.

Micro-crack

The next area examined was the micro-crack in the seal body. Appendix 7.15 Figure 8 is a BSE image of that area. The micro-crack extends from the exterior surface (which is actually a larger white-coated crack) on the upper left of the BSE image roughly 800 microns (0.8 mm) into the solid steatite matrix of the seal (the muted horizontal striping are marks across the matrix are from the saw used to cut the section). There is some loose talc-like platy material in the wide portion of the micro-crack near the surface. Deeper in the interior there a white material filling the voids created by the fissure. There are also several dark gray patches within the solid steatite matrix near the micro-crack. EDS scans were made at eight points in this area (Appendix 7.15 Figure 9 top). One was of the solid steatite of the seal interior (Point 1), another was of one of the dark gray patches near the crack (Point 2), six were of the white substance within the crack (points 3 through 7) and one final scan was made of the loose material toward the exterior surface. The spectra for those scans are displayed in the lower portion of Appendix 7.15 Figure 9.

The EDS spectrum of the solid steatite interior showed peaks for Mg and Si (MgSi - magnesium

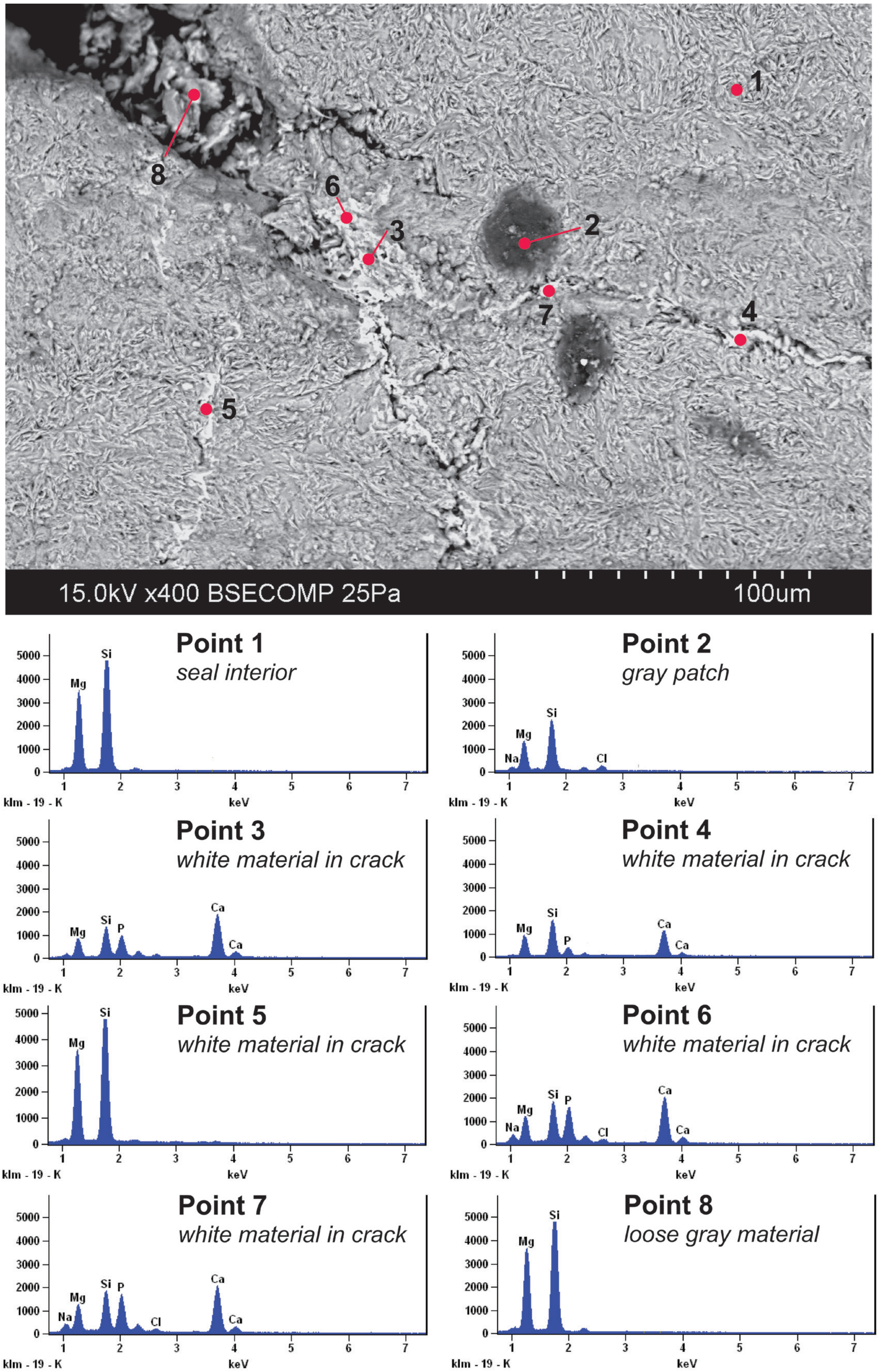

Appendix 7.15 Figure 9 Top - The eight points where EDS scans were made in and around the micro-crack. Bottom - The spectra for the eight EDS scans.

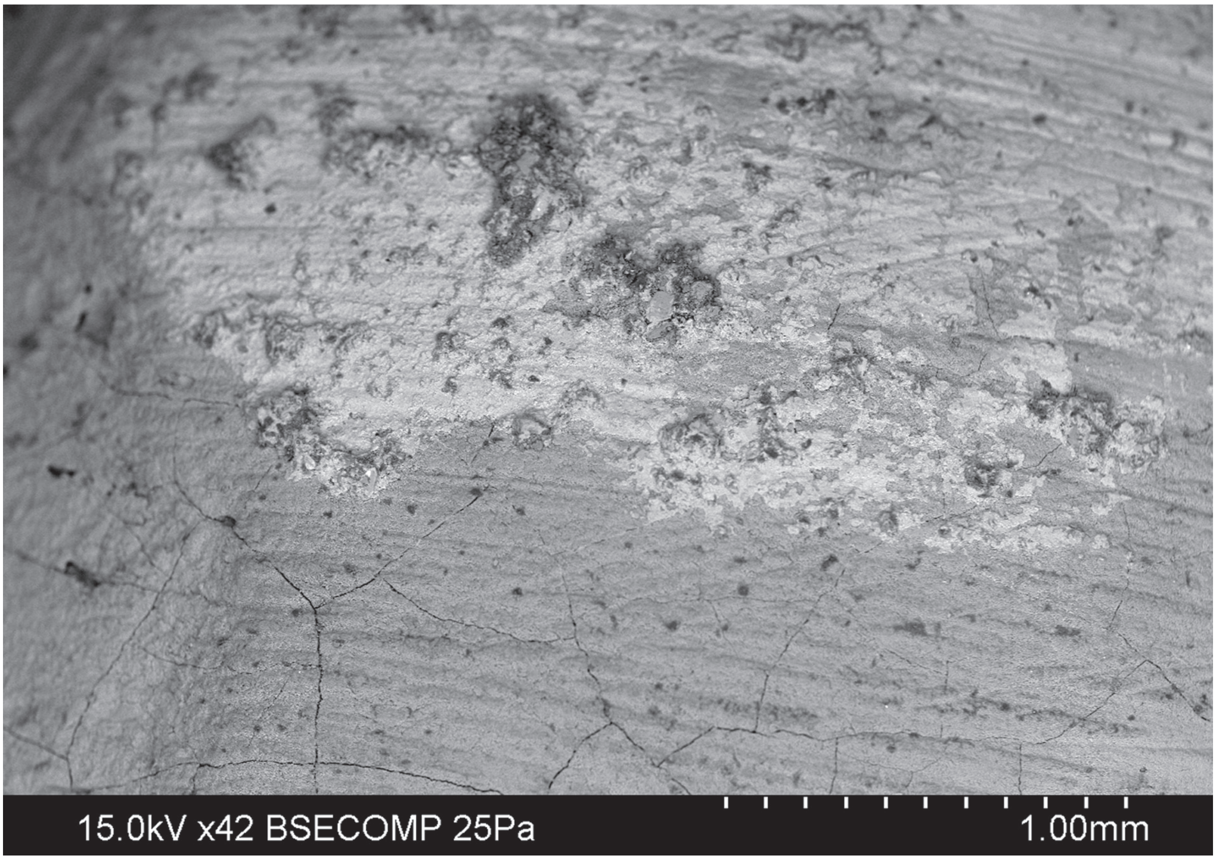

Appendix 7.15 Figure 10 BSE image of the patchy area on the boss' surface examined using VP-SEM/EDS.

silicate) as expected. Along with MgSi, minor peaks for Na & Cl (sodium chloride) were detected in the gray patch, which indicates the presence of salt. This salty phase may have naturally occurred in the steatite body or it could have formed following the artifact's deposition in the saline soil of Harappa. Along with MgSi, peaks of Ca and P (calcium phosphate) was detected in all of the EDS scans of the white material filling the deeper potion of the crack, save for Point 5. The calcium phosphate detected could be powdered bone or bone ash. Only MgSi was detected in the spectra for Point 5. Unlike the other scans made on the white substance, the white phase here was in a crack-like area that, at least in this section, does not appear to have reached the surface of the seal. It is, therefore, probably not a crack fill with a white substance but rather a lighter phase of steatite. The loose material toward the exterior surface was also only MgSi or just talcose material.

Patchy exterior surface

The final area examined with the VP-SEM/EDS was a place on the seal boss' exterior where there are intact patches of the treated surface as well as patches where it was missing. These are clearly visible in the BSE image of the area (Appendix 7.15 Figure 10) as bright white phases (the applied material) and gray phases (the areas where it is missing). There are also numerous large and small dark gray crusty dark patches of sediment that remained on the surface despite repeated sonic baths. An important feature to notice in the BSE image is the way in which the manufacturing striations on seal's surface continue unobscured as they pass from the applied surface areas to the places where the applied material is missing and vice versa. The fact that such marks were visible on the surface of seals has been argued to indicate that a bleach rather than a slip or glaze was responsible for the white exteriors of these objects. As we have seen,

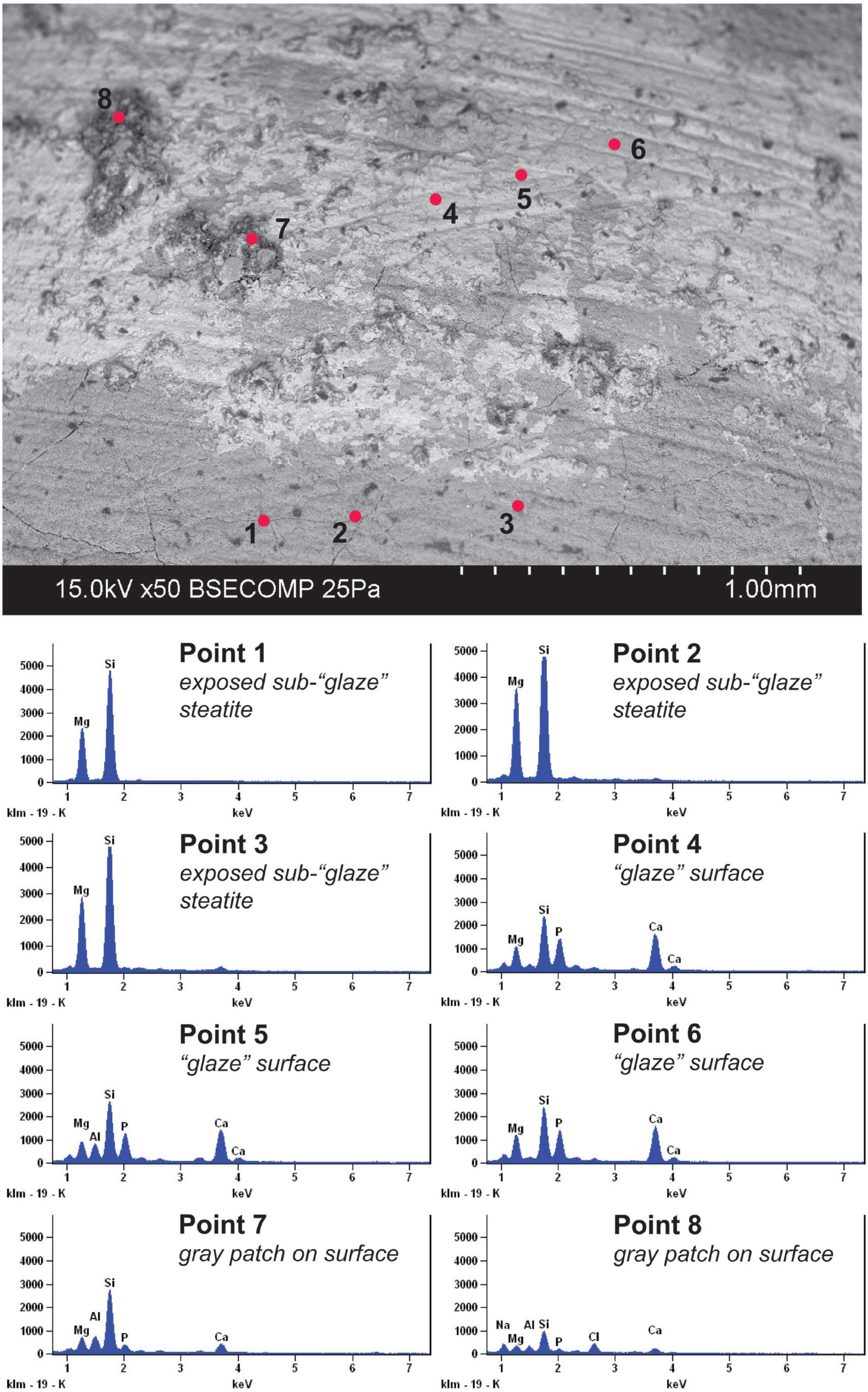

Appendix 7.15 Figure 11 Top - The eight points where EDS scans were made in the patchy area. Bottom - The spectra for the eight EDS scans.

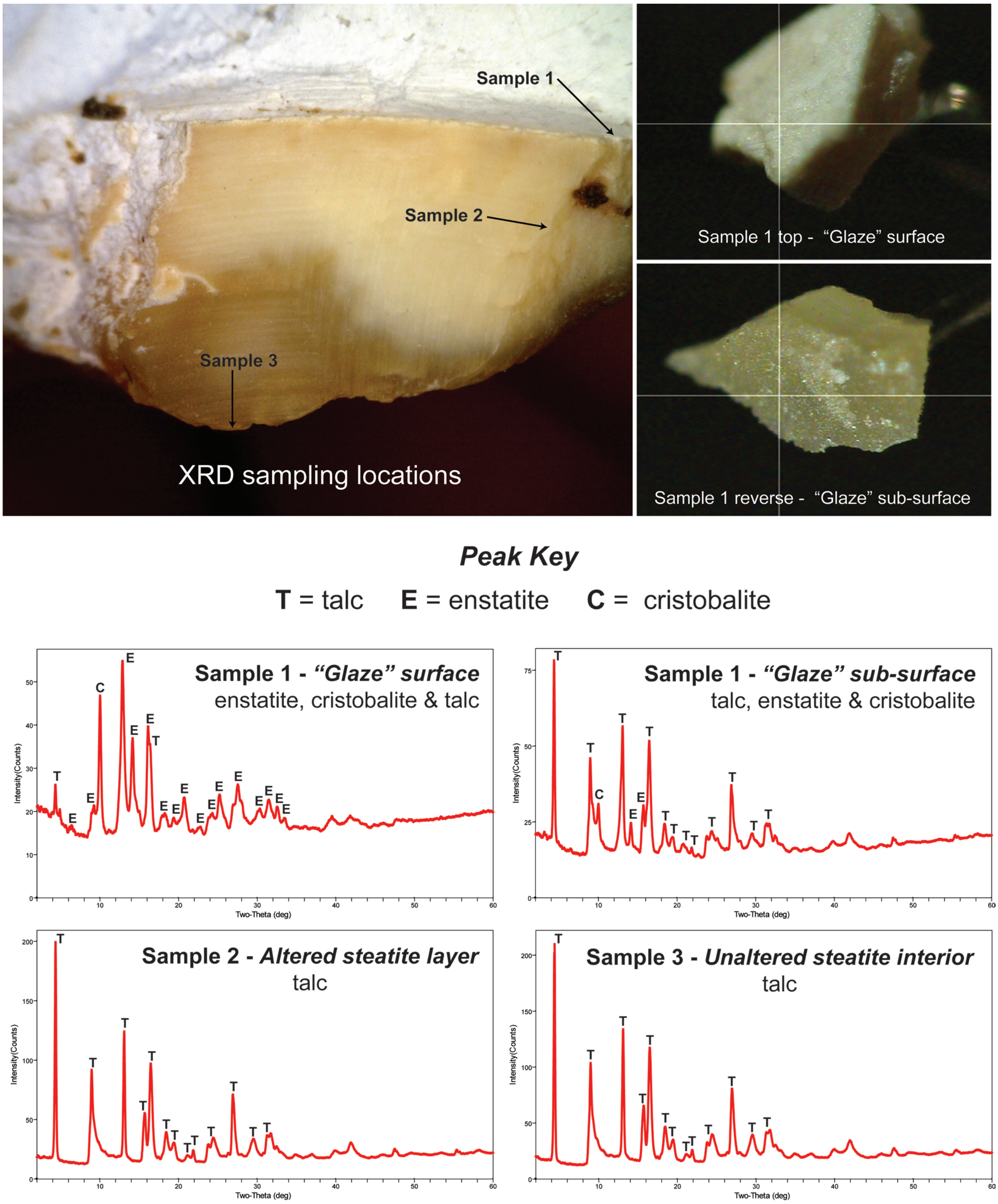

Appendix 7.15 Figure 12 Top left - Three areas on the seal boss' section where small sample of material were removed for XRD analysis. Top right two images - The surface layer sample exterior and interior side. Bottom - The XRD spectra for the three samples.

however, a distinct layer of talcose material covers the surface. That layer was obviously thin enough to adhere to the contours of the manufacturing marks without obscuring them.

EDS scans were made at eight points in this area (Appendix 7.15 Figure 11 top). Three were made where the applied surface was missing (points 1 to 3), another three were made on the applied surface itself (points 4 to 6) and two were on the dark gray crusty patches thought to be adhered sediment (points 7

Appendix 7.15 Figure 13 Left - Carver at the shrine of Shah Noorani producing talc powder as he saws a block of steatite. Right - Bags of talc powder for sale at Shah Noorani.

and 8). The spectra for those scans are displayed in the lower portion of Appendix 7.15 Figure 10. They reveal that, as expected, the bare areas where the original, pre-application surface is exposed are wholly magnesium silicate (talcose) material. The spectra for three scans made on the applied surface, however, exhibit peaks for calcium phosphate in addition to magnesium silicate, just like the white material found deep in micro-crack. It is significant that calcium phosphate was not detected in the spectra of scans made of the applied surface in section. Those scans ran down the center of that 20 to 30 micro thick surface layer rather than along the exterior edge. This suggests that the calcium phosphate is found only on the immediate surface and was applied subsequent to the talcose layer. It almost certainly was applied as a liquid slip, which would account for the presence of the calcium phosphate within the micro-crack. Lastly, although their rough surfaces resulted in poor EDS spectra for the dark gray crusty patches, peaks of Al (aluminum) were evident, which indicates that the patches are indeed composed of clay sediments.

XRD

Although the EDS scans of the seal boss' applied surface revealed that the layer was composed of magnesium silicate (topped-off with a calcium phosphate slip), it was not possible to tell what mineralogical form it took. In order to determine this, as well as to characterize the discolored, seemingly heat-altered sub-surface zone of steatite, samples from the boss were analyzed in December 2009 on the Rigaku Rapid II X-ray diffractometer at the S. W. Bailey X-ray Diffraction Laboratory, Department of Geology and Geophysics, University of Wisconsin–Madison. Using the tip of an X-Acto knife, tiny (sub-millimeter) pieces were removed in three places along the section cut for EMPA

(Appendix 7.15 Figure 12 top left). Sample 1 is a piece of the applied white surface layer. Sample 2 is a piece of the seal's interior removed from a point about halfway down the discolored zone. Sample 3 is a piece of the unaltered interior steatite. The XRD spectra for the three samples are shown on the bottom half of Appendix 7.15 Figure 12.

Sample 1 was X-rayed twice – once on the exterior surface and once on the reverse, sub-surface side (Appendix 7.15 Figure 12 top right two images). Enstatite, well-developed cristobolite and a minor talc phase were detected on the exterior side. On the reverse, sub-surface side of Sample 1, talc was the primary mineral phase detected along with minor phases of cristobolite and enstatite. It is important to note at this point that, although I attempted to remove just the applied surface layer for analysis, some of the underlying steatite of the original seal came off with the sample (notice the light khaki-colored appearance of the sample in the lower of the top right two images in Appendix 7.15 Figure 12). The minor talc phase detected in the spectra of surface XRD scan was almost certainly some of this interior material. Conversely, as the X-ray beam passed through the steatite that adhered to the reverse side of the applied surface, talc was main phase detected. The minor phases of enstatite and cristobalite observed in that scan, in all likelihood, represent the applied talcose surface layer, which is probably composed solely of those two minerals.

The spectrum for Sample 2 indicates that, despite the discoloration of the steatite in this area, the composition of the material is pure talc. Recall from Appendix 7.12 the steatite chips that were fired at 800°C for up to three hours. The appearance of those experimental samples lightened somewhat but XRD analysis indicated that their talc component remained unchanged. The spectrum for Sample 3 – the unaltered khaki-colored raw steatite beneath the lighter zone – is absolutely identical to the spectrum for Sample 2. It therefore appears that below the thin enstatite-cristobolite surface layer the seal is entirely talc.

CONCLUSION

Although much remains to be learned about the technology and process of Harappan seal manufacture, the EMPA, VP-SEM and XRD observations made here have provided a great deal of information about the surface of this particular seal boss fragment. The carved steatite body of the object is covered by an extremely thin (≈ 20 microns) layer composed of talc that has been heated to a temperature of 1200°C or greater (and, thus, it is no longer talc but rather the minerals enstatite and cristobalite) as well as a calcium phosphate slip. There are several indications that the talcose layer is an applied surface rather than the result of bleaching or in situ heat-treatment. The texture of the layer in section is very distinct when compared to the compact steatite of the seal body and, in certain places, the platy grains of material making it up are oriented in ways that appear as if they flowed in a viscous form into grooves in the seal's carved steatite body. Most importantly, however, it that given the intensity of the cristobolite peaks detected and the extreme thinness of the surface layer in which that mineral phase is found, this transformation could not have taken place in situ. Published analyses (see Wesolowski 1984 for a review of various steatite heating studies) as well as my own experimental work (appendices 7.12 and 7.16; Jamison and Law 2007) demonstrates that it takes temperatures in the range of 1200°C or greater in order to for well-developed cristobolite phases to develop in steatite (weak peaks of cristobolite may develop at temperatures closer to 1100°C). Although heat evidently penetrated the seal body enough to lighten the appearance of the raw steatite to a depth of up to 4 mm immediately below the surface layer, it clearly was not of sufficient intensity or duration to cause any mineralogical change in that zone (not even minor peaks of enstatite). One centimeter thick chips cut from Daradar deposit samples (the very deposit the INAA studies predicted to be the source of the boss fragment) that were experimentally heated by Gregg Jamison and myself (Jamison and Law 2007) showed that it took 5 minutes at 1100°C for the steatite to be fired completely throughout. Those and other (appendices 7.12 and 7.16) experiments also demonstrated that it takes a considerably longer time and higher temperatures than that for well-developed cristobalite to develop. So what it comes down to is this: If the seal had been exposed to heat of the intensity and duration required for that mineral to form on its surface then the interior would have been altered, at least to enstatite, throughout. It has not been, however. In fact, the XRD analysis showed that talc directly abuts the enstatite-cristobalite layer. Based on these observations, I have concluded that the surface layer is composed of previously high-fired steatite that was ground[1)] (or talc was first ground and then fired) into a fine powder and applied to carved seal's surface.

The calcium phosphate detected on the outer surface of the seal and preserved in a micro-crack within its body is perhaps a bone-ash slip/treatment of some kind that was added after the talcose layer was applied. Bone ash is added to certain kinds of porcelains "as a way of enhancing whiteness, translucency and strength" (Pishch *et al*. 1997: 61). It may have been applied to Harappan seals for those very same purposes.

---

1) Actually, Harappans had no need to deliberately grind steatite as an abundance of extremely fine powder is produced during the sawing and drilling of that stone. Massimo Vidale believes (2000: 63) that "talc working craftspeople used to live and work surrounded by 'clouds' and mud of white talc powder." Today, the steatite carvers at the shrine of Shah Noorani collect, package and sell this powder (Appendix 7.15 Figure 13) for a variety medicinal uses (Vidale and Shar 1990: 64).

APPENDIX 7.16

HEATING AND CHARACTERIZATION OF STEATITE FROM VARIOUS GEOLOGIC SOURCES

Barthélémy de Saizieu and Bouquillon (1994: 51) heated “raw steatite flakes found at Mehrgarh” and observed that their color turned from black to white between 800°C to 900°C. I heat-treated four steatite fragments (unworked and unprovenienced pieces turned in by a workman) from Harappa that were of varying colors including jet black (Appendix 7.16, Figure 1). After a one hour static firing at 1200° C, all four had become bright white, just like the tens of thousand of heat-treated steatite artifacts recovered at the site. That the color of these unfired scraps of raw steatite left behind by Indus Tradition craftspeople should transform in this way is not at all surprising as a white appearance was what was evidently sought when objects made from this variety of stone were fired. The debris from manufacturing such objects should naturally become white also. However, can we conclude that all steatite fires white? In this appendix, I provide an overview of my attempts to answer this question. In addition, I detail the effort to characterize the quality/workability of steatite from different geologic sources in Pakistan and India.

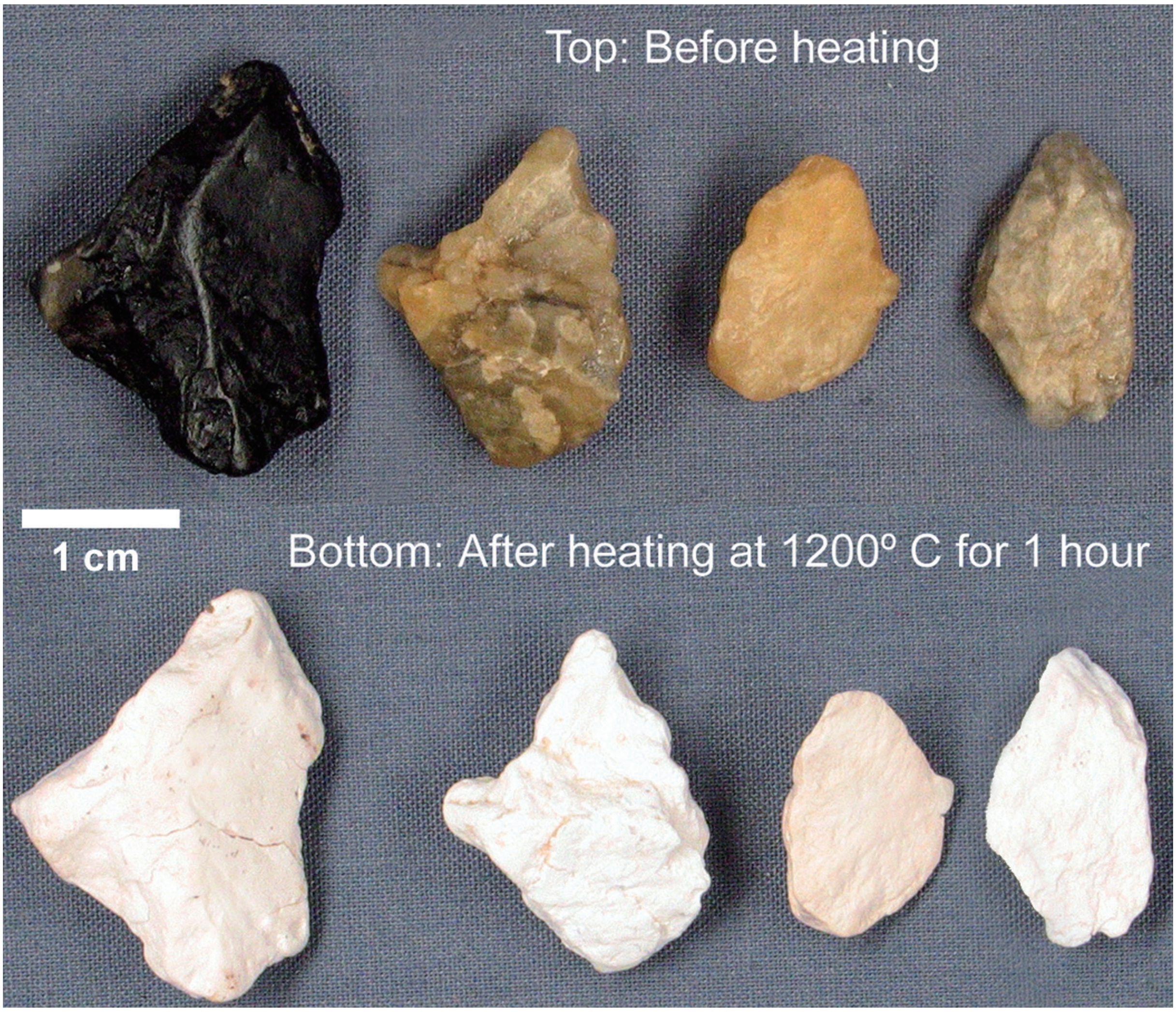

Appendix 7.16 Figure 1 Experimental heating for four unworked steatite fragments from Harappa (surface finds).

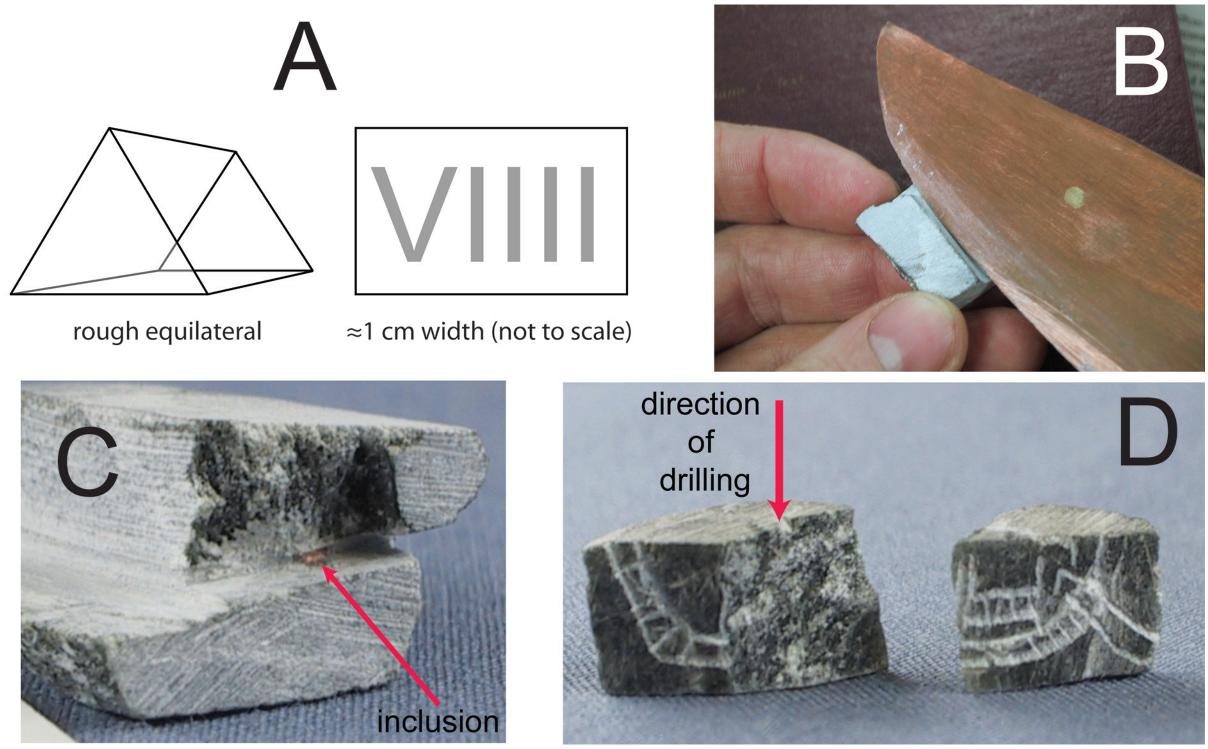

Appendix 7.16 Figure 2 **[A]** Experimental steatite tablet dimensions. **[B]** Replica copper saw. **[C]** Inclusion in Jamrud (NWFP) deposit steatite. **[D]** A seal replica using Shiv Bola (southern Rajasthan) steatite that split during drilling.

My initial steatite heating and characterization experiments were conducted in the Spring of 2002. At that time, samples from only 20 locations were available for study (these are listed in Appendix 7.16, Figure 4). Sixteen were from steatite sources that would go on to be included in the geologic dataset (their source codes correspond to those used in Chapter 7 and listed in Appendix 7.2). Two others were from sources in Pakistan – Jamrud in the Khyber Agency, FATA and Kund from the Peshawar District, NWFP. Neither of these would be analyzed for the provenience study due, in large part, to the observations reported in this appendix. The final two samples were taken from steatite purchased in shops. Sample "shop 1" was obtained from the workshop of a steatite carver named Ravi Soni in Udaipur, Rajasthan. Sample "shop 2" was purchased from the main bazaar in Attock City, northern Punjab Province, Pakistan.

In order to gauge the quality/workability of the stone from each of the different sources, the blanks to be heat-treated were fashioned into replicas of prism-shaped incised steatite tablets in dimensions (Appendix 7.16, Figure 2 A) approximating those reported in Meadow and Kenoyer (2000). The tablets were cut using a replica of a Harappan period bronze saw (Appendix 7.16, Figure 2 B) that was reconstructed by Dr. J. Mark Kenoyer based on scanning electron microscopy (SEM) studies of steatite debitage (Kenoyer 1997b). The Harappan sign "VIIII" was incised onto one face of each of the tablets using a copper stylus with a beveled end. The 20 completed, unfired replicas can be seen in Appendix 7.16, Figure 3 A.

As is evident on Appendix 7.16, Figure 3 A, not all of the experimental tablets could be carved into prism-like shapes with nice even edges. While many (or most) of the problems had to do, no doubt, with my lack of skill as a carver, much of the difficulty was attributable to the varying quality of raw material from different sources. The heavily foliated steatite from Kund kept splitting. Ultimately the tablet from

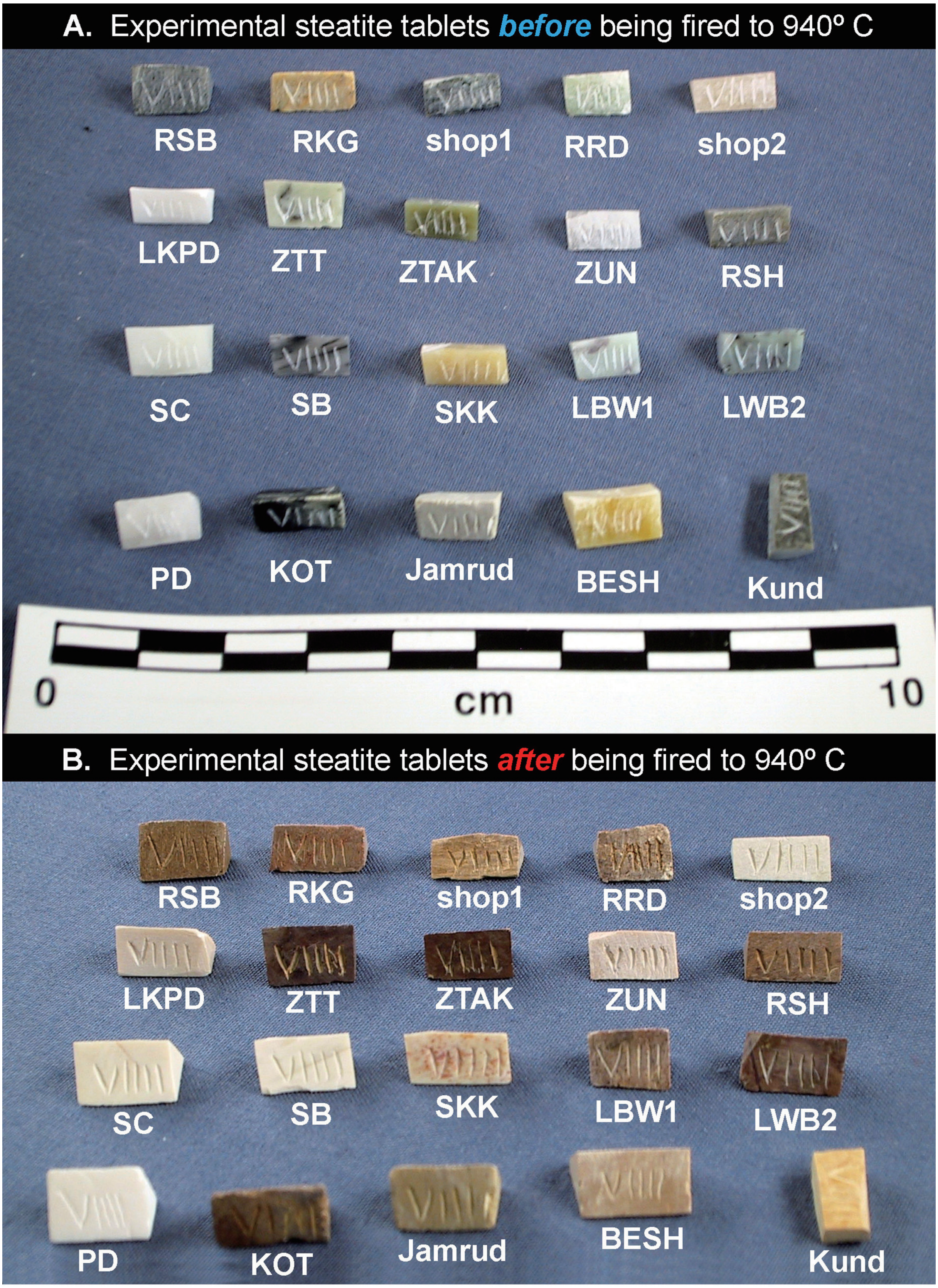

Appendix 7.16 Figure 3 Heating experiment using steatite from 20 South Asian deposits.

Appendix 7.16 Figure 4 Descriptions of the 20 geologic steatite samples used in the initial heating experiment.

Source	*Parent-Rock*	*Pre-fire color*	*fired color*	*volume change*	*weight change*	*final hardness*
PD	Dolomite	Very light gray N 8	White N 9	9.00%	-1.48%	6
KOT	Ultramafic	Greenish black 5 G 2/1 to Greenish gray 10 GY 5/2	Dark yellowish brown 10 YR 4/2	-5.00%	-3.20%	5 to 6
Jamrud	Dolomite	Very light gray N 8	Pale yellowish brown 10 YR 6/2	1.75%	-1.44%	5
BESH	Dolomite	Yellowish gray 5 Y 8/1	Yellowish gray 5 Y 8/1	-4.00%	-0.76%	5 to 6
Kund	Dolomite	Dark greenish gray 5 GY 4/1	Grayish orange 10 YR 7/4	n/a	n/a	5 to 6
SC	Dolomite	Very light gray N 8	Very light gray N 8	-0.75%	-2.28%	6
SB	Dolomite	Med. Light gray N 6 to Dark gray N 3	White N 9	-0.75%	-1.49%	6
SKK	Dolomite	Yellowish gray 5 Y 8/1	Yellowish gray 5 Y 8/1	-2.00%	-2.32%	6
LBW1	Ultramafic	Very pale green 10 G 8/2 to Med. Dark gray N 4	Dark yellowish brown 10 YR 4/2	-2.75%	-2.03%	5 to 6
LBW2	Ultramafic	Greenish gray 5 G 6/1 to Black N 1	Dark yellowish brown 10 YR 4/2	-0.75%	-2.60%	6
LKPD	Dolomite	White N 9	Pinkish gray 5 YR 8/1	-3.75%	-1.56%	5 to 6
ZTT	Ultramafic	Light greenish gray 5 G 6/1 to Grayish black N 2	Dusky yellowish brown 10 YR 2/2	-13.50%	-2.07%	6
ZTAK	Ultramafic	Dusky yellow green 5 GY 5/2	Dusky yellowish brown 10 YR 2/2	2.00%	-1.85%	6
ZUN	Ultramafic	Med. Light gray N 6	Yellowish gray 5 Y 8/1	0.25%	-1.38%	6
RSH	Ultramafic	Dusky yellow green 5 GY 5/2 to 5 GY 3/2	Dark yellowish brown 10 YR 4/2	-2.00%	-2.33%	5 to 6
RSB	Ultramafic	Dark greenish gray 5 GY 4/1	Dark yellowish brown 10 YR 4/2	-12.00%	-3.89%	5 to 6
RKG	Ultramafic	Grayish orange 10 YR 7/4 to Dark yellowish orange 10 YR 6/6	Dark yellowish brown 10 YR 4/2	-11.00%	-2.12%	5 to 6
Shop1	unknown	Pale green 5 G 7/2	Grayish orange pink 5 YR 7/2	3.00%	-3.25%	6
RRD	Ultramafic	Dark greenish gray 5 GY 4/1 to Greenish black 5 GY 2/1	Grayish orange pink 5 YR 7/2	9.00%	-2.46%	5 to 6
Shop2	unknown	Grayish orange pink 5 YR 7/2	Pinkish gray 5 YR 8/1	3.75%	-0.47%	5 to 6

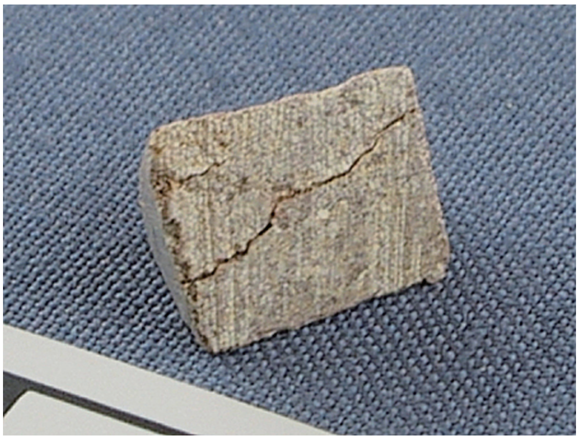

Appendix 7.16 Figure 5 Cracked tablet RRD (post-firing).

that source had to be made flat and rectangular. The Jamrud steatite had a great many quartz inclusions in it that made sawing difficult (Appendix 7.16, Figure 2 C). A rough-looking tablet from that source was shaped only after considerable effort and material waste. Problematic inclusions were encountered in the KOT and "shop 1" samples. Most of the remaining tablets were fairly easily carved and incised. I also attempted to make several rectangular replica seals using stone from various sources. Most also carved fairly well but one from the Shiv Bola deposit of Rajasthan quickly split when I tried to drill a hole through its center (Appendix 7.16, Figure 2 D).

Prior to firing, each of the 20 prism-shaped tablets was weighed, measured and its color characterized using a Munsell Rock Color Chart. The surfaces of all of them could be scratched using a calcite crystal and thus each had a hardness of 2½ or less on the Mohs' Mineral Hardness Scale (Appendix 2.1). They were then placed in a muffle furnace and the temperature was slowly raised 60°C per hour to 940° C. The tablets were held at this temperature for one hour and then the furnace was turned off and allowed to cool slowly overnight. The next day all were re-weighed, measured and color-characterized. The post-firing hardness of the tablets was scratch-tested using apatite (hardness 5), feldspar (hardness 6), quartz (hardness 7).

The post-firing appearance of the incised tablets is pictured in Appendix 7.16, Figure 3 B (the before and after Munsell characterizations are listed in columns three and four of Appendix 7.16, Figure 4). Only five of them (PD, SC, SB, LKPD, ZUN and "shop 2") exhibited a post-firing color that was white (or anything close to it). It is important to note that all but one (SB) of those was white or near-white in appearance to begin with. The color of most of the remaining tablets had become a dull rusty red.

Post-firing changes in volume, weight and hardness for each tablet are listed in the fourth through sixth columns of Appendix 7.16, Figure 4. Most of them held up well physically, meaning that heat-induced changes in weight and volume (due to water being driven off during the conversion of talc to enstatite) did not cause them to split, crack or flake. Only the tablet carved using steatite from RRD (from Rishab-der in southern Rajasthan) exhibited any significant cracking (Appendix 7.16, Figure 5). Mineral scratch tests indicated that the Mohs hardness for most tablets was just around 6 while some fell between 5 and 6.

A series of XRD analyses were performed on select tablets – from PD, LKPD, RSB and ZTT. Each of these was sawn into two pieces, one of which was re-heated to 1150ºC for one hour. No further macroscopic changes were evident after the halves were reheated (i.e, they did not become any whiter) but their hardness increased to between 6 and 7 (PD and LKPD) to 7 (RSB and ZTT). Unheated powder from the carving of tablets PD and RSB was also X-rayed. PD was pure talc to being with but steatite from RSB contained a minor chlorite phase.

Composites of all XRD scans for the three tablets can be seen in Appendix 7.16, Figure 6. In each one, talc had begun to transform into enstatite by 940ºC, although the decomposition/formation of those minerals was different from tablet to tablet. In ZTT, talc had all but disappeared (there is a minor peak at around 9.75º) while in LKPD it was still the dominant mineral. Talc had entirely decomposed in each of the

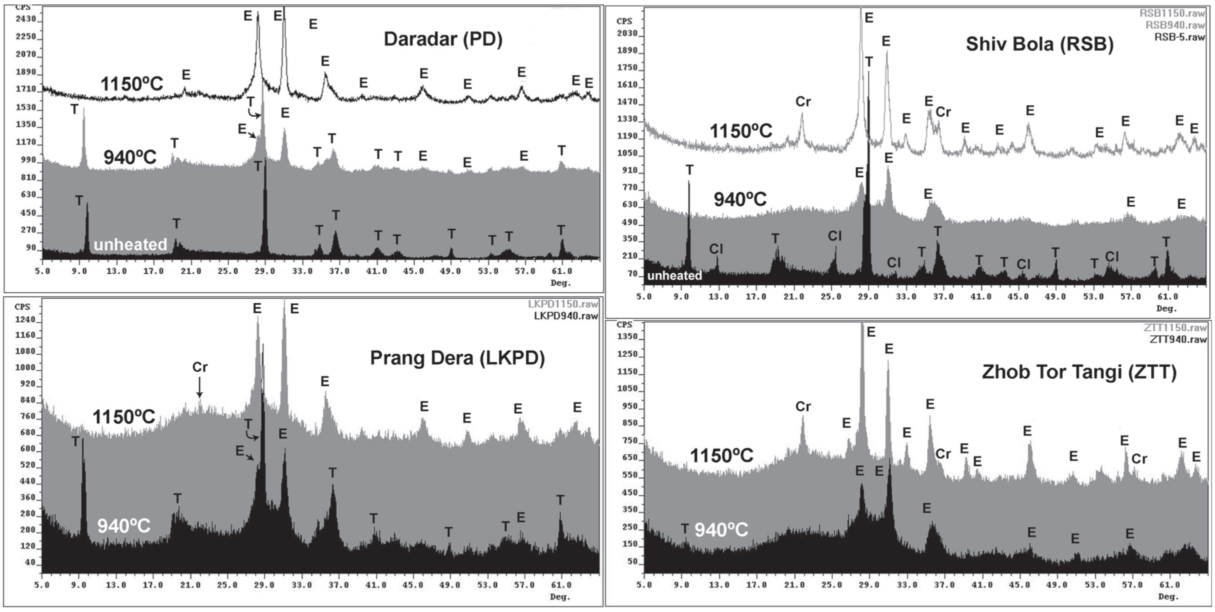

Appendix 7.16 Figure 6 XRD scans of heated steatite samples from three sources. Peak Key: T = talc, Cr = cristobalite, E = enstatite, Cl = chlorite.

tablet halves that were heated to 1150ºC. Cristobalite had begun to form in RSB and ZTT as well as, just barely, in LKPD. No cristobalite peaks were evident in the scan for PD, however. The varying Mohs hardness values in the heated samples are attributable to the differential formation of these minerals.

The results of the initial heating experiment indicated several things. First and most importantly, it was quite clear that not all steatite becomes white when it is heat-treated. It was also apparent that mineral composition, inclusions, foliation and bonding of raw steatite were all things that affected the ease to which steatite was carved and, probably, how well it held together when fired. Lastly, the hardness of fired steatite is a function of the temperature to which it was heated (and to a lesser extent how long it was heated). The formation of enstatite will impart a steatite object with a hardness of around 5 to 6. Only those tablets that were re-heated to 1150ºC exhibit a hardness of higher than 6.

Ernest Mackay documented (1933) the ancient process for bleaching white designs onto carnelian beads that involved heat in combination with an alkali-based solution. Upon seeing the results of the initial steatite heating experiment, Dr. J. Mark Kenoyer suggested that I attempt to bleach that stone using the same technique. I agreed to try. Raw steatite from three sources – LBW1, SB and KOT, were cut into three pieces each. These can be seen in the figure below (Appendix 7.16, Figure 7). The pieces labeled "1" are the raw, unfired stones. Those labeled "2" were treated with the carnelian bleaching solution recorded by Mackay. This consisted of sodium carbonate (Na_2CO_3) and juice from the "kikar" plant (*Capparis aphylla* – a type of caper native to South Asia) that was carefully mixed and strained. The steatite pieces were allow to soak in this solution for five days after which they were placed (while the exterior was still damp) into the muffle furnace. The temperature was slowly raised 60°C per hour to 1150° C, allowed to dwell there for one hour and then turned off to cool overnight. The pieces on the figure labeled "3" were soaked for five days in a paste of consisting of calcium carbonate ($CaCO_3$ – which Massimo Vidale [2000: 62] has previously suggested might have been used to whiten steatite) and potassium hydroxide (KOH) or "potash," which was added on the suggestion of Dr. Kenoyer. These were heated along with those soaked in the Na_2CO_3-kikar solution.

Appendix 7.16 Figure 7 Experimental heating in combination with bleaching of steatite from three sources. 1 = unfired steatite, 2 = fired after being soaked in sodium carbonate and "kikar" juice, 3 = fired after being soaked in calcium carbonate and potash.

The photograph for Appendix 7.16, Figure 7 was taken after the bleaching/heating experiment was completed. Compare the pieces labeled "2" and "3" on that figure to the post-fired appearance of their corresponding tablets pictured in Appendix 7.16, Figure 3 B. Those from LBW1 and KOT exhibit exactly the same dull red post-fired appearance that they did in the initial heating experiment. The piece from source SB did fire white this time but it also fired white in the initial experiment in which it was untreated. There is nothing to indicate that the two alkali solutions affected any color change in the samples at all. Of course, this does not prove that Indus Tradition craftspeople were incapable of bleaching steatite. I may have incorrectly prepared and/or applied the solutions. However, new data began to come light around the time these experiments were conducted that suggested there was probably little need for Harappans to bleach steatite white.

The results of the provenience study of steatite that are detailed in Chapter 7 indicated that, of the 139 artifacts analyzed from Harappa (I exclude the BMAC wig and the seal boss sample), 138 appear to have been derived from sources of dolomitic origin (see Figure 7.14). An emphasis on the use of this type of raw material was seen at several of the other Indus Tradition sites from which steatite artifacts were analyzed. Furthermore, the majority of the dolomitic steatite artifacts from Harappa and Mohenjo-daro appear to have been derived from a select few deposits in northern Pakistan and India. Of those, samples from PD, LKPD, SB, SC and SKK were heat-treated in the initial experiment (Appendix 7.16, Figure 3). The post-firing appearance of all of them, save for the tablet made from SKK steatite, was white. None of the tablets from ultramafic sources had become that color except for the one from ZUN. That one was white to begin with and was actually became an off-white shade it was fired. So it seemed as if Harappans were very deliberately exploiting white-firing stone from dolomitic while ignoring non-white-firing ultramafic stone. However, except for the stone from SB, all of the white-firing dolomitic samples were also white to begin with. Raw steatite of that color has never been found at Harappa.

It was decided to heat a series of dolomitic steatite samples that, in appearance, were more like the raw material recovered at Harappa, that is – colorful (recall Figure 7.4). At the time I did this

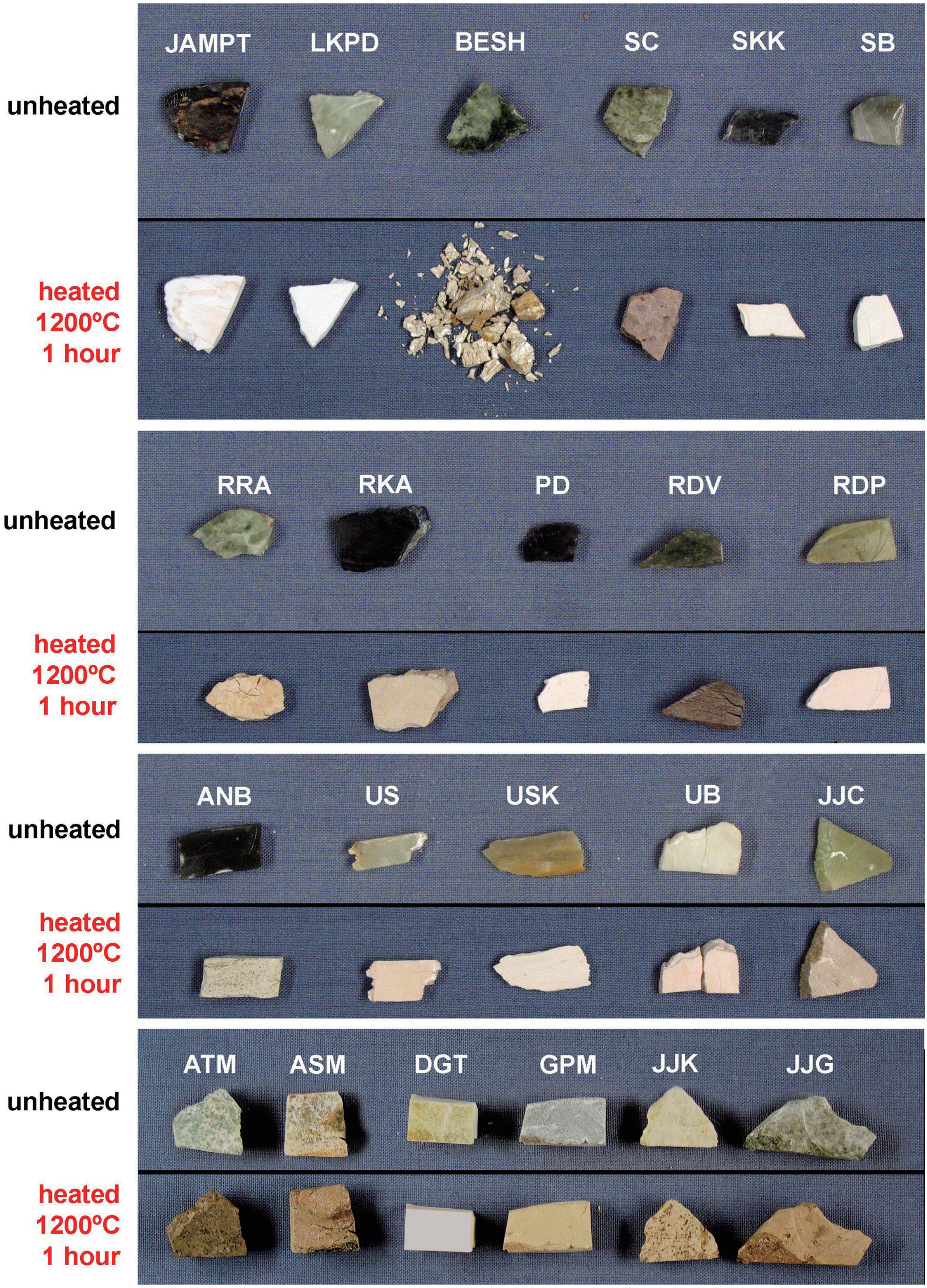

Appendix 7.16 Figure 8 Experimental firing of steatite chips from select dolomitic sources.

(Fall 2003), samples from 22 dolomitic sources had been obtained. Unfired chips taken from these are pictured in Appendix 7.16, Figure 8 in the rows marked "unheated." These chips were placed in the muffle furnace and the temperature was raised quickly (200°C per hour) to 1200° C and left to dwell for one hour. This time and temperature was sufficient to turn any kind steatite white if it was predisposed to do so.

Post-firing images of the steatite chips are visible in the rows directly beneath the "unheated" ones in Appendix 7.16, Figure 8. The majority of them did not become white after being fired. Most of those that did are from sources in northern Pakistan and India (JAMPT. LKPD, SKK, SB and PD) that were predicted in Chapter 7 to have been ones used by residents of Harappa. Three chips from sources in Uttaranchal and Rajasthan also became white (USK and DGT) or near white (RDP). Although it was not my intent to the examine quality/workability of steatite from different sources, most seem to have held up well in this quicker and hotter firing. Three chips (RRA, RDV and UB) showed signs of cracking and one from BESH exhibited what can only be described as catastrophic failure.

A few important observations can be made as a result of this firing. Firstly, just as it is not possible to say that all steatite fires white it is also not possible to say that all dolomitic steatite fires white. Materials from some sources clearly will not. Moreover, there are good indications that even within individual steatite deposits there are raw materials that fire in different ways. Note that the SC chip did not become white in this last heating experiment but the SC tablet from the initial one did. The JAMPT chip fired bright white in Appendix 7.16, Figure 8 but recent (May 2007) studies with Gregg Jamison (Jamison and Law 2007) using material from that source only produced light grayish-colored results. These observations actually fit well with my suggestion in Chapter 7 that highly compositionally similar groups within the set of steatite artifacts analyzed from Harappa might represent raw materials extracted from a very restricted area *within* an individual occurrence. In order to obtain white-firing stone for their beads and seals, Harappans had to be (and clearly were) highly selective.

APPENDIX 7.17

IS IT POSSIBLE TO SOURCE FIRED STEATITE ARTIFACTS USING INAA?

INTRODUCTION

All of the artifacts characterized using INAA in Chapter 7 are composed of unmodified or "raw" steatite. Once cleaned and desalinated it is, materially speaking, as if the stone has come directly from the source. Harappa, Mohenjo-Daro and Mehrgarh are sites where there were extensive steatite craft activities and, thus, there is an abundance of such raw manufacturing debris that can be sampled for studies of this kind. I have found that most other Harappan settlements are not nearly as rich in this regard, however. For example, out of the tens of thousands of stone artifacts at the Indus city of Dholavira I have recorded only a dozen or so pieces of steatite manufacturing debris. Most site assemblages contain even fewer, if any, such fragments. On the other hand, heat-treated or "fired" steatite beads are found, often by the hundreds or even thousands, at practically every Harappan settlement. If it could be determined from where the raw material used make those beads was derived then it might be possible to identify different production centers and reconstruct, in great detail, distribution networks for beads made from this stone. We might even be able to examine exchange networks between Indus Civilization peoples and the non-Harappan peoples outside of the greater Indus region who have frequently been found to have possessed such beads. But is it possible to source fired steatite artifacts using INAA?[1)]

I thought that it might be. Although heating substantially alters the mineralogical character of steatite (recall Appendices 7.12 and 7.16), other than driving off it's water component the major and, importantly with regard to this study, the trace element composition of the stone should, in theory at least, remain unchanged. If a fired steatite bead were fashioned from a solid piece of stone (rather than a paste that could contain additives) and was unmodified by a bleach, glaze or some other treatment, then analyzing it should produce results roughly the same as analyzing unheated raw material from the same source. This seemed like a plausible scenario so I decided to conduct a small pilot study in order to test it.

My idea for the study was simple. I would heat a set of steatite samples from known deposits that I had been previously characterized using INAA. The heat-treated samples would then be re-characterized and compared, as ungrouped cases (i.e., as if they were of unknown provenience) using canonical discriminant analysis (CDA), to the database of South Asian steatite sources that I had assembled. Relative success would be judged based on what percentage of the fired samples were correctly assigned to the source or source region from which they actually came.

EXPERIMENTAL HEATING AND INAA

Small chips were cut from twenty steatite samples – two each from ten different deposits – that were previously subjected to INAA. These can be seen in the left-hand image of Appendix 7.17 Figure 1. Each is labeled with a two or three letter code

1) The title and subject of this appendix is the same as a paper I presented at the 38th Conference on South Asia, University of Wisconsin-Madison, October 23–25, 2009.

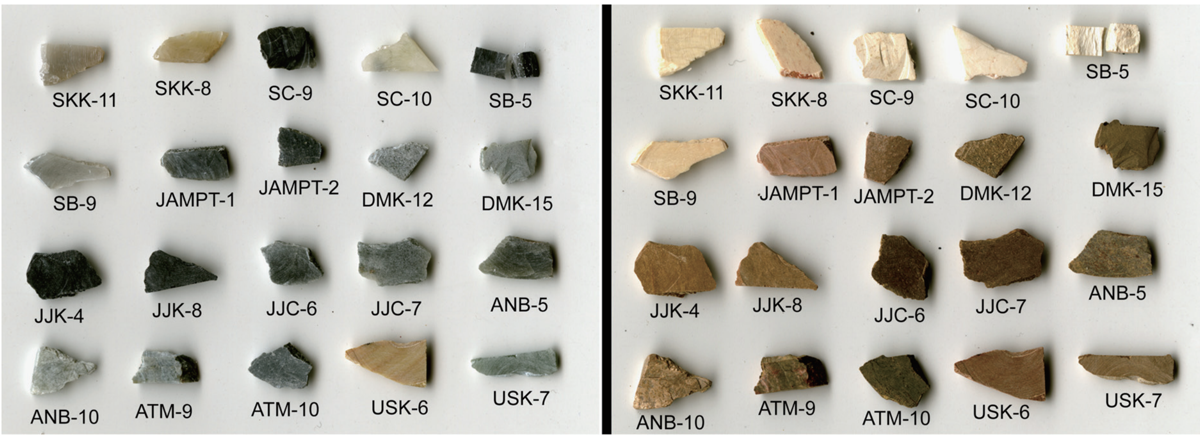

Appendix 7.17 Figure 1 Left - A set of chips taken from 20 geologic samples previously subjected to INAA. Right - The same 20 chips after being fired at 1200ºC for one hour.

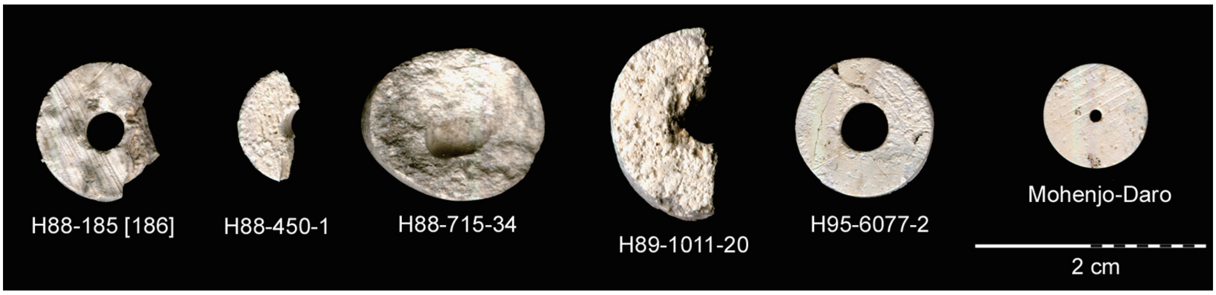

Appendix 7.17 Figure 2 The five fired steatite artifacts (beads or bead fragments) from Harappa and one from Mohenjo-Daro subjected to INAA for this pilot study.

that corresponds to sources listed in Appendix 7.2. The letter codes are followed by a sample numbers. These (letter codes + numbers) correspond to the individual samples listed in Appendix 7.3, which is the original INAA results table for the geologic samples. All twenty chips were placed together in a muffle furnace and heated in a single static firing for one hour at 1200ºC. This is long enough and hot enough to produce the mineralogical features (enstatite and cristobalite) exhibited by high-fired Harappan steatite beads (recall Appendix 7.14). The post-firing appearance of the chips can be seen in the right-hand image of Appendix 7.17 Figure 1. It is interesting and important to note that the only geologic samples that became white and/or lightened significantly were those from the Sherwan deposits of the NWFP (source codes SKK, SC and SB), which is the regional occurrence shown in Chapter 7 to have been the major source of steatite for residents of Harappa. After being fired, the 20 chips were prepared and subjected to INAA following the procedures outline in Chapter 3.

Along with the heat-treated geologic samples, five fired steatite beads from Harappa and one from Mohenjo-Daro (Appendix 7.17 Figure 2) were prepared and subjected to INAA. These artifacts were selected from among the thousands that have been recovered during surface surveys at those sites. All had clearly been carved from solid steatite and did not appear to have been glazed. I was interested to learn which deposits they would be predicted to belong when they were compared to the steatite sources database using CDA. Around 95% of the steatite acquired by residents of Harappa appears to have come from sources to the north of the city while most of the remaining 5% was derived from deposits in northern Rajasthan. At Mohenjo-Daro, the ratio of raw material exploited from those two broad source regions was more like 60% to 40% respectively. If the six steatite beads are predicted to belong to deposits in altogether different regions then that might be an indication that it is not possible to accurately source such artifacts using INAA.

RESULTS

The INAA data for the heat-treated geologic samples are listed in Appendix 7.17 Figure 3 and those for the six steatite beads are listed in Appendix 7.17 Figure 4. Using CDA, these data were compared to the steatite sources database (Appendix 7.3) as ungrouped cases and plotted by their discriminant scores (Appendix 7.17 Figure 5). The heated geologic samples fell on the plot basically where expected. The two fired chips taken from the Dev Mori Kundol (DMK) deposit in northeastern Gujarat, which was the only ultramafic source fired and analyzed, plotted with the large cluster of ultramafic source samples on the right-hand side of the plot. The two fired chips from the Painthal deposit in Jammu (JAMPT) fell close by the distinct cluster of geologic samples from that source.

Appendix 7.17 Figure 3 INAA data for chips taken from previously analyzed raw steatite samples and then heat-treated. Elemental data in parts per million (PPM).

Sample	Al	Co	Cr	Eu	Fe	La	Mn	Na	Sc	V	Zn
SKK-11 FIRED	4341	0.76	4.03	0.023	3216	0.107	7.93	159	0.255	7.85	8.4
SKK-8 FIRED	2266	0.833	1.76	0.032	2328	2.262	7.37	187	0.116	3.82	4.75
SC-9 FIRED	57290	3.409	36.12	0.113	8685	12.56	18.3	245	2.636	42.1	25.19
SC-10 FIRED	1186	1.178	1.51	0.047	2447	1.598	7.49	122	1.144	5.23	16.52
SB-5 FIRED	4899	2.281	6.24	0.069	5751	1.454	8.71	140	0.297	7.48	9.43
SB-9 FIRED	14480	0.907	8.17	0.026	4444	0.1947	8.35	149	0.324	11.75	9.81
JAMPT-1 FIRED	1130	0.218	0.98	0.016	9236	0.0202	7.96	119	0.029	3.27	13.07
JAMPT-2 FIRED	1029	0.4	1.24	0.016	14250	0.0614	14.6	221	0.024	4.06	21.26
DMK-12 FIRED	19090	73.75	2427	0.051	41600	0.0624	398	164	6.049	40.6	38.69
DMK-15 FIRED	6071	81.35	2139	0.042	39450	0.0251	341	132	6.184	30.8	38.47
JJK-4 FIRED	17430	3.316	31.85	0.051	24980	0.1909	83	239	3.199	135.4	27.87
JJK-8 FIRED	12770	4.273	24.91	0.031	26060	0.1312	70.1	144	2.348	113	24.29
JJC-6 FIRED	8281	18.07	25.02	0.644	40080	3.246	173	148	8.622	9.76	46.54
JJC-7 FIRED	2665	16.5	9.14	0.033	34340	0.224	99.4	300	2.227	4.22	24.46
ANB-5 FIRED	3329	4.358	11.21	0.032	17550	0.2109	23.1	2846	0.402	14.7	10.96
ANB-10 FIRED	366.5	6.601	2.3	0.023	18870	0.0633	22.1	146	0.257	18.5	9.14
ATM-9 FIRED	2068	2.826	20.47	0.025	29450	0.2202	23.2	229	0.923	8.21	16.01
ATM-10 FIRED	9041	2.187	20.06	0.051	39340	0.2848	37.8	6282	0.936	4.43	17.7
USK-6 FIRED	1051	5.659	1.92	0.034	20280	0.0797	23.5	127	0.114	3.84	35.96
USK-7 FIRED	8306	11.33	9.68	0.032	22880	0.1836	9.89	174	0.73	8.89	27.39

Appendix 7.17 Figure 4 INAA data for fired steatite beads from Harappa and Mohenjo-Daro. Elemental data in parts per million (PPM)

Artifact	Al	Co	Cr	Eu	Fe	La	Mn	Na	Sc	V	Zn
Harappa H95-6077-2	1111	2.681	8.81	0.0576	3028	0.719	87.53	1401	0.2118	6.5	44.22
Harappa H89-1011-20	6454	1.553	5.81	0.0864	5136	1.084	37.13	9259	0.436	5.68	14.38
Harappa H88-715-34	2514	0.482	12.27	0.0271	7045	0.119	9.29	1075	0.1157	6.06	39.55
Harappa H88-450-1	1106	0.705	84.54	0.1035	13680	0.563	47.22	1734	0.1233	13.08	127.4
Harappa H88-185[186]	1243	3.235	8.18	0.1256	3483	3.471	94.67	2979	0.1679	4.19	44.56
Mohenjo-Daro Disc-bead	1410	0.569	12.33	0.1277	3534	0.18	42.52	4325	0.556	16.5	23.84

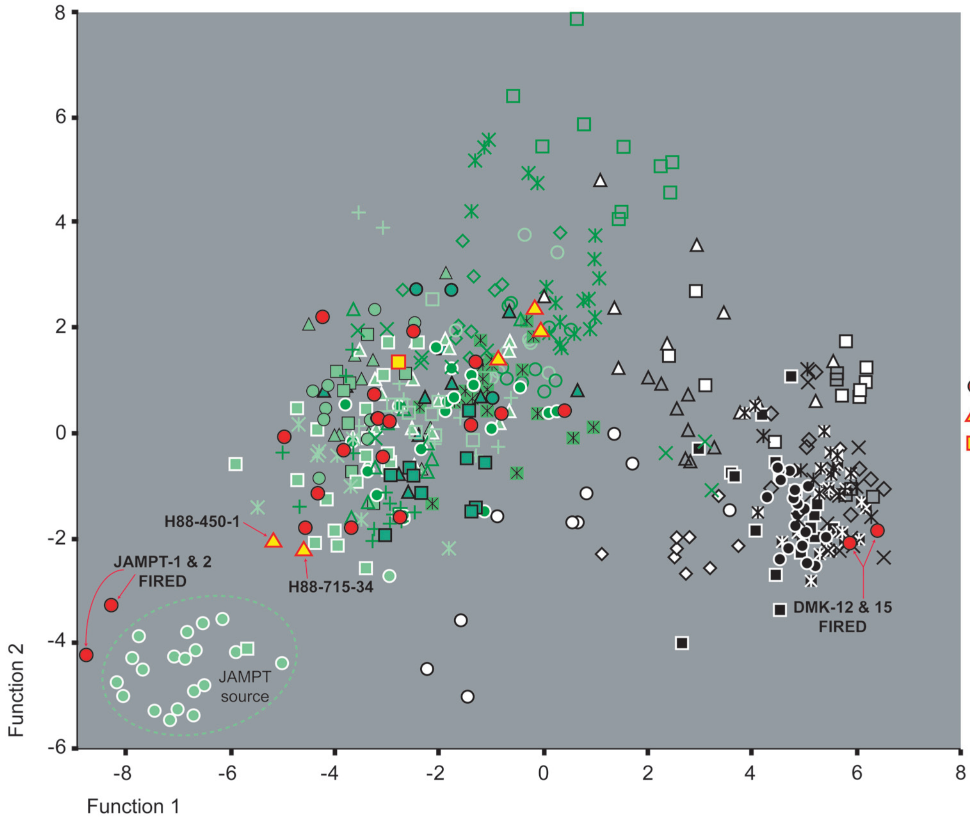

Appendix 7.12 Figure 5

Fired geologic samples and steatite beads plotted as ungrouped cases in relation to the 442 geologic samples.

Discriminant functions generated using the elements Al, Co, Cr, Eu, Fe, La, Mn, Na, V, Zn

KEY

- **Fired geologic samples**
- **Harappa beads**
- **Mohenjo-daro bead**

Symbols representing samples from **dolomitic** parent-rock are those in shades of green (some of them have black or white elements). Symbols that represent steatite from **ultramafic** sources are in black and/or white only.

For **key** to source symbols see figures 7.2, 7.10, 7.15 and 7.22 A to D

The remaining heat-treated geologic samples fell among the large cluster of dolomitic steatite source samples in the upper middle potion of the plot. The six steatite beads from Harappa and Mohenjo-Daro also plotted among this cluster, which, at this level of analysis, clearly indicates that these ornaments were each fashioned out of stone from a dolomitic source.

The first and second predicted group memberships (PGMs) generated by CDA for the heat-treated chips are listed in the second and third columns of Appendix 7.17 Figure 6. The fourth column heading of that figure is labeled "1st PGM spot on," which means that the fired geologic samples noted with an "X" in the column below had PGMs in the exact deposits from which they were taken. For example, the first PGM of chip SB-5 was the Sherwan-Banda (SB) deposit. Nine of the 20 samples, or 45%, had "spot on" PGMs. The next column is labeled "1st PGM regionally correct." This means that those fired samples noted with an "X"

Appendix 7.17 Figure 6 Predicted group memberships (PGMs) of the 20 fired geologic samples.

Sample	1st PGM	2nd PGM	1st PGM spot on	1st PGM regionally correct	1st or 2nd PGM correct
SKK-11 FIRED	SB	JJK		X	X
SKK-8 FIRED	SC	SKK		X	X
SC-9 FIRED	JJG	UB			
SC-10 FIRED	US	SC			X
SB-5 FIRED	SB	SC	X	X	X
SB-9 FIRED	SB	PD	X	X	X
JAMPT-1 FIRED	JAMPT	JJK	X	X	X
JAMPT-2 FIRED	JAMPT	ATM	X	X	X
DMK-12 FIRED	DMK	RSB	X	X	X
DMK-15 FIRED	DMK	RSB	X	X	X
JJK-4 FIRED	JJK	JJG	X	X	X
JJK-8 FIRED	JJK	JJG	X	X	X
JJC-6 FIRED	UB	RDP			
JJC-7 FIRED	DGT	ZTAK			
ANB-5 FIRED	ATM	ANB		X	X
ANB-10 FIRED	JJK	US		X	X
ATM-9 FIRED	JJK	ATM		X	X
ATM-10 FIRED	ATM	ANB	X	X	X
USK-6 FIRED	JJK	USK			X
USK-7 FIRED	PD	USK			X
percentage of 20 samples correct			45%	70%	85%

in the column had a PGM in a deposit that is in the same related geologic source region from which the raw material it is composed of derived. For example, fired sample SKK-8 is from the Sherwan-Khanda Khu deposit but was predicted to belong to the Sherwan-Chelethar (SC) deposit, which is in the same zone of dolomitic steatite mineralization just a few kilometers away. Fourteen of the 20 samples, or 70%, had "regionally correct" PGMs. Because some of the samples selected for firing could have been compositional outliers of the deposits from which they came (and, thus, potentially misassigned [given a 1st PGM] to a compositionally similar deposit in another region), I decided to include in Appendix 7.17 Figure 6 a sixth column that included the second PGM of samples along with the first. By doing this, I hoped to catch some of those potential outliers. Seventeen of the 20 samples, or 85%, had either their "1st or 2nd PGM correct." The remaining three fired samples were assigned first and second PGMs in sources that, other than being dolomitic, had no geologic relation to the deposit from which they actually derived.

At first glance, the results of the CDA comparison of the heat-treated geologic samples to the steatite source database appear mediocre at best. It seems that slightly less than half the time you can expect to correctly determine the exact deposit from which a fired steatite object came. Just over two-thirds of the time you might be able to assign such an artifact to a regionally correct source. If you decide to take second PGMs into consideration then it might be possible to push the number of correctly assigned artifacts to 85%, which is not great but it is respectable. Although these results seem less than outstanding, it is important to note

Appendix 7.17 Figure 7 Predicted group memberships (PGMs) of the original geologic samples prior to heat-treatment.

Sample	1st PGM	2nd PGM	1st PGM spot on	1st PGM regionally correct	2nd PGM correct
SKK-11 RAW	SKK	UB	X	X	X
SKK-8 RAW	SC	SKK		X	X
SC-9 RAW	SB	SKK		X	X
SC-10 RAW	US	SB			X
SB-5 RAW	SC	SKK		X	X
SB-9 RAW	SKK	SC		X	X
JAMPT-1 RAW	JAMPT	USK	X	X	X
JAMPT-2 RAW	RSA	USK			
DMK-12 RAW	DMK	KOT	X	X	X
DMK-15 RAW	DMK	RSH	X	X	X
JJK-4 RAW	JJK	JJG	X	X	X
JJK-8 RAW	JJK	JJG	X	X	X
JJC-6 RAW	JJG	RDP		X	X
JJC-7 RAW	JJG	RDP		X	X
ANB-5 RAW	ANB	ATM	X	X	X
ANB-10 RAW	JJK	ANB			
ATM-9 RAW	ATM	JJK	X	X	X
ATM-10 RAW	ATM	ANB	X	X	X
USK-6 RAW	USK	RSA	X	X	X
USK-7 RAW	USK	UB	X	X	X
percentage of 20 samples correct			55%	85%	90%

that the fired samples were compared to the entire source database and there significant overlap between certain deposits. Recall that the overall "leave-one-out" cross validation success rate at this level ("full set") of analysis was 69%. This is certainly much better than the 45% "spot on" success rate I got but it based on the cross validation of a substantially more diverse set of geologic samples. There is, however, the possibility that is being explored in this appendix – the heat-treatment of the 20 samples may altered their chemical compositions enough to affect their PGMs. In order to judge that possibility, I went back to the original database of geologic samples and compared the INAA data for same 20 samples prior to them being fired to the "full set" database. Those results are in Appendix 7.17 Figure 7. This time the "spot on" success rate was 55%, the "regionally correct" rate was 85%, and the "1st or 2nd correct" combined was 90%. This is better in all instances but not substantially different and still not perfect. These reason that the PGMs made in the INAA study of unfired steatite artifacts presented in Chapter 7 were

Appendix 7.17 Figure 8 First and second predicted group memberships (PGMs) for fired steatite beads from Harappa and Mohenjo-Daro.

Sample	1st PGM	2nd PGM
H88-185[186]	ANB	JJC
H88-450-1	ATM	JJK
H88-715-34	ATM	JAMPT
H89-1011-20	ATM	ANB
H95-6077-2	JJC	ANB
MD disc bead	ATM	ANB

convincing is because there was an overall consistency in their patterning over the large artifact set and throughout multiple scales of comparison. Only six steatite beads have been analyzed at this point. It may require the analysis of many more such artifacts before the same convincing patterns become obvious for fired steatite objects.

The INAA data for the five fired steatite beads from Harappa and one from Mohenjo-Daro were first compared to the full set of geologic samples and then to a set comprised of the dolomitic steatite deposits. The PGMs for these two analyses are listed in Appendix 7.17 Figure 8. Both sets of results are almost identical. In the "full set" analysis a single bead from Harappa (H88-715-34) had a second PGM in the Painthal deposit of Jammu (JAMPT) but in the "dolomitic sources only" analysis the second PGM for the same bead was the Kho deposit in the Jhunjhunu District (JKK) of northern Rajasthan. Otherwise, in every other instance, both the first and second PGMs of the beads were northern Rajasthan sources. These findings do not leave a lot of room for alternate interpretations. That is, if all or many had second PGMs in the one of the Sherwan deposits for example, then I could, perhaps, argue that they were compositional outliers of those deposits. It is not possible to do that, however. Two of the beads from Harappa (H88-715-34 and H88-450-1) do plot on Appendix 7.17 Figure 5 apart from the other four beads in an area where Shewan assigned raw steatite artifacts tend to plot as well. But this is not enough to disregard their assigned PGMs and say they actually belong to the Sherwan zone. The beads' PGMs are based their distances to the various groups' centroids in multi-dimensional space. In Appendix 7.17 Figure 5 we are only seeing two dimensions (discriminant functions 1 and 2). If a multi-dimensional "cloud" of datapoints were viewable then the PGMs assignments for the two beads would likely make more sense visually. In any case, the results strongly suggest that all six beads were made from steatite that was acquired from deposits in northern Rajasthan

So what does this mean? Well, the INAA study presented in Chapter 7 did indicate that raw steatite from the deposits of northern Rajasthan was being acquired by residents of both Harappa and Mohenjo-Daro. So in this regard the findings are consistent with the patterns of source area exploitation at those sites. Based the limited study of Mohenjo-Daro steatite fragments there was roughly a 40% chance that the disc bead from that site would be made from northern Rajasthan stone. Its PGM is, therefore, not difficult to accept. However, the fact that all five of the beads from Harappa were also predicted to be from northern Rajasthan deposits causes me to view those results, while with not skepticism, at with least caution. Fewer than 5% of the 141 raw steatite fragments and artifacts analyzed from Harappa were attributable to those sources. Detecting a single example made from northern Rajasthan steatite among the beads was, for that reason, statistically unlikely. Having all five predicted to come from that source area is then very unusual. Of course, it could be a mere matter of chance that the five randomly selected artifacts happened to be made of the same, much more infrequently used raw material. The analysis of a larger set of fired steatite artifacts from Harappa should help to determine if that is the case or if the results represent a genuine pattern of raw material use.

Another aspect of the results that gave me pause was that none of the experimental chips of northern Rajasthan steatite fired white. The six beads from Harappa and Mohenjo-Daro clearly could not have been made by only heat-treating raw materials like the ones I sampled from deposits across that region. Those materials would have needed to be bleached or by some other process whitened and this would have, presumably, altered their chemical compositions. This finding does not is not necessarily rule out northern Rajasthan as a Harappan steatite source area, however. The deposits I visited in that region were all recently abandoned mines. All high-quality material had been removed and I was left with only poor-to-mediocre quality stone to sample. Even so, it is likely that white-firing steatite existed at these or related locations in the region at some point in the past.

CONCLUSION

The answer to the question posed in the title of this appendix is a qualified yes, it is probably possible to source fired steatite artifacts using INAA. Although the success rate for correctly classifying the experimentally heated geologic samples was not what I had hoped it would be, in light of the overall cross-validation success rate for the raw steatite artifact provenience study, it is not too bad, especially on the regional level. I cautiously accept the results of the artifact pilot study, which suggests that the fired steatite beads from Harappa and Mohenjo-Daro were made from raw material that originated in northern Rajasthan.

APPENDIX 8.1

INAA DATA FOR AGATE SAMPLES FROM RATANPUR, GUJARAT

Data in parts per million (PPM)

sample	Al	Co	Cr	Eu	Fe	La	Na	Sb	Sc	V
GRTP-01	1850	0.5172	10.935	0.0799	2902	0.0812	174	0.3827	0.0517	2.12
GRTP-02	3401	0.7281	11.944	0.1589	2997	0.6739	187	1.1616	0.8657	13.43
GRTP-03	2971	0.6626	9.104	0.1173	2532	0.2722	313	0.7013	0.3903	6.644
GRTP-04	2645	0.3994	8.081	0.1026	2190	0.115	350	0.6715	0.4669	6.21
GRTP-05	2235	0.3284	3.402	0.0729	974	0.0065	243	0.3304	0.0499	1.331
GRTP-06	1501	0.5769	6.972	0.0948	1996	0.1841	142	0.4123	0.2103	3.30
GRTP-07	1896	0.3891	5.328	0.0503	1210	0.0638	100	0.4977	0.0725	1.537
GRTP-08	3378	0.9297	15.977	0.1438	4353	0.7066	202	0.2559	0.8286	9.192
GRTP-09	1924	0.3305	4.592	0.067	1234	0.0896	200	0.529	0.0272	1.557
GRTP-10	2113	0.4627	3.878	0.0707	1913	0.113	189	0.469	0.1628	3.037
GRTP-11	1852	0.4095	5.724	0.0827	1531	0.1084	202	0.5406	0.0257	1.654
GRTP-12	2250	0.6177	6.852	0.0838	2306	0.0639	177	0.2773	0.5736	4.328
GRTP-13	1984	0.248	0.679	0.0428	317	0.113	197	0.4413	0.0126	1.304
GRTP-14	1747	0.1183	0.954	0.0401	139	0.013	49	0.2171	1.5517	0.916
GRTP-15	2070	0.3017	11.942	0.0548	1052	0.0867	127	0.2432	0.0948	3.092
GRTP-16	2301	0.3953	0.804	0.0441	375	0.0555	263	0.5963	0.4464	1.082
GRTP-17	2559	0.3455	0.938	0.0466	604	0.1011	323	0.2978	0.2451	2.875
GRTP-18	2692	0.8421	12.279	0.0618	5875	0.165	162	0.1217	0.856	23.252
GRTP-19	2637	0.3066	0.906	0.0353	124	0.0384	469	0.171	0.2384	0.827
GRTP-20	1962	0.2064	3.774	0.0262	490	0.0788	99	0.0821	0.1758	1.101

APPENDIX 8.2

INAA DATA FOR AGATE SAMPLES FROM MARDAK BET, GUJARAT

Data in parts per million (PPM)

sample	Al	Co	Cr	Eu	Fe	La	Na	Sb	Sc	V
GMB-01	1868	0.4005	3.56	0.0829	860	0.2008	337	0.1445	0.617	1.208
GMB-02	1906	0.3403	6.861	0.0571	1664	0.0868	351	0.3705	0.0597	2.009
GMB-03	1960	0.3792	4.576	0.0815	1194	0.1086	404	0.2321	0.0265	1.614
GMB-04	2287	0.3765	2.704	0.0976	543	0.5745	392	0.1494	6.4109	0.833
GMB-05	1992	0.5975	7.095	0.0802	1788	0.1391	528	0.4998	0.8002	2.258
GMB-06	2014	0.3433	5.507	0.0495	1677	0.2123	379	0.1427	6.9568	0.958
GMB-07	2101	0.3493	4.339	0.1207	1048	0.5624	441	0.1298	0.0698	0.965
GMB-08	2052	0.6978	4.663	0.0733	957	0.2293	507	0.3478	4.678	0.927
GMB-09	2291	0.7152	10.936	0.0919	2501	0.2803	575	0.1863	0.4679	3.368
GMB-10	2010	0.4439	5.695	0.0453	1267	0.2117	370	0.6212	5.307	1.276
GMB-11	2058	0.4207	5.094	0.0754	1321	0.1195	331	0.6476	0.101	2.742
GMB-12	1917	0.4063	8.021	0.0700	1712	0.006	319	0.3900	0.0638	2.297
GMB-13	2305	0.1207	1.476	0.0534	213	0.9033	570	0.6653	4.9204	1.319
GMB-14	1946	0.1867	1.24	0.0376	260	0.117	434	1.4944	3.7008	0.060
GMB-15	3426	0.4849	1.762	0.0250	2626	0.1205	572	0.0496	0.5073	9.910
GMB-16	6360	1.4611	3.647	0.0790	3597	0.5723	1551	0.2252	1.3634	14.253
GMB-17	3806	0.6573	1.805	0.0374	7683	0.3522	879	0.0040	0.311	15.854
GMB-18	7844	1.4600	12.873	1.4685	4735	11.3524	1787	0.1413	3.9293	40.162
GMB-19	2394	0.2484	2.945	0.0400	822	0.3356	477	0.1104	3.926	1.390
GMB-20	2567	0.1867	3.117	0.0178	773	0.0688	629	0.2699	0.1194	1.344

APPENDIX 8.3

INAA DATA FOR AGATE SAMPLES FROM KHANDEK, GUJARAT

Data in parts per million (PPM)

sample	Al	Co	Cr	Eu	Fe	La	Na	Sb	Sc	V
GKK-01	1907	0.1946	0.284	0.0175	99	0.0065	165	0.1555	0.0296	0.934
GKK-02	1828	0.6039	0.833	0.0623	418	0.7129	78	0.0306	0.1315	0.942
GKK-03	3295	1.9164	6.802	0.1652	1590	0.8768	373	0.8363	0.4134	6.583
GKK-04	1747	0.4720	0.771	0.0269	236	0.0078	100	0.8305	0.0217	1.026
GKK-05	2324	0.4518	0.778	0.0313	365	0.0079	337	1.0483	0.0514	1.155
GKK-06	1955	0.4812	0.732	0.0550	489	0.3148	167	0.1913	0.0914	0.998
GKK-07	1910	0.7033	1.625	0.0799	595	0.4479	209	0.6103	0.0670	1.029
GKK-08	1766	0.2286	1.010	0.0227	149	0.1082	90	0.1865	0.0146	0.915
GKK-09	1985	0.2501	0.667	0.0284	223	0.0099	184	0.2774	0.0390	0.771
GKK-10	2520	0.7402	0.979	0.0336	1043	0.1650	304	0.1318	0.3259	2.624
GKK-11	2293	0.5263	0.818	0.0290	636	0.2094	334	0.2622	0.0990	1.943
GKK-12	3317	0.5683	1.032	0.0252	1048	0.2047	641	0.0836	0.4024	3.307
GKK-13	3482	0.4799	0.625	0.0814	974	0.7775	659	0.0988	0.1929	2.105
GKK-14	2322	0.1029	0.270	0.0241	90	0.0930	363	1.1208	0.0074	0.060
GKK-15	2351	0.2027	0.475	0.0530	300	0.6555	325	0.2968	0.0473	1.057
GKK-16	1963	0.1583	0.245	0.0173	138	0.0563	200	0.4982	0.0162	1.010
GKK-17	2900	0.7813	1.032	0.0485	988	0.3550	271	0.0588	0.2051	6.838
GKK-18	2064	0.8594	1.745	0.0231	1080	0.3374	301	0.1531	0.1952	4.384
GKK-19	2727	0.4311	0.677	0.0329	647	0.1992	348	0.6055	0.1841	3.354
GKK-20	2338	0.4700	1.029	0.0256	907	0.2174	335	0.3701	0.0860	2.293

APPENDIX 8.4

INAA DATA FOR AGATE ARTIFACTS FROM SHAHR-I-SOKHTA, IRAN

Data in parts per million (PPM)

sample	Al	Co	Cr	Eu	Fe	La	Na	Sb	Sc	V
S-i-S_01	2409	0.5995	5.404	0.0718	5013	0.6939	632	3.4254	0.2027	0.754
S-i-S_02	2005	0.5482	7.577	0.0712	2099	1.9471	475	2.9873	0.1325	2.097
S-i-S_03	2159	0.3412	5.310	0.0736	1367	0.4809	469	3.0094	0.0965	1.482
S-i-S_04	3799	0.3242	7.035	0.0793	2584	2.6748	1172	2.9185	0.3235	1.169
S-i-S_05	1761	0.3868	5.303	0.0471	2263	0.2711	415	1.8996	0.0801	0.908
S-i-S_06	1834	0.5544	7.959	0.0785	2666	3.1115	602	4.1397	0.1636	2.304
S-i-S_07	2015	0.3247	4.248	0.0430	1753	0.5431	574	2.6235	0.1795	1.828
S-i-S_08	1692	0.3087	4.121	0.0537	1193	1.8038	648	1.5142	0.0324	1.535
S-i-S_09	1837	0.2828	4.240	0.0818	1139	1.4178	463	1.6454	0.0906	0.916
S-i-S_10	1704	0.2969	4.016	0.0650	1217	0.6882	242	1.7668	0.0868	1.121
S-i-S_11	1863	0.4209	7.320	0.0582	1634	0.3332	950	0.5608	0.0600	1.592
S-i-S_12	1662	0.4611	9.765	0.0766	1929	0.1483	593	4.427	0.0562	1.364
S-i-S_13	1611	0.2977	3.950	0.0617	790	0.1098	1037	2.6625	0.0360	0.930
S-i-S_14	1911	0.3488	4.835	0.0626	1100	0.1263	747	0.3519	0.0938	0.927

APPENDIX 8.5

INAA DATA FOR AGATE ARTIFACTS FROM HARAPPA

Data in parts per million (PPM).

sample	Artifact #	Site location	Period	Al	Co	Cr	Eu	Fe	La	Na	Sb	Sc	V
AH-1	HM-2397	unknown	unknown	1863	0.1323	0.381	0.0015	341	0.6693	517	0.2701	0.2998	0.934
AH-2	HM-12414	unknown	unknown	1814	0.1143	0.457	0.0214	585	0.2731	622	0.2938	0.0149	1.295
AH-3	H90/3011-154	survey, Mound E	S&D	3186	0.3578	1.246	0.0574	636	0.0722	999	0.1714	0.0168	1.564
AH-4	H90/3011-153	survey, Mound E	S&D	3274	0.4720	2.504	0.0628	1233	0.0961	732	0.1073	0.2342	1.294
AH-5	H90/3030-87	Tr. 58, Mound E	S&D	2070	0.3554	2.562	0.0733	921	0.1679	420	0.3633	0.0453	1.209
AH-6	H90/3037-63	Tr. 58, Mound E	S&D	1936	0.3948	5.633	0.0750	1449	0.1111	469	0.2651	0.1820	2.150
AH-7	H90/3122-12	Tr. 58, Mound E	Period 3B	2053	0.1341	0.381	0.0203	171	0.0329	344	0.1725	0.0199	0.818
AH-8	H90/3070-6	Tr. 58, Mound E	S&D	6576	1.9976	5.360	0.0554	3426	2.2976	1321	0.3103	1.3337	13.607
AH-9	H90/3048-505	Tr. 58, Mound E	S&D	1997	0.5095	4.363	0.0669	1578	0.0723	837	0.6152	0.0378	1.976
AH-10	H90/3068-19	Tr. 58, Mound E	S&D	1983	0.4604	5.100	0.0759	1839	0.1258	599	0.2579	0.0997	1.519
AH-11	H90/3072-1	Tr. 58, Mound E	Period 3C	2115	0.3336	3.815	0.0805	1269	0.2167	392	0.2629	0.0618	0.978
AH-12	H90/3200-36	Tr. 59, Mound E	S&D	1741	0.3147	1.993	0.0512	605	0.0243	917	0.2766	0.0399	0.892
AH-13	H90/3257-20	Tr. 58, Mound E	S&D	1889	0.3713	4.390	0.0603	1244	0.1735	683	0.2784	0.0552	2.921
AH-14	H90/3124-13	Tr. 56, Mound E	Period 3B	2552	1.0451	6.319	0.0359	3466	0.1431	459	0.2230	0.2133	19.490
AH-15	H90/3048-506	Tr. 58, Mound E	S&D	3036	0.5456	0.748	0.0438	1107	0.1264	960	0.6165	0.2289	3.300
AH-16	H88/353-3	Tr. 51	Period 3C	1869	0.1512	1.001	0.0262	153	0.0345	973	0.2746	0.0734	1.806
AH-17	H88/715-47	Tr. 52	Period 3C	1730	0.1238	0.921	0.0229	158	0.0248	625	0.1568	0.0369	0.970
AH-18	H88/725-22	Tr. 52	Period 3C	2028	0.2671	0.325	0.0273	343	0.0679	340	0.5850	0.0300	1.112
AH-19	H89/2023-9	Tr. 52	Period 3B	1908	0.1890	0.411	0.0015	447	0.0063	162	0.3254	0.0093	1.047
AH-20	H90/3064-20	Tr. 58	Period 3B	1685	0.1154	0.401	0.0184	491	0.1503	533	0.4243	0.1292	0.061
AH-21	H88/567-14	Tr. 50	Period 3C	1965	0.1989	0.331	0.0230	468	0.0809	101	1.0273	0.0054	1.253
AH-22	H88/178-20	Cemetery area	Period 3C	2120	0.1176	0.437	0.0330	231	0.0350	384	0.3175	0.0149	3.625
AH-23	H90/3022-28	Tr. 58, Mound E	S&D (likely 3B or 3C)	2289	0.3177	0.547	0.0433	354	0.1890	578	0.1430	0.0554	2.571
AH-24	H96/7484-1	Tr. 39, Mound AB	Period 2	1888	0.2943	0.494	0.0406	401	0.0628	623	0.1530	0.1183	1.076

APPENDIX 8.6
INAA DATA FOR AGATE ARTIFACTS FROM MEHRGARH (AMR) AND NAUSHARO (ANS).

Data in parts per million (PPM).

artifact	Context [number]	Al	Co	Cr	Eu	Fe	La	Na	Sb	Sc	V
AMR-1	MR2 Surface	2520	0.0886	0.270	0.0259	80	0.0296	608	0.9750	0.0116	0.726
AMR-2	MR2 Surface	1952	0.0658	0.269	0.0218	93	0.0217	625	2.6377	0.0367	0.851
AMR-3	MR2 Surface	2499	0.1827	0.424	0.0193	149	0.1161	511	0.8508	0.2733	1.082
AMR-4	MR2 Surface	2048	0.0895	0.357	0.0151	67	0.0248	635	0.4956	0.0028	0.820
AMR-5	MR2 Surface	1893	0.0636	0.192	0.0189	37	0.0356	495	0.1006	0.0089	1.507
AMR-6	MR2 Surface	2146	0.0822	0.270	0.0184	31	0.0879	439	0.9987	0.0029	0.670
AMR-7	MR2 Surface	1727	0.0736	0.269	0.0011	57	0.0146	264	0.2232	0.1371	0.553
AMR-8	MR2 Surface	1859	0.0877	0.424	0.0245	74	0.0416	320	3.9236	0.0853	0.528
ANS-1	Nausharo IC/ID [NS I G8F 88.01.38]	2227	0.1234	0.192	0.0012	208	0.0285	437	0.1786	0.3155	1.805
ANS-2	Nausharo III [NS.90.09.06.26]	1952	0.2160	0.725	0.0218	194	0.0662	541	0.2278	0.0348	1.212
ANS-3	Nausharo IC [NS G4C (1) 86.18.26]	2433	0.1274	0.220	0.0228	287	0.0057	659	0.3759	0.0426	1.378
ANS-4	Nausharo III [NS.89.06.153]	2024	0.0806	0.251	0.0178	193	0.0058	225	0.2820	0.0588	0.679
ANS-5	Nausharo IC [NS I 87.4D.53]	1784	0.0839	1.250	0.0522	465	9.9652	160	1.3486	0.0360	0.695
ANS-6	Nausharo III [NS.96.06.35.13]	1789	0.0868	0.364	0.0274	156	0.0910	458	1.7987	0.0141	0.744
ANS-7	Nausharo III [NS.87.14.92]	1871	0.1400	0.315	0.0190	640	0.0799	243	0.2837	0.0319	1.328

APPENDIX 8.7

INAA DATA FOR AGATE ARTIFACTS FROM MOHENJO-DARO (AMD), CHANHU-DARO (ACD) AND NAGWADA (ANGW)

Data in parts per million (PPM)

artifact	Al	Co	Cr	Eu	Fe	La	Na	Sb	Sc	V
AMD-1	3234	0.3865	3.105	0.0715	1175	0.0925	1372	0.4993	0.0279	3.177
AMD-2	3514	0.2594	3.032	0.0715	803	0.0480	1671	1.2017	0.0199	1.811
AMD-3	2579	0.3747	1.833	0.3127	539	2.1685	822	0.1345	0.0983	1.797
AMD-4	1850	0.1835	0.757	0.0479	200	0.0901	992	0.1407	0.0462	1.871
AMD-5	2456	0.2908	2.622	0.0394	672	0.0450	908	0.118	0.3899	5.594
AMD-6	2072	0.2022	0.938	0.065	189	0.1038	1800	0.1649	0.0738	2.348
AMD-7	2041	0.1605	0.579	0.0399	246	0.0873	806	0.1596	0.0756	1.749
ACD-1	3444	0.6120	4.386	0.1439	1876	2.4948	705	0.2566	0.0528	6.439
ACD-2	3046	0.4871	4.056	0.0844	1405	0.1699	2374	0.1067	0.0705	3.596
ACD-3	1849	0.1639	1.223	0.0261	393	0.1031	1821	0.4212	0.0229	4.300
ACD-4	1642	0.1259	0.462	0.0198	541	0.0689	377	0.2913	0.0346	1.173
ACD-5	2710	0.2080	0.359	0.0239	320	0.0692	1162	0.6208	0.3494	2.811
ACD-6	3125	0.2691	0.854	0.025	714	0.0390	1165	0.2161	0.1478	20.457
ACD-7	2168	0.3536	1.607	0.0662	556	0.0684	1344	0.2148	0.142	8.426
ANGW-1	2892	0.3448	2.727	0.0522	1029	0.1254	335	0.113	0.0332	2.431
ANGW-2	2290	0.2878	5.831	0.0395	753	0.6066	325	0.0977	0.103	4.382
ANGW-3	2313	0.4096	3.028	0.0387	890	0.1768	722	0.2556	0.6969	3.040

APPENDIX 8.8

FIRST PREDICTED GROUP MEMBERSHIPS (PGMS) FOR AGATE ARTIFACTS GENERATED FROM THREE CDAS IN CHAPTER 8

Artifact	Figure 8.34	Figure 8.35	Figure 8.36 B	Artifact	Figure 8.34	Figure 8.35	Figure 8.36 B
AH-1	S-i-S	S-i-S	n/a	ACD-1	GMB	Gujarat	GMB
AH-2	S-i-S	S-i-S	n/a	ACD-2	GMB	Gujarat	GMB
AH-3	GMB	Gujarat	GMB	ACD-3	S-i-S	S-i-S	n/a
AH-4	GMB	Gujarat	GMB	ACD-4	S-i-S	S-i-S	n/a
AH-5	GMB	Gujarat	GMB	ACD-5	GMB	Gujarat	GMB
AH-6	GMB	Gujarat	GMB	ACD-6	GMB	Gujarat	GMB
AH-7	GKK	Gujarat	GKK	ACD-7	GMB	Gujarat	GMB
AH-8	GKK	Gujarat	GKK				
AH-9	S-i-S	S-i-S	n/a	AMD-1	GMB	Gujarat	GMB
AH-10	GMB	Gujarat	GMB	AMD-2	GMB	S-i-S	n/a
AH-11	GMB	Gujarat	GMB	AMD-3	GMB	Gujarat	GMB
AH-12	GMB	Gujarat	GMB	AMD-4	GMB	Gujarat	GMB
AH-13	GMB	S-i-S	n/a	AMD-5	GMB	Gujarat	GMB
AH-14	GRTP	Gujarat	GMB	AMD-6	GMB	Gujarat	GMB
AH-15	GKK	Gujarat	GKK	AMD-7	GMB	Gujarat	GMB
AH-16	GMB	Gujarat	GMB				
AH-17	GMB	Gujarat	GMB	AMR-1	GKK	Gujarat	GKK
AH-18	GKK	Gujarat	GKK	AMR-2	S-i-S	S-i-S	n/a
AH-19	GKK	Gujarat	GKK	AMR-3	GKK	Gujarat	GKK
AH-20	S-i-S	S-i-S	n/a	AMR-4	GKK	Gujarat	GKK
AH-21	GKK	Gujarat	GKK	AMR-5	GKK	Gujarat	GMB
AH-22	GRTP	Gujarat	GRTP	AMR-6	GKK	Gujarat	GKK
AH-23	GKK	Gujarat	GKK	AMR-7	GKK	Gujarat	GKK
AH-24	GMB	Gujarat	GMB	AMR-8	GRTP	Gujarat	GRTP
ANGW-1	GRTP	Gujarat	GRTP	ANS-1	GKK	Gujarat	GKK
ANGW-2	GMB	Gujarat	GMB	ANS-2	GKK	Gujarat	GMB
ANGW-3	GMB	Gujarat	GMB	ANS-3	GMB	Gujarat	GMB
				ANS-4	GRTP	Gujarat	GRTP
				ANS-5	S-i-S	S-i-S	n/a
				ANS-6	S-i-S	S-i-S	n/a
				ANS-7	GKK	Gujarat	GKK

APPENDIX 8.9

STANDARDIZED CANONICAL DISCRIMINANT FUNCTION COEFFICIENTS FOR THE SCATTER AND BOX PLOTS IN CHAPTER 8 GENERATED USING CANONICAL DISCRIMINANT ANALYSIS

Figures 8.33 & 34	Function 1	Function 2
Log Al	-.812	-.511
Log Co	-1.231	.766
Log Cr	.725	-.529
Log Eu	.183	-.586
Log Fe	.679	-.060
Log La	.018	.895
Log Na	1.008	.406
Log Sb	.009	.557
Log Sc	.403	-.578
Log V	-.047	-.067

Figure 8.35	Function 1
Log Al	-.682
Log Co	-.318
Log Cr	.025
Log Eu	-.333
Log Fe	.594
Log La	.689
Log Na	.667
Log Sb	.681
Log Sc	-.386
Log V	.077

Figure 8.36 A & B	Function 1	Function 2
Log Al	-.619	.899
Log Co	-1.280	-.845
Log Cr	1.062	.095
Log Eu	.461	.317
Log Fe	.246	.785
Log La	-.512	-.394
Log Na	1.052	-1.207
Log Sb	-.493	.383
Log Sc	.627	.053
Log V	-.045	.142

APPENDIX 9.1

EMPA OF ARCHAEOLOGICAL AND GEOLOGIC VESUVIANITE-GROSSULAR SAMPLES

Seven vesuvianite-grossular ornament manufacturing debris fragment from Harappa and five geologic samples from two vesuvianite-grossular sources in Pakistan (Muslimbagh ophiolite, Balochistan and Sakhakot-Qila ophiolite, FATA) were examined using electron microprobe analysis (EMPA). Both the energy dispersive spectrometry (EDS) and the wavelength dispersive spectrometry (WDS) capabilities of the probe, as described in Chapter 3, were employed in these analyses.

Phases of vesuvianite and grossular garnet were distinguishable from one another because of their differing Mg contents (< 1% for grossular vs. 2 to 3 % for vesuvianite) as well as the consistently low composition totals (»94-95%) for vesuvianite phases. The low vesuvianite totals are likely due in part to fact that Fluorine (F) was not one of the elements analyzed. Groat and others (1992) found F ranged up to 3.15% of the total in vesuvianites.

ARCHAEOLOGICAL FRAGMENTS

XRD had previously indicated that four fragments H2000/9999-87, H2000/9999-88, H2000/9999-89 and H2000/9999-93 were composed of solely of vesuvianite. No inclusions or additional phases were identified during in the WDS analyses (Appendix 9.1 Figure 1).

XRD analysis indicated that fragment H2000/9999-90 was primarily composed of vesuvianite and a significant secondary component of grossular garnet. This was confirmed by WDS (Appendix 9.1 Figure 2).

XRD analysis indicated that fragment H98/8499-353 was composed of vesuvianite. Chlorite in fissures within the stone was detected by WDS (Appendix 9.1 Figure 3). No other phases were identified.

XRD analysis indicated that fragment H2000/9999-91 was primarily grossular garnet with traces of chlorite

Appendix 9.1 Figure 1 WDS compositional data for four vesuviantite fragments from Harappa.

	H2000/ 9999-87 (n=7)	H2000/9999-88 (n=7)	H2000/9999-89 (n=7)	H2000/9999-93 (n=5)
MgO	2.75 %	2.99 %	2.77 %	2.61 %
Al_2O_3	17.62 %	18.36 %	17.73 %	17.22 %
SiO_2	35.86 %	36.32 %	35.89 %	36.18 %
CaO	36.21 %	36.33 %	36.45 %	35.71 %
TiO_2	0.01 %	0.00 %	0.01 %	0.03 %
MnO	0.03 %	0.08 %	0.07 %	0.05 %
FeO	2.32 %	0.97 %	2.08 %	2.82 %
Na_2O	0.00 %	0.00 %	0.00 %	0.01 %
K_2O	0.01 %	0.00 %	0.00 %	0.01 %
Cr_2O_3	0.01 %	0.01 %	0.00 %	0.07 %
Totals	94.82 %	95.07 %	95.01 %	94.71 %
Phase	vesuvianite	vesuvianite	vesuvianite	vesuvianite

Appendix 9.1 Figure 2 WDS compositional data for fragment H2000/9999-90

	primary phase (average of 7 analyses)	**secondary phase (average of 3 analyses)**
MgO	2.75 %	0.19 %
Al_2O_3	18.85 %	21.84 %
SiO_2	36.16 %	38.45 %
CaO	36.28 %	37.13 %
TiO_2	0.02 %	0.03 %
MnO	0.01 %	0.07 %
FeO	0.74 %	0.95 %
Na_2O	0.00 %	0.00 %
K_2O	0.00 %	0.00 %
Cr_2O_3	0.02 %	0.02 %
Totals	94.84 %	98.69 %
Phase	**vesuvianite**	**grossular**

Appendix 9.1 Figure 3 WDS compositional data for fragment H98/8499-353

	primary phase (average of 7 analyses)	fissure (1 analysis)
MgO	2.77 %	17.73 %
Al_2O_3	17.56 %	0.64 %
SiO_2	35.75 %	54.78 %
CaO	35.98 %	25.36 %
TiO_2	0.00 %	0.01 %
MnO	0.03 %	0.10 %
FeO	2.18 %	1.13 %
Na_2O	0.00 %	0.16 %
K_2O	0.00 %	0.00 %
Cr_2O_3	0.02 %	0.02 %
Totals	94.30 %	99.92 %
Phase	**vesuvianite**	**chlorite**

Appendix 9.1 Figure 4 [**A**] WDS compositional data for fragment H2000/9999-90 [**B**] BSE image of fragment showing the where WDS scans were made on 12 points for three analyses (**0** = phase A, **+** = phase B, ♦ = phase C).

A	**analysis phase A (average of 6 analyses)**	**analysis phase B (average of 5 analyses)**	**fissure (phase C) (n=1)**
MgO	0.01 %	2.55 %	18.1 %
Al_2O_3	22.03 %	17.83 %	0.2 %
SiO_2	38.64 %	35.46 %	55.0 %
CaO	37.19 %	36.09 %	25.4 %
TiO_2	0.03 %	0.02 %	0.0 %
MnO	0.08 %	0.04 %	0.0 %
FeO	1.01 %	2.13 %	0.6 %
Na_2O	0.00 %	0.01 %	0.0 %
K_2O	0.00 %	0.00 %	0.0 %
Cr_2O_3	0.02 %	0.01 %	0.0 %
totals	99.01 %	94.14 %	99.4 %
Phase	**grossular**	**vesuvianite**	**chlorite**

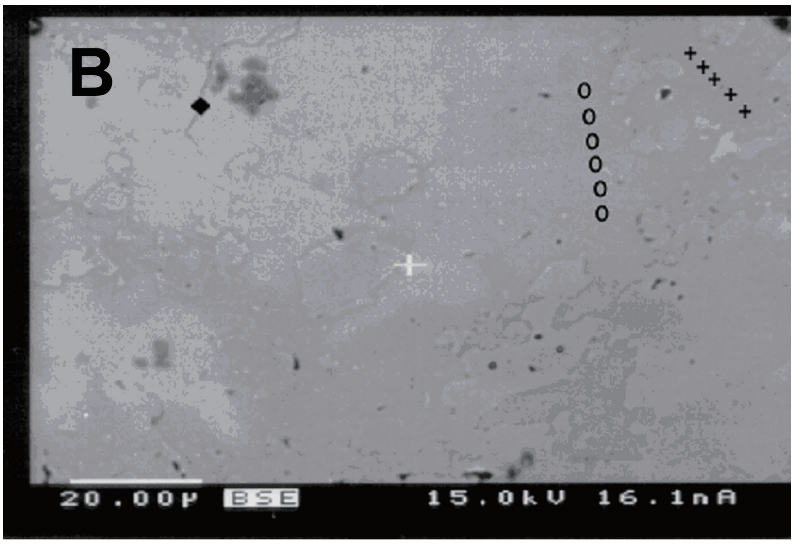

Appendix 9.1 Figure 5 [**A**] WDS compositional data for sample SQ-1. [**B**] BSE image of fragment showing the where WDS scans were made on 11 points for three analyses (**0** = phase A, **+** = phase B, □ = phase C). *Note that the black patches in the image are voids rather than mineral phases.*

A	**analysis phase A (n=3)**	**analysis phase B (n=5)**	**analysis phase C (n=3)**
MgO	0.01 %	0.00 %	2.46 %
Al_2O_3	22.49 %	22.44 %	18.30 %
SiO_2	38.80 %	38.73 %	36.13 %
CaO	37.04 %	37.08 %	36.14 %
TiO_2	0.02 %	0.02 %	0.02 %
MnO	0.04 %	0.06 %	0.03 %
FeO	0.70 %	0.77 %	1.92 %
Na_2O	0.01 %	0.01 %	0.03 %
K_2O	0.01 %	0.01 %	0.01 %
Cr_2O_3	0.01 %	0.02 %	0.00 %
totals	99.13 %	99.15 %	95.04 %
Phase	**grossular**	**grossular**	**vesuvianite**

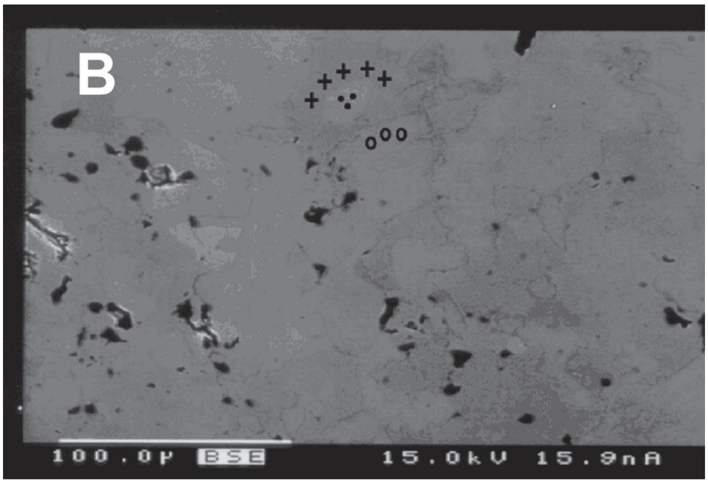

Appendix 9.1 Figure 6: WDS compositional data for sample SQ-2

	primary phase (average of 7 analyses)	**black inclusion (n=1)**
MgO	0.01 %	7.99 %
Al_2O_3	22.84 %	23.79 %
SiO_2	38.61 %	0.06 %
CaO	37.02 %	0.17 %
TiO_2	0.03 %	0.30 %
MnO	0.07 %	0.00 %
FeO	0.20 %	26.61 %
Na_2O	0.01 %	0.01 %
K_2O	0.01 %	0.01 %
Cr_2O_3	0.00 %	39.11 %
totals	98.79 %	98.06 %
Phase	**grossular**	**chromite**

Appendix 9.1 Figure 7: WDS compositional data for sample SQ-3

	primary phase (average of 7 analyses)
MgO	3.10 %
Al_2O_3	17.65 %
SiO_2	35.41 %
CaO	36.39 %
TiO_2	0.03 %
MnO	0.07 %
FeO	1.75 %
Na_2O	0.01 %
K_2O	0.01 %
Cr_2O_3	0.00 %
totals	94.42 %
Phase	**vesuvianite**

Appendix 9.1 Figure 8 WDS compositional data for samples QB-1 and TMJ-1

	QB-1 (average of 7 analyses)	TMJ-1 (average of 7 analyses)
MgO	2.51 %	2.8 %
Al_2O_3	17.40 %	15.9 %
SiO_2	36.11 %	35.7 %
CaO	35.50 %	35.3 %
TiO_2	0.39 %	0.3 %
MnO	0.03 %	0.1 %
FeO	2.52 %	3.7 %
Na_2O	0.00 %	0.0 %
K_2O	0.00 %	0.0 %
Cr_2O_3	0.01 %	0.0 %
totals	94.47 %	93.8 %
Phase	vesuvianite	vesuvianite

(variety clinochlore). WDS analyses confirmed the presence of both minerals and also detected a secondary vesuvianite phase (Appendix 9.1 Figure 4 A & B).

GEOLOGIC SAMPLES

Three samples (SQ-1, SQ-2, SQ-3) from the Sakhakot-Qila Ophiolite (Kot), FATA source formation were probed along with two samples (QB-1, TMJ-1) from the Taleri Mohammed Jan occurence in the Muslimbagh Ophiolite , Balochistan.

SQ-1. Specific gravity = 3.51. XRD analysis indicated that this sample was grossular. This was confirmed by WDS and a minor phase of vesuvianite was also detected (Appendix 9.1 Figure 5 A & B).

SQ-2. Specific gravity = 3.40. XRD analysis indicated that this sample was pure grossular. Small black inclusions are apparent in the stone's translucent milky green matrix. WDS confirmed that grossular was the primary component of this sample and revealed the inclusions to be chromite (Appendix 9.1 Figure 6).

SQ-3. Specific gravity = 3.32. XRD analysis indicated that this sample was vesuvianite. This was confirmed was by WDS (Appendix 9.1 Figure 7). No other phases or inclusions were identified.

QB-1. Specific gravity = 3.33. XRD analysis on a sample of this material indicated that it is composed of vesuvianite and grossular. WDS analysis was only performed on the sample's major phase, which was vesuvianite (Appendix 9.1 Figure 8 *column 1*).

TMJ-1. Specific gravity = 3.26. XRD analysis indicated that the sample was composed of vesuvianite with some chlorite (variety clinochlore). EDS and WDS confirmed this but found no evidence of grossular phases or chromite inclusions (Appendix 9.1 Figure 8 *column 2*).

APPENDIX 9.2

ANALYSES OF VESUVIANITE-GROSSULAR FRAGMENTS FROM MOHENJO-DARO

Six vesuvianite-grossular ornament manufacturing debris fragments from Mohenjo-daro were examined using XRD analysis and SG testing (Appendix 9.2 Figure 1).

The XRD scan for sample MDV-1 (Appendix 9.2 Figure 2 left) was conducted at 2-theta 5° to 65°. All others were run only from 2-theta 25° to 45° as this was sufficient to identify and distinguish both vesuvianite and grossular. Only MDV-2 is presented here (Appendix 9.2 Figure 2 right) as the scans for MDV-2 through MDV-6 are basically identical.

Mineralogically, all six of the fragments from Mohenjo-Daro fall within the range of variation exhibited by vesuvianite-grossular artifacts from Harappa.

Appendix 9.2 Figure 1: XRD & SG testing results for six greenstone fragments from Mohenjo-Daro

Sample	***Phase(s)***	***Specific gravity***
MDV 1	grossular-vesuvianite	3.41
MDV 2	vesuvianite	3.28
MDV 3	vesuvianite	3.30
MDV 4	vesuvianite	3.28
MDV 5	vesuvianite	3.29
MDV 6	vesuvianite	3.24

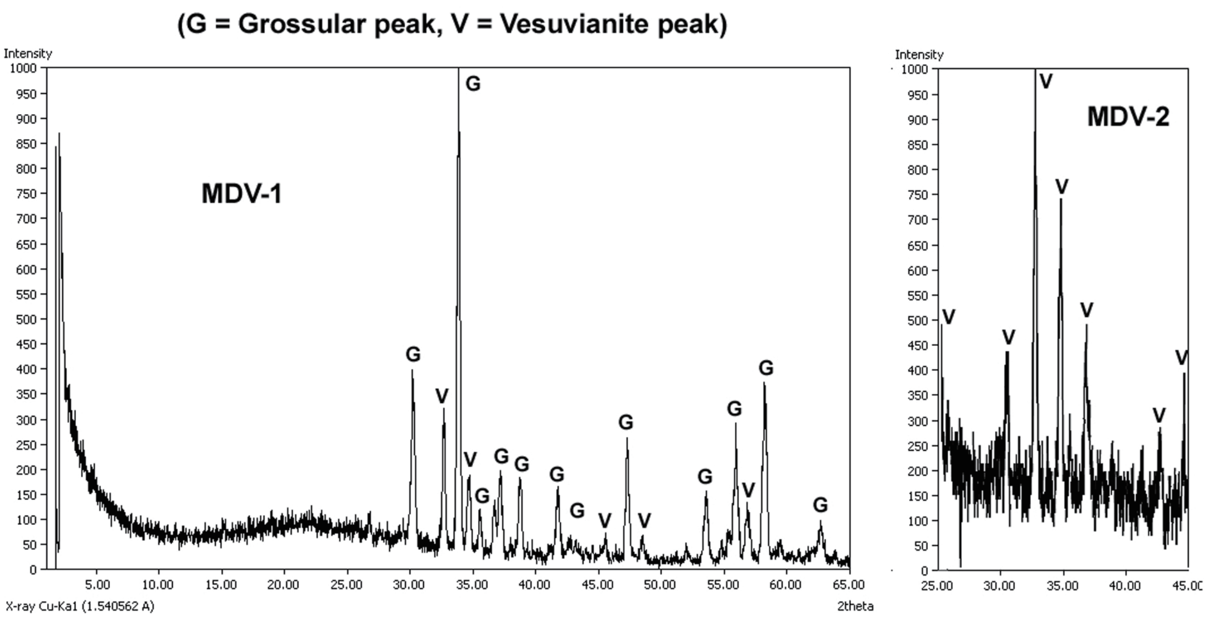

Appendix 9.2 Figure 2 XRD spectra for two Mohenjo-Daro green stone fragments (MDV-1 and MDV-2).

APPENDIX 9.3

XRD OF MASSIVE VESUVIANITE FROM KUMBHALGARH FOREST, RAJASTHAN

The XRD spectrum (Appendix 9.3 Figure 1) for a sample of massive green rock from Kumbalgarh Forest Reserve, Rajasthan confirms that it is composed of vesuvianite. No grossular peaks are present in this particular sample, however.

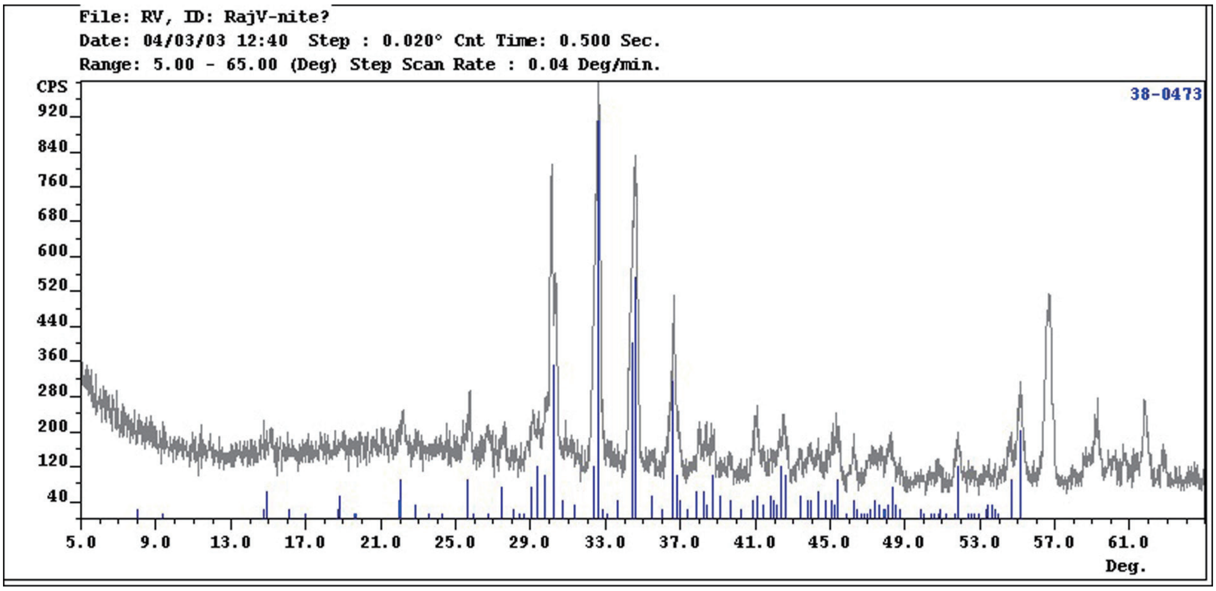

Appendix 9.3 Figure 1 Sample of (vertical blue lines indicate vesuvianite peaks).

APPENDIX 9.4

INAA DATA FOR VESUVIANITE-GROSSULAR SAMPLES FROM HARAPPA AND MOHENJO-DARO (MDV)

Elemental concentrations in parts per million.

Artifact	Period	Mound	Trench	Al	Ce	Co	Cr	Eu	Fe	Mn	Na	Sc	Sm	Sr	U	V
H96/7327-2	5	AB	38	110623	2.74	18.99	586	0.224	20302	715	79.9	74.66	0.05	650	0.507	341
H99/9730-11	3C	F	43	109543	0.89	12.63	33	0.051	13280	870	53.1	3.95	0.006	623	0.132	36.2
H96/7129-1	3C	E	36	92188	3.61	27.2	878	0.414	20792	470	109	134.5	0.06	518	0.642	471
H94/5302-81	3C	ET	22	96097	1.59	24.53	269.5	0.126	19943	572	103	24.6	0.009	509	0.252	108
H94/4898-83	3C	ET	27	93140	0.80	10.78	3.72	0.093	18619	359	73.7	0.32	0.006	432	0.094	5
H96/6958-41	3B	E	11	101568	1.93	40.74	686	0.154	28103	593	151	32.99	0.075	536	0.308	86
H98/8908-8	1	AB	39	108235	0.96	21.96	27	0.087	22530	475	144	3.19	0.005	485	0.133	23.2
MDV-1	Surface	Moneer Area	n/a	95973	1.28	16.56	103	0.108	18567	452	301	18.23	0.021	443	0.194	79.6
MDV-2	Surface	Moneer Area	n/a	93137	1.62	17.13	163	0.141	19151	418	329	27.52	0.021	465	0.255	115
MDV-3	Surface	Moneer Area	n/a	96364	0.85	13.7	13.6	0.086	18387	442	72.3	2.15	0.004	466	0.109	14.2

APPENDIX 9.5

INAA DATA FOR VESUVIANITE-GROSSULAR SAMPLES FROM SAKHAKOT-QILA (FATA-SQ) AND TALERI MOHAMMED JAN (B-TMJ)

Elemental concentrations in parts per million.

Sample	Al	Ce	Co	Cr	Eu	Fe	Mn	Na	Sc	Sm	Sr	U	V
FATA-SQ-01	136093	0.84	2.67	44.3	0.142	7595	524	203	1.585	0.037	556	0.119	7.8
FATA-SQ-02	137086	0.72	1.44	9.64	0.137	5254	440	208	0.44	0.021	528	0.09	6.58
FATA-SQ-03	110213	0.86	11.9	6.84	0.113	15295	723	87.8	2.499	0.078	582	0.128	18.3
FATA-SQ-04	112945	0.95	14.4	41.2	0.11	13266	470	63	4.637	0.096	520	0.151	27.9
FATA-SQ-05	155226	0.91	4.21	209.1	0.134	5714	918	76.9	2.139	0.061	689	0.121	14.4
FATA-SQ-06	164444	0.85	1.6	120	0.234	6087	649	74.1	2.083	0.114	611	0.119	11.6
B-TMJ-01	94495	0.96	22.3	3.21	0.883	35350	772	71.5	0.375	0.254	549	0.14	18.8
B-TMJ-02	87390	0.75	10.3	1.22	0.279	26161	574	29.9	0.177	0.005	495	0.111	17.8
B-TMJ-03	87073	0.96	13.1	2.22	0.551	35870	813	48.3	0.722	0.489	562	0.168	28.2
B-TMJ-04	89308	0.53	3.37	0.72	0.278	7814	703	12.2	0.694	0.019	529	0.098	61
B-TMJ-05	86622	0.96	13.2	3.65	0.649	36781	839	53.7	1.828	0.187	571	0.184	36.8
B-TMJ-06	85458	0.87	12.5	3.69	0.541	34712	814	47.9	0.338	0.065	567	0.208	16
B-TMJ-07	91995	0.92	16.9	2.79	0.767	35987	733	70.8	0.402	0.238	546	0.222	19.7
B-TMJ-08	94171	1.22	10.1	10.4	0.379	17953	283	119	24.18	0.331	402	0.253	11.8
B-TMJ-09	95638	1.09	9.26	6.58	0.292	18015	331	125	18	0.227	421	0.223	10.9

APPENDIX 9.6

INAA DATA FOR VESUVIANITE-GROSSULAR SAMPLES FROM KUMBHALGARH FOREST RESERVE, RAJASTHAN (RAJ-K)

Elemental concentrations in parts per million.

Sample	Al	Ce	Co	Cr	Eu	Fe	Mn	Na	Sc	Sm	Sr	U	V
RAJ-K-01	75650	6.77	3.89	18.3	0.509	24501	313	28.8	7.266	1.072	939	0.378	18.7
RAJ-K-02	75342	9.25	8.82	47.7	1.169	38017	315	43.3	13.2	4.327	1076	0.791	15.5
RAJ-K-03	73890	14.67	7.45	70.1	0.811	40296	313	43.2	16.23	3.238	738	0.916	23.1
RAJ-K-04	73184	41.06	8.09	11.9	0.712	35635	317	58.1	3.843	2.628	1132	0.737	9.81
RAJ-K-05	74511	8.41	12.4	33.3	0.555	41636	350	41.8	4.816	1.256	931	0.44	20.1
RAJ-K-06	72398	8.75	10	18.7	0.61	40853	351	47.6	4.763	1.291	761	0.494	19.3
RAJ-K-07	80427	116.3	8.48	59.9	1.253	42754	338	55	18.2	7.021	1446	2.485	18

APPENDIX 9.7

STANDARDIZED CANONICAL DISCRIMINANT FUNCTION COEFFICIENTS FOR FIGURE 9.8

Element	Function 1	Function 2
Log Al	2.164	-.723
Log Ce	.066	.855
Log Co	.357	-1.367
Log Cr	-1.227	1.814
Log Eu	-1.243	-1.776
Log Fe	.304	.598
Log La	-2.079	-1.297
Log Mn	.811	-.985
Log Na	1.843	1.386
Log Sc	-.341	-2.036
Log Sm	1.420	2.271
Log U	-.163	1.238
Log V	.818	-.922

APPENDIX 9.8

SIX ALTERNATE CLUSTERING STRATEGIES USING THE VESUVIANITE-GROSSULAR COMPARATIVE DATA

Average Linkage (Between Groups)

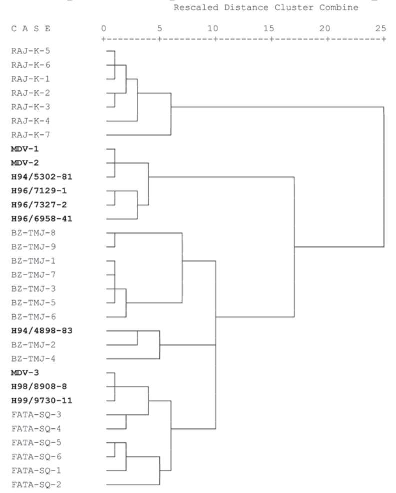

Average Linkage (Within Group)

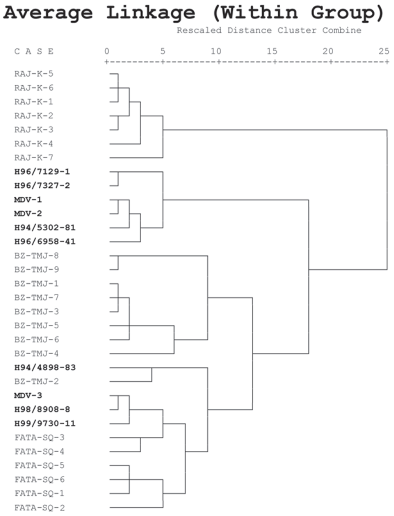

Single Linkage (Nearest Neighbor)

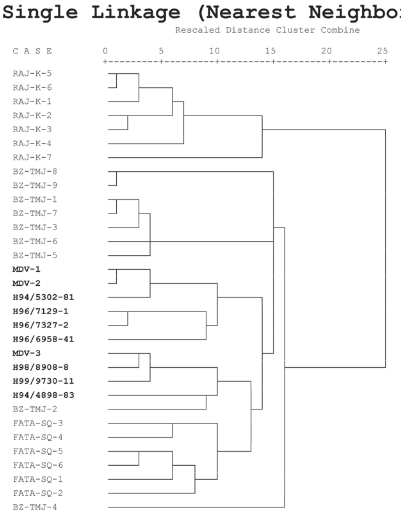

Complete Linkage (Furthest Neighbor)

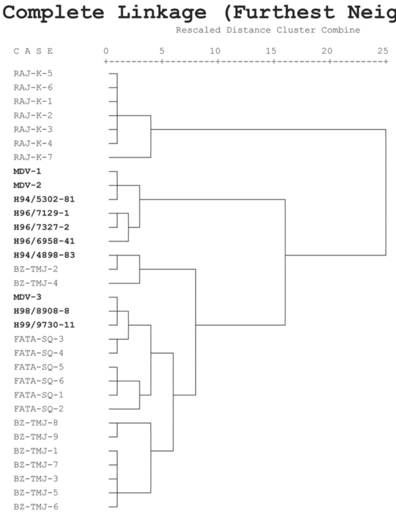

Centroid Method

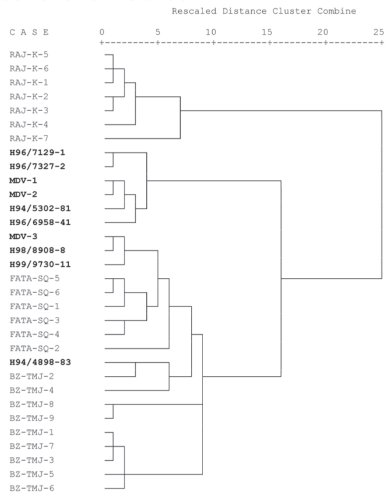

Median Method

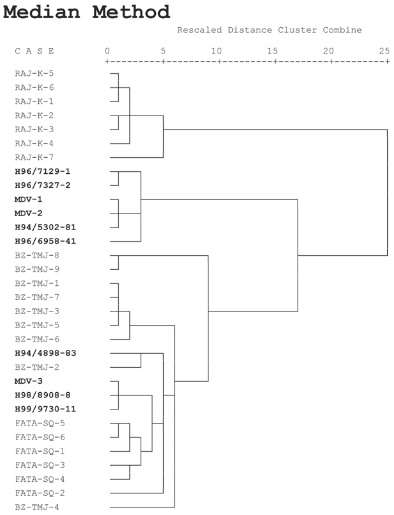

APPENDIX 9.9

IS THE VESUVIANITE-GROSSULAR / "ERNESTITE" ASSOCIATION GENUINE?

In Chapter 9, I showed that the spatial and temporal distribution patterns of "Ernestite" and vesuvianite-grossular artifacts at Harappa are practically mirror images of one another. With the exception of a single and possibly anomalous vesuvianite-grossular flake in Period 1 levels, each variety of stone begins to appear in the site's archaeological record around periods 3B and 3C. Both are varieties are found mainly on mounds E and ET. Moreover, when association at the level of shared stratigraphically secure excavation lot is considered, we see that in roughly one out of every three lots (32.4%) in which an "Ernestite" artifact was recovered a vesuvianite-grossular artifact was also present. I argue that it is no coincidence that each material appears at exactly the same time *when* (ca. periods 3B and 3C) and, largely, in the same places *where* (Mound E/ET) beadmakers were using the other one. Simply put, the reason is that vesuvianite-grossular beads could not have been drilled without use of "Ernestite" bits. Whether or not the discovery of "Ernestite" and its unique drilling properties (discussed in Appendix 4.5) finally allowed beadmakers to use vesuvianite-grossular or if desire to use vesuvianite-grossular necessitated the development of "Ernestite" is a "chicken and egg" type question. Who knows? They both appear at the same time and place.

However, is this association indeed *genuine*? That is, does the evident spatial and temporal pattern stem from the actual behaviors of Harappans? Or, could it be a product of something else? As I discussed in detail in Chapter 4, Harappa's rock and mineral assemblage is unevenly distributed through time and space. Some of this is due to the physical constraints of the site (Harappa's deeply buried early occupation levels) while some is due to the research strategies of the HARP excavators (an early and sustained focus on mounds E and ET). Although I think that in Chapter 9 I satisfactorily demonstrated the vesuvianite-grossular / "Ernestite" association to be valid despite the possibility of recovery bias, here I present some additional, supplementary observations regarding this issue.

First recall Figure 4.10, which in its second column shows how all of Harappa's rock and mineral artifacts from secure contexts (n = 32,365) are distributed through each chronological phase. The distributional bias toward Period 3C at the expense of earlier levels is clear. Now look at Figure 4.12, which shows the spatial and temporal presence or absence of all rock and mineral varieties at Harappa in order of decreasing abundance in the assemblage. The rock and mineral sub-assemblages from the early levels are clearly not as diverse as Period 3C. Part of the reason for this, I have argued, is because the less abundant overall varieties (those at the bottom of the table) were not as apt to be recovered in the early levels. However, "Ernestite" and, in particular, vesuvianite-grossular have fairly sizeable sub-assemblages. If those stones were used to any significant degree (or if at all) prior to Period 3B then I would expect at least a few examples to have been recovered from Early Harappan and Period 3A levels. For Appendix 9.9 Figure 1 (next page), I used the overall rock and mineral assemblage temporal distribution percentages from the second column of Figure 4.10 as a formula for making (admittedly) crude predictions of the number of artifacts that might be expected in each phase for those material varieties and a select number of others. If vesuvianite-grossular was used and discarded throughout the entire sequence at Harappa, then perhaps 45 or so examples out of the 180

Appendix 9.9 Figure 1 The predicted temporal distribution of select rock and mineral varieties in secure contexts based on overall assemblage distribution versus the actual temporal distribution of those varieties

Period	*rock & mineral assemblage Distribution (n = 32,365)*	predicted **vesuvianite** distribution (n=180)	actual **vesuvianite** distribution (n=180)	predicted **“Ernestite”** distribution (n=40)	actual **“Ernestite”** distribution (n=40)
1	11.59%	21	1	4.6	0
2	7.95%	14	0	3.2	0
3A	6.10%	11	0	2.4	0
3B	10.88%	20	4	4.4	2
3C	62.81%	113	174	25.1	38
4/5	0.67%	1	1	0.3	0

Period	*rock & mineral assemblage Distribution (n = 32,365)*	predicted **igneous** distribution (n=252)	actual **igneous** distribution (n=252)	predicted **alabaster** distribution (n=212)	actual **alabaster** distribution (n=212)
1	11.59%	29.2	3	24.6	3
2	7.95%	20.0	13	16.9	3
3A	6.10%	15.4	7	12.9	9
3B	10.88%	27.4	34	23.1	18
3C	62.81%	158.3	192	133.2	179
4/5	0.67%	1.7	3	1.4	0

Period	*rock & mineral assemblage Distribution (n = 32,365)*	predicted **lapis lazuli** distribution (n=75)	actual **lapis lazuli** distribution (n=75)	predicted **amazonite** distribution (n=12)	actual **amazonite** distribution (n=12)
1	11.59%	8.7	4	1.7	3
2	7.95%	6.0	11	1.2	2
3A	6.10%	4.6	2	0.9	0
3B	10.88%	8.2	24	1.6	2
3C	62.81%	47.1	32	9.4	5
4/5	0.67%	0.5	2	0.1	3

artifacts in that material sub-assemblage from secure-contexts might be expected to have been recovered from levels prior to Period 3B. However, with the exception of the single and possibly anomalous flake from Period 1 (this instance detailed in Chapter 9), none were. Likewise, no “Ernestite” artifacts whatsoever were recovered from the early periods in question, although perhaps around ten examples might have been expected. For the purpose of comparison, I have applied the same formula to other rock and mineral varieties having sub-assemblages of comparable sizes – igneous rock and alabaster for vesuvianite-grossular and lapis lazuli and amazonite for “Ernestite.” Although the predicted versus the actual distributions for those materials did not always correspond to one another (indicating that overall assemblage distribution is not a good predictor of the distribution of any one material type), it was almost always the case that some examples of those materials were recovered from pre-Period 3B chronological phases. This suggests to me that the absence (or near absence) of vesuvianite-grossular and “Ernestite” from

Appendix 9.9 Figure 2 The predicted spatial distribution of select rock and mineral varieties across the mounds at Harappa based on overall assemblage distribution versus the actual spatial distribution of those varieties.

Mound	*rock & mineral assemblage Distribution (n=56,350)*	predicted **vesuvianite** distribution (n=534)	actual **vesuvianite** distribution (n=543)	predicted **"Ernestite"** distribution (n=75)	actual **"Ernestite"** distribution (n=75)
AB	19.54%	106.1	5	14.7	4
E	40.14%	218.0	300	30.1	30
ET	26.51%	143.9	190	19.9	37
F	6.73%	36.5	5	5.0	1
Off	7.08%	38.4	43	5.3	3

Mound	*rock & mineral assemblage Distribution (n=56,350)*	predicted **igneous** distribution (n=455)	actual **igneous** distribution (n=455)	predicted **alabaster** distribution (n=422)	actual **alabaster** distribution (n=422)
AB	19.54%	88.9	95	82.5	154
E	40.14%	182.6	158	169.4	61
ET	26.51%	120.6	76	111.9	124
F	6.73%	30.6	97	28.4	55
Off	7.08%	32.2	29	29.9	28

Mound	*rock & mineral assemblage Distribution (n=56,350)*	predicted **lapis lazuli** distribution (n=174)	actual **lapis lazuli** distribution (n=174)	predicted **amazonite** distribution (n=21)	actual **amazonite** distribution (n=21)
AB	19.54%	34.0	74	3.9	13
E	40.14%	69.8	48	8.0	0
ET	26.51%	46.1	15	5.3	4
F	6.73%	11.7	12	1.3	3
Off	7.08%	12.3	25	1.4	1

early levels at Harappa is probably not due to recovery bias alone. These rock varieties were simply not used at during those phases.

Next we turn to my contention that Harappans living and working on mounds E and ET were the primary users of vesuvianite-grossular and "Ernestite." Figure 4.9 from Chapter 4 indicates that 66% of the rock and mineral assemblage at Harappa was recovered from excavation or survey on the combined area of those two mounds (Mound E/ET). This shows that there is unquestionably a recovery bias toward the area of the site where vesuvianite-grossular and "Ernestite" artifacts are most heavily concentrated. However, is it enough to account for the fact that around 90% of both rock varieties were recovered from those mounds? For Appendix 9.9 Figure 2 (next page), I have used the used the assemblage spatial distribution percentages for the entire assemblage of rock and mineral artifacts (Figure 4.9) to make crude predictions about how vesuvianite-grossular, "Ernestite," and the selected sub-assemblages of comparable size was be distributed if they were being used more or less to the same degree in all parts of the site. Although once again the predicted distributions and the actually distributions for the comparable sub-assemblages do not always match perfectly, none of them are as sharply biased toward mounds E-ET as vesuvianite-grossular and "Ernestite" clearly area. This leads me to conclude that the spatial patterning of the latter two materials is, at least partially, a genuine product of behaviors of ancient residents of Harappa.

APPENDIX 10.1

SULFUR AND STRONTIUM ISOTOPE VALUES FOR ALABASTER ARTIFACTS FROM HARAPPA, MOHENJO-DARO, REHMAN DHERI AND MUSA KHEL

Site	Artifact	Sample number	Period	Mound-Trench	δ34S ‰	Sr 87/86
Harappa	fragment	H2000/9572-22	2	AB - 39	34.769	0.710059
Harappa	fragment	H98/8486-84	2	AB - 39	28.664	0.711125
Harappa	bangle	H2000/2126-9	3A	E - 54	14.245	0.711609
Harappa	fragment	H95/4686-7	3B	ET - 10	26.488	0.714056
Harappa	fragment	H94/4469-406	3B	ET - 10	23.402	0.712165
Harappa	fragment	H95/7018-11	3C	AB - 31	25.756	0.712064
Harappa	fragment	H98/8308-170	3C	AB - 39	36.223	0.708499
Harappa	fragment	H98/8310-64	3C	AB - 39	20.128	0.709541
Harappa	fragment	H98/8327-16	3C	AB - 39	23.602	0.708272
Harappa	ringstone	H98/7715-9	3C	AB - 42	21.971	0.709034
Harappa	fragment	H2001/11502-3	3C	E - 11	27.465	0.710068
Harappa	vessel	H99/8890-93	3C	E - 11	21.293	0.712989
Harappa	bangle	H2000/2207-20	3C	E - 54	21.116	0.710131
Harappa	plug	H2000/2733-16	3C	E - 55	18.674	0.713016
Harappa	fragment	H94/3987-32	3C	E - 7/8	14.933	0.708542
Harappa	fragment	H95/4731-2	3C	ET - 19	20.039	0.709318
Harappa	fragment	H95/4921-12	3C	ET - 28	21.260	0.711188
Harappa	fragment	H95/4954-19	3C	ET - 28	23.624	0.708876
Harappa	fragment	H95/5729-151	3C	ET -32	19.640	0.711863
Harappa	fragment	H2000/10046-5	3C	F - 43	21.460	n/a
Harappa	fragment	H98/8631-2	3C	F - 43	23.358	0.707956
Harappa	fragment	H99/9765-2	3C	F - 43	21.615	0.708487
Harappa	fragment	H99/8387-107	surface	AB - 39	23.624	0.713547
Harappa	vessel	H2000/2102-907	surface	E - 54	21.249	n/a
Harappa	bangle	H2000/2139-128	surface	E - 54	20.505	0.712308
Harappa	fragment	H96/7218-10	surface	F - 37	22.881	0.708216
Harappa	pendent	H94/4999-511	unknown	unknown	19.784	0.709347
Harappa	ball	Vats 3558	unknown	AB?	19.107	n/a
Harappa	weight	Vats 13799	unknown	AB?	22.459	0.708033
Mohenjo-daro	vessel	MD-1	surface	DK area	16.820	0.708719
Musa Khel	fragment	MK-1	surface	n/a	31.128	0.708490
Musa Khel	fragment	MK-2	surface	n/a	26.832	0.712666
Rehman Dheri	fragment	RD-1	surface	n/a	25.500	0.709975

APPENDIX 10.2

SULFUR AND STRONTIUM ISOTOPE VALUES FOR GEOLOGIC SAMPLES OF ALABASTER FROM SOURCES IN THE SULAIMAN MOUNTAINS, SALT RANGE AND KOHAT

Sample	Region (Province)	Source/Location	Age	$\delta^{34}S$ ‰	Sr 87/86
BG19	Sulaimans (Balochistan)	Bala Dhaka - Karher	Eocene	22.337	0.707846
BG-20	Sulaimans (Balochistan)	Bala Dhaka - Karher	Eocene	22.193	0.707778
BG21	Sulaimans (Balochistan)	Barkhan	Eocene	22.725	0.707793
BG-13	Sulaimans (Balochistan)	Chamlang Mari	Eocene	22.559	0.707784
BG-14	Sulaimans (Balochistan)	Chamlang Mari	Eocene	22.592	0.707805
BG-04	Sulaimans (Balochistan)	Dera Bugti	Eocene	23.414	0.707750
BG-05	Sulaimans (Balochistan)	Dera Bugti	Eocene	23.458	0.707817
BG-03	Sulaimans (Punjab)	DG Khan - Zinda Pir	Eocene	24.102	0.707766
DGK-2	Sulaimans (Punjab)	DG Khan - Zinda Pir	Eocene	23.769	n/a
BG-08	Sulaimans (NWFP)	DI Khan - Drazinda	Eocene	22.415	0.707825
BG-09	Sulaimans (NWFP)	DI Khan - Drazinda	Eocene	20.594	0.707835
DIK-3	Sulaimans (NWFP)	DI Khan - Drazinda	Eocene	23.025	n/a
DIK-4	Sulaimans (NWFP)	DI Khan - Drazinda	Eocene	22.847	n/a
BG17	Sulaimans (Balochistan)	Kore More	Eocene	23.402	0.707825
BG18	Sulaimans (Balochistan)	Kore More	Eocene	23.669	0.707824
BG-22	Sulaimans (Balochistan)	Kurcha-Rakni	Eocene	22.792	0.707745
BG-06	Sulaimans (Balochistan)	Lakha Kach-Rakni	Eocene	22.903	0.707824
BG-07	Sulaimans (Balochistan)	Lakha Kach-Rakni	Eocene	23.214	0.707805
BG-10	Sulaimans (Balochistan)	Nisau-Vitakri	Eocene	23.769	0.707779
BG-11	Sulaimans (Balochistan)	Nisau-Vitakri	Eocene	23.647	0.707804
BG-15	Sulaimans (Balochistan)	Nodo	Eocene	23.824	0.707785
BG-16	Sulaimans (Balochistan)	Nodo	Eocene	24.202	0.707795
BG-01	Sulaimans (Balochistan)	Spintangi	Eocene	24.890	0.707704
BG-02	Sulaimans (Balochistan)	Spintangi	Eocene	24.612	0.707748
KJ-1	Kohat (NWFP)	Jatta	Eocene	19.173	0.707906
KJ-2	Kohat (NWFP)	Jatta	Eocene	19.029	0.708949
KBK-1	Kohat (NWFP)	Bahad-ur-Khel	Eocene	19.118	0.707747
KBK-2	Kohat (NWFP)	Bahad-ur-Khel	Eocene	20.084	n/a

Sample	Region (Province)	Source/Location	Age	$\delta^{34}S$ ‰	Sr 87/86
SRL-1	Salt Range (Punjab)	6km north of Lille	Infra-Cambrian	37.699	0.709053
SRL-2	Salt Range (Punjab)	6km north of Lille	Infra-Cambrian	37.400	0.709021
BK-1	Salt Range (Punjab)	Buri Khel	Infra-Cambrian	36.745	0.708139
BK-2	Salt Range (Punjab)	Buri Khel	Infra-Cambrian	36.722	0.708048
BK-3	Salt Range (Punjab)	Buri Khel	Infra-Cambrian	36.878	0.708152
SRDK-1	Salt Range (Punjab)	Daud Khel	Eocene	25.278	0.711878
SRDK-2	Salt Range (Punjab)	Daud Khel	Eocene	25.467	0.711899
SRDK-3	Salt Range (Punjab)	Daud Khel	Eocene	25.334	n/a
JSR-1	Salt Range (Punjab)	Jalalpur	Infra-Cambrian	31.539	0.710204
JSR-2	Salt Range (Punjab)	Jalalpur	Infra-Cambrian	34.036	0.708770
JSR-3	Salt Range (Punjab)	Jalalpur	Infra-Cambrian	34.480	n/a
KDSR-1	Salt Range (Punjab)	Katha Dome	Infra-Cambrian	30.151	0.708570
KDSR-2	Salt Range (Punjab)	Katha Dome	Infra-Cambrian	30.751	0.708543
KDSR-3	Salt Range (Punjab)	Katha Dome	Infra-Cambrian	30.762	n/a
SRK-2	Salt Range (Punjab)	Khewra	Infra-Cambrian	35.957	0.708059
SWN-1	Salt Range (NWFP)	Saiduwali Nala	Eocene	26.488	0.711462
SWN-2	Salt Range (NWFP)	Saiduwali Nala	Eocene	26.444	0.710686
SWN-3	Salt Range (NWFP)	Saiduwali Nala	Eocene	26.621	0.711447

APPENDIX 10.3

LIST OF PINK BI-PYRAMIDAL QUARTZ CRYSTALS (MARI "DIAMONDS") FROM HARAPPA

artifact (year-lot-record)	mound / area	trench / context	period
H86/0.031-20	E - western slope	surface	unknown
H86/17-8	Cemetery	Harappan dump	3C
H89/2024-16	E	52	3B
H89/2025-5	E	52	3B
H93/3516-34	E	4	3 or later
H94/4814-53	ET	19	3 or later
H95/5166-55	E	7_8	3C
H96/6219-36	ET	35	3C
H96/7401-60	AB	39	2/3 mix
H96/7467-613	AB	39	2/3 mix

APPENDIX 11.1

ARCHAEOLOGICAL LIMESTONE SAMPLES FROM HARAPPA ANALYZED FOR THIS STUDY

UPPERCASE text indicates analysis variety.

sample #	artifact #	artifact type	texture	color
HLS-001	H89/1063-28	fragment	sandy	BANDED Dark yellowish orange 10YR 6/6 to Grayish orange 10YR 7/4
HLS-002	H2000/9999-72	fragment	sandy	BANDED Dark yellowish orange 10YR 6/6 to Grayish orange 10YR 7/4
HLS-003	H2000/2091-35	fragment	MICRITIC	Very pale orange 10YR 8/2 rapidly blending to Grayish red 5Y 4/2
HLS-004	H2000/2500-3	fragment	sandy	BANDED Dark yellowish orange 10YR 6/6 to Grayish orange 10YR 7/4
HLS-005	H2000/2085-7	ringstone fragment	sandy	Dark GOLDEN orange 10YR 6/6 to Pale reddish brown 10R 5/4
HLS-006	H95/7008-12	fragment	sandy	BANDED Dark yellowish orange 10YR 6/6 to Grayish orange 10YR 7/4
HLS-007	Vats (no #)	ringstone	sandy	BANDED Dark yellowish orange 10YR 6/6 to Pale brown 5YR 5/2
HLS-008	Vats (no #)	ringstone	sandy	BANDED Dark yellowish orange 10YR 6/6 to Pale brown 5YR 5/2
HLS-009	H95/7110-4	fragment	MICRITIC	Grayish orange 10YR 7/4 with some black spots
HLS-010	H2001/9613-7	shaped stone	MICRITIC	Pale yellowish brown 10YR 6/2 mottled Grayish orange 10YR 7/4
HLS-011	H86/0.025-123	fragment	sandy	Dark yellowish orange 10YR 6/6 (BANDED group)
HLS-012	H93/3862-9	fragment	sandy	BANDED Dark yellowish orange 10YR 6/6 to Pale brown 5YR 5/2
HLS-013	H93/3892-15	fragment	sandy	Dark yellowish orange 10YR 6/6 (BANDED group)
HLS-014	H93/3892-56	ringstone fragment	sandy	Dark GOLDEN orange 10YR 6/6 to Pale reddish brown 10R 5/4
HLS-015	H94/667-1	ringstone fragment	sandy	Dark GOLDEN orange 10YR 6/6
HLS-016	H94/3937-1	fragment	sandy	Dark yellowish orange 10YR 6/6 (BANDED group)
HLS-017	H95/4940-106	fragment	sandy	Dark yellowish orange 10YR 6/6 (BANDED group)
HLS-018	H95/5170-57	fragment	sandy	Grayish red 10R 4/2 (BANDED group)
HLS-019	H95/5170-58	fragment	sandy	Grayish red 10R 4/2 to Moderate yellowish brown 10YR 5/4 (BANDED group)
HLS-020	H95/5195-12	ringstone fragment	sandy	Dark GOLDEN orange 10YR 6/6
HLS-021	H95/7017-3	fragment	sandy	Dark yellowish orange 10YR 6/6 (BANDED group)
HLS-022	H96/7150-5	fragment	sandy	Dark yellowish orange 10YR 6/6 to Moderate reddish brown 10R 4/6 (BANDED group)
HLS-023	H96/7218-5	fragment	sandy	Dark yellowish orange 10YR 6/6 to Moderate reddish brown 10R 4/6 (BANDED group)
HLS-024	H98/8306-20	ringstone fragment	sandy	Dark GOLDEN orange 10YR 6/6
HLS-025	H98/8334-261	fragment	sandy	Dark GOLDEN orange 10YR 6/6 to Moderate reddish brown 10R 4/6
HLS-026	H98/8324-19	fragment	sandy	Dark GOLDEN orange 10YR 6/6 to Grayish orange 10YR 7/4
HLS-027	H98/8324-14	fragment	sandy	Dark GOLDEN orange 10YR 6/6 to Grayish orange 10YR 7/4
HLS-028	H98/8310-147	fragment	sandy	Dark yellowish orange 10YR 6/6 (BANDED group)
HLS-029	H98/8308-138	fragment	sandy	BANDED Dark yellowish orange 10YR 6/6 to Pale brown 5YR 5/2

sample #	artifact #	artifact type	texture	color
HLS-030	H98/8313-116	fragment	sandy	Dark yellowish orange 10YR 6/6 (BANDED group)
HLS-031	H98/8323-49	fragment	sandy	Dark GOLDEN orange 10YR 6/6
HLS-032	H98/8335-37	fragment	sandy	Dark yellowish orange 10YR 6/6 (BANDED group)
HLS-033	H98/8331-68	fragment	sandy	Dark yellowish orange 10YR 6/6 (BANDED group)
HLS-034	H98/8321-2	ringstone fragment	sandy	Dark GOLDEN orange 10YR 6/6 to Moderate reddish brown 10R 4/6
HLS-035	H98/8306-257	fragment	sandy	Dark yellowish orange 10YR 6/6 (BANDED group)
HLS-036	H98/8303-36	fragment	sandy	Moderate yellowish brown 10YR 5/4 (BANDED group)
HLS-037	H99/9724-50	fragment	sandy	Moderate yellowish brown 10YR 5/4 to Dark yellowish brown 10YR 4/2
HLS-038	H99/9722-16	fragment	sandy	Dark GOLDEN orange 10YR 6/6
HLS-039	H2000/2091-36	fragment	sandy	Dark yellowish orange 10YR 6/6 (BANDED group)
HLS-040	H2000/2520-3	fragment	sandy	BANDED Dark yellowish orange 10YR 6/6 to Pale brown 5YR 5/2
HLS-041	Vats (T#148)	shaped stone	sandy	Dark GOLDEN orange 10YR 6/6
HLS-042	Vats (T#149)	shaped stone	sandy	Dark GOLDEN orange 10YR 6/6
HLS-043	Vats (T#150)	shaped stone	sandy	Dark GOLDEN orange 10YR 6/6
HLS-044	Vats # 4534	shaped stone	sandy	Dark GOLDEN orange 10YR 6/6
HLS-045	Vats (T#152)	shaped stone	sandy	Dark GOLDEN orange 10YR 6/6
HLS-046	HM#10548	shaped stone	sandy	Dark GOLDEN orange 10YR 6/6
HLS-047	HM#88798	door pivot?	fine sandy	Grayish Orange 10YR 7/4 (BANDED group)
HLS-048	H96/7401-2	fragment	fine sandy	Moderate reddish brown 10R 3/4 (GOLDEN group)
HLS-049	H96/7307-1	ringstone fragment	fine sandy	Moderate reddish brown 10R 3/4 (GOLDEN group)
HLS-050	H98/8334-4	fragment	fine sandy	Pale reddish brown 10R 5/4 (GOLDEN group)
HLS-051	H98/8334-3	fragment	fine sandy	Pale reddish brown 10R 5/4 (GOLDEN group)
HLS-052	H2000/2088-101	fragment	MICRITIC	Pale brown 5YR 5/2 to Grayish red 5R 4/2
HLS-053	H2000/2109-19	fragment	MICRITIC	Grayish orange 10YR 7/4
HLS-054	H95/4962-27	fragment	MICRITIC	Grayish orange 10YR 7/4 with some black spots
HLS-055	H93/3892-82	drain cover?	MICRITIC	Pale yellowish brown 10 YR 6/2 to Grayish orange 10YR 7/4
HLS-056	H93/4051-12	fragment	sandy	Grayish Orange 10YR 7/4 (BANDED group)
HLS-057	H96/6251	fragment	MICRITIC	Grayish Orange 10YR 7/4 to Very pale orange 10YR 8/2
HLS-058	H94/3990-19	fragment	MICRITIC	Grayish Orange 10YR 7/4
HLS-060	H95/4719-1	fragment	MICRITIC	Dark yellowish orange 10YR 6/6 to Grayish Orange 10YR 7/4
HLS-061	H99/8394-20	fragment	MICRITIC	Grayish Orange 10YR 7/4
HLS-062	Vats (6098)	shaped stone	sandy	Very dusky purple 5RP 2/2 to GRAYish red purple 5RP 4/2
HLS-063	Vats (T#146)	shaped stone	sandy	Very dusky purple 5RP 2/2 to GRAYish red purple 5RP 4/2
HLS-064	Vats (T#141)	shaped stone	fine sandy	Brownish GRAY 5YR 4/1
HLS-065	T#130 (B-7)	shaped stone	sandy crystalline	GRAYish purple 5P 4/2 to Grayish red purple 5RP 4/2
HLS-066	H2001/11810-4	ringstone broken	sandy crystalline	GRAYish purple 5P 4/2 to Grayish red purple 5RP 4/2
HLS-067	Vats (T#140)	shaped stone	sandy crystalline	GRAYish purple 5P 4/2 to Grayish red purple 5RP 4/2

sample #	artifact #	artifact type	texture	color
HLS-068	H98/8313-117	fragment	MICRITIC	Dark reddish brown 10R 3/4
HLS-069	H98/8306-126	ringstone fragment	fine sandy	Dark yellowish orange 10YR 6/6 (GOLDEN group)
HLS-071	H99/8759-3	fragment	chalky	WHITE N9
HLS-072	H98/8603-41	fragment	chalky	WHITE N9
HLS-073	H2003-9904-16	fragment	chalky	WHITE N9
HLS-075	H2000/2748-13	fragment	chalky	WHITE N9
HLS-076	H2000/9846-20	fragment	chalky	WHITE N9
HLS-077	H2000/2763-28	fragment	chalky	WHITE N9
HLS-079	Vats (no #)	large cone	chalky	WHITE N9
HLS-080	Vats (no #)	large cone	chalky	WHITE N9
HLS-081	Vats (B1514)	bull sculpture fragment	fine sandy crystalline	Brownish GRAY 5YR 4/1
HLS-082	H2000/9880-75	shaped stone	fine sandy crystalline	GRAYish red purple 5RP 4/2
HLS-083	H99/9413-73	fragment	fine sandy	Moderate reddish brown 10R 4/6 (GOLDEN group)
HLS-084	H99/8387-96	fragment	MICRITIC	Moderate yellowish brown 10YR 5/4
HLS-085	H99/8939-228	shaped stone	crystalline	Dark yellowish brown 10YR 4/2 (BANDED group)
HLS-086	H98/8331-69	fragment	fine sandy	GRAYish red 10R 4/2
HLS-087	H98/8307-2	shaped stone	fine sandy	Moderate reddish brown 10R 4/6 (GRAY group)
HLS-088	H98/8323-12	fragment	fine sandy	GRAYish red purple 5RP 4/2
HLS-089	H98/8324-11	shaped	fine sandy	GRAYish red purple 5RP 4/2
HLS-090	H98/8438-8	shaped stone	fine sandy crystalline	Brownish GRAY 5YR 4/1
HLS-091	H98/8321-1	ringstone fragment	fine sandy crystalline	GRAYish red purple 5RP 4/2
HLS-093	Vats (T#121)	shaped stone	sandy crystalline	Dark reddish brown 10R 3/4 (GRAY group)
HLS-094	Vats (T#143)	shaped stone	fine sandy crystalline	GRAYish red 10R 4/2 to Pale reddish brown 10R 5/4
HLS-096	Vats (T#99)	shaped stone	fine sandy	Moderate reddish brown 10R 4/6 (GRAY group)
HLS-097	H98/8306-21	wavy ringstone fragment	fine sandy crystalline	Brownish GRAY 5YR 4/1
HLS-098	Vats (T#105)	shaped stone	fine sandy	Pale reddish brown 10R 5/4 (GRAY group)
HLS-099	Vats (T#142)	shaped stone	fine sandy crystalline	GRAY red purple 5RP 4/2
HLS-100	Vats (T#133)	shaped stone	fine sandy crystalline	Brownish GRAY 5YR 4/1
HLS-101	H98/8306-256	fragment	sandy crystalline	GRAYish red purple 5RP 4/2
HLS-102	H98/8306-23	shaped stone	fine sandy crystalline	Medium GRAY N5
HLS-103	H98/9724-50	fragment	sandy crystalline	Grayish red 10R 4/2 (BANDED group)
HLS-104	Vats (T#116)	shaped stone	sandy crystalline	Medium GRAY N5
HLS-105	Vats T#123	shaped stone	sandy crystalline	Medium GRAY N5
HLS-106	Vats (T#124)	shaped stone	sandy crystalline	Medium GRAY N5
HLS-107	Vats (T#125)	shaped stone	sandy crystalline	Medium GRAY N5
HLS-108	Vats (T#126)	shaped stone	sandy crystalline	Medium GRAY N5

sample #	artifact #	artifact type	texture	color
HLS-109	Vats (T#128)	shaped stone	sandy crystalline	Medium GRAY N5
HLS-110	Vats (T#134)	shaped stone	sandy crystalline	Medium GRAY N5
HLS-111	Vats (T#136)	shaped stone	sandy crystalline	Medium GRAY N5
HLS-112	Vats (T#138)	shaped stone	sandy crystalline	Medium GRAY N5
HLS-113	Vats (T#139)	shaped stone	sandy crystalline	Medium GRAY N5

APPENDIX 11.2

RESULTS OF ICP-MS ANALYSIS OF THE INITIAL LIMESTONE SET

Elemental data in parts per million (ppm).

Sample	Ca	Sr	Ba	La	Ce
DLS-001	126265	111.97	17.37	11.133	19.082
DLS-002	157405	105.69	9.21	4.446	8.1
DLS-003	161388	115.74	22.57	10.248	11.392
DLS-004	99358	72	10.81	5.513	9.442
DLS-005	143223	172.17	2.57	7.791	11.947
DLS-006	133571	87.46	4.77	8.914	11.397
DLS-007	165081	109.55	14.22	12.909	16.916
DLS-008	194331	144.58	7.54	8.428	12.008
DLS-009	152483	148.9	17.15	15.346	23.635
DLS-010	174448	142.9	17.94	12.623	21.246
DLS-011	140829	119.04	10.03	9.405	15.091
DLS-012	129642	103.62	10.05	9.353	15.044
DLS-013	106197	93.09	16.27	25.333	40.449
DLS-014	158871	110.27	9.86	5.012	9.196
DLS-015	133821	102.24	4.77	5.654	7.965
JLS-001	115093	94.06	30.71	8.998	13.122
JLS-002	122255	59.73	12.32	2.566	5.343
JLS-003	127799	75.06	40.12	14.717	23.336
JLS-004	100394	57.25	23.75	12.64	22.023
JLS-005	104493	52.84	8.71	2.729	5.638
JLS-006	113054	31.39	13.85	2.641	5.521
JLS-007	111399	36.48	14.41	2.132	3.672
JLS-008	158288	50.41	22.13	3.14	6.747
JLS-009	134817	50.39	32.36	2.13	4.57
JLS-010	130113	37.68	19.87	4.837	8.714
JLS-011	161734	54.85	27.52	4.015	7.23
JLS-012	127905	62.45	14.29	3.529	6.058
JLS-013	126719	42.05	13.62	2.769	5.856
JLS-014	124329	47.82	10.47	1.97	3.84
JLS-015	114492	43.7	10.35	1.697	3.288
HLS-1	128037	123.43	6.22	11.757	20.015
HLS-2	162785	130.42	3.18	7.276	9.281
HLS-3	211961	282.91	1.16	3.589	6.5
HLS-4	140026	106.84	27.59	1.271	2.319
HLS-5	123213	85.05	14.29	8.217	10.153
HLS-6	114826	57.9	13.55	4.17	4.939

APPENDIX 11.3

RESULTS OF INAA ANALYSIS OF THE INITIAL LIMESTONE SET

Elemental data in parts per million (ppm).

Sample	Al	Ca	Eu	Fe	La	Lu	Mg	Mn	Sr	V
DLS-001	2953	387460	1.33	34363	27.1	0.333	1375	1254	226.1	85.5
DLS-002	2343	408878	0.35	29846	9.7	0.099	838	477	165.6	22.7
DLS-003	6115	335005	1.68	115292	25.8	0.461	1828	837	111.7	84.2
DLS-004	2385	330933	1.11	72417	37.3	0.184	980	1447	137.3	96.2
DLS-005	1743	422005	0.49	11532	9.7	0.095	800	506	114	18.3
DLS-006	1613	412840	0.44	15918	8.9	0.095	538	500	60.4	13.7
DLS-007	1062	385372	0.30	8931	6.1	0.066	730	397	101.2	15.1
DLS-008	1515	386199	0.37	19605	8.1	0.087	603	458	158	18
DLS-009	1084	375720	0.32	12390	6.6	0.061	592	506	206.2	11.2
DLS-010	3706	375126	0.78	32575	12.8	0.149	713	511	85.4	43
DLS-011	1572	375008	0.31	8983	8.6	0.079	689	474	141.9	18.8
DLS-012	835	380274	0.32	29853	10.2	0.069	741	776	513.9	18.6
DLS-013	1484	371777	0.39	20953	9.2	0.087	641	434	140.2	16.3
DLS-014	947	388769	0.30	9908	8.9	0.059	623	388	207.2	12.3
DLS-015	1162	426359	0.27	10819	7.2	0.061	827	496	168.7	14
JLS-1	3784	342954	1.66	69959	31.0	0.399	1627	1197	442.8	103.1
JLS-2	3274	405748	0.60	11131	8.9	0.14	1000	633	593.1	62.3
JLS-3	1527	399216	0.77	14250	19.4	0.208	1509	885	552.4	23.5
JLS-4	13750	276295	0.78	10512	21.3	0.171	1430	1225	671.7	34.8
JLS-5	2659	379185	0.93	14376	19.0	0.215	1827	921	973.9	37.6
JLS-6	2008	410254	1.04	12230	23.9	0.246	958	691	363.4	28
JLS-7	2350	393629	1.04	12776	27.4	0.225	1057	691	317.9	26.6
JLS-8	1873	336543	0.60	12989	18.0	0.147	1184	644	412.8	13.6
JLS-9	4388	289262	1.47	49190	33.8	0.445	1347	1083	405.9	111.2
JLS-11	3584	311337	1.14	66718	26.6	0.347	1447	1129	381.6	87
JLS-12	3526	304023	1.15	53360	30.9	0.344	1528	924	444.2	80.1
JLS-13	3264	300605	1.20	81419	31.2	0.332	1094	1274	360	95.4
JLS-14	3627	317203	0.53	38173	8.5	0.213	1173	730	775.8	98.2
JLS-15	1794	350108	0.60	12216	16.7	0.129	1022	648	363.7	12.8
HLS-1	4119	344665	1.78	14462	7.1	0.071	1773	784	650.4	99.4
HLS-2	1811	396031	1.02	16654	7.7	0.088	1539	589	499.2	27.1
HLS-3	254	391304	0.85	178904	27.4	0.241	1128	285	738.8	307.2
HLS-4	1245	399206	0.06	14667	7.1	0.071	1101	563	313.2	15.7
HLS-5	1382	368002	0.61	11476	16.1	0.123	1572	623	213.9	22.7
HLS-6	1251	416175	0.49	10618	12.5	0.102	1165	682	159.3	13.3

APPENDIX 11.4

RESULTS OF ICP-AES ANALYSIS OF THE EXPANDED GEOLOGIC LIMESTONE SAMPLE SET

Elemental data in parts per million (ppm).

Sample#	Region	Location	Ca	Ba	Sr	Fe	Mg
DLS-001	Kutch/Khadir Island	Harappan quarry	331063	112.13	360	17894	2726
DLS-002	Kutch/Khadir Island	Harappan quarry	397579	283.45	244	7753	1962
DLS-003	Kutch/Khadir Island	Harappan quarry	367466	108.52	287	6714	1971
DLS-004	Kutch/Khadir Island	Harappan quarry	226195	50.21	168	4987	1195
DLS-005	Kutch/Khadir Island	Harappan quarry	353926	145.2	532	12601	2985
DLS-006	Kutch/Khadir Island	Harappan quarry	365226	20.57	269	7637	1831
DLS-007	Kutch/Khadir Island	Harappan quarry	367289	117.81	276	7611	1913
DLS-008	Kutch/Khadir Island	Harappan quarry	390535	98.91	323	8403	2034
DLS-009	Kutch/Khadir Island	Harappan quarry	277943	152.26	272	22480	2544
DLS-010	Kutch/Khadir Island	Harappan quarry	351698	63.38	312	8230	3493
DLS-011	Kutch/Khadir Island	Harappan quarry	337063	37.82	310	15197	2427
DLS-012	Kutch/Khadir Island	Harappan quarry	336488	49.62	311	10661	2502
DLS-013	Kutch/Khadir Island	Harappan quarry	379955	44.2	361	14142	2911
DLS-014	Kutch/Khadir Island	Harappan quarry	359622	40.87	242	25333	2259
DLS-015	Kutch/Khadir Island	Harappan quarry	415959	28.04	348	8111	2205
DLS-016	Kutch/Khadir Island	Harappan quarry	434542	41.27	300	4813	2623
DLS-017	Kutch/Khadir Island	Harappan quarry	463583	37.95	377	6323	3332
DLS-018	Kutch/Khadir Island	Harappan quarry	299004	143.82	500	23211	3162
DLS-019	Kutch/Khadir Island	Harappan quarry	462375	30.16	360	8223	3060
DLS-020	Kutch/Khadir Island	Harappan quarry	441406	26.83	354	8192	3087
DLS-021	Kutch/Khadir Island	Harappan quarry	448342	22.67	344	8070	3074
DLS-022	Kutch/Khadir Island	Harappan quarry	407298	133.77	298	15167	3363
DLS-023	Kutch/Khadir Island	Harappan quarry	428826	29.34	299	27596	2596
DLS-024	Kutch/Khadir Island	Harappan quarry	410185	26.42	378	11325	2849
DLS-025	Kutch/Khadir Island	Harappan quarry	352952	37.39	287	8285	2489
DLS-026	Kutch/Khadir Island	Harappan quarry	387533	57.5	262	7264	2382
DLS-027	Kutch/Khadir Island	Harappan quarry	374897	29.57	393	14845	5600
DLS-028	Kutch/Khadir Island	Harappan quarry	276460	44.4	201	2436	1682
DLS-029	Kutch/Khadir Island	Harappan quarry	275510	18.45	243	1785	2504
DLS-030	Kutch/Khadir Island	Harappan quarry	259520	21.69	230	1748	1971
LTH-001	Kutch/Khadir Island	Limdiwali Tari	341565	13.26	264	2217	1867
LTH-002	Kutch/Khadir Island	Limdiwali Tari	332137	37.03	313	1550	2141
LTH-003	Kutch/Khadir Island	Limdiwali Tari	313953	41.56	225	1207	1645
LTH-004	Kutch/Khadir Island	Limdiwali Tari	328832	58.41	270	1367	2110

Sample#	Region	Location	Ca	Ba	Sr	Fe	Mg
LTH-005	Kutch/Khadir Island	Limdiwali Tari	341857	23.9	264	2835	2180
LTH-006	Kutch/Khadir Island	Limdiwali Tari	319302	56.21	399	1906	1999
LTH-007	Kutch/Khadir Island	Limdiwali Tari	305745	29.39	245	1654	1985
LTH-008	Kutch/Khadir Island	Limdiwali Tari	317857	34.49	258	2223	1827
LTH-009	Kutch/Khadir Island	Limdiwali Tari	301952	118	241	1183	1262
LTH-010	Kutch/Khadir Island	Limdiwali Tari	310043	18.19	247	1494	1915
LTH-011	Kutch/Khadir Island	Limdiwali Tari	318406	105	255	1314	1487
LTH-012	Kutch/Khadir Island	Limdiwali Tari	316330	38.11	277	1555	2025
LTH-013	Kutch/Khadir Island	Limdiwali Tari	310133	28.79	241	1908	1696
LTH-014	Kutch/Khadir Island	Limdiwali Tari	299548	50.96	233	1919	1841
LTH-015	Kutch/Khadir Island	Limdiwali Tari	321422	57.56	391	1836	2027
P-001	Kutch/Pachchham I.	near Juni Kuran	268205	35.22	337	2864	2466
P-002	Kutch/Pachchham I.	near Juni Kuran	224788	35.53	263	2904	1674
P-003	Kutch/Pachchham I.	near Juni Kuran	330452	3.53	354	2205	1476
P-004	Kutch/Pachchham I.	near Juni Kuran	318651	7.23	343	1226	1401
P-005	Kutch/Pachchham I.	near Juni Kuran	303873	18.25	271	1296	1309
P-006	Kutch/Pachchham I.	near Juni Kuran	333266	6.18	341	1409	1392
P-007	Kutch/Pachchham I.	near Juni Kuran	240965	127	323	2778	36712
P-008	Kutch/Pachchham I.	near Juni Kuran	316300	41.45	293	1454	1542
P-009	Kutch/Pachchham I.	near Juni Kuran	309071	180	404	2448	2067
P-010	Kutch/Pachchham I.	near Juni Kuran	283928	53.86	285	1475	1418
P-011	Kutch/Pachchham I.	near Juni Kuran	267741	11.99	446	4733	1760
P-012	Kutch/Pachchham I.	near Juni Kuran	207755	10.99	261	3129	1271
P-013	Kutch/Pachchham I.	near Juni Kuran	300556	66.75	245	12203	1602
P-014	Kutch/Pachchham I.	near Juni Kuran	199705	10.85	329	4454	1526
P-015	Kutch/Pachchham I.	near Juni Kuran	133109	6.57	97	1871	658
P-016	Kutch/Pachchham I.	near Juni Kuran	135284	13.75	226	2718	927
P-017	Kutch/Pachchham I.	near Juni Kuran	133096	5.95	178	5115	1278
P-018	Kutch/Pachchham I.	near Juni Kuran	233959	23.49	200	12019	1946
P-019	Kutch/Pachchham I.	near Juni Kuran	187688	12.33	218	3294	1276
P-020	Kutch/Pachchham I.	near Juni Kuran	125505	16.02	206	1921	979
JLS-001	Rajasthan-Jaisalmer	Mool Sagar Khan	389975	319	316	10946	2503
JLS-002	Rajasthan-Jaisalmer	Jethway	414757	33.63	262	6327	1794
JLS-003	Rajasthan-Jaisalmer	Mool Sagar Khan	338291	131	241	15292	2486
JLS-004	Rajasthan-Jaisalmer	Mool Sagar Khan	309427	59.57	239	13406	1659
JLS-005	Rajasthan-Jaisalmer	Jethway	376232	19.86	208	3827	1400
JLS-006	Rajasthan-Jaisalmer	Jethway	405651	24.06	127	2981	935
JLS-007	Rajasthan-Jaisalmer	Jethway	386713	58.17	141	3606	1061
JLS-008	Rajasthan-Jaisalmer	Jethway	359132	71.78	135	3316	955
JLS-009	Rajasthan-Jaisalmer	Jethway	359295	128.9	155	3222	1024
JLS-010	Rajasthan-Jaisalmer	Mool Sagar Khan	332607	62.93	105	5300	979

Sample#	Region	Location	Ca	Ba	Sr	Fe	Mg
JLS-011	Rajasthan-Jaisalmer	Mool Sagar Khan	387637	50.9	151	3345	1190
JLS-012	Rajasthan-Jaisalmer	Mool Sagar Khan	367296	27.97	198	3649	1623
JLS-013	Rajasthan-Jaisalmer	Jethway	374355	27.64	135	3439	955
JLS-014	Rajasthan-Jaisalmer	Jethway	354914	43.08	150	3901	943
JLS-015	Rajasthan-Jaisalmer	Jethway	383276	17.98	164	4437	1012
JLS-016	Rajasthan-Jaisalmer	Jethway	417839	158.6	243	4353	2086
JLS-017	Rajasthan-Jaisalmer	Jethway	464355	76.82	190	3566	2016
JLS-018	Rajasthan-Jaisalmer	Jethway	515504	20.29	281	3148	2163
JLS-019	Rajasthan-Jaisalmer	Jethway	462682	96.23	208	3483	2814
JLS-020	Rajasthan-Jaisalmer	Jethway	277235	85.01	152	1140	1468
JLS-021	Rajasthan-Jaisalmer	Jethway	284176	47.59	117	729	1161
JLS-022	Rajasthan-Jaisalmer	Jethway	303138	24.64	134	665	1143
JLS-023	Rajasthan-Jaisalmer	Habur	271288	66.41	129	630	1146
JLS-024	Rajasthan-Jaisalmer	Habur	280923	38.85	167	932	1283
JLS-025	Rajasthan-Jaisalmer	Habur	314692	43.75	199	2709	1727
JLS-026	Rajasthan-Jaisalmer	Habur	276003	30.13	142	786	1329
JLS-027	Rajasthan-Jaisalmer	Habur	220158	32.1	127	647	1076
JLS-028	Rajasthan-Jaisalmer	Habur	279734	27.42	148	1177	1310
JLS-029	Rajasthan-Jaisalmer	Habur	258038	29.78	150	3109	1234
JLS-030	Rajasthan-Jaisalmer	Habur	371593	31.4	151	2788	1071
JLS-031	Rajasthan-Jaisalmer	Habur	273143	59.61	197	2147	1516
JLS-032	Rajasthan-Jaisalmer	Habur	346034	40.67	152	1133	996
JLS-033	Rajasthan-Jaisalmer	Habur	296821	39.86	191	1005	1410
JLS-034	Rajasthan-Jaisalmer	Habur	338900	79.17	231	1731	1615
JLS-035	Rajasthan-Jaisalmer	Habur	348362	32.21	107	788	868
JLS-036	Rajasthan-Jaisalmer	Mool Sagar Khan	308686	64.13	146	1019	1287
JLS-037	Rajasthan-Jaisalmer	Mool Sagar Khan	340784	37.42	127	826	948
JLS-038	Rajasthan-Jaisalmer	Mool Sagar Khan	140094	77.9	104	694	622
JLS-039	Rajasthan-Jaisalmer	Mool Sagar Khan	337400	20.66	103	730	855
JLS-040	Rajasthan-Jaisalmer	Mool Sagar Khan	296738	31.69	96	880	1194
JLS-041	Rajasthan-Jaisalmer	Jethway	337982	61.65	219	2024	1631
JLS-042	Rajasthan-Jaisalmer	Jethway	347986	42.89	153	1139	996
JLS-043	Rajasthan-Jaisalmer	Jethway	361109	27.27	158	1155	1069
JLS-044	Rajasthan-Jaisalmer	Habur	340108	28.28	209	1196	1441
JLS-045	Rajasthan-Jaisalmer	Habur	344640	21.11	146	1114	1003
JLS-046	Rajasthan-Jaisalmer	Habur	350774	20.56	148	1136	1022
JLS-047	Rajasthan-Jaisalmer	Habur	323617	36.96	120	834	885
JLS-048	Rajasthan-Jaisalmer	Habur	330826	48.3	154	1077	1157
JLS-049	Rajasthan-Jaisalmer	Habur	343405	11.19	192	745	1297
JLS-050	Rajasthan-Jaisalmer	Habur	319604	73.75	234	2245	1819
JLS-051	Rajasthan-Jaisalmer	Amar Sagar	208001	107.12	202	1003	1526

Sample#	Region	Location	Ca	Ba	Sr	Fe	Mg
JLS-052	Rajasthan-Jaisalmer	Amar Sagar	348387	33.19	130	886	951
JLS-053	Rajasthan-Jaisalmer	Amar Sagar	318835	33.13	135	970	992
JLS-054	Rajasthan-Jaisalmer	Amar Sagar	290826	37.75	112	941	1220
JLS-055	Rajasthan-Jaisalmer	Amar Sagar	306224	46.43	182	1552	1448
JLS-056	Rajasthan-Jaisalmer	Amar Sagar	309604	37.19	194	1042	1512
JLS-057	Rajasthan-Jaisalmer	Amar Sagar	321373	30.57	167	1056	1144
JLS-058	Rajasthan-Jaisalmer	Amar Sagar	331589	48.96	219	1705	1744
JLS-059	Rajasthan-Jaisalmer	Amar Sagar	334251	38.44	189	1237	1362
JLS-060	Rajasthan-Jaisalmer	Amar Sagar	474903	46.64	190	2762	1763
RHLS-001	Sindh - Rohri Hills	Nara near Thari	487384	60.82	691	320	2125
RHLS-002	Sindh - Rohri Hills	Nara near Thari	519208	29.14	925	524	2366
RHLS-003	Sindh - Rohri Hills	Kandarki	500046	27.45	870	341	1622
RHLS-004	Sindh - Rohri Hills	Adam Sultan	493414	30.81	1540	873	2265
RHLS-005	Sindh - Rohri Hills	Adam Sultan	452711	23.79	2074	1053	6753
RHLS-006	Sindh - Rohri Hills	Rohri	507840	23.01	746	334	1713
RHLS-007	Sindh - Rohri Hills	Rohri	499546	21.32	597	4468	1451
RHLS-008	Sindh - Rohri Hills	Kot Diji	493205	36.77	984	730	1946
RHLS-009	Sindh - Rohri Hills	Kot Diji	512351	62.04	1270	906	1965
RHLS-010	Sindh - Rohri Hills	Kot Diji	538777	46.84	1447	834	2510
RHLS-011	Sindh - Rohri Hills	Kot Diji	522827	36.52	1282	686	2437
RHLS-012	Sindh - Rohri Hills	Kot Diji	479314	40.9	1363	767	3787
RHLS-013	Sindh - Rohri Hills	Kot Diji	486996	28.03	1707	769	2200
RHLS-014	Sindh - Rohri Hills	Kot Diji	506259	41.62	1251	545	1737
RHLS-015	Sindh - Rohri Hills	Kot Diji	502324	36.76	654	749	1642
RHLS-016	Sindh - Rohri Hills	Kot Diji	495404	36.62	618	487	1548
RHLS-017	Sindh - Rohri Hills	Adam Sultan	451690	22.28	1968	913	6821
RHLS-018	Sindh - Rohri Hills	Nara near Thari	509239	27.13	865	567	2342
RHLS-019	Sindh - Rohri Hills	Kot Diji	506344	50.86	769	629	1676
RHLS-020	Sindh - Rohri Hills	Kot Diji	498539	57.28	1695	557	2039
RHLS-021	Sindh - Rohri Hills	Kot Diji	475943	45.82	1825	1214	2649
RHLS-022	Sindh - Rohri Hills	Kot Diji	509014	31.26	1203	521	2269
RHLS-023	Sindh - Rohri Hills	Kot Diji	491319	34.7	978	571	1723
RHLS-024	Sindh - Rohri Hills	Kot Diji	488056	39.32	1215	865	2242
RHLS-025	Sindh - Rohri Hills	Kot Diji	493299	75.23	1449	596	2111
GJLS-1	Gujarat - Junagadh	Adityana	486320	53.6	2214	1996	5618
GJLS-2	Gujarat - Junagadh	Adityana	427030	76.03	857	2799	4893
GJLS-3	Gujarat - Junagadh	Adityana	431957	103.49	1928	4502	7307
GJLS-4	Gujarat - Junagadh	Adityana	416530	75.67	1028	3389	5449
GJLS-5	Gujarat - Junagadh	Adityana	464294	114.38	2754	3892	7937
LPLS-1	Balochistan - Loralai	Loralai Town	423434	80.54	886	1252	1909
LPLS-2	Balochistan - Loralai	Loralai Town	452280	80.01	957	1094	1734

Sample#	Region	Location	Ca	Ba	Sr	Fe	Mg
LPLS-3	Balochistan - Loralai	Loralai Town	502506	90.63	1096	1241	1913
KRLS-001	Sindh - Kirthar	Ranikot	455785	334.21	679	8764	2867
KRLS-002	Sindh - Kirthar	Ranikot	446144	619.91	631	7162	2547

APPENDIX 11.5

RESULTS OF ICP-AES ANALYSIS OF THE EXPANDED HARAPPAN LIMESTONE SAMPLE SET

Elemental data in parts per million (ppm).

MSK = Mool Sagar Khan (Jaisalmer Formation)

Sample#	Mound	Trench	Period	Probable geologic provenience	Ca	Ba	Sr	Fe	Mg
HLS-001	AB-E	53	3+	Pachchham Fm. – Khadir quarry	357994	16.91	400.1	23213	2541
HLS-002	n/a	n/a	n/a	Pachchham Fm. – Juni Kuran	379903	7.59	335	7285	2099
HLS-003	E	54	3+	Unclear at this time * not Rohri Hills	398604	0.01	600.4	773	1177
HLS-004	E	56	3+	Pachchham Fm. – Khadir quarry	406386	139.78	353.1	7384	2098
HLS-005	E	54	3+	Pachchham Fm. – Khadir * possibly MSK	373805	88.14	296.2	8190	2231
HLS-006	AB	31	3+	Pachchham Fm. – Khadir quarry	405231	34.94	273.8	9520	1784
HLS-007	n/a	n/a	n/a	Pachchham Fm. – Khadir quarry	403443	33.5	366.1	9868	3585
HLS-008	ET	Thana	n/a	Pachchham Fm. – Khadir quarry	455098	30.71	376.6	8306	3035
HLS-009	E	36	3C	Sindh – Rohri Hills	522709	29.77	668.8	635	2068
HLS-010	E	46	3C	Sindh – Rohri Hills	536330	119.5	255.7	407	2345
HLS-011	ET	surf	3+	Pachchham Fm. – Khadir quarry	471586	30.01	337.9	6470	2722
HLS-012	E	7	3+	Pachchham Fm. – Khadir quarry	430884	24.95	381.1	7914	3381
HLS-013	E	8	3C	Pachchham Fm. – Khadir quarry	458575	29.32	344.2	8126	2745
HLS-014	E	8	3C	Pachchham Fm. – Khadir quarry	466838	25.84	336.1	6934	3170
HLS-015	AB	mosque	3+	Pachchham Fm. – Khadir * possibly MSK	502028	29.49	318	4894	2614
HLS-016	E	7_8	3C	Pachchham Fm. – Khadir quarry	469517	33.91	427.2	8303	3965
HLS-017	ET	28	3C	Pachchham Fm. – Juni Kuran	475755	52.13	450.5	5945	2931
HLS-018	E	7_8	3+	Pachchham Fm. – Khadir quarry	433480	39.56	318.6	16011	3311
HLS-019	E	7_8	3+	Pachchham Fm. – Khadir quarry	436903	163.6	344.1	8640	3280
HLS-020	E	7_8	3C	Jaisalmer Fm. – Mool Sagar Khan	481506	94.33	302.4	7358	2440
HLS-021	AB	31	3C	Pachchham Fm. – Khadir quarry	437755	46.3	329.3	7861	2816
HLS-022	E	36	3+	Pachchham Fm. – Juni Kuran	455274	36.98	516.1	7217	4976
HLS-023	F	37	3+	Jaisalmer Fm. – Mool Sagar Khan	419655	105.34	292.3	7727	2588
HLS-024	AB	39	3+	Pachchham Fm. – Khadir * possibly MSK	294439	33.41	199.3	3960	1892
HLS-025	AB	39	3+	Pachchham Fm. – Khadir quarry	495416	58.79	388.8	7411	2438
HLS-026	AB	39	3C	Pachchham Fm. – Limdiwali Tari	489313	31.27	372.7	4957	2606

Sample#	Mound	Trench	Period	Probable geologic provenience	Ca	Ba	Sr	Fe	Mg
HLS-027	AB	39	3C	Pachchham Fm. – Khadir quarry	509927	23.13	341.5	6270	2996
HLS-028	AB	39	3C	Pachchham Fm. – Juni Kuran	477468	24.12	363	4559	2596
HLS-029	AB	39	3C	Pachchham Fm. – Khadir quarry	418869	49.56	524.4	13356	3401
HLS-030	AB	39	3+	Pachchham Fm. – Khadir quarry	493072	49.68	368.9	9005	2944
HLS-031	AB	39	3C	Pachchham Fm. – Khadir quarry	426012	62.91	370.8	13621	3087
HLS-032	AB	39	3C	Pachchham Fm. – Khadir quarry	432848	29.21	310.5	6001	2539
HLS-033	AB	39	3+	Pachchham Fm. – Khadir quarry	449283	21.94	299.4	4610	2615
HLS-034	AB	39	3C	Pachchham Fm. – Khadir quarry	411862	23.31	307.6	7671	3188
HLS-035	AB	39	3+	Pachchham Fm. – Juni Kuran	462867	55.6	462.7	6686	2428
HLS-036	AB	39	3+	Pachchham Fm. – Khadir quarry	419103	29.07	404.5	8677	4373
HLS-037	F	43	3C	Pachchham Fm. – Khadir quarry	409903	34.95	353	14722	3562
HLS-038	F	43	3C	Pachchham Fm. – Khadir * possibly MSK	455116	25.57	294.6	5114	2532
HLS-039	E	54	3+	Jaisalmer Fm. – Mool Sagar Khan	491088	75.53	333.8	6808	2670
HLS-040	E	56	3+	Pachchham Fm. – Khadir quarry	429730	60.62	309.6	11222	2629
HLS-041	AB	B	3C+	Pachchham Fm. – Khadir * possibly MSK	490547	28.21	330.6	7478	2958
HLS-042	AB	B	3C+	Pachchham Fm. – Khadir * possibly MSK	379237	36.78	258.8	4079	2304
HLS-043	AB	B	3C+	Jaisalmer Fm. – Mool Sagar Khan	449342	53.06	259.9	7175	2455
HLS-044	AB	B	3C+	Pachchham Fm. – Khadir * possibly MSK	460706	136.71	386.5	6080	2930
HLS-045	AB	B	3C+	Pachchham Fm. – Khadir quarry	499251	24.02	365.4	5328	2922
HLS-046	AB	B	3C+	Jaisalmer Fm. – Mool Sagar Khan	497680	283.14	435.5	5755	3343
HLS-047	AB	B	3C+	Jaisalmer Fm. – Mool Sagar Khan	454710	147.01	347	7952	3380
HLS-048	AB	39	3+	Jaisalmer Fm. – Mool Sagar Khan	470980	168.86	267.6	10698	2480
HLS-049	AB	38	3+	Pachchham Fm. – Khadir * possibly MSK	489322	54.49	471.8	10000	3130
HLS-050	AB	39	3+	Pachchham Fm. – Khadir quarry	467789	51.62	431.6	7392	2739
HLS-051	AB	39	3+	Pachchham Fm. – Khadir quarry	519683	248.09	584.6	4485	1885
HLS-052	E	54	3+	Unclear at this time * not Rohri Hills	542850	268.41	565.6	1639	1773
HLS-053	E	54	3+	Unclear at this time * not Rohri Hills	540505	26.7	663	749	2107
HLS-054	ET	28	3+	Sindh – Rohri Hills	12058.4	141.01	62.5	2785	747
HLS-055	E	8	3C	Unclear at this time * not Rohri Hills	491707	30.58	578.2	1890	6025
HLS-056	ET	10W	3+	Pachchham Fm. – Juni Kuran	514765	101.62	622.4	865	2230
HLS-057	E	36	3+	Sindh – Rohri Hills	527199	66.14	481.4	1157	1777

Sample#	Mound	Trench	Period	Probable geologic provenience	Ca	Ba	Sr	Fe	Mg
HLS-058	E	7_8	3C	Sindh – Rohri Hills	54114.8	171.38	108.2	589	732
HLS-060	ET	19W	3C	Sindh – Rohri Hills	529073	173.03	778.9	476	2123
HLS-061	AB	39	3+	Sindh – Rohri Hills	262116	43.52	375.6	400	1076
HLS-062	AB	B	3C+	Pachchham Fm. – Juni Kuran	482366	66.02	643.7	8119	3906
HLS-063	AB	B	3C+	Pachchham Fm. – Juni Kuran	483640	105.46	734.6	8454	4397
HLS-064	AB	B	3C+	Pachchham Fm. – Khadir quarry	454805	43.39	402	10315	3249
HLS-065	AB	B	3C+	Pachchham Fm. – Juni Kuran	494695	38.9	539.7	7560	4804
HLS-066	E	11	3C	Pachchham Fm. – Juni Kuran	527899	193.84	968.2	9021	4597
HLS-067	AB	B	3C+	Pachchham Fm. – Juni Kuran	534131	36.48	869.1	7237	3978
HLS-068	AB	39	3+	Unclear at this time * not Rohri Hills	152550	138.23	492.7	47100	5491
HLS-069	AB	39	3+	Pachchham Fm. – Khadir quarry	526037	30.59	381.4	6143	3131
HLS-071	F	43	3C	Unclear * possibly Rohri Hills or Parh Fm.	557303	60.45	1305	447	2686
HLS-072	F	43	3+	Unclear * possibly Rohri Hills or Parh Fm.	510501	32.98	1210.7	262	4577
HLS-073	n/a	n/a	3C+	Unclear * possibly Rohri Hills or Parh Fm.	493182	30.71	572.4	294	2191
HLS-075	E	55	3C	Unclear * possibly Rohri Hills or Parh Fm.	554604	53.8	1180.9	192	2778
HLS-076	E	43	3C	Unclear * possibly Rohri Hills or Parh Fm.	498653	30.81	1839.4	300	3332
HLS-077	E	55	3C	Unclear * possibly Rohri Hills or Parh Fm.	502045	61.41	1217.6	217	2585
HLS-079	AB	Vats III & IV	3C+	Unclear * possibly Rohri Hills or Parh Fm.	417142	32.67	422.1	306	1749
HLS-080	AB	Vats III & IV	3C+	Unclear * possibly Rohri Hills or Parh Fm.	518853	46.43	556.3	397	2229
HLS-081	AB	B	3C+	Pachchham Fm. – Khadir * possibly not	445348	44.44	471.1	13837	19884
HLS-082	E	43	3C	Pachchham Fm. – Juni Kuran	476886	42.8	483	4875	5415
HLS-083	AB	39	3+	Pachchham Fm. – Khadir * possibly MSK	487541	51.92	319.9	10566	2655
HLS-084	AB	39	3+	Unclear at this time * not Rohri Hills	7965.74	81.28	38.8	5574	836
HLS-085	AB	39	3+	Pachchham Fm. – Juni Kuran	488421	32.83	495.5	7686	3282
HLS-086	AB	39	3+	Pachchham Fm. – Juni Kuran	514209	32.09	826.8	9036	4441
HLS-087	AB	39	3C	Pachchham Fm. – Khadir quarry	439958	217.85	338.9	10937	3114
HLS-088	AB	39	3C	Pachchham Fm. – Juni Kuran	458675	39.1	738.5	7308	3816
HLS-089	AB	39	3C	Pachchham Fm. – Juni Kuran	445316	41.13	788.2	12129	4833

Sample#	Mound	Trench	Period	Probable geologic provenience	Ca	Ba	Sr	Fe	Mg
HLS-090	AB	39	3+	Pachchham Fm. – Juni Kuran	506587	32.06	761.5	8886	4521
HLS-091	AB	39	3+	Pachchham Fm. – Juni Kuran	493961	38.02	664.1	8327	4275
HLS-093	AB	B	3C+	Pachchham Fm. – Juni Kuran	369045	45.71	415.7	5582	2555
HLS-094	AB	B	3C+	Pachchham Fm. – Khadir * possibly JK	489640	54.93	452.5	6579	3084
HLS-096	AB	B	3C+	Pachchham Fm. – Juni Kuran	488596	80.25	514.1	10877	3686
HLS-097	AB	39	3+	Pachchham Fm. – Khadir * possibly JK	476179	83.25	550	10686	4537
HLS-098	AB	B	3C+	Pachchham Fm. – Khadir * possibly JK	475619	53.55	295.3	5037	3147
HLS-099	AB	B	3C+	Jaisalmer Fm. – Mool Sagar Khan	469359	55.42	647.4	9283	4075
HLS-100	AB	B	3C+	Pachchham Fm. – Juni Kuran	477057	38.56	802	9060	4308
HLS-101	AB	39	3+	Pachchham Fm. – Juni Kuran	438168	36.1	663.5	10465	4741
HLS-102	AB	39	3+	Pachchham Fm. – Juni Kuran	443389	33.68	583.9	9103	4079
HLS-103	F	43	3C	Pachchham Fm. – Juni Kuran	452980	37.38	776.9	6697	3640
HLS-104	AB	B	3C+	Pachchham Fm. – Khadir * possibly not	305759	9.42	334.5	9873	11071
HLS-105	AB	B	3C+	Pachchham Fm. – Juni Kuran	318474	11.54	518.6	7435	4579
HLS-106	AB	B	3C+	Pachchham Fm. – Juni Kuran	317632	14.38	506.6	6883	4099
HLS-107	AB	B	3C+	Pachchham Fm. – Juni Kuran	322710	9.13	771.7	5249	3115
HLS-108	AB	B	3C+	Pachchham Fm. – Juni Kuran	316082	10.15	526.5	5629	2608
HLS-109	AB	B	3C+	Pachchham Fm. – Juni Kuran	301710	11.63	652.8	4694	2952
HLS-110	AB	B	3C+	Pachchham Fm. – Juni Kuran	244254	9.85	396.2	4157	2261
HLS-111	AB	B	3C+	Pachchham Fm. – Juni Kuran	297134	8.46	458.6	5285	2614
HLS-112	AB	B	3C+	Pachchham Fm. – Juni Kuran	322926	13.43	395.9	7221	3500
HLS-113	AB	B	3C+	Pachchham Fm. – Juni Kuran	309994	52.55	575.7	5403	4153

APPENDIX 11.6

STANDARDIZED CANONICAL DISCRIMINANT FUNCTION COEFFICIENTS FOR FIGURES IN CHAPTER 11 GENERATED USING CANONICAL DISCRIMINANT ANALYSIS

Figure 11.24

	Function 1	Function 2
Log(Sr/Ca)	0.538854	-0.263662
Log(Ba/Ca)	-0.515918	0.632779
Log(La/Ca)	2.049668	1.390571
Log(Ce/Ca)	-1.504577	-0.910055

Figure 11.25

	Function 1	Function 2
Log Al	-0.056874	0.749801
Log Ca	-0.576539	0.134206
Log Eu	0.122040	-0.401635
Log Fe	-1.077745	0.440063
Log La	0.218032	0.290513
Log Lu	2.207798	-1.296973
Log Mg	-0.587172	1.065233
Log Mn	-0.632225	0.721394
Log Sr	1.218172	-0.332209
Log V	-0.437484	-0.647896

Figure 11.27

	Function 1	Function 2
Log(Sr/Ca)	0.073614	0.464596
Log(Ba/Ca)	0.211263	-1.461557
Log(La/Ca)	0.650717	0.909790
Log(Ce/Ca)	0.211846	0.326597

Figures 11.30, 11.31, 11.32, 11.34, 11.37, & 11.39

	Function 1	Function 2
Log(Ba/Ca)	-0.058470	-0.342616
Log(Sr/Ca)	1.135848	0.240759
Log(Mg/Ca)	-0.467101	0.446292
Log(Fe/Ca)	-0.469716	0.689877

Figure 11.36

	Function 1
Log(Sr/Ca)	0.844995
Log(Mg/Ca)	0.610469
Log(Fe/Ca)	0.420370
Log(Ba/Ca)	-0.209630

Figure 11.33

	Function 1	Function 2
Log(Ba/Ca)	-0.364807	0.084021
Log(Sr/Ca)	0.907554	-0.696177
Log(Mg/Ca)	0.098317	0.238141
Log(Fe/Ca)	0.188085	1.045765

Figures 11.35 & 11.38

	Function 1	Function 2
Log(Ba/Ca)	-0.438160	-0.066719
Log(Sr/Ca)	1.000905	-0.440645
Log(Mg/Ca)	0.139384	0.083884
Log(Fe/Ca)	-0.054452	1.106942

Figure 11.40

	Function 1	Function 2
Log(Ba/Ca)	0.319044	0.637698
Log(Sr/Ca)	0.255953	0.084343
Log(Mg/Ca)	0.192665	-0.852032
Log(Fe/Ca)	0.703255	0.367320

Figure 11.41

	Function 1	Function 2
Log(Ba/Ca)	-0.031867	-0.290917
Log(Sr/Ca)	1.136319	0.170960
Log(Mg/Ca)	-0.422515	0.540320
Log(Fe/Ca)	-0.443741	0.658560

APPENDIX 11.7

HIERARCHICAL CLUSTER ANALYSIS OF INITIAL LIMESTONE SAMPLES SET INAA DATA

Dendrogram generated using median clustering and Pearson correlation.

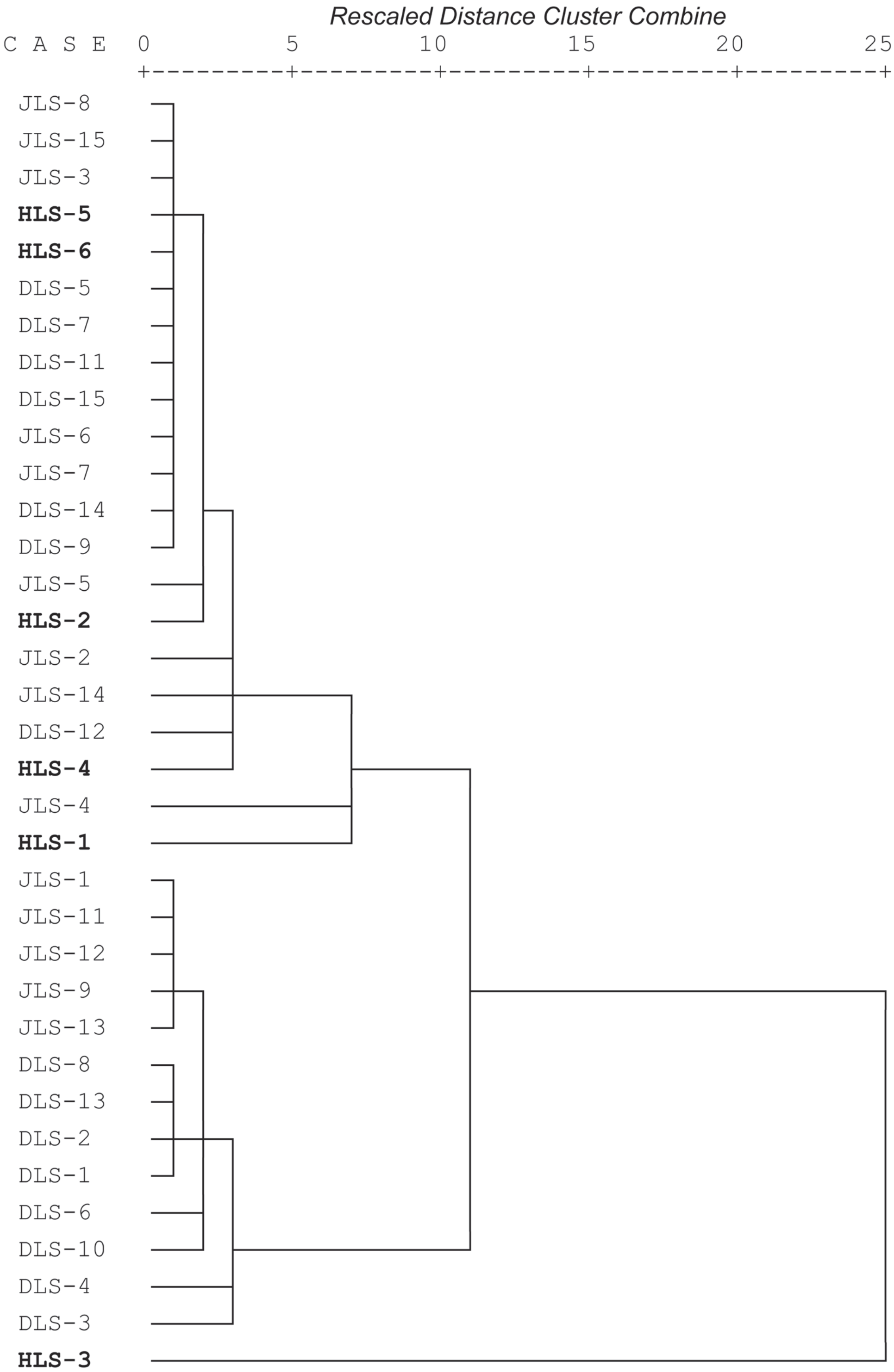

APPENDIX 12.1

PB ISOTOPE DATA FOR ORE SAMPLES FROM LEAD DEPOSITS IN INDIA, PAKISTAN AND OMAN

region - deposit	reference	sample	208/207	207/206	207/204
Balochistan - Chagai (Koh-i-Sultan)	LARCH	ch1	2.4816	0.8439	15.604
Balochistan - Chagai (Koh-i-Sultan)	LARCH	ch1.2	2.482	0.8433	15.635
Balochistan - Chagai (Koh-i-Sultan)	LARCH	ch2	2.4756	0.8418	15.636
Balochistan - Chagai (Koh-i-Sultan)	LARCH	ch2.2	2.4807	0.8417	15.639
Balochistan - Chagai (Koh-i-Sultan)	LARCH	ch3	2.4817	0.8435	15.633
Balochistan - Chagai (Koh-i-Sultan)	LARCH	ch3.2	2.4854	0.8412	15.64
Balochistan - Chagai (Rekodiq)	LARCH	ch4	2.4856	0.8362	15.665
Balochistan - Chagai (Rekodiq)	LARCH	ch4.2	2.4872	0.8366	15.655
Balochistan - Chagai (Rekodiq)	LARCH	ch5	2.4833	0.8374	15.66
Balochistan - Chagai (Rekodiq)	LARCH	ch5.2	2.4857	0.8375	15.713
Balochistan - Chagai (Rekodiq)	LARCH	ch6	2.4847	0.8367	15.689
Balochistan - Chagai (Rekodiq)	LARCH	ch6.2	2.4849	0.8355	15.634
Balochistan - Khuzdar (Gunga)	LARCH	KHZ1	2.4578	0.845	15.614
Balochistan - Khuzdar (Gunga)	LARCH	KHZ2	2.4499	0.8493	15.607
Balochistan - Khuzdar (Gunga)	Siddiqui 1994: Table 7.4	SGL-101	2.4693	0.8459	15.733
Balochistan - Khuzdar (Gunga)	Siddiqui 1994: Table 7.4	SGL-102	2.4697	0.8461	15.721
Balochistan - Khuzdar (Gunga)	Siddiqui 1994: Table 7.4	SGL-103	2.4656	0.8447	15.646
Balochistan - Las Bela - Kanrach Valley (Kharrari)	Bhutta 1992: Table 3	AB258	2.463	0.85	15.703
Balochistan - Las Bela - Kanrach Valley (Duddar)	Bhutta 1992: Table 3	AB269	2.4667	0.8497	15.699
Balochistan - Las Bela - Kanrach Valley (Kharrari)	Bhutta 1992: Table 3	AB295	2.4643	0.8489	15.694
Balochistan - Las Bela - Kanrach Valley (Kharrari)	LARCH	3P-9	2.4619	0.8482	15.704
Balochistan - Las Bela - Kanrach Valley (Kharrari)	LARCH	3P9B	2.4612	0.8472	15.692
Balochistan - Las Bela - Kanrach Valley (Bamph)	LARCH	hppb9	2.4588	0.8494	15.68
Balochistan - Las Bela - Kanrach Valley (Kharrari)	LARCH	KAN2	2.4526	0.8512	15.733
Balochistan - Las Bela - Kanrach Valley (Kharrari)	LARCH	KAN22	2.4631	0.8481	15.527
Balochistan - Las Bela - Kanrach Valley (Kharrari)	LARCH	KAN23	2.4573	0.8533	15.764
Balochistan - Las Bela - Kanrach Valley (Kharrari)	LARCH	KAN24x2	2.4436	0.8544	15.662
Balochistan - Las Bela - Kanrach Valley(Kharrari)	LARCH	KAN25	2.4501	0.8463	15.637
Balochistan - Las Bela - Kanrach Valley (Bamph)	LARCH	KAN3	2.4542	0.8479	15.632
Balochistan - Las Bela - Kanrach Valley (Bamph)	LARCH	KAN33	2.4593	0.8433	15.613
Balochistan - Las Bela - Kanrach Valley (Bamph)	LARCH	KAN34	2.4585	0.8444	15.69

region - deposit	reference	sample	208/207	207/206	207/204
Balochistan - Las Bela - Kanrach Valley (Bamph)	LARCH	KAN35	2.4718	0.8524	15.673
Balochistan - Las Bela - Kanrach Valley (Duddar)	Siddiqui 1994: Table 7.4	SGL-104	2.4702	0.8467	15.722
Bihar - Amjhor	Balasubrahmanyan & Chandy 1976	11	2.4029	0.8915	15.61
Bihar - Amjhor	Balasubrahmanyan & Chandy 1976	12	2.3959	0.896	15.76
Bihar - Amjhor	Balasubrahmanyan & Chandy 1976	13	2.3931	0.8977	15.62
Bihar - Hesatu-Pindara	Singh *et al.* 2001: Table 1	TQ97-22	2.319	0.9564	15.494
Bihar - Hesatu-Pindara	Singh *et al.* 2001: Table 1	TQ97-23	2.3203	0.9573	15.564
Bihar - Hesatu-Pindara	Singh *et al.* 2001: Table 1	TQ97-24	2.3201	0.9571	15.537
Bihar - Hesatu-Pindara	Singh *et al.* 2001: Table 1	TQ97-25	2.3184	0.9563	15.498
Bihar - Hesatu-Pindara	Singh *et al.* 2001: Table 1	TQ97-26	2.3238	0.9574	15.567
Gujarat - Ambadongar	Venkatasubramanian *et al.* 1982: Table I	n/a	2.4685	0.8379	15.56
Gujarat - Banejnes (Gir Forest)	LARCH	GIR-1	2.6496	0.7789	15.657
Gujarat - Banejnes (Gir Forest)	LARCH	GIR-2	2.6628	0.779	15.704
Gujarat - Banejnes (Gir Forest)	LARCH	GIR-3	2.6547	0.7795	15.711
Gujarat - Banejnes (Gir Forest)	LARCH	GIR-4	2.6485	0.7803	15.717
Gujarat - Banejnes (Gir Forest)	LARCH	GIR-5	2.6638	0.7789	15.727
Gujarat - Khandia	LARCH	GK1	2.324	0.9508	15.691
Gujarat - Khandia	LARCH	GK2	2.3237	0.9506	15.702
Gujarat - Khandia	LARCH	GK3	2.327	0.95	15.692
Gujarat - Khandia	LARCH	GK4	2.3241	0.9518	15.699
Gujarat - Khandia	LARCH	GK5	2.326	0.9508	15.706
Gujarat - Khandia	LARCH	GK6	2.3249	0.9515	15.71
Gujarat/Rajasthan - Ambaji-Sendra - Ambaji	Deb *et al.* 1989: Table III	BH115/11A	2.3876	0.9019	15.616
Gujarat/Rajasthan - Ambaji-Sendra - Ambaji	Deb *et al.* 1989: Table III	BH115/7	2.3883	0.9026	15.613
Gujarat/Rajasthan - Ambaji-Sendra - Ambaji	Deb *et al.* 1989: Table III	BH16/2	2.3869	0.9039	15.615
Gujarat/Rajasthan - Ambaji-Sendra - Ambaji	Deb *et al.* 1989: Table III	BH89/9	2.3875	0.9041	15.615
Gujarat/Rajasthan - Ambaji-Sendra - Ambaji	Deb *et al.* 1989: Table III	TQ85-29	2.3873	0.9034	15.616
Gujarat/Rajasthan - Ambaji-Sendra - Ambaji	LARCH	Ambaji Pb	2.3761	0.9127	15.833
Gujarat/Rajasthan - Ambaji-Sendra - Amli Mal	Deb *et al.* 2001:Table 4	TQ90-11	2.3928	0.907	15.612
Gujarat/Rajasthan - Ambaji-Sendra - Amli Mal	Deb *et al.* 2001:Table 4	TQ90-12	2.3929	0.907	15.608
Gujarat/Rajasthan - Ambaji-Sendra - Basantgarh	Deb *et al.* 2001:Table 4	TQ91-43	2.3719	0.9151	15.476
Gujarat/Rajasthan - Ambaji-Sendra - Birantiya	Deb *et al.* 2001:Table 4	TQ92-74	2.3952	0.8977	15.68
Gujarat/Rajasthan - Ambaji-Sendra - Danva	Deb *et al.* 2001:Table 4	TQ92-75	2.3617	0.927	15.351
Gujarat/Rajasthan - Ambaji-Sendra - Deri	Deb *et al.* 1989: Table III	DR14/4	2.3867	0.9039	15.626
Gujarat/Rajasthan - Ambaji-Sendra - Deri	Deb *et al.* 1989: Table III	DR9/14	2.3881	0.9035	15.623
Gujarat/Rajasthan - Ambaji-Sendra - Deri	Deb *et al.* 1989: Table III	DR9/9	2.3871	0.9039	15.622

region - deposit	reference	sample	208/207	207/206	207/204
Gujarat/Rajasthan - Ambaji-Sendra - Deri	Deb *et al*. 1989: Table III	Dupl.	2.3888	0.9035	15.628
Gujarat/Rajasthan - Ambaji-Sendra - Kumbariya	Deb *et al*. 2001:Table 4	4	2.3853	0.9019	15.656
Haryana - Tosham	Deb *et al*. 2001:Table 4	TQ89-8	2.4165	0.8833	15.727
Himachal Pradesh - Amba Kala	LARCH	AKHP1	2.4409	0.8498	15.732
Himachal Pradesh - Amba Kala	LARCH	AKHP2	2.4381	0.8542	15.716
Himachal Pradesh - Amba Kala	LARCH	AKHP3	2.4388	0.8496	15.754
Himachal Pradesh - Amba Kala	LARCH	AKHP4	2.4385	0.8518	15.728
Himachal Pradesh - Amba Kala	LARCH	AKHP5	2.4407	0.8495	15.748
Himachal Pradesh - Panuh	LARCH	HPP-1	2.4526	0.8416	15.872
Himachal Pradesh - Panuh	LARCH	HPP-1B	2.4513	0.8416	15.866
Himachal Pradesh - Panuh	LARCH	HPP-2	2.4522	0.8435	15.939
Himachal Pradesh - Panuh	LARCH	HPP-2C	2.4509	0.8427	16.021
Himachal Pradesh - Panuh	LARCH	HPP-3	2.4588	0.8431	15.95
Himachal Pradesh - Panuh	LARCH	HPP-3B	2.4529	0.8408	15.885
Himachal Pradesh - Panuh	LARCH	HPP-4	2.4535	0.8446	15.934
Himachal Pradesh - Panuh	LARCH	HPP-4B	2.4559	0.8419	15.911
Himachal Pradesh - Panuh	LARCH	HPP-5	2.4531	0.8448	15.944
Himachal Pradesh - Panuh	LARCH	HPP-5B	2.4606	0.8419	15.911
Himachal Pradesh - Tal	LARCH	HPT-1	2.4538	0.8329	16.133
Himachal Pradesh - Tal	LARCH	HPT-2	2.4597	0.8308	16.072
Himachal Pradesh - Tal	LARCH	HPT-3	2.4608	0.8306	16.02
Himachal Pradesh - Tal	LARCH	HPT-4	2.4525	0.8318	16.087
Himachal Pradesh - Tal	LARCH	HPT-5	2.4538	0.8314	16.059
Himachal Pradesh - Uchich	LARCH	HPU-1	2.5775	0.7102	15.832
Himachal Pradesh - Uchich	LARCH	HPU-2	2.572	0.7119	15.499
Himachal Pradesh - Uchich	LARCH	HPU-3	2.5665	0.7081	15.501
Himachal Pradesh - Uchich	LARCH	HPU-5	2.5758	0.7135	16.145
Himachal Pradesh - Uchich	LARCH	HPU-4	2.5828	0.7059	15.299
Jammu & Kashmir - Buniyar	LARCH	RB2	2.3525	0.9066	15.473
Jammu & Kashmir - Buniyar	LARCH	rb2-2	2.3346	0.9115	15.381
Jammu & Kashmir - Buniyar	LARCH	RB3	2.3605	0.9093	15.538
Jammu & Kashmir - Buniyar	LARCH	RB3-2	2.3601	0.906	15.557
Jammu & Kashmir - Buniyar	LARCH	RB3B	2.3513	0.908	15.592
Jammu & Kashmir - Buniyar	LARCH	RB4	2.3434	0.9084	15.425
Jammu & Kashmir - Buniyar	LARCH	RB4-2	2.3554	0.9101	15.575
Jammu & Kashmir - Riasi (Kheri Kot)	LARCH	KK1	2.3589	0.9108	15.6
Jammu & Kashmir - Riasi (Kheri Kot)	LARCH	KK2	2.3572	0.9127	15.602
Jammu & Kashmir - Riasi (Kheri Kot)	LARCH	KK3	2.358	0.9112	15.599
Jammu & Kashmir - Riasi (Kheri Kot)	LARCH	KK4	2.3586	0.9109	15.576
Jammu & Kashmir - Riasi (Kheri Kot)	LARCH	KK5	2.3583	0.911	15.603

region - deposit	reference	sample	208/207	207/206	207/204
Jammu & Kashmir - Riasi (Kheri Kot)	LARCH	KK6	2.3571	0.9115	15.599
Jammu & Kashmir - Riasi (Darabi)	LARCH	RD1	2.3472	0.9282	15.66
Jammu & Kashmir - Riasi (Darabi)	LARCH	RD1A	2.339	0.9278	15.983
Jammu & Kashmir - Riasi (Darabi)	LARCH	RD2	2.3528	0.9164	16.78
Jammu & Kashmir - Riasi (Darabi)	LARCH	RD3	2.3591	0.9169	15.824
Jammu & Kashmir - Riasi (Darabi)	LARCH	RD4	2.3578	0.9172	16.168
Jammu & Kashmir - Riasi (Sersendu)	Raha *et al*. 1978: Table II	0.25	2.3686	0.9171	15.6
Jammu & Kashmir - Riasi (Sersendu)	Raha *et al.* 1978: Table II	I/3	2.3697	0.9138	15.47
Jammu & Kashmir - Riasi (Sersendu)	Raha *et al.* 1978: Table II	II/2	2.3631	0.9105	15.56
Jammu & Kashmir - Riasi (Sersendu)	Raha *et al.* 1978: Table II	II/I	2.3688	0.9178	15.51
NWFP - Besham (Lahor)	Shah *et al*. 1992: Table 1	n/a	2.2878	1.0193	15.085
NWFP - Besham (Lahor)	Shah *et al*. 1992: Table 1	n/a	2.2883	1.0172	15.097
NWFP - Besham (Lahor)	Shah *et al*. 1992: Table 1	n/a	2.2892	1.0192	15.106
NWFP - Besham (Pazang)	Shah *et al*. 1992: Table 1	n/a	2.2864	1.0131	15.116
NWFP - Besham (Pazang)	Shah *et al*. 1992: Table 1	n/a	2.2865	1.017	15.096
NWFP - Chitral	Tahirkheli *et al*. 1997: Table 1	Tz203	2.493	0.8361	15.66
NWFP - Chitral	Tahirkheli *et al*. 1997: Table 1	Tz5	2.4971	0.8371	15.73
NWFP - Chitral	Tahirkheli *et al*. 1997: Table 1	Tz8	2.4962	0.8349	15.68
Oman - Qumayrah	Calvez and Lescuyer 1991: Table 1	JL90-35	2.481	0.8376	15.689
Oman - Ibra (Semail Ophiolite)	Chen and Pallister 1981: Table 1	OMG-15	2.4766	0.8408	15.719
Oman - Wadi Mayh	Calvez and Lescuyer 1991: Table 1	C533	2.4535	0.8624	15.734
Oman - Wadi Nujum	Keck Isotope Laboratry	OWN-1	2.4795	0.8378	15.654
Oman - Wadi Nujum	Keck Isotope Laboratry	OWN-2	2.4792	0.8385	15.655
Oman - Wadi Nujum	Keck Isotope Laboratry	OWN-3	2.4793	0.838	15.643
Oman - Wadi Nujum	Keck Isotope Laboratry	OWN-4	2.4795	0.8377	15.655
Rajasthan - Khera Mawal	Keck Isotope Laboratry	RKM-1	2.4623	0.8606	15.774
Rajasthan - Khera Mawal	Keck Isotope Laboratry	RKM-2	2.4619	0.8608	15.774
Rajasthan - Khera Mawal	Deb *et al*. 2001:Table 4	TQ95-45	2.4641	0.8609	15.778
Rajasthan - Lohakhan	LARCH	point119	2.3106	0.9544	15.65
Rajasthan - Punagarh Hill	Deb *et al*. 2001:Table 4	TQ96-3	2.4031	0.8851	15.787
Rajasthan - Punagarh Hill	Deb *et al*. 2001:Table 4	TQ96-4	2.3942	0.8863	15.78
Rajasthan - Rajpura-Dariba	Balasubrahmanyan & Chandy 1976	5	2.305	0.961	15.51
Rajasthan - Rajpura-Dariba	Balasubrahmanyan & Chandy 1976	6	2.2688	0.9635	15.59
Rajasthan - Rajpura-Dariba	Balasubrahmanyan & Chandy 1976	7	2.3059	0.9682	15.53
Rajasthan - Rajpura-Dariba	Balasubrahmanyan & Chandy 1976	8	2.3155	0.9706	15.53
Rajasthan - Rajpura-Dariba	Balasubrahmanyan & Chandy 1976	9	2.2995	0.9621	15.49
Rajasthan - Rajpura-Dariba	Balasubrahmanyan & Chandy 1976	10	2.2987	0.9592	15.5
Rajasthan - Rajpura-Dariba	Deb *et al*. 1989: Table III	Dupl.	2.3102	0.966	15.486
Rajasthan - Rajpura-Dariba	Deb *et al*. 1989: Table III	Dupl.	2.311	0.966	15.492

region - deposit	reference	sample	208/207	207/206	207/204
Rajasthan - Rajpura-Dariba	Deb *et al*. 1989: Table III	Dupl.	2.3112	0.9657	15.494
Rajasthan - Rajpura-Dariba	Deb *et al*. 1989: Table III	RD400/208	2.3116	0.966	15.49
Rajasthan - Rajpura-Dariba	Deb *et al*. 1989: Table III	RD400/224	2.3114	0.9658	15.488
Rajasthan - Rajpura-Dariba	Deb *et al*. 1989: Table III	RD400/231	2.3097	0.9658	15.488
Rajasthan - Rajpura-Dariba	Deb *et al*. 1989: Table III	RD400/247	2.3109	0.966	15.485
Rajasthan - Rajpura-Dariba	Deb *et al*. 1989: Table III	RD400/263	2.3109	0.966	15.494
Rajasthan - Rajpura-Dariba	Deb *et al*. 1989: Table III	RD400/27	2.3115	0.9655	15.488
Rajasthan - Rajpura-Dariba	Deb *et al*. 1989: Table III	RD400/28	2.3099	0.9659	15.499
Rajasthan - Rajpura-Dariba	Deb *et al*. 1989: Table III	RD400/305	2.3109	0.9658	15.49
Rajasthan - Rajpura-Dariba	Deb *et al*. 1989: Table III	RD400/52	2.3109	0.9658	15.489
Rajasthan - Rajpura-Dariba	Deb *et al*. 1989: Table III	RD400/8	2.311	0.9662	15.492
Rajasthan - Rampura-Agucha	Deb *et al*. 1989: Table III	Dupl.	2.3106	0.9657	15.503
Rajasthan - Rampura-Agucha	Deb *et al*. 1989: Table III	Dupl.	2.311	0.9655	15.506
Rajasthan - Rampura-Agucha	Deb *et al*. 1989: Table III	Dupl.	2.3111	0.9657	15.505
Rajasthan - Rampura-Agucha	Deb *et al*. 1989: Table III	Dupl.	2.3112	0.9659	15.507
Rajasthan - Rampura-Agucha	Deb *et al*. 1989: Table III	Dupl.	2.3114	0.9659	15.506
Rajasthan - Rampura-Agucha	Deb *et al*. 1989: Table III	Dupl.	2.3124	0.9658	15.498
Rajasthan - Rampura-Agucha	Deb *et al*. 1989: Table III	RA/OD/5	2.3111	0.9657	15.499
Rajasthan - Rampura-Agucha	Deb *et al*. 1989: Table III	RA/OD/7	2.3104	0.9658	15.495
Rajasthan - Rampura-Agucha	Deb *et al*. 1989: Table III	RA84/A	2.3117	0.9657	15.507
Rajasthan - Rampura-Agucha	Deb *et al*. 1989: Table III	RA84/B	2.3109	0.9656	15.509
Rajasthan - Rampura-Agucha	Deb *et al*. 1989: Table III	RA84/C	2.3117	0.9658	15.504
Rajasthan - Rampura-Agucha	Deb *et al*. 1989: Table III	RD400/8	2.312	0.9658	15.512
Rajasthan - Saladipura	Deb *et al*. 1989: Table III	Dupl.	2.3118	0.9642	15.492
Rajasthan - Saladipura	Deb *et al*. 1989: Table III	TQ 85-24	2.3126	0.9642	15.498
Rajasthan - Sawai Madhopur	LARCH	RSM-1	2.3187	0.9464	15.805
Rajasthan - Sawai Madhopur	LARCH	RSM-2	2.3114	0.9494	15.788
Rajasthan - Sawai Madhopur	LARCH	RSM-3	2.314	0.9502	15.802
Rajasthan - Sawai Madhopur	LARCH	RSM-4	2.3227	0.9494	15.731
Rajasthan - Sawai Madhopur	LARCH	RSM-5	2.3128	0.9524	15.831
Rajasthan - Zawar	Balasubrahmanyan & Chandy 1976	1	2.3195	0.952	15.68
Rajasthan - Zawar	Balasubrahmanyan & Chandy 1976	2	2.3152	0.9462	15.64
Rajasthan - Zawar	Balasubrahmanyan & Chandy 1976	3	2.3227	0.9456	15.65
Rajasthan - Zawar	Balasubrahmanyan & Chandy 1976	4	2.3179	0.9512	15.6
Rajasthan - Zawar Mines	LARCH	Zawar Pb	2.3227	0.9479	15.674
Rajasthan - Zawar-Baroi	Deb *et al*. 1989: Table III	BM4	2.3234	0.9483	15.706
Rajasthan - Zawar-Baroi	Deb *et al*. 1989: Table III	BM6	2.3253	0.9479	15.723
Rajasthan - Zawar-Baroi	Deb *et al*. 1989: Table III	BM7	2.3217	0.9488	15.683
Rajasthan - Zawar-Baroi	Deb *et al*. 1989: Table III	Dupl.	2.3232	0.9478	15.721
Rajasthan - Zawarmala	Deb *et al*. 1989: Table III	Dupl.	2.3237	0.9477	15.725

region - deposit	reference	sample	208/207	207/206	207/204
Rajasthan - Zawarmala	Deb *et al*. 1989: Table III	Dupl.	2.3241	0.9467	15.698
Rajasthan - Zawarmala	Deb *et al*. 1989: Table III	Dupl.	2.3248	0.9471	15.708
Rajasthan - Zawarmala	Deb *et al*. 1989: Table III	ZM14	2.3249	0.9469	15.708
Rajasthan - Zawarmala	Deb *et al*. 1989: Table III	ZM22	2.3225	0.9476	15.694
Rajasthan - Zawarmala	Deb *et al*. 1989: Table III	ZM27	2.3245	0.9489	15.694
Rajasthan - Zawarmala	Deb *et al*. 1989: Table III	ZM5	2.3233	0.9479	15.722
Rajasthan - Zawar-Mochia	Deb *et al*. 1989: Table III	BL5	2.3215	0.9499	15.666
Rajasthan - Zawar-Mochia	Deb *et al*. 1989: Table III	BL9	2.3215	0.95	15.66
Rajasthan - Zawar-Mochia	Deb *et al*. 1989: Table III	Dupl.	2.3209	0.9499	15.657
Rajasthan - Zawar-Mochia	Deb *et al*. 1989: Table III	Dupl.	2.3221	0.9503	15.67
Rajasthan - Zawar-Mochia	Deb *et al*. 1989: Table III	ZMC15	2.3219	0.9502	15.663
Rajasthan - Zawar-Mochia	Deb *et al*. 1989: Table III	ZMC2	2.3222	0.9502	15.672
South India - Andhra Pradesh - Agnigundala	Srinivasa 1999: Table 2	1	2.3053	0.9415	15.721
South India - Andhra Pradesh - Agnigundala	Srinivasa 1999: Table 2	2	2.3057	0.9408	15.736
South India - Andhra Pradesh - Agnigundala	Srinivasa 1999: Table 2	3	2.3052	0.9408	15.731
South India - Andhra Pradesh - Agnigundala	Srinivasa 1999: Table 2	4	2.3077	0.9418	15.77
South India - Andhra Pradesh - Agnigundala	Srinivasa 1999: Table 2	5	2.3042	0.9402	15.718
South India - Andhra Pradesh - Agnigundala	Srinivasa 1999: Table 2	6	2.3055	0.9408	15.738
South India - Andhra Pradesh - Agnigundala	Srinivasa 1999: Table 2	7	2.3043	0.9405	15.714
South India - Andhra Pradesh - Agnigundala	Srinivasa 1999: Table 2	8	2.3074	0.9421	15.758
South India - Andhra Pradesh - Agnigundala	Srinivasa 1999: Table 2	9	2.3061	0.9419	15.744
South India - Andhra Pradesh - Chelima	Venkatasubramanian *et al*. 1982: Table I	n/a	2.323	0.9466	15.42
South India - Karnataka - Arothikoppal	Venkatasubramanian *et al*. 1982: Table I	n/a	2.3234	0.95	15.4
South India - Karnataka - G.R. Halli	Venkatasubramanian *et al*. 1982: Table I	n/a	2.2724	1.0903	14.61
South India - Karnataka - Kolar	Venkatasubramanian *et al*. 1982: Table I	n/a	2.268	1.0475	15
South India - Karnataka - Kunchiganahalu	Venkatasubramanian *et al*. 1982: Table I	n/a	2.3008	1.1392	13.83
South India - Karnataka - Kurubaramaradikere	Venkatasubramanian *et al*. 1982: Table I	n/a	2.2855	1.0813	14.5
South India - Karnataka -Bukkambudhi	Venkatasubramanian *et al*. 1982: Table I	n/a	2.3156	1.1272	13.91
South India - Tamil Nadu - Kurichi	Venkatasubramanian *et al*. 1982: Table I	n/a	2.3497	0.9318	15.44
South India - Tamil Nadu - Mamandur	Venkatasubramanian *et al*. 1982: Table I	n/a	2.2692	1.05	15.12
South India - Tamil Nadu - Metri	Venkatasubramanian *et al*. 1982: Table I	n/a	2.3491	0.9296	15.44
South India - Andhra Pradesh - Chelima	Venkatasubramanian *et al*. 1982: Table I	n/a	2.323	0.9466	15.42
Sikkim - Rangpo	Sarkar *et al*. 2000: Table 1	MAHW/17/B/7	2.303	0.974	15.41
Sikkim - Rangpo	Sarkar *et al*. 2000: Table 1	MAHW/17/R/6	2.2805	0.9736	15.457
Sikkim - Rangpo	Sarkar *et al*. 2000: Table 1	NAB-3/P/5	2.3009	0.9735	15.386
Sikkim - Rangpo	Sarkar *et al*. 2000: Table 1	NAFW/2/R/8	2.3012	0.9736	15.4
Uttaranchal - Askot	LARCH	AS28B	2.297	0.97	15.457

region - deposit	**reference**	**sample**	**208/207**	**207/206**	**207/204**
Uttaranchal - Askot	LARCH	RR-84-B2	2.288	0.9718	15.329
Uttaranchal - Askot	LARCH	RR85	2.3001	0.9727	15.966
Uttaranchal - Bageshwar	Sarkar *et al*. 2000: Table 1	B6-1	2.3121	0.9576	15.551
Uttaranchal - Bageshwar	Sarkar *et al*. 2000: Table 1	B6-2	2.3176	0.9471	15.555
Uttaranchal - Bageshwar	Sarkar *et al*. 2000: Table 1	B6-3	2.3127	0.9572	15.541
Uttaranchal - Khansue	LARCH	GK74/1	2.372	0.8513	15.729
Uttaranchal - Khansue	LARCH	GK74/3	2.3803	0.854	15.743
West Bengal - Gorubathan	Sarkar *et al*. 2000: Table 1	D2/6/4	2.2955	0.9726	15.511
West Bengal - Gorubathan	Sarkar *et al*. 2000: Table 1	K5/6/1	2.3011	0.9729	15.428
West Bengal - Gorubathan	Sarkar *et al*. 2000: Table 1	S/31/6/3	2.3028	0.9741	15.42

APPENDIX 12.2

CONTEXT AND PB ISOTOPE DATA FOR 19 ARCHAEOLOGICAL LEAD ORE FRAGMENTS FROM HARAPPA

artifact number	material	mound-trench	context	208/207	207/206	207/204	probable geologic provenience
H93/4001-1	galena	ET - 10	surface	2.3666	0.91	15.616	Jammu and Kashmir
H96/7512-10	galena	AB - 39	Period 1	2.3432	0.91	15.578	Jammu and Kashmir
H89/1038-21	galena	AB / E - 53	disturbed	2.3577	0.9086	15.641	Jammu and Kashmir
H90/3011-147	galena	E - survey	surface	2.4411	0.8584	15.759	unclear at this time
H90/3011-148	galena	E - survey	surface	2.4366	0.8613	15.763	unclear at this time
H99/7649-31	galena	F- 41	Period 3C	2.3556	0.9107	15.599	Jammu and Kashmir
H98/8158-62	galena	E - 11	Period 3C	2.3543	0.9116	15.576	Jammu and Kashmir
H2000/2102-143	galena	E - 54	disturbed	2.3548	0.9141	15.603	Jammu and Kashmir
H2000/2101-1726	galena	E - 54	disturbed	2.3577	0.9055	15.628	Jammu and Kashmir
H2000/2226-111	galena	E - 54	disturbed	2.3545	0.9099	15.626	Jammu and Kashmir
H2000/9999-73	galena	E - survey	surface	2.3562	0.9115	15.579	Jammu and Kashmir
H99/8857-1	cerussite-anglesite	E - 11	disturbed	2.4721	0.8469	15.701	southern Balochistan
H99/8755-152	cerussite-anglesite	F - 43	Period 3C	2.4608	0.8474	15.738	southern Balochistan
H2000/2139-141	cerussite-anglesite	E - 54	disturbed	2.4731	0.8455	15.635	southern Balochistan
H2000/2342-40	massicot	E - 54	disturbed	2.4351	0.8586	15.815	unclear at this time
H88/715-15	massicot	E - 52	Period 3C	2.4677	0.8466	15.704	southern Balochistan
H90/3030-1	massicot	E - 1	disturbed	2.4197	0.8673	15.758	unclear at this time
H2001/9091-1	massicot	E - 11	Period 3C	2.4443	0.8651	15.639	unclear at this time
H90/3193-6	massicot	E - 58	Period 3C	2.4629	0.8443	15.636	southern Balochistan

APPENDIX 12.3

PB ISOTOPE DATA FOR LEAD ARTIFACTS, SLAGS, LUMPS AND RESIDUES FROM HARAPPA

artifact number	material	mound-trench	context	208/207	207/206	207/204	probable geologic provenience
H93/3506-43	lead rod	E - 1	disturbed	2.4368	0.8689	15.797	Unclear at this time
H88/197-1	wulfenite rod	cemetery	Period 3B	2.3479	0.9093	15.585	Jammu and Kashmir
H2000/2174-321	inscribed lead bar	E - 54	surface	2.4631	0.8486	15.634	southern Balochistan
H94/4891-214	lead piece	ET - 27	Period 3C	2.4497	0.8653	15.72	unclear at this time (Oman?)
H2000/2102-1555	lead bar	E - 54	disturbed	2.449	0.8644	15.606	unclear at this time (Oman?)
H2000/2226-50	lead bar/chisel	E - 54	disturbed	2.4505	0.846	15.667	southern Balochistan
H88/446-04	lead repair plug in shell ladle	cemetery	Period 3B	2.4379	0.8662	15.69	Unclear at this time
H93/3892-69	porous slag with lead inclusions	E - 8	surface	2.4654	0.8433	15.701	southern Balochistan
H93/3563-13	slag with yellow encrustation	E - 4	Period 3C	2.4555	0.8634	15.679	Unclear at this time
H95/6006-1	melted lead lump	north of F	surface	2.4689	0.8436	15.731	southern Balochistan
H2001/11701-6	melted lead lump	E - 11	surface	2.3575	0.914	15.548	Jammu and Kashmir
H93/3511-37	slag w/ green and yellow encrustation	E - 1	disturbed	2.4136	0.8738	15.514	Unclear at this time
H93/3804-5	slag w/ green and yellow encrustation	E - 5	disturbed	2.4573	0.8556	15.597	southern Balochistan
H87/539-80	lead residue inside "surma" bottle	AB - 50	Period 3C	2.3558	0.9074	15.806	Jammu and Kashmir
H98/8158-26	lead residue inside "surma" bottle	E - 11	Period 3C	2.369	0.9115	15.753	Jammu and Kashmir
[HM 9697 V3906]	lead residue inside "surma" bottle	Unknown	Unknown	2.3472	0.9114	15.799	Jammu and Kashmir

APPENDIX 12.4

PB ISOTOPE DATA FOR LEAD ARTIFACTS FROM SHAHR-I-SOKHTA, MUNDIGAK, MEHRGARH, NAUSHARO, GOLA DHORO AND MOHENJO-DARO

site	analysis # / artifact number	artifact type	208/207	207/206	207/204
Shahr-i-Sokhta	SiS151	galena fragment	2.4704	0.8497	15.606
Shahr-i-Sokhta	SiS11390	galena fragment	2.4747	0.8412	15.599
Mundigak	MGK-1 / MGB 36 CLXXXVII (3)	galena fragment	2.4727	0.8510	15.714
Mundigak	MGK-2 / MG G91 (3)	galena fragment	2.4678	0.8517	15.704
Mundigak	MGK-3 / no #	galena fragment	2.4792	0.8488	15.665
Mundigak	MGK-4 / MGA XXXII *a*	galena fragment	2.4629	0.8488	15.630
Mundigak	MGK-5 / MGA XXXII *b*	galena fragment	2.4609	0.8488	15.661
Mundigak	MGK-6 / MGA XXXII *c*	galena fragment	2.4653	0.8480	15.596
Mundigak	MGK-7 / no #	galena fragment	2.4793	0.8504	15.664
Mundigak	MGK-8 / no #	galena fragment	2.4691	0.8501	15.659
Mundigak	MGK-9 / no #	galena fragment	2.4763	0.8497	15.663
Mundigak	MGK-10 / MG J12 Tepe A	lead sheet	2.4658	0.8412	15.562
Mundigak	MGK-11 / MG J12 Tepe A	lead sheet	2.4744	0.8390	15.611
Mundigak	MGK-12 / MG 6.1	lead ring	2.4774	0.8459	15.643
Mundigak	MGK-14 / no #	galena fragment	2.4811	0.8503	15.681
Mehrgarh	MR-L1 / MR4 F6B (2) – large (MR 78 04 11 24)	galena fragment	2.4641	0.8467	15.755
Mehrgarh	MR-L2 / MR4 F6B (2) – small (MR 78 04 11 25)	galena fragment	2.4710	0.8482	15.767
Mehrgarh	MR-L3 / MR4 F6B (2) *c* (MR 78 04 11 26)	galena fragment	2.4585	0.8485	15.749
Mehrgarh	MR-L4 / MR79.04.73.59	galena fragment	2.4657	0.8469	15.708
Mehrgarh	MR-L5 / L31121	galena fragment	2.4698	0.8458	15.702
Mehrgarh	MR-L6 / L31122	galena fragment	2.4800	0.8446	15.708
Mehrgarh	MR-L7 / MR4 F6B (1) 78 (MR 78 04 10 31)	galena fragment	2.4759	0.8442	15.681
Gola Dhoro	BRS-5930	lead lump	2.4669	0.8471	15.674
Nausharo	NS-L1 / NS-9111 6303 loc. XII	lead ring	2.4719	0.8447	15.697
Mohenjo-daro	MD-S / no #	"surma" bottle residue	2.4316	0.8660	15.516
Mohenjo-daro	MD-L1 / MD-88 711	galena fragment	2.4668	0.8437	15.672

APPENDIX 12.5

PB ISOTOPE DATA FOR SILVER ARTIFACTS FROM ALLAHDINO, MOHENJO-DARO, MUNDIGAK, GOLA DHORO AND NAGWADA

Site	analysis number	accession number	artifact type	208/207	207/206	207/204
Mundigak	MGK-13	MGB 40 CXCIX	ring	2.4938	0.8353	15.629
Nagwada	NGW-1	n/a	ring fragment	2.4677	0.8522	15.685
Gola Dhoro	BSR-7053	n/a	ring	2.4797	0.8397	15.696
Mohenjo-daro	NM-1	50.47, S. no 12	bangle	2.4462	0.8636	15.624
Mohenjo-daro	NM-1	NMP#8	bead	2.4468	0.8652	15.577
Mohenjo-daro	NM-1	NMP#8	bead	2.4437	0.8629	15.538
Mohenjo-daro	NM-1	NMP#8	bead	2.4420	0.8672	15.548
Mohenjo-daro	NM-1	NMP#50.22/6	button or nose stud	2.4304	0.8701	15.473
Allahdino	AD-1	2070 A	large flat bead with triple hole	2.4695	0.8455	15.666
Allahdino	AD-2	2070 B	large flat bead with triple hole	2.4651	0.8494	15.583
Allahdino	AD-3	2101 A	small bead	2.4647	0.8520	15.343
Allahdino	AD-4	2101 B	small bead	2.4608	0.8500	15.474
Allahdino	AD-5	2101 C	bead	2.4429	0.8539	15.487
Allahdino	AD-6	2101 E	bead	2.4478	0.8569	15.623
Allahdino	AD-7	2101 F	bead	2.4607	0.8511	15.604
Allahdino	AD-8	2111 A	toe ring	2.4709	0.8466	15.674
Allahdino	AD-9	2111 B	bead	2.4409	0.8705	15.747
Allahdino	AD-10	2111 B	lump of twisted bands	2.4561	0.8481	15.655

APPENDIX 12.6

PB ISOTOPE DATA FOR THE ARGENTIFEROUS GALENA DEPOSIT AT NAKHLAK, IRAN

(extrapolated from Stos-Gale 2001: Table 4.1)

Sample number	Material	208/207	207/206	207/204
Pb-835	Litharge	2.4738	0.84509	15.690
Pb-833	Pb slag/litharge	2.4715	0.84479	15.647
Pb-832	Cerussite	2.4743	0.84480	15.645
Pb-834	galena	2.4710	0.84525	15.670
PI 1b	Pb slag	2.4712	0.84468	15.654
PI 2	Pb slag	2.4706	0.84466	15.651
PI 1a	Pb slag	2.4710	0.84463	15.655

APPENDIX 12.7

XRD AND PB ISOTOPE ANALYSES OF MODERN LEAD OBJECTS AND SUBSTANCES

During the course of my research on the acquisition and use of lead in ancient northwestern South Asia, I frequently came across of modern lead objects and lead substances that, for informational and comparative reasons, were worth analyzing along with the artifacts and geology samples I was examining. The results of analyses are summarized here.

I picked up numerous samples of the cosmetic known across South Asia "surma" (and nearly everywhere else as "kohl") in the bazaars of Pakistan and India. In many places it is available in both finished and raw form. For example, in the Ajmer bazaar one shop sold boxes of Gulab Sada brand surma right next to a tagari filled with raw chunks of galena (Appendix 12.7 Figure 1 A). In the Harappa town bazaar I purchased a vial of the popular Hashmi brand surma (Appendix 12.7 Figure 1 B), which, along with samples of the cosmetic from several other places, was analyzed when I returned to Madison. The XRD spectrum of the Hashmi surma (and most of the others too) indicated that it contained the lead mineral galena (Appendix 12.7 Figure 1 C). This finding is consistent with other studies on present-day samples of the cosmetic by al-Hazzaa and Krahn 1995, Hardy et al. 1998, Parry and Eaton 1991, and Vaishnav 2001.

I conducted Pb isotope analysis on seven samples taken from modern lead items in Pakistan. These data are listed in Appendix 12.7 Figure 2. Three of the samples were pieces of galena purchased in traditional medicine shops, or *pansaris*. I obtained galena from such shops in Karachi, New Attock City (this sample can be seen in Chapter 3 Figure 2 C) and Harappa Town. At the cave shrine of Lahoot La Makan in the Las Bela District, southern Balochistan, I purchased a small bottle of homemade surma from a herbalist who had a small stand there. The remaining three samples were taken from modern era lead musket balls found on the surface at Harappa.

In Appendix 12.7 Figure 3, the Pb isotope data for the seven modern lead samples are plotted in relation to South Asian lead ore fields. For comparative purposes, datapoints for lead analyzed from Harappa and Mohenjo-Daro are plotted on the figure as well. The three pansari-purchased galenas and the surma from the herbalist fall in and around what I have called the "ambiguous" area. Although many Harappan lead artifacts plot in that area, it is poorly characterized with regard to lead sources. The galenas from the Karachi and Harappa Town pansaris do fall adjacent to datapoints for two minor lead occurrences in Oman and southern Rajasthan. However, to my knowledge neither of those deposits are being worked today. The surma sample obtained from the herbalist at Lahoot La Makan plots near the lead sources of southern Balochistan, which would seem to indicate that it was made from regionally acquired galena. While the galena sample from the New Attock City pansari does not resemble any lead deposit in the database, it does share almost identical Pb isotope values with the surma sample analyzed from Mohenjo-Daro. The proprietor of the New Attock City pansari where I bought the samples did not know from where the sample he sold me originated. Still, the fact a modern piece of galena meant to be powdered for surma is isotopically analogous to ancient surma from Mohenjo-Daro is a very important finding, as are the associations of the other modern samples. Together they serve to further demonstrate that the "ambiguous" area is represented by multiple lead deposits in locations,

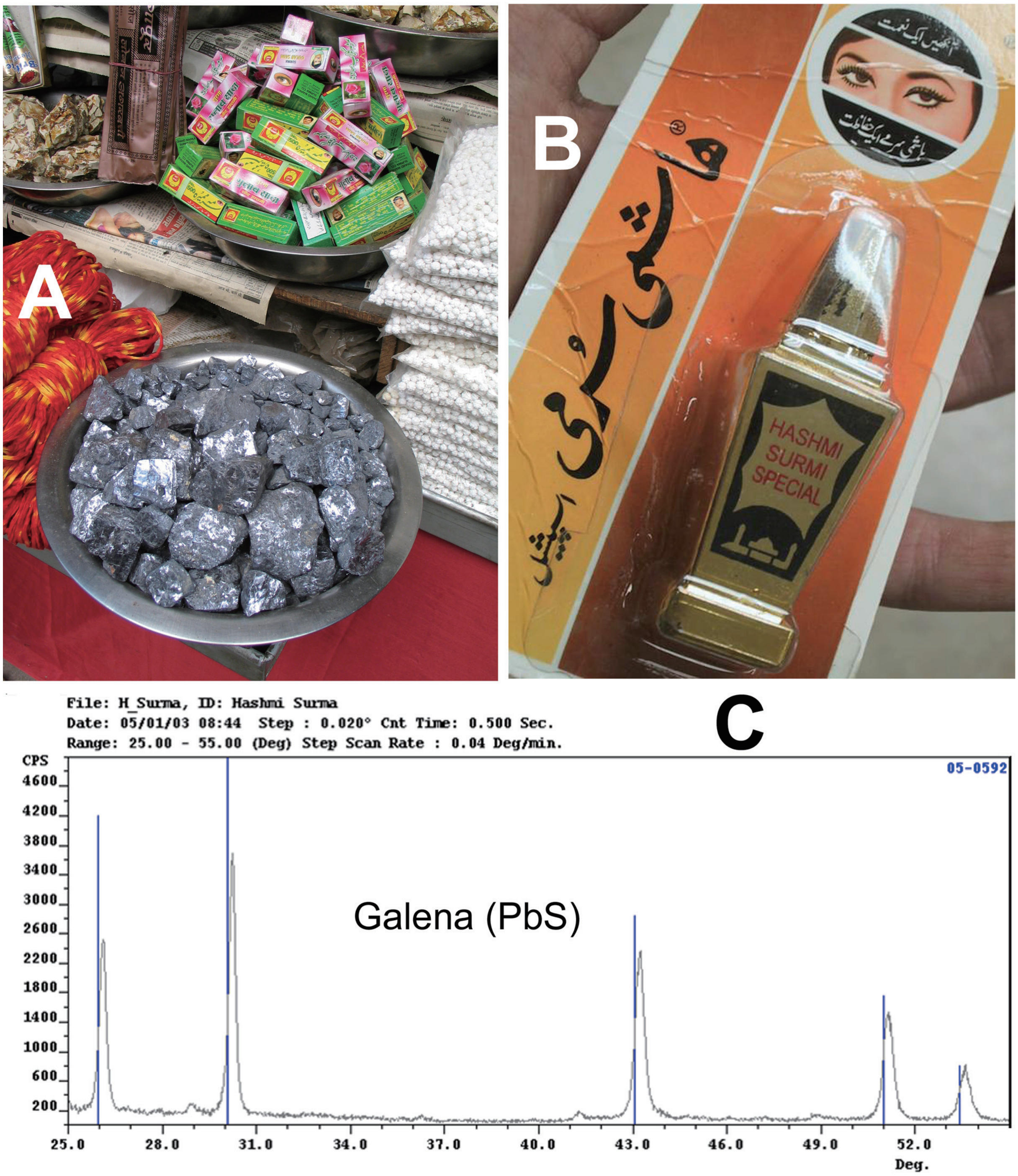

Appendix 12.7 Figure 1 **[A]** Surma and galena for sale in the Ajmer bazaar, Rajasthan.
[B] Hashmi brand surma purchased in the Harappa Town bazaar.
[C] The XRD spectrum for the Hashmi surma purchased in Harappa Town.

very likely in northwestern South Asia, that remain to be located and isotopically characterized. Unlike the Wadi Mayh lead showing in Oman and the Khera Mawal deposit in southern Rajasthan, which as I have pointed out above are both minor in nature, the sources represented by the "ambiguous" are probably significant as they were exploited during the Harappan Phase and continue to be today. This is assuming, of course, they are even the same deposits at all. It is certainly possible that the modern galenas are from altogether different sources that just happen to have identical isotopic characteristics as the old ones used by the Harappans. For the time being, however, I will assume that the modern and ancient sources are

Appendix 12.7 Figure 2 Pb isotope data for modern lead artifacts from Pakistan		**208/207**	**207/206**	**207/204**
New Attock Pansari	galena	2.4329	0.8659	15.594
Harappa Town Pansari	galena	2.4547	0.8613	15.618
Karachi Pansari	galena	2.4597	0.8588	15.633
Lahoot La Makan herbalist	surma	2.4489	0.8563	15.634
Harappa Mound ET (H93-3803-24)	lead shot	2.3377	0.9294	15.607
Harappa Mound F (H2000-9848-4)	lead shot	2.4258	0.8623	15.647
Harappa Mound F (H99-8764-101)	lead shot	2.4736	0.8456	15.616

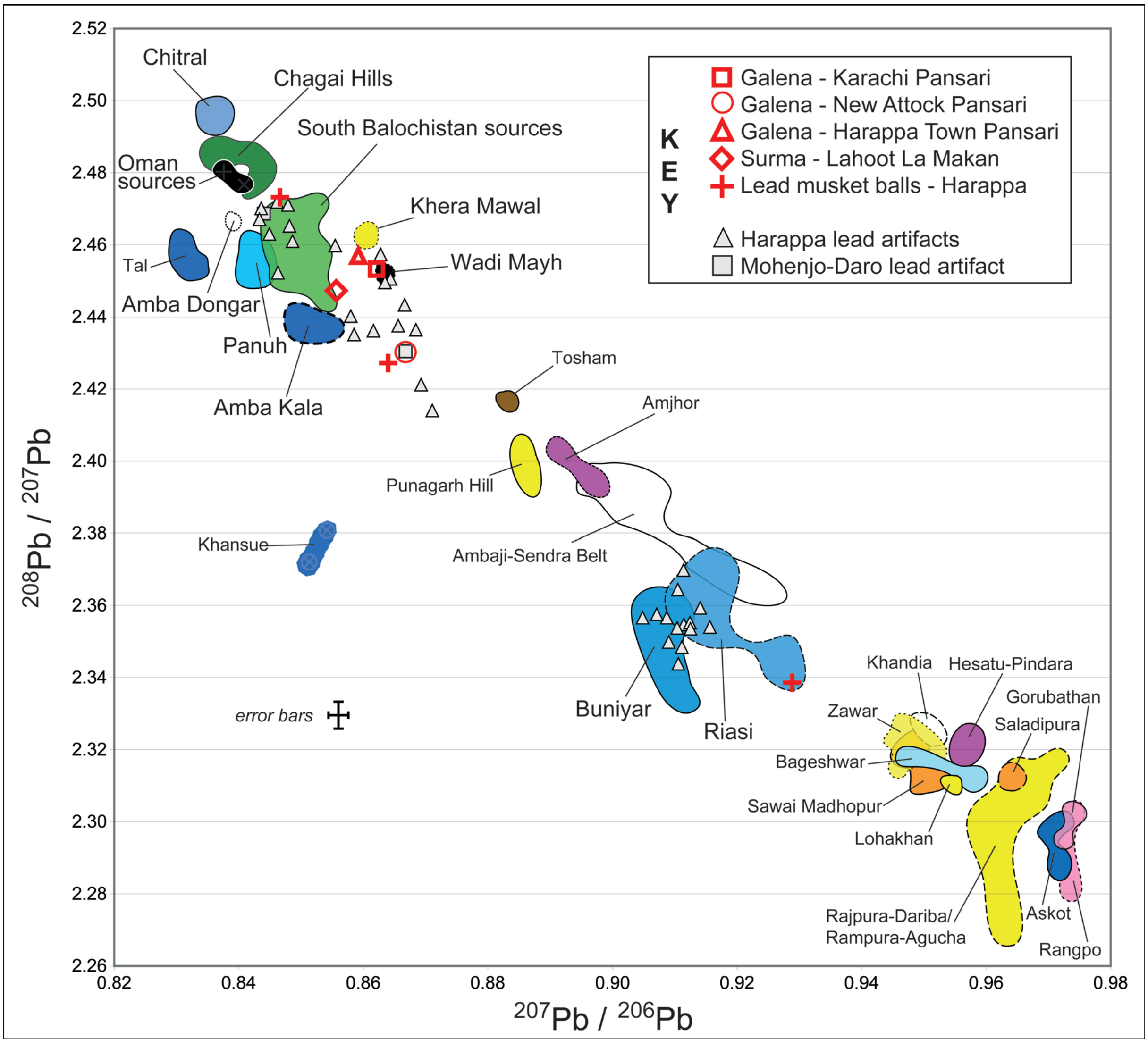

Appendix 12.7 Figure 3 Pb isotope data for modern lead from Pakistan plotted against South Asian lead ore fields.

one and the same and continue searching for them. The shop owner in Harappa Town was also unable to say from where the galena he sold me originated but I was told at the Karachi pansari that their galena came from Balochistan. This then seems like the most promising region to focus on initially, followed by Afghanistan and the great many uncharacterized lead deposits there.

The three musket balls from Harappa each plot with a different lead source area: southern Balochistan, Jammu and the "ambiguous" area. Any or all of these the balls could, of course, contain metal from multiple deposits and, thus, their positions on the isotope plot may represent points on different source mixing lines. It is, nevertheless, interesting how these lead objects suggest that the same three main source areas exploited during the Harappan Phase continued to be used in the modern (relatively) era.

APPENDIX 12.8

PB ISOTOPE DATA FOR COPPER ORES AND SLAGS FROM DEPOSITS IN INDIA, PAKISTAN, IRAN AND OMAN

(*archaeological ore)

Region	source	material	reference	analysis #	208/207	207/206	207/204
Balochistan	Chagai-Saindak	ore	LARCH	ChCu1	2.4878	0.8327	15.782
Balochistan	Chagai-Saindak	ore	LARCH	ChCu2	2.4802	0.8407	15.828
Balochistan	Chagai-Saindak	ore	LARCH	ChCu3	2.4763	0.8421	15.729
Balochistan	Chagai-Saindak	ore	LARCH	ChCu4	2.4697	0.8424	15.758
Balochistan	Chagai-Saindak	ore	LARCH	ChCu5	2.4728	0.8447	15.797
Balochistan	Chagai-Saindak	ore	LARCH	ChCu6	2.4838	0.8434	15.704
Balochistan	Chagai-Saindak	ore	LARCH	ChCu7	2.4911	0.8315	15.807
Gujarat	Ambaji	ore	LARCH	GN-01	2.395	0.9111	15.89
Gujarat	Ambaji	ore	LARCH	GN-02	2.4027	0.9106	15.396
Gujarat	Ambaji	ore	LARCH	GN-03	2.4035	0.9079	15.862
Gujarat	Ambaji	ore	LARCH	GN-04	2.3916	0.8995	15.771
Gujarat	Ambaji	ore	LARCH	GN-05	2.4041	0.8795	15.706
Gujarat	Ambaji	ore	LARCH	GN-06	2.3977	0.8976	15.685
Gujarat	Ambaji	ore	LARCH	GN-07	2.3889	0.8991	15.693
Gujarat	Ambaji	ore	LARCH	GN-08	2.3861	0.8972	15.647
Gujarat	Ambaji	ore	LARCH	GN-09	2.3858	0.897	15.647
Gujarat	Ambaji	ore	LARCH	GN-10	2.3879	0.8991	15.677
Gujarat	Ambaji	ore	Hegde and Ericson 1985	no #	2.3891	0.904	15.649
Himachal Pradesh	Chargaon	ore	LARCH	HP1	2.6692	0.6834	16.639
Himachal Pradesh	Chargaon	ore	LARCH	HP2	2.6706	0.6801	16.662
Himachal Pradesh	Chargaon	ore	LARCH	HP3	2.6701	0.6813	16.69
Himachal Pradesh	Chargaon	ore	LARCH	HP4	2.6756	0.6801	16.678
Himachal Pradesh	Chargaon	ore	LARCH	HP5	2.665	0.6812	16.702
Iran	Shahr-i-Sokhta	ore*	Hauptmann et al. 2003	SS 96	2.4891	0.8348	15.639
Iran	Shahr-i-Sokhta	ore*	Hauptmann et al. 2003	SS 101/1	2.4935	0.8341	15.643
Iran	Shahr-i-Sokhta	ore*	Hauptmann et al. 2003	SS 137	2.4934	0.8336	15.631
Iran	Shahr-i-Sokhta	ore*	Hauptmann et al. 2003	SS 145	2.4861	0.812	15.661
Iran	Shahr-i-Sokhta	ore*	Hauptmann et al. 2003	SS 148	2.4933	0.8319	15.617
Iran	Shahr-i-Sokhta	ore*	Hauptmann et al. 2003	SS 156A	2.4898	0.8193	15.656
Iran	Shahr-i-Sokhta	ore*	Hauptmann et al. 2003	SS 161	2.495	0.8329	15.624
Iran	Chechel Kureh	ore	Hauptmann et al. 2003	E 127/4111	2.4899	0.8394	15.657
Iran	Chechel Kureh	ore	Hauptmann et al. 2003	E 128/4112	2.4879	0.8389	15.659

Region	source	material	reference	analysis #	208/207	207/206	207/204
Iran	Qaleh Zari	ore	Hauptmann et al. 2003	E 128/4286	2.4913	0.8349	15.662
Iran	Qaleh Zari	ore	Hauptmann et al. 2003	E 130/4661	2.4906	0.8347	15.665
Oman	Aarja	ore	Chen and Pallister 1981	Aarja	2.4484	0.8601	15.459
Oman	Al Ajal	ore	Calvez and Lescuyer 1991	PS12	2.4104	0.8797	15.668
Oman	Al Ajal	ore	Calvez and Lescuyer 1991	PS18	2.4435	0.8699	15.501
Oman	Al Ajal	ore	Calvez and Lescuyer 1991	PS17	2.4446	0.8615	15.515
Oman	Bayda	ore	Chen and Pallister 1981	Bayada	2.4433	0.8627	15.438
Oman	Daris 1	ore	Calvez and Lescuyer 1991	PS5	2.4507	0.8559	15.488
Oman	Daris 1	ore	Calvez and Lescuyer 1991	PS4	2.4532	0.8557	15.443
Oman	Daris 2	ore	Calvez and Lescuyer 1991	PS2	2.4676	0.8454	15.6
Oman	Daris 2	ore	Calvez and Lescuyer 1991	PS1	2.467	0.8459	15.547
Oman	Gaddamah (near Lasail)	ore	Calvez and Lescuyer 1991	CU54	2.4593	0.8545	15.533
Oman	Hayl as Safil	ore	Calvez and Lescuyer 1991	CJ55	2.4647	0.8453	15.603
Oman	Hayl as Safil	ore	Calvez and Lescuyer 1991	PS16	2.455	0.8535	15.461
Oman	Lasail	ore	Chen and Pallister 1981	Lasail	2.4412	0.8564	15.427
Oman	Maqa'il	ore	Calvez and Lescuyer 1991	CU73	2.4613	0.853	15.544
Oman	Rakah	ore	Calvez and Lescuyer 1991	PS9	2.465	0.8466	15.62
Oman	Rakah	ore	Calvez and Lescuyer 1991	CJ58	2.4678	0.8444	15.602
Oman	Rakah	ore	Calvez and Lescuyer 1991	CJ57	2.468	0.8438	15.606
Oman	Rakah	ore	Calvez and Lescuyer 1991	PS6	2.4682	0.8431	15.608
Oman	Rakah	ore	Calvez and Lescuyer 1991	PS8	2.4683	0.8437	15.608
Oman	Rakah	ore	Calvez and Lescuyer 1991	PS7	2.4691	0.8438	15.593
Oman	Rakah	ore	Calvez and Lescuyer 1991	PS10	2.4701	0.8454	15.607
Oman	Zuha	ore	Calvez and Lescuyer 1991	CU24	2.4439	0.8568	15.451
Rajasthan	Ganeshwar	slag	LARCH	RNSG_13	2.4613	0.8513	15.754
Rajasthan	Ganeshwar	slag	LARCH	RNSG2.2	2.4481	0.856	15.701
Rajasthan	Ganeshwar	slag	LARCH	RNSG2.2_14	2.4345	0.8682	15.849
Rajasthan	Ganeshwar	slag	LARCH	RNSG2.5	2.4249	0.8674	15.567
Rajasthan	Ganeshwar	slag	LARCH	RNSG2_10	2.4534	0.8552	15.717
Rajasthan	Ganeshwar	slag	LARCH	RNSG2_11	2.4304	0.8689	15.745
Rajasthan	Ganeshwar	slag	LARCH	RNSG2_12	2.4392	0.8662	15.723
Rajasthan	Ganeshwar	slag	LARCH	RNSG7	2.4281	0.8728	15.538
Rajasthan	Ganeshwar	slag	LARCH	RNSG6	2.4304	0.8688	15.679
Rajasthan	Ganeshwar	slag	LARCH	RNSG8	2.4218	0.8654	15.824
Rajasthan	Ganeshwar	slag	LARCH	RNSG9	2.4246	0.8634	15.565
Rajasthan	Singhana	slag	LARCH	RNSS4	2.3798	0.8856	15.853
Rajasthan	Singhana	slag	LARCH	RNSS5	2.3845	0.8863	15.608
Rajasthan	Singhana	slag	LARCH	RNSS7	2.4338	0.8603	15.723
Rajasthan	Singhana	slag	LARCH	RNSS8	2.4354	0.8637	15.616
Rajasthan	Piplawas	ore	Hegde and Ericson 1985	no #	2.2803	0.9844	15.444

Region	source	material	reference	analysis #	208/207	207/206	207/204
Rajasthan	Kankaria	ore	Hegde and Ericson 1985	no #	2.3141	0.963	15.524
Uttaranchal	Askot	ore	LARCH	UT1	2.3351	0.9547	15.746
Uttaranchal	Askot	ore	LARCH	UT10	2.3094	0.9755	15.659
Uttaranchal	Askot	ore	LARCH	UT2	2.3013	0.9813	15.727
Uttaranchal	Askot	ore	LARCH	UT4	2.3034	0.9823	15.518
Uttaranchal	Askot	ore	LARCH	UT5	2.3017	0.9841	15.708
Uttaranchal	Askot	ore	LARCH	UT6	2.3001	0.982	15.686
Uttaranchal	Askot	ore	LARCH	UT7	2.3023	0.9799	15.639
Waziristan	Shinkai	ore	LARCH	WAZ-1	2.4671	0.8467	15.668
Waziristan	Shinkai	ore	LARCH	WAZ-2	2.4674	0.8478	15.664
Waziristan	Shinkai	ore	LARCH	WAZ-3	2.4768	0.8462	15.644
Waziristan	Shinkai	ore	LARCH	WAZ-4	2.4812	0.8444	15.573
Waziristan	Shinkai	ore	LARCH	WAZ-5	2.4799	0.8465	15.603

APPENDIX 12.9

PB ISOTOPE DATA FOR SEVEN COPPER ORES FROM HARAPPA

artifact number	ore type	Context	208/207	207/206	207/204
H94/4999-529	chalcocite	misc. surface find period unknown	2.4454	0.8485	15.312
H90/3008-13	chalcocite	Mound E – survey, Period 3 or Later	2.4678	0.8434	15.309
H90/2070-12	chalcocite	Mound E – survey, Period 3 or Later	2.4593	0.8452	15.479
H90/3008-14	chalcocite	Mound E – survey, Period 3 or Later	2.4373	0.8610	15.148
H90/3022-98	malachite	Mound E – Tr. 58 Period 3 or later	2.4652	0.8470	15.531
H95/4943-8	malachite	Mound ET – Tr. 28 Period 3 or later	2.4642	0.8473	15.203
H90/3126-1	malachite	Mound E – Tr. 56 Period 3C	2.4639	0.8450	15.419

APPENDIX 13.1

POSSIBLE ROUTES FROM THE INDUS BASIN TO THE SITE OF SHORTUGHAÏ

There are numerous possible routes that Indus Civilization peoples may have taken when traveling to the site of Shortughaï in northern Afghanistan. The major ones emanating from the upper Indus Basin were depicted on Figure 13.9 in Chapter 13. Before reviewing the routes that I believe are suggested by rock and mineral acquisition patterns at Harappa, it is important to at least briefly acknowledge some alternate possibilities. First of all, when journeying to the Shortughaï it is not impossible that Harappans circumvented the Hindu Kush Mountains of Afghanistan altogether, traveling instead toward the west-northwest through the Helmand region and then north to southern Central Asia (Turkmenia). From there they could have continued due east to Bactria and, eventually, Shortughaï. Although this is a circuitous way to get to northern Afghanistan, Francfort points out that (1984a: 172) the Helmand route "is the most probable one between the Harappan world and Turkmenia," where Indus materials have been found at sites like Altyn Depe (Masson 1981). For this reason it should not be ruled out. It is also possible that Harappans utilized a northerly route to Shortughaï but bypassed the highland regions directly west and north of the upper Indus Basin. They could have began such a journey in the lower Indus Basin, traveled via the Bolan and Khojak passes of Balochistan into southeastern Afghanistan and from there moved northward to their destination through the Tarnak Valley and over the Sher-i-Dana and Saling passes. The shortest and most direct routes to Shortughaï from Harappan territory, however, would have originated in the upper Indus Basin. Below I discuss several possibilities.

Harappans from the upper Indus Basin might have embarked on their journey to Shortughaï by first traveling due west, through the Sanghar Pass in the central Sulaiman Range and into northern Balochistan. Travel in this direction would likely have taken them past the large Indus Civilization site of Dabar Kot in the Loralai Valley and, eventually, into the southern Zhob Valley. From there they could have continued west to the Khojak Pass and picked up the second alternate route described in the preceding paragraph or turned north toward the Gomal route, which will be discussed next. Much of the grindingstone, alabaster and some of the vesuvianite-grossular utilized at Harappa (and maybe even white Parh limestone from Loralai too) could have been acquired directly along this northern Balochistan route.

The Gomal Plain may have been an important embarkation area for Harappans traveling to northern Afghanistan. A number of Indus Civilization settlements are now known to have existed in that region including Ghandi Umar Khan, which is located near the Gomal River itself. Harappans could have followed that river to its headwaters, crossed into eastern Afghanistan via the Gomal Pass and then traveled north to their destination from there. Along the way they would have passed not far from the highland Harappan site of Periano Ghundai. Some of the grindingstone and alabaster acquired by residents of Harappa came from sources near the beginning of this route, which Markham noted (1879: 53) was one of the more historically important links between Central Asia and India.

Two main routes lead from the Bannu Basin into eastern Afghanistan – one follows the Tochi River and the other the Kurram River (Thomas and Knox 1994: 93). From their termini near the modern cities of Ghazni and Kabul (respectively) the traveler could continue on to regions in the north. Although the Kurram route, in particular, was a major thoroughfare for traders and invaders alike during the historic period (Markham 1879: 47-50), it is unclear if it might have also been for Indus Civilization peoples. Some of the raw steatite acquired by residents of Harappa and Mohenjo-Daro may well have come from a source in the Safed Koh Range, which forms part of the northern boundary of the Kurram River Valley. However, no trace of a Harappan presence within the Bannu Basin has been detected in over two decades of archaeological exploration there (Khan et al. 2002: 89).

No Indus Civilization sites (save for Shortughaï) have been discovered north of the Salt Range either. However, there is good reason to suppose that an important route for Harappans journeying to and from northern Afghanistan may have traversed those mountains and proceeded across the Potwar Plateau and through the Peshawar Valley. It has been shown that, during Period 3 at Harappa, site residents acquired alabaster (along with Mari "Diamonds") from the Salt Range, large amounts of steatite from sources not far to the north of the Potwar Plateau, and steatite, vesuvianite-grossular and, perhaps, some chert from occurrences on the margins of the Peshawar Valley. It is highly likely (but not yet confirmed) that they acquired gold, amazonite, mica, nephrite, serpentine and many other varieties of stone and metal from those regions as well. Although Harappans might have obtained these raw materials through one of the other interaction scenarios discussed on pp. 487-489, it is probable that, at least at times, they traveled to or near the actual sources themselves. I have argued (pp. 235 & 239) that in order to identify deposits of white-firing steatite it would have been necessary conduct high-temperature experimental firings and that this would have required technological expertise that Northern Neolithic peoples may not have possessed. If Harappans were the ones who conducted such firings then it is likely that, rather than transport samples hundreds of kilometers to the south, they would have tested them at or near potential sources in the north.

From the Peshawar Valley, Harappans had several options for their onward journey to Shortughaï. They could have traveled west into Afghanistan via the Khyber Pass (passing just 10 km north of the Landi Kotal steatite deposit) and then, upon reaching the Kabul Valley, headed north over the Saling Pass into northern Afghanistan. Or they might have turned eastward before Saling and traveled up the Panjshir Valley and over the Anjuman Pass to the lapis lazuli mines of Badakhshan. From there they would have needed only to have followed the Kokcha River 200 km downstream to its confluence with the Oxus River. Shortughaï is located less than 20 km from that point. Harappans could have also left the Peshawar Valley by a northerly route, passed through the Swat and Chitral valleys (over the Malakand and Lowari passes respectively) and the took the Dorah pass eastward toward Badakhshan and the lapis lazuli mines. A variation on this route would have them exiting the Peshawar Valley from the east, following the Indus River north for a ways and entering the Swat Valley via the Shangla Pass. By doing so, they would have passed nearby the Sherwan steatite deposits in the Hazara region, which is where the large majority of steatite used at Harappa is now known to have been derived.

Indus Civilization peoples may have journeyed to Shortughaï by any or all of the routes described above. However, I would argue that the evidence presented here most favors those routes that first passed through either the Potwar Plateau / Peshawar Valley regions or the Gomal Plain.